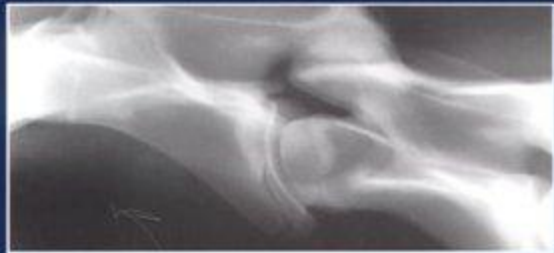# Clinical Radiology of the Horse

Second Edition

JANET A. BUTLER, CHRISTOPHER M. COLLES,
SUE J. DYSON, SVEND E. KOLD AND PAUL W. POULOS

Blackwell Science

Clinical Radiology of the Horse

Clinical Radiology of the Horse

Second Edition

JANET A. BUTLER
Lansdown Veterinary Surgeons, Willesley Equine Clinic, Nr Tetbury, UK

CHRISTOPHER M. COLLES BVetMed, PhD, MRCVS
Avonvale Veterinary Group, Banbury, UK

SUE J. DYSON MA, VetMB, PhD DEO, FRCVS
Centre for Equine Studies, Animal Health Trust, Newmarket, UK

SVEND E. KOLD DVM, Dr Med Vet, MRCVS
Lansdown Veterinary Surgeons, Willesley Equine Clinic, Nr Tetbury, UK

PAUL W. POULOS JR, DVM, PhD
Poulos Veterinary Imaging, Ukiah, California, USA

Blackwell
Science

Contents

Contents

Preface

As the knowledge of equine radiology and radiography progressed, the need for a textbook specifically in this field became more obvious. We set out with the intention of creating such a book, but more particularly a book that would be of practical help to general practitioners, as well as providing specialist information. The authors all practise equine radiography and radiology daily, and we have pooled our knowledge to write a book by consensus, rather than a multiauthor text with chapters contributed by different people. There is no doubt that writing this way has tested the patience and endurance of us all, but we hope that it has enhanced the value of the book to the reader.

This second edition of the book has been significantly enlarged to include new information, to provide additional illustrations and line diagrams, and to incorporate the most recent relevant literature references. The authors have collectively gained considerably more experience in a variety of clinical situations, and in some instances have changed their opinions in the light of new knowledge; the text has been updated accordingly.

The authors recognize that there have also been advances in other complementary imaging techniques such as nuclear scintigraphy, diagnostic ultrasonography, magnetic resonance imaging and computed tomography. Where appropriate, brief references have been made to these techniques, but the authors have continued to focus the text on radiography and radiology, and advise the reader to consult other more specialized texts for information on these methods.

We would particularly like to thank J. G. Lane, BVetMed, DES, FRCVS, of the University of Bristol, and I. G. Mayhew, BVSc, DipOVC, PhD, MRCVS, DACVIM, of the University of Edinburgh, for their assistance in reading and providing specialist advice on parts of the text.

Radiographs have been provided primarily from the Animal Health Trust, and the Faculty of Veterinary Medicine, University of Florida. We also thank the School of Veterinary Science, University of Bristol, for several radiographs of the head, and the College of Veterinary Medicine, Swedish University of Agricultural Sciences, Uppsala, for a number of radiographs of the thorax and feet. We thank J. Weaver, S. Stover and T. O'Brien (University of California, Davis) and the *Equine Veterinary Journal* for figures illustrating soft tissue attachments in the fetlock and pastern regions. Finally we must thank D. R. Ellis, BVetMed, DEO, FRCVS (Greenwood, Ellis and Partners, Newmarket), M. Nowak DVM (Tierklinik Hochmoor), P. Dixon MVB, PhD, MRCVS (University of Edinburgh) and E. Santschi, DVM (Peterson and Smith, Florida) for providing radiographs of a number of conditions that other archives could not provide.

Without the willing support of all the above, and our wives, partners, families, and friends, this book could never have been written.

Chapter 1
General Principles

INTRODUCTION

There are many books which describe the principles of radiographic imaging. This book does not attempt to provide detailed information in this area, and readers who do not have a working knowledge of radiography are advised to consult one of the standard texts in order to obtain the necessary understanding of radiographic physics. This book does aim to provide up to date information specific to the horse. As various forms of competitive and pleasure riding become more popular, the demand on veterinarians to provide the highest quality of treatment is increasing. Radiography of the horse in sickness as well as in health, for insurance and purchase examinations, is increasing. The book is intended for all who radiograph horses, be they equine specialist, general practitioner or student. It gives information on radiographic techniques, equipment, positioning, and views required to visualize the various areas of the horse adequately. It also provides information on the normal radiographic anatomy of the immature and skeletally mature horse, variations, and incidental findings. Finally it gives information on the types of lesion that may be detected, with examples of as many of the more common problems as practicable, as well as brief clinical remarks where appropriate. The 'Further reading' lists at the end of each chapter are not intended to be complete lists of every paper written on the subject of the chapter. They list references that the authors consider of particular interest, and that are complementary to the text. Many of these references give more detailed information in specific areas than can be justified in a textbook of this type.

Interpreting the clinical significance of radiographic changes is always difficult. We set out to indicate certain lesions which may always be regarded as clinically significant, and some which are known to have no clinical significance. The section in each chapter on 'Normal variation and incidental findings' attempts to differentiate between variations which have no clinical significance at any time (e.g. unossified radiolucent lines in the fibula) and those that may be clinically significant for a specific but limited period of time, and therefore require further clinical investigation to determine their significance (e.g. entheseophyte formation). The radiograph is only a reflection of the state of the tissues at the fraction of a second when they were radiographed. There are many findings which indicate a past event that has 'left its mark', but which is no longer clinically significant. For example, entheseophyte formation at the insertion of a ligament may indicate a sprain to that ligament at some time in the past. As entheseophytes take time to form, once they are visible on radiographs they no

longer represent an acute injury, but are the result of an incident which occurred at least several weeks previously.

Radiography is a continually developing science, and as more powerful and sophisticated equipment becomes generally available, the diagnostic possibilities for veterinary practitioners become ever greater. It is hoped that this book will enable veterinarians to get the best out of their equipment, to obtain diagnostic radiographs, and to give a correct and meaningful diagnosis from the radiographs. The information in the text where possible has been collated from the literature, and complemented by the authors' experiences. In some areas, however, there is no published work, or published information is contradictory. In these circumstances the authors have relied on their own collective experience, but have only presented information if all the authors are in agreement. (For example, reported physeal closure times for some physes vary widely between texts. The times given are based on the authors' experience of radiographic closure, in some cases backed up by radiographic examinations of animals specifically to aid completion of this text.) The authors are experienced clinicians who routinely obtain and read equine radiographs, and it is hoped that the broad range of experience which they offer to the reader will prove to be of practical value. It is important to remember that, as radiography is a developing science, 'new' lesions and radiographic views are continually being found and described, and no text can hope to be complete when published, let alone as time progresses.

This text has made use of current terminology. *Nomina Anatomica Veterinaria* (3rd edition, 1983) was consulted for anatomical names. Radiological views are described using the method advocated by the American College of Veterinary Radiologists. Reference to Figure 1.1 may help to elucidate the current terminology used. While at first sight this may appear cumbersome, it does provide a specific description of the views, which allows them to be reproduced accurately. Terminology in common usage is included in parentheses and serves only to maintain continuity with other texts and references. A glossary (Appendix C) is also included and lists former and current scientific terminology as well as common lay terms.

We have not set out to provide radiographs of every variation of all lesions. Rather we have given typical examples of lesions, and in the text have indicated how these may vary. We also hope that the reader will use this text as a basis to understand why certain types of lesions form, and the processes that are likely to cause them, so that an inexhaustible supply of radiographic variations would be superfluous. Although we have done our utmost to find radiographs that reproduce well, we ask the reader to remember that inevitably some detail is lost in the process of transferring radiographs to print, and in some cases the lesions depicted are far easier to detect on original films.

PRINCIPLES OF RADIOLOGY

The following paragraphs serve only as a reintroduction to the subjects of image production and differentiation. For more detailed information the
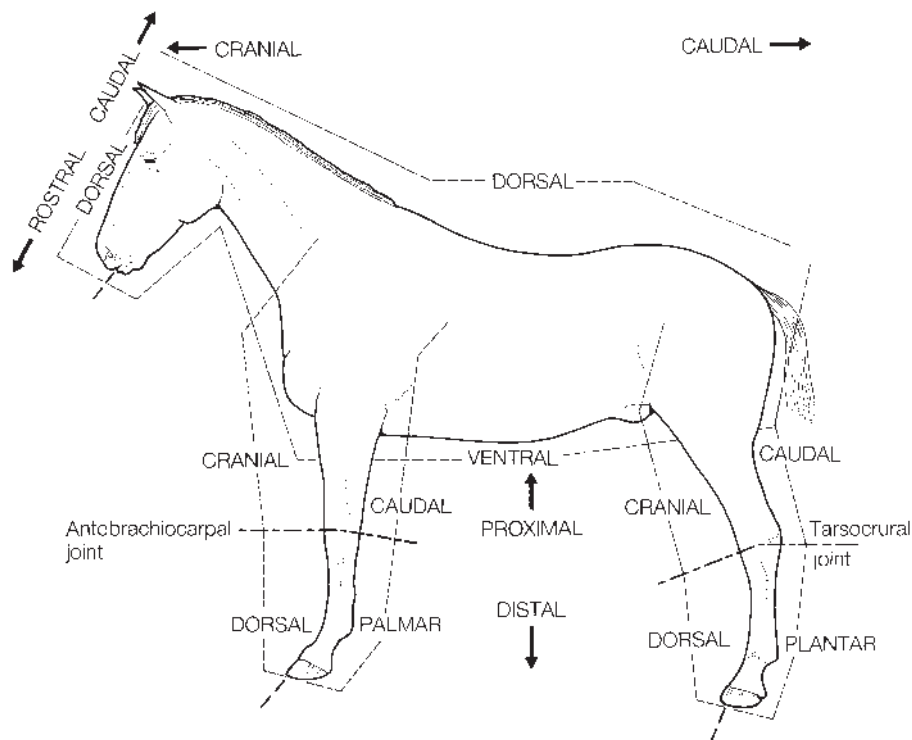
Figure 1.1 Correct nomenclature to describe various aspects of the horse.

reader is referred to the standard radiology texts. It is important that any radiograph is of maximum quality and yields sufficient detail to allow subtle radiographic lesions to be detected.

An x-ray beam is produced by acceleration of electrons onto a tungsten target. An image is created by the x-rays that penetrate an object placed in the path of the x-ray beam. This image is dependent, in part, on the total number of x-rays produced (milliamperage multiplied by the time of the exposure in seconds, mAs), the distance from the focal spot of the x-ray tube to the film (focal–film distance, FFD), and the ability of the x-rays to penetrate the tissue, which is dependent upon kilovoltage (kV) or kilo-voltage peak (kVp).

Other important variables include the type of film being used and the compatibility of the screens, which intensify the image. The large number of film and screen combinations available makes a discussion of this subject beyond the scope of this book. The clinician should rely on a veterinary radiologist or knowledgeable sales person to help decide which film–screen combination is best suited to the x-ray machine and the practice, although Appendix B gives some guidelines. With a high output x-ray machine (100 kV, 100 mAs) it is well worthwhile investing in high definition screens, for use with single emulsion, relatively slow film for distal extremity work. This will give the best quality detail. This system is unsuitable for low output machines, because exposure times would be too long, resulting in loss of definition through movement blur. Rare earth screens are essential for obtaining high quality images proximal to the carpus and tarsus. Old screens are like old horses, they collect scars and lose performance as they age, and some should be replaced on a regular basis

in order to obtain the optimum level of performance. It is also important that screens are cleaned regularly, to prevent the build-up of dust and extraneous materials within the cassette, which results in white spots and lines on processed films.

The image produced on the x-ray film is dependent on the ability of the x-ray beam to penetrate a given volume of a specific tissue. It is more difficult to penetrate bone than air, and therefore less x-rays will reach the film if they have to penetrate bone rather than air. The areas of film exposed to unobstructed x-rays will be black, whereas the areas protected by bone, which absorbs or deflects a proportion of the x-rays, will be relatively white and unexposed. Intermediate densities of tissues produce variable shades of grey. Fat is the least dense tissue, and will give almost black tones, with soft tissues and bone giving increasingly light tones. It is the juxtaposition of these tissues of varying densities that allow for differentiation of form and structure.

It is advantageous to record the exposure settings used each time, and gradually to build up an exposure chart. This should include a record of the size and age of the horse, the area radiographed, and the exposures and the film–screen combination used. This allows better radiographs to be obtained, and also provides a basis for estimating the required exposures for animals of different sizes and ages. Once this chart has been created, it is important to maintain a constant FFD. A reduction in FFD increases the radiation reaching the screen by a factor of the square of the change in distance (necessitating a reduction in the exposure factors), whereas an increase in distance has the opposite effect. Generally in equine radiography a FFD of 75–100 cm is used. Note that single emulsion film is particularly sensitive: a slight change in FFD can have a relatively big effect on exposure.

In a well-positioned radiograph, the x-ray beam is perpendicular to the cassette to avoid image distortion. Most of the radiation passes through the tissues and exposes the film, or is absorbed by the tissues. Some of the radiation is always deflected (termed 'scatter') and this results in reduced film contrast. A grid is placed in front of a cassette to absorb scatter radiation when the thickness of the area being radiographed is sufficient to produce enough scatter to interfere with interpretation of the radiograph. This is usually when the body exceeds 11 cm in thickness. Thus equine extremities below the carpus and tarsus usually do not require the use of a grid. Grids are generally not required for soft-tissue evaluation, and may be contraindicated in this situation. There are numerous types of grid, but their function is always to reduce the effect of scatter on the film. In equine radiology, parallel grids are normally used. The disadvantages of a grid are that they increase the exposure required and produce lines on the films, which are sometimes found objectionable when reading the radiograph. If a focused grid is used, the x-ray beam must be perpendicular to the grid, centred on it, and at the correct FFD. When grids are of value, this is noted in the discussion of the projections described in the following text.

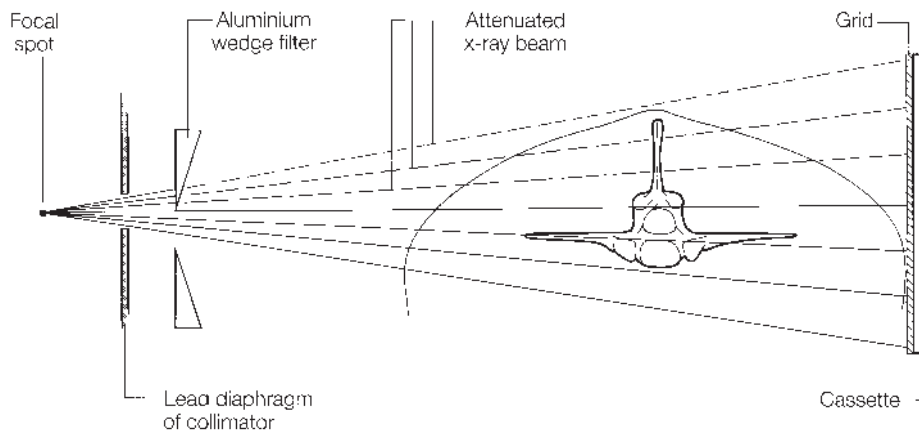In several parts of the following text, reference is made to an aluminium

Focal spot — Aluminium wedge filter — Attenuated x-ray beam — Grid —

Lead diaphragm of collimator

Cassette

Figure 1.2 Use of an aluminium wedge filter placed between the x-ray machine collimator and the object to be radiographed. The upper leaves of the filter placed in the x-ray beam reduce the exposure of the upper part of the beam.

wedge filter (Figure 1.2). This is placed immediately in front of the x-ray tube, and absorbs a proportion of the x-rays. It allows the intensity of the beam to be reduced in specific areas. It is of particular value when radiographing parts of the horse that show a marked change in soft-tissue thickness from one side of the film to the other, e.g. the thoracolumbar spine or stifle.

Preparation of the patient is essential to good radiography. Quiet and careful handling will reduce movement, and sedation may be beneficial in some cases. Blinkers, blocking the horse's line of vision, may make it less apprehensive. Cotton wool ear plugs, or background music, may make the horse less aware of the noise of the x-ray machine. Areas to be radiographed should be brushed to remove mud from the coat, which can produce confusing artefacts. For radiographs of the feet, the shoes normally need to be removed and the feet trimmed to remove loose horn and dirt.

A high-quality radiograph is also dependent upon good darkroom technique. The developer and fixer must be kept clean, replenished, and replaced regularly. When hand processing, the solutions should be agitated before and during processing a film. It is important that developing should be carried out at a constant temperature and for set times. The film should be rinsed thoroughly after developing, and washed well in running water after completing fixing, before being dried. Automatic processing undoubtedly gives more consistent results than manual processing, and allows marked improvement in radiographic standards. The reader is urged to consider the use of automatic processing as soon as the volume of work permits it.

Radiation safety, i.e. ensuring that personnel around the horse do not receive doses of radiation, is extremely important. There are codes of practice available in different countries, but the basic principles can be summarized as follows:

1   Keep the number of people present when radiographing a horse to the absolute minimum required for its safe handling.

2   Use appropriate restraint of the horse to keep it still during exposures (so that repeat exposure to radiation is not necessary). Sedation may be required in some cases.

3   Use cassette holders whenever possible. Certain views, where 'patient

tolerance' is low, may prompt the hand holding of cassettes. This may be justified if it reduces the repetition of radiographs or prevents the horse panicking. If it is essential to hand hold a cassette, then large cassettes should be used, with the x-ray beam well collimated, and the holder's gloved hands as far from the primary x-ray beam as possible.

4 The x-ray beam should be collimated, and a light beam diaphragm used to enable maximum collimation. *No part of any attending person, even if covered with protective clothing, should be placed in the primary beam.* Protective lead clothing protects from scattered radiation only, not the primary beam. Remember that the primary beam will continue past the patient and cassette, and personnel standing on the opposite side of the patient are at risk.

5 All personnel who must remain present during radiography must wear protective gowns, and if near the primary beam should also wear gloves or similar hand and arm protection, and a thyroid protector.

6 All personnel working with and around x-ray machines should be monitored using a film badge system.

With the increasing use of radiography, and the rise in litigation against veterinarians, it is essential that radiographs are carefully labelled. This should be done photographically on the film, either by the use of one of the special tapes produced for this purpose, attached to the cassette when the film is exposed, or by a labelling light-box system in the darkroom. Labels should include at least the identity of the horse, the limb radiographed, the date, and lateral or medial markers where relevant. Ideally the veterinary practice and view employed should also be identified. It is also essential that a complete examination is carried out, with an adequate number of films and views of the area involved. The exposures must be correct to demonstrate the lesions present, and the radiographs must be of diagnostic quality. An inadequate examination may be at best inconclusive and at worst totally misleading.

PRINCIPLES OF RADIOGRAPHIC INTERPRETATION

It is important to read radiographs when they are dry. The emulsion swells when wet and detail cannot be appreciated on wet films.

It is helpful if radiographs are always viewed using the same orientation, i.e. with the horse facing to the viewer's left, medial on the left, and when appropriate the left side on the right. This aids interpretation, as only one image need be remembered for each area radiographed. (This varies slightly from the convention that any film should be viewed as if the examiner was looking at the patient face on, e.g. the left forelimb is viewed with medial to the left, and the right forelimb with medial to the right.) The number of views required for any area varies, and is mentioned in the text. It is important to obtain an adequate number of views to ensure that no lesion is missed, and an attempt to compromise with fewer views is a false economy. The use of 'special' views, e.g. obliques and skylines, of suspected lesions can be remarkably rewarding.

Adequate radiographic interpretation is dependent on complete and systematic evaluation of all of the information that is found on the film. Films should be viewed on a viewing box, in a room with subdued light. This optimizes the ability of the reader to differentiate structures and to obtain the maximum information from a film. The darker the film, the more important it becomes that the conditions under which it is read are ideal. Initially the film should be evaluated from a distance of several feet before viewing closely, in order to get an overall impression before concentrating on details. Masking the light around the edge of the radiograph also improves the ability to read a film, as do high-intensity illumination devices.

Start by assessing the radiograph itself:
- Is the quality of the film adequate for interpretation?
- Are there any processing artefacts or other artefacts (e.g. mud on the horse) which will influence interpretation?

Then move on to assess the area radiographed:
- What is the approximate age of the patient?
- Is there any soft-tissue abnormality such as swelling?

Finally look at the outline of the bones and their detailed internal structure:
- If an 'abnormality' is identified, ensure that it is real – can it be seen on another view? Can it be explained by positioning or overlap of other bones or soft-tissue structures? Is it a variation rather than an abnormality, e.g. the position and shape of a nutrient foramen can vary considerably. Could a radiolucent zone be explained by introduction of air during a previously performed local analgesic technique (Figure 1.3)? Intra-articular gas appears as a semicircular or more diffuse radiolucent area, often in the proximal part of a joint, whereas extra-articular gas appears as a linear radiolucency. These lucencies may persist for up to 48 hours after injection.

Would additional views aid or complete adequate evaluation?
- If it is a true radiographic lesion, describe it in radiographic terms. In this process of description it is often possible to determine if it is an active or inactive process. In general, terms like smooth, regular and well marginated (defined) lead towards a conclusion of normal, benign or long-standing lesions. Terms such as roughened, irregular, sharp, poorly demarcated, or destructive lead to a conclusion of active disease. If the process is considered to be pathological, then think what pathological process could cause this change and then consider what diseases could cause this type of pathology.

If films are obtained to confirm the presence of a specific disease or disease process and are not completely evaluated, the severity of the condition, complications of the process or other concurrent lesions may be overlooked. Thus to read radiographs successfully, it is important to relate the changes seen to known behaviour of the tissues under consideration, rather than relating the radiographic appearance to a clinical condition seen before. The latter method relies heavily on experience and does not allow interpretation of changes that have not been previously encountered. It is important to remember that each radiograph can only represent a fraction

Figure 1.3 Dorsopalmar view of the distal metacarpal region and metacarpophalangeal joint of a mature horse. There are radiolucent areas superimposed over the third metacarpal bone. These gas shadows are the result of inadvertent introduction of air into the metacarpophalangeal joint while performing intra-articular analgesia. Such lucent areas may persist for up to 48 hours.

of a second in the life of the patient, and the development of a disease process. It is a static image of a dynamic process. When a radiograph is read, all the changes from the normal should be considered and used to build up an impression which can then be related to disease processes known to occur in the region. For accurate interpretation it is important to take into account factors such as the period of time for which the clinical signs have been present, the age, sex and breed of the patient, and the validity of the history and possible complicating factors. A working diagnosis can then be formed, which will complement any laboratory findings and other imaging techniques, and help to confirm a clinical diagnosis. There is no substitute for a good clinical history and examination, and radiographs should only be used as an aid to the clinical diagnosis.

It is beneficial to have bone specimens available when reading radiographs, particularly oblique views. An anatomy book and a library of normal radiographs of each anatomical area at different ages are invaluable. If problems are encountered in evaluating an area, it is often

helpful to obtain a similar radiograph of the contralateral limb for comparison, thus providing a perfect age, sex, and breed matched radiograph. Remember that, in the neonate, some structures are not ossified and therefore cannot be visualized. More confusing is the appearance of partially ossified structures (e.g. incompletely ossified subchondral tissues have an irregular opacity, which may seem similar to the radiographic appearance of infection). The normal radiographic appearance of the structures of immature animals is therefore described in each chapter.

Radiographs are only one part of a jigsaw puzzle and may be used for several purposes:
- To confirm, refute or suggest a diagnosis.
- To give information on progression and severity of a condition, and aid formation of a prognosis.
- To add information regarding size, shape, position, alignment and possibly duration of a lesion.

When reading a radiograph the result must be fitted into the general picture presented to the clinician. It is one aid to diagnosis that the clinician has available. In some cases special views or contrast studies may provide valuable additional information. There are many other complementary imaging techniques (e.g. ultrasonography and scintigraphy) and other sources of clinical information that are available. The radiograph is an aid to diagnosis and not the ultimate diagnosis in itself.

One of the most difficult questions to answer is how long a lesion has been present. This is often of importance, but can seldom be answered with any degree of certainty. Minimum times for certain lesions to develop can be estimated, but the time for which a lesion has been present often remains uncertain. The following pointers may be of value:
- Osteophyte formation of any type is not normally visible, even under optimum conditions, in less than 3 weeks.
- Treatment after injury may delay osteophyte formation.
- Incomplete or fissure fractures may take up to 2 weeks to become visible.
- Active bone changes are characterized by lesions with irregular or fuzzy margins, which may be less opaque than the parent bone.
- Inactive bone changes are generally smooth, regular and uniformly opaque.
- Large productive changes may take months to form and become smooth in outline.
- An old inactive bone lesion may not indicate current disease, although it may be present in the same region as a current problem.
- Bone models due to the stress applied to it (Wolff's law). Non-stressed bone does not model.
- Scars in bone, as in any other tissue, do not model.

It should be noted that the terms remodel and model are frequently used incorrectly in radiology (see Appendix C: Glossary). In this text, the term remodel is frequently employed because of its common usage. Modelling is, however, a more correct term, compatible with changes detectable radiographically and histologically.

[9]

RADIOLOGICAL APPEARANCE OF PHYSIOLOGICAL
CHANGES AND SOME COMMON PATHOLOGICAL
LESIONS

Bone changes

The basic ability of bone to respond to stimuli is affected by various factors, such as diet, disease, and the physiological state of other organs such as the lungs, kidneys and gastrointestinal tract.

It is important to remember that the normal bone status varies throughout life. During the period of skeletal growth, there is increased bone formation relative to resorption. The skeleton of the young individual lacks density and is more pliable (35% mineral to 65% matrix and cells). As the individual matures, the density gradually increases (approaching 65% mineral and 35% matrix and cells). With advancing age the bone mineral balance changes towards decreased formation and increased resorption.

Although it is common to think of bone as being largely calcium, the mineral content of bone is roughly 35% calcium, 17% phosphorus, and 12% copper and other minerals. Radiologically it is not possible to detect a decrease in mineralization of less than approximately 30% of the total mineral content, and therefore changes in bone mineralization may be undetectable radiographically early in a disease process.

It is important to remember that some changes reflect past history, rather than the response to current stimuli; thus some radiographic lesions may no longer have clinical significance, but persist as incidental findings.

Wolff's law states that bone models in relation to the stresses placed on it, and modelling is dependent upon bone function and the distribution of the load. Forces are applied to bone at the sites of attachment of ligaments and tendons or through the joints. Application of a load may deform the part concerned. Deformity is dependent upon the degree of the stress and the number of loading cycles.

When evaluating radiographs it should be remembered that bone is a living dynamic tissue which can only respond in a finite predictable way to an infinite number of outside stimuli or insults.

Demineralization of bone

GENERALIZED DEMINERALIZATION

Generalized demineralization or osteopenia may be recognized by: thinning of the cortices; coarser, more obvious trabecular pattern; apparent radiographic overexposure due to reduced bone density (check the FFD, exposure values and processing technique).

Generalized demineralization (Figure 1.4) may result from a mobilization of minerals because of a need elsewhere in the body, e.g. in

Figure 1.4 Slightly oblique lateromedial view of the distal limb of a mature pony, showing generalized demineralization due to secondary nutritional hyperparathyroidism. Note the thin poorly defined cortices and the very prominent trabecular pattern (compare with Figure 2.63c–f, pages 111–14, of a normal metacarpophalangeal joint).

Figure 1.5 Dorsolateral-plantaromedial oblique view of a metatarsophalangeal joint of a mature horse. Note the extremely obvious trabecular pattern in the lateral proximal sesamoid bone due to disuse osteopenia. The horse had not borne full weight on the left hindlimb for the preceding 6 months due to severe navicular disease and adhesions between the deep digital flexor tendon and the navicular bone. Note also the opacities on the plantar distal aspect of the joint, which represent the ergot.

pregnancy, dietary inadequacy or metabolic imbalance (e.g. secondary nutritional hyperparathyroidism), or renal disease. Alternatively the lack of mineral may indicate that the patient is very young or very old.

LOCALIZED DEMINERALIZATION

Loss of mineral in a single limb indicates a process limited to that area, e.g. the loss of mineral in one leg may relate to disuse osteopenia (Figure 1.5). Mineral is lost due to muscular inactivity and/or reduction in weight bearing.

Figure 1.6 Lateral view of the summits of the dorsal spinous processes in the mid-thoracic region. There is extensive demineralization of the dorsal spinous process of the ninth thoracic vertebra. The cortex is also irregular in outline.

It should be compared with the contralateral limb if a generalized disease might be implicated.

FOCAL DEMINERALIZATION

Focal loss of bone (Figure 1.6) may indicate the presence of infection, neoplastic invasion, or replacement of bone by fibrous tissue as a result of a previous disease process (this may be considered to be equivalent to a scar in bone). It is also seen as an osteochondral defect in osteochondrosis, in osseous cyst-like lesions, as subchondral bone loss in degenerative joint disease, in association with vascular abnormalities, and along fracture lines. It may also result from continuous pressure on bone, as in chronic proliferative synovitis.

Increased bone production

This may result in increased bone density and thus radiopacity.

A generalized increase in bone density may be due to fluorine poisoning or a hereditary disease such as osteopetrosis. In some species, but as far as is known not the horse, mineral deposition could indicate hypervitaminosis A.

[12]

Wolff's law states that bone models in relation to the stresses placed on it, and is dependent on its function and the distribution of the load. Cortical thickness, particularly of the third metacarpal and metatarsal bones, changes from a young, skeletally immature, untrained horse to a mature trained horse. The dorsal cortex becomes significantly thicker than the palmar cortex. If a horse has a marked conformational abnormality, such as 'off set knees', the distal limb bones will model accordingly, resulting in increased thickness of the cortices of the bones carrying increased load.

FOCAL NEW BONE FORMATION

Osteophyte formation occurs in response to various stimuli. The time for osteophyte development after a stimulus varies between individuals and depends upon the inciting cause. It may take as little as 2 weeks, or take several weeks. Osteophyte formation with uniform opacity and a smooth outline is likely to be longstanding and inactive. More lucent osteophyte formation, or a formation with a more lucent tip, is likely to be actively developing.

Osteophyte formation may be categorized in relation to its location. *Periarticular osteophytes* may be associated with articular pathology, and develop at the margins of articular cartilage and periarticular bone. They also develop as a consequence of joint instability. *Entheseophytes* are seen where tendons, ligaments or joint capsules attach to bone. They represent the response of bone to stress applied through these structures, whether it is tearing of a portion of a ligament, chronic stress applied by a tendon, capsular traction, or chronic capsular distension. It may be difficult to differentiate between osteophytes and entheseophytes in some areas.

PERIOSTEAL OR ENDOSTEAL BONE

Periosteal or endosteal new bone formation results from inflammation of the periosteum or endosteum. This may result from a fracture (the callus forming endosteal and periosteal new bone), trauma, infection, inflammation or tumour.

SCLEROSIS

Sclerosis is a localized increased opacity of the bone due to increased bone mass within existing bone. It is most readily recognized in trabecular bone, and occurs in response to several stimuli including:
- Stress (e.g. subchondral sclerosis in degenerative joint disease).
- In an attempt to wall off infection (e.g. in the medullary cavity adjacent to an area of osteomyelitis, in response to osteitis of cortical bone adjacent to the site of infection, or adjacent to sequestration).
- To protect a weakened area (e.g. sclerosis surrounding an osseous cyst-like lesion).

Bone lesions

Physitis (epiphysitis)

Physitis (or physeal dysplasia) is the term which should be used to describe abnormal widening and bony irregularity at the epiphyseal and meta-physeal margins of the growth plate in skeletally immature horses. The metaphysis of the bone is broadened and asymmetrical. There is sclerosis of the metaphysis adjacent to the physis, which may be more irregular in appearance than normal. The cortices of the metaphysis may be abnormally thick. Soft-tissue swelling over the area of involvement is usually present, and there may be an associated angular limb deformity. These changes are secondary either to rapid cartilage production or to defects in mineraliza-tion within the primary spongiosa.

Although any physis may be involved in this process, it is most commonly associated with the distal radius (see Figure 4.16, page 196) and distal metacarpal/metatarsal bones in the horse. Focal osteochondral defects have been noted histologically and result from repeated haemorrhage and/or microfractures which interfere with the blood supply to the mineralizing cartilage. Osteochondrosis-like defects have also been described.

Widened metaphyseal and physeal bone that is produced during the acute stage of the disease may persist through life, resulting in an irregular or flared appearance at the location of the physeal scar.

Neoplasia

Primary tumours and metastatic malignancy of the long bones of horses are rare. The majority of tumours that involve bone occur in the skull (see Chapter 8, pages 353 and 379) or occasionally the spine (see Chapter 9, page 425). Tumours result in space occupying lesions that may be radiopaque or radiolucent. Adjacent bone may be distorted in outline, and there may be associated new bone production. It is frequently not possible to differentiate specific tumour types by their radiographic appearance. A malignant tumour may be similar radiographically to the result of infection, and differentiation is based on history, clinical signs, laboratory tests, and biopsy.

Osteitis and osteomyelitis

Osteitis is inflammation of bone, and osteomyelitis is inflammation of cortical bone and its myeloid cavity. In bones that do not have a myeloid cavity (e.g. the distal phalanx), it is not appropriate to use the term osteomyelitis. Osteitis is usually the result of trauma, or inflammation in adjacent soft tissues. It is characterized by new bone formation and some-times bone resorption. Differentiation should be made between aseptic osteitis and infectious osteitis (see below).

Infectious osteitis and infectious osteomyelitis

Infectious osteitis (inflammation of bone due to infection) and infectious osteomyelitis (inflammation of the bone involving the myeloid cavity) are common in the horse. In the adult, infectious osteitis is more common and is usually seen at a single site often related to trauma such as wire cuts or puncture wounds. The hallmarks of infection are:

- Soft-tissue swelling with bone destruction and new bone formation.
- An attempt to wall off infection resulting in radiopaque bone being laid down adjacent to the area of bone infection and destruction.
- Infection of bone may result in the formation of a sequestrum (a piece of dead radiopaque bone) surrounded by an involucrum (an area of lucent granulation tissue) (see Figure 3.18, page 157). A radiolucent tract may be visible extending from the infected area (a sinus).
- The distal phalanx, navicular bone and skull show a slightly different reaction to infection. In these bones, infection tends to cause destruction of bone with little evidence of new bone formation.
- In the foal, osteomyelitis is more common and may occur simultaneously at several sites, often extending into adjacent joints. The converse is also true, and septic arthritis commonly extends into adjacent bone causing an osteomyelitis. Osteomyelitis in the foal tends to be very destructive and there is usually very little response by the bone to wall off the infection.

A useful classification of infection of bone and joints has been devised by Firth (see 'Infectious arthritis', pages 23–4).

Hypertrophic osteopathy

This condition, formerly known as Marie's disease, hypertrophic pulmonary osteoarthropathy or hypertrophic osteoarthropathy, is now termed hypertrophic osteopathy, since it has been shown that pulmonary involvement is not a prerequisite for the development of the disease, as was once thought. Hypertrophic osteopathy principally affects the metaphyses and diaphyses of the long bones, while sparing the joints. The disease is typified by periosteal new bone which often appears to be perpendicular to the cortices of the bone and irregular in outline in the acute stage (Figure 1.7). In the early stages, soft exposures must be used to avoid overexposure of this relatively lucent new bone. Later the margins of the new bone become more opaque and smoother, and the appearance of the original cortex of the bone becomes less clear. The bony lesions develop secondarily to a primary lesion, usually in the thorax or occasionally the abdomen, such as a tumour, an abscess or diffuse granulomatous disease. The cause and distribution of the bony lesions are not understood; however, the bone changes may regress and model if the primary disease can be identified and successfully treated.

Enostosis-like lesions and other circumscribed opacities

An enostosis is defined as bone developing within the medullary cavity or on the endosteum, resulting in a relatively sclerotic region. In the horse

Figure 1.7 Dorsolateral-palmaromedial oblique view of a metacarpophalangeal joint of a 3-year-old Thoroughbred with a history of raised plasma fibrinogen for the preceding 4 months, and very recent onset forelimb stiffness associated with diffuse oedematous painful swellings of the distal limbs. There is soft-tissue swelling and active periosteal new bone on the distal diaphysis of the third metacarpal bone (arrows) and the proximal metaphysis/diaphysis of the proximal phalanx (white arrow). Note its palisade-like appearance perpendicular to the cortex. This is typical of hypertrophic osteopathy. The horse had a dissecting aneurysm of the thoracic aorta. Diagnosis: hypertrophic osteopathy.

Figure 1.8 Lateromedial view of the mid radius of a mature horse. There is a discrete, rounded radiopacity apparently within the medulla (arrow), an enostosis.

enostosis-like lesions have been described as focal or multifocal, intramedullary sclerosis, in the diaphyseal region of long bones, near the nutrient foramen, often developing on the endosteal surface of the bone. The most common sites are the tibia, radius and humerus (Figure 1.8). The aetiology and clinical significance of the lesions are unknown. Such sclerotic reactions should be differentiated from endosteal callus secondary to a fatigue fracture. Small focal opacities in the proximal metaphyseal or diaphyseal region of the tibia have been recognized. Their aetiology and clinical significance are unknown.

[16]

A fracture is a discontinuity of the bone seen radiographically as a lucent line or lines. Radiography is performed to establish the type, severity and degree of displacement of the fracture, and to assess the damage to adjacent joints and surrounding soft tissues. Later radiographs may be obtained to assess the degree of reduction achieved and to monitor healing. In order to establish the presence of a fracture, at least two projections, preferably obtained at right angles to each other, are essential. Many more views may be necessary to establish the exact configuration of the fracture.

Fatigue (stress) fractures and other non-displaced and/or incomplete fractures can be extremely difficult to detect in the acute stage. Mach lines due to edge enhancement should not be confused with fractures. For best visualization of a fracture, the x-ray beam must be parallel with the plane of the fracture, and thus detection may necessitate obtaining many views at 5° angles to each other. Two radiolucent lines often represent a single complete fracture, which traverses through two cortices, e.g. dorsal and palmar, and should not be confused with two fractures. During the normal healing process there is osteoclasis along the fracture line within 5–10 days, resulting in apparent broadening of the lucent fracture line. Thus a fracture line which was not readily apparent in the initial radiographs may be detected on follow-up films obtained 5–10 days later. In the acute stage, nuclear scintigraphy may be a better method of detecting the presence of an incomplete fracture or a fatigue fracture. Some fractures are never visible radiographically, despite there being strong evidence of a fracture from nuclear scintigraphic evaluation. Some radiographically detectable stress (fatigue) fractures may be preceded by the development of sclerosis (see page 13) before the fracture becomes apparent.

A fracture should be evaluated to establish whether it is simple, multiple or comminuted, whether there is articular involvement, the degree of displacement of the fracture fragments and to identify any concurrent pathology which may adversely influence the prognosis.

Fractures involving the physis of a bone may be classified according to Salter-Harris, based upon the configuration and relationship of the fracture plane to the growing cells of the metaphyseal growth plate. The fractures are classified by Salter-Harris as follows (Figure 1.9):

Type I A fracture through the zone of hypertrophied cells without involvement of the adjacent epiphysis or metaphysis.

Type II A fracture through the physis across part of the width of the bone and through the metaphysis, leaving a segment of the metaphysis attached to the epiphysis.

Type III A fracture through the physis across part of the width of the bone and through the epiphysis, entering the joint.

Type IV A fracture across the epiphysis, physis and a portion of the metaphysis, perpendicular to the plane of the physis.

Type V A compression fracture of the physis with minimal displacement.

Although this classification has now been further extended, we feel that the above classification is adequate for practical clinical purposes.
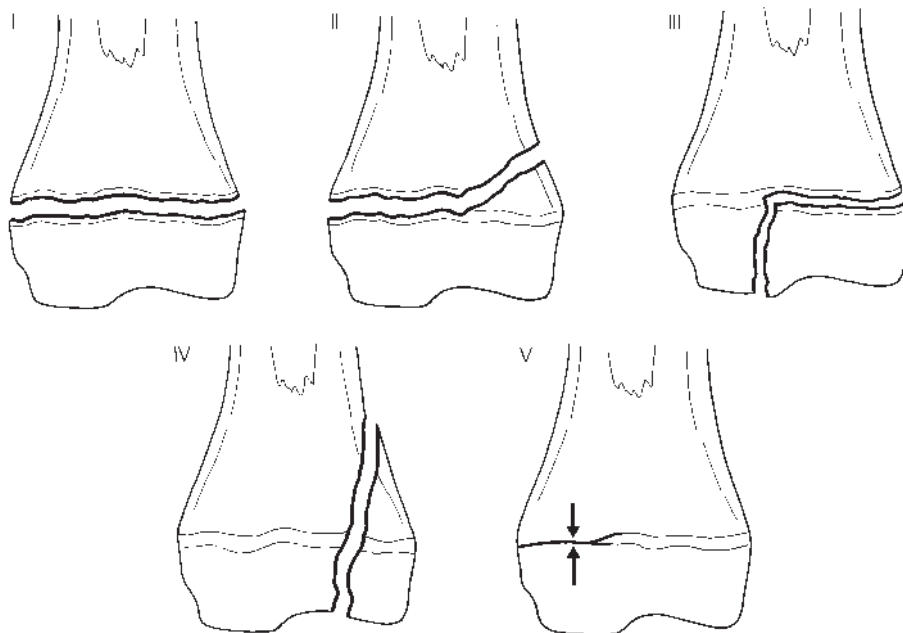
Figure 1.9 Salter-Harris classification of physeal fractures.

Fracture healing should be monitored radiographically to determine the progression of healing. The time interval between re-examinations will depend on the severity of the fracture, the type of repair and the clinical reassessment of the patient. Following initial mineral resorption along the fracture line, and formation of a fibrous callus, calcified periosteal and endosteal callus develops. The amount and quality of callus which develops depends upon the degree of stability at the fracture site and the presence or absence of concurrent infection. Endosteal callus is more difficult to visualize radiographically, but ultimately results in disappearance of the fracture line. Stability of the fracture may develop long before the fracture line disappears radiographically. Some bones (e.g. the distal phalanx, proximal and distal sesamoid bones and the accessory carpal bone) tend to heal by fibrous union, resulting in a persistent lucent line. The rate of healing varies and is dependent on many factors, including the age of the horse, its nutritional and metabolic status, the degree of stability of the fracture, the site of the fracture, the presence or absence of periosteum, the blood supply to the bone, and the presence or absence of infection. Infection is likely to be progressive and impair osseous union unless there is stability at the fracture site.

If a fracture is repaired by internal fixation, and there is adequate stability at the fracture site, healing should be predominantly by primary union, with minimal periosteal callus. Instability at the fracture site will result in secondary union by the production of periosteal callus.

If a fracture has been repaired by internal fixation, the implants and surrounding bone should be examined carefully on follow-up radiographs. The development of localized lucent zones around the implants indicates loosening of the implant, or infection, and it may be necessary to remove one or more selected portions of the implant. Diagnostic ultrasonography

may be helpful in early detection of osteomyelitis in some cases, e.g. detection of fluid around a screw head.

If implants are removed when there is stability at the fracture site, radiolucent tracts will persist for 8–12 weeks. These tracts may act as stress points until adequate remineralization has occurred, and are potential sites for fracture to recur.

Whether a fracture is treated conservatively or surgically, once initial mineral resorption along the fracture line has occurred, there should be progressive narrowing of the fracture line or lines, and they should gradually disappear. Healing may be complete within 6–12 weeks, but some fractures will take considerably longer. A horse may be sound and be able to withstand work, despite the persistence of a radiolucent fracture line. In some locations (e.g. third metacarpal condylar fractures) the long term persistence of a lucent line is commonly associated with recurrent lameness. If a fracture line persists beyond 6 months it can be considered to be a delayed union. There may be sclerosis of the bone adjacent to the fracture line, and the ends of the bone may become slightly flared (Figure 1.10). Although delayed union is not uncommon in the horse, non-union (complete failure of osseous union after 12 months) is rare, except in the areas previously

Figure 1.10 Lateromedial view of the carpus of a mature Thoroughbred steeplechaser, 8 months after the onset of acute lameness. There is a delayed union fracture of the accessory carpal bone. Note the flaring of the fracture margins proximally and the sclerosis along the fracture edges, especially distally. There is no evidence of osseous union proximally. Note also the periosteal new bone on the distal caudal radius, of questionable clinical significance. The horse made a functional recovery, although bony union was not achieved. Diagnosis: delayed union fracture of the accessory carpal bone.

mentioned where healing is usually by fibrous union. If there is apparent healing by fibrous union, it is usually impossible to state when the original fracture occurred. Fractures of the navicular bone usually heal by fibrous union, and frequently lucent zones develop adjacent to the fracture line. These lucent zones are indicative of a fracture of at least 6–8 weeks' duration.

Joint lesions

Swelling

Soft-tissue swelling in and around joints may be classified as shown below.

INTRA-ARTICULAR SWELLING

The joint capsule is distended and in the non-weight-bearing patient there may be a widened joint space. In some locations (e.g. the carpus) a normal lucent fat pad may disappear due to compression. Joint distension is usually associated with inflammation and may be septic or aseptic. If several joints are involved in the neonatal animal, septic arthritis should be considered. If several joints are involved in older animals, immune mediated disease should be suspected, especially if the occurrence is cyclic in nature.

PERIARTICULAR SWELLING

This does not involve the joint space, but may involve the joint capsule as is seen in sprains. Periarticular swelling may also be caused by conditions that are more obvious on examination of the patient than on the radiograph, such as wire cuts, puncture wounds and external trauma. With cuts and wounds, gas may be evident within the soft-tissue swelling.

GENERALIZED PERIARTICULAR SWELLING

This may result in the inability to differentiate between intra-articular and extra-articular fluid accumulation. The inability to differentiate may result from massive swelling or the loss of soft-tissue fat which is normally found in the pericapsular, peritendinous and periligamentous areas.

Trauma

Joint trauma may be classified as shown in Table 1.1.

SPRAIN

Joint sprain is the wrenching of a joint with partial rupture or other injury of its attachments, and without luxation of bones. There is usually rapid swelling, heat and pain. Sprains must be differentiated from fissure fractures and other causes of acute joint swelling. Sprains may be classified as shown in Table 1.1.

Table 1.1 Classification of sprains

Type of tissue damage	Radiographic finding
Ligament strain or partial rupture	Soft-tissue swelling
Ligament rupture	Soft-tissue swelling
Ligament avulsion	Soft-tissue swelling and the presence of a bone fragment

If ligament rupture or avulsion is suspected, stressed radiographs (Figures 1.11a and 1.11b; see below) should be obtained to assess the integrity of the joint and the possibility of subluxation.

SUBLUXATION AND LUXATION (DISLOCATION)

Luxation is the complete loss of contact between the articular surfaces of the joint. Subluxation of a joint is partial loss of contact between joint surfaces, and may be intermittent. Luxation and subluxation in the horse are usually the result of trauma, although congenital luxation of the patella occurs in rare cases. Subluxation of the proximal interphalangeal joint may develop without an obvious cause. Luxation is usually easily identified radiographically, but multiple radiographic views are required in order to assess whether or not there is a concurrent fracture which may adversely influence the prognosis. If luxation is incomplete (i.e. subluxation), radiographic assessment is more difficult. Radiographs should be obtained in the weight-bearing position and compared carefully with the normal anatomy. When luxation or subluxation is suspected clinically, so-called 'stress radiographs' may be helpful to determine the integrity of the periarticular soft tissues such as the collateral ligaments. Stress radiographs are obtained with the limb not weight-bearing, with force applied to the joint in either a mediolateral or dorsopalmar direction to determine whether the bones may be moved abnormally relative to each other (Figures 1.11a and 1.11b).

INTRA-ARTICULAR FRACTURES

Intra-articular fractures exist when there is a break in the articular surface. Unless there is some degree of displacement, damage to the articular cartilage may not be seen, but is assumed to exist. A small degree of displacement will be indicated by the presence of a slight 'step' in the two sides of the articular portion of the fracture line. Fissure fractures are not displaced and many views may be required in order to visualize the fracture, as the x-ray beam must be exactly aligned in the plane of the fissure.

Fractures of the articular margin are termed chip fractures. Radiographs should be carefully inspected for evidence of additional chips, pre-existing degenerative joint disease, or other concurrent pathology, which may adversely affect the prognosis. Differentiation between chip fractures, ectopic mineralization and separate centres of ossification may not

(a)
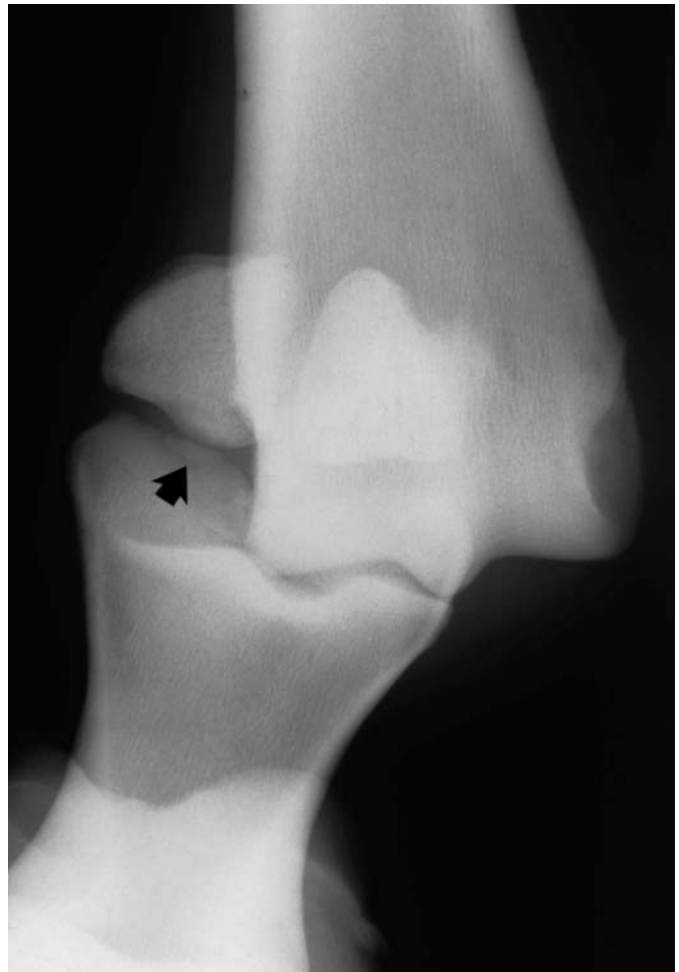
(b)

Figure 1.11(a) Dorsoplantar view of a metatarsophalangeal joint of an event horse with acute onset severe lameness 3 weeks previously. The horse was bearing full weight on the limb without discomfort. The bones are in normal alignment.

Figure 1.11(b) Stressed dorsoplantar view of the same horse as in Figure 1.11a. There is luxation of the metatarsophalangeal joint, and disruption of the proximal articular margin of the proximal phalanx (arrow).

be possible. The position of the mineralized body relative to the articular margin, the size and shape of the body, and the contour of the articular margin should all be assessed carefully. A recent chip fracture may have a sharp edge, and a fracture 'bed' may be discernible. Separate centres of ossification, or old chip fractures, may be very well-rounded uniformly opaque bodies, and a fracture bed is usually not detectable. Ectopic mineralization may be present within the joint capsule.

A slab fracture is a fracture extending from one joint surface to another, e.g. from the proximal to distal articular surface of the third carpal or tarsal bones. These fractures may be extremely difficult to detect radiographically in the acute stage if not displaced. Oblique views are invaluable in the carpus. In the tarsus it may be necessary to re-radiograph the joint after 7–10 days when some demineralization has occurred along the fracture line.

[22]

Infectious arthritis is most commonly seen in young foals, and frequently involves several joints. It may occur in the adult, usually associated with trauma, but may be iatrogenic. Radiographic features of joint infection include:

● Periarticular soft-tissue swelling.
● Joint capsule distension with or without apparent widening of the joint space.
● Irregularity of outline of the subchondral bone.
● Lucent zones in the subchondral bone, with or without sclerosis.
● Periarticular osteophyte formation, due to secondary joint disease.
● Partial collapse of the subchondral bone.

The presence of bony abnormalities indicates that the disease is advanced and warrants a guarded prognosis. The absence of detectable radiological abnormalities does not preclude a diagnosis of infection. The speed of development and degree of cartilage and bone destruction depend on the causative organism.

In the neonate, care should be taken to differentiate the radiographic appearance of incompletely ossified bones, which may have an irregular outline and granular opacity, similar to that seen in infection. Reference should be made to the text in the subsequent chapters, which describes the appearance of incomplete ossification where it is a normal feature at birth. In the foal, joint infection may develop secondarily to infection of an adjacent physis, or may spread from a joint to an adjacent epiphysis.

Firth classified infectious polyarthritis of foals into several syndromes as follows:

1 Physeal type P osteomyelitis. There are areas of irregularity and focal widening in the physis. At this point the term physitis may appear more appropriate than physeal osteomyelitis; however, once the changes are sufficiently far advanced to be seen radiographically there is usually also involvement of the metaphyseal or epiphyseal bone adjacent to the site of origin. Infection may continue to extend into the epiphysis or metaphysis, where the infection is characterized by relatively opaque areas of bone surrounded by lucent areas. These are frequently triangular in shape. As the condition progresses, soft-tissue swelling associated with the joints may be seen, and this may develop into infectious arthritis secondary to underlying osteomyelitis.

2 Type E begins in the epiphysis and progression is similar. The classification is only used to denote where the nidus of infection was established.

3 Type S actually begins in the synovium, and extends from there, rapidly becoming septic arthritis.

4 Type T osteomyelitis is limited to the tarsus and must be differentiated from aseptic necrosis of the central and third tarsal bones. Type T cases usually present because of generalized tarsal enlargement or tarsocrural joint capsule distension. Although the central and third tarsal bones are occasionally involved, the majority of pathology is noted in the distal tibial

[23]

physis and or tarsocrural joint. The main radiographic findings include soft-tissue swelling, distension of the tarsocrural joint and irregularity of the distal tibial physis (type P osteomyelitis). When the central and third tarsal bones are involved, they are normal in shape but have a mottled lucent appearance.

5 Type C osteomyelitis. Recently osteomyelitis of the carpal bones has been noted, and appears similar in many respects to tarsal osteomyelitis. It may therefore be appropriate to include a fifth category in Firth's classification – osteomyelitis identical to type T, but localized to a single carpal bone.

Osseous cyst-like lesions (bone cyst)

Osseous cyst-like lesions (OCLLs) are usually solitary, circular lucent areas in a bone, which may be surrounded by a narrow rim of sclerosis. They are usually unicameral (single chambered) but may be multicameral. They are often close to the articular surface of the bone and sometimes a 'neck' connecting the cyst-like lesion with the joint surface can be identified. Some OCLLs ultimately fill in radiographically, but others persist virtually unchanged. Osseous cyst-like lesions occurring near the articular margin in young horses may appear to migrate progressively away from the joint surface, as normal endochondral ossification occurs.

The aetiology of OCLLs is obscure. Some are true subchondral bone cysts and have a fibrous cystic lining, but there are probably a number of causes, despite their similar radiographic appearance. It has been suggested that they are part of the osteochondrosis syndrome, but the evidence for this is limited. There is increasing evidence that some OCLLs are traumatic in origin.

Osseous cyst-like lesions may or may not be associated with lameness. Cyst-like lesions which occur deep within bone, such as in the carpal bones, are rarely associated with lameness, whereas those close to an articular surface, such as in the medial femoral condyle, are frequently associated with lameness, although lameness may resolve despite radiographic persistence of the lesion.

An OCLL may first be identified as a small lucent depression in the articular surface (see Chapter 7, page 305). This progressively enlarges and a sclerotic margin may develop around the cyst-like lesion. The radiographs should be carefully examined for evidence of concurrent secondary degenerative joint disease.

Osteochondrosis

Osteochondrosis is considered to be a disturbance of endochondral ossification, but there is increasing evidence to show that there may also be primary subchondral bone lesions. The disease may be generalized, although only evident radiographically in certain joints. The femoropatellar, tarsocrural, fetlock and scapulohumeral joints are the most commonly affected in the horse (see Chapters 7, 6, 2 and 5, respectively). The radiographic

appearance of osteochondritic lesions is variable between individuals, and the joints involved, but the changes normally include:

- Discrete osteochondral fragments.
- Alterations in the contour of the articular surface, e.g. flattening or a depression.
- Irregularly shaped lucent zones in the subchondral bone.
- Sclerosis surrounding the lucent zones.
- Secondary remodelling of joints.

Lesions are not always of clinical significance but must be interpreted in the light of the clinical signs. Some lesions remodel gradually and become increasingly sclerotic. Clinical signs are generally recognized in horses less than 3 years of age, but occasionally horses remain asymptomatic until later in life.

Degenerative joint disease

Degenerative joint disease (DJD), osteoarthrosis, osteoarthritis and secondary joint disease are often used synonymously in veterinary medicine, yet distinctions can be made in some cases.

Arthritis simply means inflammation of a joint, and if recognized radiographically is seen as joint capsule distension without evidence of new bone involvement. There is inflammation of the synovial lining and changes in the quantity and quality of synovial fluid. Osteoarthritis or osteoarthrosis indicate that bone has become involved and that a soft-tissue component may (itis) or may not (osis) be present. The term secondary joint disease is used when the primary cause is known, such as in osteochondrosis or intra-articular fracture. Degenerative joint disease is used to refer to any number of causes that affect the joint and its supporting structures. In the horse, the degenerative process which results in DJD may be associated with poor conformation and/or hard use. Advanced DJD, however, is sometimes seen in immature horses, less than 3 years of age, with no identifiable predisposing cause. Any condition that damages cartilage directly, causes joint instability, or subjects the joint to abnormal directional forces, can cause DJD. Immune mediated joint disease should be considered whenever there is polyarthritis, and sepsis can be ruled out.

Radiographic abnormalities associated with DJD included:

- Periarticular osteophyte formation.
- Subchondral bone sclerosis, and loss of trabecular pattern.
- Ill-defined small lucent zones in the subchondral bone.
- Small well-defined osseous cyst-like lesions.
- Narrowing of the joint space.
- Joint capsule distension.
- Periarticular soft-tissue swelling.

One or more of the above may be seen in association with DJD in any joint. If possible, periarticular osteophyte formation should be differentiated from entheseophyte formation. Small periarticular osteophytes are not necessarily synonymous with clinically significant DJD. It must also be borne in mind that the absence of detectable radiographic abnormalities

does not preclude the presence of cartilage degeneration. As DJD progresses, radiographic abnormalities become more obvious.

Dystrophic and metastatic mineralization (calcification)

Calcium is seldom deposited alone. Even in bone the opacity seen on radiographs is due to a mixture of calcium, phosphorus, zinc, manganese and magnesium, and therefore dystrophic and metastatic calcification is more correctly termed mineralization.

Mineralization in soft tissue can occur in association with inflammation, neoplasia, trauma or metabolic disease. The most reliable indication of the cause of the mineralization is the location in which it occurs. This, combined with knowledge regarding the organs or structures located in the area in which the mineral opacity is seen, and knowing what diseases will result in mineralization of a particular organ, will provide valuable information and occasionally a definite diagnosis. The size, shape and pattern of mineralization may vary, and therefore are poor indications of a specific aetiology.

Soft-tissue mineralization has been classified as being metastatic or dystrophic. Metastatic mineralization is the deposition of minerals in tissues that have not previously been damaged. It is associated with hypercalcaemia, hypercalciurea and hyperphosphataemia.

Dystrophic mineralization is the process whereby mineral is deposited in injured, degenerating or necrotic tissue, and is more commonly seen in the horse. It can occur secondary to any injury to soft tissue, e.g. in tumours that have become necrotic, at the site of fat necrosis, subsequent to infarction, and in association with inflammation or haemorrhage. Either type of mineralization may eventually result in the formation of mature bone.

FURTHER READING

Armstrong, S. (1990) *Lecture Notes on the Physics of Radiology.* Clinical Press Ltd., Bristol

Carlson, W.D. (1967) *Veterinary Radiology*, 2nd edn, Lea and Febiger, Philadelphia

Douglas, S.W. and Williamson, H.D. (1970) *Veterinary Radiological Interpretation*, 1st edn, Heinemann Veterinary Books, London

Greet, G. and Greet, T. (1966) The use of specific radiographic projections to demonstrate three intra-articular fractures. *Equine Vet. Educ.* **8**, 208–211

Harrison, L. and Edwards, G. (1996) Radiographic investigation of osteochondrosis. *Equine Vet. Educ.* **8**, 172–176

Kirberger, R., Gottschalk, R. and Guthrie, A. (1996) Radiological appearance of air introduced during regional limb anaesthesia. *Equine Vet. J.* **28**, 298–305

Mair, T., Dyson, S., Fraser, J. *et al.* (1996) Hypertrophic osteopathy (Marie's disease) in Equidae: a review of twenty-four cases. *Equine Vet. J.* **28**, 256–262

May, S. (1996) Radiological aspects of degenerative joint disease. *Equine Vet. Educ.* **8**, 114–120

Meredith, W.J. and Massey, J.B. (1971) *Fundamental Physics of Radiology*, 2nd edn, John Wright, Bristol

Smallwood, J., Shiveley, M., Rendano, V. and Habel, R. (1985) A standard nomenclature for radiographic projections used in veterinary medicine. *Vet. Radiol.* **26**, 2–9

Chapter 2
Foot, Pastern and Fetlock

The foot is a complex area, involving several bones as well as the hoof wall. This chapter has therefore been subdivided into anatomical areas in order to make description easier. Although several of these areas may be obtained on a single radiograph, radiographs centred on the area of interest are required for accurate appraisal.

Except where stated otherwise, the text refers to front and hind feet.

Distal phalanx (pedal bone)

RADIOGRAPHIC TECHNIQUE

Equipment

Radiographs of the distal phalanx (third phalanx, pedal bone) can be obtained with low output (minimum 15 mA) portable x-ray machines. Slow, high detail screens with compatible film are recommended to obtain maximum definition. If machines with an output of 100 mA or less are used, slow, high detail rare earth screens are appropriate.

Prior to obtaining radiographs, the shoe should be removed and the sole and hoof wall cleaned of mud and dirt. Loose flakes of horn from the sole and frog should be trimmed. Particular care should be taken if the frog clefts are deep. A sharp pointed instrument such as a rat tail file is particularly useful for removal of packed debris, followed by a stiff brush. Radiographs of the distal phalanx do not normally require the foot to be packed, although packing the sole will eliminate air shadows from the foot and may avoid confusion in some cases, especially if a fracture is suspected. Care must be taken to ensure that the sole is packed evenly, as the low exposures required to visualize the solar margin of the distal phalanx can also result in images of uneven packing. Loose packing may mimic, or mask, fractures; excessive packing may create radiopaque artefacts.

Lateromedial and dorsopalmar or plantarodorsal views of the distal phalanx should normally be obtained using a grid (see relevant view for details). Oblique views, particularly palmaroproximal-palmarodistal oblique and dorsoproximal-palmarodistal oblique views of the palmar processes, and soft exposures, e.g. radiographs to visualize separation of the hoof wall from the distal phalanx, lucent lines in the dorsal hoof wall, or subtle remodelling of the extensor process are best obtained without a grid.

Positioning

Any examination of the foot should always include lateromedial and dorsoproximal-palmarodistal oblique views. Mediolateral views have a similar appearance to lateromedial views and may be used if preferred. For hind feet it may be easier to obtain plantarodorsal rather than dorsoplantar views.

Lateromedial view

Lateromedial views of the distal phalanx normally require the foot to be raised on a block of sufficient thickness to bring the solar surface of the foot level with the centre of the x-ray beam. This also allows the bottom of the cassette to be placed lower than the solar surface of the foot, so that it is included on the film. The cassette can be supported on the floor, or on a second block, to minimize the risk of movement blur. The x-ray beam should be maintained horizontal, and centred on the distal phalanx. Care must be taken when assessing the hoof pastern axis with this technique, since this will be altered if the horse is not fully weight-bearing on a level surface. An 8:1 ratio grid will give the best results for this view, but acceptable results can be obtained without the use of a grid.

A survey lateromedial view of the entire foot and pastern may be obtained. In this case the maximum information will be obtained if the x-ray beam is centred on the navicular bone – the beam should be centred approximately 1 cm below the coronary band, and midway between the most dorsal and most palmar aspects of the foot at the level of the coronary band. The x-ray beam should be aligned parallel with a line drawn across the bulbs of the heel. The importance of a true lateromedial view cannot be overemphasized for proper interpretation. This may be difficult to obtain on horses with a deviating toe axis. If specific lesions of the distal phalanx are anticipated, the x-ray beam should be centred on the lesion, or on the distal phalanx, at approximately the region of insertion of the deep flexor tendon – a point approximately midway between the coronary band and the ground surface at the junction of the dorsal and middle thirds of the hoof. The beam should be aligned parallel with a line drawn across the bulbs of the heel.

Dorsoproximal-palmarodistal oblique view

For hind feet it is often preferable to obtain a plantarodorsal view of the foot rather than a dorsoplantar. This gives good visualization of the structures within the foot and makes little difference to interpretation of radiographs of the distal phalanx.

A dorsoproximal-palmarodistal oblique view gives good visualization of the body, solar margin, and palmar processes (wings) of the bone, and is suitable for use as a routine view. It may be obtained in one of two ways. The technique giving least distortion is the 'upright pedal' view. The toe of the

foot is placed on a wooden block with a groove cut along its top surface (referred to as a 'navicular block', see Figure 2.30c, page 66), and the limb is manipulated until the sole of the foot is vertical. A horizontal x-ray beam is centred on the coronary band and aligned perpendicular to the sole of the foot (Figure 2.1a). This view can be enhanced by the use of an aluminium wedge filter to reduce the exposure at the toe of the foot (see Chapter 1, page 5). A low ratio grid (6:1) is ideal for this view, but acceptable results can be obtained without the use of a grid (Figure 2.1b).

A similar view, a dorsoproximal-palmarodistal (high coronary) oblique, may be obtained with the horse standing on a tunnel containing the cassette. The x-ray beam is angled in a dorsoproximal-palmarodistal oblique direction, at approximately 65° to the horizontal, centred on the coronary band (Figure 2.2a). This technique has the disadvantage that the beam is oblique to the cassette, and therefore results in some distortion. It may be useful for visualizing fractures, and is helpful in some horses which resent placing the foot in a 'navicular block'. A parallel 6:1 ratio grid is used if the x-ray beam can be aligned with the grid lines; otherwise a better result is obtained without a grid (Figure 2.2b).

Dorsopalmar (weight bearing) view

A dorsopalmar weight bearing view is useful in selected cases, e.g. sagittal fractures of the distal phalanx, lateromedial foot imbalance. The horse
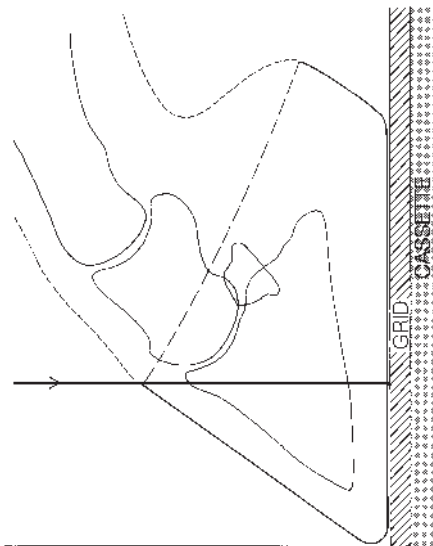
Figure 2.1(a) Positioning to obtain a dorsoproximal-palmarodistal oblique ('upright pedal') view of the distal phalanx. The x-ray beam (arrow) is centred on the coronary band.

Figure 2.1(b) Dorsoproximal-palmarodistal oblique radiographic view of the distal phalanx of a normal adult horse, obtained using the 'upright pedal' technique.
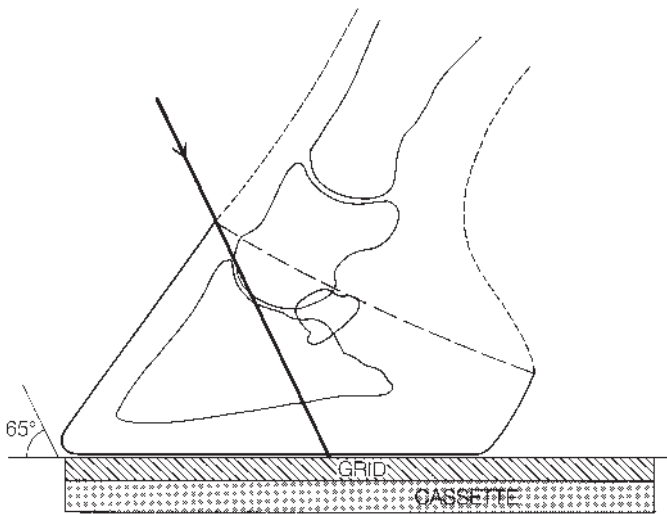
Figure 2.2(a) Positioning to obtain a dorsoproximal-palmarodistal oblique ('high coronary') view of the distal phalanx. The x-ray beam (arrow) is centred on the coronary band.

Figure 2.2(b) Dorsoproximal-palmarodistal oblique radiographic view of the distal phalanx of a normal adult horse (the same horse as Figure 2.1b), obtained using the 'high coronary' technique. Note the apparent elongation of the bone (compare with Figure 2.1b).

stands weight bearing on the limb, on a flat block, so that the cassette may be placed lower than the solar surface of the foot. A horizontal x-ray beam is centred midway between the coronary band and the ground surface, at the midline of the hoof (Figure 2.3). It should be aligned at right angles to a line drawn across the bulbs of the heel. This will ensure a straight dorsopalmar view of the foot. If it is desired to record medial or lateral deviation of the distal limb, the beam should be aligned craniocaudal to the antebrachium. A 6:1 ratio grid is preferred.

Palmaroproximal-palmarodistal oblique view

This view is used to give good visualization of the palmar processes of the distal phalanx, particularly for separation of the laminae of the heel of the foot.

The horse stands on a cassette tunnel, flat on the floor. The foot to be radiographed is positioned as far caudally under the horse as is consistent with the horse standing flat on the foot. The x-ray machine is placed ventral to the thorax of the horse and the x-ray beam centred between the bulbs of the heel (Figure 2.4). The angle of incidence of the x-ray beam to the cassette is 45°–70°, dependent upon the slope of the pastern and the positioning of the foot. The beam is angled so that the image of the fetlock is not superimposed over the palmar processes of the distal phalanx. If the foot is positioned too far forward, it is impossible to avoid superimposition
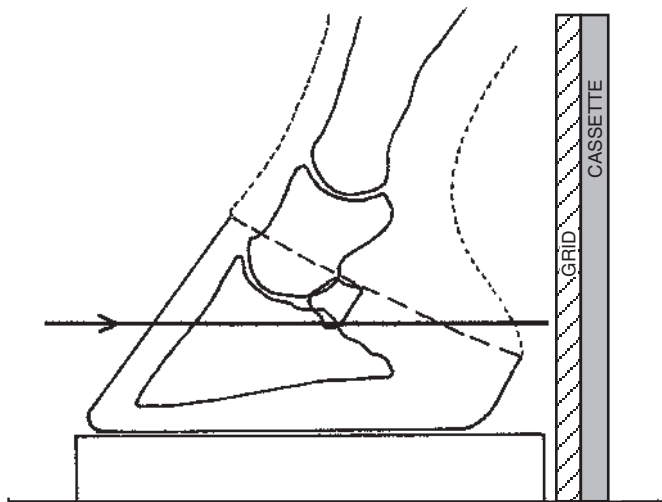
Figure 2.3 Positioning to obtain a dorsopalmar (weight-bearing) view of the distal phalanx and navicular bone (see Fig. 2.7c, page 36). The x-ray beam (arrow) is centred midway between the coronary band and the ground surface of the hoof.
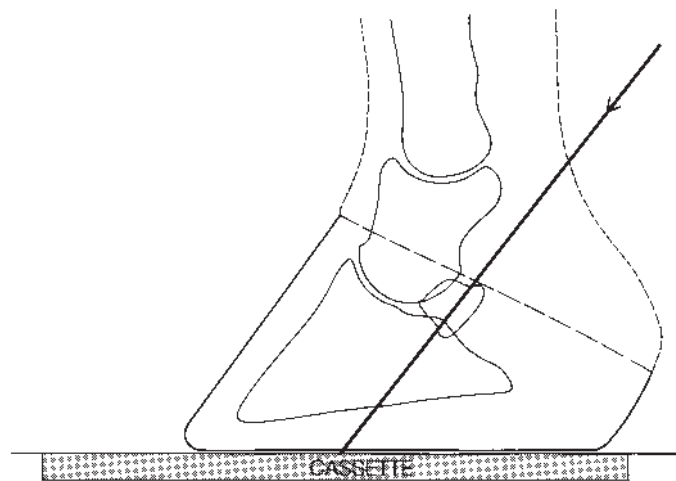

Figure 2.4 Positioning to obtain a palmaroproximal-palmarodistal view of the distal phalanx (see Fig. 2.7d, page 37). The x-ray beam is centred between the bulbs of the heels.

of the image of the fetlock over the foot, especially if the ergot is prominent. This view is obtained without a grid.

Other oblique views

Oblique views of the distal phalanx and hoof wall are often required. These are particularly valuable if fractures involving the body or palmar processes of the distal phalanx are suspected, and if new bone is present on the dorsal wall of the distal phalanx, or there is mineralization in the dermal laminae. They also help to identify entheseophytes on the dorsomedial and dorsolateral aspects of the distal interphalangeal joint. Obliquity is determined by one of two factors:

1   An attempt to align the x-ray beam parallel with the line of a fracture.
2   Positioning the x-ray beam so that new bone will be 'skylined' (i.e. the beam will form a tangent to the surface of the distal phalanx). For this purpose, reduced exposures should be used, and a grid is unnecessary.

Osteophyte or entheseophyte formation on the dorsolateral or dorsomedial aspects of the distal phalanx are often best seen on flexed oblique views, which open the distal interphalangeal joint. The toe of the foot is placed in a navicular block with the sole of the foot approximately vertical. Dorsal 60° lateral-palmaromedial oblique and dorsal 60° medial-palmarolateral oblique views are obtained. A horizontal x-ray beam is used, centred on the coronary band (Figure 2.5). To highlight the lateral and medial palmar processes, dorsal 45° lateral-palmaromedial oblique and dorsal 45° medial-palmarolateral oblique views respectively should be obtained.

Alternatively, to image the palmar processes, stand the horse on a tunnel containing the cassette. Angle the beam at 45° proximally and centre on the
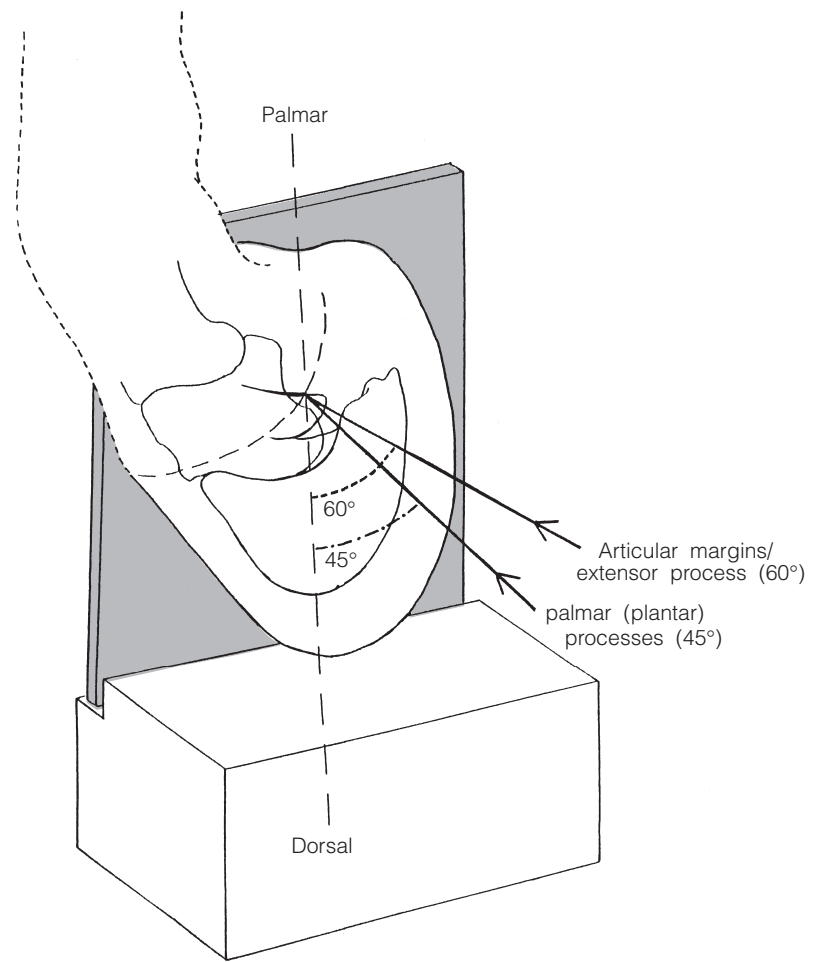
[31]

Palmar

60°

45°

Articular margins/
extensor process (60°)

palmar (plantar)
processes (45°)

Dorsal

Figure 2.5 Positioning to obtain a dorsolateral-palmaromedial oblique (flexed) view of the distal phalanx and interphalangeal joints. The x-ray beam (arrow) is centred on the coronary band. An angle of 45° from dorsal highlights the lateral palmar process of the distal phalanx (see Fig. 2.7f, page 40). The dorsal margins of the interphalangeal joints are best imaged with an angle of 60° from the dorsal plane (see Fig. 2.7e, page 38).

coronary band on the lateral or medial aspect of the foot (Figure 2.6). A lateral 45° proximal-mediodistal oblique highlights the lateral palmar process, a medial 45° proximal-laterodistal oblique images the medial side.

The frog clefts should be carefully packed to avoid radiolucent artefacts mimicking a fracture.

NORMAL ANATOMY

The front and hind distal phalanges have a similar appearance, but the bones of the hind feet are slightly narrower mediolaterally than those of the forefeet.

Immature horse

The distal phalanx develops from a single centre of ossification, which is present at birth. It continues to enlarge and model until at least 18 months

[32]

Medial

Lateral

45°

CASSETTE IN PROTECTIVE TUNNEL
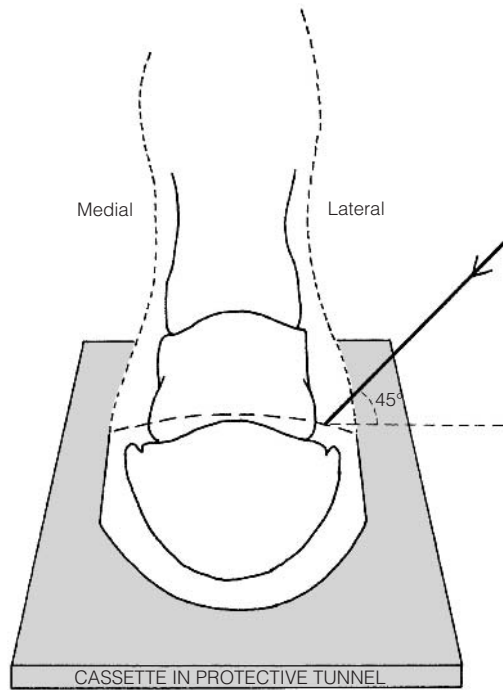
Figure 2.6 Technique to obtain a lateral 45° proximal-mediodistal oblique view of the distal phalanx to skyline the lateral palmar process. The x-ray beam is centred on the coronary band. See also Figure 2.7(g).

of age. The palmar processes are not evident at birth, but gradually ossify over 12 months.

Skeletally mature horse

Lateromedial view

The dorsal surface of the distal phalanx is smooth and opaque (Figure 2.7a). It may be slightly convex from the solar margin to the base of the extensor (pyramidal) process, and should meet the solar margin at a sharp angle. In horses with a large crena marginis solearis (Figure 2.8a, page 42), a radiolucent indentation or a double line may be seen at the junction of these margins (Figure 2.8b, page 42). There are considerable variations in the shape of the extensor process, but they are usually bilaterally symmetrical (Figure 2.9, page 43).

The solar surface of the distal phalanx is smooth in outline and is normally at a 5–10° angle to the sole, sloping proximally toward its palmar aspect. The solar canal of the distal phalanx (through which runs the terminal arch of the digital arteries) is seen between the solar surface of the bone and the distal interphalangeal joint. It is seen with a variable degree of clarity, depending on the exposure factors used and the direction of the x-ray beam. It may appear as a very distinct radiolucent zone in the middle of the bone, proximal to the solar surface, but in some bones it is barely evident. Palmar to the solar canal is a sharply defined, smoothly outlined relatively sclerotic band of bone, the facia flexoria. The deep digital flexor tendon attaches to the palmar aspect (Figure 2.7a).

The articular surfaces of the middle and distal phalanges are reasonably

[33]
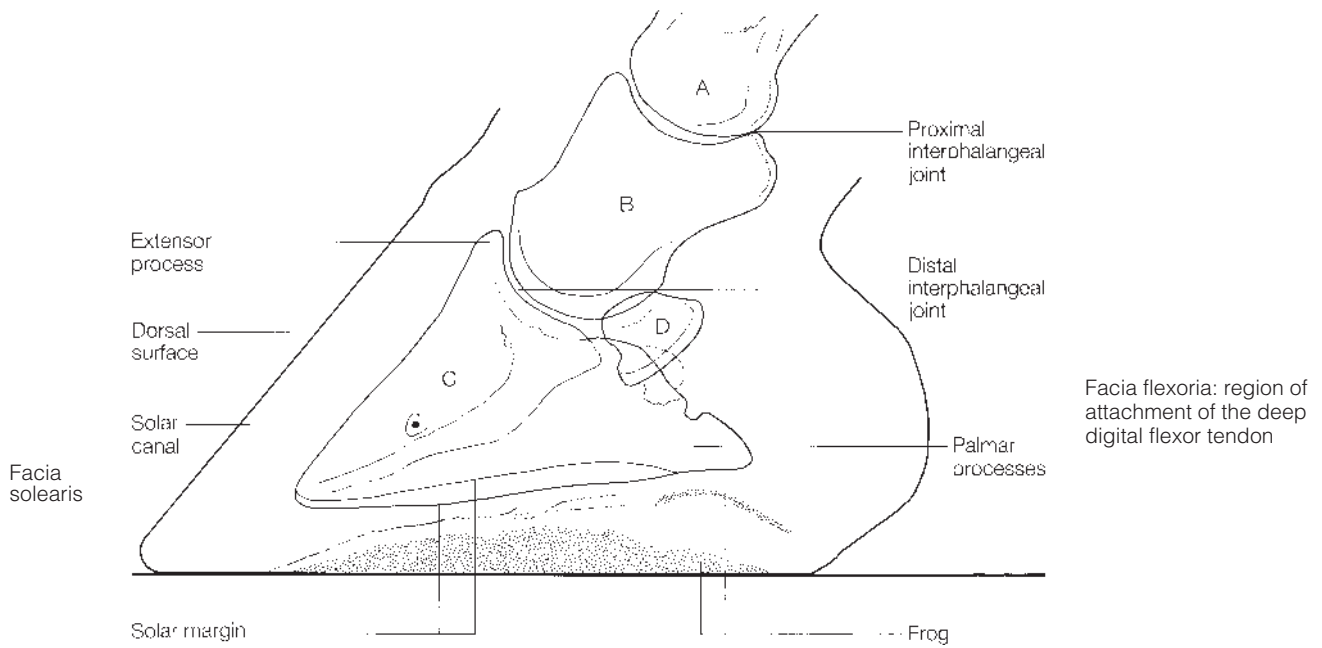
Figure 2.7(a) Lateromedial radiograph and diagram of a normal adult foot. A = proximal phalanx, B = middle phalanx, C = distal phalanx, D = navicular bone.
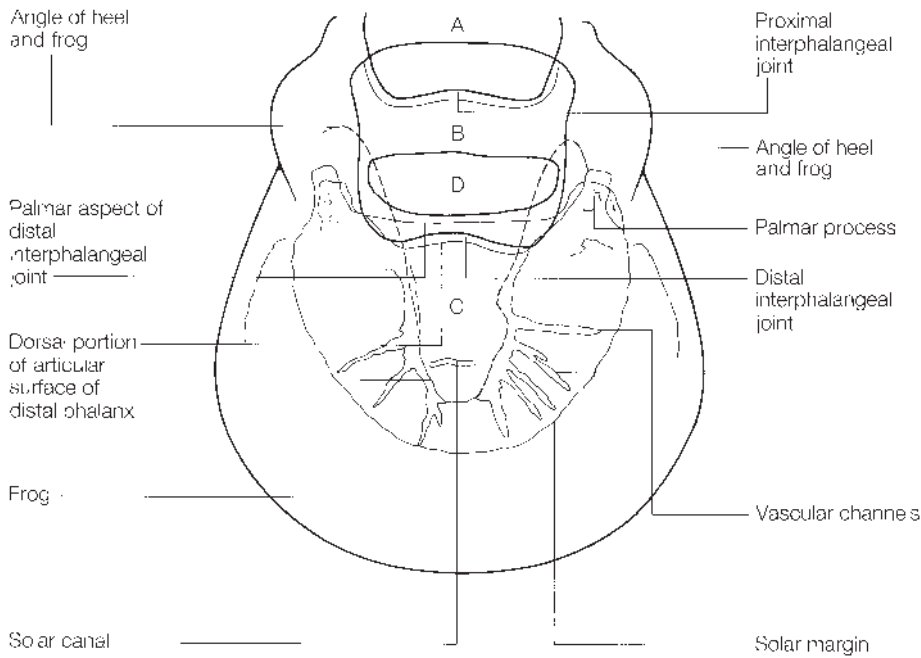
Diagram labels:
- A
- B
- C
- D
- Proximal interphalangeal joint
- Extensor process
- Dorsal surface
- Solar canal
- Facia solearis
- Solar margin
- Distal interphalangeal joint
- Facia flexoria: region of attachment of the deep digital flexor tendon
- Palmar processes
- Frog

Figure 2.7(b) Dorsoproximal-palmarodistal oblique ('upright pedal') radiograph and diagram of a normal adult front foot. A = proximal phalanx, B = middle phalanx, C = distal phalanx, D = navicular bone.
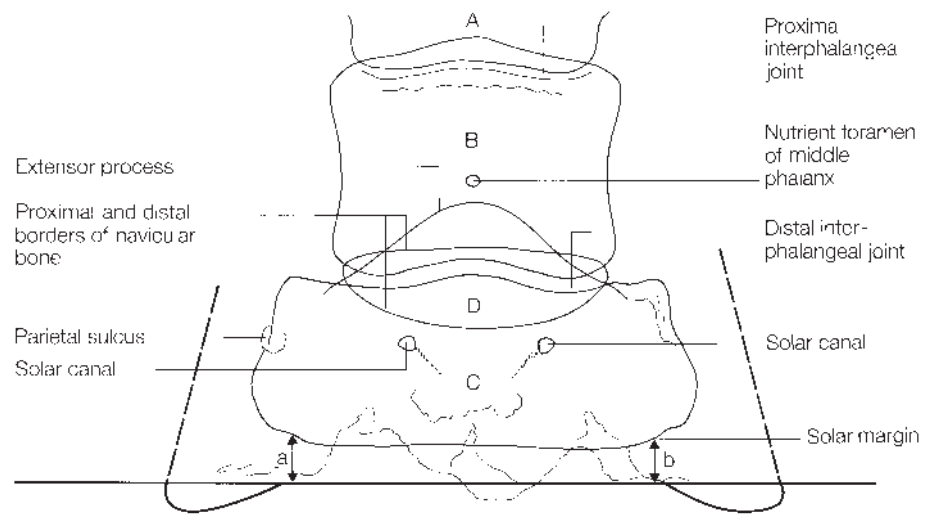
Figure 2.7(c) Dorsopalmar (weight bearing) radiograph and diagram of a normal adult foot. Arrows a and b indicate the height between the distal border of the distal phalanx and the ground surface. A = proximal phalanx, B = middle phalanx, C = distal phalanx, D = navicular bone.

congruous. There is sometimes a smoothly outlined V-shaped notch in the articular margin of the distal phalanx (Figure 2.8c, page 42). The middle of the articular margin of the middle phalanx may be slightly flattened. The width of the joint space will depend on the amount of weight being borne on the foot, and the presence of any effusion within the joint.

[36]
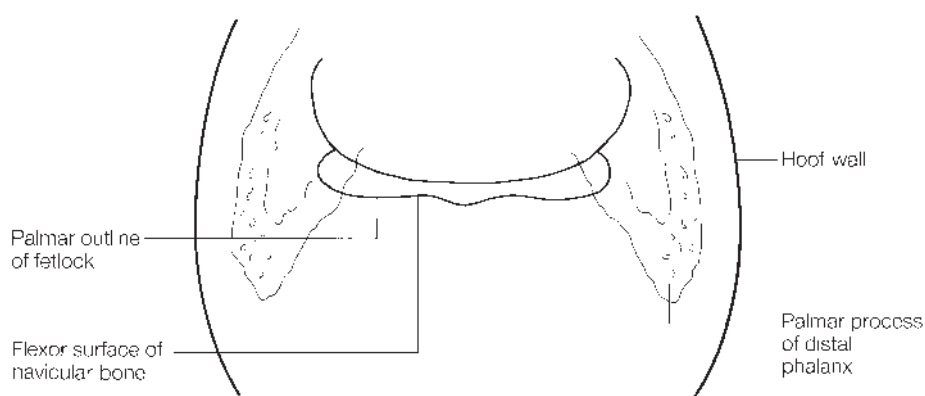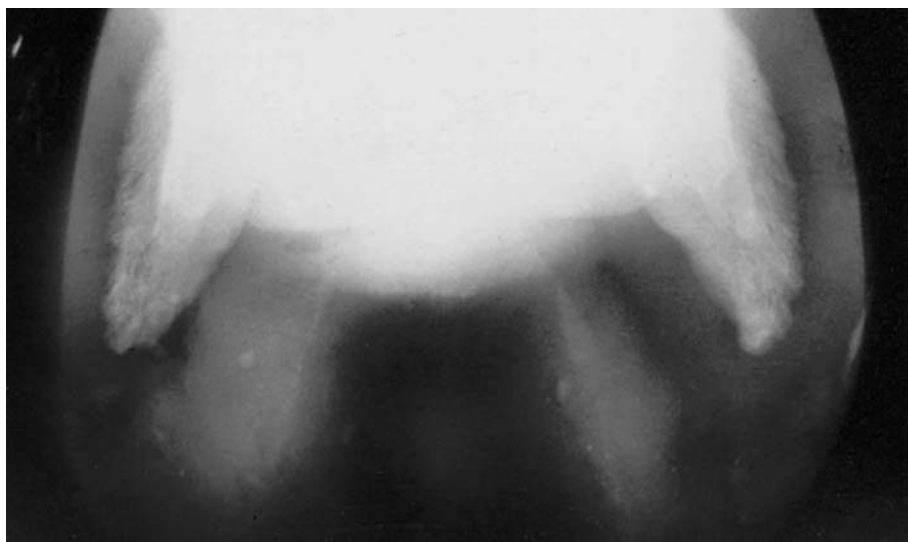
Figure 2.7(d) Palmaroproximal-palmarodistal radiograph and diagram of a normal adult distal phalanx.

Dorsoproximal-palmarodistal oblique view

The appearance of the distal phalanx on the dorsoproximal-palmarodistal oblique upright pedal and high coronary views is essentially the same (Figure 2.7b, page 35). The solar margin is well defined, describing a regular curved outline. Some irregularity may be present. The distal phalanges of the hind feet are narrower and have a slightly more pointed outline at the toe than those of the front feet.

A distinct somewhat blunted V-shaped notch (crena marginis solearis) may be present in the midline in the dorsal aspect of the solar margin of the bone. This is usually present bilaterally, and is variable in size (up to 1.5 cm in depth).

Vascular channels are evident as radiolucent lines, radiating between the solar canal and the solar margin. They are variable in number and width, and may appear to narrow or widen slightly close to the solar margin.

The solar canal is evident as an irregular, roughly U-shaped lucency running through the centre of the distal phalanx, extending from the level

Figure 2.7(e) A flexed dorsal 60° lateral-palmaromedial oblique view and diagram of the pastern and foot of a normal adult horse. A = proximal phalanx, B = middle phalanx, C = distal phalanx, D = navicular bone.

of the distal interphalangeal joint to approximately midway between the joint and the solar margin of the bone.

The distal interphalangeal joint is evident as two distinct lines, the uppermost representing the palmar aspect of the articulation of the distal phalanx with the middle phalanx, close to its articulation with the distal sesamoid (navicular) bone. The lower of the two lines represents a more dorsal portion of the articular surface of the distal phalanx, its exact position depending on the angulation of the bone when radiographed.

[38]

Eminence for
attachment
of collateral
ligaments
of distal inter-
phalangeal joint

Extensor process
of distal phalanx

Proximal angle of
palmar process

Lateral aspect of
navicular bone

Variably sized notch
or foramen

Lateral palmar
process of
distal phalanx

Distal angle of
palmar process

Line created by
superimposition
of a frog shadow
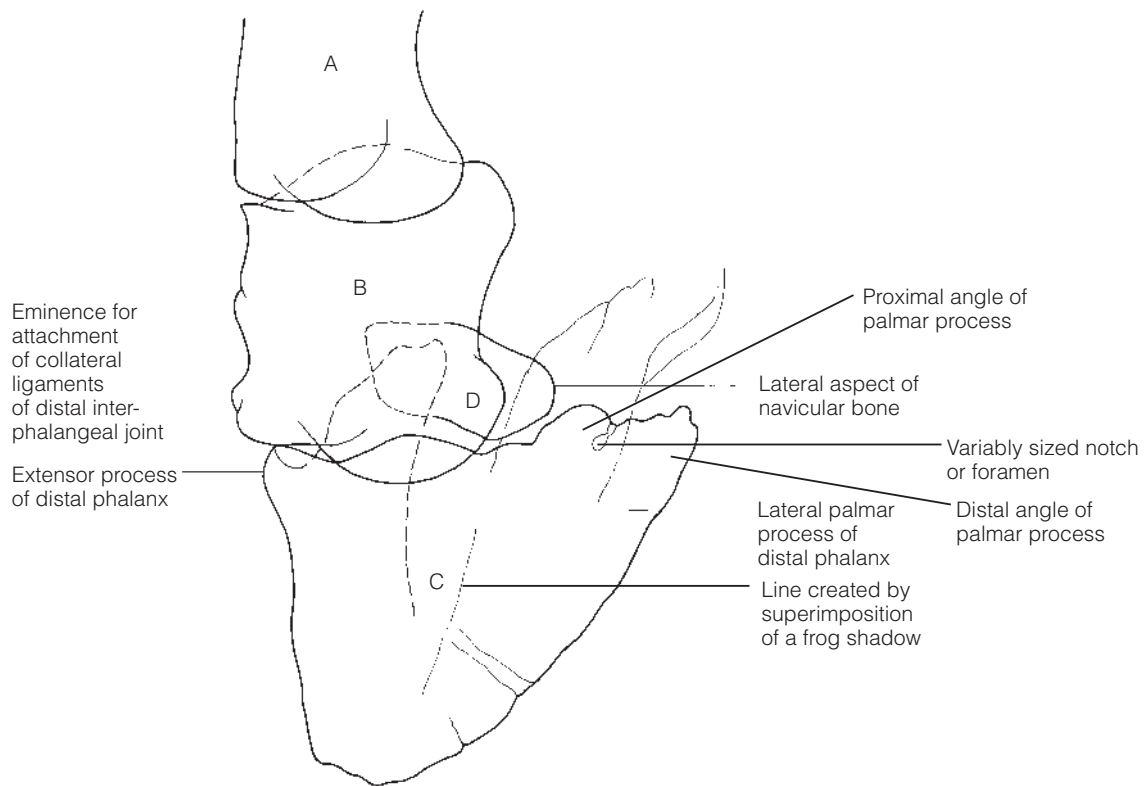
Figure 2.7(e) *Cont'd*

Dorsopalmar (weight bearing) view

In the dorsopalmar (weight bearing) view (Figure 2.7c, page 36), the openings of the solar canal are seen as two distinct circular foramina distal to the articular surface.

The extensor process may be difficult to visualize as it lies superimposed over the distal end of the middle phalanx and the navicular bone.

The parietal sulci (dorsal grooves) of the distal phalanx are seen as notches on the lateral and medial aspects of the bone.

The solar margin of the bone should be an equal distance from the ground surface of the foot laterally and medially.

Palmaroproximal-palmarodistal oblique view

The palmar aspect of the palmar processes of the distal phalanx are seen on either side of the navicular bone (Figure 2.7d, page 37). The axial and abaxial surfaces have a relatively smooth appearance, although some irregular lucencies within the body of each process are often present. An oval opaque ring may be present in the processes, representing mineralization in the base of the hoof cartilage (collateral cartilage) (see also 'Ossification of the hoof cartilages', page 49). A lucent halo is evident in the hoof wall immediately adjacent to the bone, representing the dermal tissue and laminae of the hoof.

[39]

Figure 2.7(f) Dorsal 45° lateral-palmaromedial oblique (flexed) view of a pastern and foot of a normal adult horse.

Flexed dorsal 60° lateral-palmaromedial oblique and dorsal 60° medial-palmarolateral oblique views

The contour of the extensor process of the distal phalanx is smoothly curved. Depending on the degree of flexion, one of the condyles of the middle phalanx may be partially superimposed over the extensor process. The eminence for the attachment of a collateral ligament on the distal aspect of the middle phalanx on the opposite side is also seen (Figure 2.7e). A lucent line courses obliquely across the distal phalanx. This may be either an edge effect created by the superimposition of the contralateral palmar process, or a frog shadow, depending on the projection angle. It should not be confused as a fracture. There is a variably sized notch or foramen on the palmar aspect of the palmar process, the parietal incisure or foramen of the palmar process, leading to the parietal sulcus (dorsal groove).

The dorsal 60° lateral-palmaromedial oblique view (Figure 2.7e) allows better evaluation of the proximal and distal interphalangeal joint margins

[40]

Lateral aspect of
navicular bone

Articular margin of
distal interphalangeal joint

Lateral palmar
process

Lateral condyle
of middle phalanx

Extensor process
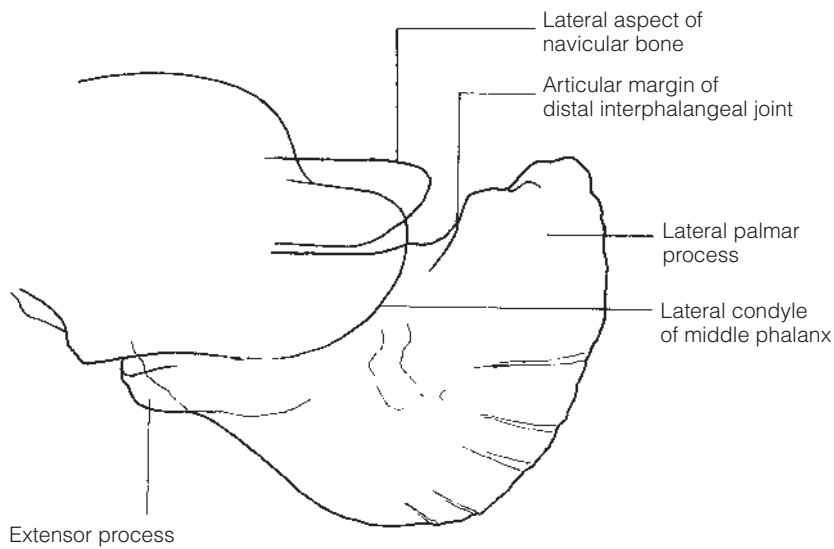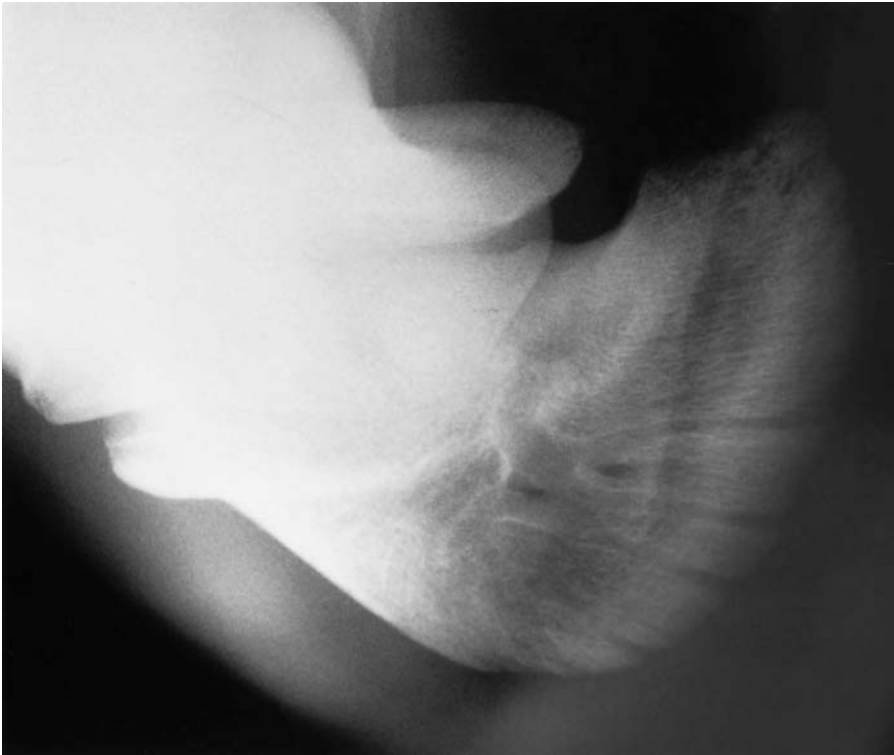
Figure 2.7(g) Lateral 45° proximal-medial distal oblique view to highlight the lateral palmar process of the distal phalanx.

than the dorsal 45° lateral-palmaromedial oblique view (Figure 2.7f). The lateral 45° proximal-medial distal oblique view permits more assessment of the lateral palmar process (Figure 2.7g).

NORMAL VARIATIONS AND INCIDENTAL FINDINGS

A small circumscribed bony 'fragment' palmar to the palmar processes of the distal phalanx may represent a separate ossification centre or possibly

(a)

(b)

Figure 2.8(a) Dorsoproximal-palmarodistal oblique view of a normal adult horse. There is a large notch at the toe of the distal phalanx, the crena solearis.

Figure 2.8(b) Lateromedial view of the distal phalanx of a normal adult horse, the same horse as Figure 2.8(a). Note the irregular appearance of the dorsal margin of the bone at the toe (arrow). This is created by the large crena solearis.

Figure 2.8(c) Lateromedial view of a distal interphalangeal joint of an adult horse. There is a V-shaped notch in the middle of the articular surface of the distal phalanx, of questionable clinical significance.

(c)

a fracture sustained early in life. When present they are usually evident palmar to both palmar processes of both feet, although they may only occur in one foot or at one process. Their diameter may vary between approximately 1 and 10mm. They should not be confused with clinically significant fractures of the palmar process, which are usually larger, and tend to have a sharper division from the body of the bone (see pages 54 and 56).

A small radiopaque 'fragment' less than approximately 6mm in
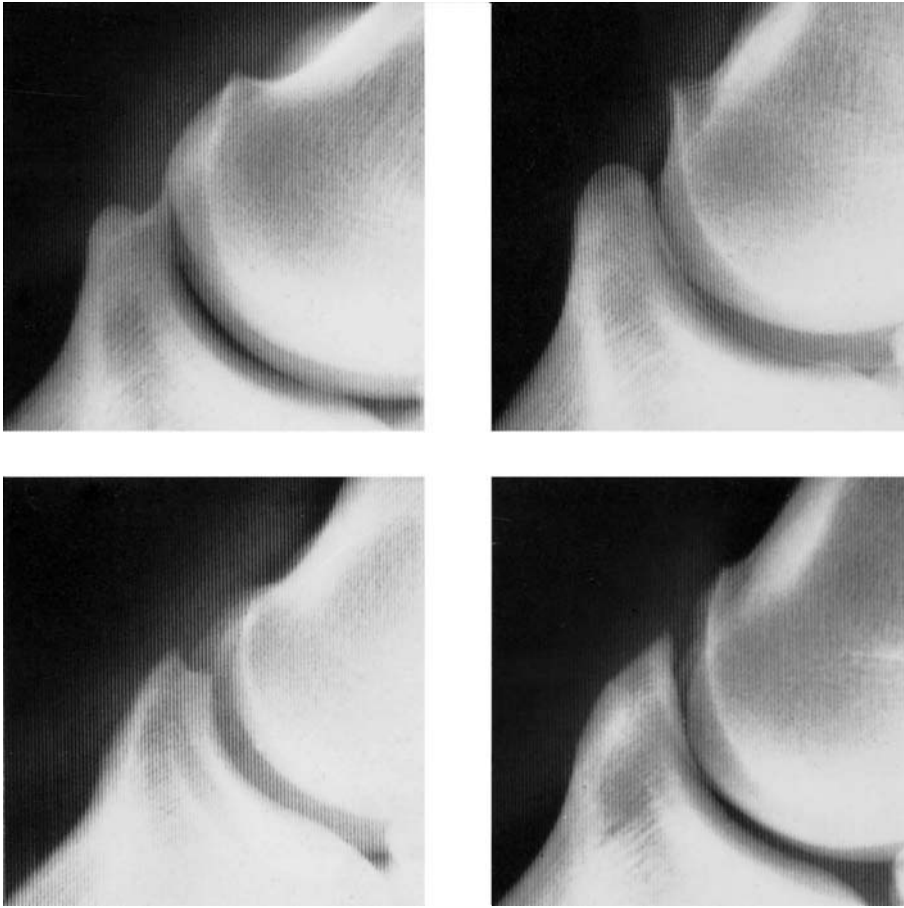
Figure 2.9 Lateromedial radiographs of the extensor process of normal distal phalanges, showing the variation in shape that may occur.

diameter is sometimes present proximal to the extensor process (Figure 2.10). This is usually present in the midline, and may represent a separate centre of ossification, a fracture, or dystrophic mineralization within the tendon. They may be present bilaterally. Many of these fragments have a smooth outline, but trabeculation of the fragment may be seen. They may be of no clinical significance, although some may cause lameness (see 'Significant findings', pages 56–7).

Some degree of ossification of the hoof cartilages may be regarded as normal. Fusion between the ossified cartilage and the distal phalanx may not be present, may be incomplete or be complete. One or several ossification centres may be present, either proximally, midway or distally in the cartilage. The lateral cartilage is ossified more frequently than the medial cartilage (see page 49).

In some cases the parietal sulci of the distal phalanx appears as a foramen rather than a notch.

SIGNIFICANT FINDINGS

Pedal osteitis

The term *pedal osteitis* strictly means inflammation of the distal phalanx, and has been widely used to describe a broad spectrum of radiographic

Figure 2.10 Lateromedial radiograph showing a radiopaque body proximal to the extensor process of the distal phalanx (these fragments are of variable clinical significance – see pages 56–7.

abnormalities of the distal phalanx. It is likely that there are both septic and aseptic forms of what has become known as 'pedal osteitis', but there is currently a dearth of information concerning the aetiology of some of the radiographic changes described. The authors acknowledge that there is a wide variation in the radiographic appearance of the distal phalanx in apparently normal horses, and that any radiographic changes that develop in the distal phalanx tend to persist. Because of the present lack of knowledge, the authors have elected to describe several discrete radiographic findings and their associated clinical signs under the general heading of 'pedal osteitis complex', without ascribing a specific name or aetiology to them. Other conditions with a known aetiology are then discussed under separate subheadings.

Pedal osteitis complex

The most common change referred to as part of the pedal osteitis complex is remodelling of the solar margin of the bone. Changes are most obvious on dorsoproximal-palmarodistal oblique views (Figure 2.11a). The solar margin of the bone loses its relatively smooth, opaque outline due to demineralization. In mild cases the bone near the solar margin may have some increased radiolucency, making its visualization difficult. In more severe or long-standing cases, larger areas of bone may be resorbed from the solar margin of the bone, resulting in apparent widening of the vascular channels primarily at the solar margin.

On lateromedial views these changes may be evident as remodelling of the tip of the bone, the solar margin no longer showing a straight outline but curving proximally towards the dorsal aspect of the bone. This change

Figure 2.11(a) Pedal osteitis complex. Dorsoproximal-palmarodistal oblique ('upright pedal') view of the distal phalanx, showing demineralization of the solar margin and discrete circular lucent areas in the palmar processes.

appears to be exaggerated if the radiograph is not a true lateromedial projection. In more advanced cases new bone may be laid down on the dorsal surface of the bone at the toe. This change is frequently seen in animals that, over a period of time, have taken an increased pressure on the sole, e.g. after laminitis, or in horses with badly dropped soles. Active bone formation along the distal portion of the dorsal cortex is nearly always considered abnormal. Slight new bone formation seen in oblique views along the middle portion of the dorsal cortex is sometimes seen in horses not displaying lameness and may not be of clinical significance.

A second change associated with the pedal osteitis complex is seen in the palmar processes of the distal phalanx. It is best visualized on dorsoproximal-palmarodistal oblique or palmaroproximal-palmarodistal oblique radiographs. Discrete circular radiolucent areas, 2 mm or 3 mm in diameter, are present in the palmar processes of the bone, and these may be associated with new bone, particularly on the axial surfaces of the palmar processes (Figure 2.11a). Modelling changes of the palmar processes may also be seen in a lateromedial view. The solar aspect of the palmar processes may have an irregular outline (Figure 2.11b). There may be a change in shape with elongation of the palmar processes, seen also in a flexed dorsolateral-palmaromedial (or dorsomedial-palmarolateral) oblique view (Figure 2.11c). These changes are sometimes seen in association with an abnormally thin sole and/or abnormal orientation of the solar surface of the distal phalanx seen in a lateromedial view. The solar surface of the distal phalanx may be horizontal, or the palmar processes may be lower than the toe (see also 'Long-toe, low-heel syndrome', page 60).

These changes, and those described above, are probably associated with concussion of the bone and may be related to poor foot conformation and shoeing imbalances. They may be associated with lameness that is most marked on hard surfaces. Treatment is by corrective trimming and shoeing. Although the condition may resolve clinically, the radiological changes

Figure 2.11(b) Lateromedial view of the distal phalanx of a 12 year old Selle Francais with low, collapsed heels and foot pain. There is modelling and irregularity in outline of the solar margin of the distal phalanx. Nuclear scintigraphic examination confirmed increased bone activity in this area. Note also the small radiolucent zone immediately distal to the extensor process.

[45]

(c)
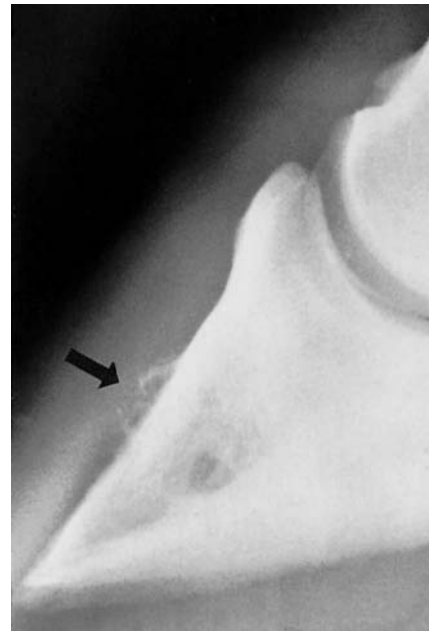
(d)

Figure 2.11(c) Dorsal 60° medial-palmarolateral (flexed) oblique view of the distal phalanx of a 10 year old Dutch Warmblood with low, collapsed heels and foot pain. There is modelling and elongation of the medial palmar process of the distal phalanx. Nuclear scintigraphic examination confirmed increased bone activity in this region.

Figure 2.11(d) Pedal osteitis complex. Lateromedial radiograph of the dorsal surface of the dorsal phalanx, showing mineralization (arrow) in the dermal laminae. (N.B. This is a slightly oblique view.)

usually remain throughout life. Nuclear scintigraphy may help to determine the significance of these radiographic changes within the distal phalanx.

Mineralized lesions on the dorsal wall of the distal phalanx may be seen (Figure 2.11d). These are usually approximately midway between the proximal border and solar margins of the bone on its dorsal surface, either in the midline or slightly to either side of it. These lesions are best visualized on a lateromedial or slightly oblique lateromedial view. Slight irregularities associated with the parietal sulci may be normal. The aetiology of this lesion is uncertain. It may represent new bone on the dorsal surface of the distal phalanx, or mineralization within the dermal tissue or dermal laminae. Although slight roughening of the dorsal cortex may be an incidental finding, mineralization in the laminae is usually associated with lameness.

Infectious osteitis

The pedal bone has no medullary cavity and therefore infection of this bone is, strictly speaking, an infectious osteitis, not osteomyelitis. Infections of the foot are common, but only infrequently do they involve the distal phalanx, with a resultant infectious osteitis. When present, infection most commonly involves the dorsal or solar surfaces of the distal phalanx, where it may cause
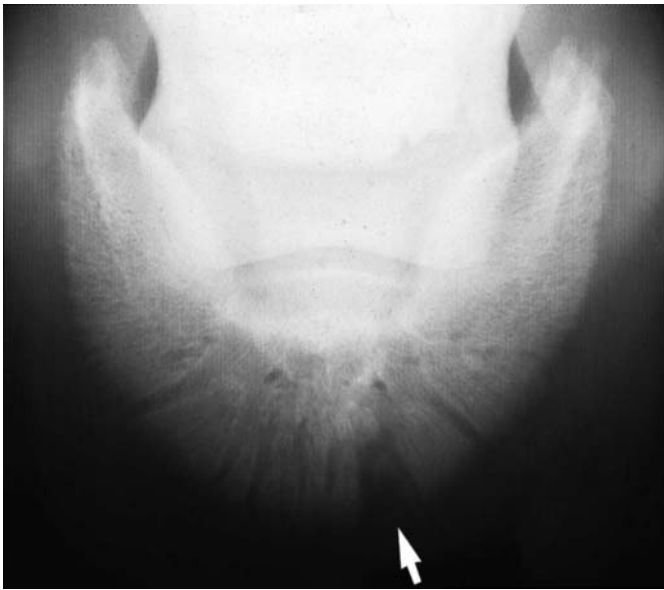
(a)
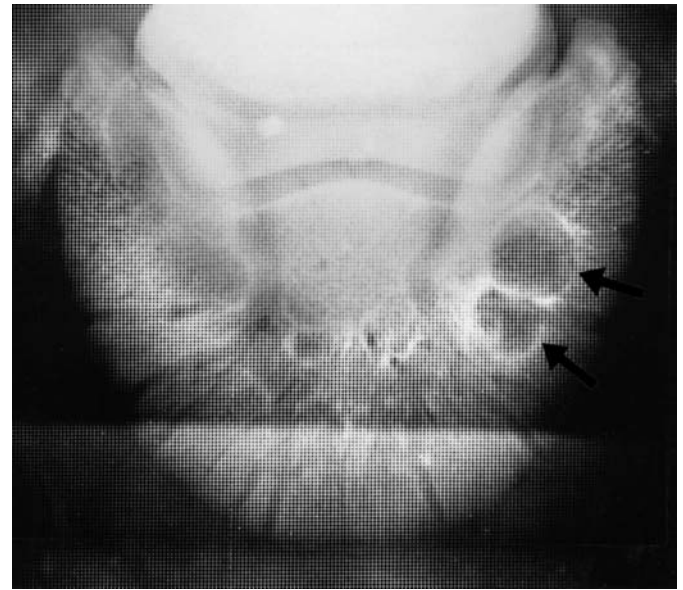
(b)

Figure 2.12(a) Infection of the distal phalanx. Dorsoproximal-palmarodistal oblique view of the distal phalanx, showing modelling of the toe of the bone (arrow) due to infection.

Figure 2.12(b) Infection of the distal phalanx. Dorsoproximal-palmarodistal oblique view of the distal phalanx, showing lucent areas (arrowed) surrounded by sclerosis. These represent inspissated pus within the distal phalanx. (The increased opacity at the toe of the bone is due to superimposition of the block supporting the foot.)

Figure 2.12(c) Osseous cyst-like lesion. Dorsoproximal-palmarodistal oblique view of the distal phalanx, showing an osseous cyst-like lesion (arrow) in the distal phalanx. The lesion is surrounded by sclerosis, and in this case no connection to the distal interphalangeal joint is evident.

(c)

focal demineralization (this may appear on a dorsoproximal-palmarodistal oblique view as a defect in the solar margin of the bone; Figure 2.12a). The lucent lesion usually has an irregular margin and there is seldom surrounding sclerosis, although new bone may be present at its margins (most easily seen on tangential views). There may be signs of chronic bone inflammation including a focal or generalized loss of radiopacity and widening of the vascular channels. Early lesions are more difficult to detect and are seen as an irregular margin or ill-defined lucent area in the solar margin of the distal phalanx. High quality radiographs are essential. In more advanced cases a radiopaque sequestrum is sometimes seen, surrounded by a lucent border.

Infectious osteitis is extremely painful and usually requires surgical

[47]

treatment. The prognosis following surgery is fair to guarded (see also 'Infection', pages 60–61).

Penetrating wounds through the sole of the foot may result in infectious osteitis of the solar surface of the distal phalanx. Initially this will show as a lucent area of bone on a dorsoproximal-palmarodistal oblique view. Occasionally antibiotic treatment of these lesions will result in a pocket of inspissated pus being walled off within the distal phalanx. This may result in a well-defined radiolucent zone appearing as an osseous cyst-like lesion (Figure 2.12b). These lesions may cause intermittent lameness when the horse is worked on a hard surface. Close examination of these lesions will show no connection with the distal interphalangeal joint, which may help to differentiate them from other osseous cyst-like lesions.

Osseous cyst-like lesions

Osseous cyst-like lesions not connected to the distal interphalangeal joint may be associated with infectious osteitis (see above).

Solitary osseous cyst-like lesions (see Chapter 1, page 24) close to or associated with the distal interphalangeal joint are occasionally seen. Care should be taken not to confuse this with a lucency created by a cavity frequently seen in the centre of the frog. They are generally most easily visualized on the dorsopalmar or dorsoproximal-palmarodistal oblique views (Figure 2.12c). When cysts are present, the distal interphalangeal joint should be carefully inspected for evidence of secondary degenerative joint disease. Lameness associated with osseous cyst-like lesions in the midline rarely resolves with conservative treatment. Surgical treatment of the cyst has proved successful in some cases. Small osseous cyst-like lesions (1–3 mm diameter) may occur at the lateral or medial border of the distal interphalangeal joint, and a better prognosis may be given for conservative treatment in these cases. Osseous cyst-like lesions may occasionally be seen at a pre-purchase examination in a clinically sound horse. Their significance is unpredictable.

An ill-defined osseous cyst-like lesion may be seen in the axial aspect of a palmar process of the distal phalanx in association with tearing of one of the collateral ligaments of the distal interphalangeal joint.

Tumours

The most common tumour to involve the distal phalanx is a keratoma. Typically it is seen on a dorsoproximal-palmarodistal oblique view. Additional oblique views may be required for better visualization. Pressure from the tumour on the dorsal wall of the distal phalanx causes resorption of bone. This is most easily seen at the solar margin of the bone, where a distinct semicircular notch is evident. This has a smooth outline, the bone underlying the keratoma frequently being sclerotic, which helps to differentiate this lesion from infection. There is usually no new bone associated with the lesion (Figure 2.13a).

Keratomas may occur at any point in the hoof wall, causing

(a)

(b)

Figure 2.13(a) Keratoma. Dorsoproximal-palmarodistal oblique view of the distal phalanx. There is a large, smoothly outlined defect in the distal phalanx (arrow) resulting from resorption of bone due to pressure caused by a keratoma.

Figure 2.13(b) Fibrosarcoma. Dorsolateral proximal-palmaromedial distal oblique view of the distal phalanx, showing modelling of the bone resulting from a fibrosarcoma.
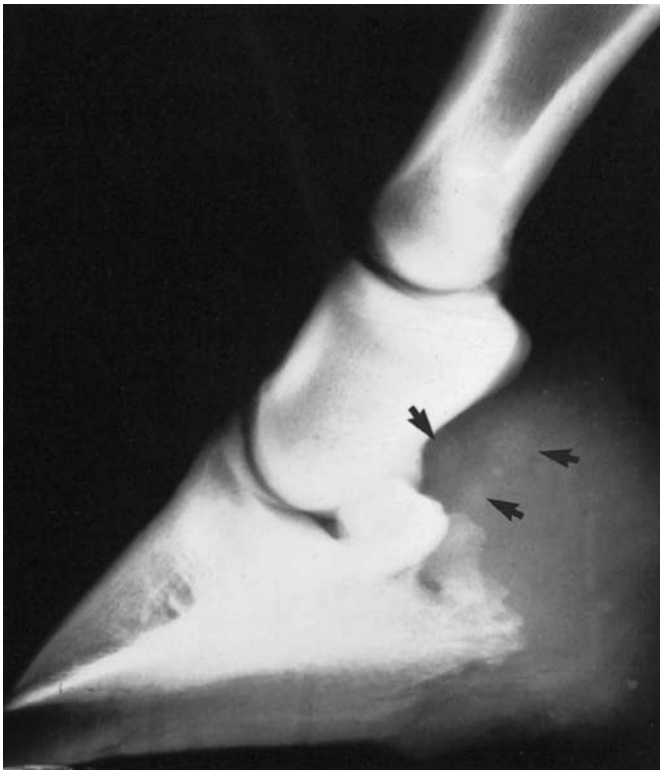
deformation of the wall, sole and white line. They are most commonly seen in the dorsal half of the foot. A keratoma may cause lameness as it enlarges, and may be associated with secondary infection. Treatment is by surgical removal of the keratoma and carries a reasonable prognosis, although the tumour may recur up to several years later.

Other tumours have been recorded infrequently (e.g. neurofibroma, haemangioma). They tend to be associated with remodelling of adjacent bone (Figure 2.13b).

Ossification of the hoof cartilages (side bone)

A degree of mineralization of the hoof cartilages is a very common finding, particularly in heavy breeds, and is frequently not associated with clinical signs. Ossification, or mineralization progressing from the distal aspect of the cartilage proximally to the level of the proximal border of the navicular bone, may be considered a normal process in any animal of 2 years of age or more (Figure 2.14). Ossification may commence in the proximal half of the cartilage and spread outwards. This is usually asymptomatic (Figure 2.15). Although these changes are unlikely to cause overt lameness, they may result in some shortening of the forelimb stride. The proximal half of the cartilage is directed slightly axially, and where ossification occurs from the base and from the proximal half of the cartilage simultaneously, a radiolucent line may be apparent at the point where the two meet (Figure 2.16, page 51), frequently at the level where the axial deviation in the cartilage occurs. This may be difficult to differentiate from a fracture of the cartilage. Fracture of an ossified cartilage is a rare occurrence, but will cause acute onset of lameness which normally resolves with rest. Completely ossified cartilages are rarely seen, and may extend proximally to the level of the proximal interphalangeal joint (Figure 2.17, page 51).

(a)

(b)

Figure 2.14 Ossification of the cartilages of the foot. Ossification from the distal aspect of the cartilages: (a) lateromedial view; (b) dorsoproximal-palmarodistal oblique view.
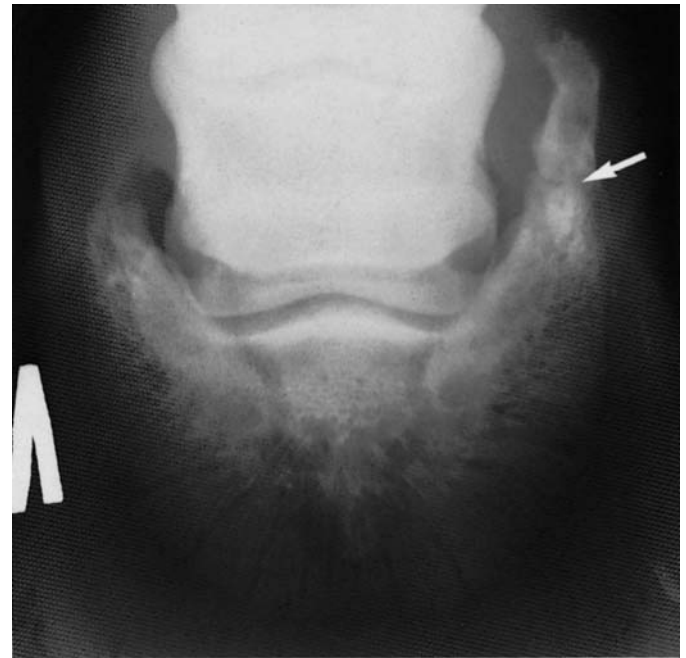

(a)

(b)

Figure 2.15 Ossification of the cartilages of the foot. Separate centres of ossification in the proximal half of the cartilages and in the distal aspect of the cartilages: (a) slightly oblique lateromedial view – note that the proximal areas of ossification are seen as poorly defined radiopaque areas (arrowed) proximal to the navicular bone; (b) dorsoproximal-palmarodistal oblique view.

[50]

(a)

(b)

Figure 2.16 Ossification of the lateral cartilage of the foot. Separate centres of ossification in the proximal and distal aspects of the cartilage have met to give almost complete ossification of the cartilage. Note that there is a lucent line where the two areas meet (arrow). This is not a fracture of the ossified cartilage. (a) Lateromedial view; (b) dorsoproximal-palmarodistal oblique view.

(a)

(b)

Figure 2.17 Complete ossification of the cartilages of the foot: (a) lateromedial view; (b) dorsoproximal-palmarodistal oblique view.
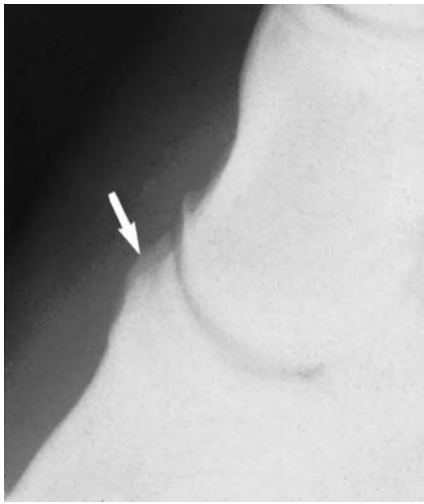
[51]

Entheseophytes on the extensor process of the distal phalanx

The common digital extensor tendon inserts on the extensor process of the distal phalanx. Tearing of the insertion will result in lameness, and entheseophyte formation on the dorsal aspect of the extensor process, rather than at its apex (Figure 2.18). This change must be distinguished from the normal variation in shape of the extensor process (see Figure 2.9, page 43). The outline caused by formation of entheseophytes is irregular, and there may be alteration in the opacity and trabecular structure of the underlying bone. Its significance must be interpreted in the light of clinical signs, since the radiographic changes persist despite resolution of lameness.

Entheseophytes at the insertion of the deep digital flexor tendon

The deep digital flexor tendon inserts on the facia flexoria of the distal phalanx, in a smoothly outlined concavity (Figure 2.7a, page 34). The cortex of the bone at this site should be smooth and regular as it meets the more proximal site of the insertion of the distal sesamoidean impar ligament. Tearing of the attachment of the deep digital flexor tendon may result in irregular new bone formation, or ill-defined lucent areas in the normally uniformly opaque bone. It may be associated with lameness.

Degenerative joint disease of the distal interphalangeal joint

Degenerative joint disease of the distal interphalangeal joint is a common cause of lameness, although frequently associated with little, if any, radiographic change. Radiographic abnormalities are seen most easily on lateromedial (Figure 2.19) and flexed oblique views (Figure 2.20). Remodelling of the extensor process of the distal phalanx is commonly, but not invariably, associated with degenerative joint disease (see 'Entheseophytes on the extensor process of the distal phalanx' above), and its presence should alert the clinician to examine the joint carefully. Radiographic changes of degenerative joint disease include periarticular and periosteal osteophytes on the proximal articular margin of the distal phalanx, on the distodorsal and/or distal palmar aspects of the middle phalanx, and slight irregularity and incongruity of the joint surfaces, particularly the articular surface of the extensor process. Periarticular osteophytes on the dorso-proximal aspect of the navicular bone may also be an indicator of arthritis, but should not be confused with entheseophyte formation. Non-articular new bone on the dorsal diaphysis of the middle phalanx (see page 94 and Figure 2.53, page 100) should not be confused with periarticular osteophyte formation, and is not necessarily associated with degenerative joint disease. In more advanced cases some subchondral bone lucency may be visible at the dorsal aspect of the joint, and there may be narrowing or unevenness of the joint space visible on a dorsopalmar (weight bearing) view. (This should not be confused with the distal interphalangeal joint space being widened on one side due to a hoof imbalance. A mediolateral hoof imbalance may result in this appearance on dorsopalmar views, despite the horse bearing full weight on the limb, and this is not synonymous with

Figure 2.18 Entheseophytes on the extensor process of the distal phalanx (arrow) (slightly oblique lateromedial view).

Figure 2.19 Lateromedial view of the distal phalanges of a 7-year-old Warmblood showjumper with lameness substantially improved by analgesia of the distal interphalangeal joint. There is considerable modelling of the extensor process of the distal phalanx. This view is slightly oblique; thus accurate evaluation of the distal dorsal aspect of the middle phalanx is difficult.
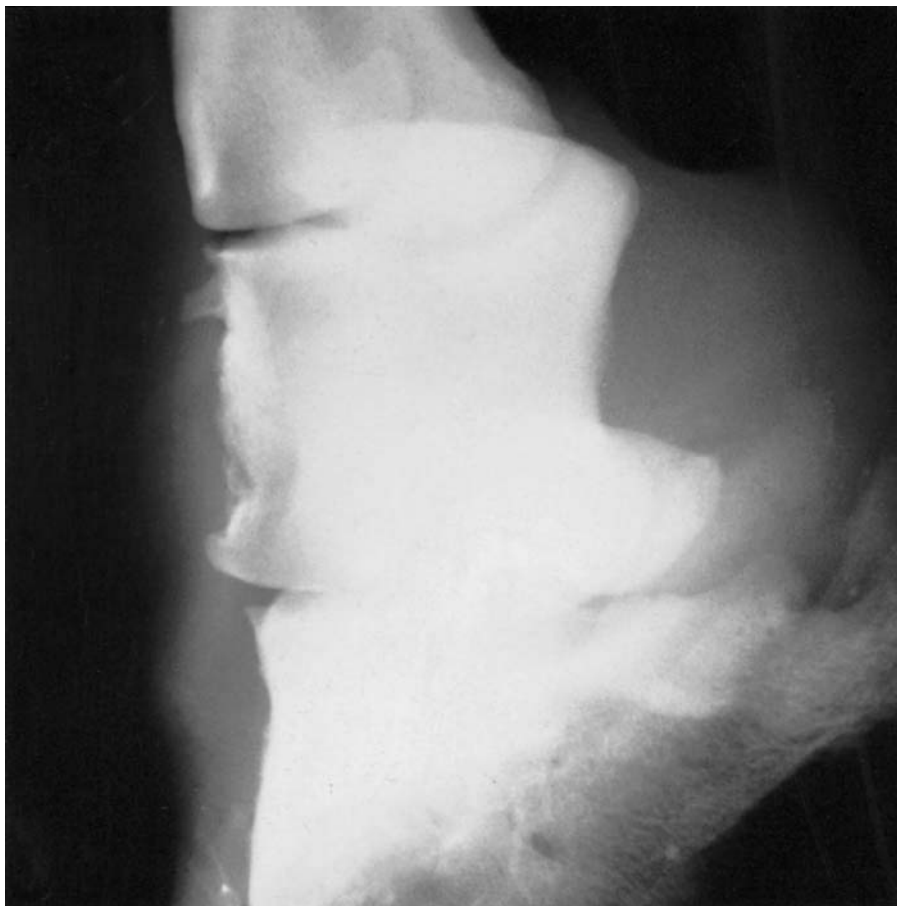
Figure 2.20 Flexed dorsolateral-palmaromedial oblique view of the pastern and foot of a 6-year-old Warmblood with degenerative joint disease of the proximal and distal interphalangeal joints. There is osteophyte formation on the dorsoproximal medial aspects of the middle and distal phalanges. The distal dorsomedial aspect of the middle phalanx is also modelled. Note also the rather irregular contour of the entire dorsomedial aspect of the middle phalanx and the distal palmarolateral aspect of the proximal phalanx. This may suggest that trauma was the inciting cause of degenerative joint disease.

degenerative joint disease. A mediolateral hoof imbalance may also make it difficult to obtain true lateromedial views.)

Degenerative joint disease carries a poor prognosis once radiographic changes are present, although remodelling of the extensor process alone may not be associated with current lameness. Some cases will respond for a time to careful balancing of the feet, and the use of anti-inflammatory drugs and intra-articular medication. Modelling changes of the distal interphalangeal joint are sometimes seen in association with navicular disease.

Subluxation of the distal interphalangeal joint

Subluxation of the distal interphalangeal joint is usually the result of partial or complete disruption of the deep digital flexor tendon. It is best identified on a lateromedial projection. There is widening of the joint space and the middle phalanx is displaced in a palmar direction.

Fractures

Common fracture sites of the distal phalanx are shown in Figure 2.21. A fracture through the body or a palmar process of the distal phalanx may initially be difficult to visualize on radiographs, but after 7–10 days some rarefaction adjacent to the fracture occurs making identification easier.

[53]
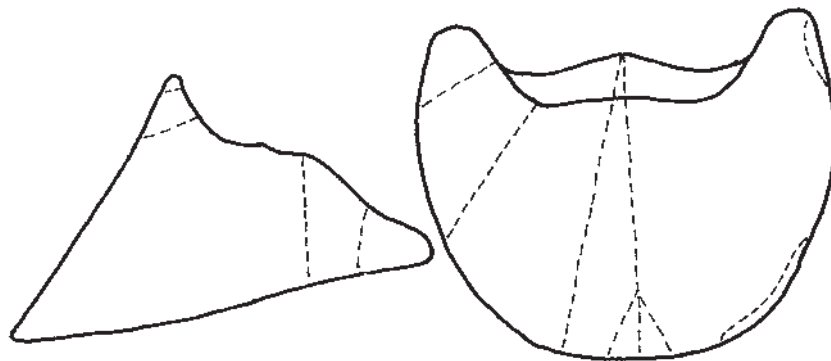
Figure 2.21 The common fracture sites of the distal phalanx.

Sagittal, parasagittal and marginal fractures are normally best visualized on a dorsoproximal-palmarodistal oblique view (Figure 2.22a), although a fracture of a palmar process may first be suspected on the lateromedial view (Figure 2.22b). When a fracture is suspected it may be necessary to obtain a number of oblique views in order to visualize the fracture clearly. A fracture of a palmar process may require a number of oblique views in order to demonstrate the fracture line and to ascertain if the fracture is articular or non-articular. Such fractures may not be detectable in a standard dorso-proximal-palmarodistal oblique projection. Occasionally a fracture may be suspected either on clinical grounds, or as the result of nuclear scintigraphic examination, but it is not detectable on these standard radiographic views. In these circumstances a palmaroproximal-palmarodistal oblique view and weight bearing lateral 45° proximal-medial distal oblique or medial 45° proximal-lateral distal oblique view may be helpful.

A fracture is best seen as a lucent line when the x-ray beam is in line with the plane of the fracture (Figure 2.22c). Frequently it will appear as two lines, representing the break through each surface of the bone. By careful comparison of a number of slightly different oblique views, it is possible to establish whether the fracture is simple or comminuted. It should also be remembered that more than one fracture may be present.

Clinically, a fracture of the distal phalanx presents as acute lameness, pain to pressure and concussion of the hoof, although there may be limited reaction if there is a palmar process fracture. Fractures of the distal phalanx which enter the distal interphalangeal joint, occurring in animals more than 18 months old, respond best to internal fixation. Fractures which do not enter the distal interphalangeal joint, fractures of the palmar processes of the bone and fractures in animals of less than 18 months of age have a good prognosis with conservative treatment, shoeing the affected foot with a broad-webbed bar shoe. A number of cases will never show bony union radiographically, even though clinically sound.

Non-articular osseous fragments at one or both palmar processes may occur in foals from a few weeks to 1 year of age. These are often associated with a club foot appearance and lameness, but are occasionally seen without associated clinical signs. These are believed to be the result of fractures and not secondary centres of ossification. They appear as a triangular shaped bone

(a)

(b)

(c)
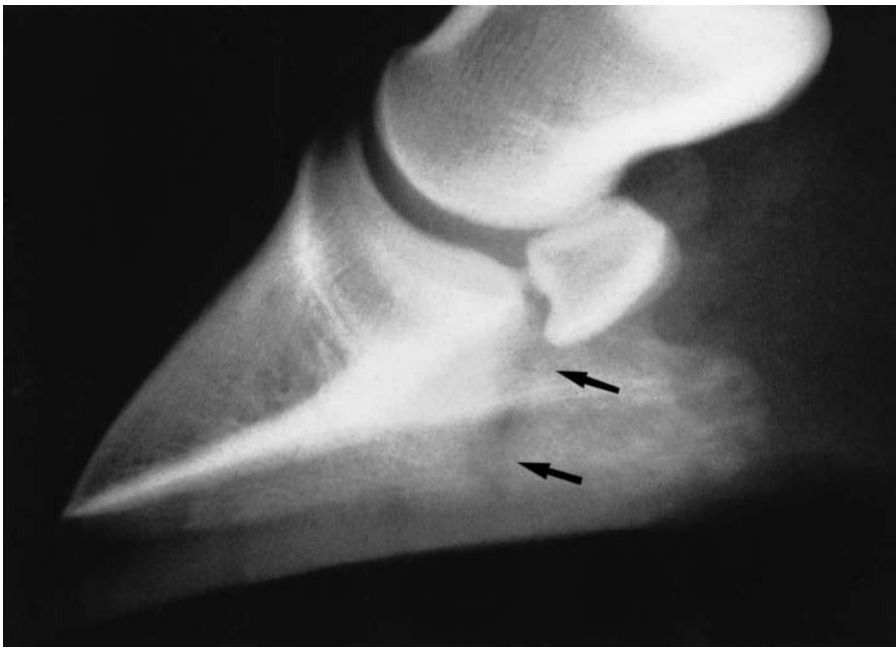
Figure 2.22(a) Sagittal fracture of the distal phalanx (dorsoproximal-palmarodistal oblique view). Note the separate lucent lines which represent the fracture through the dorsal and solar cortices. The shoe was left in place to give support to the foot until the injury was fully assessed.

Figure 2.22(b) Palmar process fracture (arrows) of the distal phalanx (lateromedial view).

Figure 2.22(c) Palmar process fracture of the distal phalanx (dorsoproximal lateral-palmarodistal medial oblique view).

[55]

fragment of the distal angle of the palmar process, or an oblong bone fragment extending from the incisure of the palmar process to the solar margin. These fractures heal by osseous union, with rapid resolution of lameness.

A fracture of the solar margin of the bone (running parallel and adjacent to the margin of the bone) is best visualized on the dorsoproximal-palmarodistal oblique view (Figure 2.23). This fracture frequently occurs in animals that are flat footed and suffer repeated bruising of the sole. These horses are frequently footsore and several sources of pain may contribute to the lameness. There is seldom a history of acute onset of lameness. Many of these fracture fragments persist radiographically, although some heal and others appear to be resorbed. Treatment is usually by shoeing with a broad-webbed seated-out shoe, to give increased protection to the sole. Occasionally the fracture may become secondarily infected and may require surgical removal of the fragment. A reasonable outcome can be given for these fractures, but their presence often indicates that the foot is prone to concussion and this must be taken into account when giving a prognosis.

A fracture of the extensor process is best visualized on a lateromedial radiograph. A small radiopaque fragment proximal to the extensor process may represent a recent fracture, a fracture sustained early in life, a separate ossification centre, or dystrophic mineralization within the extensor tendon (see Figure 2.10, page 43). A fragment may be homogeneously radiopaque, with a smooth outline or have a cortex and medullary pattern. However, it is often not possible to determine radiographically the significance of such
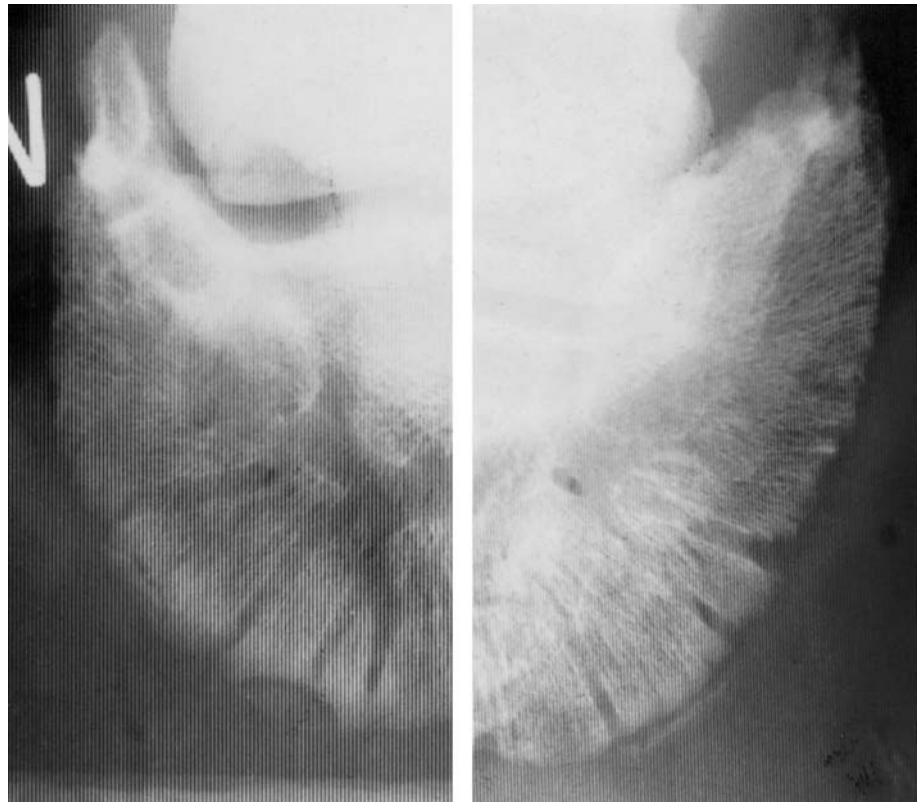
Figure 2.23 Fracture of the solar margin of the distal phalanx of two horses (dorsoproximal-palmarodistal oblique view).

[56]

fragments. Local analgesic techniques should be used to determine their clinical significance. Lameness associated with a fragment less than approximately 5 mm in diameter, or not involving the joint surface, frequently resolves with conservative treatment, although the fragment may persist radiographically. Lesions approximately 5–10 mm in diameter, which are shown clinically to be causing lameness, may require surgical removal. A fracture of the extensor process more than 10 mm from its proximal border carries a poor prognosis. A large discrete osseous fragment proximal to the extensor process, often occurring bilaterally, may be seen as an incidental finding.

Hoof

RADIOGRAPHIC TECHNIQUE

The radiographic views for examination of the hoof wall are similar to those for the distal phalanx (see page 27); however, the exposures should be considerably reduced in order to visualize the hoof wall, and it is preferable not to use a grid. It is frequently useful to place a radiodense marker on the hoof wall in order to mark its outer surface. This can be done using tape and a piece of wire, or with barium paste. The barium is difficult to remove completely if plain radiographs are required subsequently. In cases where separation of the distal phalanx from the hoof wall is suspected, the use of a small screw or thumb tack to mark a precise location on the hoof wall may be beneficial.

For assessing hoof conformation on radiographs, care must be taken to ensure that exact lateromedial and dorsopalmar radiographic views are obtained. In particular, dorsopalmar (weight bearing) views must be obtained with the horse standing squarely and bearing weight evenly on the foot to be radiographed. To evaluate foot imbalance the x-ray beam should be perpendicular to the foot, whereas to assess distal limb deviation the x-ray beam should be perpendicular to the antebrachium.

NORMAL ANATOMY

Hoof shape and conformation are dependent upon hoof trimming, and feet which are incorrectly trimmed (out of balance) may result in intermittent lameness, due to foot pain or pain elsewhere in the limb caused by uneven weight bearing. Assessment of hoof conformation on lateromedial and dorsopalmar (weight bearing) radiographs can frequently aid the clinician in diagnosing imbalance. On lateromedial views, the solar border of the distal phalanx is closer to the bearing surface of the foot at the toe than at the heels, sloping 5°–10° (Figure 2.24). The centre of the radius of curvature of the distal interphalangeal joint should be vertically above the middle of the bearing surface of the foot. The horn at the toe should be parallel to that of the heels (this is often easier to assess clinically than on radiographs). On dorsopalmar (weight bearing) views, the solar margin of the distal phalanx should be the same height from the ground on the lateral and medial aspects of the foot (Figure 2.7c, page 36).
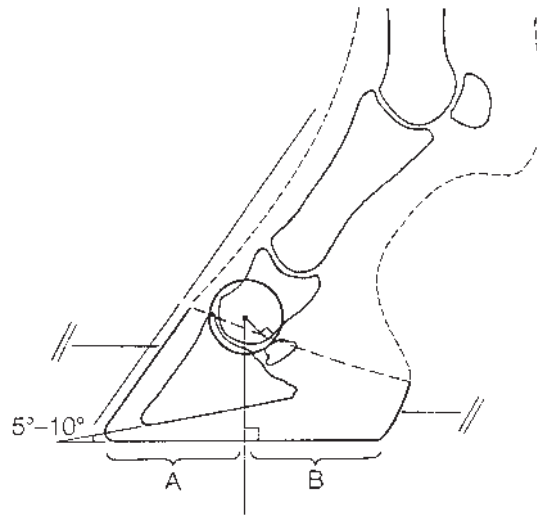
Figure 2.24 Normal hoof conformation. Lateromedial view. Note that A = B.

The tissues of the dermal laminae are slightly less dense than the horn of the hoof wall. For this reason a halo effect is always seen immediately around the distal phalanx on correctly exposed radiographs.

NORMAL VARIATIONS AND INCIDENTAL FINDINGS

Slight variation in hoof conformation is acceptable. The normal thickness of the dorsal wall varies, with a mean of 16mm in Thoroughbreds and a mean of 18mm in Warmbloods. There is also considerable individual variation in the thickness of the sole. No other normal variations have been recognized.

SIGNIFICANT FINDINGS

Laminitis

The primary radiographic changes detected in laminitis relate to separation of the distal phalanx from the hoof wall. Most commonly this is evident as a distal rotation of the toe of the bone, resulting in the dorsal wall of the hoof ceasing to be parallel to the dorsal wall of the distal phalanx. As the condition progresses, a faint radiolucent line may appear between the distal phalanx and the sole or hoof wall. This initially represents serum collected between the dermal and epidermal laminae, and is visible because of the slight difference between fluid and horn densities. This can only be seen on very high-quality radiographs. Subsequently this area may become more lucent, mimicking the appearance of gas. This may develop within 12–18 days of an initial laminitis episode. This line represents necrotic laminar tissue. The lucent lines move distally relative to the coronary band with hoof wall growth (Figure 2.25). However, increasing width of this lucent line is indicative of progressive rotation or laminar necrosis. With extension of the lucent line to the sole, a portal for infection may be established (see also 'Infectious osteitis', pages 46–8).

[58]

Figure 2.25 Lateromedial view of the foot of a horse with laminitis. There is rotation of the distal phalanx and a radiolucent line under the horn of the hoof capsule. A radiopaque marker has been placed on the dorsal hoof wall. The marker on the solar surface of the foot locates the point of frog.

The degree of rotation may be important in assessing prognosis, but this is subject to dispute. It is a subjective measurement and recent trimming of the dorsal hoof wall will make the degree of rotation appear less. It may be helpful to place a radiodense marker on the dorsal hoof wall in order to delineate its position in relation to the distal phalanx. Since laminitis may affect all four feet, lateromedial radiographs of all feet may be required. If progressive rotation is suspected, radiographs obtained at regular intervals may be valuable to monitor progress. The more marked the rotation and the more rapidly it progresses, the worse the prognosis. Attention should also be paid to the toe of the distal phalanx. Radiographic changes include increased lucency of the solar margin at the toe, followed by new bone formation on the dorsal surface of the bone (Figure 2.26). The presence of these changes justifies a more guarded prognosis for return to full athletic function.

In 'the sinker syndrome' (a very severe form of laminitis), the entire distal phalanx drops within the horny capsule. This is difficult to visualize on a single episode radiograph, as the dorsal wall of the hoof and distal phalanx remain parallel. Assessment of the vertical distance between the coronary band and the extensor process of the distal phalanx compared with the contralateral limb, or previous radiographs, may allow a more objective assessment to be made (Figure 2.27a, page 61). There may be soft tissue swelling at the coronary band, which appears more opaque at its dorsal aspect. This is followed by the development of a distinct depression immediately above the coronary band (Figure 2.27b, page 61). A small screw placed in the dorsal hoof wall in these cases will help in the comparison of repeat radiographs obtained on successive days. Further dropping of the distal phalanx can be assessed by measuring from the marker to a set point on the distal phalanx (usually the proximal border of the extensor process; however, care must be taken to monitor positioning and magnification factors when measurements are made.)

Radiographic evidence of previous laminitis is sometimes seen in a

Figure 2.26 Laminitis. Lateromedial view of a case of chronic laminitis, showing rotation of the distal phalanx. Note the mottled lucent areas in the separated laminae at the toe of the foot, and new bone formation on the dorsal aspect of the toe of the distal phalanx (arrow). There is new horn growth below the coronary band with divergence of the horn distally.

clinically normal horse. This includes increased thickness of the dorsal hoof wall, with or without a radiolucent line, and modelling of the toe of the distal phalanx.

Treatment of laminitis must include both systemic treatment and corrective farriery. Lateromedial radiographs are helpful to the farrier when dressing the dorsal wall of the hoof parallel with the dorsal surface of the distal phalanx.

Long-toe low-heel syndrome

On lateromedial radiographs of a normal foot, the centre of the radius of curvature of the distal interphalangeal joint should be vertically above the centre of the bearing surface of the foot (see Figure 2.24, page 58). If the joint is over the palmar third of the bearing surface, this indicates poor dorsopalmar hoof balance which may result in lameness. On a standing latero-medial radiograph it is also important to assess the position of the solar margin of the distal phalanx relative to the ground. If the palmar processes of the distal phalanx are closer to the ground than the toe, this indicates extremely poor hoof balance and is usually associated with lameness (Figure 2.28a, page 62). Palmaroproximal-palmarodistal oblique views of the distal phalanx should be obtained in these cases, to look for increased lucency around the palmar processes indicative of separation of the laminae at the heels (Figure 2.28b, page 62). New bone formed on the axial or abaxial surfaces of the palmar processes of the distal phalanx is suggestive of repeated trauma to this area (see also 'Pedal osteitis complex', pages 44–6).

Infection

Infection of the foot is usually easily diagnosed clinically, but the extent of the area involved can be difficult to assess. Radiographically lucent zones may be seen within the hoof. These vary in shape and size, but with the
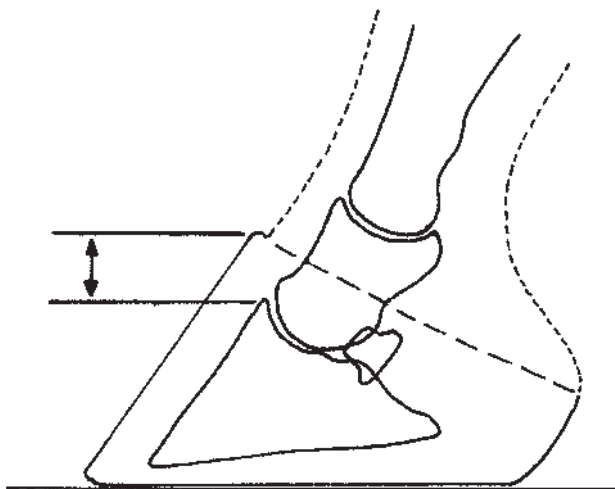
Figure 2.27(a) Diagram to show a method to evaluate 'sinking' of the distal phalanx. Monitor the distance between horizontal lines drawn at the levels of the coronary band and the proximodorsal aspect of the extensor process of the distal phalanx.
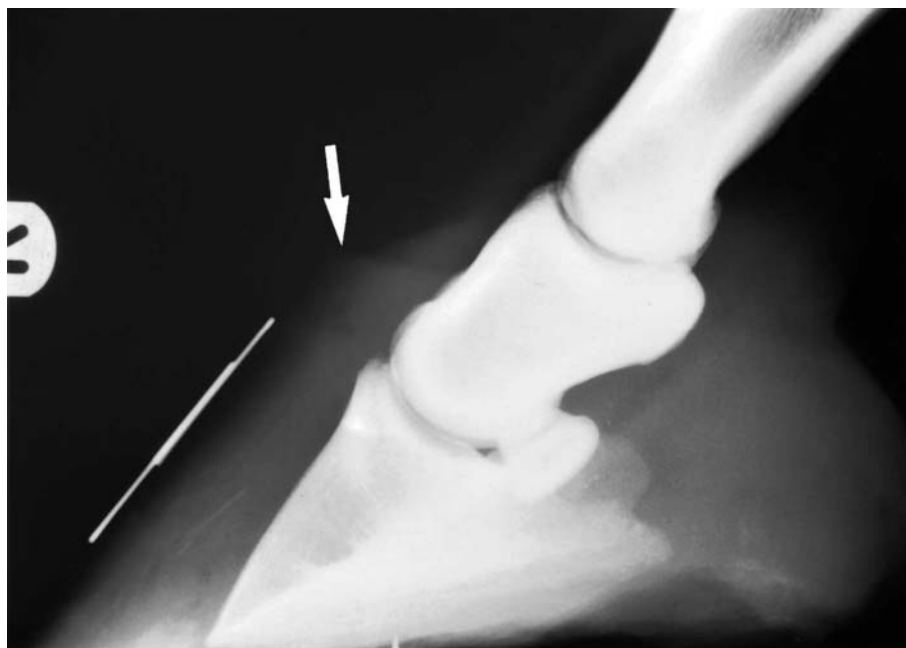
Figure 2.27(b) Lateromedial view of the front foot of a horse with severe laminitis. The distal phalanx has sunk within the hoof capsule. Note the position of the distal phalanx relative to the coronary band (large arrow). The dorsal hoof wall is abnormally thick, and there is also very slight rotation of the distal phalanx. There is a radiopaque marker on the dorsal hoof wall.

careful use of oblique views the extent of hoof separation can be determined. They must be distinguished from the lucent lines seen with separation of the hoof wall in laminitis (see page 58). The margin of the distal phalanx should be inspected carefully for evidence of infectious pedal osteitis (see pages 46–8), particularly if infection is recurrent.

In some cases, clinical signs may indicate the presence of infection, but a discharging sinus may be slow to occur. This is most common if the sole is hard or unusually thick. In these cases radiographs may reveal a lucent zone beneath or adjacent to the distal phalanx, indicating infection.

Hoof wall separation

Separation of the hoof wall may occur for a number of reasons other than laminitis (see page 58) and infection (see above). Excessive length of horn

Figure 2.28(a) Low heel conformation. Lateromedial view. The solar surface of the distal phalanx is abnormally aligned with the ground (compare with Figure 2.7a). Note two clenches left in the hoof when the shoe was removed.
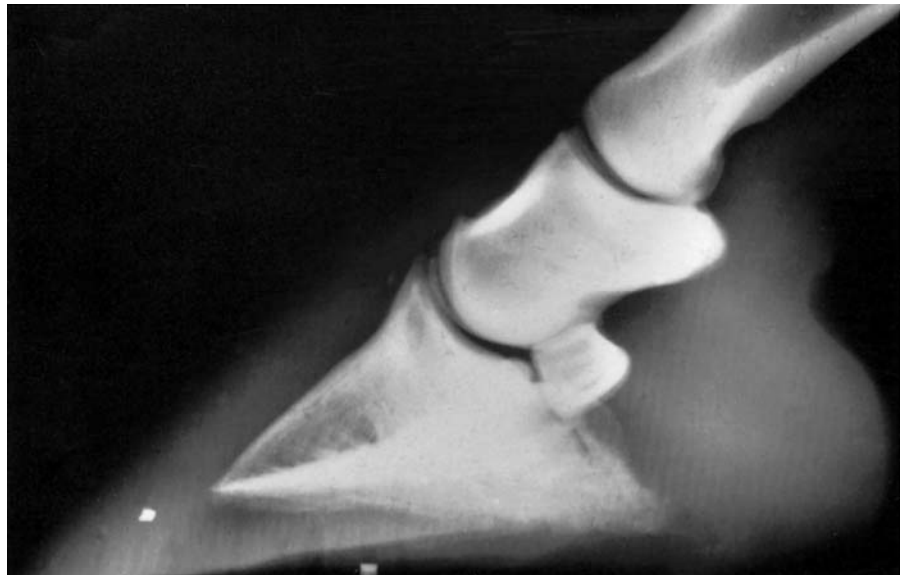
Figure 2.28(b) Low heel conformation. Palmaroproximal-palmarodistal view of the distal phalanx, showing separation of the laminae around the medial palmar process seen as an area of increased lucency (arrow).

at the toe may result in the dorsal aspect of the hoof wall lifting away from the distal phalanx. A radiolucent area will be evident under the hoof wall (Figure 2.29). Separation can also occur as a result of an acute traumatic incident, e.g. jumping on hard uneven ground.

The term 'seedy toe' is used to describe a condition in which there appears to be separation of the dermal and epidermal laminae, or there is poor horn formation from the dermal laminae. The aetiology of this condition is uncertain. It may initially be detected proximally and, as the horn grows down, the separated area moves distally. Seedy toe can be seen radiographically as a lucent area in the laminar portion of the hoof wall. It may have no apparent opening through the hoof wall or white line when first detected. When the distal margin of the separated area reaches the bearing surface, trimming the foot will open into the separation which may

[62]
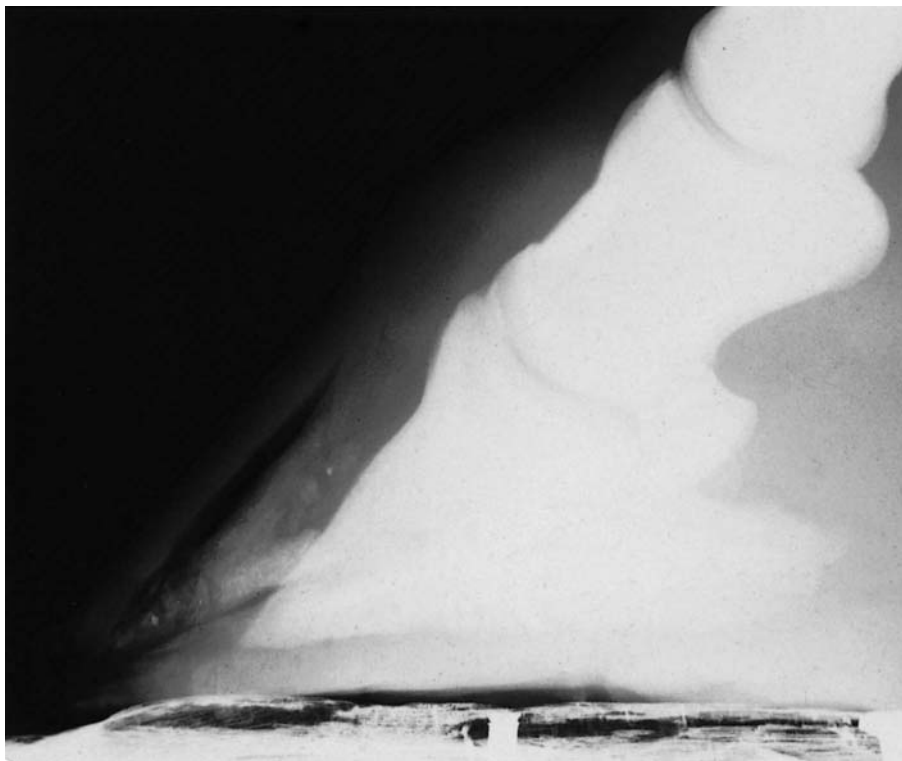
Figure 2.29 Laminar separation at the toe. Lateromedial view, showing separation of the hoof wall at the toe of the foot. This extends up the dorsal wall and laterally around the toe. The granular opaque material is dirt packed into the separated area.

then act as a portal for infection. If the lesion is extensive, the increased loading on the adjacent laminae may result in lameness, particularly on hard ground. The extent of the lesion may be determined by the careful use of oblique views. (The term seedy toe is sometimes used to refer to the separated laminae seen in the hoof after rotation of the distal phalanx in laminitis. These two conditions should be distinguished from each other, as they have different aetiologies and require different treatments.)

Navicular bone

RADIOGRAPHIC TECHNIQUE

In this chapter the distal sesamoid bone is referred to as the navicular bone.

Equipment

Adequate radiographs of the navicular bone can be obtained using portable x-ray equipment, but a minimum output of 15 mA at 80 kV is required. With machines of low output (less than 40 mA at 80 kV), rare earth screens and appropriate films are essential to avoid movement blur. Machines with a high milliamperage output allow short exposure times, and therefore fine-grain high-definition screens and compatible films can be used to obtain more detail. All radiographs of the navicular bone should be obtained using a grid (8:1 ratio), with the exception of the palmaroproximal-palmarodistal oblique view for which a grid may not be required. Careful collimation of the x-ray beam will also enhance the quality of the radiographs.

[63]

It is essential that the shoes are removed and the feet carefully cleaned prior to radiography. Loose horn in the sole and irregular growth of the frog should be removed. Scrubbing the feet with water can result in artefacts due to loose packing in the frog clefts (see below).

The frog clefts need to be packed to eliminate air shadows being cast over the navicular bone for at least one dorsoproximal-palmarodistal view, and for the palmaroproximal-palmarodistal oblique view. This can be achieved using Playdoh or equivalent, Vaseline or soft soap. However, the latter two may trap air bubbles creating artefacts which may mimic pathology. There is also the danger of the horse slipping. Packing should be kept to a minimum, to avoid creating artefacts. The use of a water bath is not recommended as this increases scatter, resulting in reduced contrast on the final radiograph.

Positioning

For complete evaluation of the navicular bone it is recommended that lateromedial, dorsoproximal-palmarodistal oblique and palmaroproximal-palmarodistal oblique views should be obtained. A second dorsoproximal-palmarodistal oblique may be required to rule out artefacts. In some cases a dorsopalmar (weight bearing) view should also be obtained.

Lateromedial view

This radiograph is obtained with the foot to be examined placed on a flat block. It is preferable, but not essential, for the foot to be weight bearing. The x-ray beam should be horizontal and centred on the end of the navicular bone (approximately 1 cm below the coronary band at a point midway between the most dorsal and most palmar aspects of the coronary band). The beam is aligned parallel to a line drawn across the bulbs of the heel, so that it traverses the navicular bone through its long axis.

Dorsoproximal-palmarodistal oblique views

Two dorsoproximal-palmarodistal oblique views are helpful to aid recognition of artefacts. These views can be obtained using either of two techniques, the choice of which is used is largely a matter of personal preference.

DORSOPROXIMAL-PALMARODISTAL ('UPRIGHT PEDAL') OBLIQUE VIEW

The best radiographs are obtained using the dorsoproximal-palmarodistal oblique (upright pedal) view. The toe of the foot is placed on a navicular block (see page 66), and the dorsal wall of the foot and the pastern angled forwards at approximately 85° to the horizontal (Figure 2.30a). The x-ray beam is kept horizontal and centred 2–3 cm proximal to the coronary band at the midline of the foot. The beam should be well collimated. The cassette is placed behind and as close as possible to the foot. If the navicular block is placed too close to the horse, the fetlock and pastern joints will flex too much and the x-ray beam will traverse too great a distance through the middle phalanx, with resultant loss of quality of the radiograph. If

positioned too far in front of the horse, the dorsal wall of the hoof and the pastern become too upright and the distal border of the navicular bone is superimposed over the distal interphalangeal joint.

A second dorsoproximal-palmarodistal (upright pedal) oblique view may be helpful to aid interpretation and to differentiate artefacts. This view is obtained in a similar manner to the first, but with the dorsal wall of the hoof and the pastern vertical and the x-ray beam centred on the coronary band (Figure 2.30b).
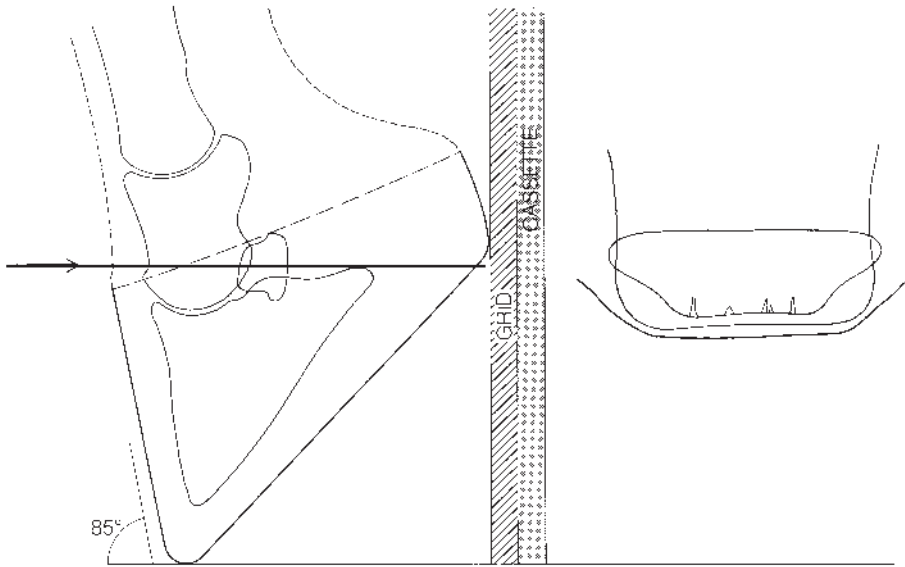
Figure 2.30(a) Positioning to obtain a dorsoproximal-palmarodistal oblique view of the navicular bone (85° upright pedal view). Inset diagram shows resultant radiographic positioning of the distal border of the navicular bone proximal to the distal interphalangeal joint.
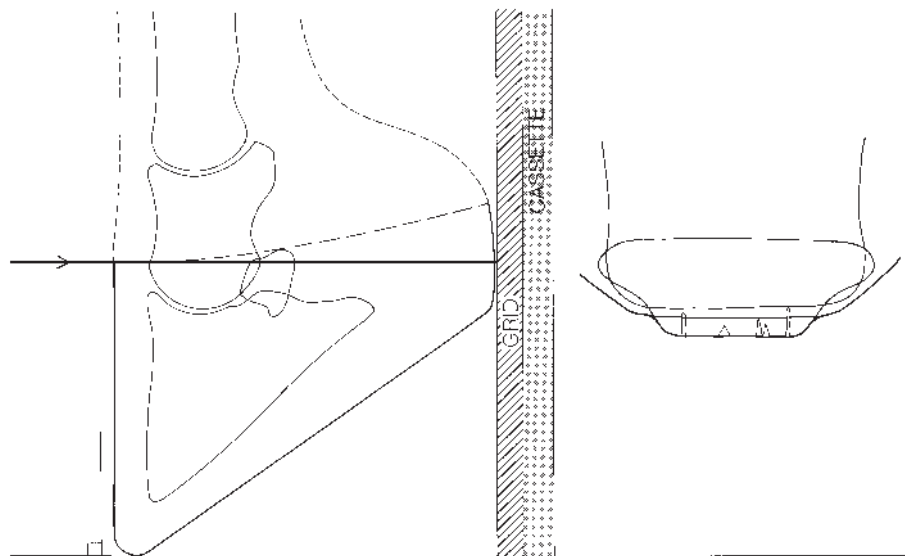
Figure 2.30(b) Positioning to obtain a dorsoproximal-palmarodistal oblique view of the navicular bone (90° upright pedal view). Inset diagram shows resultant radiographic positioning of the distal border of the navicular bone superimposed over the distal interphalangeal joint.
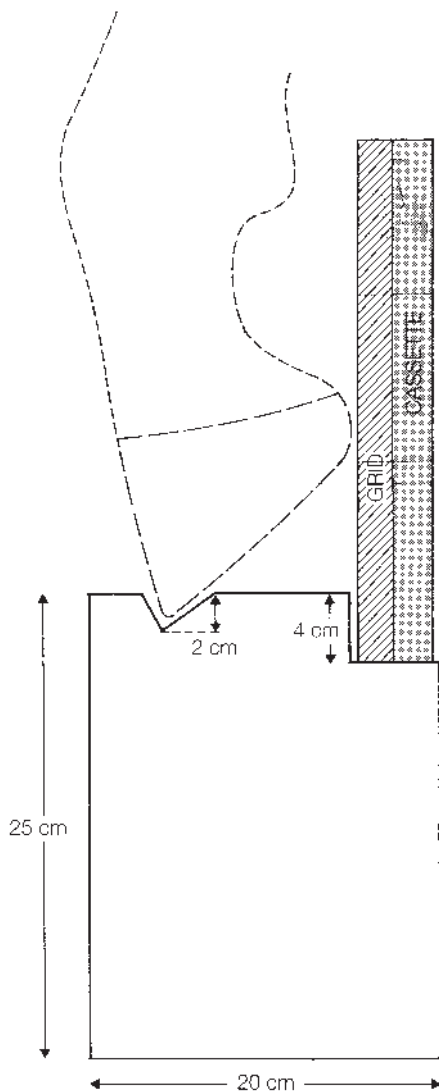
Figure 2.30(c) A 'navicular block' (used to position the foot for radiographs of the navicular bone and distal phalanx in the 'upright pedal' position).

The first of these two views will give good visualization of the distal border of the bone. The second view gives good visualization of the proximal border and the body of the navicular bone.

A 'navicular block' can take a number of forms, but is basically a solid block of wood with a groove cut in the top in which the toe of the foot can be rested (see Figure 2.30c) while the limb is held by an assistant. By moving the block forward or backward relative to the horse, the dorsal wall of the hoof can be positioned at different angles. A horse will normally stand quietly if the limb is raised on a block about 25 cm high. With a smaller block the horse will continually try to straighten the limb and stand on it.

DORSOPROXIMAL-PALMARODISTAL OBLIQUE ('HIGH CORONARY') VIEW

This technique has the disadvantage that the x-ray beam is not at right angles to the film, nor is the film parallel with the flexor surface of the navicular bone (see Figure 2.2a, page 30). This results in some distortion of the image. None the less, in some horses ease of handling the animal may outweigh other considerations, and some workers prefer to use this technique routinely. The cassette is placed in a suitable tunnel on the floor, and the horse stands on it. The x-ray beam is centred 2 cm above the coronary band in the midline, and angled distally, at an angle of at least 60° to the horizontal (i.e. a dorsal 60° proximal-palmarodistal oblique view). It is recommended that two views should be obtained with 10°–15° difference in angle of the beam.

The radiographic image is normally improved by the use of a parallel grid. A grid ratio of 6:1 is preferable to 8:1 because of the difficulty of aligning the foot, grid lines and x-ray beam. Alignment of the grid with the x-ray beam and the foot is more difficult than with the upright pedal view.

Palmaroproximal-palmarodistal oblique view

This view is used to give good visualization of the medulla, flexor cortex and flexor surface of the navicular bone.

The foot to be radiographed is positioned caudal to the contralateral forelimb, on a cassette tunnel containing the cassette. The heels should be flat on the ground, but the weight of the horse should be forward on the contralateral limb. The x-ray machine is placed ventral to the thorax of the horse. The x-ray beam is centred between the bulbs of the heel at the base of the pastern at an angle of 45° to the horizontal (Figure 2.31a).

Alternatively, the horse stands on a cassette tunnel which is placed on a wedge-shaped block, which has a slope of approximately 10°. The contralateral limb is raised to restrict movement. The x-ray beam is angled at approximately 30° from the horizontal, centring as above (Figure 2.31b). In both techniques it is important to avoid superimposition of the palmar aspect of the fetlock over the navicular bone.

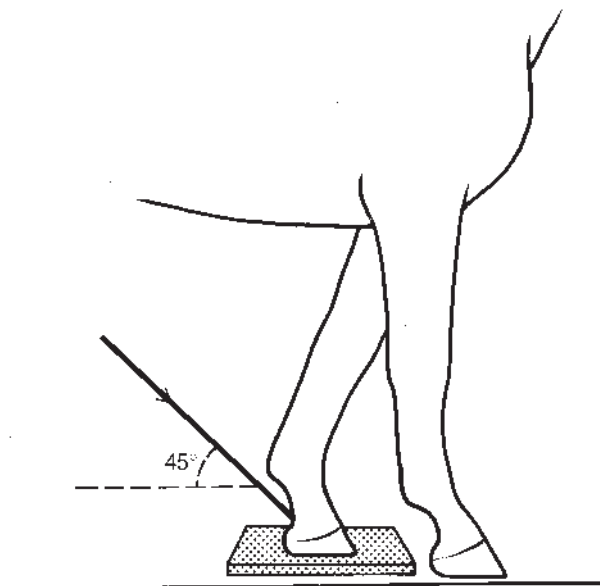The angle of the x-ray beam should be parallel to the flexor surface of

[66]

Figure 2.31(a) Positioning to obtain a palmar 45° proximal-palmarodistal oblique view of the navicular bone. The heel of the foot to be examined should be on the ground, caudal to the contralateral foot, with the weight of the horse forward on the opposite limb. The x-ray beam (arrow) is centred on the midline between the bulbs of the heel, at the distal aspect of the pastern.
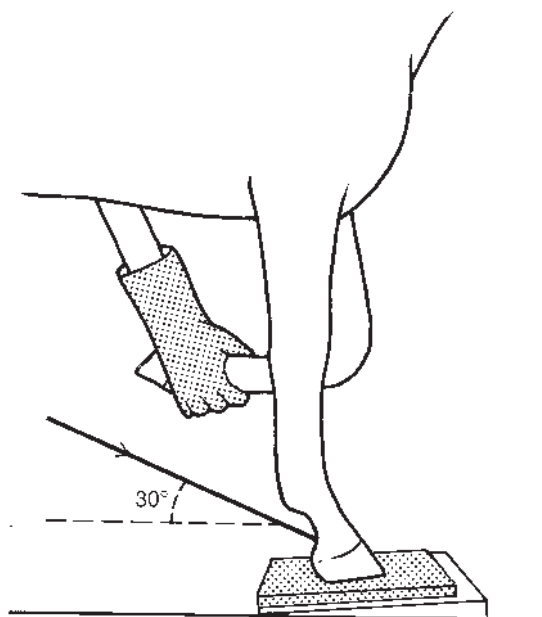
Figure 2.31(b) Positioning to obtain a palmar 30° proximal-palmarodistal oblique view of the navicular bone, with the foot on a wedge-shaped block, with the toe elevated. The x-ray beam (arrow) is centred on the midline, between the bulbs of the heel.

the navicular bone. Both foot conformation and limb placement will have an effect on the optimum angle of the x-ray beam. An upright foot conformation will require a larger angle, whereas if the heels are low the angle should be reduced. Poor technique can create artefacts and mimic pathology, especially poor corticomedullary definition and loss of medullary trabeculation (Figure 2.34c,d, page 74).

Dorsopalmar (weight bearing) view

The true dorsopalmar radiograph is obtained with the horse bearing weight on the limb (see Figure 2.3, page 31). The x-ray beam is kept horizontal, and

[67]

centred approximately 2 cm below the coronary band at the dorsal aspect of the foot. It is aligned perpendicular to a line tangential to the bulbs of the heel. The cassette is placed vertically behind the foot, at a right angle to the x-ray beam.

This is not recommended as a standard view for examining the navicular bone, but can give valuable additional information about a fracture of the navicular bone, and about new bone on its proximal border.

Dorsoplantar views of the hind feet

It is normally easier to obtain plantarodorsal rather than dorsoplantar views of the hind feet. The positioning of the limb for these views is the same as for the dorsoproximal-palmarodistal oblique view of the forefeet, except that a low flat block (5 cm) is recommended for supporting the toe. The cassette is placed in front of the foot, and the x-ray beam is centred in the midline of the bulbs of the heel, level with the dorsal aspect of the coronary band.

NORMAL ANATOMY

Immature horse

The navicular bone usually ossifies from a single centre, and at birth has an oval outline on dorsopalmar views. It continues to ossify until about 18 months of age, at which time it has acquired its adult shape.

Skeletally mature horse

Lateromedial view

Lateromedial radiographs of the navicular bone show the joint surfaces which articulate with the middle and distal phalanges (Figures 2.32a–2.32d). The flexor surface is visualized as two lines, the more palmar representing the sagittal ridge of the bone, and the more dorsal representing the main flexor surface. A smooth edged depression is frequently seen in the central part of the sagittal ridge (Figure 2.32c, page 70). The dorsal third of the distal border of the bone articulates with the distal phalanx. At the distal palmar aspect is a smoothly defined ridge which is the region of origin of the distal sesamoidean impar (interosseous) ligament. There is usually a notch of variable depth between the articular surface and the ridge on the distal border of the bone, which has been referred to as a synovial fossa. Lucent zones (also referred to as nutrient foramina and synovial invaginations of the distal interphalangeal joint) extending proximally from this notch are generally not evident in a normal horse on the lateromedial view. A clear linear trabecular pattern is seen within the medulla. The medulla and cortices of the bone are distinct. In some horses the outline of the deep digital flexor tendon is seen as a faint opacity palmar to the navicular bone.
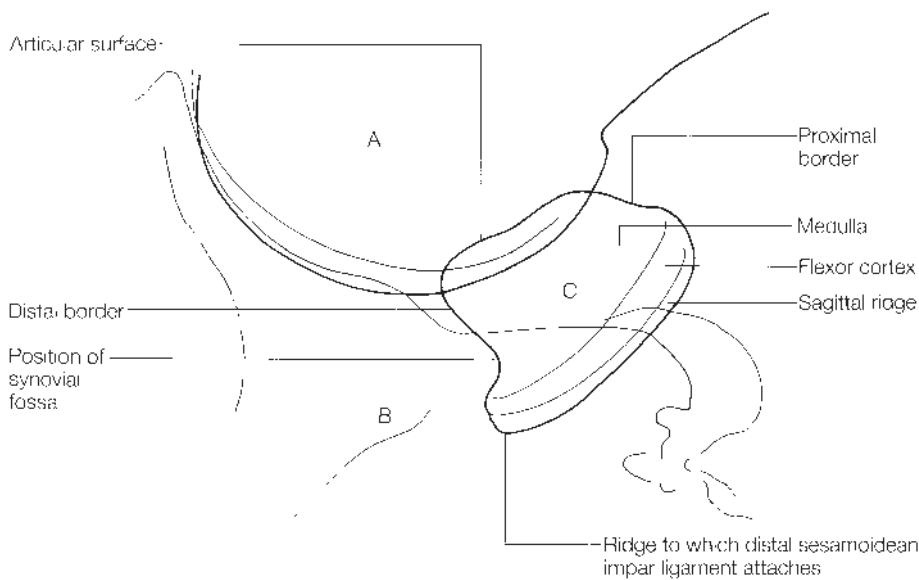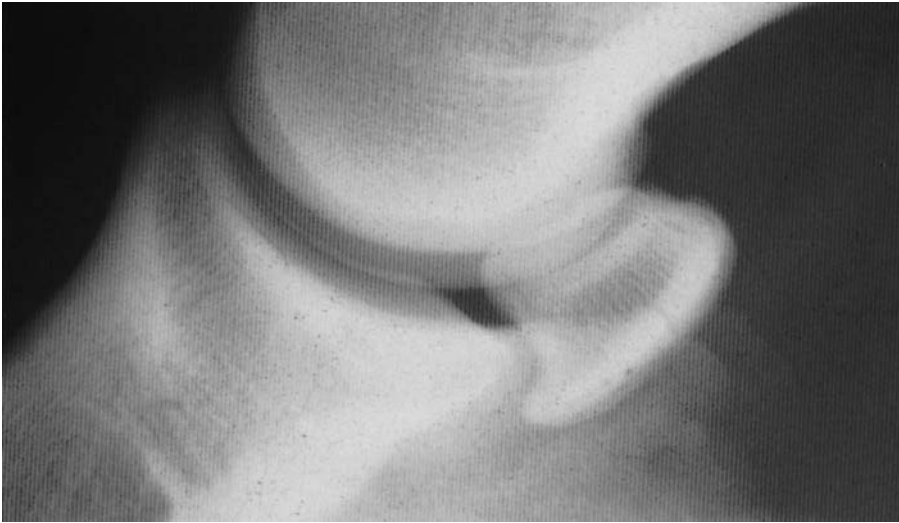
Figure 2.32(a) Lateromedial view and diagram of a normal adult navicular bone. A = middle phalanx, B = distal phalanx, C = navicular bone. Note the distal elongation of the flexor surface of the navicular bone and compare with Figure 2.7(a). The joint space between the distal aspect of the navicular bone and the distal phalanx is convergent.

Dorsoproximal-palmarodistal oblique views

DORSOPROXIMAL-PALMARODISTAL OBLIQUE ('UPRIGHT PEDAL') VIEW

The outline of the navicular bone varies considerably between animals, but is normally a mirror image of that of the contralateral limb (Figures 2.33a and 2.33b). Several triangular shaped lucent zones are often visible along the distal border of the bone (see page 75). The distal border is visualized as two lines: one (the more prominent and more proximal) represents the articulation of the bone with the distal phalanx; the other represents the distal border of the ridge from which the distal sesamoidean impar ligament originates. On poorly positioned views the proximal border of the bone may also be evident as two lines representing the palmar and dorsal margins.

[69]

Figure 2.32(b) Lateromedial view of a normal adult navicular bone with a parallel joint space between the navicular bone and the distal phalanx (compare with Figure 2.32a).
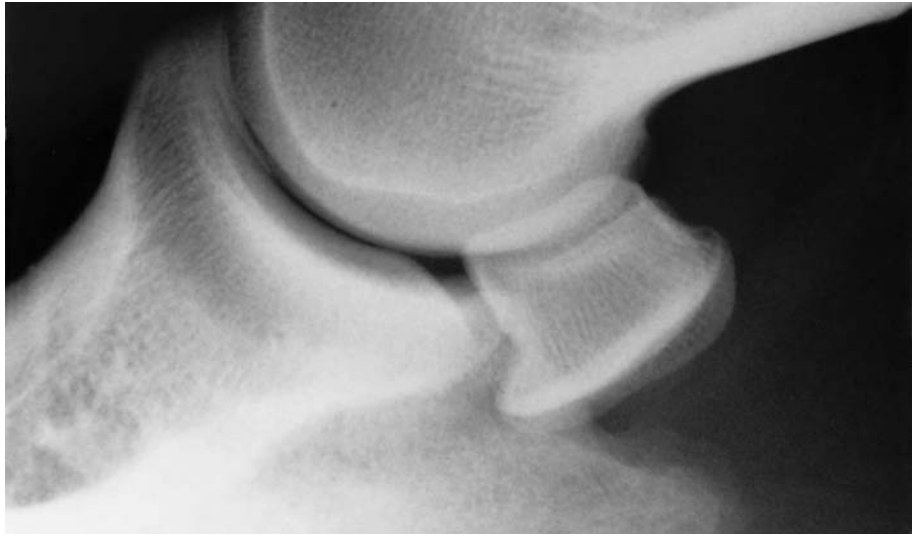
Figure 2.32(c) Lateromedial view of an adult navicular bone, showing a smooth depression in the sagittal ridge (arrow).
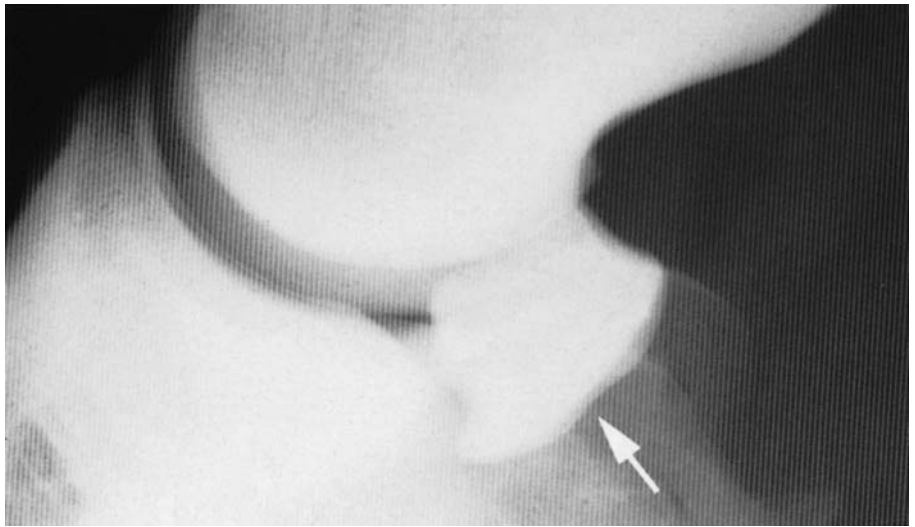
Figure 2.32(d) Lateromedial view of an adult navicular bone, showing a penetrating lesion of the flexor surface of the bone (arrow).

Figure 2.33(a) Dorsoproximal-palmarodistal oblique view of a normal adult navicular bone (upright pedal view).
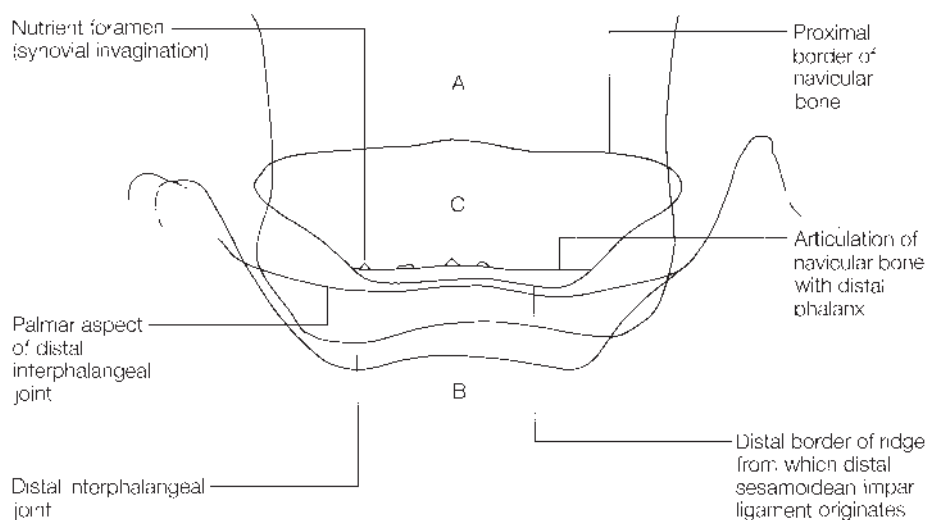
Figure 2.33(b) Diagram of a dorsoproximal-palmarodistal oblique view of a normal adult navicular bone (upright pedal view). A = middle phalanx, B = distal phalanx, C = navicular bone.

DORSOPROXIMAL-PALMARODISTAL ('HIGH CORONARY')
OBLIQUE VIEW

The image seen using this technique is distorted when compared with the upright view (Figure 2.33d), the navicular bone appearing longer in a proximodistal direction (Figure 2.33c).

Palmaroproximal-palmarodistal oblique view

The navicular bone has two distinct cortices separated by a less dense medulla, which has a distinct trabecular pattern (Figures 2.34a and 2.34b). The lucent zones seen on the distal border of the bone in dorsoproximal-palmarodistal views are visible within the medullary cavity as circular or oval lucencies. The flexor cortex has an even thickness, but a small crescentic or oval lucency may be evident in the sagittal ridge. The thickness of the cortex may vary between breeds and between individuals, but a sharp margin

Figure 2.33(c) Dorsoproximal-palmarodistal oblique view of a normal navicular bone obtained using the 'high coronary' technique. Note the slight elongation of the navicular bone in a proximodistal plane compared with Figure 2.33(d) and loss of definition of its margins.

Figure 2.33(d) Dorsoproximal-palmarodistal oblique view of the same foot as Figure 2.33(c), obtained using the 'upright pedal' technique.

between the cortex and the medulla should always be present. In horses with upright foot conformation the flexor cortex is usually thinner than in horses with more normal foot conformation.

The crescent shaped lucent zone in the sagittal ridge of the navicular bone is rarely seen in very young horses. It represents an early change of navicular bone modelling in response to stress and is of unknown clinical significance. A relatively sclerotic reinforcement line develops in the sub-chondral bone parallel with the flexor cortex in the region of the sagittal

[72]
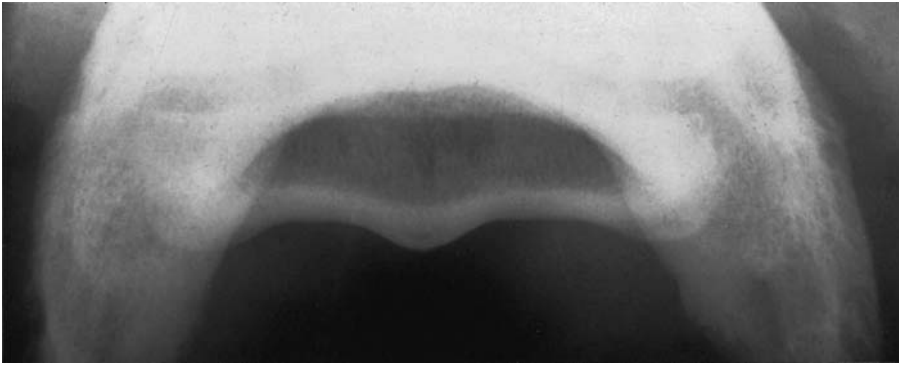
Figure 2.34(a) Palmaroproximal-palmarodistal oblique view of a normal adult navicular bone. Note the well-defined lucency in the sagittal ridge, which may or may not be present.

Palmar aspect of metacarpophalangeal joint

Palmar aspect of middle phalanx

Articular cortex of navicular bone

Articulation between navicular bone and middle phalanx

Medulla of navicular bone

Palmar process of distal phalanx

Flexor cortex of navicular bone

Distal synovial invaginations of navicular bone

Well-defined crescent-shaped lucent zone in the flexor cortex at the sagittal ridge

Sagittal ridge

Figure 2.34(b) Diagram of a palmaroproximal-palmarodistal oblique view of a normal adult navicular bone.

ridge. The intervening bone is relatively radiolucent and is projected in the palmaroproximal-palmarodistal oblique view as the crescent shaped lucent zone in the sagittal ridge. If the bone between the reinforcement line and the flexor cortex becomes compacted, then the lucent zone becomes less clear and may be obliterated.

Dorsopalmar (weight bearing) view

The navicular bone is largely obscured by the extensor process of the distal phalanx. The medial and lateral margins of the bone are seen clearly, as is its proximal border (see Figure 2.7c, page 36).

Figure 2.34(c) Palmar 45° proximal-palmarodistal oblique view of the navicular bone of a normal horse with an upright foot conformation. The medulla of the navicular bone is partially obliterated by the distal phalanx. There is apparent sclerosis of the medulla and poor corticomedullary demarcation. The x-ray beam was not parallel to the flexor surface of the navicular bone and the foot had been positioned too far forward. Compare with Figure 2.34(d).

Figure 2.34(d) Palmar 50° proximal-palmarodistal oblique view of the navicular bone of the same horse as in Figure 2.34(c). There is a clear trabecular pattern within the medulla and excellent corticomedullary demarcation. Note also that the flexor cortex appears narrower than in Figure 2.34(c). The sagittal ridge is relatively flat, a normal variation.
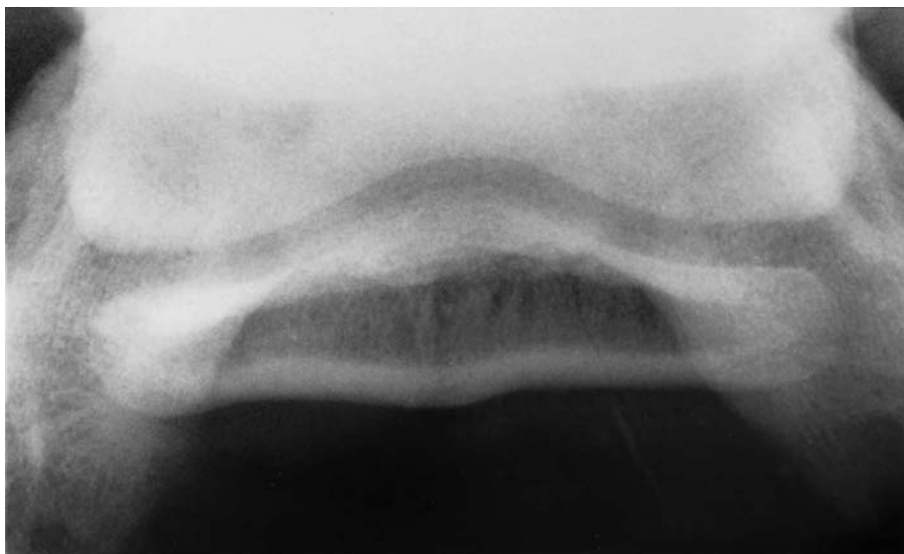
NORMAL VARIATIONS AND INCIDENTAL FINDINGS

The outline of the navicular bone is extremely variable. Occasional cases have been reported where the navicular bone was absent, bipartite or tripartite. The significance of these findings is uncertain.

Lateromedial view

The navicular bone may be trapezoid in shape (Figure 2.7a, page 34), but frequently the flexor cortex has proximal and/or distal elongations (Figure 2.32a). The joint space between the navicular bone and the distal phalanx may be parallel (Figure 2.32b) or convergent (Figure 2.32a). The thickness of the flexor cortex of the navicular bone is variable. It tends to be thinner in horses with an upright foot conformation. A small, shallow smooth-edged

depression is present in the centre of the sagittal ridge of many normal horses (Figure 2.32c, page 70).

Smooth opaque entheseophytes on the proximal border of the navicular bone may be evident at the insertions of the navicular collateral ligaments. These are best seen on the dorsopalmar views (see below and also 'Navicular disease', page 76).

Dorsopalmar ('upright pedal') view

The number and size of the lucent zones along the distal border of the navicular bone vary between individuals and between breeds. It is probably normal to have up to seven lucent zones in the bone, and these are normally conical, and taller than they are wide. The hind feet generally have two or three fewer than the front. There may be a double contour along the proximal border of the navicular bone. This may be due either to elongation of the flexor cortex proximally, or entheseophyte formation.

New bone on the proximal border of the navicular bone may be present in clinically normal horses. This is entheseophyte formation in the insertion of the navicular collateral ligaments, along the proximal border of the bone. It is normally most prominent at the medial and lateral aspects of the proximal border, where it is sometimes referred to as spurs. Spurs are more common on the lateral aspect of the navicular bone than the medial. The clinical significance of these spurs is equivocal, but they indicate previous stress to the ligaments. They are unlikely to indicate 'navicular disease' *per se*, although they may indicate a foot imbalance. Spurs or new bone along the proximal border may accompany other changes in the navicular bone, and are associated with 'navicular disease', especially if extensive. (On plantarodorsal views the navicular bone appears slightly larger relative to the middle phalanx.)

A double contour along the distal border of the bone represents the distal articular margin proximally and the distal aspect of the flexor cortex distally. Discrete mineralized fragments are sometimes detectable distal to the navicular bone (see also pages 78 and 83). Although these occur more commonly in association with navicular disease, they are sometimes present as an incidental finding.

Palmaroproximal-palmarodistal oblique view

Large nutrient foramina and synovial invaginations along the distal border of the navicular bone appear as large oval-shaped lucencies within the medulla. The thickness of the flexor cortex varies considerably between horses and is generally thinner in Thoroughbreds than in Warmbloods. It is usually bilaterally symmetrical unless there is disparity in foot shape. It tends to be thinner in horses with upright foot conformation. The prominence of the sagittal ridge varies between horses. It sometimes appears flattened.

A small well-defined crescentic or oval lucency may be evident in the sagittal ridge (see Figures 2.34a and 2.34b, page 73).

SIGNIFICANT FINDINGS

Structures overlying the navicular bone are easily misinterpreted as radiographic lesions. The following should be borne in mind:

1 There is a variable sized depression in the palmar aspect of the middle phalanx, proximal to the articular surface, which may appear relatively lucent, and is easily superimposed over the navicular bone.

2 The clefts and central sulcus of the frog are superimposed over the navicular bone on the dorsoproximal-palmarodistal oblique ('upright pedal') view. They can mimic radiolucencies or fractures, especially if poorly filled with packing, or if the packing becomes loose.

3 Excess and poorly distributed packing in the frog clefts can appear as an opacity proximal to the navicular bone, mimicking entheseophyte formation. If there is difficulty in differentiating lesions from artefacts, it is recommended that the foot be re-packed and the view repeated using a slight change in angle.

4 The marrow cavity in the middle phalanx, when present, is variable in size. It is easily superimposed over the navicular bone and care should be taken, when assessing radiographs, not to confuse it with a lucent lesion in the navicular bone.

5 There is a row of nutrient foramina in the proximal end of the middle phalanx running across the shaft of the bone, immediately distal to the transverse prominence or tuberosity. These foramina are visualized to varying degrees on the dorsoproximal-palmarodistal oblique ('upright pedal') view, depending on the angle of the projection. If the pastern is angled too far forward during radiography, these foramina may be super-imposed over the navicular bone giving the appearance of abnormal prox-imal nutrient foramina.

Navicular disease

There is no universally accepted definition of navicular disease based on pathological or radiological findings. There is, however, a clinically recognizable condition which is frequently termed navicular disease. For the purposes of this book, the term is used to describe a clinical condition, causing a bilateral (or occasionally unilateral) progressive forelimb lame-ness which is not permanently alleviated by rest or corrective shoeing alone. It is acknowledged that there are horses which show clinical signs typical of navicular disease which may have pain arising from the navicular bone or its associated soft-tissue structures, but the condition can be alleviated by rest or shoeing. The term navicular syndrome can be used to encompass these horses since they may at a later stage progress towards a less respon-sive disease. They must be differentiated from horses which have pain in the palmar aspect of the foot due to other causes (see 'Long-toe low-heel syndrome', page 60).

Considerable controversy exists over the significance of radiographic changes in the navicular bone. To relate them to the clinical situation, it is probably best to use the description given on pages 68–75 as being indicative of a normal bone, and accept that a number of apparently normal

horses do show radiographic changes in the navicular bones. When these changes are present in sound horses, their significance is equivocal. Some workers consider that they may predispose the horse to developing navicular disease at a later date, but this is by no means certain. Repeat radiographs are sometimes obtained after a period of 4–6 months, to assess the progression of such lesions. Progression, however, can occur in animals which remain clinically normal, and those that become lame may show no such progression. It is probably best, therefore, to accept that the more changes present, and the greater the degree of change, the more likely the horse is to have navicular disease. In the absence of radiographic abnormality, navicular disease should only be diagnosed with extreme caution.

Lateromedial view

There are contradictory reports that in navicular disease the bone becomes narrower in a dorsopalmar direction when viewed on lateromedial radiographs.

In some cases the synovial fossa may become more prominent. In advanced cases some lucency of the bone proximal to this notch may be seen. In the later stages of the disease the trabecular bone may appear more opaque and the cortex may increase in thickness. There is reduced corticomedullary demarcation.

When a radiolucent lesion is present in the body of the bone, it can frequently be seen on the lateromedial view. If it penetrates the flexor surface of the bone, it is evident as a sharp-edged lesion in the flexor surface (see Figure 2.32d, page 70). This lesion must be differentiated from the previously described depression in the sagittal ridge (see Figure 2.32c, page 70).

Entheseophytes can be seen on the lateromedial view on the proximal and distal borders of the bone. These are described in more detail under 'New bone formation' (see page 80).

Irregularity of the bone at the origin of the impar ligament is an indication that the dorsoproximal-palmarodistal oblique view should be carefully examined. This irregularity may be due to either entheseophyte formation in the impar ligament or to a mineralized opacity distal to the bone.

New bone on the dorsoproximal margin of the navicular bone is an indicator of degenerative joint disease of the distal interphalangeal joint, and does not reflect navicular disease, although it may be seen in association with it.

Dorsoproximal-palmarodistal oblique ('upright pedal') view

The distal lucent zones frequently show a change in shape from the normal described above (see Figures 2.33a, page 71; 2.35, page 78 and 2.36, page 78). It has been suggested that lucent zones of certain shapes have a greater significance than others, but this is still a subjective assessment. There is evidence that the greater the number of abnormally shaped lucent zones, the more likely are clinical signs of navicular disease to be present. Similarly an

[77]

Figure 2.35 Dorsoproximal-palmarodistal oblique ('upright pedal') view of a navicular bone, showing an increased number of lucent zones along the distal border of the bone. These lucent zones are of a variety of shapes, and some are positioned to the extreme edges of the bone. The lateral and medial borders of the bone are asymmetrical. If this change is seen alone, it is not necessarily of clinical significance.

Figure 2.36 Diagram of a dorsoproximal-palmarodistal oblique view of a navicular bone showing distal nutrient foramina of different shapes (after Colles, 1982). The numbers refer to the scoring system of MacGregor (1986). Larger numbers may indicate foramina of greater diagnostic significance.
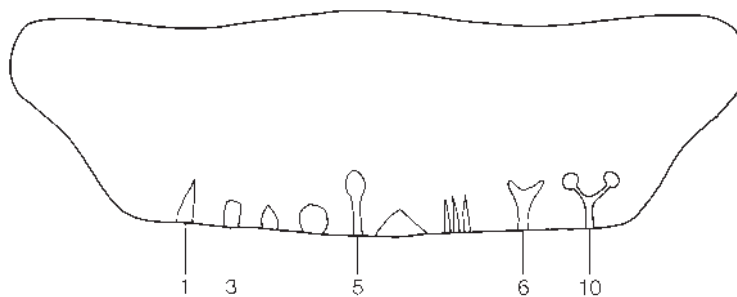
increased number of lucent zones (more than seven), and the radiographic appearance of lucent zones on the lateral, medial or proximal borders of the bone, are all indicators of abnormality. An irregular appearance of lucent zones, i.e. of many different shapes and sizes, and lucent zones surrounded by a halo of sclerosis should also be viewed with suspicion.

Distinct areas of radiolucency within the navicular bone (Figure 2.37a) which are not associated with the distal border of the bone should always be regarded with extreme caution. Although clinical signs may not be present at the time of examination, lameness is likely to develop. If these lesions are detected on dorsoproximal-palmarodistal oblique views, it is important to inspect carefully lateromedial and palmaroproximal-palmarodistal oblique views to ascertain whether they are contained within the body of the bone or penetrate the flexor surface (Figure 2.37b). If the lesion progresses to penetrate through the flexor surface of the bone, adhesion of the deep digital flexor tendon will result. Adhesions may also occur in the absence of other radiological changes in the navicular bone. Once adhesions are present, a hopeless prognosis must be given.

In advanced stages of the disease there may be an appreciable increase in opacity of the bone, with or without thickening of the flexor cortex and loss of definition between the cortex and the medulla. This is best assessed on the lateromedial or palmaroproximal-palmarodistal oblique views.

Mineralized fragments distal to the navicular bone may be seen

Figure 2.37(a) Dorsoproximal-palmarodistal oblique view of a navicular bone showing a marked lucent lesion in the bone. Note that the frog clefts are unpacked. The lesion penetrated the flexor cortex (see Figure 2.37b).
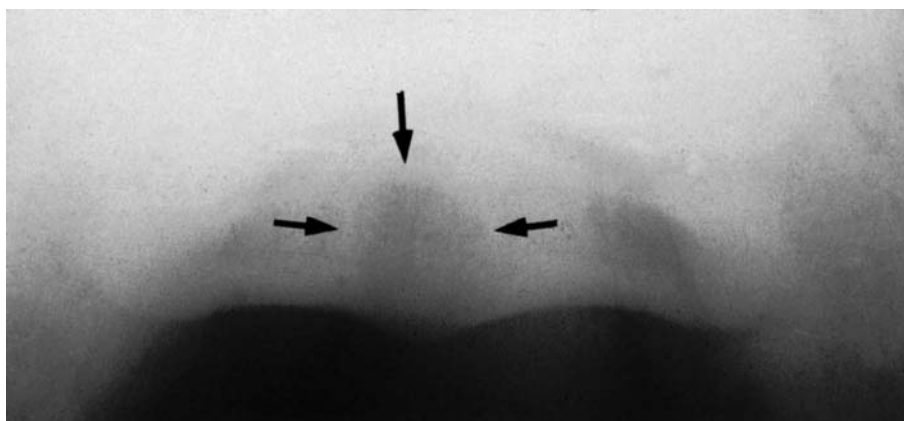
Figure 2.37(b) Palmaroproximal-palmarodistal oblique view of a navicular bone with significant radiological changes. Note: (i) the lucent lesion in the medulla and flexor cortex of the bone (arrows) (see also Figure 2.37a); (ii) the increased opacity of the medulla with resultant loss of definition between the junction of the medulla and the flexor cortex.

unassociated with clinical signs, but are seen more commonly in association with navicular disease.

Palmaroproximal-palmarodistal oblique view

On this view, alterations in the shape of the lucent zones on the distal border of the bone cannot be identified, but increased size and numbers are sometimes evident early in the course of navicular disease.

This view will help to determine whether lucent lesions are present in the medulla or flexor cortex of the bone, or both (see Figure 2.37b).

Localized thinning or reduced radiopacity of the cortex is associated with fibrocartilage degeneration, which may ultimately be associated with tendon adhesions.

The flexor cortex may become uniformly thicker, encroaching into the medulla. The trabecular pattern of the medulla may become less obvious due to sclerosis, resulting in loss of corticomedullary definition (Figure 2.37b). Apparent poor corticomedullary demarcation may be an artefact (Figure 2.34c, page 74) due to inappropriate radiographic technique; it is therefore important to compare the lateromedial and palmaroproximal-

Figure 2.38 Palmaroproximal-palmarodistal oblique radiograph of a navicular bone. Note the irregular outline of the sagittal ridge due to new bone formation.
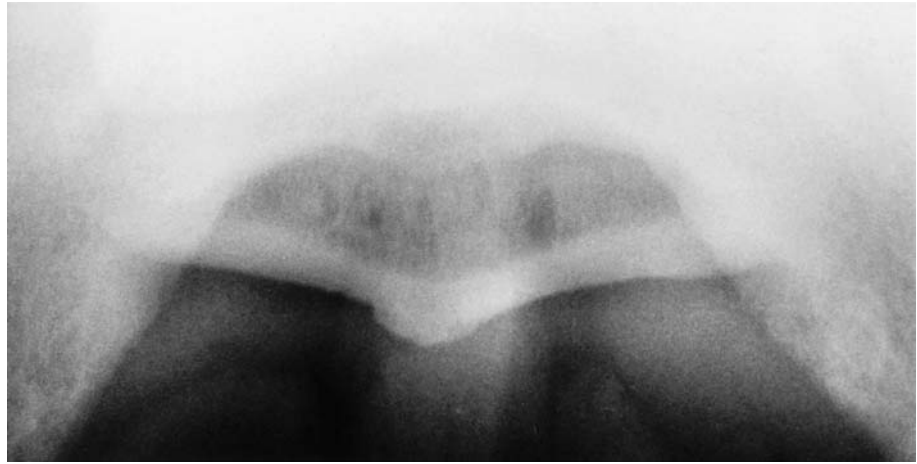
palmarodistal oblique views, and to be critical of the positioning of the palmaroproximal-palmarodistal oblique views.

Occasionally new bone is seen on the flexor cortex (Figure 2.38). This may be seen in the absence of other radiographic abnormalities, emphasizing the importance of this radiographic view in horses with suspected navicular pathology. Such new bone warrants a poor prognosis for future soundness.

A magnifying glass may be useful to study in fine detail the flexor cortex.

Positive contrast studies of the navicular bursa may enhance the interpretation of flexor cartilage changes.

New bone formation

The clinical significance of new bone along the margins of the navicular bone is questionable; however, large amounts of new bone accompanied by other changes may be significant.

Entheseophyte formation is frequently seen in the navicular collateral ligaments. This is seen on the proximal border of the bone on dorsopalmar views, and on the palmar aspect of the proximal border of the bone on lateromedial views (see page 77). Entheseophytes are believed to be evidence of abnormal tension in the suspensory apparatus of the navicular bone, and should be differentiated from osteophytes (see below). There is a significantly higher incidence on the lateral side of the foot.

Dystrophic mineralization or ossification can occur within the navicular collateral ligaments as a discrete opacity proximal to the lateral or medial border of the bone. It is often, but not always, associated with lameness (Figure 2.39).

Periarticular osteophytes are occasionally seen along the dorsal margin of the proximal border on lateromedial views (Figure 2.40, page 82). They are frequently seen in association with degenerative joint disease of the distal interphalangeal joint and warrant a poor prognosis.

Entheseophytes on the distal margin of the navicular bone at the origin of the impar ligament tend to be smaller than on the proximal border, and are thought to be more significant.

[80]

(a)

(b)

Figure 2.39 Radiographs of a navicular bone, showing dystrophic mineralization in the collateral ligaments: (a) lateromedial view; (b) dorsoproximal-palmarodistal oblique ('upright pedal') view. Note that there is some dirt in the frog clefts, and modelling of the proximal border of the navicular bone. There are a number of enlarged lucent zones along the distal border of the bone, some of which also show a change in shape.

Discrete radiopaque bodies may be seen along the distal border of the bone (Figure 2.41). These are of variable aetiology, but cannot be differentiated radiographically. They may be located within a depression in the distal border of the bone, and are more common at the medial and lateral borders of the bone. They may result from avulsion fractures, fractures of entheseophytes or dystrophic ossification in the impar ligament. Their significance is equivocal.

Mineralization in the deep digital flexor tendon

Focal mineralization occasionally occurs in the deep digital flexor tendon overlying and/or immediately proximal to the navicular bone. The cause of this is unknown (see Chapter 1, page 26). It carries a poor prognosis. It is

[81]
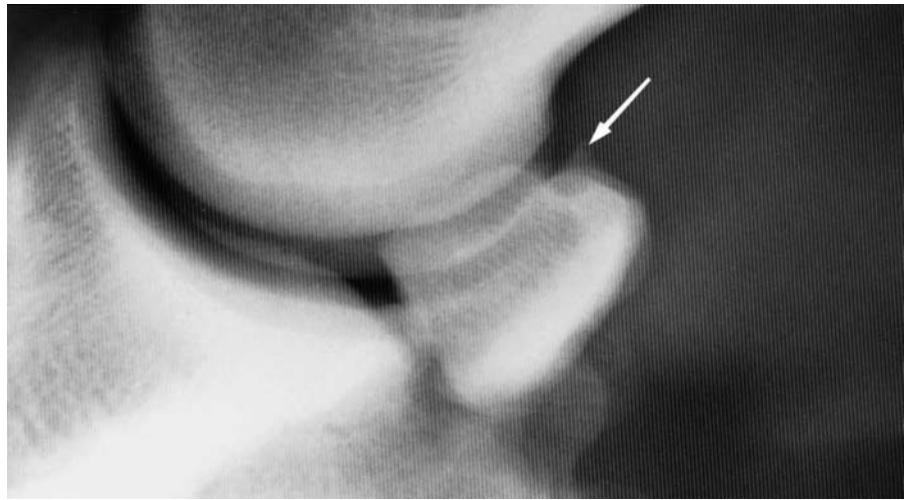
Figure 2.40 Lateromedial view of a navicular bone, showing periarticular osteophytes (arrow) on the dorsoproximal border.

Figure 2.41 Dorsoproximal-palmarodistal oblique view of a navicular bone, showing discrete radiopaque bodies on the distal border of the navicular bone (arrows). Note the presence of abnormally shaped lucent zones along the distal border of the bone. There is a radiolucent line caused by poor packing of the medial frog cleft.

most easily seen on a lateromedial view, but should not be confused with ossification of the hoof cartilages which can be differentiated on a dorsopalmar view.

Infection

Infection of the navicular bursa or bone usually occurs subsequent to a penetrating wound or after an injection into the navicular bursa. Plain radiographs obtained at the time of injury may reveal no abnormality, but if a draining sinus is present, contrast radiography may be of value (see 'Fistulography', page 581). Lateromedial and palmaroproximal-palmarodistal oblique views should be obtained. Follow-up radiographs may be helpful if lameness persists. Extensive ill-defined lucent lesions, and occasionally sclerosis of the palmar cortex of the navicular bone, warrant a very poor prognosis. If a penetrating wound has occurred, immediate and extensive flushing of the navicular bursa and antimicrobial treatment are required.

[82]

Fractures

Small radiopaque bodies in the impar ligament, adjacent to the distal border of the bone, are discussed previously (see page 78 and Figure 2.41). They are very difficult to demonstrate clearly on any radiographic view, but are most easily detected on the dorsoproximal-palmarodistal oblique view.

Fractures through the body of the navicular bone normally occur parallel to the sagittal ridge of the bone, or slightly obliquely to it, and at varying distance from it (Figure 2.42a). There is normally little or no displacement, and the fracture may be very difficult to visualize, particularly in the acute stage. After 2–4 weeks the fracture line becomes more obvious due to bone demineralization. Subsequently lucent zones develop along the fracture line (Figure 2.42b) and an increased number of lucent zones along the distal border of the bone may be seen, especially in the bone immediately adjacent to the fracture. Frequently several dorsopalmar views of slightly varying obliquity as well as palmaroproximal-palmarodistal views are required to confirm the presence of a fracture, and to differentiate it from overlying artefacts (such as lucent lines caused by the frog). It may also be necessary to adjust the packing in the frog clefts. Surgical fixation should be considered.

Fractures occasionally occur horizontally across the bone, close to and parallel with its distal border (Figure 2.42c). It is important to remember that more than one fracture may occur simultaneously.

Fractures, especially in the forelimb, carry a poor prognosis for return to work without internal fixation. A good prognosis, however, can be given for breeding purposes.

Proximal and middle phalanges

The proximal aspect of the proximal phalanx is also discussed under 'The metacarpophalangeal joint' (see page 100).

RADIOGRAPHIC TECHNIQUE

Equipment

Radiographs of the proximal and middle phalanges (pastern region) can easily be obtained using portable machines. High-definition screen and appropriate film combinations can be used even with portable equipment, since movement blur is seldom a problem. It is unnecessary to use a grid even in large horses.

Positioning

Survey radiographs of the proximal and middle phalanges will often be obtained as part of the examination of the foot or fetlock. Specific views of this area are best obtained with the horse bearing weight on the limb, and should include lateromedial, dorsopalmar and two oblique views. When

Figure 2.42(a) Dorsoproximal-palmarodistal oblique view of a navicular bone showing a sagittal fracture of the body of the bone (the fracture is of 3 weeks' duration).

Figure 2.42(b) Dorsoproximal-palmarodistal oblique view of a navicular bone, showing a sagittal fracture of the body of the bone (the fracture is of 12 weeks' duration). There are large lucent areas adjacent to the fracture line, and an increased number of lucent zones along the distal border. There is modelling of the proximal border which may have been present prior to the fracture occurring.

Figure 2.42(c) Dorsoproximal-palmarodistal oblique view of a navicular bone, showing a recent fracture of the distal border of the bone (large arrow). Note that there is also a vertical component to the fracture (small arrow).

[84]
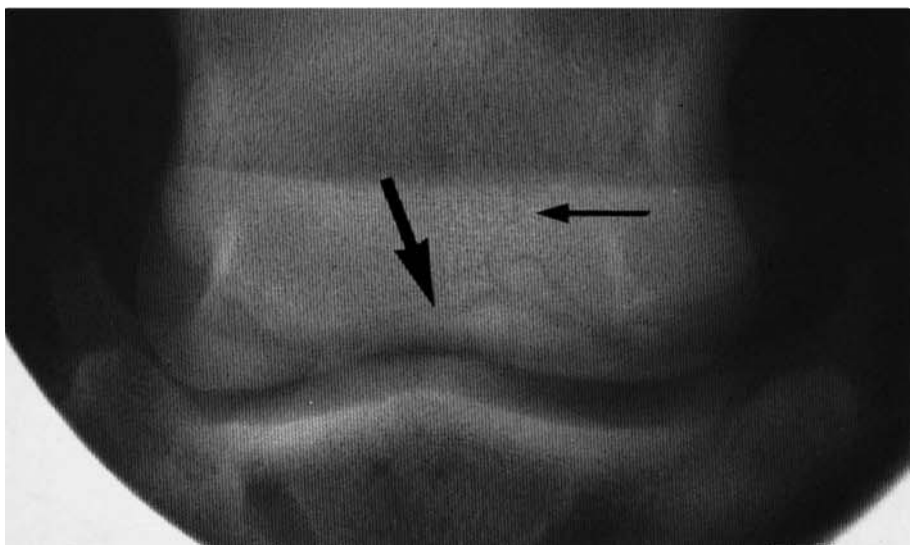
evaluating the dorsal joint margins, flexed oblique views may be more useful (see page 31). The x-ray beam is kept horizontal, and centred midway between the fetlock and coronary band. The x-ray beam should normally be aligned with reference to the bulbs of the heel in order to obtain correct lateromedial or dorsopalmar views. Dorsoproximal-palmarodistal oblique views may be obtained with the x-ray beam aligned at right angles to the dorsal surface of the pastern, and angling the cassette accordingly. This view results in less distortion, and is particularly useful for assessment of the middle phalanx and the proximal interphalangeal joint.

Chip fractures of the phalanges are best visualized on oblique views. Fractures of the phalanges are frequently spiral, and a series of oblique radiographs may be required to determine their course. Fractures, separate centres of ossification or osteochondritic lesions of the proximal palmar aspect of the proximal phalanx may best be evaluated (and/or detected) using dorsal 30° proximal 70° lateral-palmarodistomedial oblique or dorsal 30° proximal 70° medial-palmarodistolateral oblique views (see page 104).

Subtle osteophyte formation is sometimes best evaluated on flexed oblique (dorsolateral-palmaromedial and dorsomedial-palmarolateral oblique) views. These are obtained with the toe of the foot placed in a navicular block, with the sole of the foot approximately vertical (see page 31).

NORMAL ANATOMY

Immature horse

The proximal and middle phalanges both ossify from three centres. In both bones the distal epiphysis unites with the shaft before birth. In foals that are skeletally immature at birth, a lucent crescent is occasionally noted in the distal metaphysis of the bone, which represents a non-mineralized cartilage remnant of the physeal plate. The proximal physis closes at about 1 year of age in the proximal phalanx, and at 8–12 months in the middle phalanx.

Skeletally mature horse

There is an area relatively devoid of trabeculae in the central part of the proximal and middle phalanges. This is a marrow or fat cavity, and is of variable size. It appears as a lucent zone, best seen on dorsopalmar views, although the clarity with which it is seen will depend upon a number of radiographic factors. It may not be visible radiographically in the middle phalanx. On dorsopalmar views there are relatively sclerotic lines on the medial and lateral aspects of this lucent area, which extend proximally and distally. These are the areas of insertion of the oblique (middle) distal sesamoidean ligaments (Figures 2.43a, page 86; 2.43b, page 87; 2.44a, page 88 and 2.44b, page 89).

On dorsopalmar radiographs, the ergot may be recognized as a circumscribed opacity superimposed on the proximal aspect of the proximal phalanx (Figure 2.44a).

[85]

Figure 2.43(a) Lateromedial view of the proximal and middle phalanges of a normal adult horse.

Both the proximal and middle phalanges have a row of nutrient foramina across the shaft of the bone at their proximal and distal ends. These may be seen to varying degrees on dorsopalmar views depending on the angle of projection, and are a normal finding. Care should be exercised, when interpreting radiographs of the navicular bone, that the foramina of the middle phalanx are not superimposed over the navicular bone giving the appearance of abnormal proximal nutrient foramina.

On lateromedial views of the proximal phalanx, a small irregularity is evident on the palmar aspect of the bone at approximately one-third of the

Site of attachment
of oblique distal
sesamoidean ligament

Proximal interphalangeal joint

Eminence for attachment
of collateral ligament of
distal interphalangeal joint

Articular margin of
middle phalanx

* Approximate alternative positions
of nutrient vessel when present.
Not seen in this example
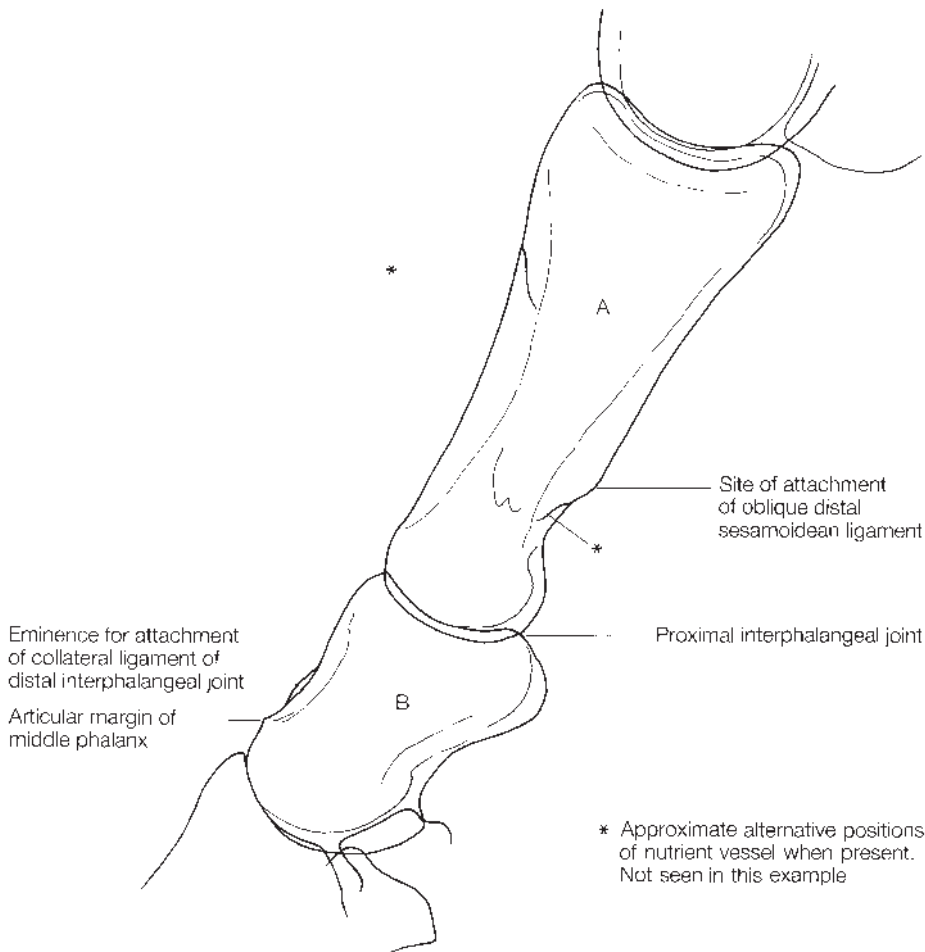
Figure 2.43(b) Diagram of a lateromedial radiograph of the proximal and middle phalanges of a normal adult horse. A = proximal phalanx, B = middle phalanx.

length of the bone from the distal end. This is the apex of the area of insertion of the oblique (middle) distal sesamoidean ligaments. The irregular bone may extend proximally in an oblique lateral and/or medial direction following the line of insertion of the ligaments, and is seen more readily on oblique radiographic views. This finding tends to be more prominent in older horses.

There may be a circular lucency or a slightly oblique radiolucent line in the centre of the middle or proximal phalanx on dorsopalmar and oblique views. This represents the normal nutrient foramen of the bone.

The middle phalanx is approximately half the length of the proximal phalanx. There are two prominent bony ridges, either side of the distal dorsal aspect of the bone, where the collateral ligaments of the distal interphalangeal joint originate. These are particularly obvious on slightly oblique views. The ligament insertions tend to be more prominent in large horses.

The articular surface of the distal end of the middle phalanx normally has a smooth curved outline, which extends dorsally into a point (see Figure 2.43). The central third of the articular surface may be relatively flatter than the more dorsal and palmar aspects. The articular surfaces of the proximal

Figure 2.44(a) Dorsopalmar view of the proximal and middle phalanges of a normal adult horse.

and middle phalanges in the proximal interphalangeal joint are otherwise reasonably congruous (see Figure 2.43).

NORMAL VARIATIONS AND INCIDENTAL FINDINGS

There is often new bone formation (entheseophytes) at the site of the ligament insertions on the distal dorsal aspect of the middle phalanx, and the palmar distal third of the proximal phalanx. This is of no long term

[88]

Opacity due to super-
imposition of ergot

A

Marrow cavity

Proximal interphalangeal
joint

Proximal nutrient foramen
(not seen in this horse)

B

Nutrient foramen

Extensor process of
distal phalanx

Site of attachment of
collateral ligament

Distal interphalangeal
joint
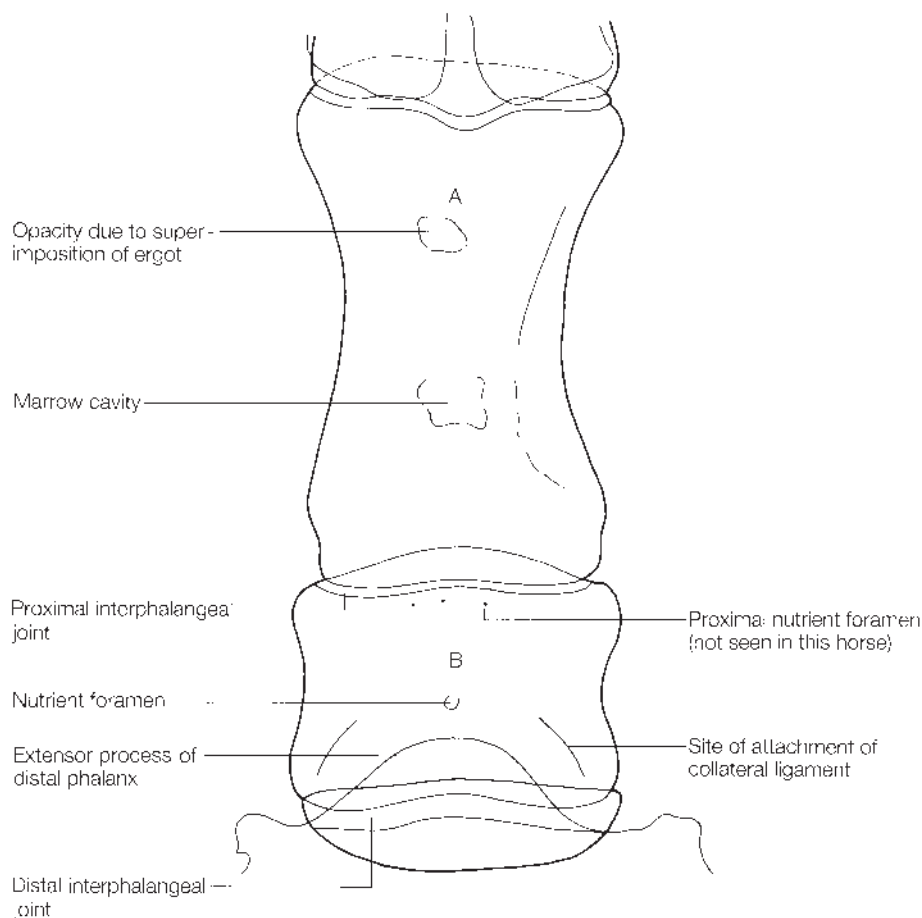
Figure 2.44(b) Diagram of a dorsopalmar radiograph of the proximal and middle phalanges of a normal adult horse. A = proximal phalanx, B = middle phalanx.

significance, but indicates that the ligaments have undergone acute or chronic trauma at some time prior to radiography. Entheseophytes should alert the clinician to a potential soft-tissue problem.

A small mineralized opacity may occasionally be present at the dorsal aspect of the proximal articular surface of the middle phalanx. Local anaesthesia may be required to assess its clinical significance.

Occasionally there are one or two small smoothly outlined, discrete opacities on the palmar proximal aspect of the proximal phalanx. These are present within the sesamoidean ligaments, and their origin is uncertain. They may represent fabellae, small chip fractures sustained early in life, or mineralization within the ligaments. Provided that they are smooth and opaque and do not involve the joint surface, they may be regarded as an incidental finding. They should not be confused with so-called Birkeland fractures (see page 120).

A small rounded osseous opacity is sometimes seen at the dorsoproximal aspect of the proximal phalanx. This may be unilateral or bilateral. If small (less than approximately 2 mm in diameter) and uniformly opaque, they may be an incidental finding (see Figure 2.72, page 125). They require selective anaesthesia to establish their significance.

[89]

On lateromedial radiographs, the distal end of the proximal phalanx may appear to be displaced dorsally relative to the proximal aspect of the middle phalanx. Although this can give the impression of subluxation, it has not been associated with any clinical abnormalities, and is most commonly seen in horses with upright conformation. The impression of subluxation of this joint may also be seen in radiographs obtained with the limb non-weight-bearing (see also 'Subluxation of the proximal interphalangeal joint').

Small periarticular osteophytes are frequently seen on the dorso-proximal aspect of the middle phalanx. Because this joint is relatively immobile, small changes may not have any clinical significance, but they cannot be differentiated from the early signs of degenerative joint disease and so should be viewed with suspicion (Figure 2.45).

A smoothly outlined spur may be present on the palmar aspect of the proximal end of the middle phalanx, pointing distally. The significance of this is uncertain, and it has been seen in lame and sound horses (Figure 2.46).

The position of the nutrient foramen is variable: in some horses it is seen on lateromedial views to enter dorsoproximally or palmarodistally.

It is important to be aware of the sites of attachment of tendons, ligaments and joint capsules (see Figures 2.47 and 2.48) in order to be able to interpret the significance of new bone formation at particular sites.

SIGNIFICANT FINDINGS

A number of the findings mentioned above as incidental may at some time have been significant. These include small discrete opacities close to the joint margins, small osteophytes (lipping) at the dorsal aspect of the proximal interphalangeal joint, and new bone formation (entheseophytes) at the attachments of ligaments (Figure 2.49, page 98). All of these findings probably result from trauma which occurred at least 3–6 weeks prior to radiography. An active osteophyte or entheseophyte may be less opaque than the parent bone, and have an irregular or 'fuzzy' outline. It is not possible to age smoothly outlined and uniformly opaque osteophytes or entheseophytes. These lesions may be regarded as an indicator of potential problems, but in chronic lameness should only be incriminated if they can be shown by other techniques to be causing lameness.

Subluxation of the proximal interphalangeal joint

Subluxation of the proximal interphalangeal joint occurs most commonly in hind limbs and may be unilateral or bilateral. It is generally seen in young horses (up to 5 years of age), but is occasionally seen in older horses. The horse may superficially appear normal at rest, although in some horses the contour of the proximal interphalangeal joint appears abnormal when viewed from the side. At the walk abnormal dorsal displacement of the distal end of the proximal phalanx may be apparent. At faster gaits usually no gait abnormality can be seen. Lateromedial radiographic views confirm slight

Figure 2.45 Lateromedial view of the pastern, showing a periarticular osteophyte on the dorsoproximal aspect of the middle phalanx.

Figure 2.46 Lateromedial view of the pastern showing a 'spur' on the palmaroproximal aspect of the middle phalanx. Note the pronounced bony ridge at the region of origin of the collateral ligaments on the dorsal aspect of the middle phalanx (arrow).

dorsal displacement of the distal aspect of the proximal phalanx (Figure 2.50, page 98). Secondary radiographic abnormalities are rarely seen. In some horses the condition resolves spontaneously.

Osseous cyst-like lesions

Single osseous cyst-like lesions occur in both middle and proximal phalanges, usually close to the proximal interphalangeal joint and sometimes respond to either conservative or surgical treatment.

Multiple small osseous cyst-like lesions may be associated with degenerative joint disease in the proximal interphalangeal joint, and warrant a poor prognosis. This has been described as juvenile degenerative joint

[91]
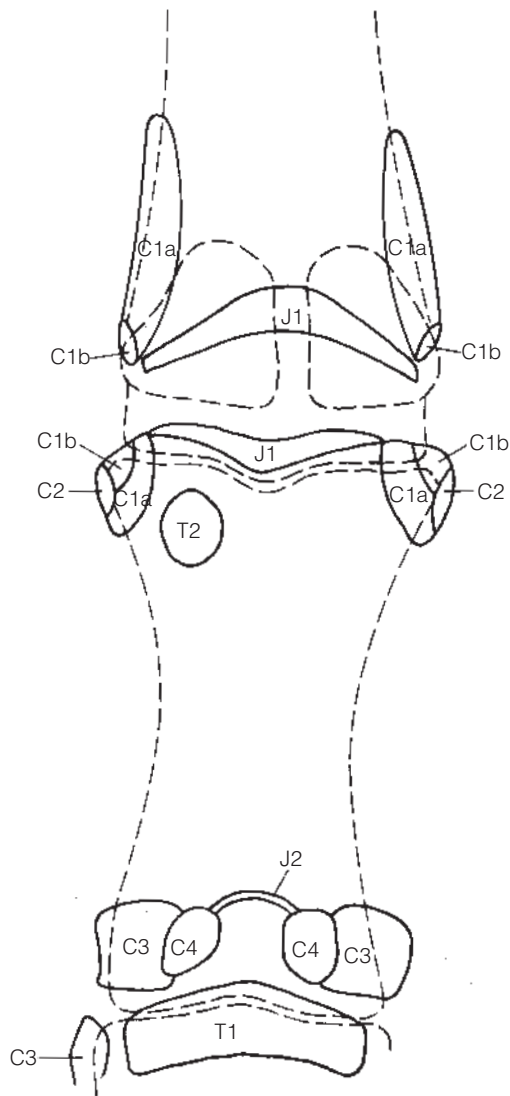
Figure 2.47(a) Diagram of a dorsal 15° proximal-palmarodistal oblique view of the fetlock and pastern regions, to illustrate the sites of attachment for those soft tissue structures attaching to surfaces seen from the dorsal aspect. Refer to Table 2.1. (Adapted figure courtesy of *Equine Vet. J.*)
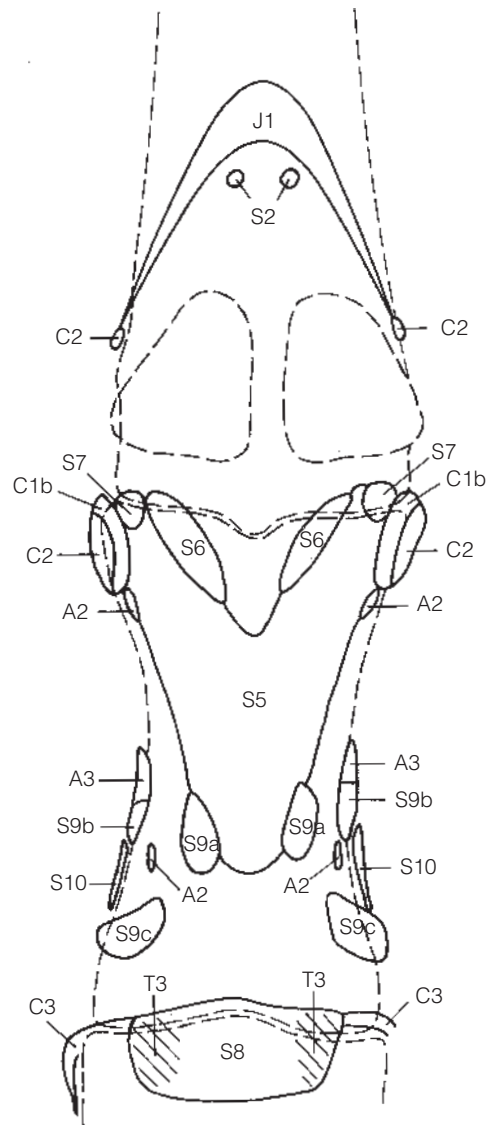
Figure 2.47(b) Diagram of a dorsal 15° proximal-palmarodistal oblique view of the fetlock and pastern regions, illustrating the site of soft tissue attachments seen from the palmar aspect. See Table 2.1. (Adapted figure courtesy of *Equine Vet. J.*)

disease following osteochondrosis in young horses. Despite the relative immobility of this joint, the prognosis is poor with or without surgical intervention.

Degenerative joint disease of the proximal interphalangeal joint

In early cases of degenerative joint disease of the proximal interphalangeal joint, there may be small osteophytes on the dorsoproximal aspect of the middle phalanx. These are evident on lateromedial and dorsolateral-palmaromedial and dorsomedial-palmarolateral oblique radiographs, and careful examination of the dorsopalmar view will often reveal other subtle

[92]
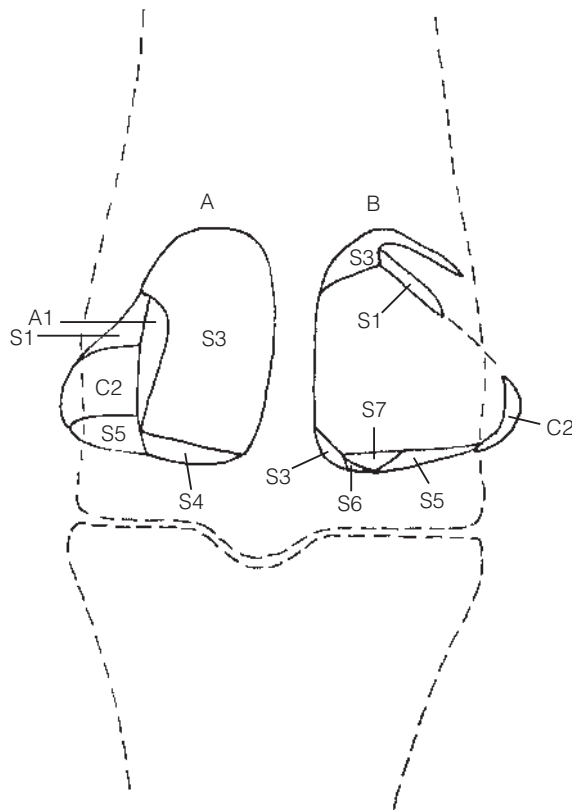
Figure 2.47(c) Diagram of a dorsal 15° proximal-palmarodistal oblique view of a fetlock joint illustrating the sites of attachment of soft tissue structures to the palmar (A) or dorsal (B) aspects of the proximal sesamoid bones. See Table 2.1. (Adapted figure courtesy of *Equine Vet. J.*)

changes at the joint margins. In some cases, osteophyte formation may be best evaluated in flexed oblique (dorsolateral-palmaromedial and dorsomedial-palmarolateral oblique) views (see page 31 and Figure 2.20, page 53). With more advanced disease there may be narrowing of the joint space, subchondral sclerosis and more extensive marginal osteophyte formation.

These latter changes are most easily seen on dorsopalmar radiographs (Figure 2.51, page 99). In advanced cases, there may be extensive new bone forming from the proximal aspect of the middle phalanx and the distal aspect of the proximal phalanx, attempting to bridge the proximal interphalangeal joint and create ankylosis.

Once radiographic changes are established the prognosis for spontaneous resolution of lameness and the response to intra-articular medication are poor. Surgical arthrodesis is an option, but the prognosis for this is guarded in competition horses.

New bone formation

The term ringbone is widely used to describe any new bone formed distal to the fetlock. It is an imprecise term, and should be avoided.

There are many causes of new bone formation in the pastern region.

Table 2.1 Legends for the soft tissue structures indicated in Figures 2.47 and 2.48

J1	Fetlock joint capsule
J2	Pastern joint capsule
C1a	Superficial part of the collateral ligaments of the metacarpophalangeal joint
C1b	Deep part of the collateral ligaments of the metacarpophalangeal joint
C2	Collateral sesamoidean ligaments of the proximal sesamoid bones
C3	Collateral ligaments of the proximal interphalangeal joint
C4	Collateral sesamoidean ligaments of the distal sesamoidean (navicular) bone
S1	Suspensory ligament
S2	Metacarpointersesamoidean ligament
S3	Intersesamoidean ligament; proximal scutum; palmar ligament of the metacarpophalangeal joint
S4	Straight sesamoidean ligament
S5	Oblique sesamoidean ligaments
S6	Cruciate sesamoidean ligaments
S7	Short sesamoidean ligaments
S8	Middle scutum
S9a	Axial palmar ligaments of the proximal interphalangeal joint
S9b	Superficial abaxial palmar ligaments of the proximal interphalangeal joint
S9c	Deep abaxial palmar ligaments of the proximal interphalangeal joint
S10	Ligaments to the cartilage of the distal phalanx
A1	Palmar annular ligament
A2	Proximal digital annular ligament
A3	Distal digital annular ligament
T1	Common digital extensor tendon
T2	Lateral digital extensor tendon
T3	Superficial digital flexor tendon

These include degenerative joint disease (see page 92), a sagittal fracture of the proximal or middle phalanx (see page 96), localized trauma, entheseophytes, localized infection, and hypertrophic osteopathy (see page 15).

New bone seen in localized areas on the diaphysis of the proximal and middle phalanges is probably due to periostitis as a result of trauma. This may be associated with lameness. The bone will normally remodel and the lameness resolve, unless the bone is forming in a position prone to repeated trauma, e.g. on the medial aspect of the limb where it is constantly struck by the contralateral limb (Figure 2.52, page 99).

Irregularly outlined pallisading new bone is sometimes seen on the dorsal diaphysis of the middle phalanx in a lateromedial view (Figure 2.53, page 100). This is generally associated with lameness relieved by intra-articular analgesia of the distal interphalangeal joint. The aetiology is unknown. The bone lies within the dorsoproximal out-pouching of the distal interphalangeal joint capsule and surgical debridement of this new bone may result in resolution of lameness. Occasionally smoothly outlined new bone is seen at the same site unassociated with clinical signs.

New bone unassociated with the interphalangeal joints may develop, encircling the phalanges. The aetiology is unknown. It is usually associated with chronic lameness.

New bone on the dorsoproximal aspect of the middle phalanx must be
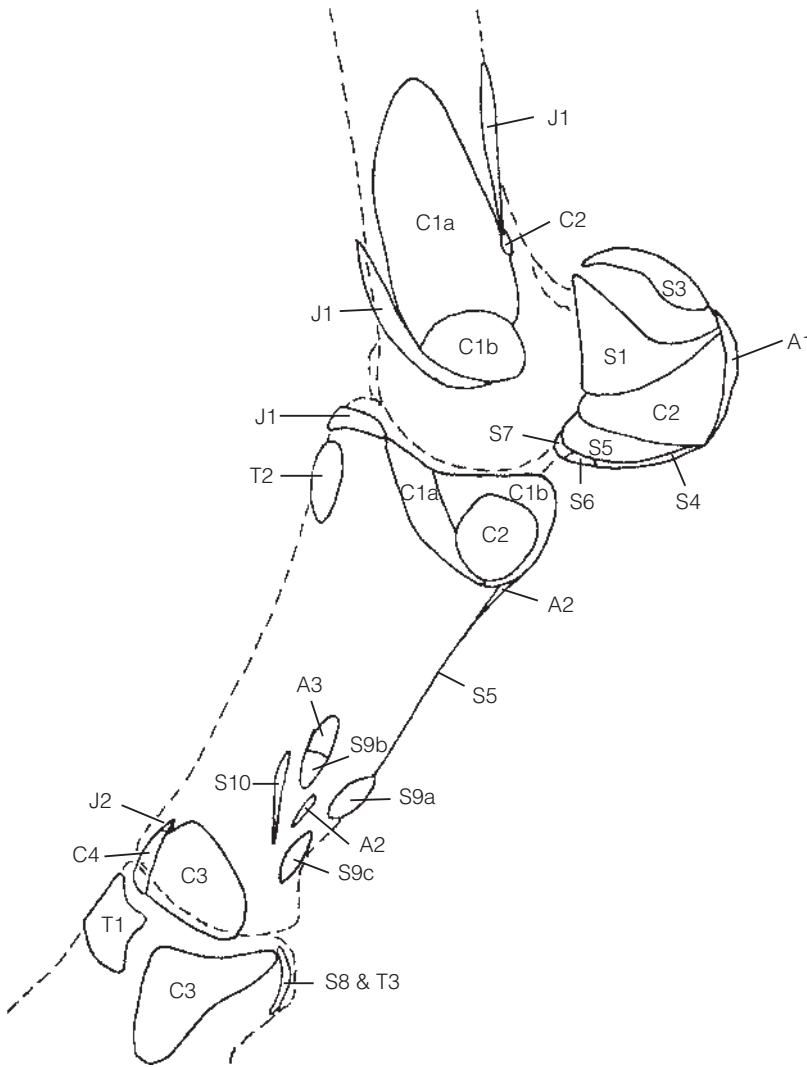
Figure 2.48(a) Diagram of a lateromedial view of the fetlock and pastern regions showing the sites of attachment of soft tissue structures. See Table 2.1. (Adapted figure courtesy of *Equine Vet. J.*)

differentiated from that associated with a partial or complete sagittal fracture of the middle phalanx (see page 96 and Figure 2.55, page 102).

There may be fairly extensive new bone on the dorsal aspect of the proximal phalanx and/or the proximal aspect of the middle phalanx, which does not extend to the joint margins. If there are no periarticular changes, this new bone is not synonymous with degenerative joint disease (see page 92), although it may be associated with lameness.

New bone (entheseophytes) is often seen at the region of insertion of the distal sesamoidean ligaments, probably due to chronic or acute stress on the ligaments (see Figure 2.49, page 98). This may cause lameness initially while actively forming, but is not of long-term significance. It should alert the clinician to the possibility of soft-tissue injury. Ultrasonography may be used to assess the ligaments.
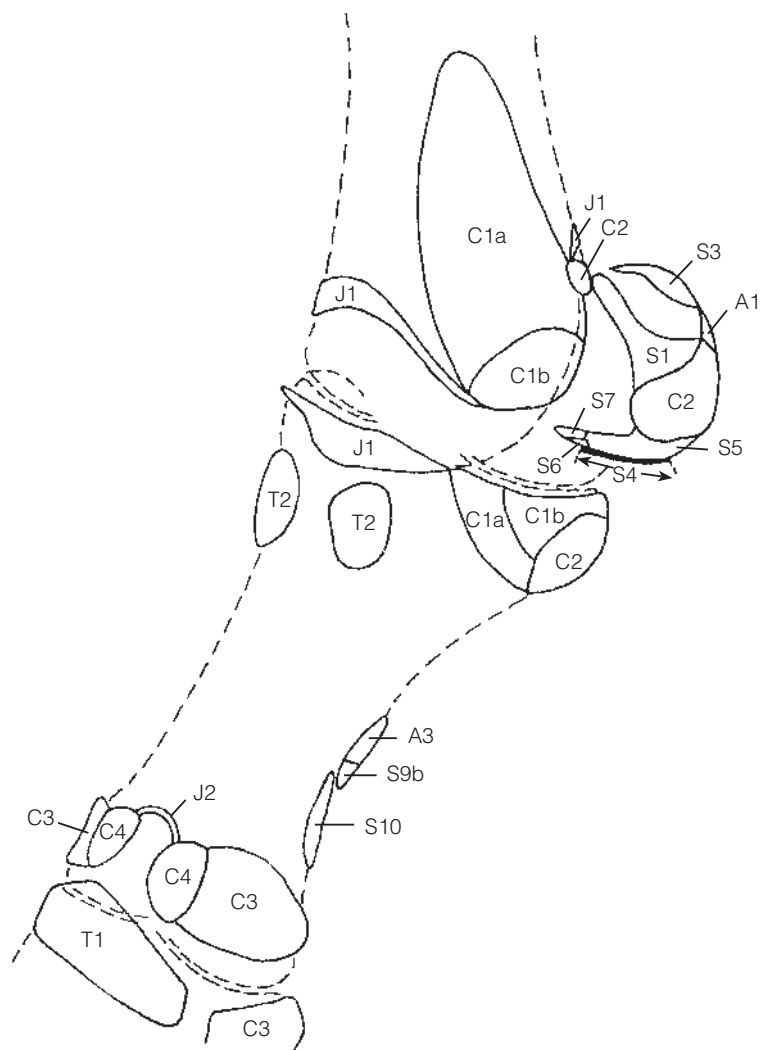
Figure 2.48(b) Diagram of an oblique view of the fetlock and pastern regions to illustrate soft-tissue attachments seen from the dorsomedial or dorsolateral aspects. See Table 2.1. (Adapted figure courtesy of *Equine Vet. J.*)

Fractures

Fractures of the proximal and middle phalanges are relatively common (see Figure 2.71, page 124). Small chip fractures of the proximal phalanx are described elsewhere (see page 124) and are of varying significance.

Midline sagittal fractures occur in both bones, but are more common in the proximal phalanx. They frequently follow a spiral course and are generally visualized as a double radiolucent line extending through the diaphysis of the bone. Each line represents cortical discontinuity (Figure 2.54, page 101). There are three principal types of midline sagittal fracture:

1 A fracture extending from the proximal to the distal joint, and entering both joints.

2 A fracture extending from either joint and exiting through the cortex.

3 An incomplete fracture extending from one of the two joints into the diaphysis of the bone (Figure 2.55a and b, page 102). These may only involve the dorsal cortex.

[96]
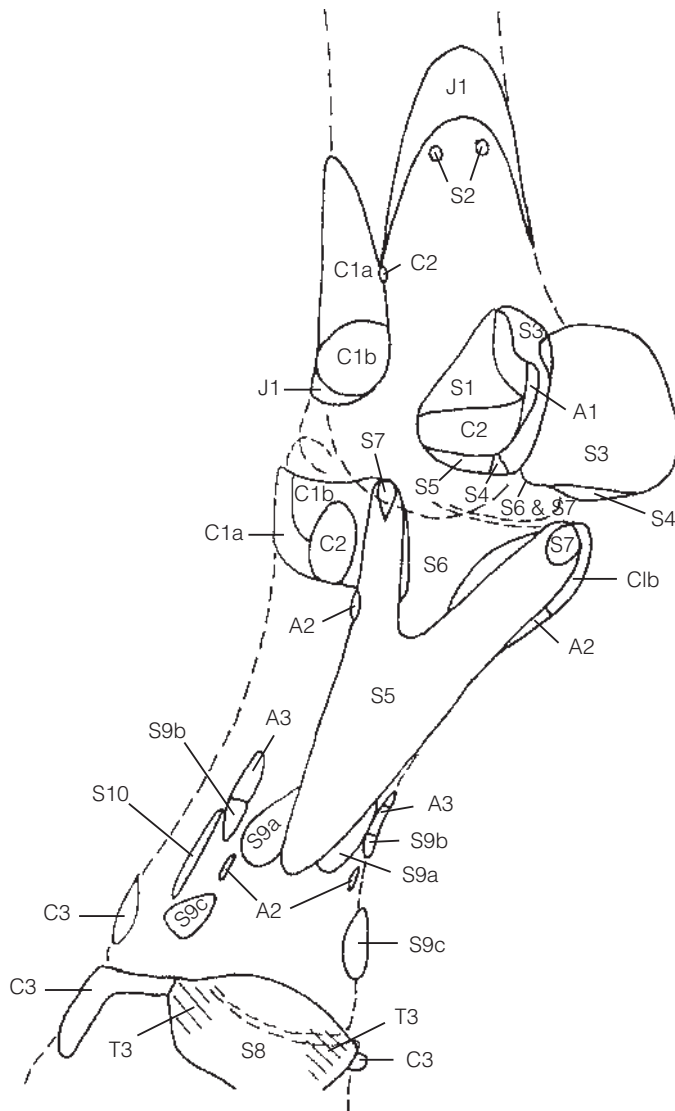
Figure 2.48(c) Diagram of an oblique view of the fetlock and pastern regions illustrating the site of soft-tissue attachments seen from the palmarolateral or palmaromedial aspects. See Table 2.1. (Adapted figure courtesy of *Equine Vet. J.*)

Initially there may be little or no displacement, and the fracture may be difficult to visualize. For this reason a series of oblique views should be obtained if there is any suspicion that such a fracture may be present. A series of oblique views may also be needed to determine the exact configuration of a fracture. Incomplete fractures may not be detected radiographically until callus forms as part of the normal healing process. This is seen as new bone on the dorsal aspect of the phalanx (Figures 2.55a and 2.55b, page 102) and may be detected on lateromedial radiographs. Reduced exposures are needed to demonstrate this poorly mineralized new bone. Non-displaced sagittal fractures may be accompanied by remarkably little lameness, and this has led to such cases being returned to work undiagnosed. The consequences of working such a case can be disastrous, and therefore suspected cases should be re-radiographed after 10 days, when rarefaction along the fracture line may be more obvious (nuclear scintigraphy may be useful for early diagnosis in these cases). Incomplete fractures have a good

Figure 2.49 Lateromedial view of the pastern (slightly oblique), showing entheseophyte formation on the palmar aspect of the proximal phalanx at the region of insertion of the distal sesamoidean ligaments.

Figure 2.50 Lateromedial view of the pastern and foot of a hind pastern of a 5 year old Arab, with a history of an audible click associated with the pastern of approximately 8 months' duration. The horse occasionally stumbled, but no lameness was detectable. The distal aspect of the proximal phalanx is positioned slightly dorsal relative to the middle phalanx, i.e. there is subluxation of the proximal interphalangeal joint.

[98]

Figure 2.51 Dorsopalmar view of the pastern, showing degenerative joint disease of the proximal interphalangeal joint. Note the narrowing of the medial aspect of the joint, and modelling of the articular margins. There is sclerosis of the proximal end of the middle phalanx, and mottled opacity of the distal end of the proximal phalanx, due to new bone on the dorsal aspect of the joint.
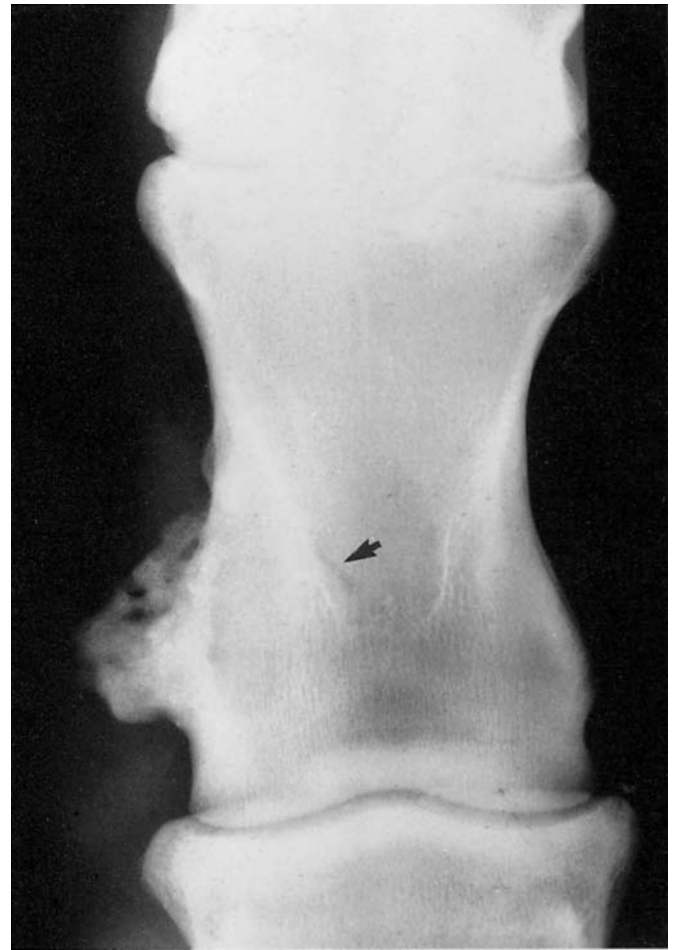
Figure 2.52 Dorsopalmar view of the pastern, showing new bone on the medial aspect of the proximal phalanx caused by repeated trauma (the oblique radiolucent line, arrowed, represents a nutrient vessel).

prognosis with conservative treatment, but repeat radiographs should be obtained to ensure healing does take place. Simple fractures of the proximal or middle phalanx respond well to internal fixation, but comminuted fractures are common and may be so extensive that any treatment is hopeless. Casting severely comminuted fractures will occasionally save an animal for breeding purposes.

Fractures of the dorsal and palmar/plantar aspects of the proximal end of the proximal phalanx occasionally occur. Dorsal 30° proximal 70° lateral-palmarodistomedial oblique and dorsal 30° proximal 70° medial-palmarodistolateral oblique views are helpful for visualization of such fractures (see page 104). These may occur as simple fractures or in combination with sagittal fractures. Palmar fractures frequently involve either the medial or lateral tuberosity of the proximal phalanx (Figure 2.56, page 103). It is possible for both tuberosities to fracture separately or for a complete fracture of the palmar/plantar aspect of the bone to occur. Fractures of the tuberosity

[99]

Figure 2.53 Lateromedial view of the middle and distal interphalangeal joints of an 8 year old horse, with lameness alleviated by intra-articular analgesia of the distal interphalangeal joint. There is pallisading new bone on the dorsal cortex of the diaphyseal region of the middle phalanx, within the distal interphalangeal joint capsule.

usually involve only a proximal fragment, but occasionally extend down the diaphysis. They may be articular or non-articular, and may require surgical fixation. Small fractures of the palmar or plantar articular margin occur on the axial aspect of the medial or lateral tuberosity, near the insertion of the cruciate sesamoidean ligaments. These are more common in hind limbs and have been referred to as Birkeland fractures. Surgical removal of these fractures may be indicated. Dorsal frontal fractures also occur, predominantly in hind limbs. They are often incomplete. Incomplete fractures have a good prognosis with conservative treatment, but complete fractures usually require surgical treatment. Articular fractures of the distal medial or distal lateral aspect of the middle phalanx, from the site of insertion of the collateral ligament of the distal interphalangeal joint, sometimes occur. Multiple flexed oblique views may be required to identify the fracture (Figure 2.57, page 104). Surgical removal usually results in a satisfactory outcome.

Dystrophic mineralization

Dystrophic mineralization occasionally occurs in the distal sesamoidean ligaments. Its significance is equivocal. Ultrasonography may be useful.

Metacarpophalangeal (fetlock) joint

RADIOGRAPHIC TECHNIQUE

Although this section refers to the metacarpophalangeal joint, it applies equally well to the metatarsophalangeal joint.

[100]

Figure 2.54 Dorsopalmar view of the pastern, showing a complete sagittal fracture of the proximal phalanx (note the double lucent line which represents the fracture through the dorsal and palmar cortices).

Equipment

Radiographs of the metacarpophalangeal joint are readily obtained with portable equipment and do not require the use of a grid. High-definition screens and compatible film are recommended when available.

Positioning

Dorsopalmar, lateromedial, dorsolateral-palmaromedial oblique and dorsomedial-palmarolateral oblique views

Standard views of the metacarpophalangeal joint are obtained with the horse weight-bearing, using a horizontal x-ray beam. The views should include a minimum of dorsopalmar (dorsoplantar), lateromedial and two 45° oblique views (D45°L-PaMO, D45°M-PaLO). Initial exposures should

(a)

(b)

Figure 2.55(a) Lateromedial view of the pastern, showing new bone on the dorsoproximal aspect of the proximal phalanx (arrow) secondary to an incomplete sagittal fracture of approximately 6 weeks' duration.

Figure 2.55(b) Dorsopalmar view of the pastern, showing an incomplete sagittal fracture of the proximal phalanx (arrow) of approximately 6 weeks' duration. Note that much of the fracture line is superimposed over the distal end of the third metacarpal bone. There is some sclerosis around the fracture in the proximal phalanx.

give good visualization of the trabecular pattern of the distal metacarpus, but may be reduced for evaluation of soft tissues, chip fractures or new bone. Although only four standard views need be obtained during a routine examination, dorsal 60° lateral-palmaromedial oblique and dorsal 60° medial-palmarolateral oblique may be necessary for better visualization of lesions on the dorsal joint margins. Superimposition of the proximal sesamoid bones over the metacarpophalangeal joint space can be avoided by angling the x-ray beam proximodistally at least 10° for the dorsopalmar view, and 15° for the dorsoplantar view. The precise angle depends on both the pastern foot axis and the position of the limb. The position of the limb (forelimb or hind limb) markedly influences the position of the proximal sesamoid bones relative to the third metacarpal or metatarsal bones and the proximal phalanx for all views. Ideally the fetlock should be extended, with the limb as far back as possible whilst weight bearing, in order to 'lift' the proximal sesamoid bones.

If there is some rotation of the distal limb, it can be difficult to achieve a true lateromedial projection. The position of the metacarpophalangeal joint relative to the foot should be assessed. Usually aligning the x-ray beam 5° palmar to a line tangential to the bulbs of the heel (i.e. L5° Pa-MDO)

Figure 2.56 Dorsomedial-palmarolateral oblique view of the metacarpophalangeal joint, showing a slightly displaced articular fracture of the medial palmar process of the proximal phalanx. There are some ill-defined opacities in the dorsal aspect of the joint.

will result in a true lateromedial view. It may help to palpate the relative positions of the medial and lateral epicondyles of the third metacarpal bone. This is particularly important in hind limbs, since many horses stand with the limb rotated toe outwards. A true lateromedial projection is required for proper assessment of the sagittal ridge of the third metacarpal bone, but slightly oblique views may sometimes be helpful for assessment of suspect lesions elsewhere in the joint.

Visualization of the proximal sesamoid bones is only partially achieved on the standard views described above. A dorsopalmar view taken at higher kilovoltage is required to visualize the axial surface of the bones. Further oblique views may also be required (see below).

Special oblique views

Standard D45°L-PaMO and D45°M-PaLO views highlight the lateral and medial proximal sesamoid bones respectively, allowing assessment of their shape, internal architecture and the apex, dorsal, palmar and distal borders. Additional information can also be obtained from a lateral 45° proximal-medial distal oblique view (L45°Pr-MDiO) (Figure 2.58a, page 105), to highlight the abaxial surface of the medial proximal sesamoid bone (Figure 2.58b, page 105) and a medial 45° proximal-lateral distal oblique view (M45°Pr-LDiO) to highlight the abaxial surface of the lateral proximal sesamoid bone.

Figure 2.57 Dorsal 45° medial-plantarolateral (flexed) oblique view of the foot and pastern of a horse with acute onset, severe lameness. There is an articular fracture (arrow) of the distal aspect of the lateral condyle of the middle phalanx. The shoe had not been removed for clinical reasons.

Evaluation of the proximal palmar (plantar) articular margins of the palmar (plantar) process of the proximal phalanx is sometimes best achieved using a dorsal 30° proximal 70° lateral-palmar distal medial oblique view (D30°Pr70°L-PaDiMO) (Figure 2.59a, page 106) or a dorsal 30° proximal 70° medial-palmar distal lateral oblique view (D30°Pr70°M-PaDiLO). This view is particularly useful for identification of palmar (plantar) fragments, and determining their source (see page 120). The D30°Pr70°L-PaDiMO view projects the lateral proximal sesamoid bone distal to the medial proximal sesamoid bone, and highlights the lateral plantar process of the proximal phalanx (Figure 2.59b, page 107).

Assessment of the lateral and medial palmar (plantar) condyles of the third metacarpal (metatarsal) bone may be facilitated by using a dorsal 45° proximal 45° lateral-palmar distal medial oblique view (D45°Pr45°L-

PaDiMO), to project the lateral condyle distal to the medial condyle (Figure 2.60, page 108). This view is particularly useful for identification of stress reactions (radiolucency or sclerosis) in the lateral condyle of the third metatarsal bone (see page 120).

Tangential dorsopalmar views

The articular surface of the distal metacarpus curves through 180°. On dorsopalmar views, only a limited part of the bone and joint tangential to the beam is clearly visualized. This means that when third metacarpal condylar

Figure 2.58(a) Technique to obtain lateral 45° proximal-medial distal oblique views to skyline the abaxial surface of the medial proximal sesamoid bone.

Figure 2.58(b) Lateral 45° proximal-medial distal oblique radiographic view and diagram of the metacarpophalangeal joint of a normal adult horse. A = third metacarpal bone, B = proximal phalanx, C = medial proximal sesamoid bone, D = lateral proximal sesamoid bone.
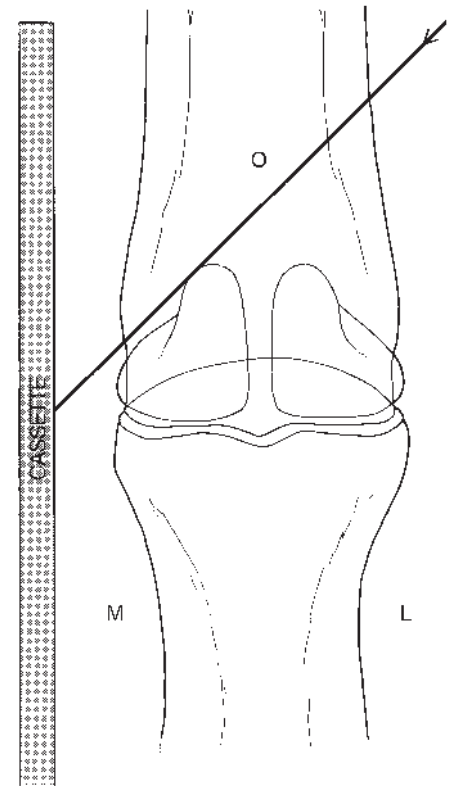
(a)
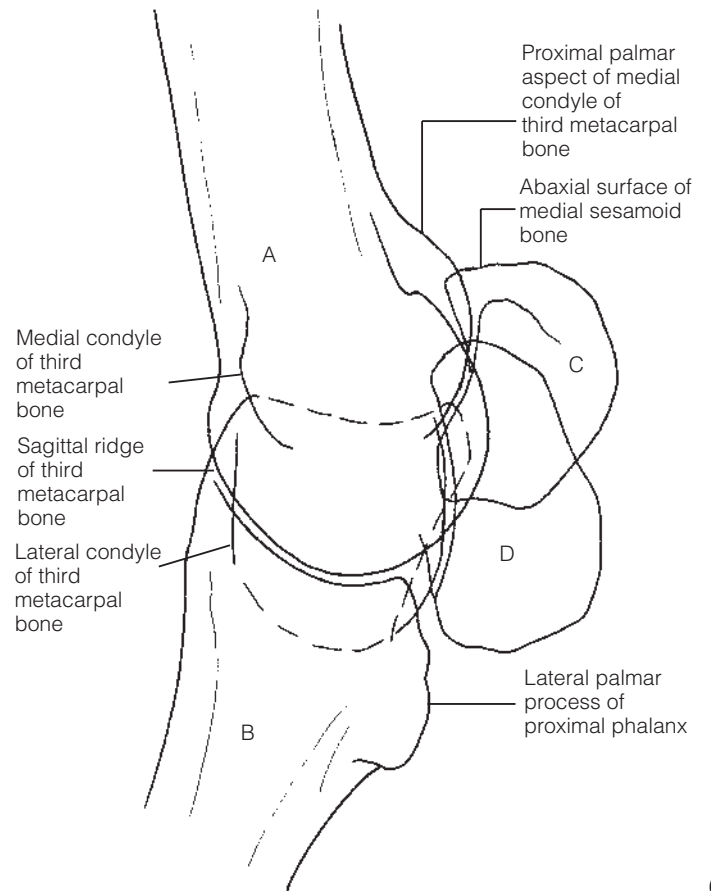
(b)
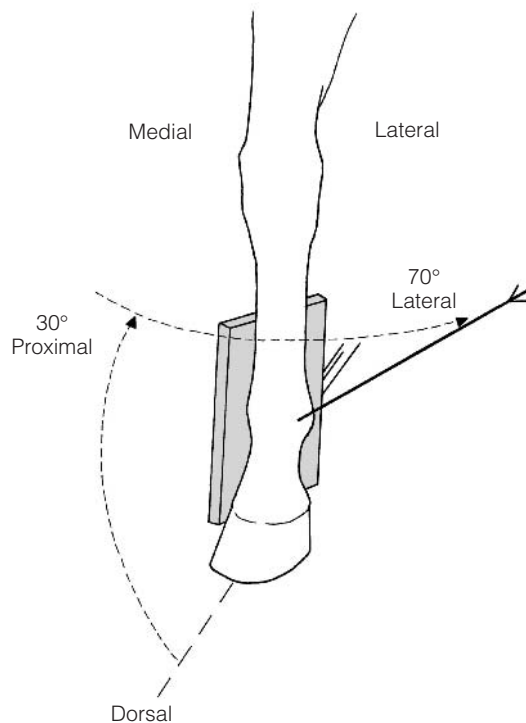
Figure 2.59(a) Positioning to obtain a dorsal 30° proximal 70° lateral-palmarodistal medial oblique view of the metacarpophalangeal joint, to highlight the lateral palmar process of the proximal phalanx.

fractures or osteochondral lesions are suspected, several dorsoproximal-palmarodistal or dorsodistal-palmaroproximal tangential views can be useful for determining the extent of such fractures and confirming possible comminution (Figure 2.61, page 108). Improved visualization may be achieved by flexing the metacarpophalangeal joint. The toe of the foot is placed in the standard navicular block (see page 66), with the dorsal hoof wall vertical. A horizontal x-ray beam is centred on the joint. The cassette is positioned as closely perpendicular to the x-ray beam as possible. This view moves the proximal sesamoid bones further proximally (Figure 3.1c, page 133), and is particularly useful when evaluating their axial margins.

The palmar articular surface may be assessed better with the limb partially extended, with the foot on a flat block (Figure 3.2, page 134). This technique has the disadvantage of resulting in magnification and geometric distortion. The cassette is positioned approximately vertically. The x-ray beam is directed distoproximally, in the plane of rotation of the metacarpophalangeal joint, at approximately 125° to the metacarpus. If the limb and x-ray beam are correctly aligned, between one-fourth and one-third of the proximal sesamoid bones are projected below the joint space (Figure 3.1d, page 133). This view is particularly important when evaluating a vertical condylar fracture; comminution of the palmar articular surface of the third metacarpal bone is usually only identifiable in this projection. It is also useful for detecting lucent lesions in the palmar aspect of the condyles of the third metacarpal bone (page 120).
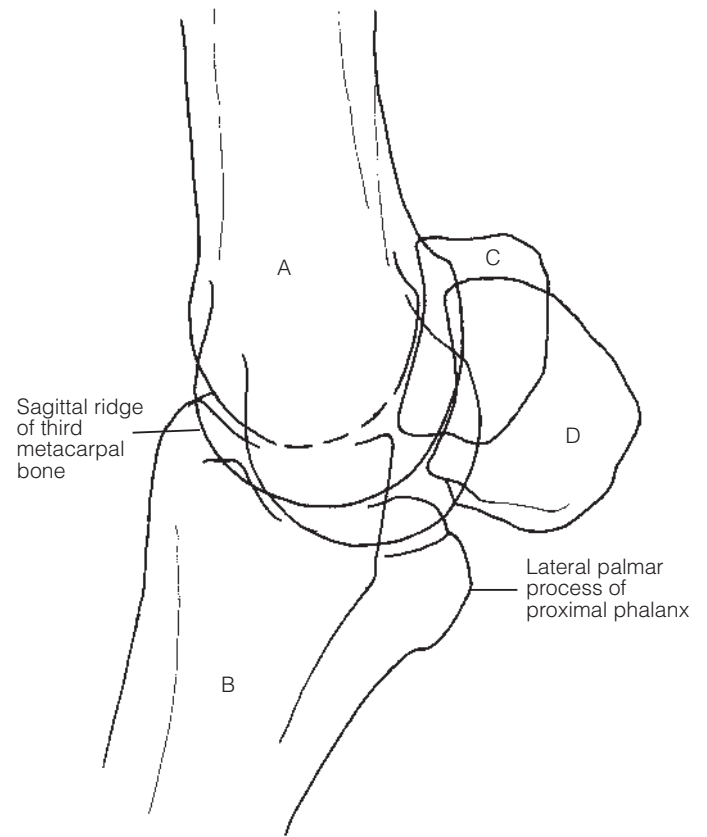
Figure 2.59(b) Dorsal 30° proximal 70° lateral-palmarodistal medial oblique radiographic view and diagram of the metacarpophalangeal joint of a normal adult horse. A = third metacarpal bone, B = proximal phalanx, C = medial proximal sesamoid bone, D = lateral proximal sesamoid bone.

Dorsoproximal-dorsodistal (flexed) view

The dorsoproximal-dorsodistal view of the metacarpophalangeal joint may be a useful view to visualize subtle lesions of the dorsal half of the distal articular surface of the third metacarpal bone. The horse is positioned with the metacarpophalangeal joint flexed and the metacarpus vertical. The cassette is placed distal to the joint and parallel to the floor. The x-ray tube is positioned dorsal to the limb, with the x-ray beam centred on the metacarpophalangeal joint, angled dorsal 45°–70° proximal-dorsodistal. A series of radiographs may be obtained at slightly different angles to visualize different areas of the joint (Figure 2.62, page 109).

Flexed lateromedial view

The flexed lateromedial view of the metacarpophalangeal joint will give better visualization of the articular surfaces of the proximal sesamoid bones and of the sagittal ridge of the third metacarpal bone. If slightly oblique, this view may aid in determining the extent of chip fractures of the sesamoids. These radiographs may be enhanced by reducing the mA s slightly from that
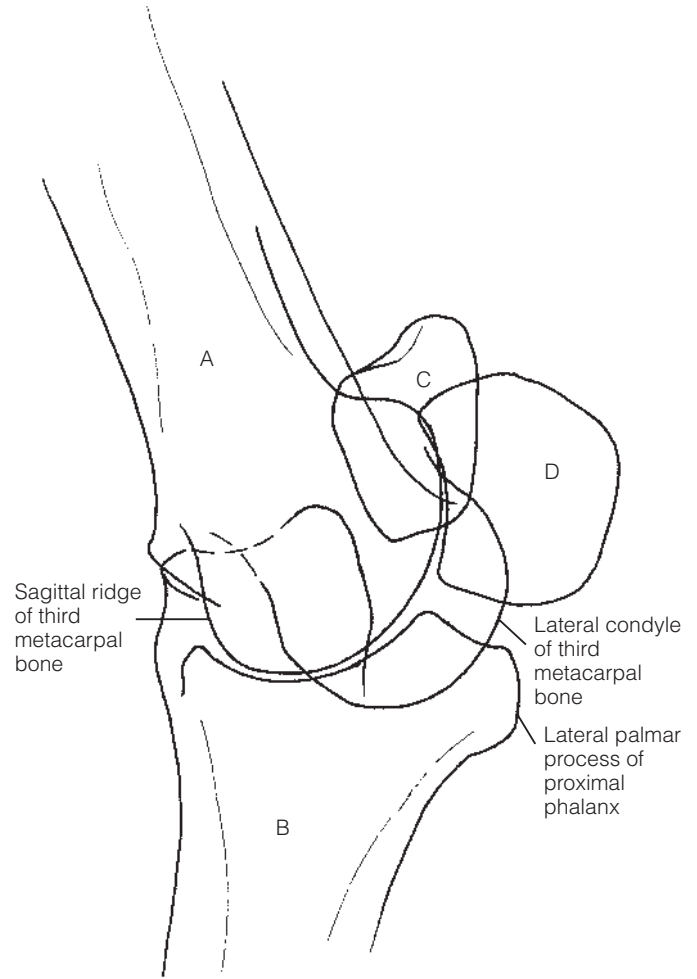
Figure 2.60 Dorsal 45° proximal 45° lateral-palmarodistal medial oblique radiographic view and diagram of the metacarpophalangeal joint of a normal adult horse. A = third metacarpal bone, B = proximal sesamoid bone, C = medial proximal sesamoid bone, D = lateral proximal sesamoid bone.
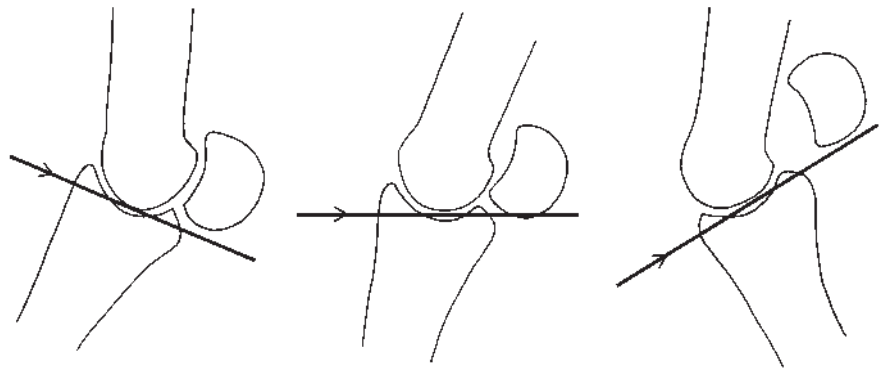
Figure 2.61 Technique to obtain flexed dorsoproximal-palmarodistal oblique and dorsodistal-palmaroproximal oblique views of the metacarpophalangeal joint. Note the different angles made by the x-ray beam to the long axis of the third metacarpal bone, in order to skyline different areas of the third metacarpal bone.

[108]

(b)

(a)
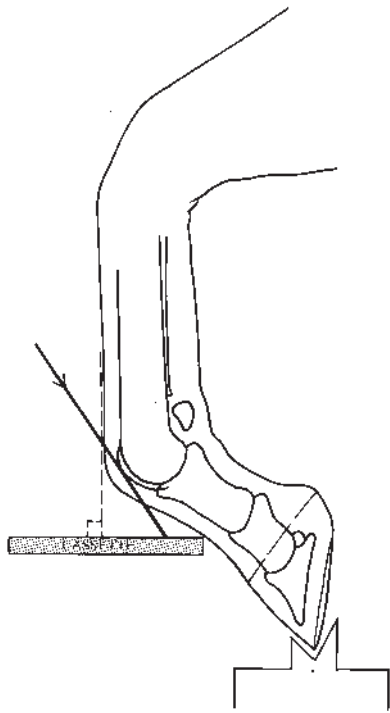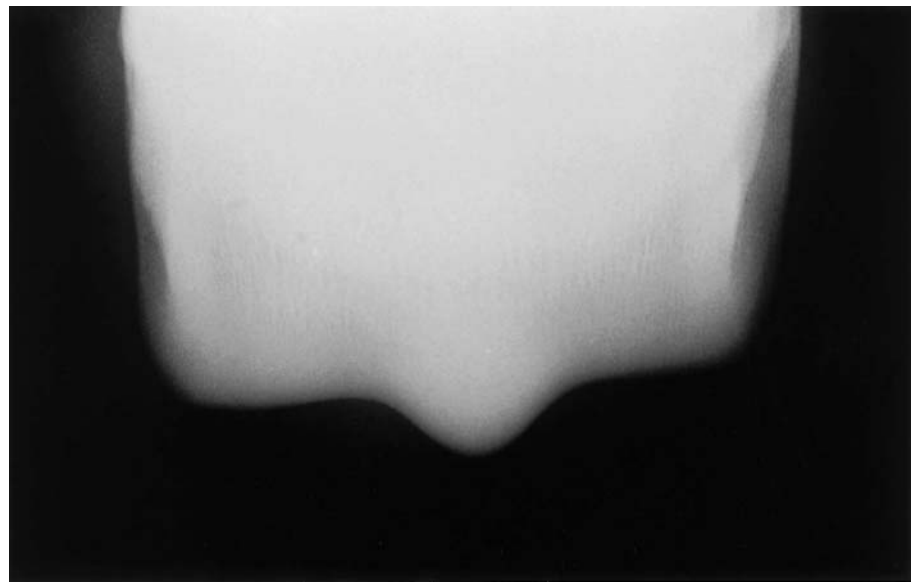
Figure 2.62(a) Positioning to obtain a dorsoproximal-dorsodistal (flexed) oblique view of the metacarpophalangeal joint, to highlight the dorsal aspect of the sagittal ridge of the third metacarpal bone.

Figure 2.62(b) Dorsoproximal-dorsodistal (flexed) oblique view of the metacarpophalangeal joint, to highlight the sagittal ridge and condyles of the third metacarpal bone.

normally required for the third metacarpus. The flexed lateromedial view is obtained by resting the horse's toe on a block, preferably 20–25 cm high, with the metacarpophalangeal joint flexed (or positioning the joint similarly, holding the limb at the toe). The x-ray beam is centred on the centre of the radius of curvature of the distal articular surface of the third metacarpal bone. The alignment of the beam may be difficult, as slight abnormalities in conformation will result in oblique views. It is most practical to take one view and realign the beam if necessary.

NORMAL ANATOMY

Immature horse

Prior to fusion of the distal physis of the third metacarpal/metatarsal bone at about 6–8 months of age, the distal metaphysis usually appears irregular (Figures 2.63a and 2.63b). The proximal physis of the proximal phalanx fuses at about 12 months of age.

Each proximal sesamoid bone usually ossifies from a single centre, which in the very young animal may have a slightly irregular margin. In a small percentage of foals there are two ossification centres, one for the proximal one-third and one for the distal two-thirds of the bone. This may occur in

[109]

Figure 2.63(a) Dorsopalmar view of the metacarpophalangeal joint of a normal foal 6 weeks of age.

Figure 2.63(b) Lateromedial view of the metacarpophalangeal joint of a normal foal 8 weeks of age. Note also the separate centre of ossification of the distal aspect of the fourth metacarpal bone.

one or several proximal sesamoid bones of the same foal. Fusion usually occurs by approximately 60 days of age. This should not be confused with a fracture of the sesamoid bone (see page 125). The cartilage precursor is fully ossified by about 3–4 months, although the bones may continue to enlarge until 18 months of age.

Skeletally mature horse

On a lateromedial view, the joint surface of the distal end of the third metacarpus describes a smooth curve, which flattens slightly on the palmarodistal aspect (Figure 2.63c). The third metacarpal bone articulates with the proximal phalanx and the proximal sesamoid bones. The distal metaphysis of the metacarpus may show some irregularity at the level of the fused physis (physeal scar).

On dorsopalmar radiographs, the metacarpophalangeal joint is approximately symmetrical about the prominent sagittal ridge of the distal metacarpus, although the medial condyle is slightly wider than the lateral. The sagittal ridge articulates with a groove in the proximal phalanx. The

[110]
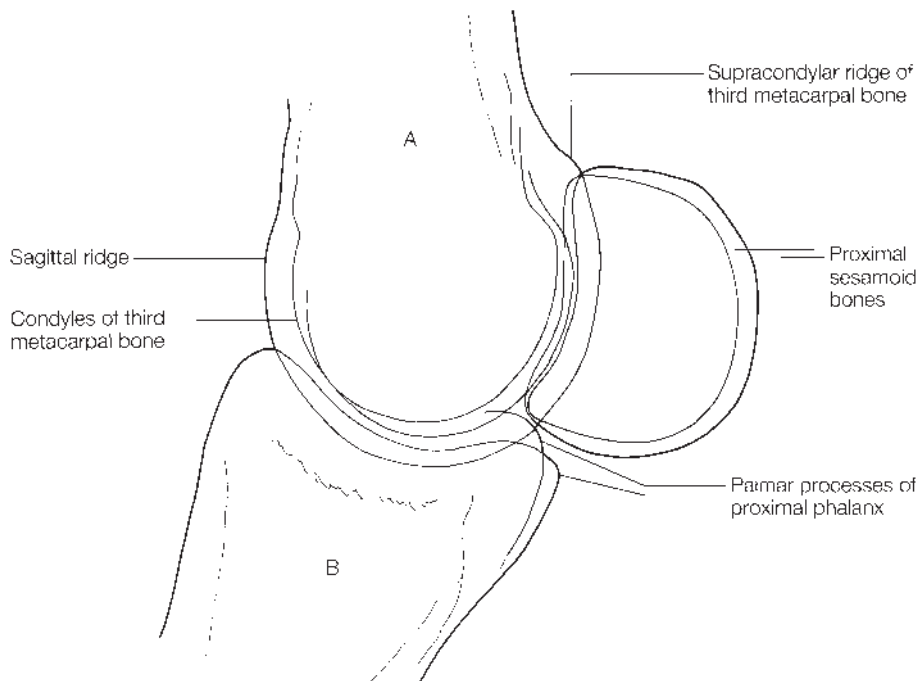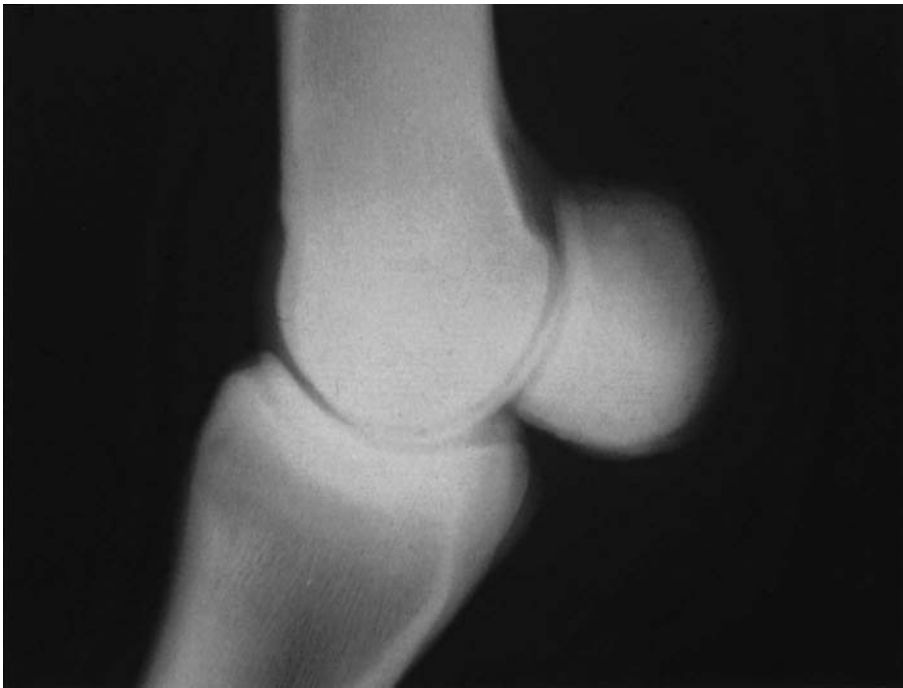
Figure 2.63(c) Radiograph and diagram of a lateromedial view of a normal adult metacarpophalangeal joint. Note that although this is a true lateromedial view of the dorsal aspect of the joint, there is some obliquity of the palmar aspect. A = third metacarpal bone, B = proximal phalanx.

joint space is approximately at right angles to the long axis of the third metacarpal bone (Figure 2.63d). Immediately proximal to the joint, the medial and lateral aspects of the third metacarpal bone have a smooth depression, above which the cortex appears slightly sclerotic.

The proximal subchondral bone plate of the proximal phalanx is best evaluated in a dorsopalmar projection. There is usually a clear demarcation between the subchondral bone plate and the underlying cancellous bone.

[111]
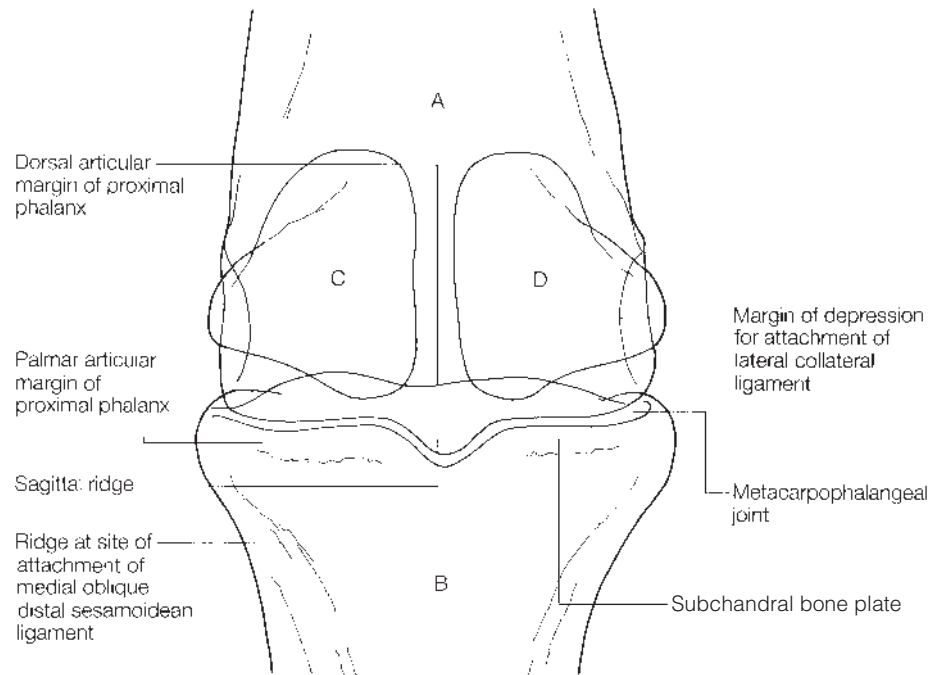
Figure 2.63(d) Radiograph and diagram of a dorsal 10° proximal-palmarodistal oblique view of a normal adult metacarpophalangeal joint. A = third metacarpal bone, B = proximal phalanx, C = medial proximal sesamoid bone, D = lateral proximal sesamoid bone.

The subchondral bone plate is of fairly uniform thickness, sometimes slightly thicker laterally than medially.

The proximal sesamoid bones are difficult to visualize clearly, as on most views they are superimposed over other bones. They are most clearly visualized on the dorsolateral-palmaromedial and dorsomedial-palmarolateral oblique views (Figure 2.63e). They normally have a smooth outline, rounded over their palmar aspects. The axial and abaxial surfaces may show some unevenness, being areas of ligament insertion, but should

[112]

Margin of depression for
attachment of medial
collateral ligament

Dorsal articular margins
of proximal phalanx

Medial condyle of the
third metacarpal bone

Medial palmar process
of proximal phalanx

Sagittal
ridge

Lateral palmar process
of proximal phalanx
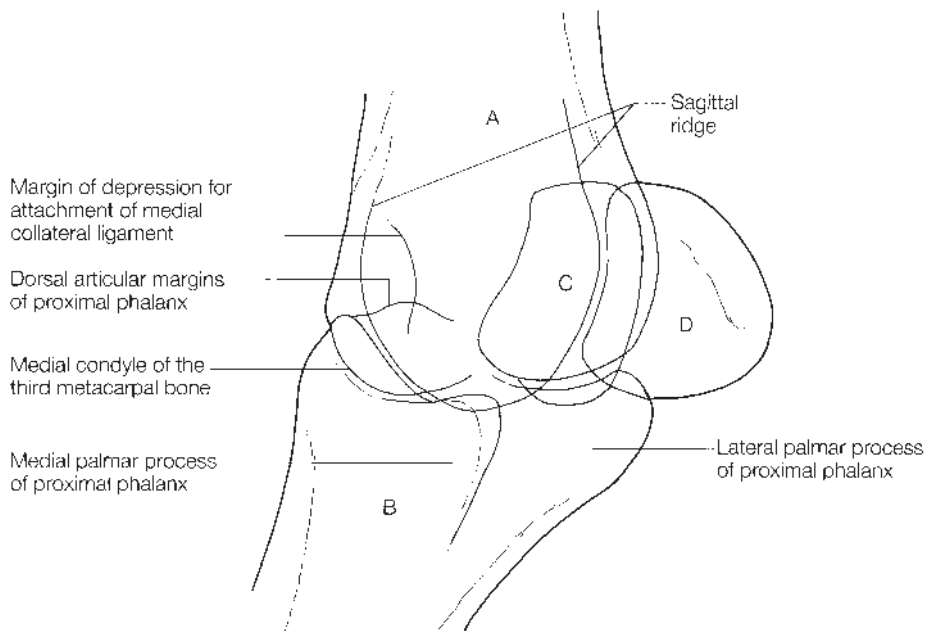
Figure 2.63(e) Radiograph and diagram
of a dorsolateral-palmaromedial oblique
view of a normal adult
metacarpophalangeal joint. A = third
metacarpal bone, B = proximal phalanx,
C = medial proximal sesamoid,
D = lateral proximal sesamoid.

not show marked roughening. There are faint radiating lucent lines within
the bones. On flexed lateromedial views, the sesamoid bones lift away from
the articular surface of the distal end of the third metacarpal bone (Figure
2.63f).

NORMAL VARIATIONS AND INCIDENTAL FINDINGS

Slight modelling of the dorsoproximal articular margins of the proximal
phalanx is a common incidental finding in older horses and is often unas-
sociated with detectable clinical signs, although it may reflect degenerative

[113]

Figure 2.63(f) Flexed lateromedial view of a normal adult metacarpophalangeal joint. Note how the proximal sesamoid bones lift away from the articular surface of the third metacarpal bone.

joint disease (see page 116). A small, smoothly rounded osseous opacity on the midline, on the dorsoproximal aspect of the proximal phalanx sometimes occurs in one or more fetlocks (see page 120). Small palmar or plantar osteochondral fragments and an ununited palmar or plantar process (see page 120) are not usually associated with clinical signs. Smoothly rounded osseous opacities are sometimes seen distal to one or both proximal sesamoid bones (Figure 2.64), presumably within the distal sesamoidean ligaments. They are usually asymptomatic and their aetiology is unknown.

An unusually long proximal sesamoid bone indicates previous fracture of the bone in the neonatal period (see page 125).

SIGNIFICANT FINDINGS

Soft-tissue swelling

Soft-tissue swelling in the fetlock region can be due to many causes and may be detected radiographically, either alone or with other radiographic abnormalities. The cause of swelling cannot usually be determined radiographically. The metacarpophalangeal joint is prone to soft-tissue injury, and although initial radiographs may show only soft-tissue swelling, radiographs obtained 3–6 weeks later may demonstrate new bone at the articular margins, at the points of attachment of the joint capsule and/or collateral ligaments. Entheseophytes and periarticular osteophytes may also develop on the proximal sesamoid bones. Accurate knowledge of the

Figure 2.64 Lateromedial view of a metacarpophalangeal joint of an adult horse. There are several small, smoothly rounded mineralized opacities distal to the proximal sesamoid bones, which are unlikely to be of clinical significance. Note that this is not a true lateromedial projection. The condyles of the third metacarpal bone are not superimposed, because the horse was not standing squarely on the limb.

anatomy of soft tissue attachments is essential for determination of the likely cause of entheseophyte formation (Figures 2.47 and 2.48, pages 92–7).

Synovitis is a common problem, visualized radiographically as a distension of the metacarpophalangeal joint capsule. This is most easily seen on the dorsal aspect of the joint on a lateromedial view. Chronic proliferative synovitis (villonodular hypertrophic synovitis) may be suspected if on lateromedial radiographs there is modelling of the dorsal distal aspect of the third metacarpal bone, associated with soft-tissue swelling. In the early stages a depression may be noted just proximal to the sagittal ridge. There may be new bone just proximal to the depression, as entheseophytes form at the capsular attachment (Figure 2.65a). In advanced cases an increased opacity may be evident dorsal to the depression, due to dystrophic mineralization or osseous metaplasia. These changes are most easily identified on a flexed lateromedial view. In most cases it is necessary to introduce positive contrast agent into the joint to outline the soft-tissue mass (Figure 2.65b, page 117). The lesion may also be confirmed ultrasonographically. Clinically there is enlargement of the dorsal pouch of the metacarpophalangeal joint. Treatment is by surgical removal of the mass, and adequate rest to allow the joint inflammation to resolve.

Soft-tissue swelling on the palmar proximal aspect of the metacarpophalangeal joint may be due to distension of the digital flexor tendon sheath. On lateromedial views a depression in the palmar contour of this swelling may indicate functional constriction by the palmar annular ligament (Figure 2.66, page 118). Occasionally mineralization in the sheath or

[115]

Figure 2.65(a) Chronic proliferative synovitis. Lateromedial view of the metacarpophalangeal joint, showing radiographic changes associated with chronic proliferative synovitis. There is a depression proximal to the sagittal ridge of the third metacarpal bone (large arrow). Proximal to this is periosteal new bone at the site of the capsular attachment (small arrow). This modelling of the dorsal distal aspect of the third metacarpal bone usually relates to chronic proliferative synovitis.

the digital flexor tendon is seen, or abnormalities of the proximal sesamoid bones. Distension of the digital flexor tendon sheath and the metacarpophalangeal joint capsule may be seen in association with infectious osteitis of a proximal sesamoid bone (see page 123). Swelling may arise after trauma to the region, and results in lameness, which may resolve with prolonged rest, or may require surgical treatment. The prognosis depends on the underlying pathology. Ultrasonographic examination may give additional information about the associated soft-tissue structures.

Degenerative joint disease

On lateromedial and/or oblique views, modelling of the proximodorsal aspect of the proximal phalanx may involve the articular margins, and may indicate early degenerative joint disease (Figure 2.67a, page 119). The proximal dorsal attachments of the joint capsule are close to the proximal end of the sagittal ridge, and entheseophyte formation at this point may result from joint trauma or chronic joint capsule distension. This is not synonymous with degenerative joint disease, but may be seen in association with it.

On dorsopalmar views, osteophytes may be seen at the articular margins on the medial or lateral aspects of the proximal phalanx, and indicate

Figure 2.65(b) Chronic proliferative synovitis. Lateromedial view of the metacarpophalangeal joint, with contrast medium in the joint (slightly oblique view). Note the filling defect (arrows) in the dorsal pouch of the joint.

degenerative joint disease. Entheseophytes at the insertion of the joint capsule develop slightly distal to a periarticular osteophyte, and indicate strain or tension of the capsular attachment. It is often difficult to differentiate these two types of osteophytes at this location, and careful clinical assessment of their significance is required.

In advanced degenerative joint disease, periarticular osteophytes on the proximal and distal margins of the proximal sesamoid bones may be seen. Associated with this, there may be a depression in the distal palmar aspect of the third metacarpal bone, proximal to the condyles. This so-called 'supracondylar lysis' is associated with fibrous proliferation of the synovial membrane in this region (Figure 2.67b, page 119). Positive contrast studies may demonstrate a filling defect in this area.

The joint space is best assessed on a dorsopalmar view. Narrowing of the joint space, particularly unilateral narrowing (usually of the medial side), may be significant. It is important, however, that this is assessed on weight-bearing views, with the horse standing evenly on all four feet, since the joint can open on either side if unevenly loaded. The relatively opaque subchondral bone should be of even thickness. Change in thickness or opacity of this bone has been associated with degenerative joint disease.

There may be thickening of the subchondral bone plate of the proximal
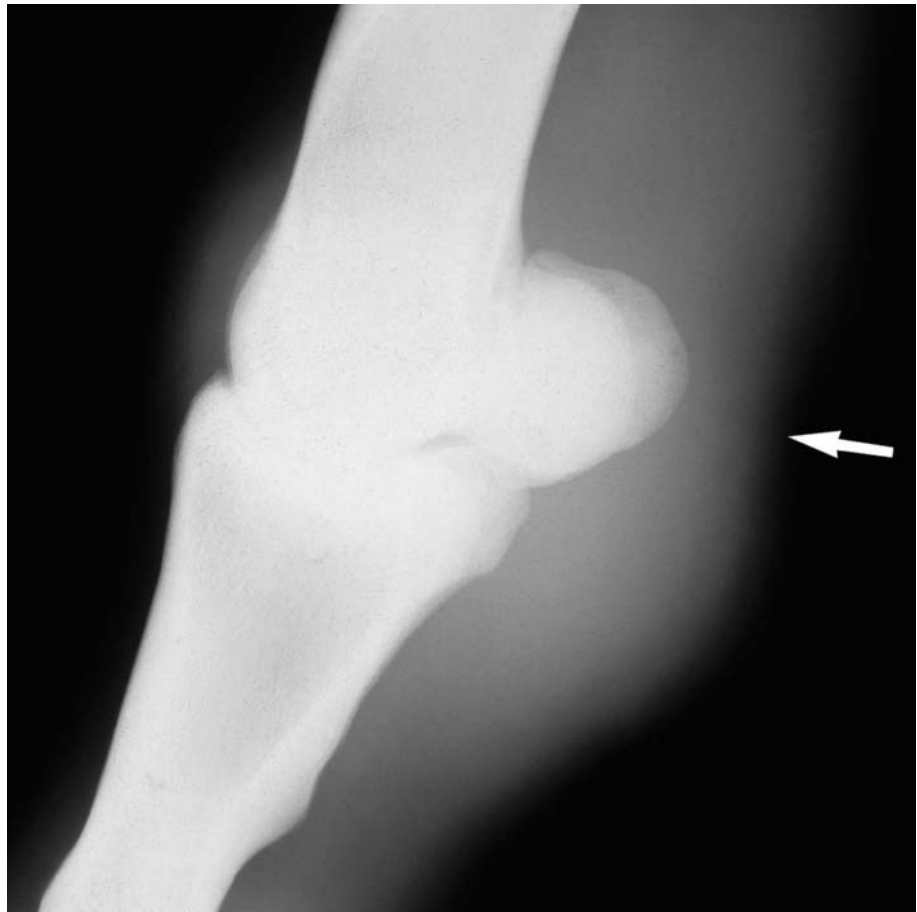
Figure 2.66 Palmar annular ligament constriction. Lateromedial view of the metacarpophalangeal joint. There is a depression in the outline of the palmar soft tissues (arrow) at the site of the constriction.

phalanx, medially and/or laterally, with decreased demarcation between it and the underlying cancellous bone.

Osteochondrosis, osteochondral fragments and stress reactions

The aetiology of some changes in the metacarpophalangeal and metatarsophalangeal joints still remains open to debate, although recent publications are helping to clarify the findings. Some abnormalities formerly thought to be due to osteochondrosis may be traumatic in origin. There appear to be breed differences in the incidence of these abnormalities, and their clinical significance is not always easy to determine. Included in this group are fragments arising from the dorsal sagittal ridge of the third metacarpal (metatarsal) bone, fragments on the dorsoproximal aspect of the proximal phalanx, palmar or plantar osteochondral fragments, an ununited palmar or plantar eminence of the proximal phalanx and flattening of the palmar or plantar condyle of the third metacarpal or metatarsal bone.

Osteochondrosis of the sagittal ridge may be seen anywhere on the ridge, but is most often seen dorsally on the proximal third. This lesion is seen early as flattening of the ridge. Later it may appear as an osteochondral fracture. This is best seen on a flexed lateromedial view, and may involve all four fetlocks. Prognosis is favourable with surgical management.

[118]

Figure 2.67(a) Degenerative joint disease. Dorsolateral-palmaromedial oblique view of the metacarpophalangeal joint, showing early changes associated with degenerative joint disease. There is modelling of the dorsomedial aspect of the proximal phalanx (arrow).
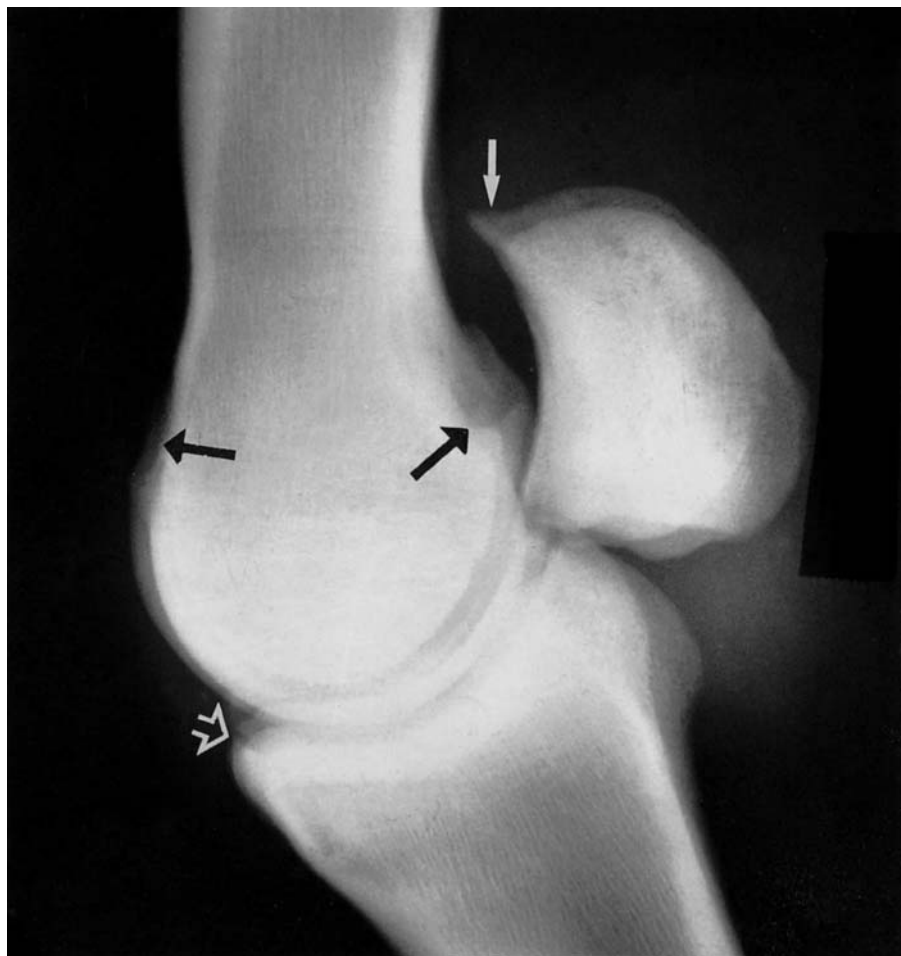
Figure 2.67(b) Degenerative joint disease. Flexed lateromedial view of the metacarpophalangeal joint, showing advanced changes associated with degenerative joint disease. There is modelling of the articular margins of the proximal sesamoid bones (white arrow), the dorsal aspect of the proximal phalanx (open white arrow), and the dorsal and palmar distal aspects of the third metacarpal bone proximal to the sagittal ridge (black arrows).

Small, well rounded fragments on the midline on the dorsoproximal aspect of the proximal phalanx (Figure 2.72, page 125), readily identifiable on a lateromedial projection, are a common radiographic finding, frequently not associated with clinical signs. They may be present in one or several fetlocks. Their aetiology is unknown but they may result from separate centres of ossification or possibly be a manifestation of osteochondrosis. Occasionally they are associated with synovial effusion and lameness, in which case surgical removal is indicated. A good prognosis is usually warranted.

Osteochondrosis involving the palmar (plantar) aspect of the condyles of the third metacarpal (metatarsal) bones usually occurs slightly palmar (plantar) to the transverse ridge. Initially the radiographic changes are flattening and sclerosis of the subchondral bone in the affected area. This may be followed by resorptive changes, resulting in focal radiolucent areas of variable shape. Although this lesion has formerly been classified as osteochondrosis, it now seems probable that it is a traumatic lesion, only seen in athletic horses. Care must be taken with interpretation, as the subchondral bone in this area is normally slightly flatter than the remainder of the condyle. Flattening of the condyle, or a triangular shaped sclerotic area in the subchondral bone, is best visualized on a lateromedial or flexed lateromedial view, or the dorsal 45° proximal 45° lateral-palmar distal medial oblique view. Nuclear scintigraphy is more sensitive for detection of early and less severe reactions. These lesions may occur bilaterally, especially in the hind limbs of Thoroughbreds and Standardbreds, causing a variable degree of lameness or loss of performance.

Palmar or plantar osteochondral fragments (Figure 2.68a) are usually seen medially or laterally (or biaxially) at the site of attachment of the short distal sesamoidean ligaments, and occur most commonly in hind limbs. They have also been referred to as Birkeland fractures. They are best identified in D30°Pr70°L-PaDiMO or D30°Pr70°M-PaDiLO views. Medial fragments are most common. These are believed to represent avulsion fractures, sustained as a foal, and are frequently asymptomatic, although they may compromise performance at high speed.

An ununited palmar or plantar process of the proximal phalanx (Figure 2.68b) usually occurs laterally, either alone, or in association with a palmar or plantar osteochondral fragment. It occurs most commonly in hind limbs, and may be articular or non-articular. It probably represents an avulsion fracture of the cruciate distal sesamoidean ligament, sustained as a foal. They are frequently asymptomatic.

Physitis

Physitis (epiphysitis) of the distal physis of the metacarpal bone occurs predominantly in rapidly growing foals. Radiographically the physis is widened and irregular in thickness, frequently with new bone (lipping) at its margins. On dorsopalmar views an angular limb deformity may be evident. The usual clinical history is of a limb deviation developing distal to the metacarpophalangeal joint. Treatment of this condition must be radical and rapid, because of the early closure of the distal physis. Usually restriction of

Figure 2.68(a) Dorsal 30° proximal 70° medial-plantarodistal oblique view of a metatarsophalangeal joint of an eight year old Danish Warmblood. There is a non-articular osteochondral fragment from the proximoplantar aspect of the medial plantar process of the proximal phalanx.

Figure 2.68(b) Dorsolateral-plantaromedial oblique view of a metatarsophalangeal joint of a 7 year old Thoroughbred. There are two smoothly rounded osseous opacities in close apposition to the plantar aspect of the lateral plantar process of the proximal phalanx. Each has a trabecular pattern. This is an ununited lateral plantar process of the proximal phalanx.

diet and exercise, coupled with corrective trimming of the foot, will be sufficient. In some cases, periosteal elevation or transphyseal bridging will be needed.

Osseous cyst-like lesions

Osseous cyst-like lesions occur near the metacarpophalangeal joint, most commonly in the third metacarpal bone. Visualization of these may require a dorsoproximal-palmarodistal angulation of the x-ray beam. Lesions often start as focal flattening of the subchondral bone, and develop through an elliptical lucent area, to an oval shaped lucency, with progressive development of surrounding sclerosis. Conservative and surgical treatments warrant a guarded prognosis.

Sesamoiditis

Sesamoiditis is a widely used term which encompasses lucent areas within the bones and new bone production. Radiographic abnormalities are best assessed in D45°M-PaLO and D45°L-PaMO views. The radiographic

appearance is variable, ranging from a number of radiolucent areas along the palmar aspect of the bones, with minimal new bone formation, to extensive new bone on the axial and abaxial surfaces, with an apparently normal internal structure to the bone. There is often poor correlation between radiological abnormalities and clinical signs.

The lucent areas are sometimes referred to as vascular channels (Figure 2.69), although the pathology is open to dispute. The number of sharply demarcated vascular channels in a normal horse may vary according to breed and work history. Wide or abnormally shaped lucent areas are likely to be associated with lameness. The greater the number of vascular channels, the more likely there is to be associated lameness. The new bone on the abaxial and distal surfaces of the bone is often associated with strain of the suspensory ligament, and distal sesamoidean ligaments. The lucent zones adjacent to the vascular channels, but outside the normal bone, are areas of fibrous tissue around nutrient vessels. The fibrous tissue resists encroachment of entheseophytes and gives a radiographic appearance of enlarged vascular channels.

In a young horse (less than 3 years) where lucent lesions are the predominant radiographic abnormality, a fair prognosis can be given if the horse receives adequate rest (although the radiographic lesions will persist). The prognosis may be more guarded when these lesions develop in older horses. Radiating lucent zones may also be seen in association with desmitis of a suspensory ligament branch.

In horses where new bone formation is the predominant radiological finding, there has probably been an associated soft-tissue injury. Ultrasonographic examination of the suspensory apparatus and palmar (plantar)

Figure 2.69 Sesamoiditis. Dorsolateral-palmaromedial oblique view of the metacarpophalangeal joint, showing the lateral proximal sesamoid bone. There are large radiating lucent zones and a slightly irregular outline of the palmar margin of the bone.

annular ligament in these cases may be useful. The prognosis depends on the amount of new bone formed and the extent of the accompanying soft-tissue injuries.

Periarticular osteophytes seen on the articular margins of the sesamoid bones are an indication of degenerative joint disease. This may be better visualized on a flexed lateromedial view (see 'Degenerative joint disease', page 116).

Lucent zones restricted to the axial aspect of the proximal sesamoid bones are easily overlooked, unless a dorsopalmar radiographic view is overexposed. For accurate evaluation of the axial margins of the proximal sesamoid bones a flexed dorsopalmar view is extremely useful. Lucent lesions on the axial aspect of the proximal sesamoid bones (Figure 2.70) have been associated with infectious osteitis in horses which have presented with severe lameness, often with distension of the digital flexor tendon sheath. The prognosis is guarded. An irregular axial margin of the proximal sesamoid bones has also been seen in association with desmitis of the inter-sesamoidean ligament. Ultrasonographic examination is indicated. The prognosis is guarded.

Luxation

Luxation of the metacarpophalangeal joint can occur in lateromedial or dorsopalmar directions. The injury may be obvious radiographically, but it may be necessary to obtain radiographs with the distal limb under stress (see

Figure 2.70 Dorsoplantar (flexed) view of a metatarsophalangeal joint of a 3 year old Thoroughbred with sudden onset of severe lameness 6 weeks previously, associated with diffuse swelling on the plantar aspects of the fetlock and pastern. There is an indistinct axial margin with underlying ill-defined lucent zones, involving the proximal half of the medial and lateral proximal sesamoid bones (arrows). This is the result of infection.

Figures 1.11a and 1.11b, page 22). The radiographs must be carefully examined for concurrent fractures. The prognosis for return to athletic function is very grave, but a hopeful prognosis may be given for breeding after casting the limb.

Fractures

The common fracture sites of the phalanges and metacarpophalangeal joint are shown in Figure 2.71. Small radiopaque bodies at the joint margins may be an incidental finding (Figure 2.72 and page 114).

Spurlock and Gabel (1983)

Henninger *et al.* (1991)
Ellis (1979)

McClure *et al.* (1998)

Barclay *et al.* (1985)

Martin (1991)

Sandgren (1993)
Whitton and Kannegeiter (1994)
Fortier *et al.* (1995)

Yovich and McIlwraith (1986)

Markel *et al.* (1985a)

Ellis *et al.* (1987)
Markel and Richardson (1985)

Bukowiecki *et al.* (1986)
Grøndahl (1992)

Markel *et al.* (1985b)

Holcombe *et al.* (1995)
Ellis *et al.* (1987)

Doran *et al.* (1987)
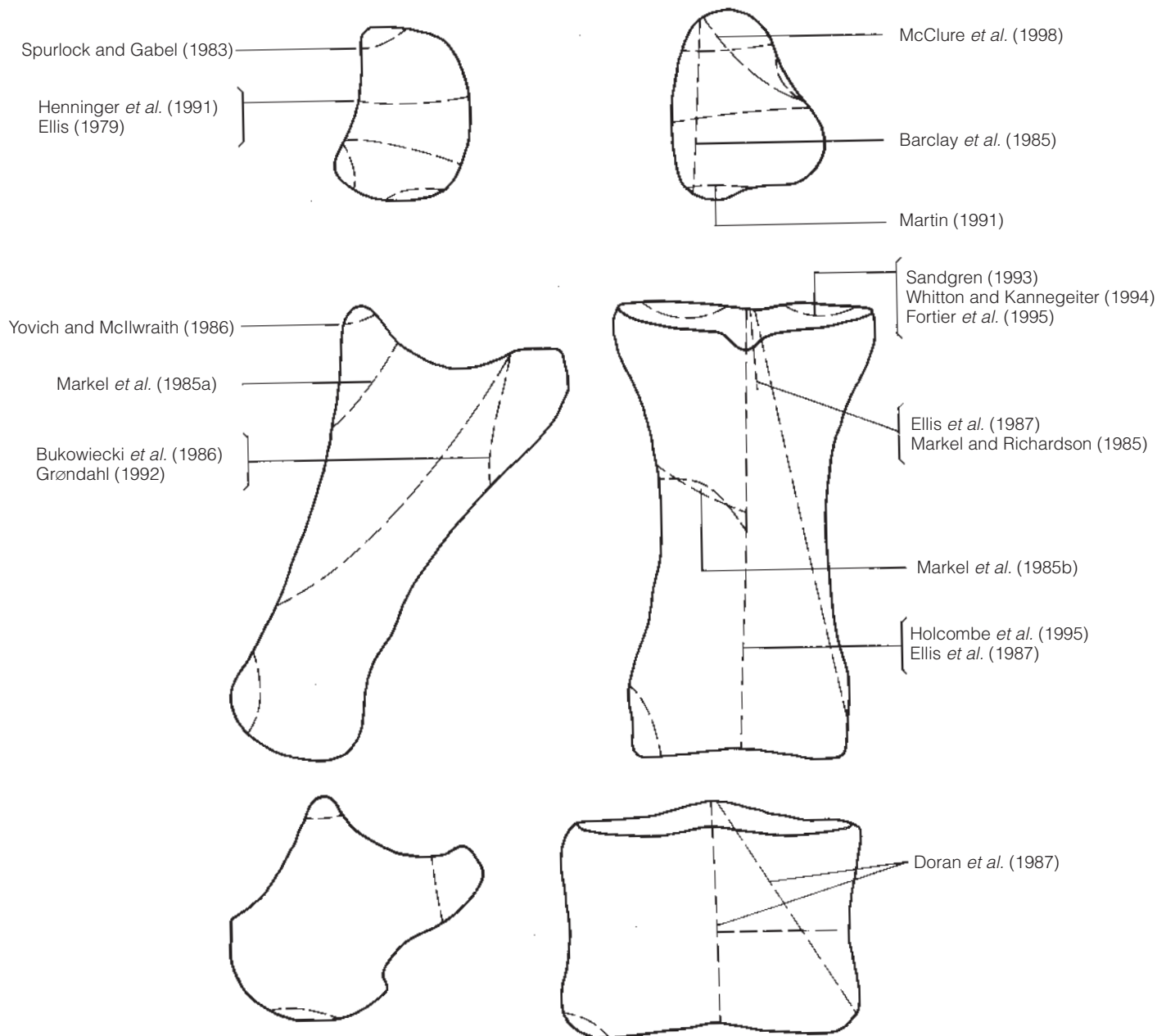
Figure 2.71 The common fracture sites for the phalanges and metacarpophalangeal joint.

Figure 2.72 Lateromedial view of the metacarpophalangeal joint, showing a discrete radiopaque body on the dorsoproximal aspect of the proximal phalanx.

Chip fractures of the proximodorsal and proximopalmar aspects of the proximal phalanx, involving the joint surface, are relatively common and, if only 2–3 mm in diameter, lameness will frequently resolve with rest, although it may be recurrent. Larger chips, chips associated with recurrent lameness, or fragments of bone with a roughened appearance or irregular and lucent base, usually need surgical removal. Other fractures of the proximal phalanx are referred to under 'Proximal phalanx' on pages 96–100. See also 'Osteochondral fragments', page 120.

Fractures of the proximal sesamoid bones occur frequently, and their significance depends on their position and the degree of associated soft-tissue injury. They may occur in association with fractures of the metacarpus and phalanges, and should not be overlooked.

Fractures of the abaxial surface of the bone are best seen on oblique tangential views (see Figure 2.58a, page 105). They carry a guarded prognosis.

Fractures of the apical region involving less than one-third of the bone generally respond well to surgical removal of the fragment. Larger fragments should normally be treated by internal fixation or bone grafting, preferably within 10 days of fracture. Even with prompt treatment the prognosis is poor. Basilar fragments of bone may be removed surgically, but even with improved arthroscopic technique, some disruption of the distal sesamoidean ligaments is inevitable, resulting in a guarded prognosis.

Sagittal fractures of the sesamoids also occur, usually concurrent with other fractures. They warrant a guarded prognosis.

Care should be taken when interpreting radiographs of foals. The sesamoid bones are not fully mineralized until 3 months of age, and the cartilage precursors may tear. This may not be seen radiographically until the

Figure 2.73 Lateromedial view of a metacarpophalangeal joint of a foal 5 weeks of age. There is a non-displaced apical fracture of the lateral proximal sesamoid bone.

sesamoid bones are more completely ossified, when the bones may appear elongated, or be visualized as two separated fragments (Figure 2.73). This is a common injury in foals under 1 month of age and may involve all four limbs. It is generally seen in foals that have exercised excessively and is associated with mild, transient lameness. With confinement to stall rest, bony union usually develops. The resulting sesamoid bone is usually larger than normal but the prognosis is good if treated promptly.

Fractures of the distal metacarpus are described in Chapter 3, page 157.

FURTHER READING

Foot

Aanes, W.A. (1984) Congenital phalangeal hypoplasia in Equidae. *J. Am. Vet. Med. Ass.*, **185**, 554–556

Ackerman, N., Johnson, J.H. and Dorn, C.R. (1977) Navicular disease in the horse. *J. Am. Vet. Med. Ass.*, **170**, 183–187

Berry, C., Pool, R., Stover, S. *et al.* (1992) Radiographic/morphologic investigation of a radiolucent crescent within the flexor central eminence of the navicular bone in Thoroughbreds. *Am. J. Vet. Res.*, **53**, 1604–1611

Campbell, J.R. and Lee, R. (1972) Radiological techniques in the diagnosis of navicular disease. *Equine Vet. J.*, **4**, 135–138

Cauvin, E. and Munroe, G. (1998) Septic osteitis of the distal phalanx: findings and surgical treatment in 18 cases. *Equine Vet. J.*, **30**, 512–519

Colles, C.M. (1979) Ischaemic necrosis of the navicular bone (distal sesamoid bone) of the horse and its treatment. *Vet. Rec.*, **104**, 133–137

Colles, C.M. (1982) The pathogenesis and treatment of navicular disease in the horse. *PhD Thesis*, University of London

Colles, C.M. and Hickman, J. (1977) The arterial supply of the navicular bone and its variations in navicular disease. *Equine Vet. J.*, **9**, 150–154

Dik, K. and Broeck, J. van den (1995) Role of navicular bone shape in the pathogenesis of navicular disease: a radiological study. *Equine Vet. J.*, **27**, 390–393

Dyson, S. (1991) Lameness due to pain associated with the distal interphalangeal joint: 45 cases. *Equine Vet. J.*, **23**, 128–135

Dyson, S. (1998) The puzzle of distal interphalangeal joint pain. *Equine Vet. Educ.*, **10**, 119–125

Gelatt, K.L., Neuwirth, L., Hawkins, D.L. and Woodard, J.C. (1996) Hemangioma of the distal phalanx in a colt. *Vet. Radiol. Ultrasound*, **37**, 275–280

Hickman, J. (1964) *Veterinary Orthopaedics*, 1st edn, Oliver and Boyd, Edinburgh, pp. 104–117

Hunt, R. (1993) A retrospective evaluation of laminitis in horses. *Equine Vet. J.*, **25**, 61–64

Jones, V.B. (1938) Veterinary radiology – navicular disease. *Vet. Rec.*, **50**, 676–677

Kaneps, A.J., O'Brien, T.R., Redden, R.F., Stover, S.M. and Pool, R.R. (1993) Characterisation of osseous bodies of the distal phalanx of foals. *Equine Vet. J.*, **25**, 285–292

Linford, R.L., O'Brien, T.R. and Trout, D.R. (1993) Qualitative and morphometric radiographic findings in the distal phalanx and distal soft tissues of sound Thoroughbred racehorses. *Am. J. Vet. Res.*, **54**, 38–51

McDiarmid, A.M. (1998) Distal interphalangeal joint lameness in a horse associated with damage to the insertion of the lateral collateral ligament. *Equine Vet. Educ.*, **10**, 114–118

MacGregor, C.M. (1986) Radiographic assessment of navicular bones based on change in the distal nutrient foramina. *Equine Vet. J.*, **18**, 203–206

Morgan, J.P. (1972) *Radiology in Veterinary Orthopaedics*, 1st edn, Lea and Febiger, Philadelphia

O'Brien, T.R., Millman, T.M., Pool, R.R. and Suter, P.F. (1975) Navicular disease in the Thoroughbred horse: a morphologic investigation relative to a new radiographic projection. *J. Am. Vet. Rad. Soc.*, **16**, 39–50

Oxspring, G.E. (1935) The radiology of navicular disease, with observations on its pathology. *Vet. Rec.*, **48**, 1445–1454

Petterson, H. (1976) Fractures of the pedal bone in the horse. *Equine Vet. J.*, **8**, 104–109

Poulos, P. (1983) Correlation of radiographic signs and histological changes in the navicular bone. *Proc. Am. Ass. Equine Pract.*, **29**, 241–255

Poulos, P. (1988) The nature of enlarged 'vascular channels' in the navicular bone of the horse. *Vet. Radiol.*, **29**, 60–64

Rendano, V. and Grant, B. (1978) The equine third phalanx: its radiographic appearance. *Vet. Radiol.*, **19**, 125–135

Richardson, G. and O'Brien, T. (1985) Puncture wounds into the navicular bursa of the horse: their radiological evaluation. *Vet. Radiol.*, **26**, 203–207

Rose, J.R., Taylor, B.J. and Steel, J.D. (1978) Navicular disease in the horse: an analysis of 70 cases and assessment of a special radiographic view. *J. Equine Med. Surg.*, **2**, 492–497

Ruohoniemi, M., Tulamo, R-M., Hackzell, M. (1993) Radiographic evaluation of ossification of the collateral cartilages of the third phalanx in Finnhorses. *Equine Vet. J.*, **25**, 453–455

Ruohoniemi, M., Karkkainen, M. and Tervahartiala, P. (1997) Evaluation of the variably ossified collateral cartilages of the distal phalanx and adjacent anatomic structures in the Finnhorse with computed tomography and magnetic resonance imaging. *Vet. Radiol. Ultrasound*, **38**, 344–351

Smallwood, J.E., Albright, S.M., Metcalf, M.R., Thrall, D.E. and Harrington, B.D. (1989) A xeroradiographic study of the developing equine foredigit and metacarpophalangeal region from birth to six months of age. *Vet. Radiol.*, **30**, 98–110

Stashak, T.S. (1987) *Adams' Lameness in Horses*, 4th edn, Lea and Febiger, Philadelphia

Vaughan, L.C. (1961) Fracture of the navicular bone in the horse. *Vet. Rec.*, **73**, 895–897

Verschooten, F. and deMoor, A. (1982) Subchondral cystic and related lesions affecting the equine pedal bone and stifle. *Equine Vet. J.*, **14**, 47–54

Verschooten, F., Waerebeek, B. Van and Verbeeck, J. (1996) The ossification of cartilages of the distal phalanx in the horse – an anatomical, experimental, radiographic and clinical study. *J. Equine Vet. Sci.*, **16**, 291–305

Wagner, I. and Hood, D. (1997) Cause of air lines associated with acute and chronic laminitis. *Proc. Am. Ass. Equine Pract.*, **43**, 363–366

Wagner, P. and Balch-Burnett, O. (1982) Surgical management of subchondral bone cysts of the third phalanx. *Equine Pract.*, **4**, 8–14

Watering, C.C. van de and Morgan, J.P. (1975) Chip fractures as a radiological finding in navicular disease of the horse. *J. Am. Vet. Rad. Soc.*, **16**, 206–210

Wright, I. (1993) A study of 118 cases of navicular disease: radiological features. *Equine Vet. J.*, **25**, 493–500

Yovich, J., Stashak, T., DeBowes, R. and Ducharme, N. (1986) Fractures of the distal phalanx of the forelimb in eight foals. *J. Am. Vet. Med. Ass.*, **189**, 550–554

Pastern

Doran, R., White, N. and Allen, D. (1987) Use of a bone plate for treatment of middle phalangeal fractures in horses: 7 cases (1979–1984). *J. Am. Vet. Med. Ass.*, **191**, 575–578

Ellis, D., Simpson, D., Greenwood, R. and Crowhurst, J. (1987) Observations and management of fractures of the proximal phalanx in young Thoroughbreds. *Equine Vet. J.*, **19** 43–49

Ellis, D. and Greenwood, R. (1985) Six cases of degenerative joint disease of the proximal interphalangeal joint of young thoroughbreds. *Equine Vet. J.*, **17**, 66–68

Holcombe, S.J., Schneider, R.K., Bramlage, L.R., Gabel, A.A., Bertone A.L. and Beard, W.L. (1995) Lag screw fixation of non-comminuted sagittal fractures of the proximal phalanx in racehorses: 59 cases (1973–1991). *J. Am. Vet. Med. Ass.*, **206**, 1195–1199

Markel, M. and Richardson, D. (1985) Non comminuted fractures of the proximal phalanx in 69 horses. *J. Am. Vet. Med. Ass.*, **186**, 573–579

Markel, M., Martin, B. and Richardson, D. (1985a) Dorsal frontal fractures of the first phalanx in the horse. *Vet. Surg.*, **14**, 36–40

Markel, M., Richardson, D. and Nunamaker, D. (1985b) Comminuted first phalanx fractures in 30 horses. Surgical versus non-surgical treatments. *Vet. Surg.*, **14**, 135–140

Trotter, G., McIlwraith, C., Nordin, R. and Turner, A. (1982) Degenerative joint disease with osteochondrosis of the proximal interphalangeal joint in young horses. *J. Am. Vet. Med. Ass.*, **180**, 1312–1318

Weaver, J., Stover, S. and O'Brien, T. (1992) Radiographic anatomy of soft tissue attachments in the equine metacarpophalangeal and proximal phalangeal region. *Equine Vet. J.*, **24**, 310–315

Fetlock

Allan, G.S. (1979) Radiography of the equine fetlock. *Equine Pract.*, **1**, 40–47

Barclay, W., Foerner, J. and Phillips, T. (1985) Axial sesamoid fractures associated with lateral condylar fractures. *J. Am. Vet. Med. Ass.*, **186**, 278–279

Barclay, W., Foerner, J. and Phillips, T. (1987) Lameness attributable to osteochondral fragmentation of the plantar aspect of the proximal phalanx: 19 cases. *J. Am. Vet. Med. Ass.*, **191**, 855–857

Birkeland, R. (1972) Chip fractures of the first phalanx in the metacarpophalangeal joint. *Acta Radiol. Suppl.*, **39**, 73–77

Bukowiecki, C., Bramlage, L. and Gabel, A. (1986) Palmar/plantar process fractures of the proximal phalanx in 15 horses. *Vet. Surg.*, **15**, 383–388

Dik, K.J. (1985) Special radiographic projections for the equine proximal sesamoid bones and the caudoproximal extremity of the first phalanx. *Equine Vet. J.*, **17**, 244–247

Ellis, D. (1979) Fractures of the proximal sesamoid bones in thoroughbred foals. *Equine Vet. J.*, **11**, 48–52

Fortier, L., Foerner, J. and Nixon, A. (1995) Arthroscopic removal of axial osteochondral

fragments of the plantar/palmar proximal aspect of the proximal phalanx in horses: 119 cases (1988–1992). *J. Am. Vet. Med. Ass.*, **206**, 71–74

Fraser, J.A. (1971) Some conditions of the proximal sesamoid bones in the horse. *Equine Vet. J.*, **3**, 20–24

Grøndahl, A. (1992) Incidence and development of ununited proximoplantar tuberosity of the proximal phalanx in Standardbred trotters. *Vet. Radiol. Ultrasound*, **33**, 18–21

Grøndahl, A., Gaustad, G. and Engeland, A. (1994) Progression and associated with lameness and racing performance of radiographic changes in the proximal sesamoid bones of young Standardbred trotters. *Equine Vet. J.*, **26**, 152–155

Hardy, J., Marcoux, M. and Breton, L. (1991) Clinical relevance of radiographic findings in proximal sesamoid bones of two-year-old Standardbreds in their first year of race training. *J. Am. Vet. Med. Ass.*, **198**, 2089–2094

Haynes, P., Root, C., Clabough, Q. and Roberts, E. (1981) Palmar supracondylar lysis of the third metacarpal bone. *Proc. Am. Ass. Equine Pract.*, **27**, 185–193

Henninger, R., Bramlage, L., Schneider, R. and Gabel, A. (1991) Lag screw and cancellous bone graft fixation of transverse proximal sesamoid fractures in horses: 25 cases (1983–1989). *J. Am. Vet. Med. Ass.*, **199**, 606–612

Hornhof, W.J. and O'Brien, T.R. (1980) Radiographic evaluation of the palmar aspect of the equine metacarpal condyles: a new projection. *Vet. Radiol.*, **21**, 161–167

McCall, D.J.M. and Kneller, S.K. (1989) Proximodorsal-distodorsal view of the equine metacarpophalangeal joint. *Vet. Technician*, **10**, 617–621

McClure, S., Watkins, J., Glickman, N. *et al.* (1998) Complete fracture of the third metacarpal or metatarsal bone in horses: 25 cases (1980–1986). *J. Am. Vet. Med. Ass.*, **213**, 847–850

Martin, B., Nunamaker, D., Evans, L., Orsini, J. and Palmer, S. (1991) Circumferential wiring of mid-body and large basilar fractures of the proximal sesamoid bones in 15 horses. *Vet. Surg.*, **20**, 9–14

Medina, L., Wheat, J., Morgan, J. and Pool, R. (1980) Treatment of basal fractures of the sesamoid bones using autogenous bone grafts. *Proc. Am. Ass. Equine Pract.*, **26**, 345–380

Morgan, J.P. (1973) Radiology of the proximal sesamoid bone in the horse after trauma. *Tijdschr. Diergeneesk.*, **98**, 995–1001

Nickels, J.F., Grant, B.D. and Lincoln, S.C. (1975) Villonodular synovitis of the equine metacarpophalangeal joint. *J. Am. Vet. Med. Ass.*, **168**, 1043–1046

Nixon, A. and Pool, R. (1995) Histologic appearance of axial osteochondral fragments from the proximoplantar/proximopalmar aspect of the proximal phalanx. *J. Am. Vet. Med. Ass.*, **207**, 1076–1080

O'Brien, T.R. (1977) Disease of the thoroughbred fetlock joint – a comparison of radiographic signs with gross pathological lesions. *Proc. Am. Ass. Equine Pract.*, **23**, 367–380

O'Brien, T.R., Morgan, J.P., Wheat, J.D. and Suter, P.F. (1971) Sesamoiditis in the thoroughbred: a radiographic study. *J. Am. Vet. Res.*, **12**, 75–87

O'Brien, T.R., Hornhof, W. and Meager, D. (1981) Radiographic detection and characterisation of palmar lesions in the fetlock joint. *J. Am. Vet. Med. Ass.*, **178**, 231–237

Palmar, S.E. (1982) Radiography of the abaxial surface of the proximal sesamoid bones of the horse. *J. Am. Vet. Ass.*, **181**, 264–265

Rick, M., O'Brien, T., Pool, R. and Meagher, D. (1983) Condylar fractures of the third metacarpal bone and third metatarsal bone in 75 horses: radiographic features, treatment and outcome. *J. Am. Vet. Med. Ass.*, **183**, 287–296

Ross, M., Nolan, P., Palmer, J. *et al.* (1991) The importance of the metatarsophalangeal joint in Standardbred lameness. *Proc. Am. Ass. Equine Pract.*, **37**, 741–756

Ross, M. (1998) Scintigraphic and clinical findings in the Standardbred metatarsophalangeal joint: 114 cases (1993–1995). *Equine Vet. J.*, **30**, 131–138

Sandgren, B. (1993) Osteochondrosis in the tarsocrural joint and osteochondral fragments in the metacarpo/metatarsophalangeal joints in young Standardbreds. *PhD Thesis*, University of Uppsala, Sweden

Shepherd, M. and Pilsworth, R. (1997) Stress reactions in the plantarolateral condyles of MT III in UK Thoroughbreds: 26 cases. *Proc. Am. Ass. Equine Pract.*, **43**, 128–131

Southwood, L., Trotter, G. & McIlwraith, C. (1998) Arthroscopic removal of abaxial fracture fragments of the proximal sesamoid bone in horses: 47 cases (1989–1997). *J. Am. Vet. Med. Ass.*, **213**, 1016–1021

Spike, D., Bramlage, L., Howard, B. *et al.* (1997) Radiographic proximal sesamoiditis in Thoroughbred sales yearlings. *Proc. Am. Ass. Equine Pract.*, **43**, 132–137

Spurlock, G. and Gabel, A. (1983) Apical sesamoid fractures in the proximal sesamoid bones in 109 Standardbred horses. *J. Am. Vet. Med. Ass.*, **183**, 76–79

Thompson, K. and Rooney, J. (1994) Bipartite proximal sesamoid bones in young Thoroughbred horses. *Vet. Radiol. Ultrasound*, **35**, 368–370

Whitton, C. and Kannegeiter, N. (1994) Osteochondral fragmentation of the plantar/palmar proximal aspect of the proximal phalanx in racing horses. *Austr. Vet. J.*, **71**, 318–321

Yovich, J., McIlwraith, C. and Stashak, T. (1985) Osteochondrosis dissecans of the sagittal ridge of the third metacarpal and metatarsal bones in horses. *J. Am. Vet. Med. Ass.*, **186**, 1186–1191

Yovich, J. and McIlwraith, C. (1986) Arthroscopic surgery for osteochondral fractures of the proximal phalanx of the metacarpophalangeal and metatarsophalangeal (fetlock) joints in horses. *J. Am. Vet. Med. Ass.*, **188**, 273–279

Chapter 3
The Metacarpus and Metatarsus

Throughout this chapter, although reference is made to the metacarpus it also applies to the metatarsus. Significant differences of the metatarsus are highlighted.

A standard radiographic examination of the metacarpus comprises lateromedial, dorsopalmar, dorsolateral-palmaromedial oblique, and dorsomedial-palmarolateral oblique views. In selected cases dorsoproximal-palmarodistal oblique views may yield valuable additional information about the distal end of the third metacarpus (see Chapter 2, page 105). Occasionally a flexed lateromedial view is helpful for identifying avulsion fractures at the origin of the suspensory ligament. Special projections for evaluating the proximal sesamoid bones are discussed in Chapter 2 (page 103).

In many instances the clinical examination will suggest which views are necessary and at which level the x-ray beam should be centred. In some cases a complete examination is not required, although many views with only slight differences in angle of projection may be needed (e.g. for evaluation of a dorsal cortical fatigue fracture of the third metacarpal bone). It is difficult to evaluate properly the entire length of the metacarpus using small (30cm) cassettes.

RADIOGRAPHIC TECHNIQUE

Lateromedial, dorsopalmar and oblique views

The metacarpus may be radiographed using a portable x-ray machine and either high-definition or rare earth screens and compatible film. A grid is unnecessary. All the standard projections are ideally obtained with the horse bearing full weight on the limb, with the metacarpus vertical. The second and fourth metacarpal bones are best evaluated using dorsomedial-palmarolateral oblique and dorsolateral-palmaromedial oblique views, respectively. The x-ray beam is centred on the area of principal interest. In some cases it may be helpful to use a long (43cm) cassette so that the entire length of the metacarpus can be seen on a single radiograph, but in an adult horse some obliquity of projection at the extremities of the bones is inevitable (see Figure 3.3, pages 136, 137 and 138). Therefore it is usually preferable to use more than one projection and create a 'jigsaw' of the length of the bone.

Many of the radiographic abnormalities in this region are subtle and are only visible with correct angulation of the x-ray beam and appropriate exposure factors. Fatigue fractures of the dorsal cortex of the third metacarpal

Figure 3.1(a) Dorsopalmar view of the distal metacarpus of a normal adult horse. The proximal sesamoid bones are superimposed over the condyles of the third metacarpal bone. Note the curved outline of the medial and lateral aspects of the distal end of the third metacarpal bone (arrows) and the variable opacity in these areas. This may be exaggerated in a slightly oblique projection.

Figure 3.1(b) Dorsal 10° proximal-palmarodistal oblique view of the distal metacarpus of a normal adult horse. The proximal sesamoid bones are projected proximally giving excellent visualization of the metacarpal condyles.

bone are readily missed unless multiple oblique views are obtained. Early periosteal proliferative reactions, less opaque than the parent bone (e.g. a 'splint') are easily overexposed. Thus reduced exposure factors should be used. The timing of the radiographic examination is also critical, since many radiographic abnormalities will not be present until at least 7–21 days after the onset of clinical signs. Sequential radiographic examinations may therefore be helpful.

Dorsoproximal-palmarodistal oblique views

In a dorsopalmar view of the distal metacarpus, the proximal sesamoid bones are projected over the distal aspect of the third metacarpal bone (Figure 3.1a) and lesions involving the condyles may easily be missed (e.g. an incomplete vertical condylar fracture). The sesamoid bones are projected further proximally if the x-ray beam is angled proximodistally at
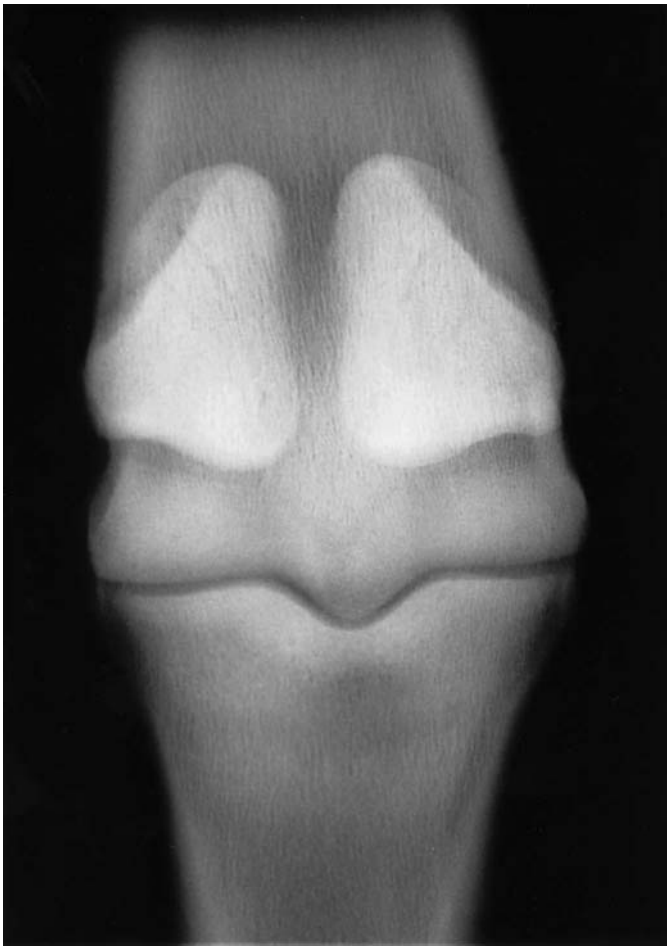
Figure 3.1(c) Dorsopalmar (flexed) view of the distal metacarpal region of a normal adult horse. The proximal sesamoid bones are projected more proximally than in Figure 3.1(b). This view highlights a more distal articular margin of the condyles of the third metacarpal bone.

Figure 3.1(d) Dorsodistal-palmaroproximal oblique view of the distal metacarpus of a normal adult horse. The proximal sesamoid bones are superimposed over the metacarpophalangeal joint, but this view gives visualization of the palmar aspect of the metacarpal condyles.

least 10°, i.e. a dorsal 10° proximal-palmarodistal oblique (D10°Pr-PaDiO) view (Figure 3.1b). This view is particularly important for the identification of incomplete, vertical articular condylar fractures, although these lesions may still be difficult to detect. Improved visualization may be achieved by flexing the metacarpophalangeal joint. The toe of the foot is placed in the standard navicular block (see page 66), with the dorsal wall vertical. A horizontal x-ray beam is centred on the joint. The cassette is positioned as closely perpendicular to the x-ray beam as possible. This view moves the sesamoid bones further proximally (Figure 3.1c).

The palmar articular surface may be assessed better with the limb partially extended with the foot on a flat block (Figure 3.2). The cassette is held approximately parallel with the metacarpus. The x-ray beam is directed distoproximally in the plane of rotation of the metacarpophalangeal joint, at approximately 125° to the metacarpus. If the limb and the x-ray beam are correctly aligned, between one-fourth and one-third of the proximal

[133]
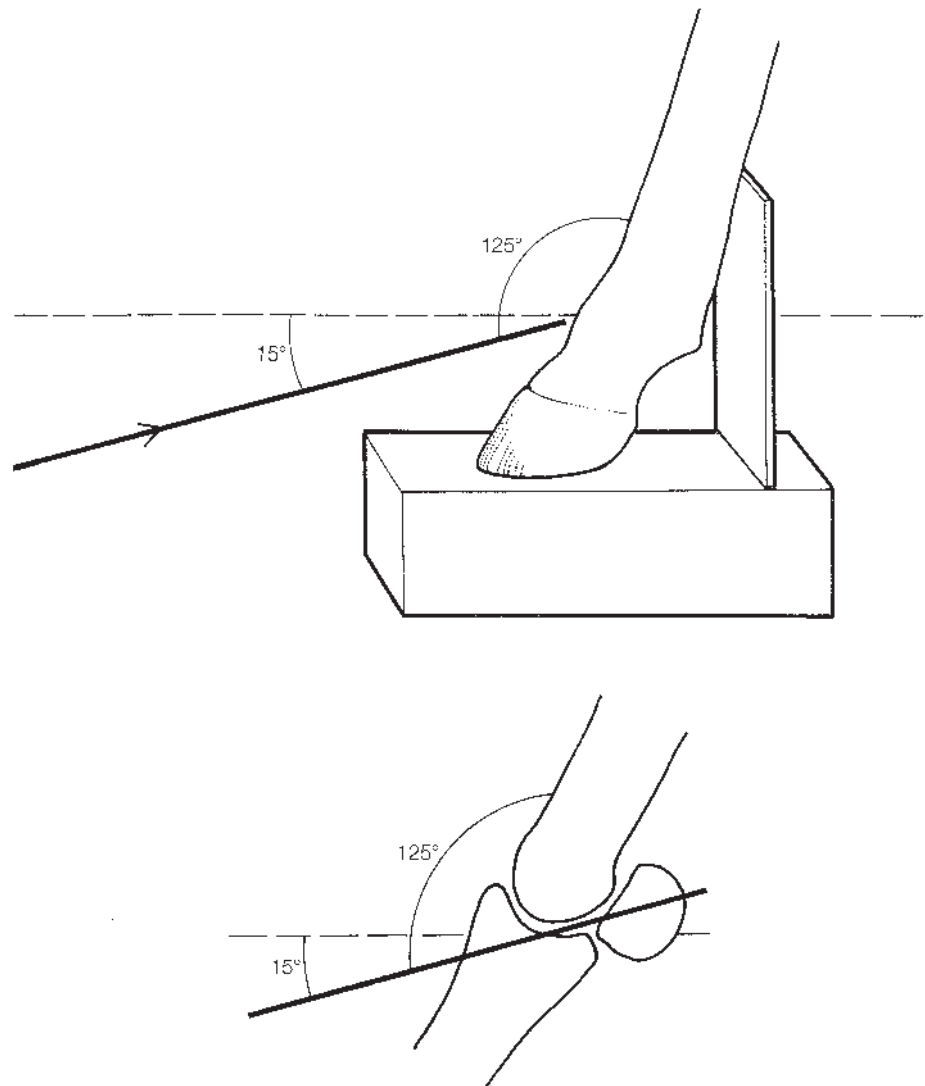
Figure 3.2 Position of the limb, x-ray machine and cassette to obtain a dorsodistal-palmaroproximal oblique view of the distal metacarpus (see Figure 3.1d).

sesamoid bones are projected below the joint space (Figure 3.1d). This view is especially important when evaluating a vertical condylar fracture; comminution of the palmar articular surface of the third metacarpal bone is usually only identifiable in this projection. It is also useful for detecting lucent lesions in the palmar aspect of the metacarpal condyles (see Chapter 2, page 120). Other oblique views of the metacarpal condyles and the proximal sesamoid bones are described in detail on pages 103–5 and 107.

Other imaging techniques

Nuclear scintigraphy offers a more sensitive method for detection of acute fatigue fractures. Ultrasonography provides a means of evaluating the metacarpal soft-tissue structures. It must be remembered that bony and soft-tissue lesions may occur concurrently and this may have an important

bearing on the prognosis (e.g. fractures of the distal one-third of the second or fourth metacarpal bones often occur together with suspensory desmitis).

NORMAL RADIOGRAPHIC ANATOMY: ITS VARIATIONS AND INCIDENTAL FINDINGS

Lateromedial view

The dorsal cortical contour of the third metacarpal bone is usually straight, but that of the third metatarsal bone is relatively convex (Figures 3.3a and 3.3b). The dorsal cortex is thicker than the palmar (plantar) cortex especially on the dorsomedial aspect of the forelimb. The smoothness of the dorsal cortex should always be evaluated carefully under high intensity illumination. The dorsal cortices of the third metacarpal or metatarsal bones may be unusually convex and thicker than normal as a result of previous trauma. Small, uniformly opaque, clinically silent osteophytes or entheseophytes are sometimes seen on the dorsoproximal aspect of the third metatarsal bone (see Chapter 6, page 252). The principal nutrient canal is sometimes seen palmarodistally, coursing horizontally or obliquely proximally.

Dorsopalmar view

The proximal articular surface of the third metacarpal bone is concave; therefore part of the carpometacarpal joint is superimposed over the third carpal bone (Figures 3.4a, page 138 and 3.4b, page 139). The subchondral bone plate is a relatively opaque band of uniform thickness. A series of small, circular lucent zones, nutrient foramina, may be seen in the subchondral bone of the proximal third metacarpus depending on the angle of projection (Figure 3.4b). The proximal and distal quarters of the third metacarpal bone have a relatively coarse, but uniformly opaque trabecular pattern (see Figures 3.1a, page 132; 3.1b, page 132; 3.1c, page 133; 3.4b, page 139 and 3.16c, page 155). The trabeculae are orientated approximately parallel to the long axis of the bone. In some horses there is a narrow, vertical, more opaque line in the middle of the proximal one-quarter of the third metacarpal bone, representing a ridge between the heads of the suspensory ligament. The principal nutrient foramen is usually seen as an oval-shaped lucent area superimposed on the medullary cavity, at the junction between the proximal and middle one-thirds of the bone (Figure 3.4a, page 138). Occasionally it may be linear in appearance or there is more than one nutrient foramen.

In this view and some oblique projections the second and fourth metacarpal bones are partially superimposed over the third metacarpus, and this may result in some confusing lucent lines. These lucent lines (Mach lines or bands) are due to edge enhancement, the effect of one bone edge crossing another (Figure 3.5, page 140), and should not be confused with fractures. The second and fourth metacarpal bones are most readily evaluated in the oblique views.

[135]

Figure 3.3(a) Lateromedial view of a normal adult metacarpus. Note the obliquity of projection at the distal end of the bone. To evaluate this area better, a view centred on this region is required.

Figure 3.3(b) Lateromedial view of a normal adult metatarsus. Due to the increased length of the bone relative to the metacarpus there is greater obliquity at the proximal and distal extremities of the bone. Note the slightly convex contour of the dorsal cortex of the third metatarsal bone.

Figure 3.4(a) Dorsopalmar projection of the metacarpus of a normal adult horse. Note the vertical lucent line on the axial aspect of the fourth metacarpal bone (arrowheads) created by an edge effect. The lucent zone in the middle of the third metacarpal bone (arrow) represents the principal nutrient foramen.

Figure 3.4(b) Dorsopalmar view of the proximal metacarpus of a normal adult horse. Note the uniform trabecular pattern and the small lucent zones in the most proximal aspect of the bone (arrows), representing nutrient foramina.

The proximal metacarpal physis is closed at birth. The distal metacarpal physis closes radiographically at approximately 3–6 months of age (Figure 3.6).

The proximal sesamoid bones are superimposed over the distal end of the third metacarpal bone. Their position depends on the angle of projection (see Figures 3.1a–3.1d, pages 132 and 133). Radiographic features of these bones are discussed in Chapter 2 (page 112).

Dorsolateral-palmaromedial oblique and dorsomedial-palmarolateral oblique views

The dorsolateral-palmaromedial oblique view (Figure 3.7a, page 142) highlights the dorsomedial cortex of the third metacarpal bone and the fourth metacarpal bone. The second metacarpal bone is superimposed over the third. The proximal end or base of the fourth metacarpal bone articulates with the fourth carpal bone. The base of the fourth metatarsal bone articulates with the fourth tarsal bone (Figure 3.7b, page 142). It may have a prominent plantar protuberance. Occasionally this protuberance has a small bony spur on its plantar aspect (Figure 3.8, page 143) which in the authors' experience is usually of no significance, although it may reflect previous injury.

The dorsomedial-palmarolateral oblique view (Figure 3.9, page 144)

[139]

Figure 3.5 Palmarolateral-dorsomedial oblique view of a normal adult metacarpus. Note the vertical lucent lines on the palmar aspect of the third metacarpal bone which are the result of edge enhancement (Mach lines).

highlights the dorsolateral cortex of the third metacarpal bone and the second metacarpal bone. The second metacarpal bone articulates with the second and third carpal bones. The second metatarsal bone articulates with the first and second tarsal bones (these are usually fused).

The principal nutrient foramen of the third metacarpal bone may be projected as a lucent line across the second or fourth metacarpal bones and should not be confused with a fracture (Figure 3.10, page 144). The second and fourth metacarpal bones are relatively straight, but may curve away from the third metacarpal bone distally. There is considerable variation in

Figure 3.6 Lateromedial view of the metacarpus of a normal foal of 8 weeks of age.

(a)

(b)

Figure 3.7(a) Dorsolateral-palmaromedial oblique view of a normal adult metacarpus. The fourth metacarpal bone is highlighted.

Figure 3.7(b) Dorsolateral-plantaromedial oblique view of a normal adult metatarsus. The fourth metatarsal bone is highlighted.

[142]

Figure 3.8 Dorsolateral-plantaromedial oblique view of the proximal metatarsal region of a clinically normal adult horse. There is a smoothly outlined bony spur (arrow) on the proximal plantar aspect of the fourth metatarsal bone, of no clinical significance.

their length and shape. There is a variably sized and shaped enlargement on the distal ends of the second and fourth metacarpal bones; the distal epiphyses are cartilaginous at birth and gradually ossify (Figure 3.6, page 141), but are separate from the body of the bone until approximately 1–9 months of age.

The contour of the second and fourth metacarpal bones is clearly defined, but many horses have smoothly outlined exostoses reflecting previous trauma to the bone (Figure 3.11a, page 145). Sometimes there is irregular periosteal new bone with distinct margins; this must not be misinterpreted as an active periosteal reaction (compare Figures 3.11b, page 145 and 3.14, page 148).

With the correct obliquity of the x-ray beam, and provided that there is no mineralization or ossification of the interosseous ligaments, a lucent space may be seen between the second and third, and fourth and third metacarpal bones. In some horses it may be necessary to obtain several views at slightly different angles in order to evaluate the entire interosseous space. Many horses have some mineralization or ossification of the interosseous ligaments (Figure 3.12, page 146). Occasionally ossification is complete. There may be an ill-defined lucent zone in the base (head) of the second metacarpal bone. This is usually seen in association with the presence of a first carpal bone (Figure 4.12b, page 188).

In some horses there is a lucent line in the proximal one-third of either or both of the second and fourth metacarpal bones. This extends distally from the medullary cavity and ends on the dorsal aspect of the bone (Figure 3.13, page 146); it represents a nutrient foramen and should not be misinterpreted as a fracture.

Figure 3.9 Dorsomedial-palmarolateral oblique view of a normal adult metacarpus. Note the oblique lucent line in the middle of the metacarpus (arrow): this represents the nutrient foramen.
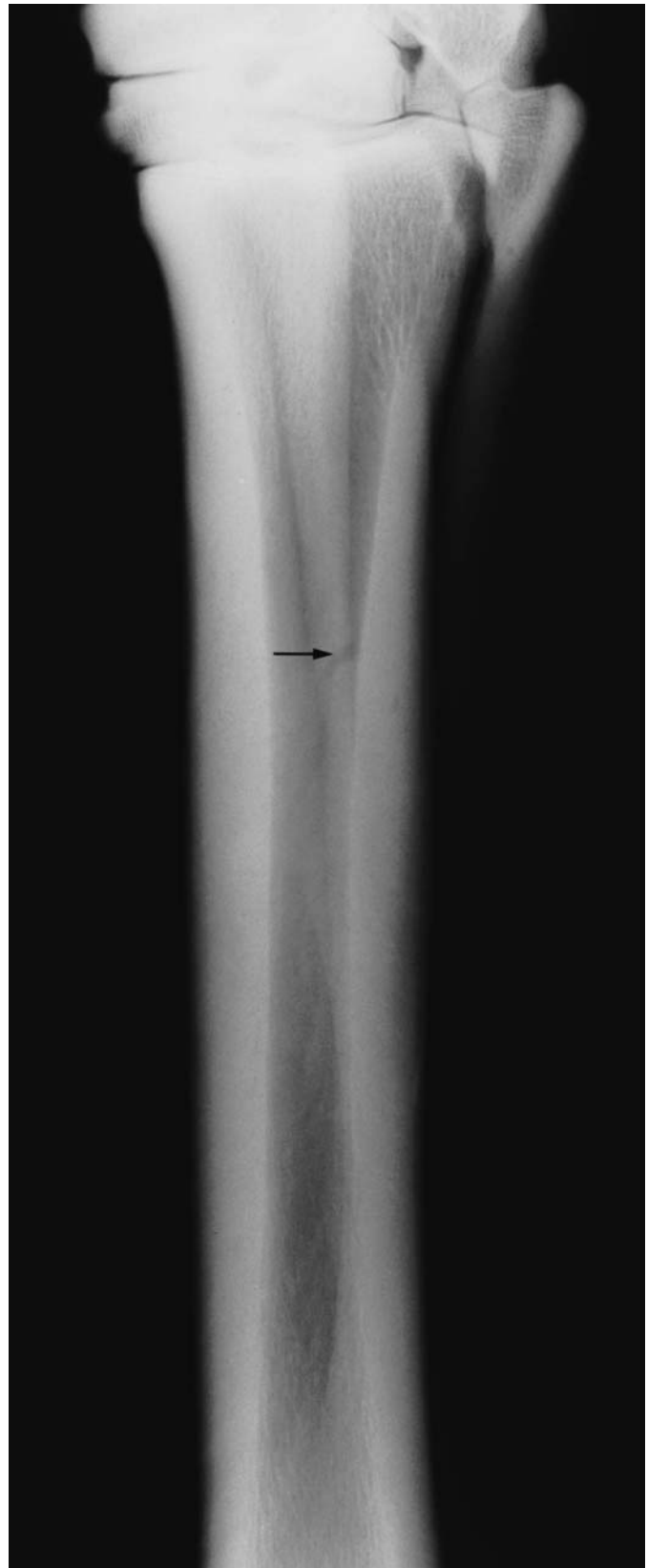
Figure 3.10 Dorsolateral-plantaromedial oblique view of a normal adult metatarsus. Note the oblique lucent line crossing the second metatarsal bone (arrow). This is the nutrient foramen and should not be confused with a fracture.

(a)

(b)

Figure 3.11(a) Dorsomedial-palmarolateral oblique view of an adult metacarpus. There is a smoothly outlined exostosis on the second metacarpal bone and some mineralization in the interosseous space, of no clinical significance.

Figure 3.11(b) Dorsomedial-palmarolateral oblique view of an adult metacarpus. There is irregular periosteal new bone with distinct margins on the proximal aspect of the second metacarpal bone (compare with Figures 3.14a and 3.14b, pages 148 and 149). Despite the irregularity the margin is distinct, which makes it likely that this change is inactive. There is also smoothly outlined new bone involving the diaphysis and mineralization in the interosseous space. This is inactive and not of current clinical significance.

[145]
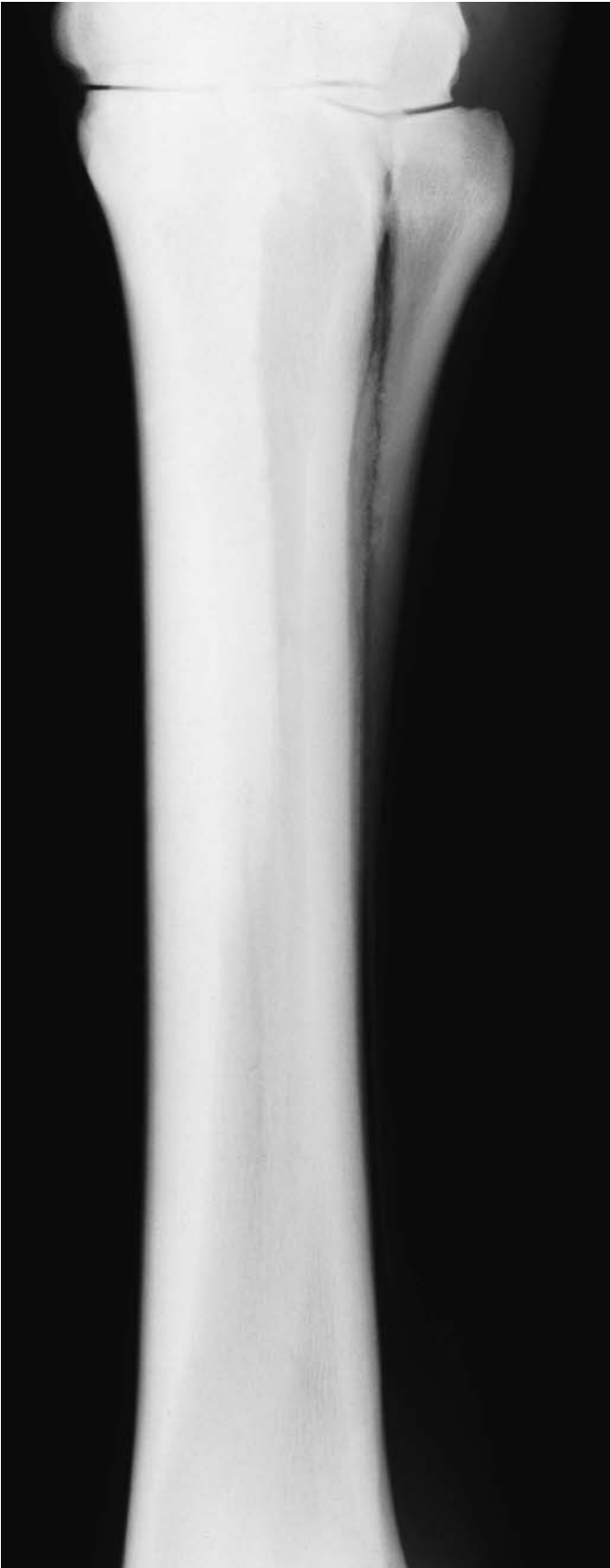
Figure 3.12 Dorsolateral-palmaromedial oblique view of an adult metacarpus. There is mineralization between the third and fourth metacarpal bones of no clinical significance.
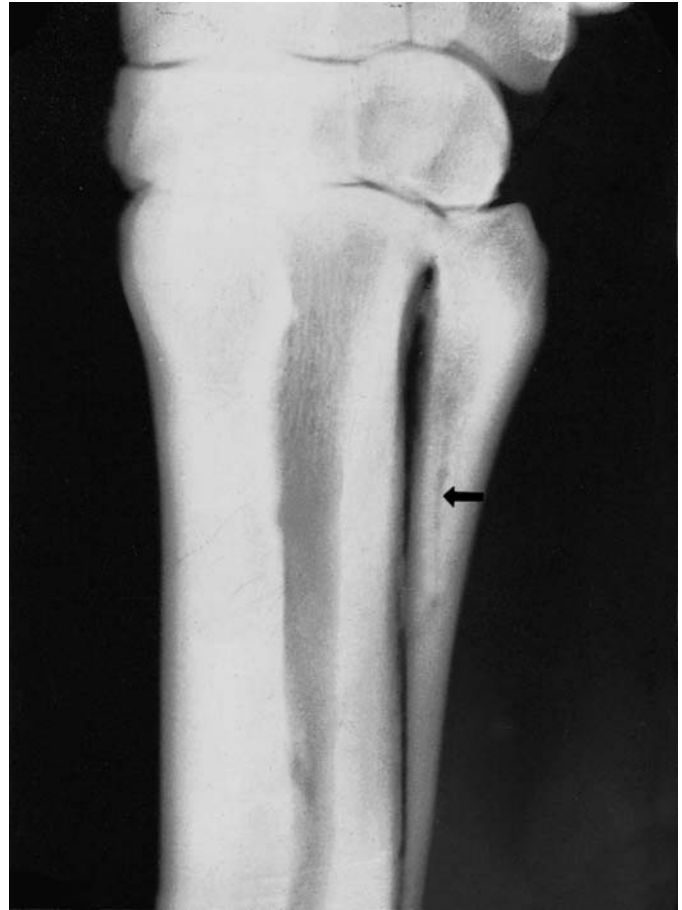
Figure 3.13 Dorsolateral-palmaromedial oblique view of a normal adult metacarpus. There is a lucent line (arrow) in the proximal one-third of the fourth metacarpal bone which represents a nutrient foramen.

Periostitis

Periostitis resulting from direct trauma to bone

Direct trauma to any of the metacarpal bones may result in inflammation of the periosteum and/or a subperiosteal haematoma and subsequent periosteal new bone. The smoothness of the margin and the opacity of the new bone help to determine the activity and chronicity of the lesion. New bone is usually not detectable for at least 14 days and appears first as slightly opaque bone in the soft tissues adjacent to the metacarpal bone, with an irregular margin (Figures 3.14a and 3.14b). The new bone becomes progressively more opaque and smoother in outline as it is modelled (see Figures 3.11a and 3.11b, page 145).

The second and fourth metacarpal bones seem particularly susceptible to production of very irregular new bone. Pillars of relatively opaque bone may be separated by more lucent bone. This pallisade-like appearance, which may be due to invasion of the proliferative new bone by some fibrous tissue, may persist when the lesion has become inactive (Figure 3.11b, page 145). The pattern of mineralization can result in a lucent line, or lines, which traverse the periosteal reaction and may mimic a fracture (Figure 3.14b).

Provided that there is no further trauma to the bone, an active periosteal reaction usually becomes quiescent within 6–12 weeks. A horse with an active periosteal reaction usually resents pressure applied to the lesion but may not be lame; nevertheless, it is likely that the reaction will heal more quickly if the horse is confined to box rest.

Periostitis produced in response to microfractures

Sore shins or 'bucked shins' is a relatively common syndrome in racing Thoroughbreds and Quarter Horses, resulting in localized heat, pain and swelling and a variable degree of lameness.

Cortical modelling is an adaptive response to increased loading during normal exercise. During training of 2- and 3-year-old horses, cortical modelling is particularly intense and often creates focal areas of porosity in the cortex. Cyclic loading of the immature third metacarpal bone may ultimately result in fatigue microfractures in the middle or distal one-thirds of the dorsal cortex which are not detectable radiographically. They may also be seen occasionally in older horses which have not previously undergone training. Microfractures may result only in periosteal and endosteal reactions, and if the training programme is moderated a fracture may never be detected radiographically. If early clinical signs are overlooked and the horse is kept in training, an overt, radiographically detectable fracture may result. Alternatively acute fractures do occur without any preceding periosteal reaction.

When clinical signs are first recognized, high-quality radiographs or xeroradiographs are essential to identify radiographic abnormalities.
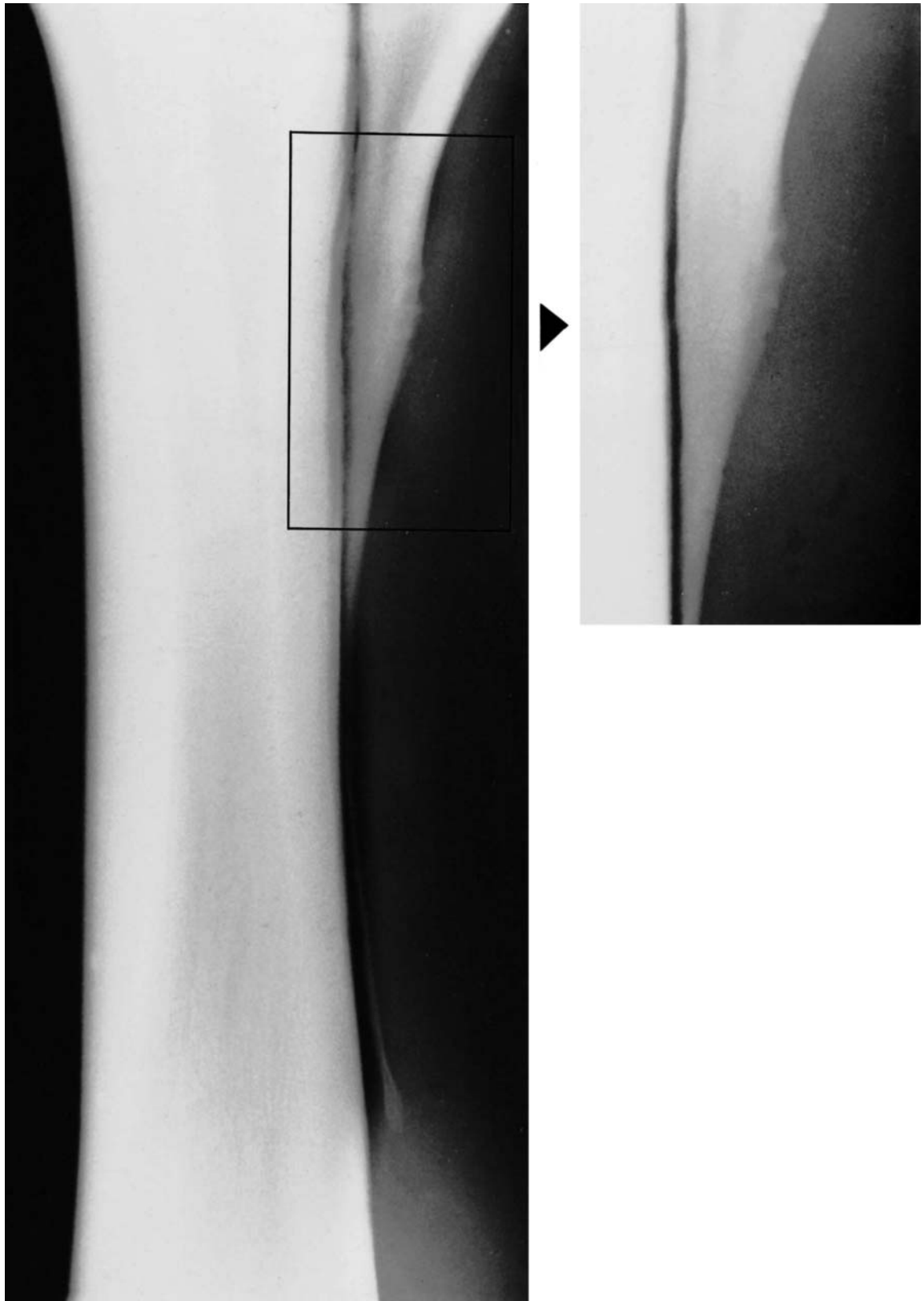
Figure 3.14(a) Dorsomedial-palmarolateral oblique view of an adult metacarpus. There is ill-defined, irregular periosteal new bone on the middle of the diaphysis of the second metacarpal bone (a 'splint'). The radiographs are deliberately underexposed in order to highlight the less opaque new bone.

[148]
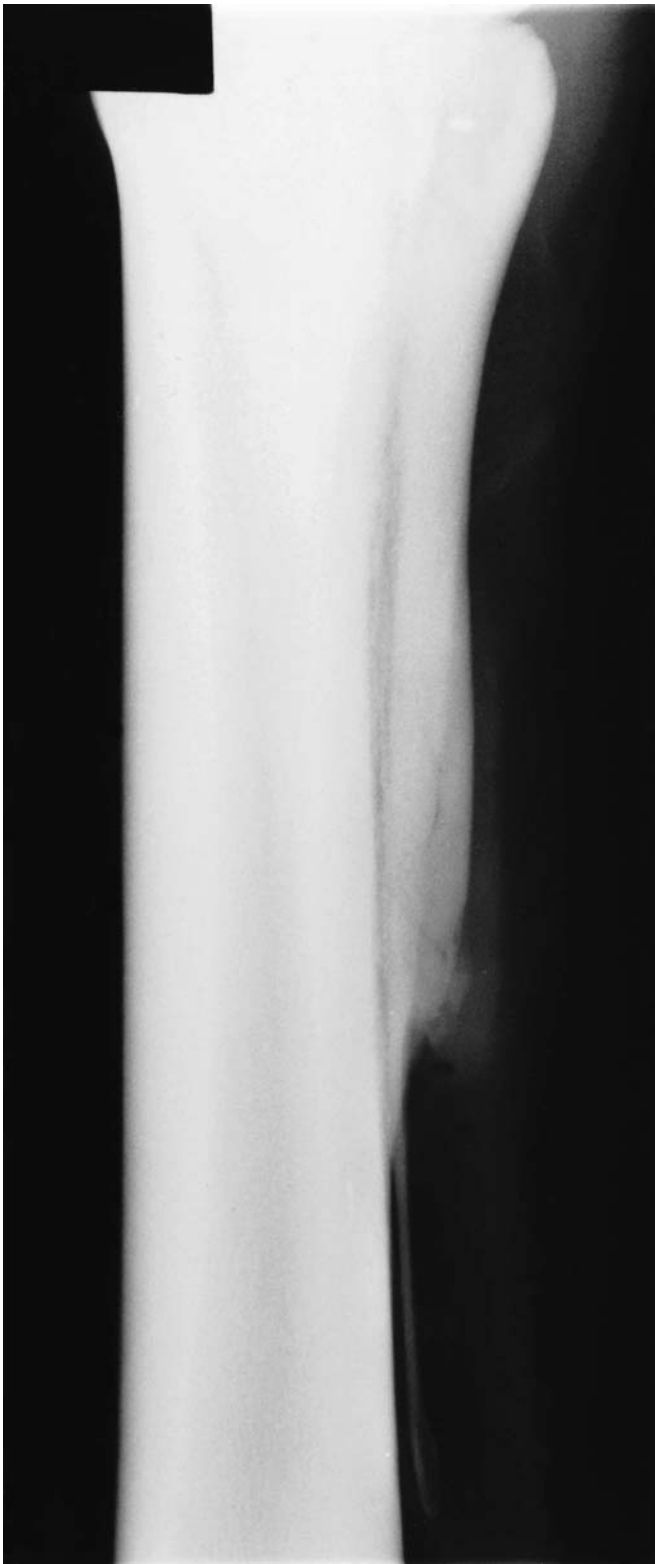
Figure 3.14(b) Dorsomedial-palmarolateral oblique view of an adult metacarpus. There is smoothly outlined enlargement of the middle of the diaphysis of the second metacarpal bone, with ill-defined irregularly outlined periosteal new bone at the distal end of the middle third of the bone. There are ill-defined lucent lines within the bone. These are the result of new bone formation and should not be confused with fractures. There is also ossification between the second and third metacarpal bones.

Nuclear scintigraphy demonstrates focal increased uptake of technetium-99m (^{99m}Tc). Intracortical fissures or indistinct lucent areas in the dorsal cortex are sometimes demonstrable, with or without localized periostitis and an endosteal reaction. Periostitis is not detectable using plain radiography until approximately 2 weeks after the onset of the clinical signs.

Using high-quality radiographic technique and multiple oblique views it may be possible to detect small fractures in the dorsal cortex of the bone. Most fractures traverse distoproximally at an angle of approximately 30° to the long axis of the bone and end at the junction of the middle and inner one-thirds of the cortex (Figures 3.15a and 3.15b). Some fractures extend to form a complete semi-circle or 'saucer'; occasionally only the proximal half of the saucer can be seen. Multiple fractures sometimes occur.

Rest results in resolution of clinical signs, but follow-up radiography or nuclear scintigraphy is important to monitor bone healing. Some fractures heal satisfactorily within 8–12 weeks and training can be resumed, but in some horses there appears to be minimal change in the radiographic appearance of the fracture and, in selected cases, surgical intervention may be necessary. In order to monitor healing it is very important to obtain identical radiographic views to those which initially best demonstrated the lesion.

Periostitis between the second and third or fourth and third metacarpal bones (splints)

Periostitis between the second and third or fourth and third metacarpal bones develops secondary to damage of the interosseous ligament. The reaction, which is of variable size, usually involves the proximal one-half of the second or fourth metacarpal bones. Splints develop most frequently between the second and third metacarpal bones in the forelimb and the fourth and third metatarsal bones in the hind limb. Several oblique views may be necessary in order to evaluate the interosseous space properly.

The condition occurs most commonly in young horses when regular work commences, but is also seen in older horses. There may be associated lameness, deteriorating with work. Careful palpation reveals a localized area of pain. If the metacarpal region is set lateral relative to the central axis of the antebrachium and carpus, or there is an angular limb deformity, the horse is particularly prone to the development of both ossification between the second and third metacarpal bones, and new bone on the medial aspect of the second metacarpal bone, as the bones model according to Wolf's law. This often develops without associated lameness. New bone formation may also occur suddenly in older horses without lameness.

In an early lesion there is some slightly opaque bone between the two metacarpal bones, and cortical bone remodelling may be detectable. With time the periosteal new bone becomes more opaque and will eventually look solid. The amount of periosteal new bone produced is extremely variable and sometimes an active bony reaction may mimic a
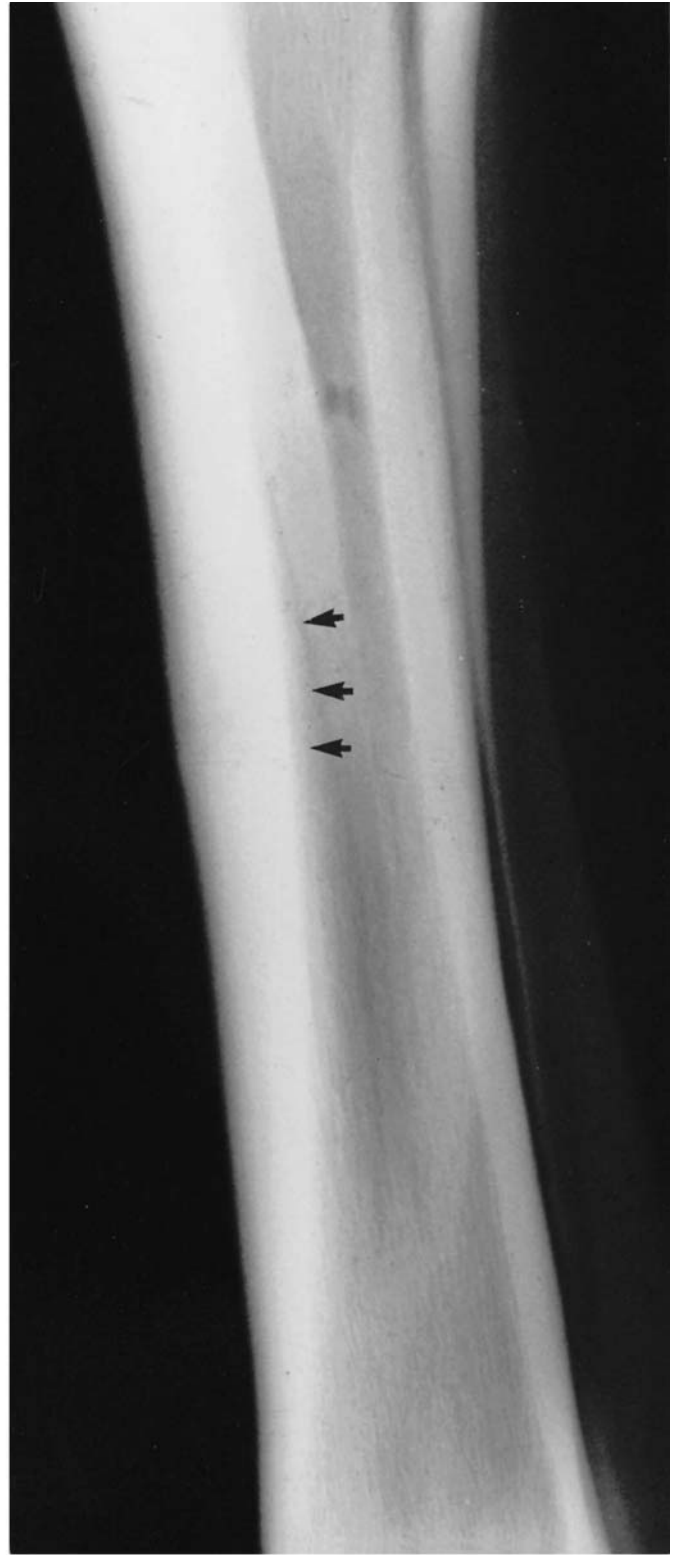
(a)   (b)

Figure 3.15(a) Lateromedial view of the metacarpus of a 3-year-old Thoroughbred. There is soft-tissue swelling over the middle of the dorsal aspect of the metacarpus and an incomplete dorsal cortical 'saucer' fracture of the third metacarpal bone.

Figure 3.15(b) Dorsolateral-palmaromedial oblique view of the same horse as in Figure 3.15(a). Note the endosteal new bone (arrows).

[151]

fracture with associated callus. It is not possible to differentiate radiographically between this condition and periostitis developing secondary to direct trauma. With rest the active bone reaction usually settles within 6 weeks, but can take several months. The new bone may model once it is no longer active. Lameness will recur if work is resumed when the periosteal reaction is still active.

Occasionally, if extensive new bone develops on the axial surface of the second or fourth metacarpal bones, this may result in associated suspensory ligament desmitis and adhesion formation. The significance of the new bone must be assessed in the light of clinical signs. Ultrasonographic examination may also be helpful.

Periostitis/entheseophyte formation in the area of attachment of the suspensory ligament

The suspensory ligament originates from the proximal palmar aspect of the third metacarpal bone. Tearing of the attachment may result in entheseophyte formation or periostitis due to subperiosteal haematoma formation. Radiographic examination may reveal a localized area of increased opacity in the proximal aspect of the bone with or without small patchy lucent zones. In the early stages this is seen only in high-quality dorsopalmar views (Figures 3.16a–d, pages 154 and 155), and comparison with the contralateral limb is often helpful. The presence of radiographic abnormalities associated with proximal suspensory desmitis is seen more commonly in hind limbs than forelimbs. However, increased opacity of the proximal third metatarsal bone may be seen as an incidental finding in dorsoplantar projections, and is not necessarily synonymous with active desmitis. In the forelimb the lesions predominantly involve the medial half of the third metacarpal bone, whereas in the hind limb the lateral half of the third metatarsal bone is more frequently involved.

If entheseophyte formation is extensive it may also be seen in a lateromedial view as an area of increased opacity superimposed over the second or fourth metacarpal bones.

Fatigue (stress) fractures of the palmar cortex of the third metacarpal bone can result in increased opacity of the proximomedial aspect of the third metacarpal bone and a lucent vertical or oblique line or lines may be detectable (Figure 3.25, page 164). The opaque region may extend further distally compared to that associated with proximal suspensory desmitis, and abnormalities are usually not detectable on a lateromedial projection.

Increased opacity seen in a dorsopalmar view may also be due to sclerosis of the trabeculae, which may be seen in the subcortical bone in a lateromedial view (Figure 3.16b). The trabeculae may be orientated more obliquely than usual. The suspensory ligament *per se* should be evaluated ultrasonographically. Nuclear scintigraphy may also be helpful to determine the degree of bony activity. Severe trauma may result in an avulsion fracture of the origin of the suspensory ligament (see page 162).

Extensive pallisading periosteal new bone involving the base and proximal metaphyseal region of the second or fourth metacarpal bones can be seen in association with localized narrowing of the carpometacarpal joint (Figure 3.17, page 156). It is usually associated with chronic lameness.

Infectious osteitis and osteomyelitis

The third metacarpal bone is only protected by a thin layer of soft tissues, and is therefore susceptible to infection following severe skin wounds and trauma to the bone. An open fracture of any of the metacarpal bones may also result in infection. The thick dorsal cortex of the diaphysis of the third metacarpal bone may predispose it to sequestrum formation in its outer one-third, since trauma to the bone may deprive it of its periosteal blood supply, and leave it dependent on medullary vessels traversing the cortex.

Radiographic signs of osteitis are not detectable until at least 7–14 days after the injury when subtle lucent areas may be seen in the cortex. These may be restricted to lucent lines parallel to the margin of the bone, in the outer one-third of the cortex. Earlier diagnosis of infectious osteitis may be possible using ultrasonography. In most cases this progresses to sequestrum formation; a central opaque piece of bone (the sequestrum) is surrounded by a lucent zone (purulent material or granulation tissue) which is in turn bordered by more sclerotic bone (the involucrum) (Figure 3.18, page 157). Periostitis may develop proximal and distal to the sequestrum but does not involve the sequestrum *per se*. Although antibiotic therapy may control clinical signs, removal of the sequestrum is usually required for complete recovery.

Angular limb deformities originating in the diaphysis of the third metacarpal or metatarsal bone

This is a rare condition, which may be congenital. The abnormal limb angulation is noted clinically, but the site of deformity is confirmed radiographically. The limb deviation usually originates in the proximal one-third of the third metacarpal or metatarsal bone. There may be cortical thickening on the concave side of the bone. To correct the condition wedge osteotomy may be considered.

Physitis of the third metacarpal bone

Physitis (physeal dysplasia) of the distal physis of the third metacarpal bone may result in enlargement of the bone and an angular limb deformity of the metacarpophalangeal joint. Radiographically the metaphysis of the bone is broadened and asymmetrical. There is sclerosis of the metaphysis adjacent

Figure 3.16(a) Lateromedial view of the proximal metatarsus of a normal adult horse. Note the regular, linear orientation of the trabeculae and the definition between the cortical and medullary bone.

Figure 3.16(b) Lateromedial view of a proximal metatarsus. There is marked thickening and sclerosis of the plantar cortex of the third metatarsal bone associated with chronic proximal suspensory desmitis. The horse had recurrent lameness.

[154]

Figure 3.16(c) Dorsoplantar view of the proximal metatarsus of a normal adult horse. Note the regular linear orientation of the trabeculae and the clear definition between the proximal subchondral bone plate and the medulla.

Figure 3.16(d) Dorsoplantar view of a proximal metatarsus (see Figure 3.16b). There is increased opacity of the lateral one-half of the third metatarsal bone resulting in loss of definition between the proximal subchondral bone plate and the medulla. This was associated with chronic proximal suspensory desmitis, but can be seen as an incidental finding.

[155]

Figure 3.17 Dorsopalmar view of the proximal metacarpal region of an aged pleasure horse, with lameness associated with pain in this area. There is narrowing of the carpometacarpal joint medially (black arrow) with ill-defined lucent areas in the adjacent subchondral bone. There is irregularly outlined new bone (white arrow) on the abaxial aspect of the second metacarpal bone.

to the physis, which may be more irregular in appearance than normal. The cortices of the bone may be abnormally thick. The epiphysis may appear wedge shaped. Surgical correction of the deviation should ideally be performed before 3 months of age.

Mineralization in the soft tissues

Dystrophic mineralization may occur in the soft tissues, particularly in the suspensory ligament or the digital flexor tendons, as the result of trauma or injection of a medicament. This may be of no clinical significance, but a more thorough clinical appraisal of the structure involved and ultrasonographic examination are indicated.

Hypertrophic osteopathy

Shifting limb lameness associated with variable oedematous swelling of a limb or limbs is the most common clinical feature of hypertrophic osteopathy (Marie's disease) (see Chapter 1, page 15). Careful palpation of the metaphyses and diaphyses of the bones may reveal unusual heat and tenderness. Radiographically the disease is typified by periosteal new bone, which often appears active and extends along the metaphyses and diaphyses (Figure 3.19, page 158). The third metacarpal and metatarsa bones

[156]
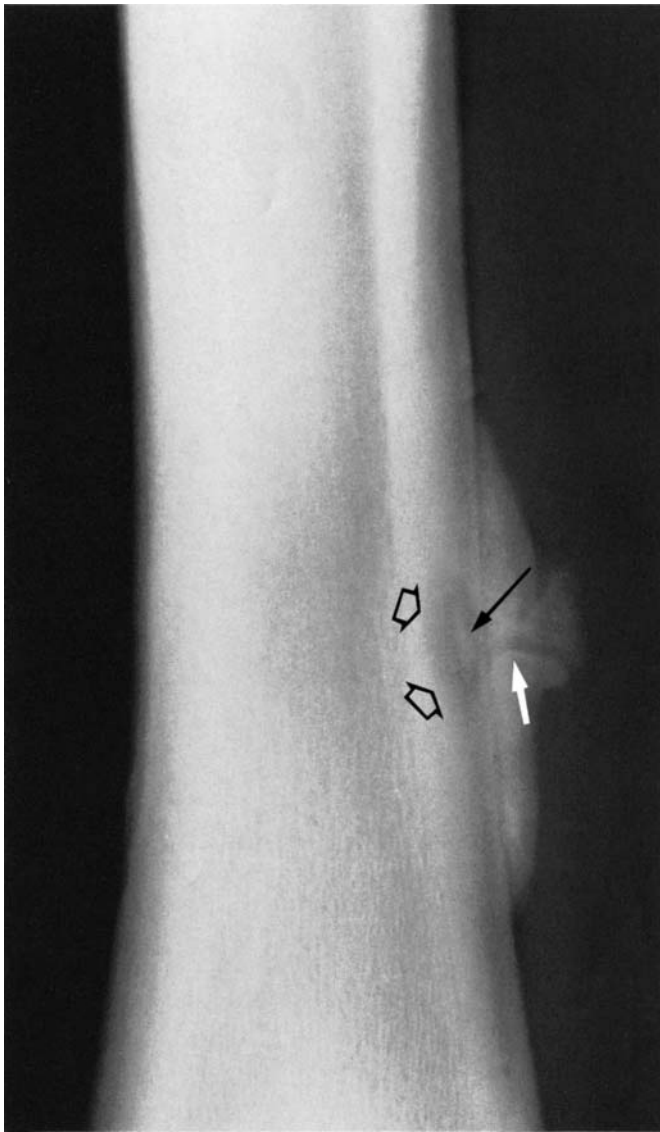
Figure 3.18 Dorsopalmar view of a metacarpus. There is a sequestrum (filled black arrow) and involucrum (open arrows), and extensive periosteal new bone formation with a lucent cloaca (white arrow) and overlying soft-tissue swelling.

are frequently involved. The periosteal reaction must be differentiated from other causes of periostitis and osteitis.

Fractures

Third metacarpal bone

FRACTURES OF THE DISTAL PHYSIS

Fractures of the distal physes of the third metacarpal and metatarsal bones are not uncommon and usually have a Salter-Harris type II configuration

Figure 3.19 Slightly oblique dorsopalmar view of the metacarpus and proximal phalanx of a 3-year-old Thoroughbred colt with hypertrophic osteopathy. There is extensive ill-defined, active periosteal new bone along the distal diaphysis and metaphysis of the third metacarpal bone and the proximal metaphysis of the proximal phalanx (arrows). The primary lesion was an aortic aneurysm (identified *post mortem*).

(see Chapter 1, page 17). Internal fixation is the treatment of choice, and provided that the foal is not less than 8 weeks of age, the longitudinal growth of the bone should not be compromised. Immobilization of the limb in a full-limb cast has been successful in some cases.

FATIGUE FRACTURES OF THE DORSAL CORTEX
('SAUCER' FRACTURES)

Fatigue fractures of the dorsal cortex have been discussed previously (pages 147 and 150).

Fractures of either the medial or, more commonly, the lateral condyle are a common injury in racehorses (Thoroughbreds, Standardbreds and Quarter Horses). There is usually distension of the metacarpophalangeal joint capsule, pain on flexion of the joint, and moderate to severe lameness. If the fracture is incomplete the lameness may resolve temporarily following rest. The fractures either occur adjacent to the sagittal ridge (Figure 3.20), or in the mid-condyles (Figure 3.22, page 162) and may be incomplete with minimal displacement. Some of these fractures extend longitudinally through the diaphysis. Many fractures are complete and 'break out' through the cortex approximately 5–8 cm proximal to the articular surface. Any fracture extending longer than 7.5 cm is likely to be complete. In both the forelimbs and the hind limbs the lateral condyle is most commonly involved (Figure 3.20). Medial condylar fractures are more often incomplete and extend into the diaphysis (Figures 3.21a and 3.21b, page 161).

If the fracture is incomplete it is very important to examine the entire metacarpus. All the standard views should be used, and extra obliques at 5° increments may be necessary to establish whether the fracture extends into the diaphysis. Even with radiographs of excellent quality it may not be possible to identify all the components of the fracture. A dorsodistal-palmaroproximal oblique view to examine the palmar articular surface is important to identify comminution, which cannot be detected in standard views. The sesamoid bones should also be inspected carefully since occasionally they suffer concurrent fractures. Some incomplete, non-displaced fractures are extremely difficult to detect radiographically in the acute stage, and nuclear scintigraphy may be useful to confirm the results of trauma to bone. Follow-up radiographs obtained after 7–10 days may demonstrate the fracture. Simple, non-displaced fractures may be successfully treated by lag screw fixation or, in selected cases, immobilization in a cast and box rest. Displaced fractures require reduction and internal fixation. The presence of Y-shaped fragments at the articular surface (Figure 3.22, page 162) is associated with a poorer prognosis. Long-term persistence of a radiographically detectable lucent fracture line is associated with reduced performance, compared to horses in which the fracture line disappears.

METAPHYSEAL AND DIAPHYSEAL FRACTURES

Incomplete transverse fractures through the palmar or dorsal aspect of the distal diaphysis or metaphysis occur occasionally, and may be bilateral (Figures 3.23a and 3.23b, page 163). They are associated with moderate to severe lameness, and pain can be induced by applying pressure on the palmar or dorsal cortex. These fractures, which are usually incomplete, are best seen in lateromedial and oblique projections. A lucent line traverses the bone horizontally from either the palmar or the dorsal cortex. Within 7–10 days some callus may be identified at the site where the fracture passes through the cortex. These fractures heal satisfactorily with rest.

Fractures of the diaphysis of the third metacarpus usually occur in

Figure 3.20 Dorsoproximal-palmarodistal oblique view of a metacarpus of a 3-year-old Thoroughbred. There is an incomplete lateral condylar fracture. Such a fracture would be obscured by the lateral proximal sesamoid bone in a dorsopalmar view. Ideally a dorsodistal-palmaroproximal oblique view is also required to evaluate better the articular surface to establish whether or not there is comminution.

transverse, spiral or comminuted configurations and are often compound. Clinical signs include severe lameness and readily detectable crepitus. Radiography is used to confirm the orientation of the fractures. In some cases many oblique views are needed to follow the complete course of the fracture(s). The radiographs should be inspected carefully to establish whether involvement of the nutrient foramen has occurred, as this will adversely influence the prognosis. Internal fixation using dynamic compression plates and lag screws may result in complete recovery.

Incomplete oblique sagittal dorsal cortical fractures occur occasionally in young Thoroughbred racehorses. These fractures are orientated in a
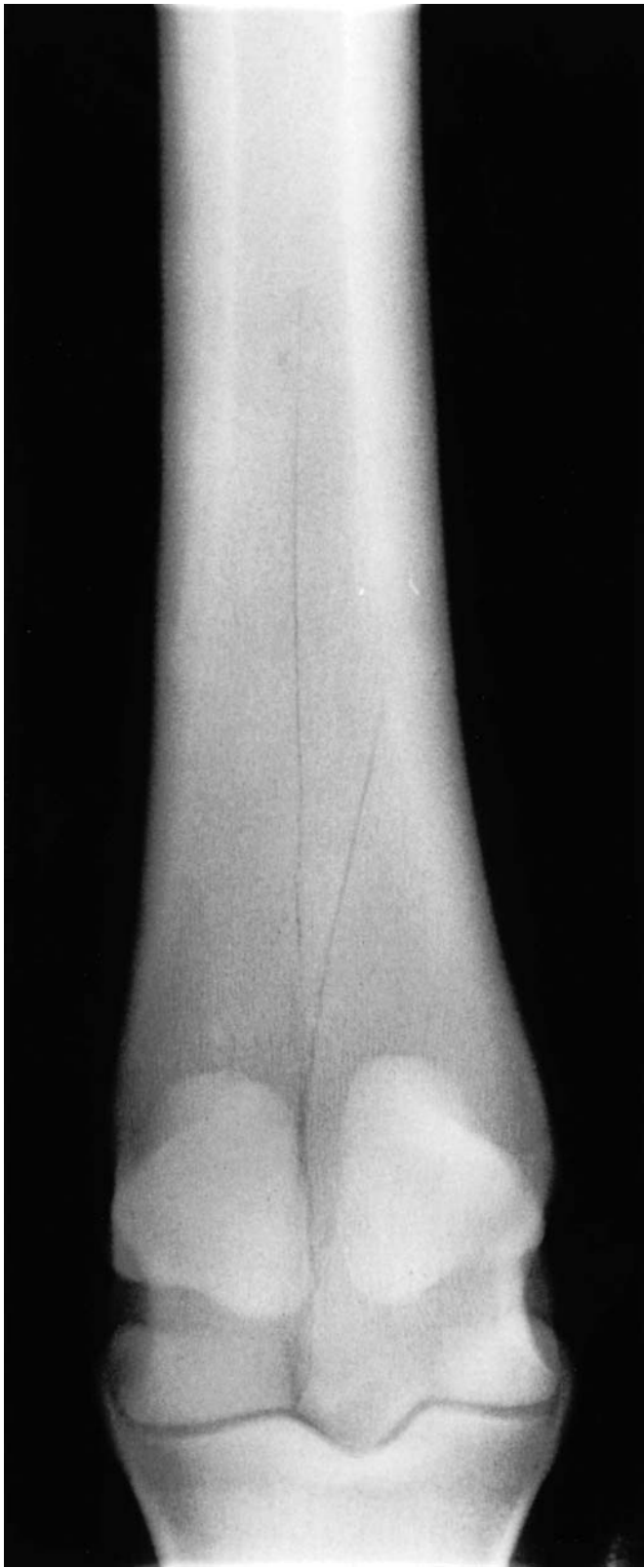
(a)
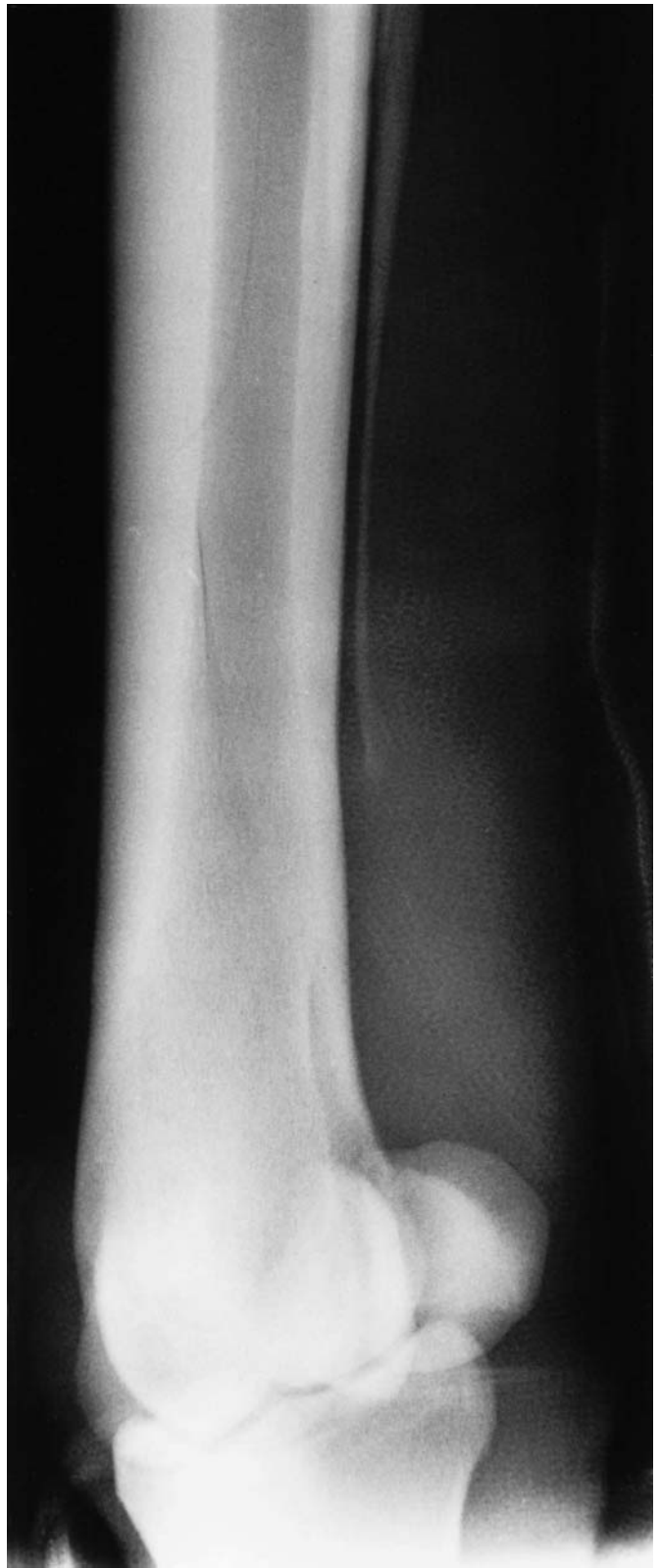
(b)

Figure 3.21 Dorsoplantar (a) and plantarolateral-dorsomedial oblique (b) views of a metatarsus of a 4-year-old Thoroughbred. There is an incomplete medial condylar fracture which spirals proximally in the diaphysis. The limb is in a cast incorporating the foot, extending to the hock.

[161]

Figure 3.22 Dorsodistal-palmaroproximal (extended) oblique view of the metacarpophalangeal joint of a 5-year-old Thoroughbred racehorse with acute onset forelimb lameness of 2 weeks' duration. There is a fracture of the lateral condyle of the third metacarpal bone. Note the Y-shaped comminution (arrows) at the articular surface. This is not visible in standard projections.

proximolateral-distomedial direction, within the dorsal cortex, at an angle of 20–30° to the long axis of the bone. They are best identified in palmarodorsal views.

Avulsion fractures of the origin of the suspensory ligament cause a variable degree of lameness which may be relieved by subcarpal local analgesia. Similar fractures may occur slightly distal to the site of attachment of the suspensory ligament; the aetiology of these is unknown. Radiographically these fractures are identified as lucent crescent-shaped lesions in the metaphysis in a dorsopalmar view (Figure 3.24, page 164) or as separate bone fragments on the palmar aspect in a lateromedial or a flexed lateromedial projection. They occur in both the forelimb and the hind limb. Ultrasonography may be more sensitive in identifying some small avulsed fragments, and is helpful to determine the presence of concurrent suspensory desmitis. Lameness usually resolves satisfactorily with rest.

Similar clinical signs may also be associated with fatigue fractures of the palmar cortex of the proximal one-third of the third metacarpal bone. In a

Figure 3.23(a) Dorsolateral-palmaromedial oblique view of the distal metacarpus of a mature riding horse who had had a sudden onset of bilateral forelimb lameness 12 days previously. There is an ill-defined lucent fracture line traversing the distal metaphysis and extensive ill-defined periosteal new bone (callus) on the dorsal and palmar aspects. The horse had sustained bilateral fractures, was treated conservatively, and made a complete recovery.

Figure 3.23(b) Dorsolateral-palmaromedial oblique view of a distal metacarpus of a 7-year-old steeplechaser with chronic lameness of several weeks' duration. There is a curved lucent line through the metaphysis of the third metacarpal bone with some surrounding sclerosis. This is an incomplete metaphyseal fracture. Note also the rather unusual configuration of the distal aspect of the fourth metacarpal bone. The horse was treated conservatively and made a complete recovery.

dorsopalmar view these are evident radiographically as subtle vertical lucent lines (the fracture seen 'end-on') in the metaphysis usually with surrounding sclerosis of the trabecular bone (Figure 3.25). Fatigue fractures occur most often in the medial one-half of the third metacarpal bone. Sometimes no fracture line is detectable, only medullary sclerosis. This is particularly so in the less lame limb of a bilaterally lame horse. Development of sclerosis, the result of microfractures, may precede the onset of lameness. Less commonly the fracture is seen only in an oblique view, although increased opacity is seen on a dorsopalmar projection. Increased opacity should be differentiated from that associated with chronic proximal suspensory desmitis (see page 152). Nuclear scintigraphy might enable

[163]

Figure 3.24 Dorsopalmar view of a metacarpus of a 6-year-old steeplechaser with sudden onset of lameness 12 days previously. Lameness was alleviated by subcarpal analgesia. There is a curved lucent line in the third metacarpal bone (arrow) which probably represents an incomplete avulsion fracture of the origin of the suspensory ligament. The horse was treated conservatively and made a complete recovery.

Figure 3.25 Dorsopalmar view of a metacarpus of a 5-year-old hurdler with recurrent lameness of several weeks' duration. Lameness was alleviated by subcarpal analgesia. There is an ill-defined approximately vertical lucent line (arrows) in the medial half of the third metacarpal bone with surrounding sclerosis of the trabecular bone. This is a palmar cortical fatigue fracture. The horse was treated conservatively and made a complete recovery.

detection of these fractures earlier and may aid interpretation of subtle alterations in the trabecular pattern of the bone. It may also provide a more accurate indicator of satisfactory healing than radiography. Lameness usually resolves satisfactorily with rest (3 months).

Articular fractures of the dorsoproximal medial aspect of the third metacarpal bone have been identified in Standardbred racehorses (pacers). These fractures are best identified in a dorsolateral-palmaromedial oblique projection. Satisfactory healing usually occurs with conservative management.

Third metatarsal bone

Incomplete articular fractures of the dorsoproximal aspect of the third metatarsal bone have been seen in association with osteophyte formation

[164]

on the dorsal aspect of the tarsometatarsal joint in young Thoroughbred racehorses, and occasionally in older performance horses. These fractures are difficult to identify radiographically unless the x-ray beam passes through the fracture plane. They are usually best seen in a projection which superimposes the lateral and medial trochlea tali. Similar complete fractures have been identified in Standardbred racehorses. Lameness is acute in onset and moderate, and is alleviated either by intra-articular analgesia of the tarsometatarsal joint or by perineural analgesia of the fibular and tibial nerves. Nuclear scintigraphy may be useful to focus attention on the proximal metatarsus. In both Thoroughbreds and Standardbreds there is frequently pre-existing periarticular new bone formation on the dorsoproximal aspect of the third metatarsal bone. Abnormal bone may predispose to fracture. The prognosis for return to full athletic function without recurrent lameness is guarded. Although the fracture may heal, there is often further development of periarticular new bone or degenerative changes within the tarsometatarsal joint.

Second and fourth metacarpal/metatarsal bones

Fractures involving the proximal one-half of the second and fourth metacarpal bones are usually the result of external trauma and may be comminuted. There is a high risk of secondary infection, especially if the fracture is open. Surgical stabilization may be required, since weight is transmitted through the second and fourth metacarpal bones. Fractures of the proximal third of the second or fourth metatarsal bone can often be conservatively treated, with success. The carpal bones should be inspected for evidence of a concurrent fracture, which will adversely influence the prognosis (see also page 203).

A fracture at the junction between the middle and distal one-thirds of the second or fourth metacarpal bones is often seen in association with suspensory desmitis, but may be the result of external trauma. The fracture may not be detectable clinically without radiographic examination, especially if there is widespread swelling. The suspensory ligament should be assessed carefully, preferably using ultrasound, and the proximal sesamoid bones radiographed if indicated. If the fracture is displaced distally (Figure 3.26a) a non-union may result. The fracture fragment often does not cause a problem if left *in situ*, but may be removed surgically. The majority of fractures which are treated conservatively do heal within 2 months (Figure 3.26b) although there may be considerable callus formation (Figure 3.26c) and small lucent defects may persist. The callus models and often reduces in size, but some enlargement of the bone persists. Simple fractures of the second and fourth metacarpal (metatarsal) bones have a good prognosis, but associated suspensory ligament desmitis warrants a more guarded prognosis. Surgical removal of the fracture may be indicated if there is a malunion with adhesion to the suspensory ligament.

Figure 3.27 (page 168) summarizes common fracture sites in the metacarpus and the metatarsus.

Figure 3.26(b) Dorsomedial-palmarolateral oblique view of a metacarpus. There is a healed fracture of the distal aspect of the second metacarpal bone. Note also the rather curved configuration of the bone, suggestive of possible adhesions with adjacent soft tissues.

Figure 3.26(a) Dorsomedial-plantarolateral oblique view of a metatarsus. There is soft-tissue swelling and an old displaced non-union fracture of the second metatarsal bone. Note also the irregular contour of the plantar cortex of the third metatarsal bone. Soft-tissue swelling is due to concurrent suspensory desmitis.
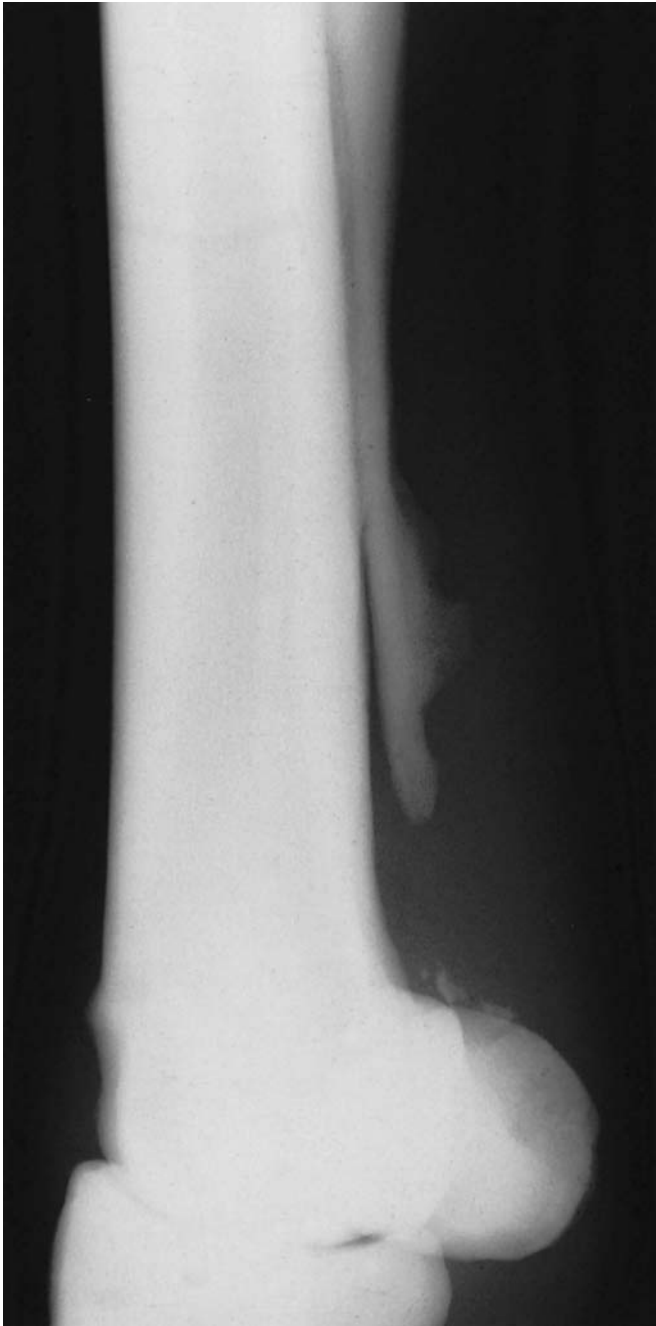
Figure 3.26(c) Dorsomedial-palmarolateral oblique view of a metacarpus. There is considerable modelling of the distal end of the second metacarpal bone, the result of a previous fracture and excessive callus formation. Note also the mineralization proximal to the proximal sesamoid bones reflecting associated suspensory desmitis.

Ross and Martin (1992)
Ross *et al.* (1993)
Pilsworth (1992)

Allen and White (1982)
Bowman and Fackleman (1982)

Bramlage *et al.* (1980)
Dyson (1988)
Ross *et al.* (1988)

Haynes (1980)
Richardson (1984)
Smallwood (1979)
Stashack (1987)

Bowman *et al.* (1982)
Verschooten *et al.* (1984)

Crawford and Fretz (1985)
Dixon and Bellinger (1968)
Grossman and Nickles (1979)
Stashack (1987)

McClure *et al.* (1998)

Embertson *et al.*
(1986)

Barclay *et al.* (1985)
Greet (1987)
Richardson (1984)
Rick *et al.* (1983)
Bassage and Richardson (1998)

Figure 3.27 Common fracture sites in the metacarpus and metatarsus, and recommended references (see 'Further reading').

FURTHER READING

Allen, D. and White, N. (1982) Management of proximal splint fractures and exostoses in the horse. *Proc. Am. Ass. Equine Pract.*, **28**, 89–95

Barclay, W., Foerner, J. and Phillips, T. (1985) Axial sesamoid injuries associated with lateral condylar fractures in horses. *J. Am. Vet. Med. Ass.*, **186**, 278–279

Bassage, L. and Richardson, D. (1998) Longitudinal fractures of the condyles of the third metacarpal and metatarsal bones in racehorses: 224 cases (1986–1995). *J. Am. Vet. Med. Ass.*, **212**, 1757–1764

Bowman, K. and Fackleman, G. (1982) Surgical treatment of complicated fractures of the splint bones in horses. *Vet. Surg.*, **11**, 121–124

Bowman, K., Evans, L. and Herring, M. (1982) Evaluation of surgical removal of fractured distal splint bones in the horse. *Vet. Surg.*, **11**, 116–120

Bowman, K., Sweeney, C. and Tate, L. (1987) Compression plating of a medial condylar fracture of the third metatarsal bone in a Thoroughbred filly. *J. Am. Vet. Med. Ass.*, **190**, 305–307

Bramlage, L., Gabel, A. and Hackett, R. (1980) Avulsion fractures of the origin of the suspensory ligament in the horse. *J. Am. Vet. Med. Ass.*, **176**, 1004–1010

Caron, J., Barber, S., Doige, C. and Pharr, J. (1987) The radiographic and histologic appearance of controlled surgical manipulation of the equine periosteum. *Vet. Surg.*, **16**, 13–20

Crawford, W. and Fretz, P. (1985) Long bone fractures in large animals: a retrospective study. *Vet. Surg.*, **14**, 259–302

Dixon, R. and Bellinger, C. (1968) Fissure fractures of the equine metacarpus and metatarsus. *J. Am. Vet. Med. Ass.*, **153**, 1289–1291

Dyson, S. (1988) Some observations on lameness associated with the proximal metacarpal region in the horse. *Equine Vet. J.*, Suppl. **6**, 43–52

Dyson, S. (1991) Proximal suspensory desmitis: clinical, radiographic and ultrasonographic features in 42 horses. *Equine Vet J.*, **23**, 25–31

Dyson, S. (1994) Proximal desmitis in the hindlimb: 42 cases. *Br. Vet. J.*, **150**, 279–291

Embertson, R., Bramlage, L. and Gabel, A. (1986a) Physeal fractures in the horse: Management and outcome. *Vet. Surg.*, **15**, 230–236

Embertson, R., Bramlage, L., Herring, D. and Gabel, A. (1986b) Physeal fractures in the horse: classification and incidence. *Vet. Surg.*, **15**, 223–229

Greet, T. (1987) Condylar fractures of the cannon bone with axial sesamoid fracture in 3 horses. *Vet. Rec.*, **120**, 223–225

Grossman, B. and Nickels, F. (1979) Repair of a metatarsal fracture with transfixation pins and plaster casts. *Equine Pract.*, **1**(6), 13–16

Haynes, P. (1980) Disease of the metacarpophalangeal joint and the metacarpus. *Vet. Clin. N. Am.: Large Anim. Pract.*, **2**(1), 33–59

Hornhof, W. and O'Brien, T. (1980) Radiographic evaluation of the palmar aspect of the equine metacarpal condyles: a new projection. *Vet. Radiol.*, **21**, 161–167

Huskamp, B. and Nowak, M. (1988) Insertion desmopathies in the horse. *Pferdheilkunde*, **4**, 3–12

Lloyd, K., Koblik, P., Ragle, C., Wheat, J. and Lakritz, J. (1988) Incomplete palmar fractures of the proximal extremity of the third metacarpal bone in the horse: ten cases (1981–1986). *J. Am. Vet. Med. Ass.*, **192**(6), 798–803

McClure, S., Watkins, J., Glickman, N. *et al* (1998) Complete fracture of the third metacarpal or metatarsal bone in horses: 25 cases (1980–1986) *J. Am. Vet. Med. Ass.*, **213**, 847–850

Moens, Y., Verschooten, F., De Moor, A. and Wouters, L. (1980) Bone sequestration as a consequence of limb wounds in the horse. *Vet. Radiol.*, **21**, 40–44

Pilsworth, R. (1992) Incomplete fracture of the dorsal aspect of the proximal cortex of the third metatarsal bone as a cause of hindlimb lameness in the racing Thoroughbred: a review of 3 cases. *Equine Vet. J.*, **24**, 147–150

Pilsworth, R., Hopes, R. and Greet, T. (1988) Use of a flexed dorsopalmar (plantar) projection of the fetlock joint to demonstrate lesions of the distal third metacarpal (tarsal) bone in the horse. *Vet. Rec.*, **122**, 332–333

Richardson, D. (1984) Dorsal cortical fractures of the equine metacarpus. *Comp. Cont. Educ.*, **6**, S248–254

Richardson, D. (1984) Medial condylar fractures of the third metatarsal bone in horses. *J. Am. Vet. Med. Ass.*, **185**, 761–765

Rick, M., O'Brien, T., Pool, R. and Meagher, D. (1983) Condylar fractures of the third metacarpal bone and third metatarsal bone in 75 horses: radiographic features, treatments and outcome. *J. Am. Vet. Med. Ass.*, **183**, 287–296

Rose, R. (1978) Surgical treatment of osteomyelitis in the metacarpal and metatarsal bones of the horse. *Vet. Rec.*, **102**, 498–500

Ross, M. and Martin, B. (1992) Dorsomedial articular fracture of the proximal aspect of the third metacarpal bone in Standardbred racehorses: seven cases (1978–1990) *J. Am. Vet. Med. Ass.*, **201**, 332–335

Ross, M., Ford, T. and Orsini, P. (1988) Incomplete longitudinal fracture of the proximal palmar cortex of the third metacarpal bone in horses. *Vet. Surg.*, **17**, 82–86

Ross, M., Sponseller, M., Gill, H. and Moyer, W. (1993) Articular fracture of the dorsoproximolateral aspect of the third metatarsal bone in five Standardbred racehorses. *J. Am. Vet. Med. Ass.*, **203**, 698–700

Smallwood, J. (1979) Evaluation of the 'bucked shin syndrome' using xeroradiography. *Equine Pract.*, **1**(2), 28–35

Stashak, T. (1987) The metacarpus and metatarsus. In *Adams' Lameness In Horses* 4th edn, Lea and Febiger, Philadelphia, pp. 596–624

Verschooten, F., Gasthuys, F. and De Moor, A. (1984) Distal splint bone fractures in the horse: an experimental and clinical study. *Equine Vet. J.*, **16**, 532–536

Watt, B., Foerner, J. and Haines, G. (1998) Incomplete oblique sagittal fracture of the dorsal cortex of the third metacarpal bone in six horses. *Vet. Surg.*, **27**, 337–341

White, K. (1983) Diaphyseal angular limb deformities in 3 foals. *J. Am. Vet. Med. Ass.*, **182**, 272–279

Chapter 4
The Carpus

RADIOGRAPHIC TECHNIQUE

The carpus consists of three principal joints – antebrachiocarpal (radio-carpal), middle carpal (intercarpal) and carpometacarpal. Articulations also exist between adjacent bones in each row of carpal bones. This causes overlying images which may confuse interpretation. Consequently it is important to obtain at least five standard views.

Equipment

Portable x-ray machines are adequate for radiography of the carpus and a grid is not required. High definition screens and films are preferable, although rare earth screens and compatible films can be used. The faster screen and film combinations tend to lack contrast and definition. A grid may be useful if the carpal region is very swollen.

Positioning

Examinations are best carried out with the horse standing, and sedation is usually unnecessary.

All examinations should include lateromedial, dorsopalmar, dorsal 45° lateral-palmaromedial oblique, dorsal 45° medial-palmarolateral oblique, and flexed lateromedial views. If degenerative joint disease is suspected it may also be helpful to obtain dorsal 75° lateral-palmarodistal oblique and dorsal 75° medial-palmarolateral oblique views to evaluate better the entire joint margins. For suspected fractures, it is often necessary to take further oblique views at different angles, as well as dorsoproximal-dorsodistal oblique ('skyline') views. Consistency of the angle of the views will greatly aid film reading.

Lateromedial, dorsopalmar and oblique views

Lateromedial, dorsopalmar and oblique views are all obtained with the horse standing bearing weight evenly on all four limbs, with the limb to be radiographed vertical. Dorsopalmar and most oblique views are obtained with the x-ray beam aligned horizontally, and the cassette held vertically, at right angles to the beam. The joints slope distally to a varying degree towards their lateral or medial aspects. For this reason the x-ray beam may need to be angled slightly up or down in order to give good visualization of the joints on lateromedial views. The x-ray beam should be centred on the middle carpal joint or on a site of particular interest. In order to obtain true

lateromedial and dorsopalmar views of the joints the x-ray beam should be orientated relative to the limb, rather than the trunk of the horse.

Flexed lateromedial views

The flexed lateromedial view is of great assistance to separate some of the overlying bone images. Chip fractures are often most easily seen on this view.

  The horse should stand squarely on all four limbs. The limb to be radiographed is then lifted by an assistant who stands against, or just behind, the shoulder of the horse, facing in the same direction as the horse. The toe of the foot is rested on the assistant's leg to help keep the limb steady and also to enable the limb to be repositioned accurately if subsequent films are needed. It is important not to rotate the limb, and the foot should be supported vertically below the elbow (Figure 4.1). The x-ray beam is initially maintained horizontal, at right angles to the long axis of the limb. Slight changes in alignment of the x-ray beam may need to be made subsequently to allow better visualization of specific lesions.

Flexed dorsoproximal-dorsodistal oblique (skyline) views

Dorsoproximal-dorsodistal oblique views of the carpus are essential to visualize some slab fractures, to establish their extent, and to detect pathology not apparent in the standard views (see also 'Degenerative joint disease' page 190, 'Sclerosis of the third carpal bone', page 194 and 'Saggital fracture of the third carpal bone', page 201).

  An assistant holds the limb to be examined with the carpus flexed, and slightly in front of the carpus of the contralateral limb, trying to keep the metacarpal region horizontal (Figure 4.2). The cassette is placed against the dorsal aspect of the third metacarpal bone, with its centre level with the carpus. The degree of flexion of the carpus which can be achieved depends on the amount of pain induced by flexion. The angle of the x-ray beam
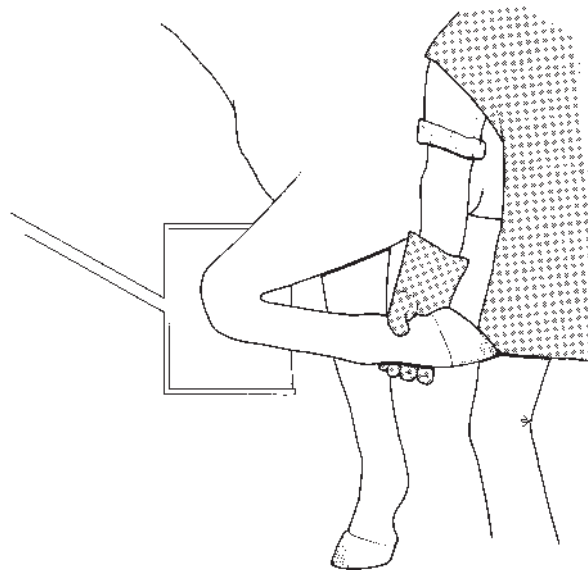
Figure 4.1 Positioning to obtain a flexed lateromedial view of the carpus.
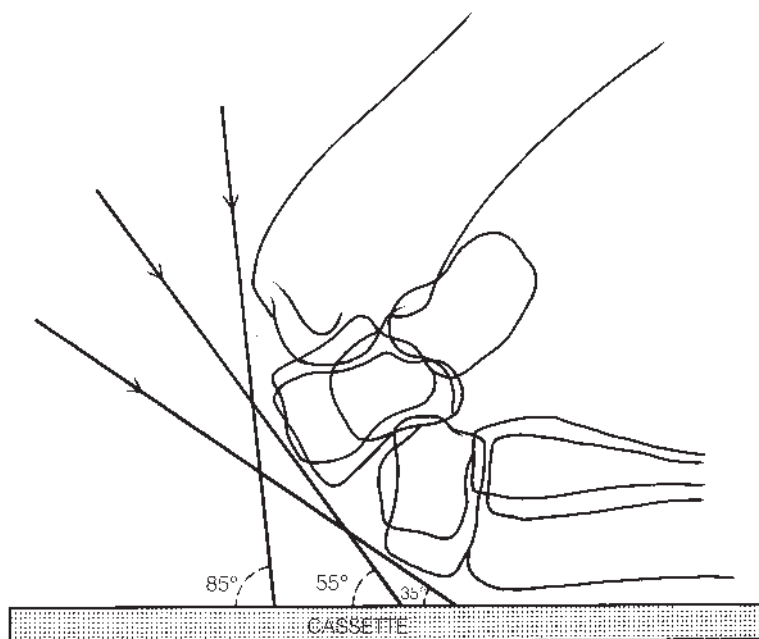
Figure 4.2 Positioning to obtain dorsoproximal-dorsodistal oblique views of the carpus. The three different angles of the x-ray beam allow visualization of the distal radius, proximal row of carpal bones, or distal row of carpal bones.

required to visualize the distal radius, and proximal and distal rows of carpal bones, is therefore variable. The radiographer must try to visualize the positions of the radius and the carpal bones in relation to the degree of flexion. In a fully flexed carpus the following guide can be given:

● To project an image of the distal radius, the x-ray beam is aligned at approximately 85° to the cassette (Figure 4.2), pointing obliquely downward through the flexed carpus. This is often most easily achieved if the carpus is allowed to drop towards the ground.

● To project an image of the proximal row of carpal bones, the beam is aligned at approximately 55° to the cassette (Figure 4.2).

● To project an image of the distal row of bones, the beam is aligned at approximately 35° to the cassette (Figure 4.2).

NORMAL ANATOMY

Immature horse

The distal radius has two ossification centres. The lateral styloid process (morphologically the distal end of the ulna) is separate at birth and fuses with the epiphysis in the first year of life. Oblique views of the carpus in a skeletally mature horse may demonstrate a radiolucent line between the styloid process and the distal radius. This line is more pronounced in young horses, but may persist to varying degrees throughout life. The distal radial physis closes at about 20 months of age.

At birth the joint spaces appear wider than in the mature horse, since endochondral ossification is incomplete and therefore the cartilage is thicker (Figures 4.3a and 4.3b). The carpal bones should be approximately cuboidal. Rounded margins to the bones indicate that they are incompletely ossified (see 'Incomplete carpal ossification', page 198).

[173]
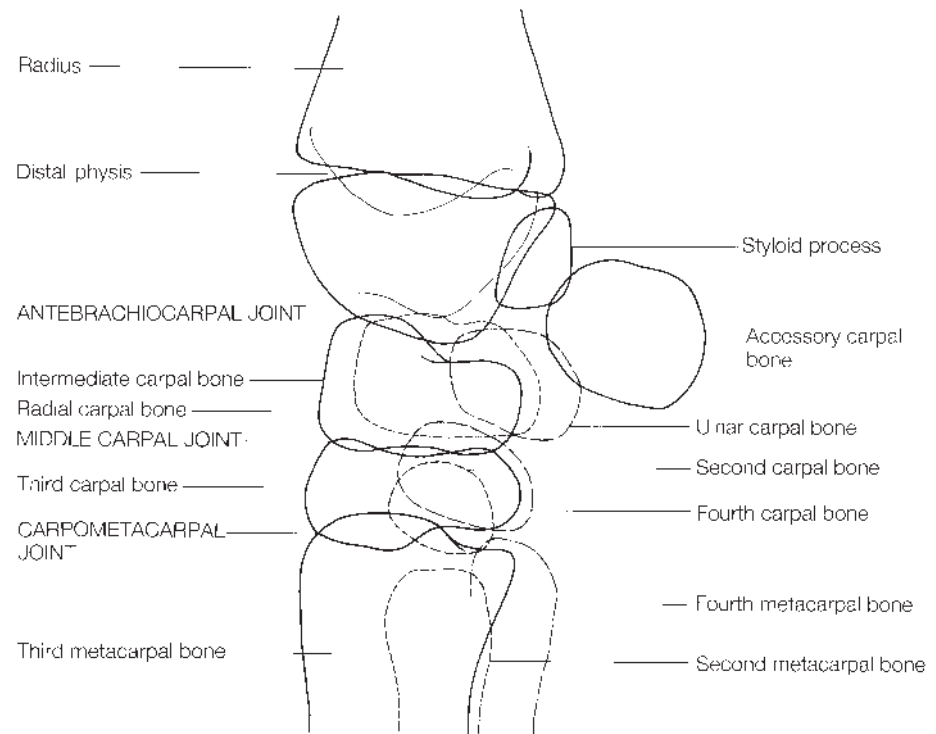
Figure 4.3(a) Lateromedial view and diagram of a carpus of a normal 5-day-old foal.

Distal physis ———

ANTEBRACHIOCARPAL JOINT

MIDDLE CARPAL JOINT ———

CARPOMETACARPAL JOINT

——— Styloid process

——— Accessory carpal bone
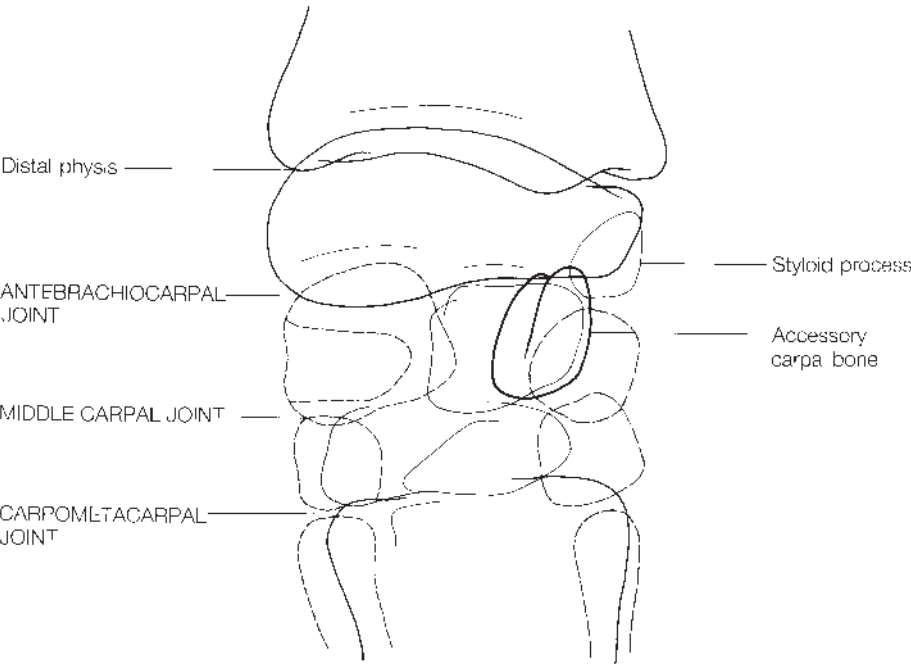
Figure 4.3(b) Dorsopalmar view and diagram of a carpus of a normal 5-day-old foal.

[175]

Each of the carpal bones ossifies from a single centre and is fully developed by 18 months of age.

The third metacarpal bone has a proximal epiphysis, which is fused with the metaphysis at birth.

Skeletally mature horse

The carpus is complex, and it may be necessary to compare images from several different views to ensure that suspected lesions are not due to overlying images.

Figure 4.4 Lateromedial view and diagram of a normal adult carpus.

The distal radius has a prominent transverse ridge caudally. Medially and laterally the medial and lateral collateral ligaments of the carpus attach. Immediately distal to the ridge are depressions for attachment of carpal ligaments. This transverse ridge is not the origin of the accessory ligament of the superficial digital flexor tendon, which arises from a longitudinal ridge approximately 10–15 cm proximal to the antebrachio-carpal joint.

The lateromedial view (Figure 4.4) demonstrates the two rows of carpal bones clearly delineated by the antebrachiocarpal, middle carpal and carpometacarpal joints. These joints are represented by double lucent lines, as they undulate, rather than forming flat parallel planes. It is possible to eliminate the double line in local areas by altering the angle of the beam and/or the point at which it is centred.

On a true lateromedial view, the bone projected most dorsally in the proximal row is the intermediate carpal. This bone has a relatively straight dorsal border, well defined proximally and distally where it meets the articular surfaces at approximately a right angle. Very slight dorsolateral-palmaromedial obliquity will make the radial carpal bone most prominent.

Figure 4.4 *Cont'd*

[177]
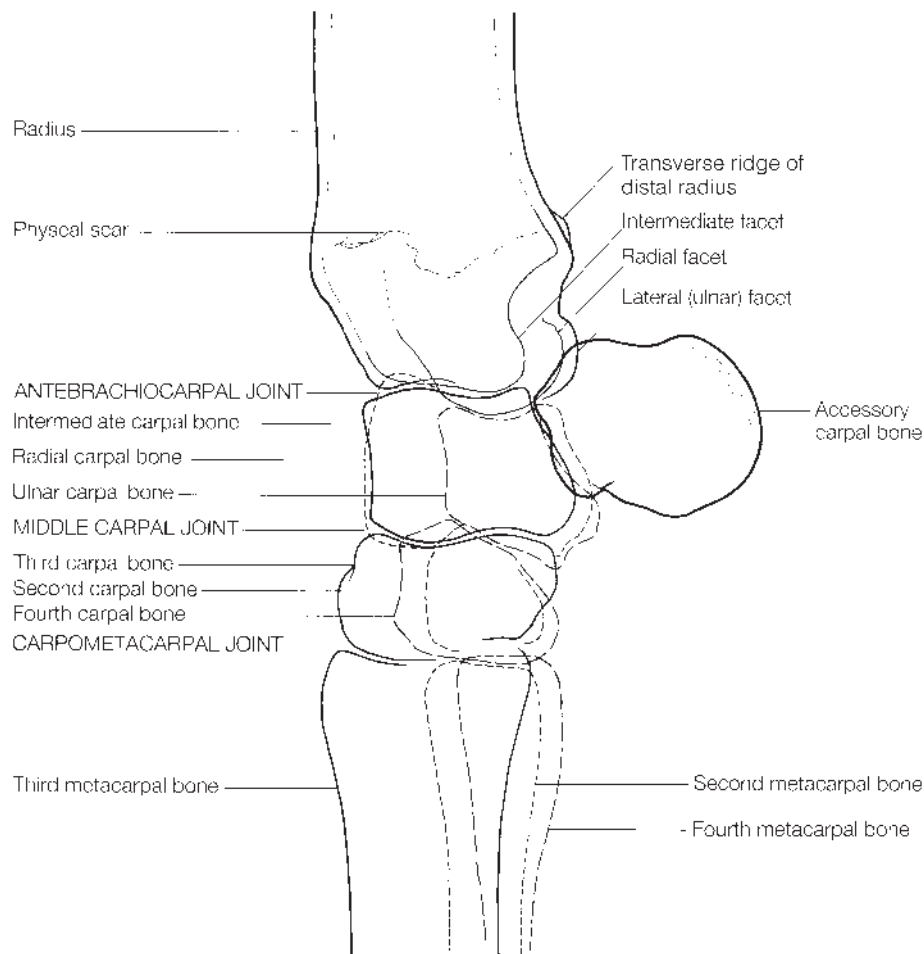
The most dorsal of the distal row of carpal bones is the third carpal. The middle third of this bone often protrudes dorsally. The dorsal surface meets the articular surfaces at approximately a right angle.

The accessory carpal bone is relatively thin, but thickens at its palmar aspect where there are tendon and ligament insertions. There is a vertical radiolucent line close to the palmar surface caused by edge enhancement.

One or two focal radiolucencies may be seen on the dorsal aspect of the antebrachiocarpal joint. These represent fat in the joint capsule, and lie palmar to the synovial sheath of the extensor carpi radialis tendon. Distension of the joint capsule may obscure these lucent areas.
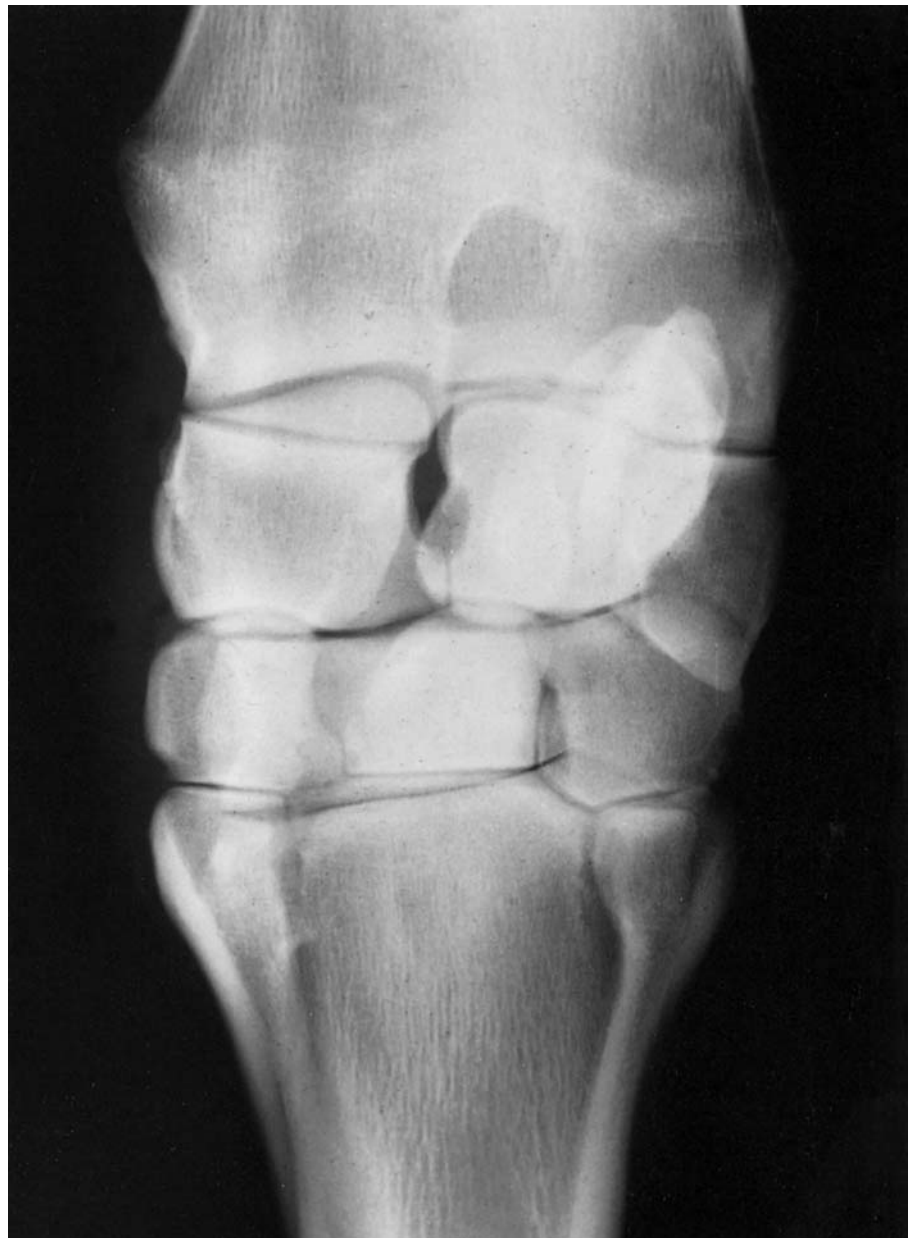
Figure 4.5 Dorsopalmar view and diagram of a normal adult carpus.

Dorsopalmar views

There is a large approximately circular lucent zone in the centre of the distal end of the radius, which is caused by a depression (between the medial and lateral styloid processes) in the caudal surface of the bone.

Figure 4.5 shows the individual carpal bones seen on the dorsopalmar radiograph, and the reader is referred to this figure for their identification. A radiolucent canal is normally seen between the radial and intermediate carpal bones on this projection.

Oblique views

Standard oblique views are shown in Figures 4.6 (page 180) and 4.7 (page 181), but their appearance is greatly affected by the degree of obliquity. Interpretation of oblique radiographs is therefore facilitated by comparison with an anatomical specimen.

Flexed lateromedial view

In the flexed lateromedial view (Figure 4.8, page 182) the distal end of the radius will normally be projected as three distinct articular surfaces, that with the largest radius of curvature being the radial facet, the smallest the intermediate facet, and the lateral or ulnar facet having an intermediate radius of curvature.

Figure 4.5 *Cont'd*

[179]

Radius -

Physeal scar

Incomplete fusion between
lateral styloid process and
distal epiphysis of radius

ANTEBRACHIOCARPAL JOINT

Radial carpal bone

Intermediate carpal bone — —

MIDDLE CARPAL JOINT

Second carpal bone

Third carpal bone

CARPOMETACARPAL JOINT

Third metacarpal bone

Second metacarpal bone

Accessory carpal bone

Ulnar carpal bone

Fourth carpal bone

Fourth metacarpal
bone

Figure 4.6 Dorsal 45° lateral-
palmaromedial oblique view and
diagram of a normal adult carpus.

Radius

Physeal scar

ANTEBRACHIOCARPAL JOINT

Intermediate carpal bone
Ulnar carpal bone
MIDDLE CARPAL JOINT
Fourth carpal bone
Third carpal bone
CARPOMETACARPAL JOINT

Third metacarpal bone

Fourth metacarpal bone

Accessory carpal bone

Radial carpal bone

Second carpal bone

Second metacarpal
bone
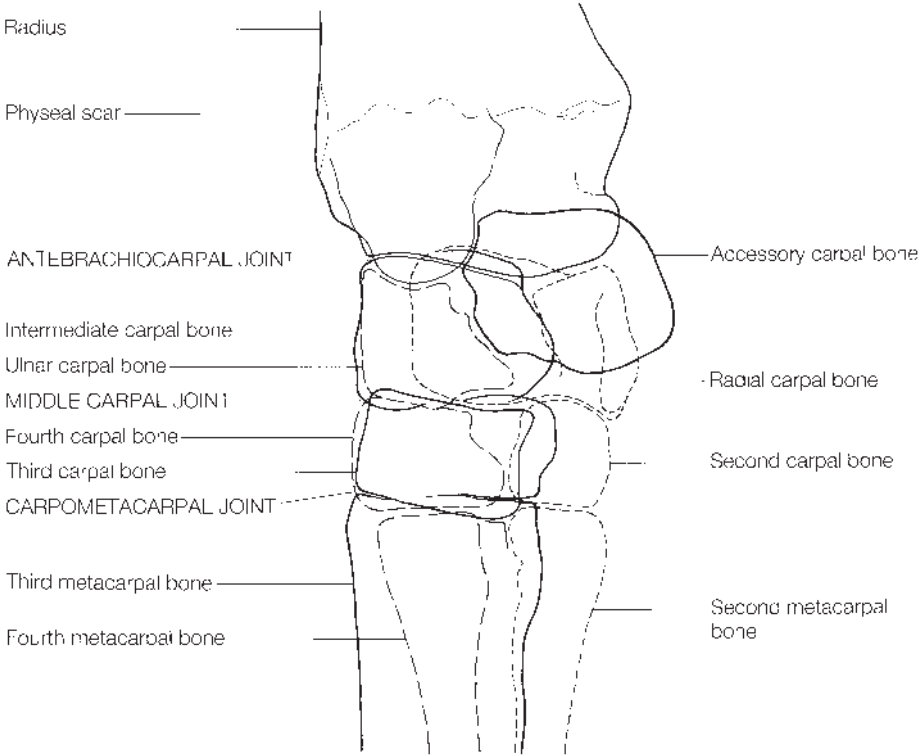
Figure 4.7 Dorsal 45° medial-palmarolateral oblique view and diagram of a normal adult carpus.

[181]

Figure 4.8 Flexed lateromedial view and diagram of a normal adult carpus.

As the carpus is flexed, the accessory carpal bone gradually rotates around a horizontal axis, and so appears slightly shorter in a proximal to distal direction than on a standing lateral view.

The majority of carpal flexion occurs at the antebrachiocarpal joint, with some flexion at the middle carpal joint. As the carpus flexes, the intermediate carpal bone moves proximally relative to the radial carpal bone. The proximal border of the fourth carpal bone is seen proximal to the third, and the dorsal surface of the third is dorsal to the fourth. The carpometacarpal joint does not open appreciably during flexion. The first and or the fifth carpal bones, if present, are easily seen.

[182]

Intermediate facet
Lateral (ulnar) facet
Radial facet
Intermediate carpal bone

Radial carpal bone
Fourth carpal bone
Third carpal bone
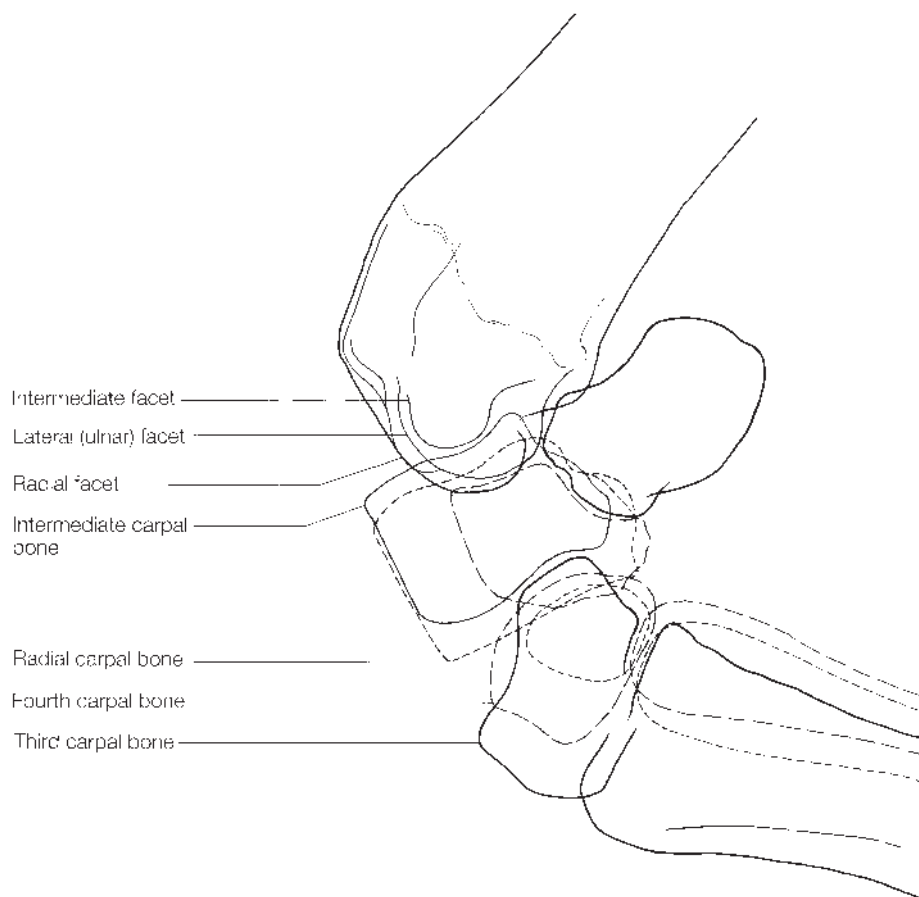
Figure 4.8 *Cont'd*

Dorsoproximal-dorsodistal oblique views

It is necessary to obtain separate views to evaluate the distal radius, and the proximal and distal rows of carpal bones.

The distal radius has a continuous outline, with two distinct grooves on the dorsal aspect (Figure 4.9a). The outline of the proximal row of carpal bones may be seen superimposed on the image of the radius on overexposed radiographs.

In the proximal row of carpal bones (Figure 4.9b) the dorsal borders of the radial and intermediate carpal bones are clearly outlined, with their articulation near the midline. The ulnar carpal bone can be seen laterally.

In the distal row of carpal bones (Figure 4.9c) the third carpal bone is central, with the second and fourth carpal bones at the medial and lateral aspects respectively.

Each carpal bone should have a smooth outline, with an even trabecular pattern and sharply defined corticomedullary border.

NORMAL VARIATIONS AND INCIDENTAL FINDINGS

In a lateromedial or slightly oblique lateromedial view there is a smoothly outlined prominence on the caudal and cranial aspects of the radius at the

(a)

(b)
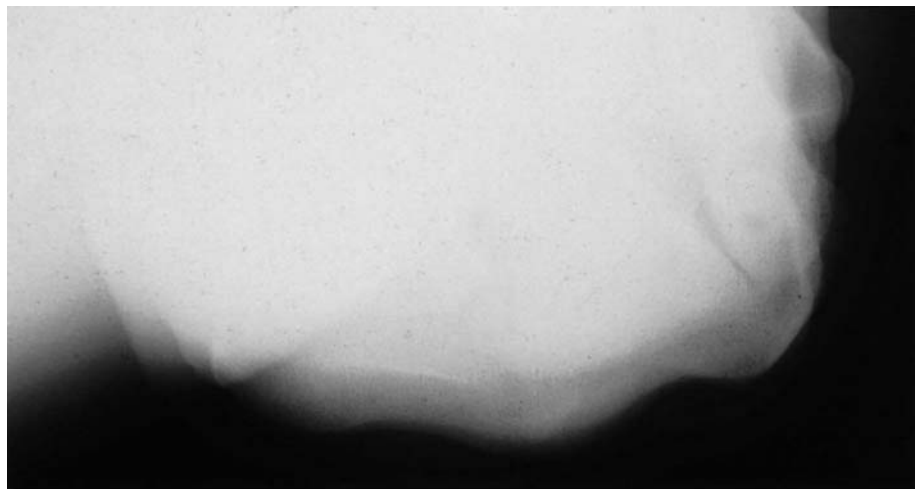
Figure 4.9 Dorsoproximal-dorsodistal oblique views and diagrams of the carpus of a normal adult horse, showing: (a) the distal radius; (b) the proximal row of carpal bones; (c) the distal row of carpal bones.

(c)

[184]

Radial carpal bone

Ulnar carpal bone

Intermediate carpal bone

Intermediate facet of radial trochlea

Dorsal articular margin of radial trochlea

Medial facet of radial trochlea

(a)

Medial border of second metacarpal bone

Proximal aspect of fourth metacarpal bone

Distal medial aspect of radius

Ulnar carpal bone

Radial carpal bone

Radial trochlea

Intermediate carpal bone

(b)

Second carpal bone

Fourth carpal bone

Third carpal bone

Superimposition of proximal row of carpal bones and third metacarpal bone

(c)

Figure 4.9 *Cont'd*

level of the fused physis. The distal caudal aspect of the radius proximal to the physis may have a rather irregular outline (Figure 4.10). The transverse ridge on the distal caudal aspect of the radius often appears slightly roughened and does not reflect previous tearing of the accessory ligament of the superficial digital flexor tendon (superior check ligament), which arises further proximally from a longitudinal ridge approximately 10–15 cm proximal to the antebrachiocarpal joint. Oblique views may demonstrate an incomplete lucent line in the distal lateral aspect of the radius (see page 173).

Although the distal end of the ulna is vestigial in the horse, it may continue to the distal tuberosity of the radius as a fibrous cord. In some cases this is partially ossified, when it can be seen on radiographs. It is variable in size and appearance (Figures 4.11a and 4.11b).
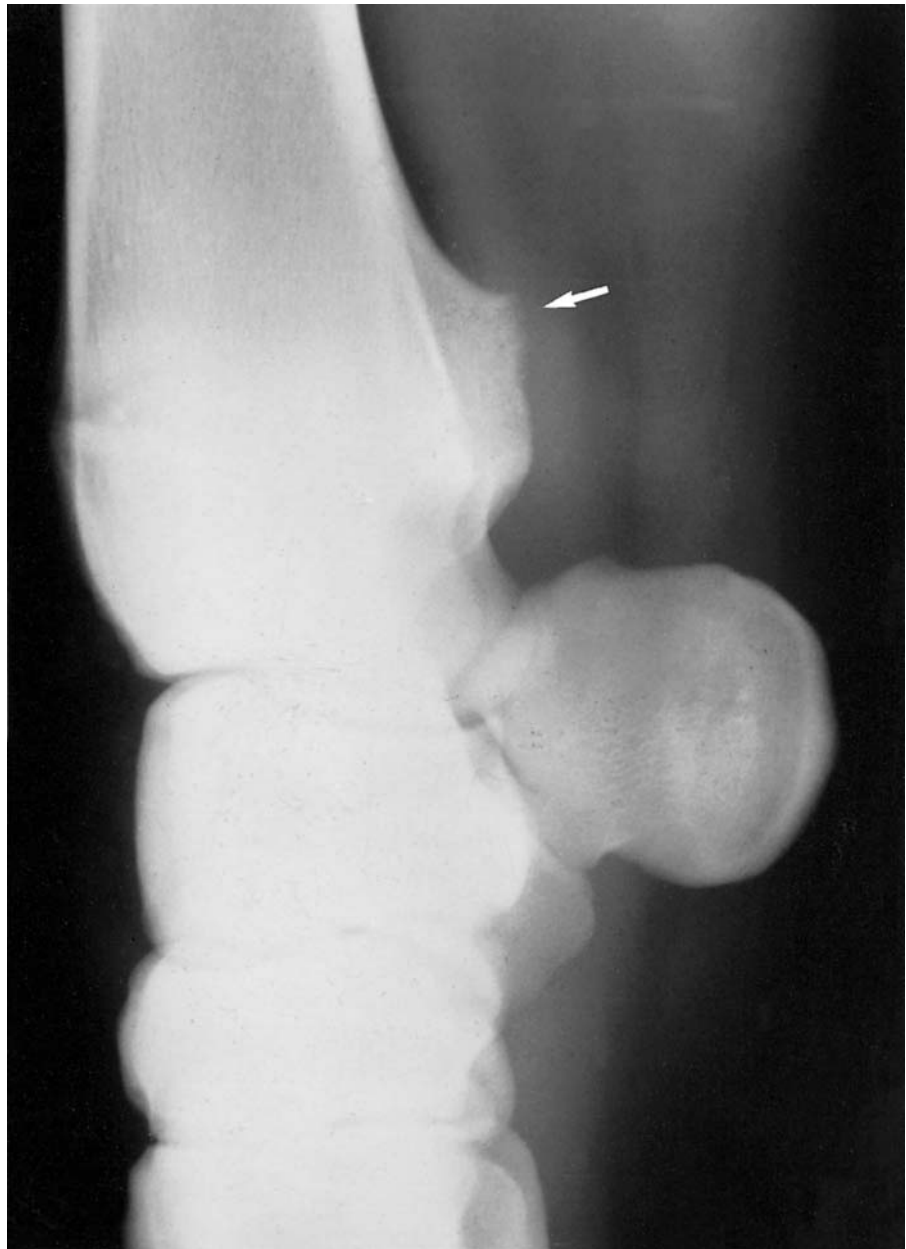
Figure 4.10 Lateromedial view of a carpus from a normal adult horse, showing marked irregularity of the caudal aspect of the radius (arrow) proximal to the level of the fused distal radial physis.

(a)

Figure 4.11 Dorsolateral-palmaromedial oblique views of the distal radius and carpus of normal adult horses showing: (a) a vestigial distal ulna – there is also a radiolucent zone (arrow) with surrounding sclerosis in the ulnar carpal bone, which is an incidental finding; (b) a vestigial distal ulna – there is also a clearly demarcated opacity (arrow) caused by the torus carpeus (chestnut).

(b)

A lucent zone is sometimes seen in the ulnar carpal bone, with or without an adjacent osseous opacity (Figure 4.11a). In a dorsopalmar projection they may appear to be on the axial border of the bone. Their aetiology is unknown, but they are not generally associated with lameness.

The first carpal bone is seen in approximately one-third of horses, in one or both limbs. It is variable in size, ranging from pinpoint to 12–15 mm in diameter. It may, but need not, articulate with the second carpal bone (Figures 4.12a, 4.12b and 4.12c), and occasionally also articulates with the second metacarpal bone. If it is separated from the second carpal bone, it

[187]

(a)

(b)

(c)

Figure 4.12 Dorsomedial-palmarolateral oblique view of the carpus of normal horses, showing variations of the first carpal bone. (a) The first carpal bone (arrow) is well separated from the second carpal bone. (b) The first carpal bone (arrow) appears to articulate with the second carpal bone. Note that the distal palmar aspect of the second carpal bone appears relatively lucent. (c) The first carpal bone appears to articulate with the second carpal bone. The distal palmar aspect of the second carpal bone is relatively lucent. There are ill-defined lucent areas within the first carpal bone.

[188]

usually has a uniformly opaque appearance. If it is in close proximity to the second carpal or metacarpal bones, then adjacent bones may show lucent areas within them.

In occasional cases a fifth carpal bone is present on the palmarolateral aspect of the distal row of carpal bones. Very occasionally there is a separate ossification centre in the proximal row of carpal bones. The size, shape and articulations of these bones are variable, but they are usually uniformly opaque. These separate ossification centres should not be confused with fractures.

Some degree of sclerosis of the radial facet of the third carpal bone may be seen in dorsoproximal-dorsodistal oblique views of horses in full work.

Marginal osteophyte formation may be seen, particularly on the medial aspect of the antebrachiocarpal and middle carpal joints in older horses with marked conformational abnormalities of the distal limb. This is most common if the metacarpal region is set on lateral to the central axis of the antebrachium. This is not necessarily associated with lameness, but this may depend on the athletic demands placed on the horse.

SIGNIFICANT FINDINGS

Soft-tissue swelling

Soft-tissue injury and swelling of the carpus is common. It can generally be appreciated radiographically, but it is frequently not possible to determine its cause. The site of maximum swelling may be located near the site of the injury, but frequently the swelling is too extensive for this to be of diagnostic assistance. Swelling may be restricted to periarticular structures or involve the carpal joint capsules. It may indicate the presence of synovitis and/or infection, or result from contusion or ligament strains.

The antebrachiocarpal joint does not communicate with the middle carpal joint. Synovitis of these joints may therefore occur separately. Distension of the antebrachiocarpal joint capsule may obscure the focal radiolucencies, which represent fat, on the dorsal aspect of the joint. If there is swelling of the middle carpal joint capsule, a dorsoproximal-dorsodistal oblique view of the distal row of carpal bones should be obtained (see 'Sclerosis of the third carpal bone', page 194). Occasionally herniation of a joint capsule may occur, to cause a synoviocele, usually on the dorsolateral aspect of the carpus. Distension of the tendon sheath of the extensor carpi radialis, common digital extensor or lateral digital extensor may result in a chronic hygroma-like swelling on the dorsal aspect of the carpus. Occasionally communication develops between two of the above structures. Positive and double contrast radiographic techniques are useful to aid differentiation of these swellings, and to identify filling defects due to synovial proliferation or adhesion formation. Ultrasonography may yield additional information. Chronic distension of the tendon sheath of extensor carpi radialis is often seen in association with irregular periosteal new bone formation on the distal cranial radius; however, this new bone is not necessarily of clinical significance.

Degenerative joint disease

The radiographic changes associated with degenerative joint disease are described elsewhere (see Chapter 1, page 25). The most frequent abnormalities identified in the carpus are periarticular osteophytes, rounding of the normally right-angled shape of the articular margins of the carpal bones, and sclerosis or lucent zones in the subchondral trabecular bone (Figures 4.13a–e). The antebrachiocarpal and middle carpal joints are most commonly affected.

Periarticular osteophytes are most commonly seen at the proximal and distal dorsal aspects of the radial carpal bone, the proximodorsal aspect of the third carpal bone, and less commonly the proximodorsal aspect of the intermediate carpal bone. Because of this positioning, examinations for degenerative joint disease of the carpus should always include dorsal 45° lateral-palmaromedial and dorsal 75° lateral-palmaromedial oblique views. Care should also be taken to evaluate the palmar margins of the joints, since periarticular osteophyte formation may also develop here, especially in more advanced cases of degenerative joint disease. Small bone spurs or modelling of the joint margins may be found in apparently sound horses in work, and their significance must be assessed in relation to the age of the horse, conformation, the work previously carried out, current lameness and future work required. Thus these would be of more significance if found at a purchase examination of a young top-grade performance horse, than if seen as an incidental finding in an old pleasure horse.

In the young Thoroughbred in training, subtle remodelling changes of the radial and third carpal bones may have important consequences. Initially there may be slight loss of opacity on the dorsal distal aspect of the radial carpal bone; the distal articular margin becomes more rounded and 'cut back'. This effectively moves the articulation with the third carpal bone in a slightly palmar direction. Subsequently the dorsoproximal aspect of the third carpal bone becomes less opaque. This modelling may predispose to fracture of the third carpal bone.

Narrowing of a joint space or ankylosis are rarely seen except in the carpometacarpal joint.

Degenerative changes are sometimes seen involving only part of the carpometacarpal joint, either the articulation between the second carpal and second metacarpal bone, or the fourth carpal and fourth metacarpal bone. There is narrowing of the joint space and subchondral lucent zones or sclerosis, often in association with irregular periosteal new bone on the metaphysis and proximal diaphysis of the second or fourth metacarpal bone (Figure 3.17, page 157).

New bone formation

New bone formation is seen in several locations:
- New bone formed at the margins of the joints (periarticular osteophytes) is associated with degenerative joint disease (see above).
- New bone formed on the dorsal aspect of one or more carpal bones, not

(a)
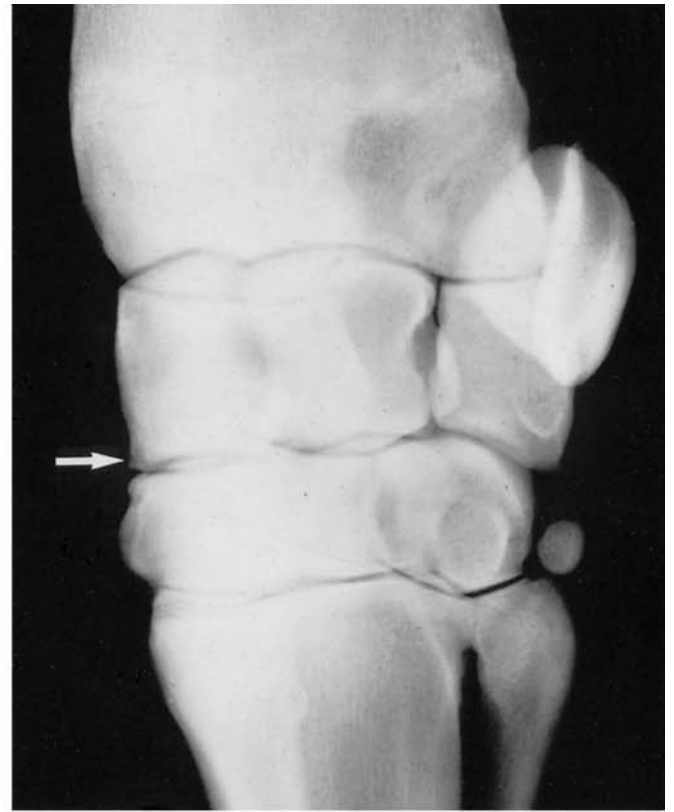
(b)

(c)

Figure 4.13 Radiographs of the carpus of adult horses, showing changes associated with early degenerative joint disease (the significance of these radiographic abnormalities must be determined in the light of the clinical examination).
(a) Dorsolateral-palmaromedial oblique view of the carpus of an 8-year-old Thoroughbred cross. There is slight osteophyte formation on the distal aspect of the radial carpal bone (arrow) and slight loss of trabecular pattern in the proximal aspect of the third carpal bone. (See also Figure 4.15a, showing a dorsoproximal-dorsodistal oblique view of the same bone.)
(b) Dorsolateral-palmaromedial oblique view of the carpus of a 3-year-old Thoroughbred. There is modelling of the distal aspect of the radial carpal bone, with alteration of the trabecular pattern (arrow) and rounding of the proximal aspect of the third carpal bone. Note also the large fifth carpal bone.
(c) Dorsolateral-palmaromedial oblique view of the carpus of a 5-year-old crossbred. There is slight osteophyte formation (solid arrow) on the medial aspect of the antebrachiocarpal joint, with more extensive modelling of the distal aspect of the radiocarpal bone (open arrow). Note the small radiolucent zone in the distal aspect of the ulnar carpal bone.
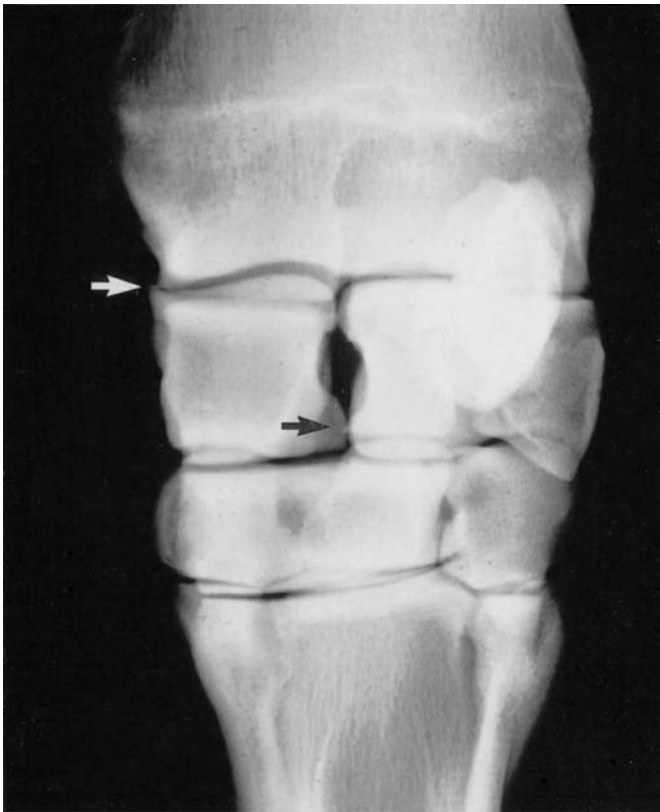
(d)

(e)

Figure 4.13 *Cont'd*
(d) Dorsopalmar view of the carpus of a 14-year-old Thoroughbred. There is osteophyte formation on the distal medial aspect of the radius and the proximal aspect of the radial carpal bone (white arrow). There is a small clearly outlined spur on the distal medial aspect of the intermediate carpal bone (black arrow), the clinical significance of which is unknown.

(e) Dorsolateral-palmaromedial oblique view of the carpus of a 3-year-old Thoroughbred. There is osteophyte formation on the dorsomedial aspect of the antebrachiocarpal joint, involving the distal radius and the radial carpal bone (solid white arrow). The dorsal aspect of the radial carpal bone is modelled at the site of the intercarpal ligament attachments (open white arrow). There is rounding of the distal aspect of the radial carpal bone. Note the apparent lucent zone in the distal aspect of the ulnar carpal bone, surrounded by a rim of sclerosis (black arrow). This is an incidental finding.

involving the joint margins, may be associated with tearing or strain of the intercarpal ligaments (entheseophyte formation), or direct trauma to the periosteum (periosteal osteophytes) (Figure 4.14). Its significance will depend to some extent on its activity at the time of examination, as well as on the amount of bone formed. The new bone will gradually remodel, but may remain irregular. If it has well-defined smooth opaque margins it is unlikely to be of long-term significance. Entheseophyte formation on the dorsal aspects of the carpal bones is often seen in association with degenerative joint disease. Entheseophyte formation reflects ligamentous damage, resulting in slight instability of the joints. This may cause secondary degenerative joint disease, but need not do so.

[192]

Figure 4.14 Dorsolateral-palmaromedial oblique view of a carpus. There is new bone on the dorsal aspect of the radial carpal bone at the site of the intercarpal ligament attachment. This is often not of long-term clinical significance.

● New bone formation is quite often seen on the transverse ridge of the distal caudal radius, unassociated with clinical signs.

● Mineralization of new bone beginning to bridge the antebrachiocarpal, middle carpal and/or carpometacarpal joints, as well as new bone between the carpal bones in either row, is usually the result of infection or repeated intra-articular administration of corticosteroids (so-called steroid arthropathy). Both steroid arthropathy and infection result in destruction of bone and thus irregular lucent areas in the bones. Infection is usually associated with sclerosis, and either condition may result in ankylosis of joints and extensive new bone formation. In either case, a poor or hopeless prognosis must be given.

● New bone formation occasionally occurs at the origin of the accessory ligament of the superficial flexor tendon (superior check ligament) at the caudal aspect of the radius. Its significance should be assessed in the light of clinical signs. Lameness, if present, will usually resolve with rest. Ultrasonographic evaluation is important to assess the integrity of the ligament.

● New bone formation may occur on the distal cranial radius, often in conjunction with distension of the tendon sheath of extensor carpi radialis. This is usually the result of repeated trauma, but is rarely of long term significance. Occasionally surgical debridement is indicated.

[193]

Sclerosis of the third carpal bone

Some degree of sclerosis of the third carpal bone is believed to be a normal modelling feature in young Thoroughbreds and Standardbreds in training and usually involves the radial facet. These changes can only be appreciated radiographically in dorsoproximal-dorsodistal oblique views, which highlight the third carpal bone. Marked sclerosis of either the radial (Figure 4.15a) or intermediate facet is abnormal. This change is appreciated radiographically as a loss of both the trabecular structure and the definition between the cortex and medulla. Often there is associated joint capsule distension of the middle carpal joint, a finding which should lead to further evaluation of the third carpal bone. Small poorly circumscribed lucent zones are abnormal (Figure 4.15b). The third carpal bone may be compared carefully with the fourth carpal bone since the trabecular pattern of the latter is generally normal. The radial facet can also be compared with the remainder of the third carpal bone. Sclerosis of the third carpal bone can be seen in conjunction with lameness alleviated by intra-articular analgesia of the middle carpal joint, with no other identifiable abnormality. Lameness usually resolves with rest, and the sclerotic bone slowly remodels. Sometimes intra-articular analgesia does not alleviate the lameness, but nuclear scintigraphic examination reveals increased modelling activity in the third carpal bone.

Excessive sclerosis, in the area of the radial facet, has been shown to predispose to subsequent fracture.

Osseous cyst-like lesions

Osseous cyst-like lesions have been described in all the carpal bones, as well as the proximal end of all three metacarpal bones and the distal radius. They are frequently incidental findings unassociated with lameness. However, in young foals osseous cyst-like lesions may represent E-type osteomyelitis (see page 23) and should lead to further diagnostic tests for 'joint ill'. Aggressive broad spectrum antimicrobial therapy may be required. Very large osseous cyst-like lesions close to a joint margin are probably more likely to be associated with lameness (see Chapter 1, page 24). Significant lesions may become clinically silent with conservative treatment, or may require surgery.

Polydactyly

Polydactyly has been recorded in the horse, arising from the carpus or distally. The extra appendage tends to cause limb deviation and therefore requires surgical removal at an early age.

Physitis (epiphysitis)

The radiographic appearance of physitis is described fully in Chapter 1 (page 14). It is relatively common in the distal radius of rapidly growing yearlings, and in young racehorses as they commence work.

[194]

(a)
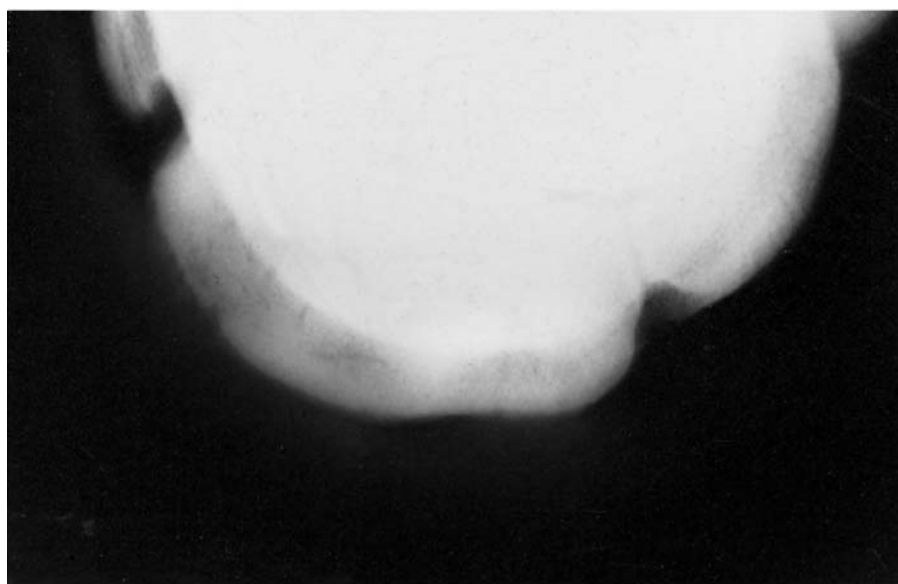
(b)

Figure 4.15 Dorsoproximal-dorsodistal oblique view of a carpus, to show: (a) sclerosis of the third carpal bone – note the loss of trabecular pattern in the medulla and poor corticomedullary demarcation (this is the same bone shown in Figure 4.13a); (b) marked sclerosis of the medulla of the third carpal bone, with ill-defined lucent areas in the radial facet – compare with the trabecular structure of the fourth carpal bone.

Physitis is characterized radiographically by an irregular widening of the physis. There may be 'lipping' medially and laterally (Figure 4.16). Frequently some limb deviation will also result. Clinically the limb may be swollen immediately proximal to the carpus, and may be hot and painful to palpation. Treatment is by restricting feed and exercise, until an adequate clinical response is seen.

Carpal angular limb deformities

Many limb deviations arise from the carpus, and may be congenital or acquired. If a deviation is severe, or a moderate deviation fails to respond

Figure 4.16 Dorsopalmar view of the distal radius of a yearling Thoroughbred, showing physitis. There is widening and an irregular outline of the physis, especially medially, with flaring of the medial aspect of the distal metaphysis and swelling of the overlying soft tissue.

to conservative treatment, radiographic examination is indicated. For valgus and varus deviations, dorsopalmar views on long (43 cm) cassettes are most useful. The extent of the deviation can be measured and monitored, by drawing the lines that bisect the radius and third metacarpal bones. These will intersect at or near the point at which the deviation arises, and the angle at the point of intersection indicates the degree of deviation (Figure 4.17).

[196]

Figure 4.17 Dorsopalmar view of a carpus of a 3-week-old foal with a carpal valgus deformity, centred close to the antebrachiocarpal joint. Deviation is approximately 12°. The lateral styloid process of the distal radius is incompletely ossified, and there is a discrete fragment distal to it. The distal radial epiphysis and the third carpal bone are wedge shaped, being shorter on their lateral aspects than medially.

Subsequent films to evaluate change in angle must be identical in position to the first set.

Radiographic abnormalities may include one or more of the following:

- Irregularity in width of the distal radial physis.
- A wedge-shaped distal radial epiphysis.
- Incomplete ossification of one or more carpal bones (see below).
- Malformation of one or more carpal bones. This probably results from weight-bearing on incompletely ossified bones.
- Delayed development of the lateral styloid process.

If the limb deformity is related to changes in the distal physis or epiphysis, surgical treatment carries a reasonable prognosis if carried out well before closure of the physis. Malformation of the carpal bones warrants a poor prognosis. Incomplete ossification requires early identification and treatment for a successful outcome (see below).

Incomplete carpal ossification

This condition is seen in young foals (often premature or twins) with a carpal angular limb deformity. On radiographs the distal radial physis usually appears normal, but one or more of the carpal bones will be small and rounded, lacking the normal cuboidal shape (Figure 4.18).

Successful treatment requires prompt action to straighten the limb and support it in a cast, until ossification of the affected bones is normal.

Figure 4.18 Dorsopalmar view of the carpus of a Quarter Horse foal, born at 323 days of gestation, obtained 6 days after birth. The carpal bones are incompletely ossified; note their rounded contour. Note also the incompletely ossified separate centre of ossification of the lateral styloid process of the ulna.

[198]

Osteochondroma

The caudodistal aspect of the radius is the site where osteochondromas are most frequently identified radiographically. They are variable in size and shape, and may have an irregular outline (Figure 4.19). It may be possible to identify a communication with the marrow cavity of the radius. Although they may be benign and not associated with clinical signs, they may result in lameness often with distension of the carpal sheath. These lesions are usually solitary, but may be associated with lesions elsewhere. They can be removed surgically, and this treatment carries a good prognosis for return to work.

Carpal fractures

Chip fractures of the carpal bones

These fractures occur frequently (Figure 4.20). They may be defined as fractures that involve only one joint surface of the bone. Their visualization may require several oblique views, although they are often most readily observed on the flexed lateromedial view. The most common sites for chip fractures are the distal border of the dorsal aspect of the radius, the radial carpal bone (slightly to the medial side of the midline) and the opposing radial facet of the third carpal bone; also, the distal dorsal aspect of the

Figure 4.19 Lateromedial view of a distal radius of a mature horse. There is a solitary osteochondroma on the caudal aspect of the distal radius, which was associated with distension of the carpal sheath and severe lameness. After surgical removal of the osteochondroma the clinical signs resolved.

[199]

Figure 4.20 Flexed lateromedial view of the carpus, showing a chip fracture of the distal border of the radial carpal bone. The fracture was poorly demonstrated on other views. Note the large first carpal bone. (The radiograph was taken with reduced exposure to highlight the fracture.)

intermediate carpal bone. Less commonly fractures occur in the proximal aspect of the radial and intermediate carpal bones. Lameness due to small fractures may resolve with rest. Surgical removal should always be considered in cases in which horses are required to return to athletic performance, and in cases with larger fragments. A good prognosis can generally be given, provided that no other lesions are present. A degree of cartilage damage will have occurred, and subsequently degenerative joint disease may develop.

Chip fractures can also involve the lateral, medial and palmar aspects of the carpal bones. These are less common and carry a more guarded prognosis.

Degenerative joint disease (see page 190) may be pre-existing and may have predisposed to a fracture. The radiographs should be carefully scrutinized to evaluate the entire carpus, both for evidence of degenerative joint disease and for the presence of more than one fracture. Since fractures frequently occur bilaterally, both carpi should be examined radiographically.

[200]

Slab fractures (involving both proximal and distal articular surfaces) occur most commonly at the dorsal aspect of the third, fourth or radial carpal bones (Figure 4.21). These fractures can usually be detected on latero-medial radiographs, but dorsoproximal-dorsodistal oblique views should also be obtained to ascertain the extent and degree of comminution of the fracture. This view will also show fractures that are not easily recognized on lateromedial views, and may show sclerosis of the third carpal bone (see page 194). Slab fractures have also been recorded at the palmar aspect of the third carpal bone.

Dorsal or oblique slab fractures of the radial and third carpal bones are usually repaired by lag screw fixation, but if the fracture fragment is very thin it may be removed.

Sagittal fractures of the third carpal bone are generally only detectable on dorsoproximal-dorsodistal oblique views (Figures 4.22a and 4.22b). Internal fixation is possible, but a fair prognosis can be given for conservative treatment provided that there is minimal displacement and no degenerative joint disease.

Fractures of the accessory carpal bone

These fractures most frequently occur in a vertical plane approximately through the middle of the bone. Although usually simple, the fractures may be comminuted and can occur in any plane. The pull of the flexor tendons which insert on the palmar aspect of the bone result in the palmar fragment being pulled proximally and medially. With prolonged rest (6–8 months), approximately 80% of cases will return to work. Healing is by fibrous union, and so a lucent line persists (Figure 1.10, page 19). However a number will

Figure 4.21 Dorsoproximal-dorsodistal oblique view of a carpus of a 2-year-old Thoroughbred. There is a frontal (slab) fracture of the third carpal bone (arrow), which probably occurred secondarily to the marked sclerosis of the radial facet. Compare the trabecular pattern of the medial aspect of the third carpal bone with that of the fourth (see also Figure 4.15).

Figure 4.22(a) Dorsolateral-palmaromedial oblique view of a 3-year-old Thoroughbred with a sagittal fracture of the third carpal bone. Note the irregular lucency of the dorsoproximal aspect of the third carpal bone (arrow).
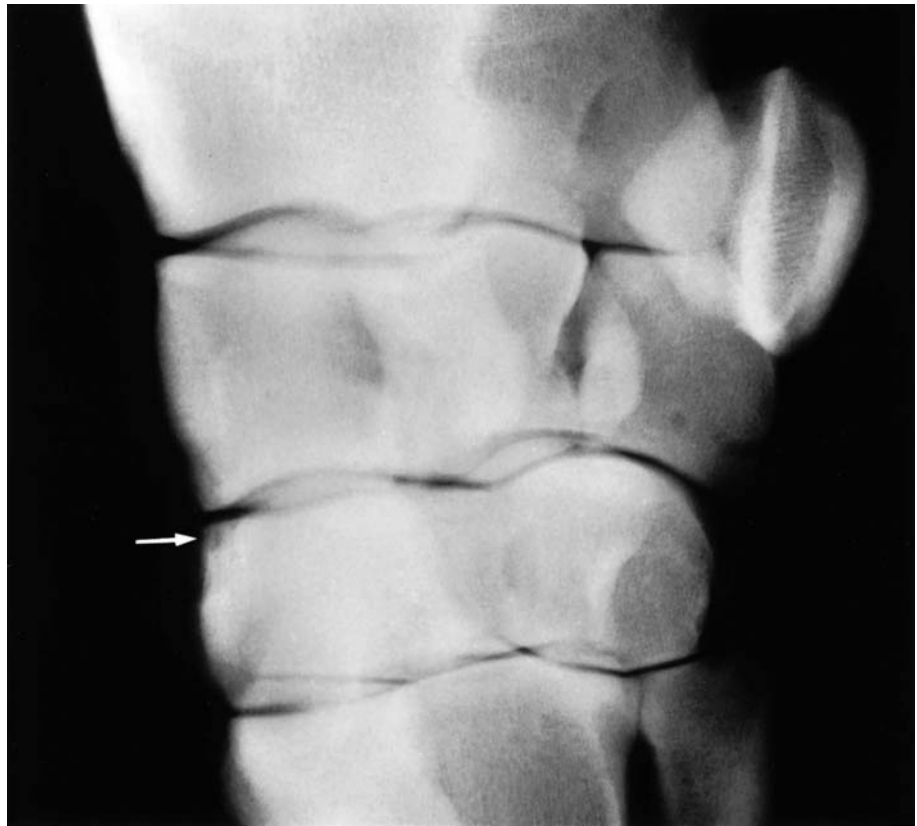
Figure 4.22(b) Dorsoproximal-dorsodistal oblique view of the same carpus to highlight the distal row of carpal bones. Note the sagittal fracture on the medial aspect of the radial facet of the third carpal bone (arrow).
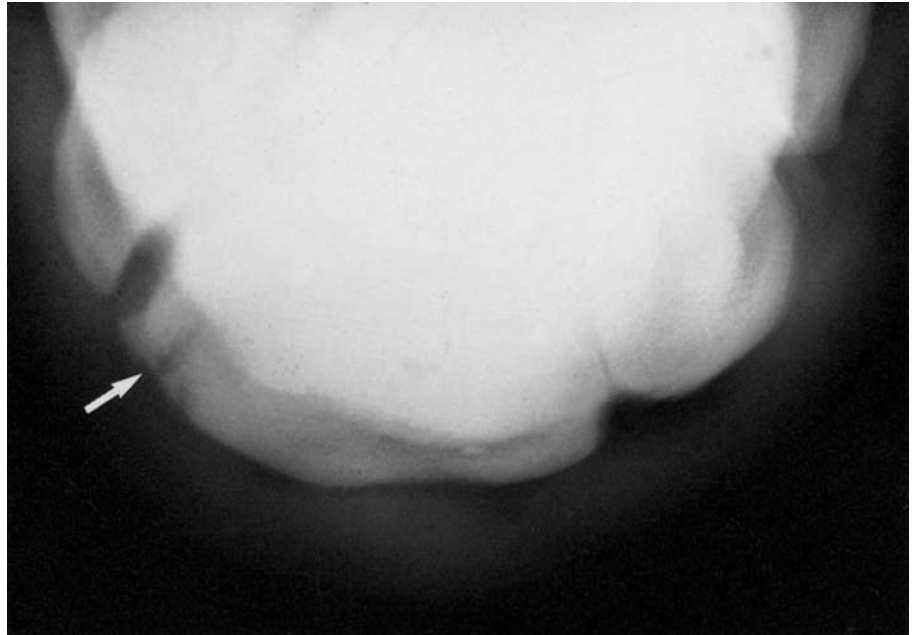
develop chronic lameness, and so internal fixation at the time of fracture may be considered.

Chip fractures may occasionally occur close to the articular surface, often proximodorsally. On a lateromedial view this may be partially super-imposed over other carpal bones, and a dorsal 80° lateral-palmaromedial

[202]
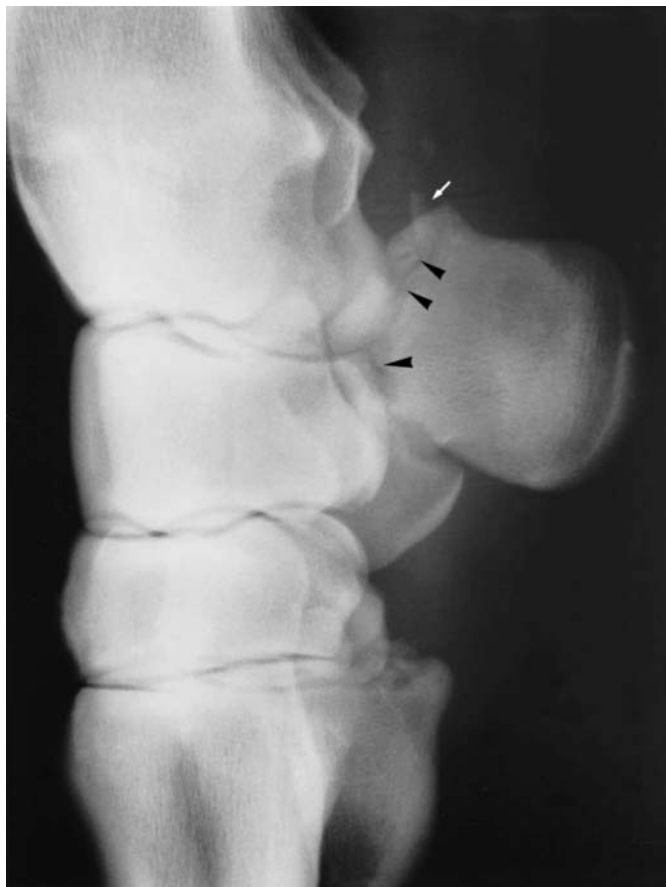
Figure 4.23 Dorsal 80° lateral-palmaromedial oblique view of a carpus of a 3-year-old Thoroughbred with acute onset of lameness of 2 days' duration. There is a comminuted articular fracture (arrow heads) of the accessory carpal bone. One small fragment (white arrow) has been displaced proximally. Note also the osseous opacity in close apposition to the fourth carpal bone, this is a fifth carpal bone.

oblique view may give better visualization (Figure 4.23). Surgical removal may be required.

Fractures of the second or fourth carpal bones

Fractures of the second or fourth carpal bones are often comminuted. These fractures are often accompanied by fractures of the proximal aspect of the second or fourth metacarpal bones. This will result in marked lateromedial instability of the carpometacarpal joint. Such fractures require internal fixation, and carry a guarded prognosis (see also 'Metacarpal fractures', page 157).

FURTHER READING

Auer, J., Smallwood, J., Morris, E., Martens, R. *et al.* (1982) The developing equine carpus from birth to 6 months. A radiographic study. *Equine Pract.*, **4**, 35–55

Barr, A., Sinnott, M. and Denny, H. (1990) Fractures of the accessory carpal bone in the horse. *Vet. Rec.*, **127**, 432–434

Bramlage, L., Schneider, R. and Gabel, A. (1988) A clinical perspective on lameness originating in the carpus. *Equine Vet. J.*, Suppl. **6**, 12–18

Burguez, P.N. (1986) Interpreting radiographs 4: the carpus. *Equine Vet. J.*, **16**, 159–163

Catcott, E.J. and Smithcors, J.F., Eds (1972) *Equine Medicine and Surgery*, 2nd edn, American Veterinary Publications, Illinois

De Haan, C., O'Brien, T. and Koblick, P. (1987) A radiographic investigation of third carpal bone injury in 42 racing thoroughbreds. *Vet. Radiol.*, **28**, 88–92

Dietze, A. and Rendano, V. (1984) Fat opacities dorsal to the equine antebrachiocarpal joint. *Vet. Radiol.*, **25**, 205–209

Dixon, R.T. (1969) Radiography of the equine carpus. *Aust. Vet. J.*, **45**, 171–174

Dyson, S (1988) Some observations on lameness associated with pain in the proximal metacarpal region. *Equine Vet. J.*, Suppl. **6**, 43–52

Dyson, S. (1990) Fractures of the accessory carpal bone. *Equine. Vet. Educ.*, **2**(4), 188–190

Ellis, D. (1985) Some observations on bone cysts in the carpal bones of young thoroughbreds. *Equine Vet. J.*, **17**, 63–65

Fischer, A. and Stover, S. (1987) Sagittal fractures of the third carpal bone in horses: 12 cases (1977–1985). *J. Am. Vet. Med. Ass.*, **191**, 106–108

Gertson, K.E. and Dawson, H.A. (1976) Sagittal fracture of the third carpal bone in a horse. *J. Am. Vet. Med. Ass.*, **169**, 633–634

Manning, J.P. and St. Clair, L.E. (1972) Carpal hyperextension and arthrosis in the horse. *Proc. Am. Ass. Equine Pract.*, **18**, 173–181

Mason, T.A. and Bourke, J.M. (1973) Closure of the distal radial epiphysis and its relationship to unsoundness in two year old thoroughbreds. *Aust. Vet. J.*, **49**, 221–228

Myers, V.S. (1965) Confusing radiological variation at the distal end of the radius of the horse. *J. Am. Vet. Med. Ass.*, **147**, 1310–1312

Park, R.D., Morgan, J.P. and O'Brien, T. (1970) Chip fractures in the carpus of the horse; a radiographic study of their incidence and location. *J. Am. Vet. Med. Ass.*, **157**, 1305–1312

Platt, D. and Wright, I. (1997) Chronic tenosynovitis of the carpal extensor tendon sheaths in 15 horses. *Equine Vet. J.*, **29**, 11–17

Schneider, R., Bramlage, A., Barone, L. and Kantrowitz, B. (1988) Incidence, location and classification of 371 third carpal bone fractures in 313 horses. *Equine Vet. J.*, Suppl. **6**, 33–42

Sisson, S. and Grossman, J.D. (1953) *Anatomy of the Domestic Animal*, 4th edn, W.B. Saunders, Philadelphia

Smallwood, U. and Shiveley, M. (1979) Radiographic and xeroradiographic anatomy of the equine carpus. *Equine Pract.* **1**, 22–38

Stashak, T.S. (1987) *Adams' Lameness in Horses*, 4th edn, Lea and Febiger, Philadelphia

Thrall, D.E., Lebel, J.L. and O'Brien, T.R. (1971) A five-year survey of the incidence and location of equine carpal chip fractures. *J. Am. Med. Ass.*, **158**, 1366–1368

Uhlorn, H., Ekman, S., Haglund, A. and Carlsten, A. (1998) The accuracy of the dorsoproximal-dorsodistal projection in assessing third carpal bone sclerosis in Standardbred trotters. *Vet. Radiol. Ultrasound*, **39**, 412–417

Wintzer, H.J. (1986) *Equine Diseases*, Paul Parey, Berlin

Young, A., O'Brien, T. and Pool, R. (1988) Exercise related sclerosis in the third carpal bone of the racing thoroughbred. *Proc. Am. Ass. Equine Pract.*, **34**, 339–346

Chapter 5
The Shoulder, Humerus and Elbow

Scapulohumeral (shoulder) joint and humerus

RADIOGRAPHIC TECHNIQUE

Equipment

The scapulohumeral joint may be radiographed with the horse standing if a high-output x-ray machine is available. Better quality radiographs are generally obtained with the horse under general anaesthesia in lateral recumbency. With the horse anaesthetized, positioning is easier and longer exposure times can be used without risk of movement, so a lower output x-ray machine may be used. The radiation hazard to personnel is also reduced. Rare earth screens and appropriate film are essential due to the high exposures required to penetrate the large muscle mass in this area. A grid is recommended to reduce the effects of scattered radiation, and lead should be placed behind the cassette to limit back scatter. There is less soft tissue to penetrate cranially; therefore it may be necessary to repeat a view with different exposure factors in order to assess properly both the cranio-proximal aspect of the humerus and the more caudally situated scapulo-humeral joint. Alternatively an aluminium wedge filter can be used to modify the exposure. For mediolateral radiographs obtained with the horse standing, the cassette should be mounted in a holder and not hand held. Both mediolateral and oblique views are required for a complete assessment of the scapulohumeral joint, and in selected cases arthrography yields valuable additional information.

Positioning

Mediolateral view

STANDING

The forelimb to be examined is positioned next to the cassette and the limb is protracted as much as the horse will comfortably allow, to avoid superimposition of the left and right shoulder joints (Figure 5.1). Some horses resist protraction of the limb and this may result in movement blur and partial superimposition of the left and right shoulder joints. Sedation may be helpful, but the horse may relax and lower its neck so that a larger proportion of the distal scapula is superimposed over the cervical and thoracic vertebrae. The use of an analgesic such as butorphanol facilitates the examination of horses suffering severe pain.
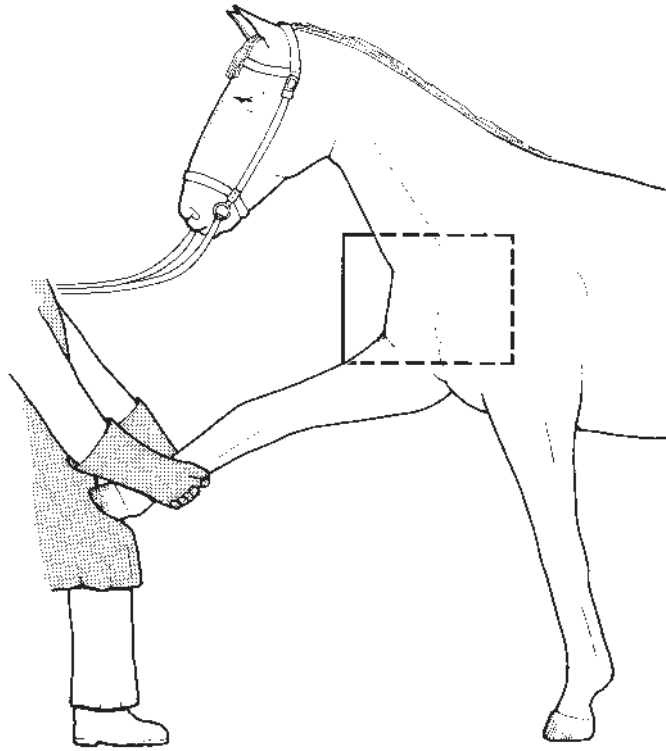
Figure 5.1 Positioning of the horse and cassette to obtain a mediolateral radiographic view of the scapulohumeral joint.

LATERAL RECUMBENCY

The anaesthetized horse is placed in lateral recumbency, lying on the limb to be radiographed. This limb is protracted, the contralateral forelimb is retracted and the neck is extended. It may be helpful to restrain the forelimbs using ropes. The position of the endotracheal tube is adjusted so that its distal end is not superimposed over the scapulohumeral joint. The examination is performed most easily if the horse is lying on a cassette tunnel, to avoid having to lift the horse in order to place the cassette beneath it. With appropriate sedation a foal may be restrained in lateral recumbency without the need for general anaesthesia.

CENTRING THE X-RAY BEAM

The x-ray beam is centred approximately 10 cm cranial to the distal aspect of the scapular spine of the limb contralateral to that being radiographed. This is approximately equivalent to centring at the level of the greater tubercle of the humerus of the protracted limb. It is helpful to mark the point at which the beam is centred (e.g. with sticky tape) so that appropriate corrections can be made for subsequent exposures.

If the scapulohumeral joint is positioned distal to the trachea, up to one-third of the distal scapula can be seen without superimposition of the cervical and thoracic vertebrae and the ribs. Evaluation of the proximal two-thirds of the scapula is difficult because of the superimposed bones and the flatness of the scapula. If either rim of the glenoid cavity of the scapula or the proximal articular surface of the humerus are superimposed over the

[206]

proximal or distal borders of the trachea, the summation of opacities makes interpretation difficult and additional radiographs may be required. It is sometimes helpful to position the scapulohumeral joint over the trachea. Although this can be achieved in the standing horse, it is most easily done if the horse is anaesthetized.

The distal two-thirds of the humerus is examined using a similar technique, but centring further distally. This examination is usually only indicated when a fracture is suspected and associated pain often makes adequate protraction of the limb very difficult. High exposure factors may therefore be required in order to obtain adequate penetration of the large muscle mass.

Cranial 45° medial-caudolateral oblique view

This view is most easily obtained with the horse standing. The forelimb to be examined is usually protracted and the cassette is held caudal to the shoulder muscle mass in order to position it sufficiently far medially. This inevitably results in some magnification. A grid is unnecessary which allows lower exposure factors. The x-ray beam is centred at the level of the greater tubercle of the humerus. Alternatively a caudolateral-craniomedial oblique view may be obtained, but this usually results in greater magnification.

These views help to clarify some intra-articular lesions, especially those in the sagittal plane. They also permit identification of some fractures not visible in a mediolateral projection and help to determine the direction of a luxation of the humerus.

Arthrography

Arthrography can be performed with the horse standing or in lateral recumbency under general anaesthesia. In the latter position the technique is more complicated because, after injecting the contrast medium with the limb to be examined uppermost, the horse must then be turned over for radiography. A small volume (7–10 ml) of a 60% mixture of sodium and meglumine amidotrizoate (Urografin 60%, Schering AG) is recommended. Dilution of the contrast agent with a balanced polyionic electrolyte solution may help definition of the articular cartilage. The technique can be used to highlight articular cartilage defects and subtle bone lesions and to identify dissecting cartilage flaps in cases of osteochondrosis.

RADIOGRAPHIC ANATOMY, NORMAL VARIATIONS AND INCIDENTAL FINDINGS

Birth to 3 years old

Scapula

The scapula has four centres of ossification: the scapular cartilage, the body of the scapula, the cranial part of the glenoid cavity of the scapula and the

Figure 5.2 Mediolateral view and diagram of a shoulder of a 12-day-old foal. The cranial centre of ossification of the glenoid cavity of the scapula and the lesser tubercle of the humerus are incompletely ossified. The curvature of the glenoid cavity of the scapula is more shallow and the ventral angle is more rounded compared with an adult.

supraglenoid tubercle (Figure 5.2). The latter two may be incompletely ossified at birth and have a fuzzy, irregular outline. The cranial part of the glenoid cavity of the scapula fuses with the body by 5 months after birth. The physis of the supraglenoid tubercle closes by 12–24 months after birth.

Humerus

The proximal humerus ossifies from three centres: the diaphysis, the humeral head and the greater tubercle. The lesser tubercle develops from the same ossification centre as the humeral head. It is usually incompletely ossified at birth and has a fuzzy outline and a granular opacity. The centres of ossification of the proximal humeral epiphysis merge by 3–4 months of age and gradually assume a more adult shape; the proximal humeral physis closes by 24–36 months.

[208]
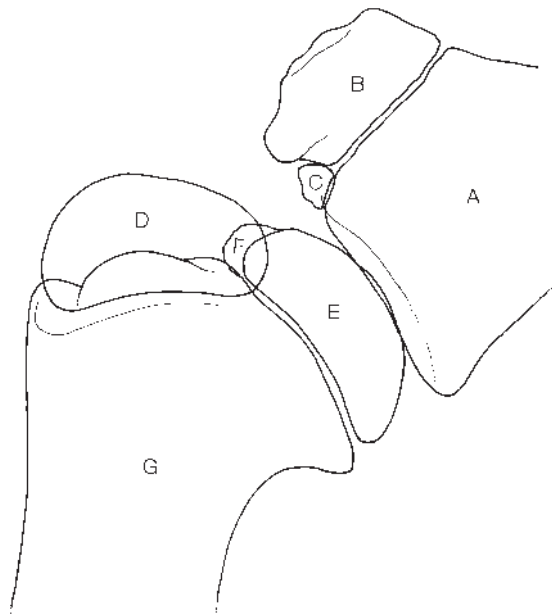
Figure 5.2 *Cont'd*
A = body of scapula, B = ossification centre for the supraglenoid tubercle and
coracoid process, C = ossification centre for the cranial part of the glenoid of the
scapula, D = ossification centre for the greater tubercle of the humerus, E =
ossification centre for the humeral head and lesser tubercle, F = incompletely ossified
lesser tubercle, G = diaphysis of humerus.

Skeletally mature horse

Mediolateral view

There is little variation in the normal radiographic anatomy of the scapu-
lohumeral joint except as a result of positioning. The medial rim of the
glenoid cavity of the scapula is projected proximal to the lateral rim and
is smoothly curved (Figure 5.3a). Its caudal edge, the ventral angle of
the scapula, is sharply pointed. The lateral rim of the glenoid cavity of
the scapula is seen as a relatively less opaque area immediately distal to the
medial rim and may make the latter appear poorly defined. It may be
superimposed over the humeral head, resulting in a relatively lucent area
in the cranial part of the humeral head which should not be mistaken for
a lucent lesion in the subchondral bone of the humeral head (Figure 5.3b,
page 211). The lateral rim of the glenoid cavity forms the proximal border
of this lucency.

There is a clearly demarcated band of opaque, sclerotic bone, of uniform
width, around the caudal two-thirds of the glenoid cavity of the scapula. In
approximately 5% of horses there is a small lucent zone (up to 0.5 cm
diameter) in the middle of the glenoid cavity of the scapula within the
opaque band (Figure 5.4, page 212). A faint vertical lucent line is sometimes
seen at the junction of the cranial and middle thirds of the glenoid cavity.
This represents the glenoid notch. Cranial to the glenoid notch the opaque
band is usually narrower.

Figure 5.3(a) Mediolateral view and diagram of a normal adult scapulohumeral joint (compare with Figure 5.5).

[210]

Supraglenoid
tubercle

Coracoid process

SCAPULA

intermediate tubercle

Glenoid notch

Cranial eminence of
greater tubercle

Cranial eminence
of lesser
tubercle

Lateral rim of
glenoid of
scapula

Medial rim of
glenoid of
scapula

HUMERUS

Deltoid tuberosity
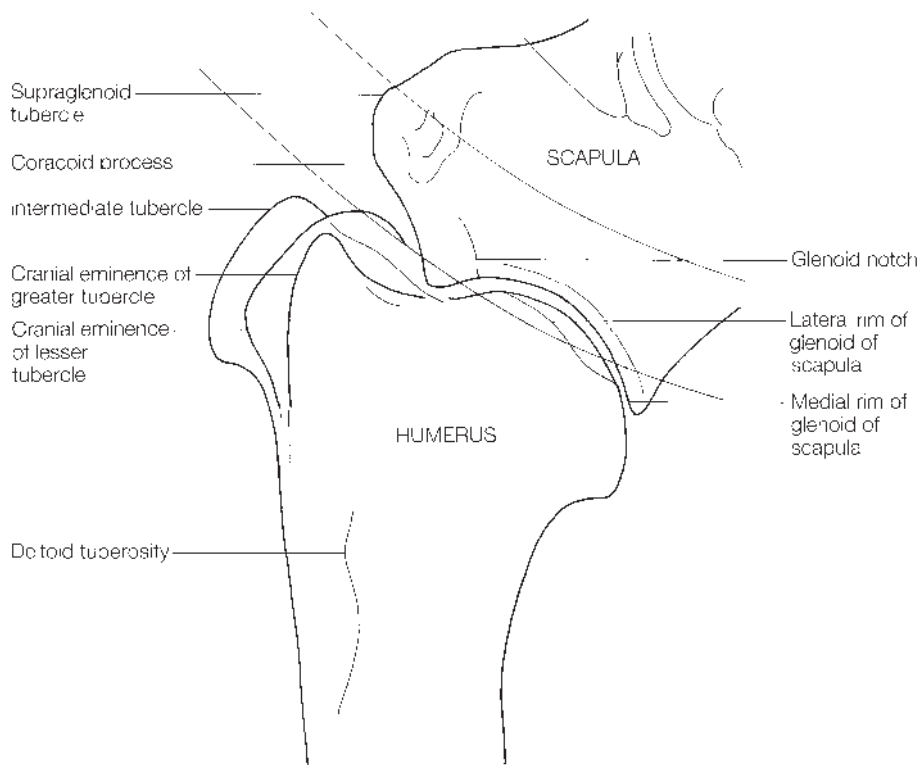
Figure 5.3(a) *Cont'd*

Figure 5.3(b) Coned down mediolateral
view of a normal scapulohumeral joint,
superimposed over the trachea. Note the
congruity of the articulation between the
scapula and the humerus and the sharply
pointed ventral angle of the scapula
(white arrow). The lucent line (black
arrows) traversing the humeral head is
normal, an edge effect created by the
overlying lateral rim of the glenoid
cavity of the scapula.

Figure 5.4 Mediolateral view of a normal adult scapulohumeral joint. There is an irregularly shaped radiolucent area (arrow) in the subchondral bone of the middle of the glenoid cavity of the scapula.

The outline of the humeral head is smoothly curved. The greater, lesser and intermediate tubercles may be slightly separated or superimposed upon each other depending on the positioning of the humerus (Figures 5.3 and 5.5).

There is reasonable congruity between the outlines of the glenoid cavity of the scapula and the humeral head, although in some horses the glenoid cavity of the scapula is more curved, resulting in apparent widening of the joint space in the middle of the joint.

Cranial 45° medial-caudolateral oblique view

In this projection the width of the scapulohumeral joint space is more variable than in the mediolateral view. The cranial eminence of the lesser tubercle, the intermediate tubercle and the intertubercular groove are highlighted and the deltoid tuberosity is outlined (Figure 5.6, page 214). The 'lip' of the deltoid tuberosity, which curves caudolaterally, may be projected in this view and should not be confused with a chip fracture (Figure 5.7, page 216).

[212]

Caudal eminence of
greater tubercle

Cranial eminence of
greater tubercle

Intermediate
tubercle

Cranial eminence of
lesser tubercle
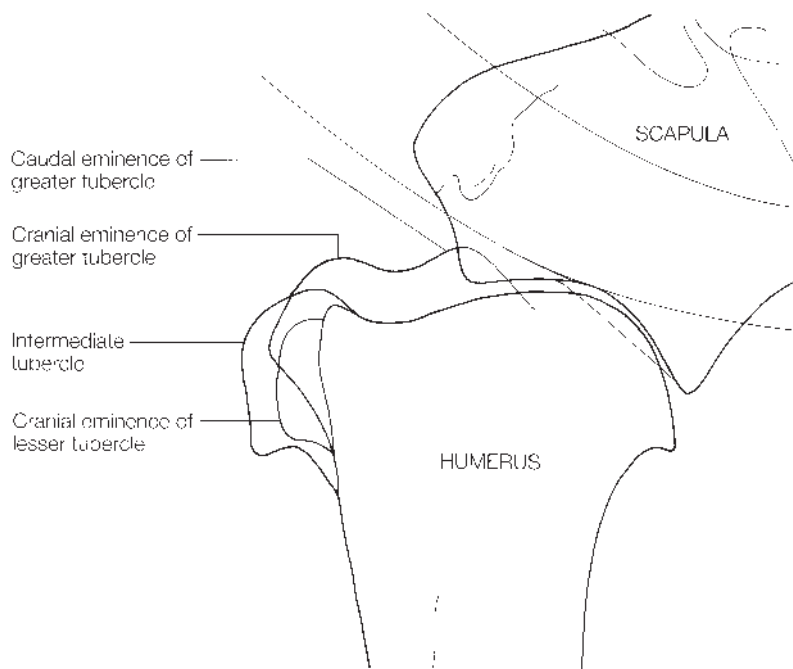
SCAPULA

HUMERUS

Figure 5.5 Mediolateral view and
diagram of a normal adult
scapulohumeral joint (compare with
Figure 5.3a). Due to slight differences in
position of the proximal humerus, the
greater tubercle appears more
prominent. Note also the slightly more
rounded ventral angle of the scapula
compared with Figure 5.3(b).

Figure 5.6 Cranial 45° medial-caudolateral oblique view and diagram of a normal adult scapulohumeral joint.

[214]

Coracoid process

Intertubercular
(bicipital)
groove

Cranial eminence of
greater tubercle

Intermediate
tubercle

Deltoid
tuberosity

Scapular spine

SCAPULA

Cranial eminence
of lesser
tubercle

Fossa of
humeral head
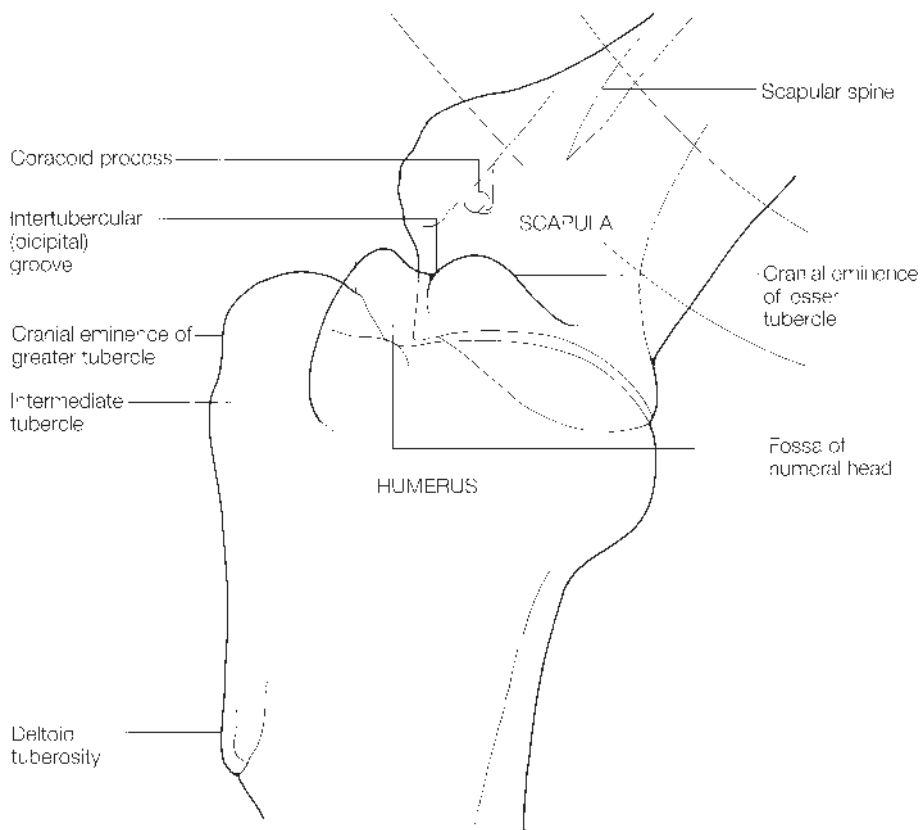
HUMERUS

Figure 5.6 *Cont'd*

Arthrography

A narrow band of contrast outlines the articular surfaces of the scapula and humerus (Figure 5.8). Some contrast may also be superimposed over the distal scapula and the humeral head. This outlines the proximal cul-de-sac of the scapulohumeral joint capsule and distal aspect of the joint capsule, respectively. In a small proportion of normal horses, arthrography will demonstrate communication between the scapulohumeral joint capsule and the intertubercular bursa.

SIGNIFICANT RADIOLOGICAL ABNORMALITIES

Osteochondrosis

Radiographic abnormalities associated with osteochondrosis are identified in either the scapula, the humerus or both. The changes predominantly involve the caudal one-half of the joint and result in loss of congruity between the subchondral bone adjacent to the articular surfaces of the scapula and humerus. In some cases there is only subtle variation in contour of the articular surfaces (Figure 5.9a, page 218). In other cases there are extensive, irregularly outlined lucent zones in the subchondral bone, which may be surrounded by some sclerosis (Figure 5.9b, page 219). There is often flattening of the subchondral bone of the humeral head and/or the glenoid cavity of the scapula (Figure 5.9c, page 220). The ventral angle of the scapula, which is usually sharply pointed, may be modelled so that it is more

[215]
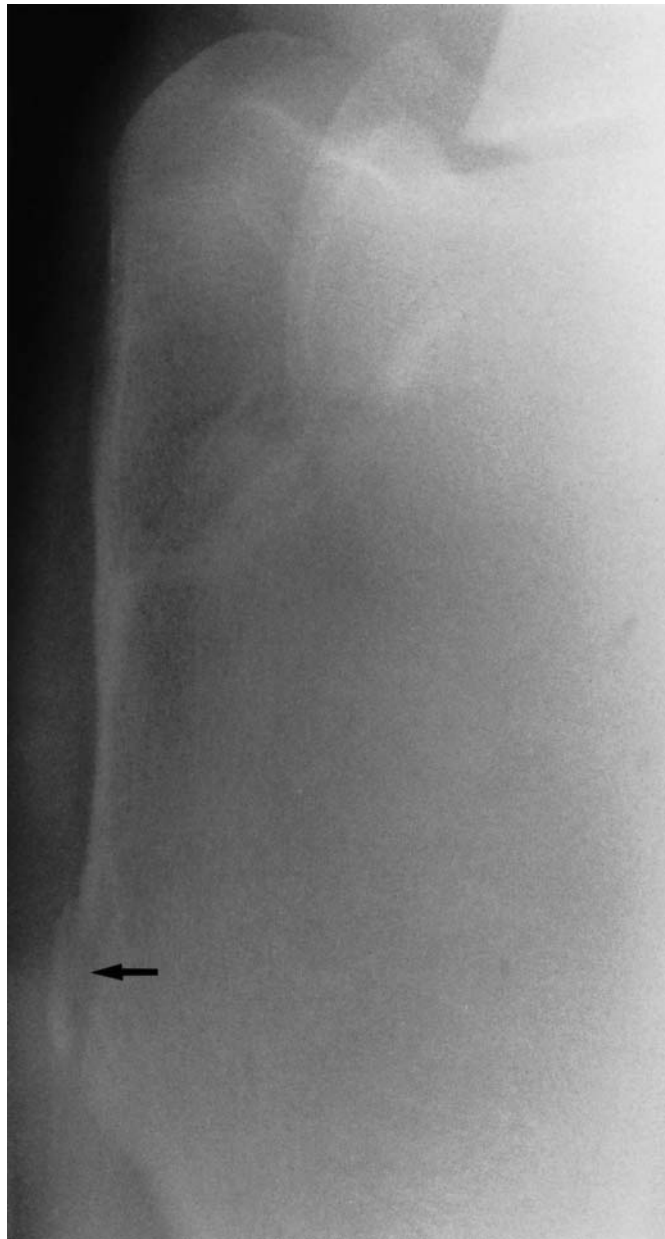
Figure 5.7 Craniomedial-caudolateral oblique view of a normal adult humerus. The 'lip' of the deltoid tuberosity is projected (arrow) and should not be confused with a chip fracture.

bulbous. The rim of the glenoid cavity of the scapula may have a blurred outline. Some of the modelling of the scapula and the humerus is due to secondary degenerative joint disease. Osteochondrosis may occur unilaterally or bilaterally, usually in horses less than 3 years of age. It causes a variable degree of lameness. Lameness may or may not be improved by intra-articular anaesthesia.

The majority of horses treated conservatively remain lame; surgical treatment has given encouraging results in immature horses.

Osseous cyst-like lesions

Poorly defined lucent zones of irregular shape in the subchondral bone of either the scapula or the humerus are a manifestation of osteochondrosis

[216]

Figure 5.8 Mediolateral arthrogram of a normal adult scapulohumeral joint.

(Figure 5.9b, page 219), but distinct, large circular lucent areas (osseous cyst-like lesions) may be a different clinical condition (or conditions) and are considered separately here.

A small lucent area within the sclerotic subchondral bone of the middle of the glenoid cavity of the scapula has been identified in normal horses (Figure 5.4, page 212) and is of questionable clinical significance. However, one case has been reported which was rendered sound by intra-articular anaesthesia and had this as the only detectable radiographic 'abnormality'.

Osseous cyst-like lesions are not common. They may occur singly or there may be more than one (Figures 5.10a and 5.10b, page 221). They occur most frequently either in the middle of the distal scapula or the middle of the humeral epiphysis, and are usually surrounded by a rim of sclerotic bone.

[217]

Figure 5.9(a) Mediolateral view of the scapulohumeral joint of a 3-year-old Thoroughbred with osteochondrosis. There is a slight depression in the humeral head (arrow).

Associated lameness is usually improved by intra-articular anaesthesia. Lesions in the distal scapula are usually close to the articular surface when first recognized, but appear to move further away with time and become surrounded by a broader rim of sclerotic bone, associated with which there may be improvement in lameness. Osseous cyst-like lesions in the distal scapula occur most commonly in young horses, but are occasionally seen in association with sudden onset lameness in mature horses. Secondary modelling of the ventral angle of the scapula is a variable feature. Not all osseous cyst-like lesions behave similarly and some in the proximal humerus 'fill in' with resolution of lameness. Occasionally modelling of the distal scapula is seen in association with an osseous cyst-like lesion in the proximal humerus.

Degenerative joint disease

Degenerative joint disease (DJD) of the scapulohumeral joint occurs rarely compared with the incidence in other joints, except as a sequel to osteochondrosis, trauma, infection or an intra-articular fracture. Some of

[218]

Figure 5.9(b) Mediolateral view of the scapulohumeral joint of a yearling Thoroughbred with osteochondrosis. There are extensive lucent areas in the subchondral bone of the distal scapula with surrounding sclerosis. There is considerable modelling of the caudal one-third of the glenoid cavity of the scapula and its ventral angle, resulting in loss of congruity between the scapula and humerus. There is an ill-defined lucent area in the subchondral bone of the middle of the humeral head, but at post mortem the overlying cartilage was intact and firmly adherent to the subchondral bone.

the modelling of the scapula and humerus described in conjunction with osteochondrosis is due to secondary DJD. Radiographic features of DJD include loss of congruity between the outlines of the distal scapula and the proximal humerus due to flattening of the humeral head and/or modelling of the ventral angle of the scapula. Subtle abnormalities of the cranial aspects of the joint may also be seen, including small periarticular osteophytes, especially on the distal scapula. In addition there may be variations in opacity of the subchondral bone. Narrowing of the joint space may be seen in advanced cases. The prognosis for return to athletic function is extremely poor.

Mineralization in the tendon of biceps brachii

Mineralization in the tendon of biceps brachii can occur as a sequel to a fracture of the supraglenoid tubercle (Figure 5.11, page 222) but has also

Figure 5.9(c) Mediolateral view of the scapulohumeral joint of a yearling Thoroughbred with osteochondrosis. There is extensive modelling of the distal scapula and proximal humerus. The outline of the caudal aspect of the glenoid cavity and of the ventral angle of the scapula is rather blurred due to new bone formation. There are ill-defined lucent zones in the caudal aspect of the distal scapula.

been described as a bilateral condition in association with DJD of the scapulohumeral joints. Mineralization is most easily identified radiographically in a mediolateral view and is seen as a variably sized opacity in the soft tissues cranioproximal to the tubercles of the humerus. The lesion is easily missed if the radiographs are overexposed. Prognosis for future soundness is guarded.

Abnormalities of the scapulohumeral joint in Shetland ponies and Miniature Horses

Dysplasia of the scapulohumeral joint, with or without subluxation of the scapulohumeral joint or secondary degenerative joint disease, has been seen in both Shetland ponies and Miniature Horses (Figure 5.12, pages 223 and 224). Unilateral degenerative joint disease, thought to be traumatic in origin, may occur in Shetland ponies and Miniature Horses associated with sudden onset, moderate to severe lameness. Radiographic abnormalities may not be present at the time of onset of lameness, and if mild may only be visible

Figure 5.10(a) Mediolateral view of a
scapulohumeral joint of a 2-year-old
Thoroughbred. There is a well-defined
single osseous cyst-like lesion in the
distal scapula, surrounded by sclerosis.
When first identified several months
previously, the lesion was smaller, closer
to the articular surface and less well
demarcated without surrounding
sclerosis. There is no detectable
modelling of the scapula (compare with
Figure 5.10b). Post-mortem examination
revealed a true subchondral bone cyst.

Figure 5.10(b) Mediolateral view of a
scapulohumeral joint of a 2-year-old
Thoroughbred with two large osseous
cyst-like lesions in the distal scapula.
Note the modelling of the ventral angle
of the scapula. The horse ultimately
raced successfully despite radiographic
persistence of the lesions.

Figure 5.11 Mediolateral view of a scapulohumeral joint of an aged horse. There are discrete mineralized areas (arrows) in the tendon of biceps brachii. Note the modelled supraglenoid tubercle, subsequent to previous fracture, the articular fracture fragment and the abnormally pointed distal cranial aspect of the scapula.

in a craniomedial-caudolateral oblique view. This view is also useful for assessment of congruity of the joint surfaces. Radiographic abnormalities include modelling of the articular margins of the glenoid cavity of the scapula, and entheseophyte formation at the insertion of the joint capsule (Figures 5.12a–d). Mild subluxation of the joint is occasionally seen. Fragmentation of the ventral angle of the scapula has also been seen in young Shetland ponies with acute onset severe lameness (Figure 5.12d). Defective bone, possibly developmental in origin, may predispose to fracture.

Infection

Septic arthritis of the scapulohumeral joint occurs most commonly in young foals and may result from osteomyelitis of the distal scapula or proximal

[222]
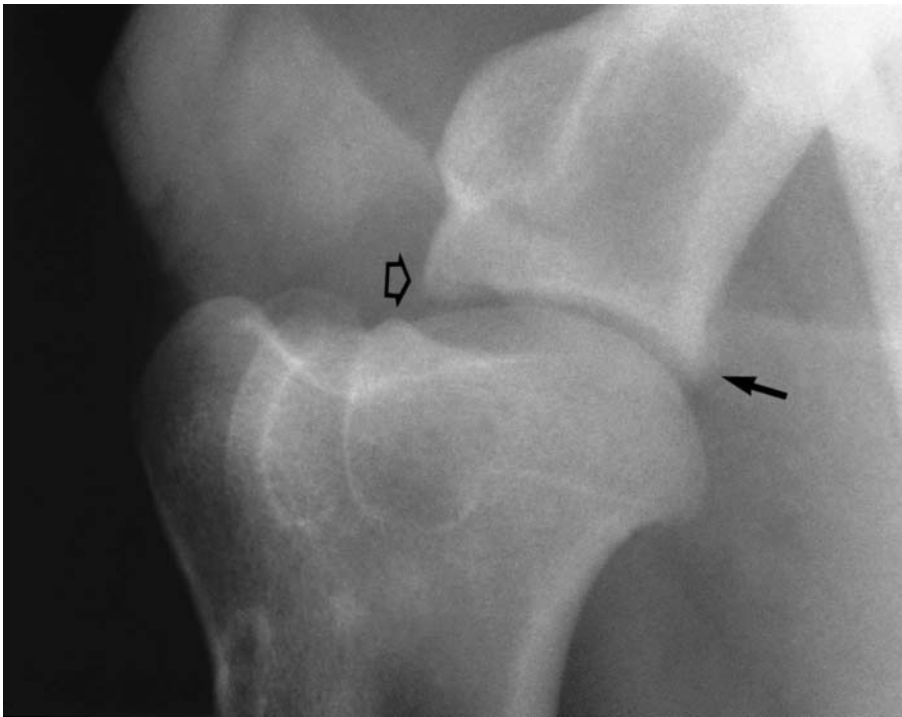
Figure 5.12(a) Craniomedial-caudolateral oblique view of a scapulohumeral joint of a Miniature Horse. No radiological abnormalities were detected in a mediolateral projection. In this oblique view there is poorly defined periosteal new bone on the ventral angle of the scapula (black arrow). The craniolateral aspect of the scapula is less sharply defined than normal (open arrow).
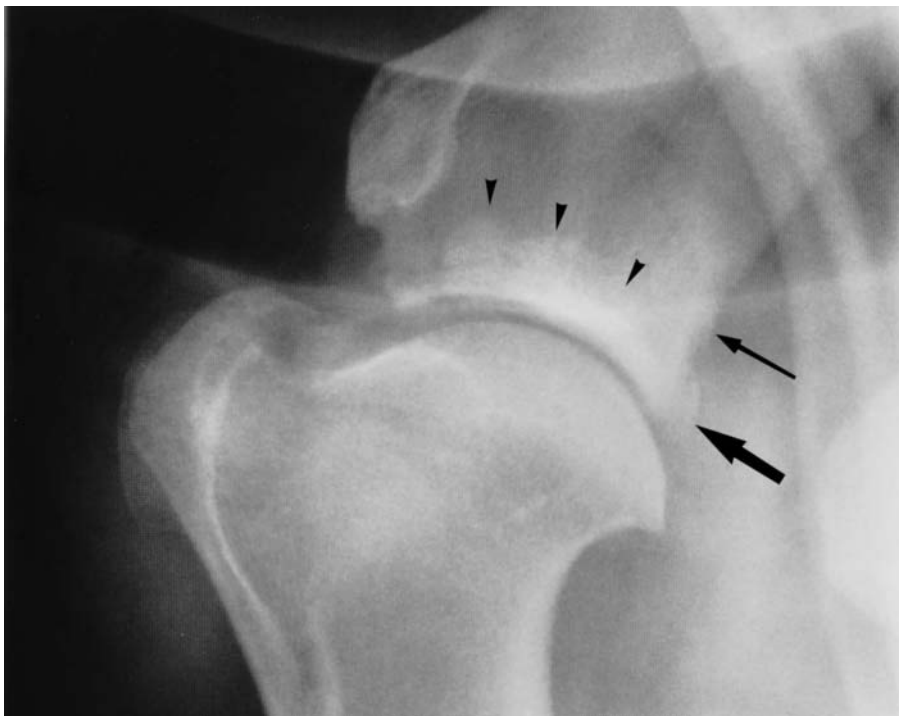
Figure 5.12(b) Mediolateral view of a scapulohumeral joint of a 4-year-old Shetland Pony. There is fairly extensive new bone on the caudal aspect of the ventral angle of the scapula (large arrow), extending proximally along the caudodistal margin of the scapula (small arrow). There is generalized increased opacity of the distal scapula (arrow heads), probably due to the extensive nature of the new bone formation around the distal scapula.

humerus (type E) or the humeral physis (type P) (see Chapter 1, page 23). In adult horses septic arthritis is usually iatrogenic. Osteomyelitis of the distal scapula is characterized by lucent zones in the subchondral bone (Figure 5.13, page 225), and an irregular outline of the glenoid cavity. There may be periosteal new bone, especially on the caudodistal aspect of the scapula. Similar changes may be seen in the proximal humeral epiphysis.

Figure 5.12(c) Mediolateral view of a scapulohumeral joint of a 4-year-old Shetland Pony. There is slight modelling on the articular margin of the proximocaudal aspect of the humerus (arrowhead). There is extensive new bone on the caudoventral aspect of the scapula, and an abnormal contour of the ventral angle of the scapula (open arrow). There is an ill-defined lucent line (arrow) crossing the ventral angle into the scapulohumeral joint. A large discrete fragment was identified at arthroscopic examination.
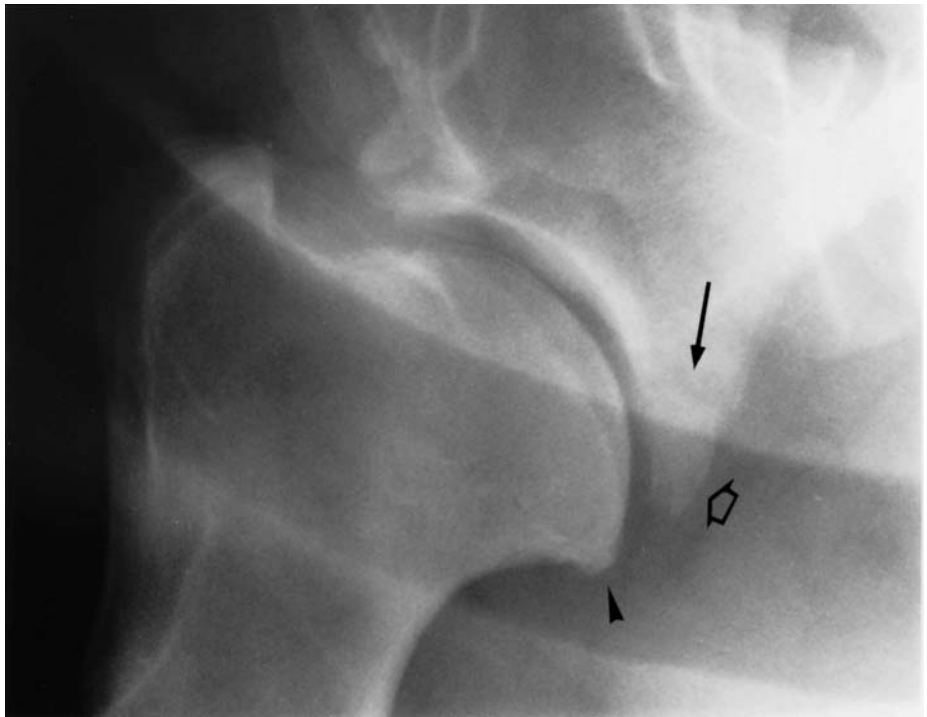
Figure 5.12(d) Mediolateral view of a scapulohumeral joint of a 5-year-old Shetland Pony. The joint surfaces of the scapula and humerus are abnormally flat and there is subluxation of the joint. There is extensive new bone on the caudoventral aspect of the scapula, and a separate mineralized opacity caudally.

Figure 5.13 Mediolateral view of a scapulohumeral joint of a 7-month-old Thoroughbred with osteomyelitis of the distal scapula and the proximal humerus and septic arthritis. Note the ill-defined lucent zones in the distal scapula, the flattened shape of the humeral head due to its partial collapse and the widened joint space. There is periosteal new bone around the ventral angle of the scapula.

Osteomyelitis of the proximal humeral physis results in areas of lucency and an irregular width of the physis. This may be focal or extend along the entire width of the physis, with or without new bone at the cortices. These changes must be differentiated from those due to osteochondrosis. Septic arthritis may result in apparent widening of the joint space due to excess synovial fluid. The granular opacity and irregular outline of incompletely ossified bones (see Figure 5.2, page 208) should not be confused with the results of infection.

Luxation of the scapulohumeral joint

Luxation of the scapulohumeral joint causes firm swelling in the shoulder region and severe lameness. The humerus may be displaced proximally and cranially (Figure 5.14) or proximally and caudally and is readily seen radiographically in a mediolateral projection, the proximal humerus being superimposed over the distal scapula. An oblique view is invaluable

Figure 5.14 Mediolateral view of a scapulohumeral joint of a mature pony with cranioproximal luxation of the humerus. Craniomedial-caudolateral oblique views should also be obtained to ensure that there is no concurrent fracture. This luxation was successfully reduced and the pony ultimately resumed full athletic function.

for determining whether the luxation is medial or lateral and for identification of any concurrent fracture. A simple luxation must be reduced rapidly, with the horse anaesthetized. Full return to athletic function has been recorded. The presence of a concurrent fracture warrants a guarded prognosis.

Fractures

Fractures of the shoulder region are usually the result of a fall, a kick or a collision with a solid object. They cause moderate to severe lameness with a variable amount of soft tissue swelling, with or without audible or palpable crepitus.

[226]

Fracture of the supraglenoid tubercle

This is the most common fracture in the shoulder region. The fracture may be simple or comminuted and there is often an articular component. There may be a separate fracture through the glenoid notch (this represents the separate centre of ossification of the cranial part of the glenoid cavity of the scapula). The supraglenoid tubercle is usually displaced cranially and distally resulting in a non-union fracture. Lameness may initially improve, but usually persists unless the fracture is treated surgically. Mineralization in the tendon of biceps brachii may be a sequel.

Other fractures

Other common sites of fractures are illustrated in Figure 5.15. Fractures restricted to the glenoid cavity of the scapula may be difficult to identify in a mediolateral view, but may be seen in an oblique projection. Fractures of the body or neck of the scapula are not uncommon and may be articular. Short fractures of the neck and body are easily overlooked due to superimposition of the cervical and thoracic vertebrae and the ribs. A fracture of the scapular spine may be very difficult to identify radiographically except in tangential views. Such fractures are sometimes associated with a chronic draining sinus due to sequestrum formation.

Fractures of the deltoid tuberosity, and the greater, lesser and intermediate tubercles of the humerus may only be identifiable in an oblique projection (Figure 5.16). Fatigue (stress or fissure) fractures of the caudal aspect of the proximal humeral metaphysis or cranial aspect of the distal humeral metaphysis occur occasionally. They can be difficult to identify
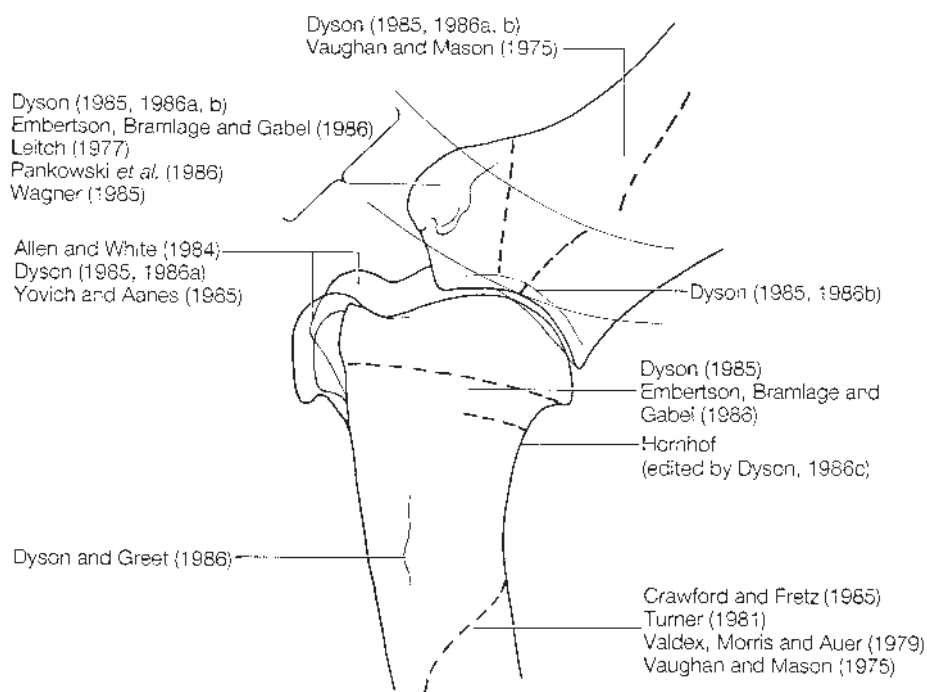
Figure 5.15 Location of common fractures of the scapula and humerus, and recommended references (see 'Further reading').

Figure 5.16 Craniomedial-caudolateral oblique view of a proximal humerus of a 3-year-old Thoroughbred. There is a non-displaced fracture of the deltoid tuberosity. No abnormality was detectable in a mediolateral view. The filly was treated conservatively and made a complete recovery.

radiographically in the acute phase, although they may be demonstrable using nuclear scintigraphy. Fractures of the humeral diaphysis are usually oblique or spiral with considerable overriding, with or without comminution. The prognosis for a fracture in the shoulder region depends on its location and configuration, and readers are advised to consult the references listed under 'Further reading'.

[228]

Humeroradial, humeroulnar and radioulnar (elbow) joints and radius

RADIOGRAPHIC TECHNIQUE

Equipment

The elbow joint and the radius are readily examined radiographically using a portable machine, with the horse standing. Sedation and administration of analgesics may facilitate positioning of the limb. Fast screens are recommended, but a grid is not essential. An aluminium wedge filter is useful, without which it may be necessary to obtain two mediolateral views to obtain correct exposures of the olecranon of the ulna and the humeroradial joint.

Positioning

Mediolateral view

For radiography of the elbow the horse is positioned with the limb to be radiographed next to the cassette. The x-ray machine is placed on the opposite side of the horse. The forelimb to be examined is protracted so that the olecranon of the ulna is cranial to the muscles of the contralateral limb. The x-ray beam is centred approximately at the junction between the cranial two-thirds and caudal one-third of the forearm, at the level of the proximal articular surface of the radius.

The majority of the radius can be examined radiographically with the horse bearing weight on the limb. The x-ray beam is centred at the point of interest and is aligned at right angles to the limb.

Craniocaudal views

Craniocaudal radiographic views of the elbow joint are usually obtained with the horse bearing weight on the limb, and the cassette held caudal to the forearm, beneath the thorax. It is helpful to rotate the cassette so that it can be held as high under the thorax as possible. It may be necessary to direct the x-ray beam approximately 10–15° from cranioproximally to caudodistally, depending on the shape of the rib cage, in order to examine the distal humerus and the humeroradial joint properly. Unfortunately this technique will cause some distortion of the radiographic image.

Alternatively the limb may be protracted, the cassette held parallel with the ulna and the x-ray beam directed perpendicular to it. There is more likely to be movement blur using this technique, and if there is a fracture of the ulna it may be difficult to straighten the limb adequately. Good quality craniocaudal views, with minimal distortion, are obtained more readily with the horse anaesthetized.

The radius is radiographed with the horse weight-bearing on the limb. The beam is centred at the area of interest.

Oblique views

A craniomedial-caudolateral oblique view is the easiest oblique view to obtain with the horse bearing weight on the limb. A craniolateral-caudomedial oblique view of the proximal radius is feasible, but due to the relative positions of the sternum and distal humerus, it is impractical to obtain a similar view of the humerus.

RADIOGRAPHIC ANATOMY, NORMAL VARIATIONS AND INCIDENTAL FINDINGS

Birth to 3 years old

The distal humerus develops from three ossification centres: the diaphysis, the distal epiphysis and the epiphysis of the medial epicondyle. Both the radius and the ulna have a single proximal epiphysis (Figure 5.17); the ulna may also have a separate centre of ossification for the anconeal process (Figure 5.18, page 232). At birth the ossification centres are rounded and may be irregular in outline because they are incompletely ossified. The epiphysis of the ulna is small and widely separated from the metaphysis. It gradually enlarges to cover the proximal ulnar metaphysis by 10–12 months. The physis appears very irregular (Figure 5.18, page 232) and remains open until 24–36 months after birth. The distal humeral physes and the proximal radial physis close between 11 and 24 months. The distal radial physis closes by between 22 and 42 months of age; there is a separate centre of ossification of the lateral styloid process which fuses with the rest of the distal epiphysis within the first year of life.

Skeletally mature horse

Mediolateral view

There is little variation in the normal radiographic appearance of the adult elbow except as a result of positioning (Figure 5.19, page 233). The anconeal process of the ulna may be sharply pointed or rounded. The trochlear notch of the ulna is divided into an articular zone proximally and a synovial fossa distally, separated by a distinct ridge. It is important to differentiate between these two areas when assessing a fracture involving the trochlear notch. The interosseous space between the ulna and radius may be clearly or poorly defined, depending upon the angle of projection. The ulna is incomplete in the majority of horses and distally fuses with the radius. Some horses have a vestigial distal ulna (see Figures 4.11a and 4.11b, page 187) and occasionally the ulna is complete. The cranial margin of the proximal articular surface of the radius has several 'lips' which must not be confused with osteophyte formation. The radial tuberosity is smoothly outlined, but may appear irregular in a slightly obliqued mediolateral projection. The medial aspect of the head of the radius is wider craniocaudally than the lateral aspect. Therefore the radioulnar articulation is not in a single plane, and in a mediolateral view the articulation of the lateral aspect of the ulna with

Diaphysis of humerus

Distal epiphysis of humerus

Proximal epiphysis of radius

Diaphysis of radius

Epiphysis of medial epicondyle of humerus

Diaphysis of ulna

Proximal epiphysis of ulna
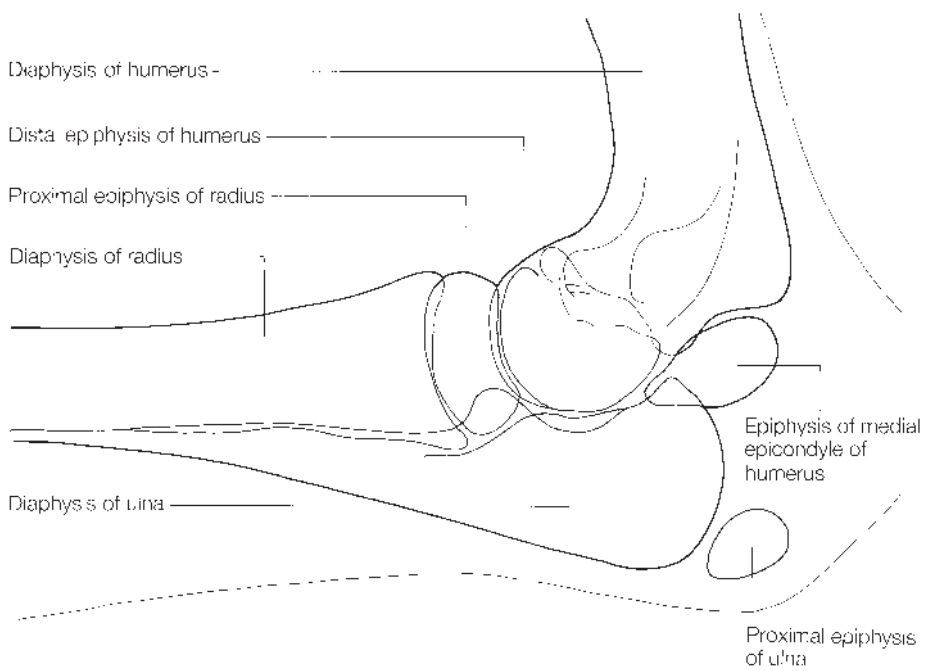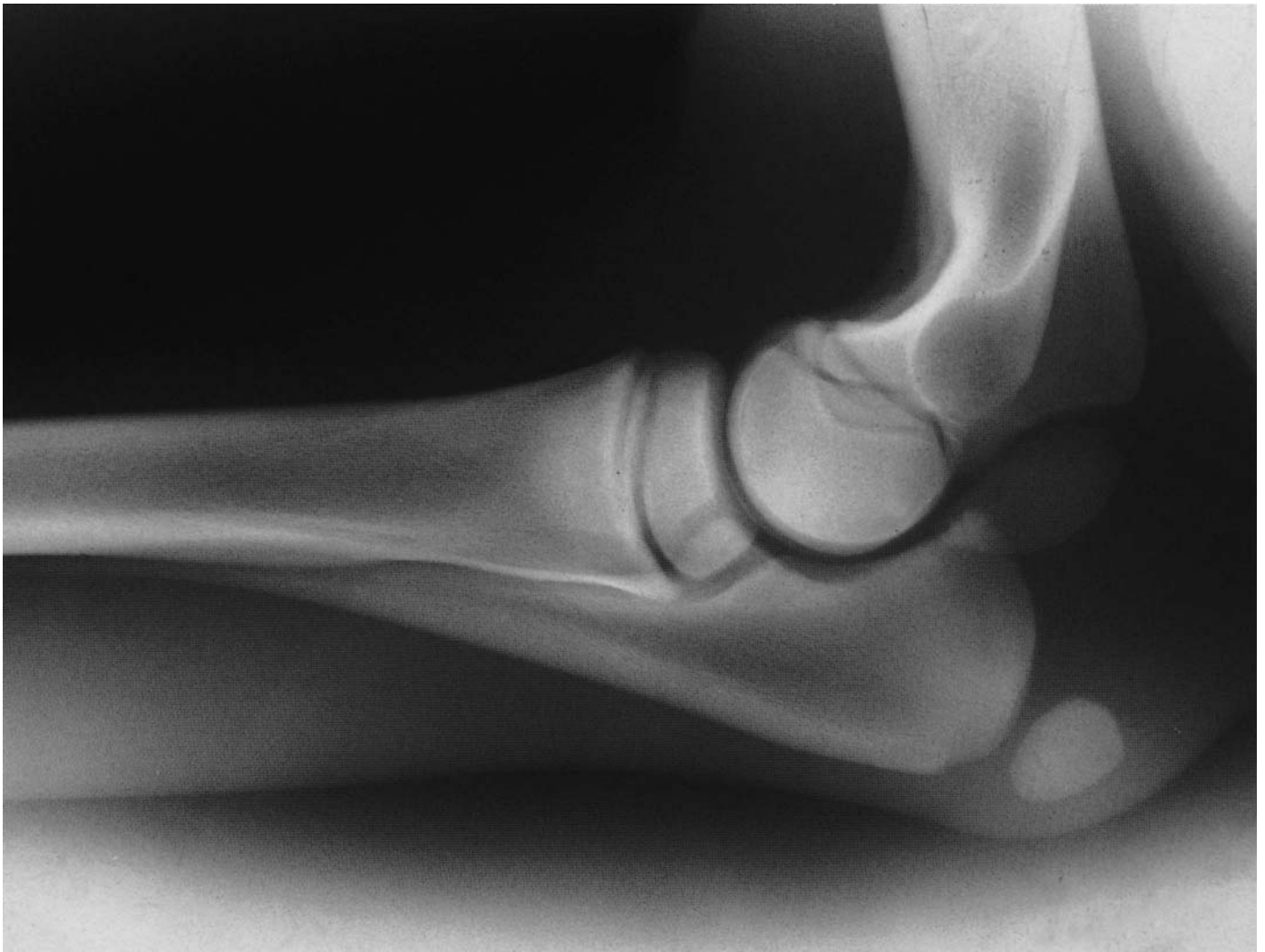
Figure 5.17 Mediolateral view and diagram of a normal elbow of a 12-day-old foal. Note the position of the incompletely ossified proximal epiphysis of the ulna.

[231]
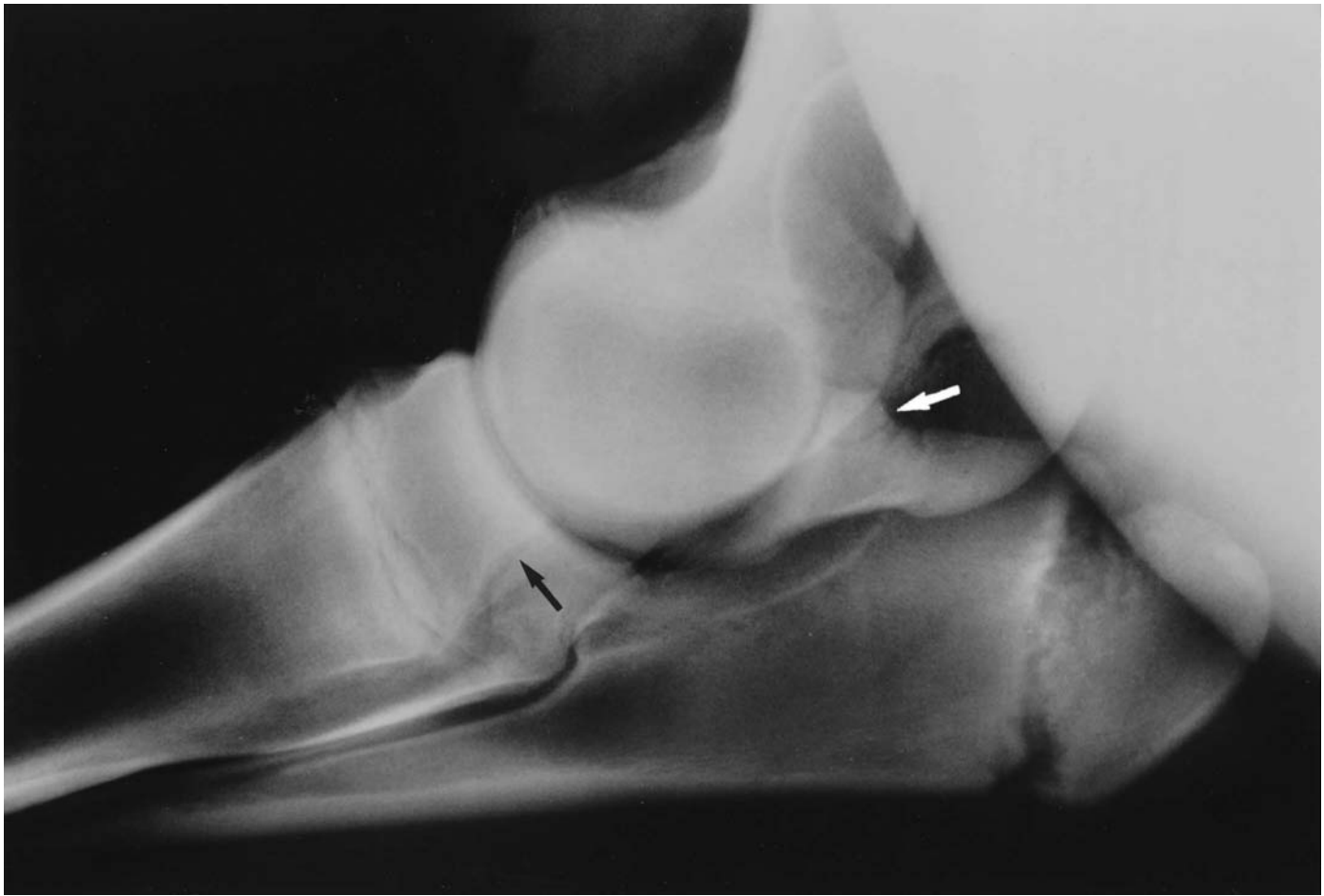
Figure 5.18 Mediolateral view of a normal elbow of an 11-month-old filly. The proximal ulnar epiphysis has enlarged compared with Figure 5.17 and is fusing with the metaphysis, but the physis is extremely irregular. There is a radiolucent line (black arrow) in the caudal aspect of the proximal radial physis which represents part of the radioulnar articulation. Positioning is not ideal, since the opacity of the pectoral muscles is superimposed over the proximal aspect of the ulna. The anconeal process (white arrow) is a separate centre of ossification.

the proximal radius is seen as a lucent line through the caudal aspect of the radius (Figure 5.18).

There is an irregularly outlined bony prominence, the transverse crest, on the distocaudal aspect of the radius. Its size depends on the angle of projection, since slight obliquity will enhance it. The mottled opacity of the torus carpeus (chestnut) on the caudal aspect of the radius must not be confused with dystrophic mineralization of soft tissues. Other radiographic characteristics of the distal radius are discussed in Chapter 4 (pages 173–86).

Craniocaudal views

The humeroradial joint space often appears wider medially than laterally. There are smoothly outlined eminences on the medial and lateral aspects of the distal humerus and proximal radius for attachment of the collateral ligaments (Figure 5.20, page 234).

[232]

Radial fossa

Humeral condyle

'Lips' of cranial margin of articular
surface of proximal radius

Radial tuberosity

Interosseous
space

Trochlear notch

Border of olecranon fossa

Medial
epicondyle

Anconeal
process

Olecranon
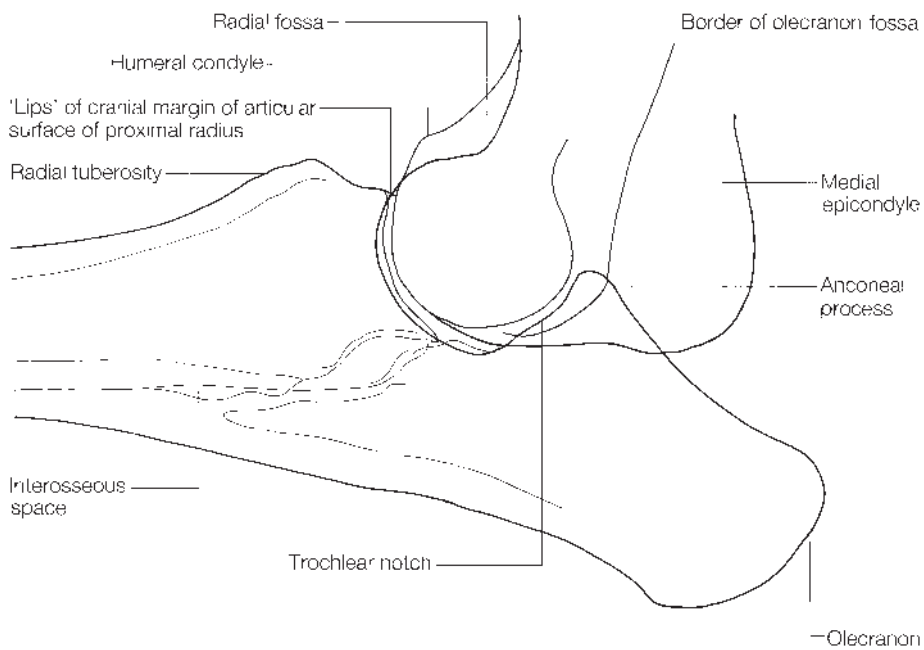
Figure 5.19 Mediolateral view and diagram of a normal adult elbow. The non-articular portion of the trochlear notch of the ulna is arrowed.

[233]

Figure 5.20 Caudocranial view and diagram of a normal adult elbow.

SIGNIFICANT RADIOLOGICAL ABNORMALITIES

Osteochondrosis

Osteochondrosis of the elbow in the horse is rare. It has been documented at post-mortem examination involving the medial condyle of the humerus and the medial proximal radius. Lameness associated with a separate bone fragment detached from the anconeal process of the ulna has been described in a 2-year-old Standardbred. The lameness was relieved by

HUMERUS

— Olecranon

Medial epicondyle
of humerus

Lateral eminences
for ligamentous
attachments

Medial eminences
for ligamentous
attachments

— ULNA

RADIUS
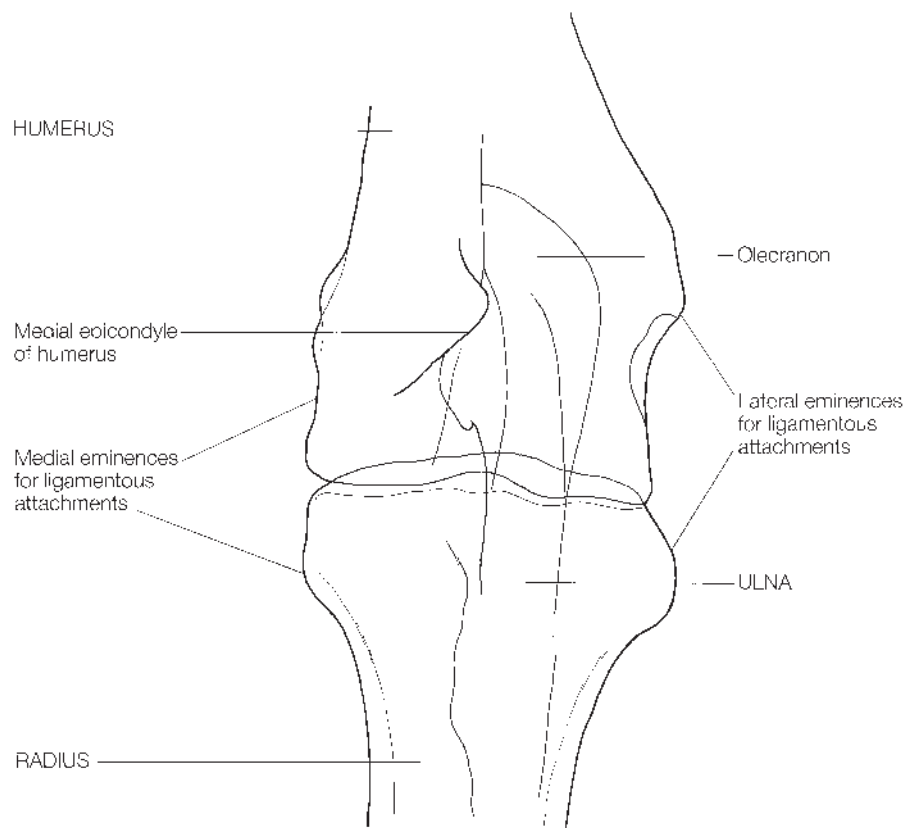
Figure 5.20 *Cont'd*

intra-articular anaesthesia of the elbow. The anconeal process is best assessed in a mediolateral view, and detachment of its apex may be an osteochondritic lesion. Care must be taken in the assessment of young foals in which the anconeal process may be a separate centre of ossification.

Osseous cyst-like lesions

Osseous cyst-like lesions occasionally occur close to the elbow joint and are usually seen in young horses. They occur most commonly in the medial aspect of the proximal radial epiphysis in association with periosteal reactions at the site of insertion of the medial collateral ligament of the humeroradial joint (Figures 5.21a and 5.21b). These cyst-like lesions may ultimately 'fill-in' radiographically, but DJD may be a sequel. The response to conservative treatment has been variable; surgical treatment might yield better results. The joint should be inspected carefully for evidence of secondary degenerative joint disease, before contemplating surgery.

Osseous cyst-like lesions occur less commonly in the distal radius. Surgical treatment may be successful.

Degenerative joint disease

Degenerative joint disease of the humeroradial, humeroulnar and radioulnar joints is uncommon except as a sequel to an osseous cyst-like lesion, collateral ligament damage or an articular fracture. In a mediolateral view
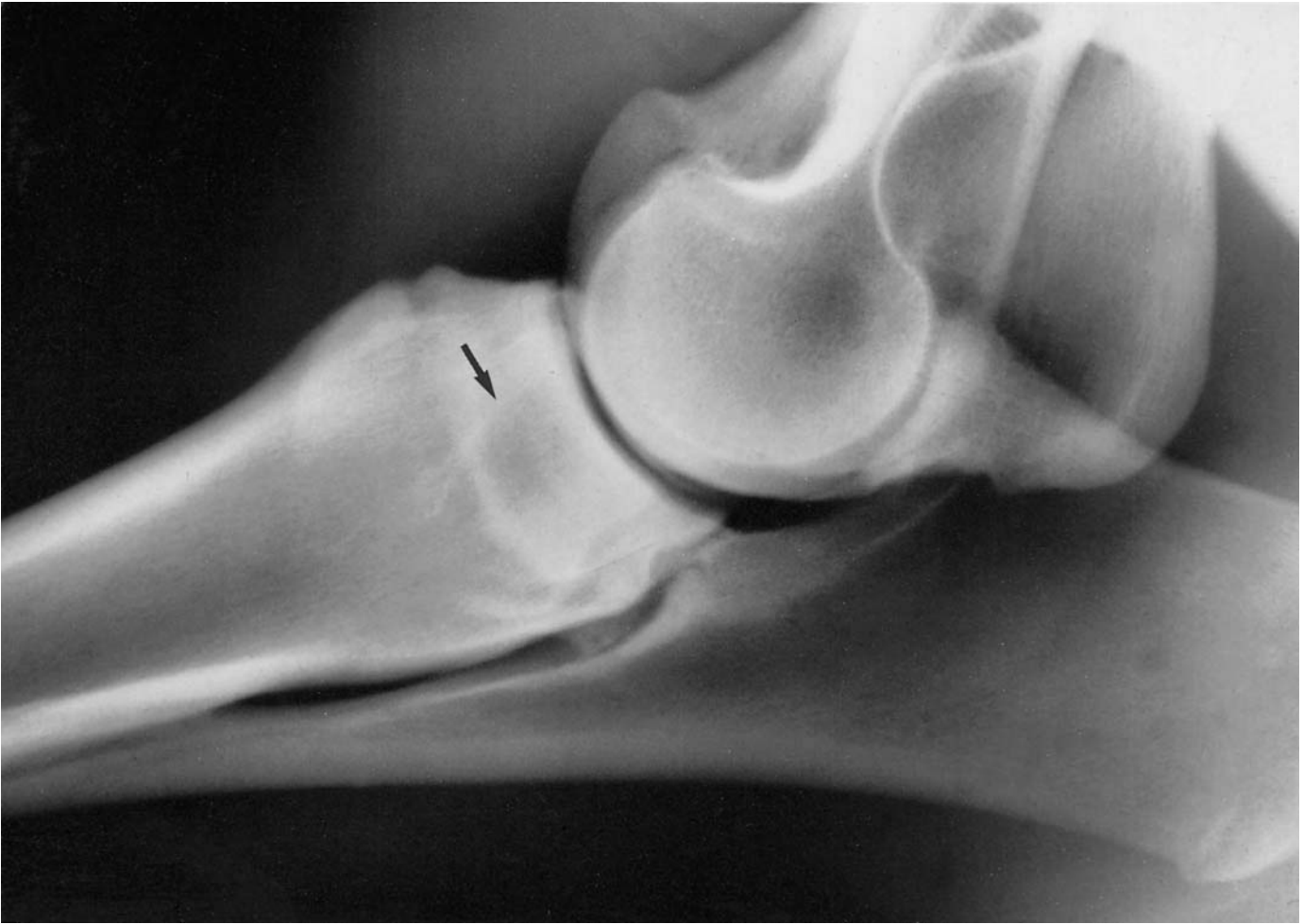
Figure 5.21(a) Mediolateral view of an elbow of a 2-year-old Thoroughbred. There is an irregularly outlined radiolucent area (arrow) in the proximal radial epiphysis and the physis is remodelled. (See also Figure 5.21(b).) The filly was treated conservatively and raced successfully.

the 'lips' of the proximal articular surface of the radius (see page 234) should not be confused with osteophytes. Craniocaudal views are more helpful for the diagnosis of degenerative joint disease. Typically, osteophyte formation is seen on the medial and lateral aspects of the distal humerus and/or the proximal radius (Figures 5.22a and 5.22b, pages 238 and 239). In advanced cases there may be narrowing of the humeroradial joint space with subchondral bone sclerosis. The prognosis for return to athletic function is poor.

Periosteal proliferative reactions (enthesopathy) at the site of insertion of biceps brachii on the radial tuberosity

Entheseous new bone, with or without discrete bony fragments, may develop at the insertion of biceps brachii on the radial tuberosity, and is best seen on a mediolateral view (Figure 5.23, page 240). New bone may not be identifiable until 3–6 weeks after the onset of lameness, so nuclear scintigraphy is more sensitive in the acute phase, and may help to interpret the significance of entheseous new bone in a horse with more chronic lameness. In the acute phase there may be some pain on manipulation of the joint, but in more chronic cases there may be no localizing signs. Lameness may resolve with rest, but often persists.

[236]
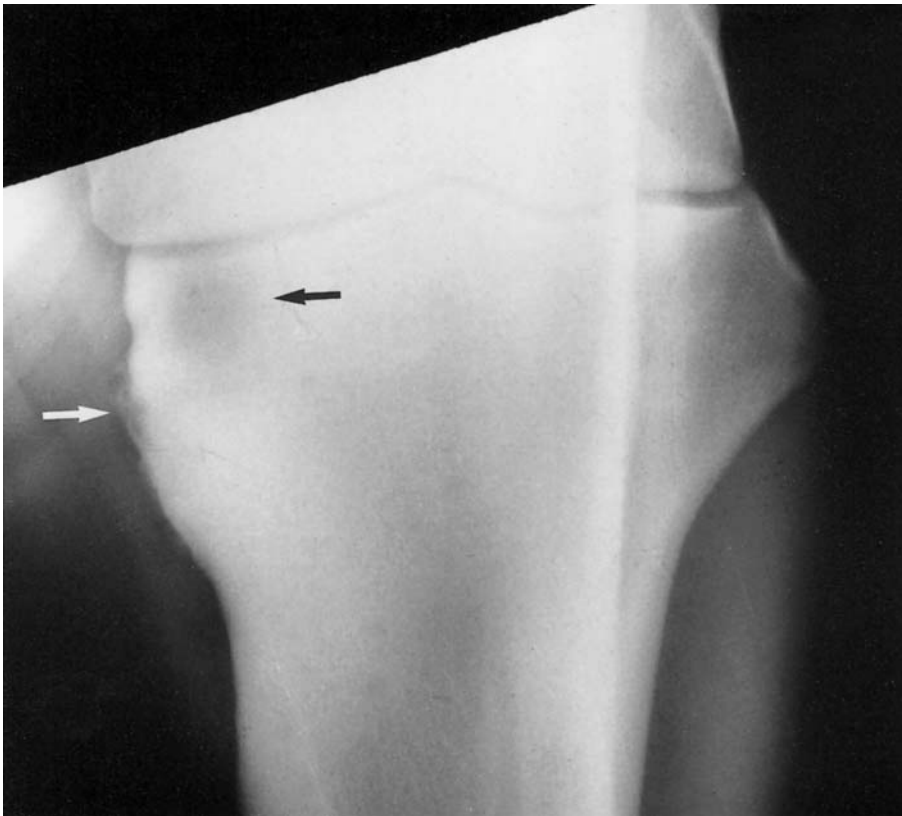
Figure 5.21(b) Craniocaudal view of the same elbow as Figure 5.21(a). The osseous cyst-like lesion (black arrow) is in the medial part of the epiphysis. There is periosteal new bone (white arrow) in the region of insertion of the medial collateral ligament.

Entheseous new bone at the sites of attachment of the collateral ligaments of the humeroradial joint

Sprain of the lateral collateral (or, less commonly, the medial collateral) ligament of the humeroradial joint may be followed by the development of entheseous new bone on the humeral epicondyle and proximal radius, best seen in a craniocaudal projection (Figure 5.24, page 241). Occasionally a fragment may be avulsed, especially from the proximal attachment. Diagnostic ultrasonography is useful to determine the degree of ligamentous damage. Chronic instability of the joint makes degenerative joint disease a likely sequel.

Periosteal reaction at the site of origin of the accessory ligament of the superficial digital flexor tendon

Periostitis may develop proximal to the transverse ridge, on the distal caudomedial aspect of the radius, secondary to tearing of the attachment of the accessory ligament of the superficial digital flexor tendon (the superior or radial check ligament). Clinical signs include very subtle lameness, sometimes associated with distension of the carpal sheath in acute cases. This injury may occur concurrently with superficial digital flexor tendonitis and it is therefore prudent to examine the tendon ultrasonographically. Radiographic changes are usually only detectable in chronic cases, and rest (for 2 months) generally results in resolution of clinical signs.

[237]

Figure 5.22(a) Mediolateral view of an elbow joint of an event horse with radiographic evidence of degenerative joint disease. There is osteophyte formation on the cranioproximal aspect of the radius (compare with Figure 5.19) and modelling of the anconeal process of the ulna. Lameness was substantially improved by intra-articular analgesia.

Luxation of the elbow joint

Luxation of the elbow joint is not common and has only been reported concurrent with a fracture of the radius or ulna.

Infection

Infection occurs most commonly in young foals but, since the lateral aspect of the radius is poorly protected by soft tissues, a deep wound in this area may penetrate the elbow joint capsule or cause localized infection. This may spread to the joint or result in osteomyelitis of the radius or ulna in an adult horse. If the degree of lameness associated with a wound in the elbow region is unexpectedly severe, or if there is a discharging sinus, radiographic examination is indicated. Injection of as much radiopaque contrast medium as possible, via a Foley catheter, should establish whether a sinus communicates with the joint capsule or with sequestered bone. It may also demonstrate a filling defect representing a foreign body.

[238]

Figure 5.22(b) Caudocranial view of an elbow (same horse as Figure 5.22a). There is considerable osteophyte formation on the medial aspect of the humeroradial joint and rather irregular opacity of the subchondral bone on the medial aspect of the joint.

Osteochondroma of the distal radius

Distension of the carpal sheath, lameness and resentment of pressure applied to the distal caudal aspect of the radius may be associated with an osteochondroma on the distal diaphysis or the metaphysis of the radius. Radiographically this appears as a variably shaped bony protuberance on the distocaudal aspect of the radius (see Figure 4.19, page 199). This mass has a thin cortex which appears to be continuous with the cortex of the radius. Sequential radiographs may demonstrate progressive enlargement of the mass. Treatment by surgical removal of the abnormal bone is usually successful in resolving both the lameness and carpal sheath swelling.
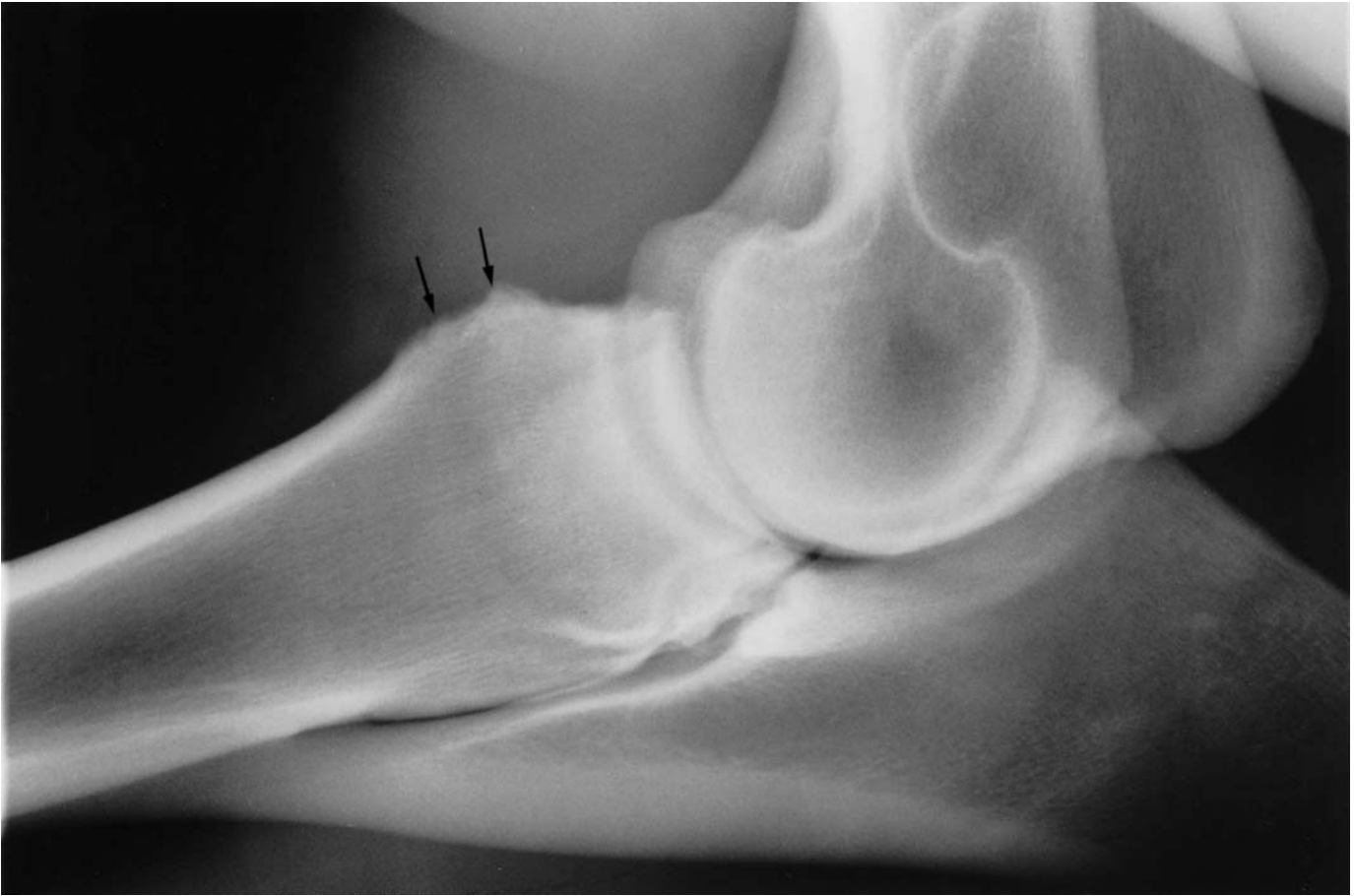
Figure 5.23 Mediolateral view of an elbow of a 7-year-old advanced event horse, with lameness of several months' duration. There is periosteal new bone formation on the cranioproximal aspect of the radius (arrows), which represents entheseophyte formation at the insertion of biceps brachii.

Hereditary multiple exostosis

Hereditary multiple exostosis is a rare condition characterized by multiple bony projections on growing long bones, the ribs, the pelvic bones and the dorsal spinous processes of the thoracic and lumbar vertebrae. These swellings are present at birth and may enlarge progressively until skeletal maturity. They may be asymptomatic unless impinging upon adjacent soft tissues, but may cause distension of synovial structures. The radiographic appearance is similar to that of solitary osteochondroma. There is no known treatment, but it is a hereditary condition, transmitted by an autosomal dominant gene.

Hypertrophic osteopathy

This condition is discussed in detail in Chapter 1 (page 15). Periosteal new bone along the diaphysis and the metaphyses of the radius may be due to hypertrophic osteopathy. The multifocal nature of the disease should help to differentiate it from other causes of periostitis.

[240]

Figure 5.24 Craniocaudal view of an elbow of a 10-year-old riding school pony with chronic lameness. There is extensive new bone on the lateral aspect of the epicondyle of the humerus (arrow heads). There is periosteal roughening and new bone on the lateral and medial aspects of the proximal radius (small white arrows). This is entheseophyte formation at the sites of attachment of the collateral ligaments of the humeroradial joint. There is also mineralization in the soft tissues laterally (large white arrow). There was also slight osteophyte formation on the articular margins of the joint, seen only in a mediolateral view.

Fractures (Figure 5.25)

Physeal fractures

Fractures of the distal physis of the humerus occur occasionally and warrant a poor prognosis. In an immature horse, the open proximal physis of the ulna should not be confused with a fracture. The apophysis may be displaced proximally (Salter-Harris type 1 fracture) (see Chapter 1, page 17) and it is important to compare its position with a horse of similar age. Radiographic examination of the contralateral limb provides an ideal comparison. These fractures and both proximal and physeal fractures of the radius have a fair prognosis.

Embertson, Bramlage and Gabel (1986)

Gaines and Auer (1983)
Embertson, Bramlage and Gabel (1986)

Auer and Watkins (1987)
Crawford and Fretz (1985)
Sanders-Shamis, Bramlage and Gabel (1986)
Vaughan and Mason (1975)

Denny (1976)
Donecker, Bramlage and Gabel (1984)
Easley *et al.* (1984)
Levine and Meagher (1980)
Monin (1978)
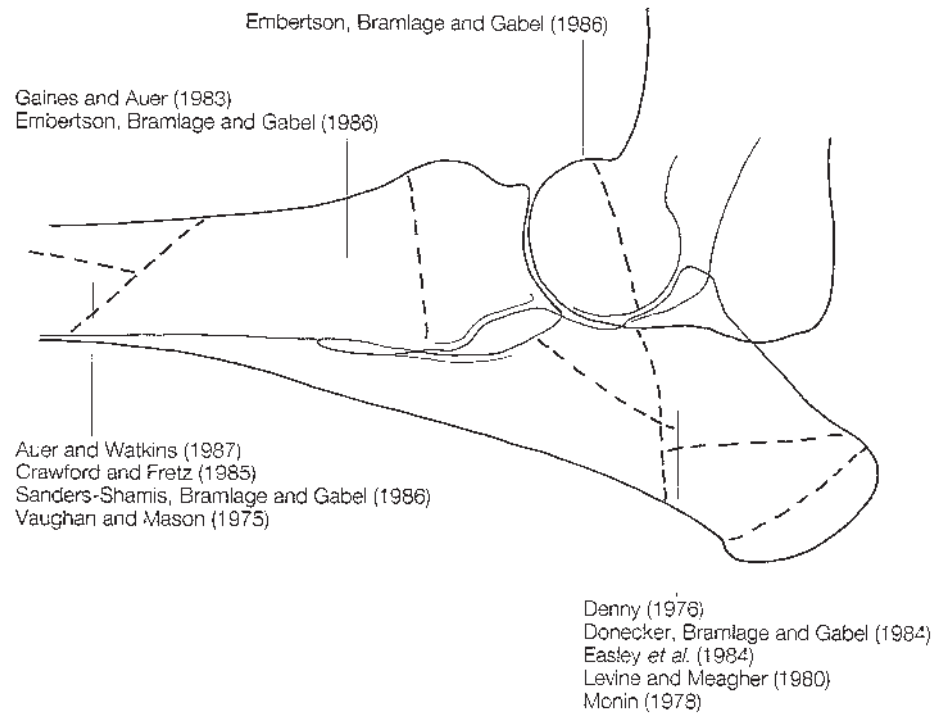
Figure 5.25 Location of common fractures in the elbow region, and recommended references (see 'Further reading').

Ulnar fractures

Fracture of the olecranon of the ulna is a common sequel to trauma in the elbow region. Lameness is usually severe and the horse may stand with the elbow 'dropped'. There may or may not be associated soft tissue swelling. Radiographic examination of a suspected facture should include both mediolateral and craniocaudal views in order to assess its configuration accurately. A fracture which enters the trochlear notch must be assessed carefully to determine whether or not it involves the articular or non-articular region (Figure 5.26). Provided that ulnar fractures are recognized and treated early, the prognosis depends primarily on whether the fracture is simple or compound, the extent of comminution and the degree of displacement of the fracture fragments. Internal fixation offers the best chance for full return to athletic function.

Radial fractures

Radial fractures are a common result of trauma and occur in many configurations, comminuted, transverse and physeal being the most frequent. Multiple radiographic views may be necessary to assess the full extent of a fracture. Repair may be successful in immature horses, but the prognosis in adult horses is extremely guarded, although an incomplete fissure (stress) fracture may heal with conservative treatment.

Fatigue or stress fractures of the radial diaphysis occur in young (2- and 3-year-old) Thoroughbreds in training. Although they may not be detectable radiographically in the acute phase, there may be localized increased opacity of the medulla. Nuclear scintigraphy is a more sensitive diagnostic

Figure 5.26 Mediolateral view of an adult elbow with a comminuted fracture of the olecranon. Although one of the fracture lines enters the trochlear notch of the ulna, it involves the non-articular area.

technique. Medullary sclerosis in the mid-diaphyseal region reflects endosteal callus.

FURTHER READING

Allen, D. and White, N. (1984) Chip fracture of the greater tubercle of a horse. *Comp. Cont. Educ.*, **6**, S39–41

Auer, J. and Watkins, J. (1987) Treatment of radial fractures in adult horses: an analysis of 15 clinical cases. *Equine Vet. J.*, **19**, 103–110

Bertone, A., McIlwraith, C., Powers, P., Stashak, T., Aanes, W. and Turner, A. (1986) Subchondral osseous cystic lesions of the elbow of horses: conservative versus surgical treatment. *J. Am. Vet. Med. Ass.*, **189**, 540–546

Brown, M. and MacCallum, F. (1974) Anconeal process of ulna: separate centre of ossification in the horse. *Br. Vet. J.*, **130**, 434–438

Chopin, J., Wright, J., Melville, L. and Robinson, W. (1997) Lateral collateral ligament avulsion of the humeroradial joint in a horse. *Vet Radiol. & Ultrasound* **38**, 50–54

Crawford, W. and Fretz, P. (1985) Long bone fractures in large animals: a retrospective study. *Vet. Surg.*, **14**, 295–302

Crawley, G. and Grant, B. (1986) Repair of elbow joint luxation without concomitant fracture in a horse. *Equine Pract.*, **8**(5), 19–26

Denny, H. (1976) The surgical treatment of fractures of the olecranon in the horse. *Equine Vet. J.*, **8**, 20–26

Donecker, J., Bramlage, L. and Gabel, A. (1984) Retrospective analysis of 29 fractures of the olecranon process of the equine ulna. *J. Am. Vet. Med. Ass.*, **185**, 183–189

Dyson, S. (1985) Sixteen fractures of the shoulder region in the horse. *Equine Vet. J.*, **17**, 104–110

Dyson, S. (1986a) Shoulder lameness in the horse: an analysis of 58 suspected cases. *Equine Vet. J.*, **18**, 29–36

Dyson, S. (1986b) The differential diagnosis of shoulder lameness in the horse. *Thesis*, Fellowship of the Royal College of Veterinary Surgeons

Dyson, S. (1986c) Interpreting radiographs 7: Radiology of the equine shoulder and elbow. *Equine Vet. J.*, **18**, 352–361

Dyson, S. and Greet, T. (1986) Repair of a fracture of the deltoid tuberosity of the humerus in a pony. *Equine Vet. J.*, **18**, 230–232

Easley, K., Schneider, J., Guffy, M. and Boero, M. (1984) Equine ulnar fractures: a review of 25 clinical cases. *Equine Vet. Sci.*, **3**(1), 5–12

Edwards, G. and Vaughan, L. (1978) Infective arthritis of the elbow joint in the horse. *Vet. Rec.*, **103**, 227–229

Embertson, R., Bramlage, L. and Gabel, A. (1986) Physeal fractures in the horse II: management and outcome. *Vet. Surg.*, **14**, 295–302

Firth, E., Dik, K., Goedegebuure, S., Hagens, F., Verberne, L., Merkens, H. and Kersjes, A. (1980) Polyarthritis and bone infection in foals. *Zbl. Vet. Med.*, **B27**, 102–124

Gaines, J. and Auer, J. (1983) Treatment of a Salter Harris Type III epiphyseal fracture in a young horse. *Comp. Cont. Educ.*, **5**, S102–106

Hardy, J., Marcoux, M. and Eisenberg, H. (1986) Osteochondrosis-like lesion of the anconeal process in 2 horses. *J. Am. Vet. Med. Ass.*, **189**, 802–803

Leitch, M. (1977) A review of treatment of tuber scapulae fractures in the horse. *J. Equine Med. Surg.*, **1**, 234–240

Levine, S. and Meagher, D. (1980) Repair of an ulnar fracture with radial luxation in a horse. *Vet. Surg.*, **9**, 58–60

Mackey, V., Trout, D., Meagher, D. and Hornhof, W. (1987) Stress fractures of the humerus, radius and tibia in horses. *Vet. Radiol.*, **28**, 26–31

Meagher, D., Pool, R. and Brown, M. (1979) Bilateral ossification of the tendon of biceps brachii muscle in the horse. *J. Am. Vet. Med. Ass.*, **174**, 282–285

Meagher, D., Pool, R. and O'Brien, T. (1973) Osteochondrosis of the shoulder joint in the horse. *Proc. Am. Ass. Equine Pract.*, **19**, 247–256

Monin, T. (1978) Repair of physeal fractures of the tuber olecranon in the horse using a tension band method. *J. Am. Vet. Med. Ass.*, **172**, 287–290

Nixon, A., Stashak, T., McIlwraith, W., Aanes, W. and Martin, G. (1985) A muscle separating approach to the equine shoulder joint for the treatment of osteochondritis dissecans. *Vet. Surg.*, **5**, 247–256

Nyack, B., Morgan, J., Pool, R. and Meagher, D. (1981) Osteochondrosis of the shoulder joint of the horse. *Cornell Vet.*, **71**, 149–163

Oikawa, M. and Narama, I. (1998) Enthesopathy of the radial tuberosity in two Thoroughbred racehorses. *J. Comp. Path.*, **118**, 135–143

Pankowski, R., Grant, B., Sande, R. and Nickels, F. (1986) Fracture of the supraglenoid tubercle: treatment and results in 5 horses. *Vet. Surg.*, **15**, 33–39

Parks, A. and Nickels, F. (1986) Scapular sequestrum in a horse: a case report. *Vet. Surg.*, **15**, 389–391

Sanders-Shamis, M., Bramlage, L. and Gabel, A. (1986) Radius fractures in the horse: a retrospective study of 47 cases. *Equine Vet. J.*, **18**, 432–437

Turner, A.S. (1981) Long bone fractures in horses Part 1. Initial management. *Comp. Cont. Educ.*, **3**, S347–353

Valdez, H., Morris, D. and Auer, J. (1979) Compression plating of long bone fractures in foals. *J. Vet. Orthop.*, **1**, 10–18

Vaughan, L. and Mason, B. (1975) *A Clinicopathological Study of Racing Accidents in Horses*, Adlard and Son, Bartholomew Press, Dorking, Surrey

Wagner, P., Watrous, B., Shires, G. and Riebold, T. (1985) Resection of the supraglenoid tubercle of the scapula in a colt. *Comp. Cont. Educ.*, **7**, S36–40

[244]

Watrous, B. and Ackerman, N. (1978) The equine shoulder: a radiographic review. *Calif. Vet.*, Feb., 7–11

Wilson, R. and Reynolds, W. (1984) Scapulohumeral joint luxation with treatment by closed reduction in a horse. *Aust. Vet. J.*, **61**, 300–301

Yovich, J. and Aanes, W. (1985) Fracture of the greater tubercle of the humerus in a filly. *J. Am. Vet. Med. Ass.*, **187**, 74–75

Chapter 6
The Tarsus

RADIOGRAPHIC TECHNIQUE

Equipment

Radiographic examination of the tarsus (hock) is easily performed using a portable x-ray machine and high-definition screens. A grid is unnecessary unless there is considerable periarticular soft tissue swelling. A minimum of four views, lateromedial, dorsoplantar, dorsolateral-plantaromedial oblique and dorsomedial-plantarolateral oblique (or plantarolateral-dorsomedial oblique), is required. In selected cases, flexed lateromedial and dorsoplantar (flexed) views yield valuable additional information. The first four views are best obtained with the horse bearing full weight on the limb, with the metatarsal region positioned vertically. It is preferable for the horse to bear weight evenly on both hind limbs. If the horse is reluctant to bear full weight on the limb due to excessive pain, administration of an analgesic such as butorphanol may be helpful. Sedation with detomidine may facilitate examination of a difficult horse, which may otherwise refuse to stand still, or may kick repeatedly.

The hind limbs should be spread apart sufficiently to allow positioning of the cassette without it touching either limb. The person holding the cassette can position it more accurately if the horse's tail is tied in a knot and the hock is not obscured. A long-handled cassette holder should be used.

Positioning

Lateromedial view

The talocalcaneal-centroquatral (proximal intertarsal), the centrodistal (distal intertarsal) and the tarsometatarsal joints are not horizontal, but slope proximodistally, from laterally to medially. In order to avoid confusing overlap of the joint spaces it is helpful to angle the x-ray beam 10° proximodistally (i.e. L10°Pr-MDiO view), centring at the approximate level of the centrodistal joint. Alternatively a horizontal x-ray beam is centred at the level of the talus (tibiotarsal bone), thus making use of a divergent x-ray beam through the lower joints of the hock. For a true lateromedial view the x-ray beam is directed parallel to a line joining the medial and lateral malleoli of the tibia, or to a line tangential to the heel of the foot.

[247]

A flexed lateromedial view can be useful to evaluate the proximal aspects of the trochlear ridges of the talus, the coracoid process of the calcaneus and the plantar distal aspect of the tibia (see Figure 6.3b, page 253). An assistant stands beside the horse's abdomen facing the tail, and holds the distal metatarsus so that the angle between the tibia and the third metatarsal bone is approximately 50°. Care should be taken to hold the limb close to the horse's body, to avoid rotation of the tarsus. The x-ray beam is centred on the talus.

Dorsoplantar view

Many horses stand slightly 'toe-out', which is helpful since it obviates the need to position the x-ray machine beneath the horse's abdomen in order to obtain a dorsoplantar view. A horizontal x-ray beam is used, centred at the centrodistal joint. In some horses it is impossible for all of the centrodistal joint to be assessed simultaneously, due to the slope of the distal joints of the hock: two views may be required. If the x-ray beam is horizontal and centred at the centrodistal joint, the lateral side of the joint may appear normal but the medial side may appear abnormally narrow. If the x-ray beam is angled 10° proximodistally, the medial side of the centrodistal joint may then look normal. Abnormalities of the medial and lateral malleoli may be missed in a dorsoplantar projection. A dorsal 15° medial-plantarolateral oblique view is useful to assess the lateral malleolus, and a dorsal 15° lateral-plantaromedial oblique projection is helpful to evaluate the medial malleolus.

Oblique views

Due to the complex structure of the equine tarsus, changes in the degree of obliquity of the x-ray beam can result in considerable alteration in the radiographs obtained. It is therefore essential to establish a consistent technique (e.g. D35°L-PLMO). The x-ray beam is centred at the site of principal interest (often the centrodistal joint). A horizontal beam is employed. It is often easier and safer to obtain a plantarolateral-dorsomedial oblique, rather than a dorsomedial-plantarolateral oblique view.

Dorsoplantar (flexed) view

The hind limb is held flexed with the hock as far behind the horse as possible (Figure 6.1). Many horses in which this view is required resent flexion of the limb and administration of an analgesic such as butorphanol will facilitate this examination. The cassette is held parallel to the plantar aspect of the tuber calcanei and the x-ray beam is directed as nearly perpendicular to it as possible. It may be easier to obtain a plantarodorsal (flexed) view depending on the degree of flexion of the hock which can be achieved. These projections are particularly useful for evaluation of the tuber calcanei and the sustentaculum tali of the calcaneus.

[248]
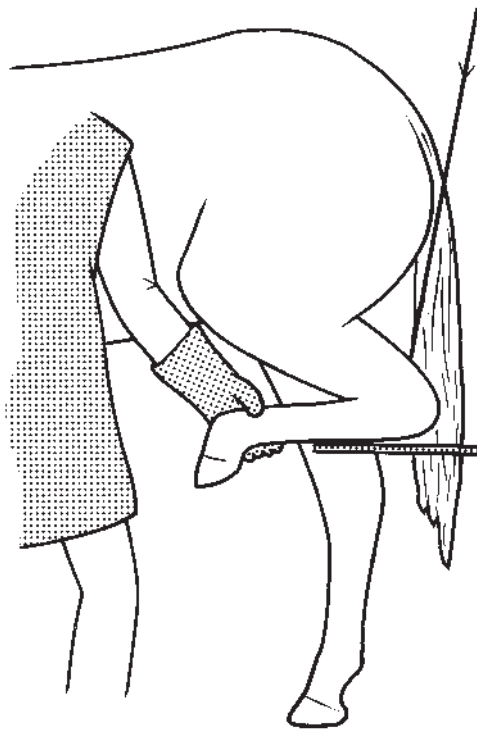
Figure 6.1 Positioning of the limb, cassette and x-ray machine to obtain a dorsoplantar (flexed) view of the calcaneus and sustentaculum tali of the fibular tarsal bone.

RADIOGRAPHIC ANATOMY: NORMAL VARIATIONS AND INCIDENTAL FINDINGS

It is important to recognize that some of the variations in radiographic appearance discussed below are the result of a previous problem which is now clinically silent. They cannot be regarded as normal, but are unlikely to be of clinical significance.

Immature horse

At birth the malleoli of the tibia and the trochlear ridges may be incompletely ossified and have an irregular, rough contour and a granular opacity (Figures 6.2a and 6.2b). There is a separate ossification centre for the lateral malleolus of the tibia, which represents the distal epiphysis of the fibula. This well-circumscribed, oval opacity fuses to the tibia by 3 months of age, and should not be misinterpreted as a fracture. Adult features such as the medial proximal and distal tubercles of the talus are undeveloped. There is a separate ossification centre for the tuber calcanei, which may be absent at birth but gradually ossifies and fuses to the calcaneus by 16–24 months of age. The centres of ossification have rounded corners, especially those of the central and third tarsal bones. The joint spaces appear wider than in an adult, because there is proportionally more cartilage present. The first and second tarsal bones may be unfused. The proximal physis of the third metatarsal bone is closed at birth.

[249]
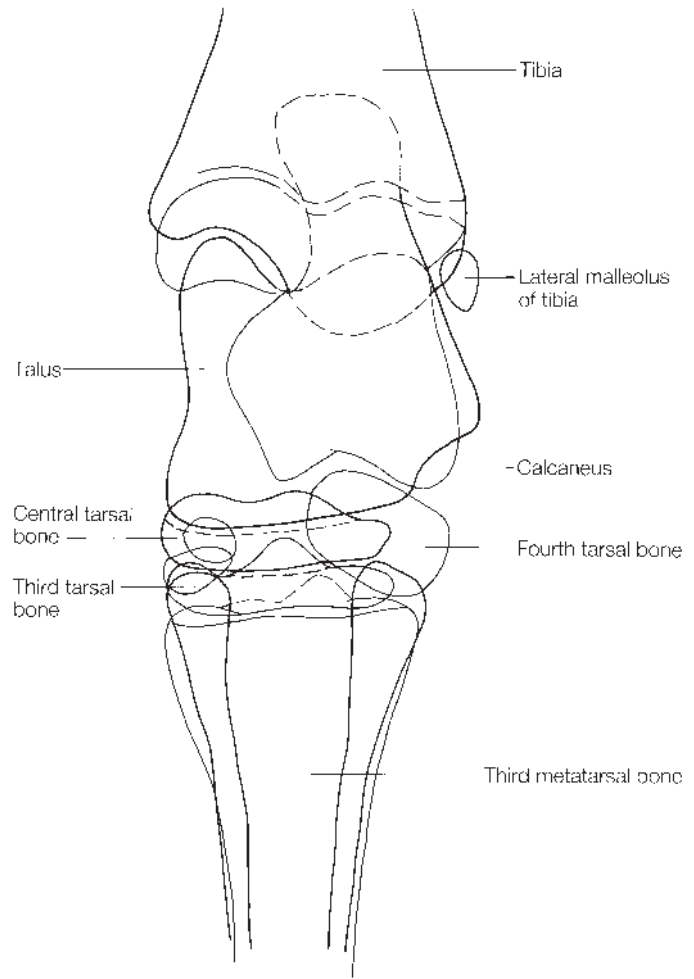
Figure 6.2(a) Dorsoplantar view and diagram of a hock of a 1-day-old foal. The small tarsal bones are rounded and the joint spaces wide compared with an adult. The medial malleolus of the tibia (white arrow) is incompletely ossified. There is a separate ossification centre of the lateral malleolus of the tibia (black arrow).

Skeletally mature horse

In order to understand the complicated radiographic anatomy of the tarsus it is useful to compare the radiographs with a bone specimen and to visualize the shapes of the individual, disarticulated bones (see Figures 6.3, 6.6, 6.7 and 6.8).

Lateromedial view

A normal lateromedial view and a flexed lateromedial view are illustrated in Figures 6.3a and 6.3b, pages 252 and 253. In some horses there is a separate bony fragment at the craniodistal aspect of the tibia: its exact location is established from the oblique views, the most common site being the distal intermediate ridge of the tibia (see Figure 6.13, page 269). This may be an

[250]
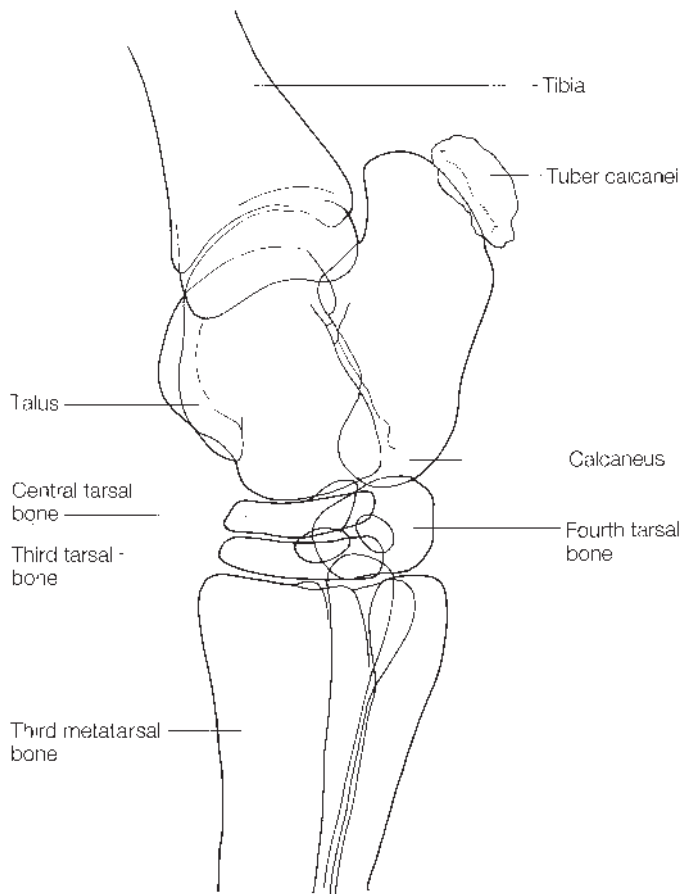
Figure 6.2(b) Lateromedial view and diagram of a hock of a 1-day-old foal. Note the relatively flat contour of the trochlear ridges of the talus compared with an adult, the widened joint spaces and the incompletely ossified tuber calcanei.

accessory ossification centre, or a manifestation of osteochondrosis. It is often clinically silent, particularly if small, although its presence may be associated with distension of the tarsocrural joint capsule (bog spavin). The medial and lateral trochlear ridges of the talus are smoothly curved, but may be slightly flattened in the mid-region, especially in Warmblood and heavy horse breeds. The lateral ridge has a distinct large notch at its distal end, whereas the medial ridge has a variably sized protuberance distally. This protuberance may be small, with or without a lucent line (a nutrient vessel) extending through it, or may be large and rounded or pointed. Sometimes there are one or two discrete bony opacities distal to it (Figure 6.4, page 254), which should not be confused with fractures. The two trochlear ridges are more widely separated in the oblique views.

Depending on the exposure factors used, a variable number of lucent lines can be identified in the region where the calcaneus and talus

[251]
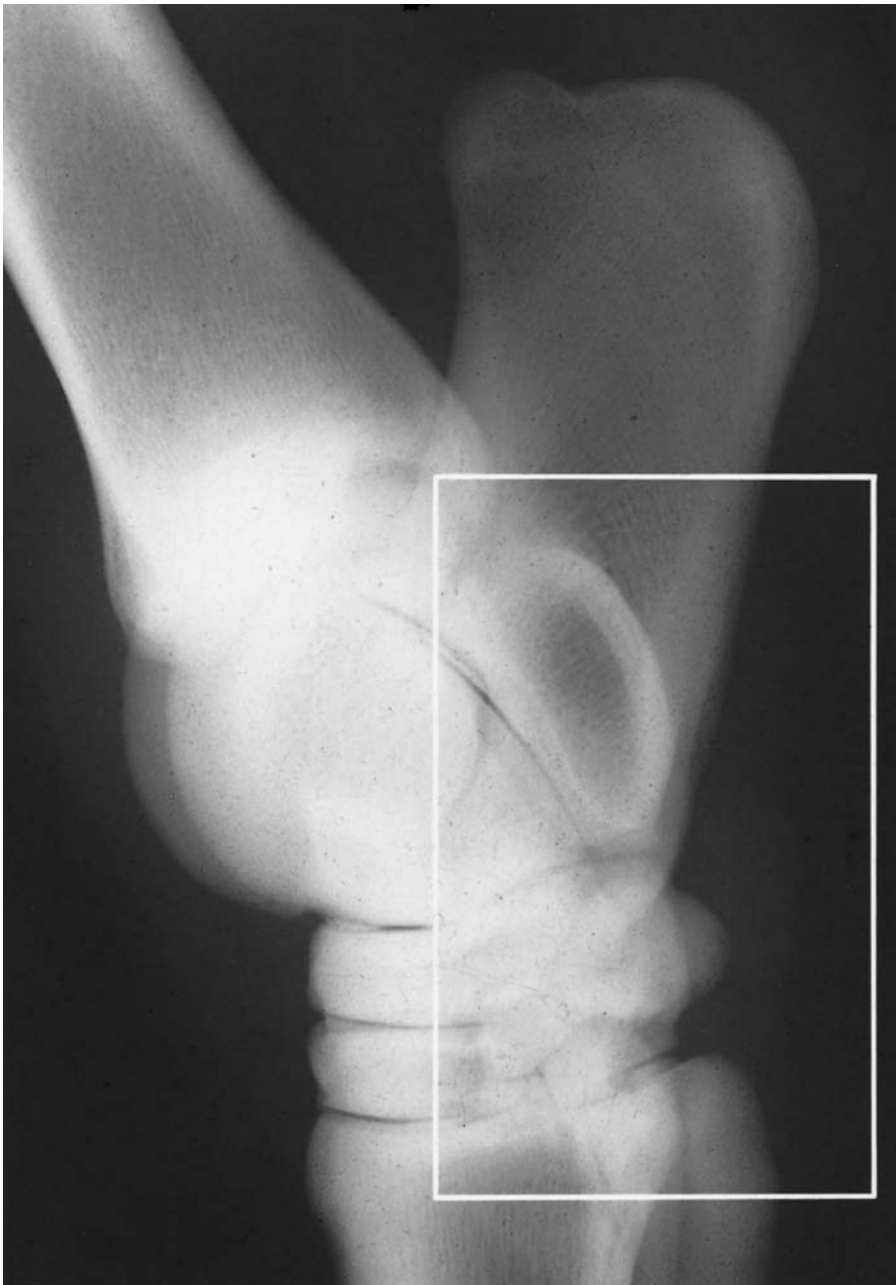
Figure 6.3(a) Inset.

Figure 6.3(a) Lateromedial view and diagram of a normal adult hock. On a soft exposure (inset) the torus tarseus (chestnut) is readily seen.

are superimposed. These represent the talocalcaneal and tarsocrural articulations and should not be confused with fractures.

The central and third tarsal bones are fairly regular in height (proximodistally) from their dorsal to plantar aspects. The first and second and fourth tarsal bones are projected superimposed upon each other; the smoothly irregular plantar contour of the fourth tarsal bone is highlighted in this view. The plantar surfaces of the calcaneus and fourth tarsal and metatarsal bones are sometimes smoothly modelled, reflecting previous tearing of the attachment of the plantar ligament ('curb').

There is sometimes a small osseous 'spur' on the dorsoproximal aspect of the third metatarsal bone (Figures 6.5a–f, pages 255 and 256). This may be an osteophyte or an entheseophyte at the site of attachment of the dorsal

[252]

Figure 6.3(a) *Cont'd*

Tarsocrural joint

Talocalcaneal-centroquatral (proximal intertarsal) joint

Centrodistal (distal intertarsal) joint

Tarsometatarsal joint

Talocalcaneal joint

Tibia

Lateral and medial trochlear tali

Central tarsal bone

Third tarsal bone

Third metatarsal bone

Calcaneus

Fourth tarsal bone

Fourth metatarsal bone
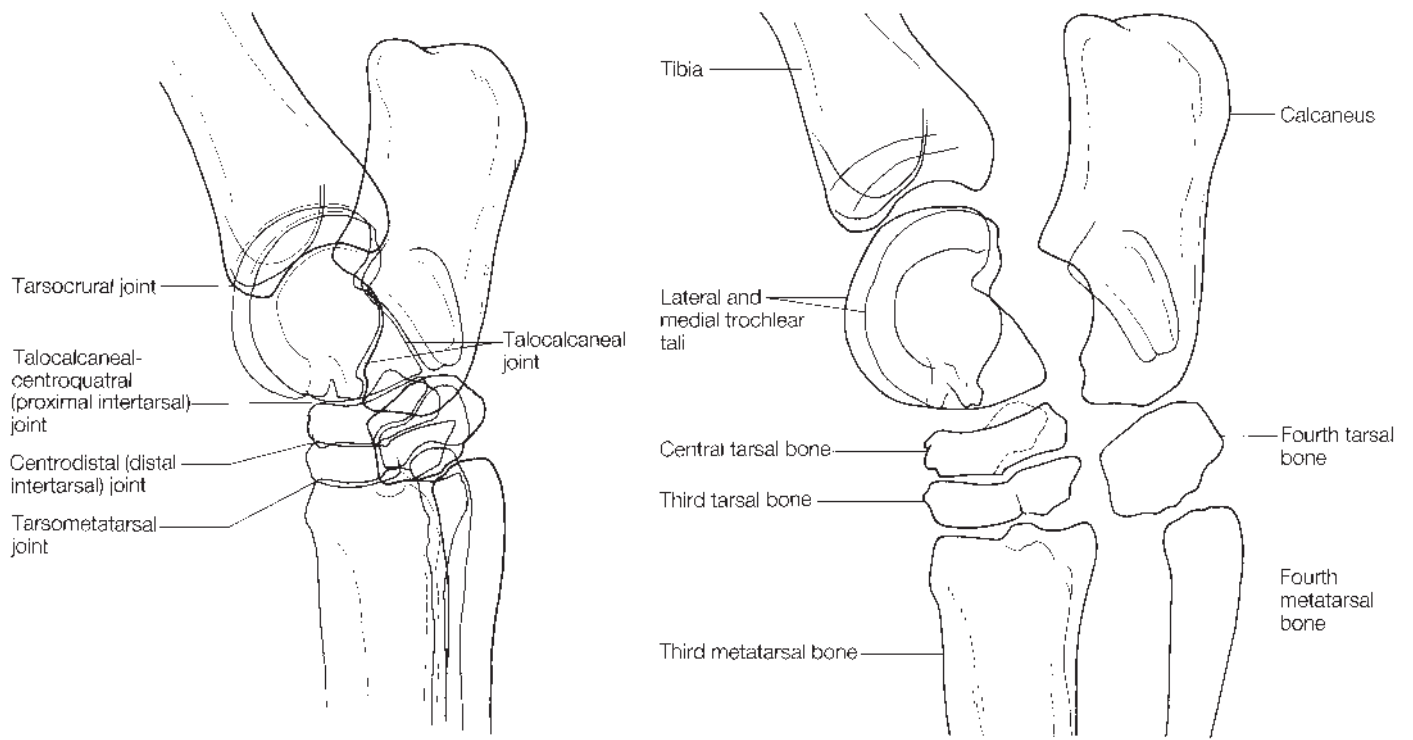
Figure 6.3(b) Flexed lateromedial view of a normal adult hock.

[253]
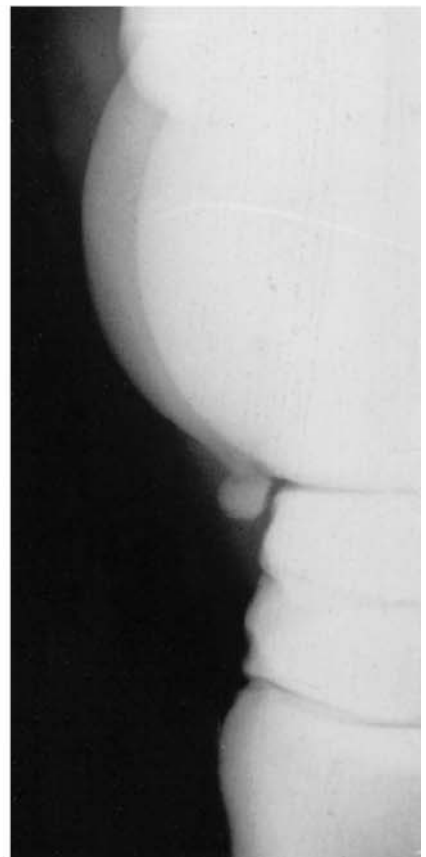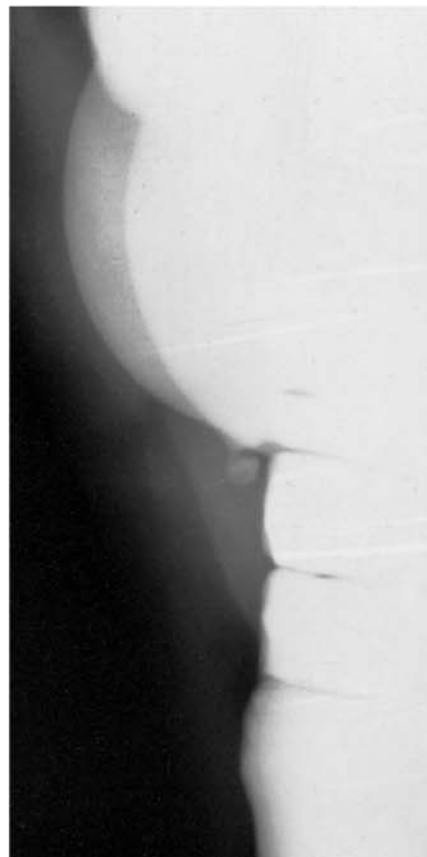
Figure 6.4 Variation in the appearance of the distal end of the medial trochlea tali (trochlear ridge).

[254]

(a)   (b)
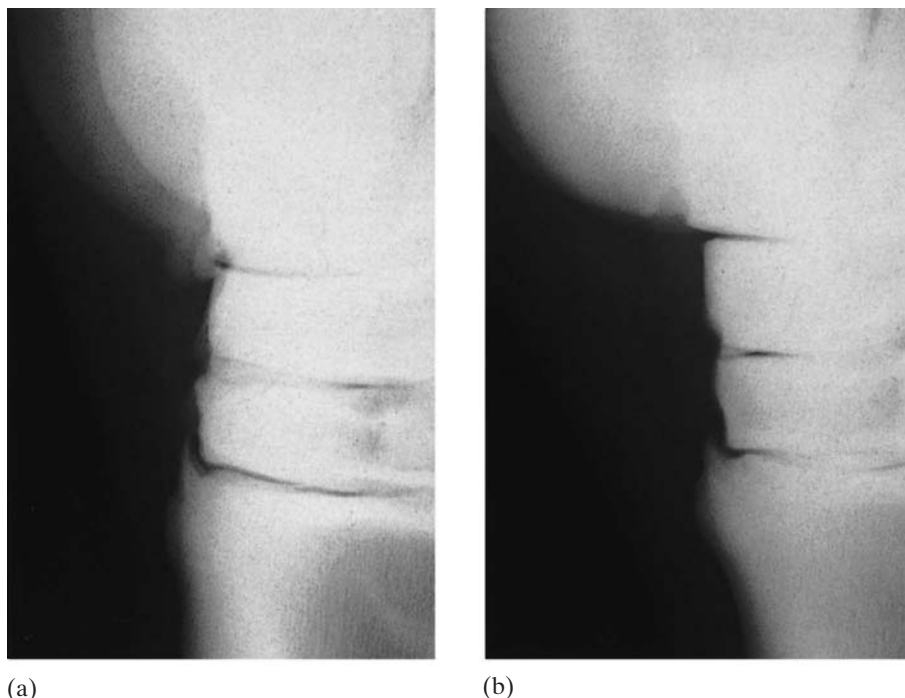
Figure 6.5(a) Lateromedial view of an adult hock. There is a large, inactive osteophyte on the dorsoproximal aspect of the third metatarsal bone. Note the protuberance on the distal aspect of the medial trochlea, a normal variation.

Figure 6.5(b) Lateromedial view of an adult hock. There is a small inactive entheseophyte on the dorsoproximal aspect of the third metatarsal bone.

tarsometatarsal ligament, peroneus (fibularis) tertius, or the cranial tibial tendon, reflecting a previous injury. In the absence of other radiographic abnormalities, an osteophyte or an entheseophyte does not necessarily signify degenerative joint disease, although they may be associated with it. An osteophyte of no significance should have a smooth margin and be of uniform opacity (Figures 6.5a and 6.5b). An irregular margin or variable opacity (both of which may only be discernible when the radiograph is viewed over high intensity illumination) suggest bony activity (Figures 6.5c and 6.5d).

The mottled opacity of the torus tarseus (chestnut) may be seen on the plantar aspect of the fourth tarsal bone (Figure 6.3a, page 252) and must not be confused with pathological mineralization of the soft tissues.

Dorsoplantar view

The medial and lateral malleoli are seen as smoothly rounded protuberances of the distal tibia (Figure 6.6, page 258). Smooth irregularity of outline may reflect previous damage to the attachment of the collateral ligaments of the tarsus.

The concave proximal articular surface of the central tarsal bone results in its plantar aspect being superimposed over the talus. There are many confusing opacities and lucent lines in the region of the central and third tarsal bones because of superimposition of the first and second and fourth tarsal bones and the bases (proximal ends) of the second and fourth metatarsal bones. The bases of the latter two bones are sloping and their articulations with the fused first and second tarsal bone and the fourth tarsal bone, respectively, are superimposed over the proximal third of the third tarsal bone. The resultant lucent lines should not be confused with

Figure 6.5(c) Lateromedial view of an adult hock. There is an active osteophyte on the dorsoproximal aspect of the third metatarsal bone. Note its relatively less opaque apex indicative of activity.

Figure 6.5(d) Lateromedial view of an adult hock. There is an active entheseophyte on the dorsoproximal aspect of the third metatarsal bone.
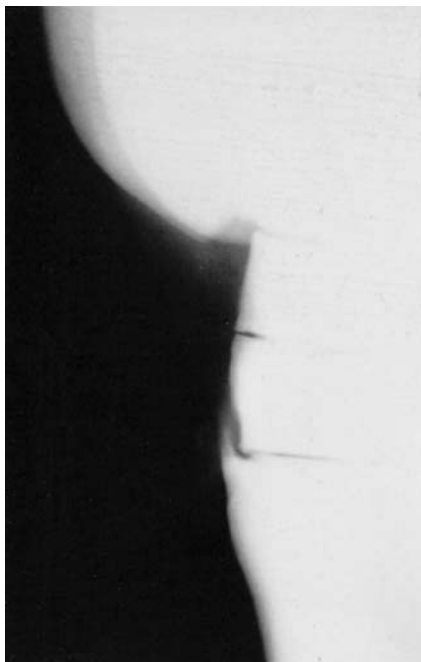
(c)
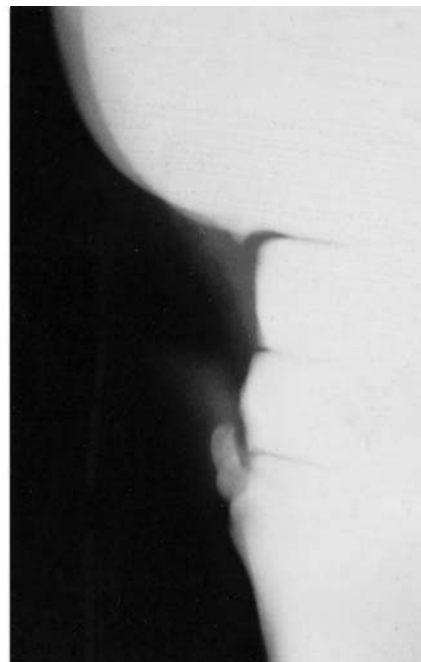
(d)

Figure 6.5(e) Lateromedial view of an adult hock (same horse as Figure 6.5c). There is dystrophic mineralization in the cranial tibial tendon.

Figure 6.5(f) Fracture of a large entheseophyte on the dorsoproximal aspect of the third metatarsal bone. Note also the osseous opacity distal to the medial trochlea tali.

(e)

(f)

pathological lesions. There are sometimes well-defined oval lucent areas centred on either or both of the talocalcaneal-centroquatral or the centrodistal joints. These represent non-articular depressions and should not be confused with osseous cyst-like lesions.

This is the best view for evaluating the width of the intertarsal articulations, provided that these joints are in the centre of the radiograph and bearing in mind the limitations imposed by the slope of the articular surfaces mentioned previously (page 247). Complete ankylosis of the

[256]

centrodistal and/or tarsometatarsal joints, in the absence of subchondral bone lysis, is sometimes seen without associated lameness.

Dorsolateral-plantaromedial oblique view

This view (Figure 6.7, page 260) highlights the medial malleolus of the tibia, the medial trochlear tali and the dorsomedial aspects of the intertarsal joints. There is a variably sized and shaped lucent area in the proximal part of the tarsal groove which represents a synovial fossa. Similar areas in the corresponding articular surface of the tibia are not seen radiographically. The distal medial tuberosity of the talus is usually smoothly rounded; it may be smoothly irregular, reflecting previous tearing of the attachment of the medial short collateral ligament. The sinus tarsi, a non-articular area between the talus and calcaneus, is seen as a relatively lucent line or oval-shaped area between the two bones, and varies with the angle of projection.

There is a bony prominence on the dorsomedial aspect of the third tarsal bone at the site of attachment of one of the dorsal tarsal ligaments. The subchondral bone of the distal talus, the central and third tarsal bones and the proximal third metatarsal bone is relatively sclerotic. There are non-articular depressions on the opposing surfaces of the talus, central and third tarsal bones and third metatarsal bones which result in relatively lucent areas in the centre of the centrodistal and tarsometatarsal joints.

In a well-positioned dorsolateral-plantaromedial oblique view, the dorsal opening of the tarsal canal, through which passes the perforating tarsal artery and a branch of the deep fibular (peroneal) nerve, is seen as a well-defined lucent area. The canal is not in the sagittal plane but courses slightly obliquely; therefore, unless the x-ray beam is parallel with the long axis of the canal, its walls will be seen as bone encroaching into the canal. This must be differentiated from new bone on the lateral aspect of the centrodistal joint (see Figure 6.18a, page 275). This new bone can usually also be seen in a dorsoplantar view. The plantar opening of the tarsal canal appears as a relatively lucent area superimposed over the fourth tarsal bone.

Plantarolateral-dorsomedial oblique view

This view (Figure 6.8, page 262) highlights the sustentaculum tali, the lateral trochlear tali, the dorsolateral aspects of the intertarsal joints, and the plantar aspect of the sustentaculum tali and the central, first and second tarsal bones. Occasionally the distal end of an incompletely ossified fibula is seen. A separate bony fragment from the distal intermediate ridge of the tibia is often best seen in this view.

Dorsoplantar (flexed) view

The proximal parts of the medial trochlear ridge, the sustentaculum tali, the tarsal groove and the tuber calcanei are highlighted in this view (Figure 6.9, page 264). Other structures are underexposed and cannot be assessed properly.

[257]

Figure 6.6 Dorsoplantar view and diagrams of a normal adult hock. Note the relative lucent areas in the central and third tarsal bones in the middle of the centrodistal joint (arrows), a normal finding.

[258]

Medial malleolus

Lateral malleolus

Calcaneus

Talus

Central tarsal bone

Fourth tarsal bone

Third tarsal bone

Fourth metatarsal bone

Second metatarsal bone

Third metatarsal bone

Figure 6.6 *Cont'd*

[259]
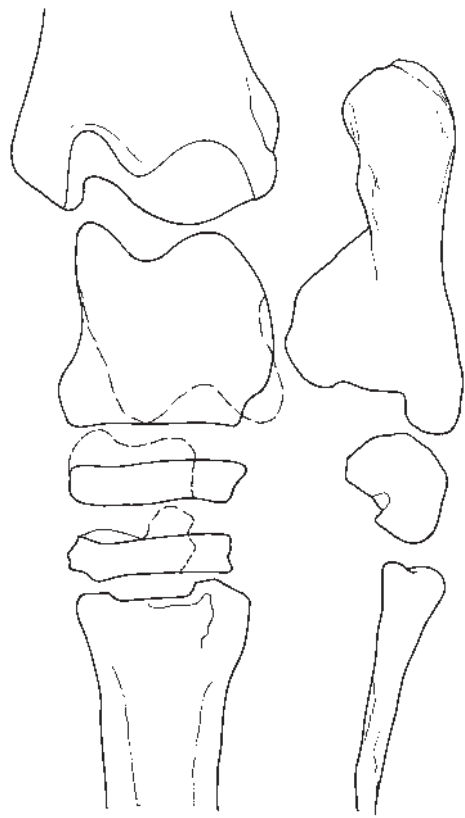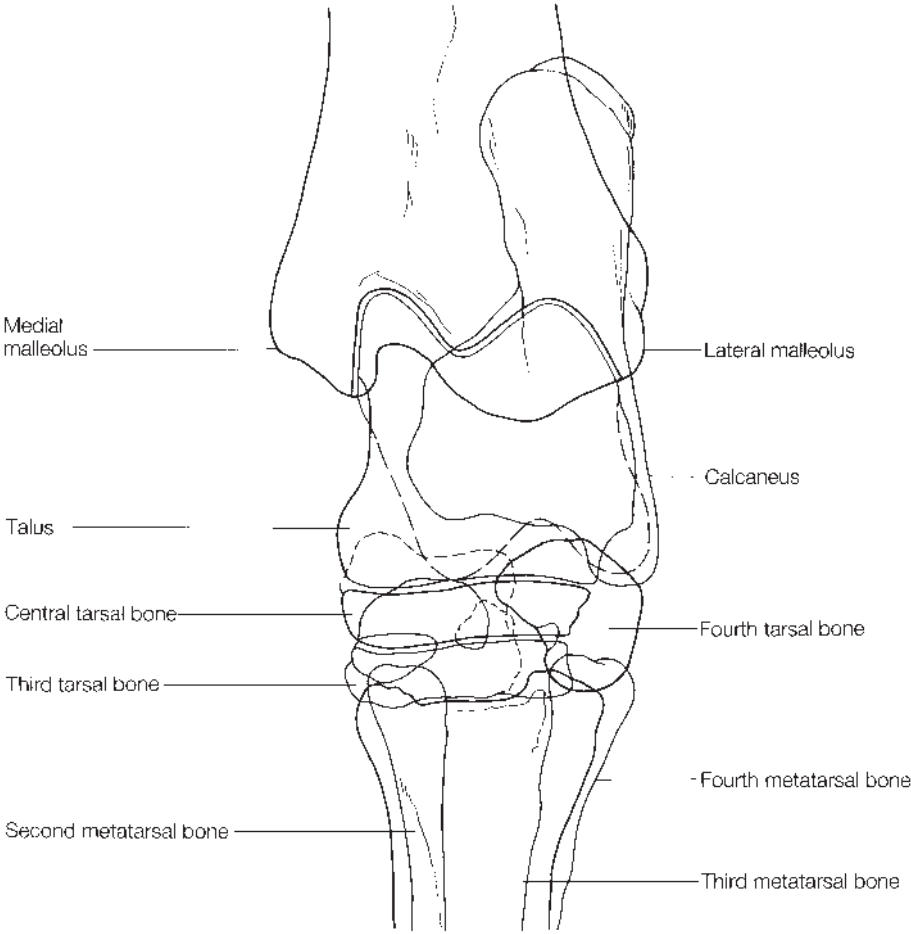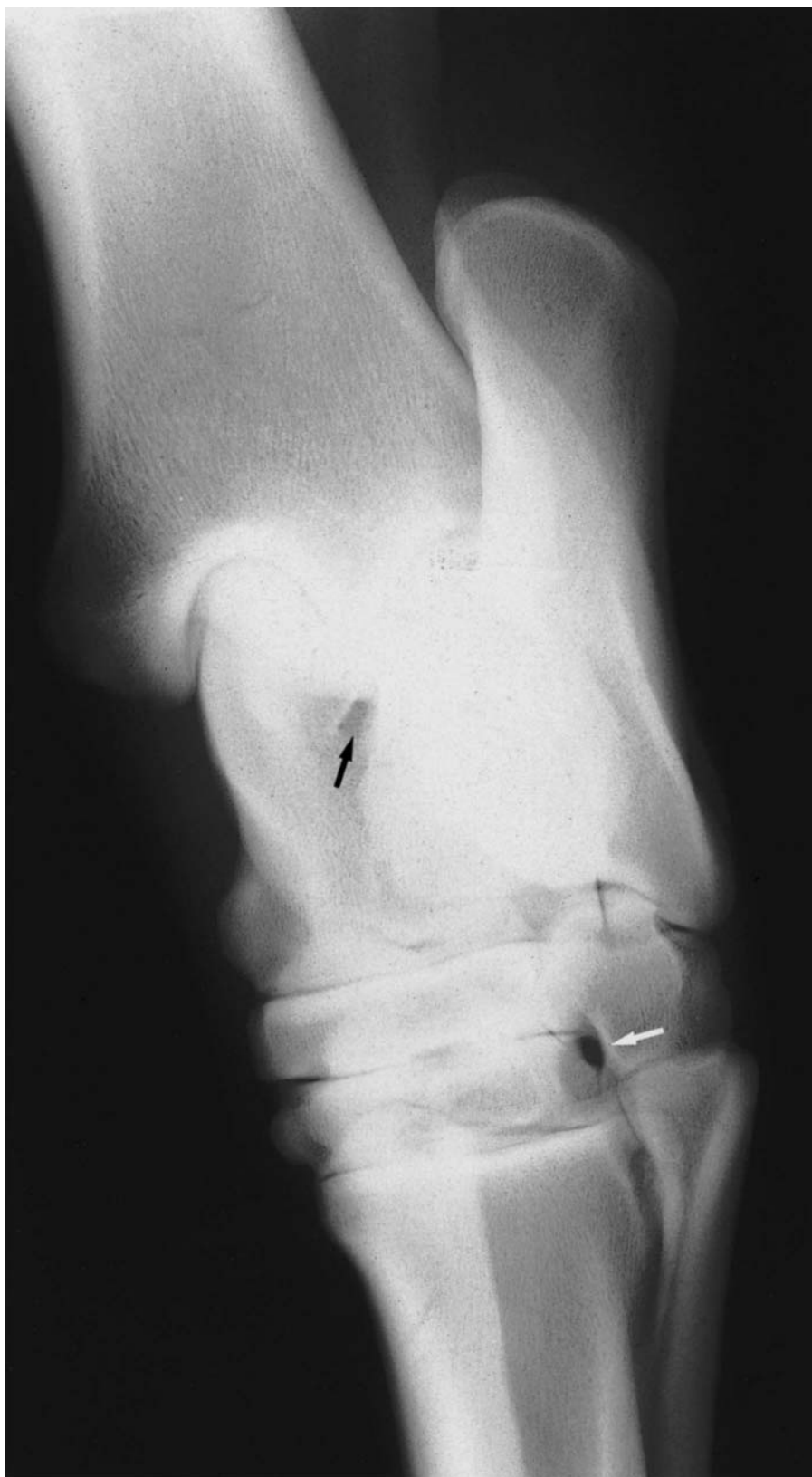
Figure 6.7 Dorsolateral-plantaromedial oblique view and diagrams of a normal adult hock. There is a radiolucent area (black arrow), a synovial fossa, in the intertrochlear groove of the talus. The third tarsal bone has a medial prominence. The dorsal opening of the tarsal canal is clearly outlined (white arrow). Note the relative lucent areas in the central and third tarsal bones in the middle of the centrodistal joint, a normal finding.

Tibia

Medial malleolus

Distal intermediate
ridge of tibia

Medial trochlea tali

Central tarsal bone

Third tarsal bone

Calcaneus

Synovial fossa

Fourth tarsal bone

Tarsal canal

Fourth metatarsal bone

Second metatarsal bone

Third metatarsal bone
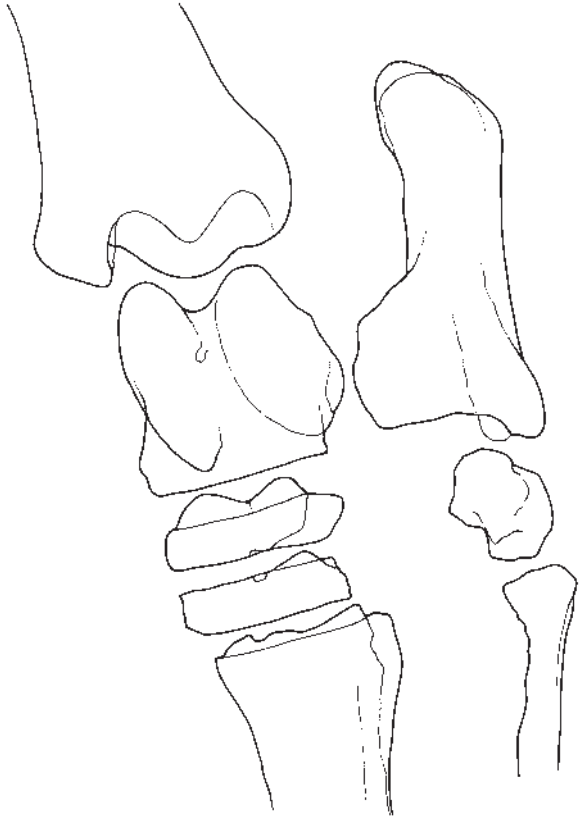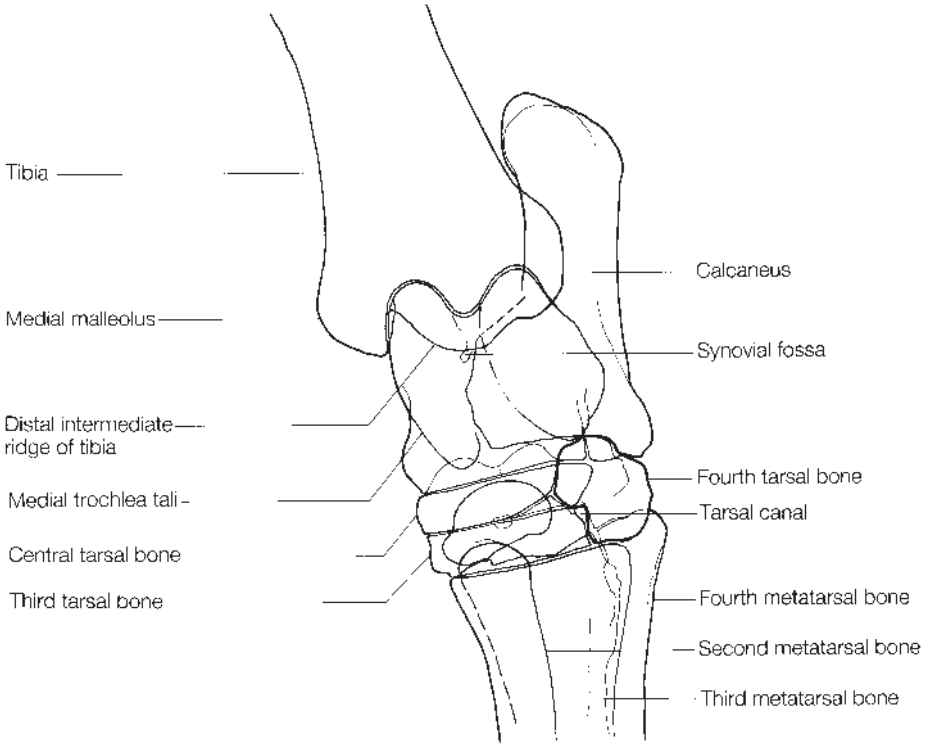
Figure 6.7 *Cont'd*

Figure 6.8 Plantarolateral-dorsomedial oblique view and diagrams of a normal adult hock. The medial trochlear tali (black arrow) and the lateral trochlear tali (white arrow) are clearly separated. The sustentaculum tali is highlighted on the plantar aspect of the talus. Note the inverted flask-shaped joint space between the third and fused first and second tarsal bones.

Lateral trochlear
tali

Sustentaculum
tali

Central tarsal bone

Fourth tarsal bone

Third tarsal bone

Fused first and second
tarsal bones

Second metatarsal
bone

Fourth metatarsal
bone
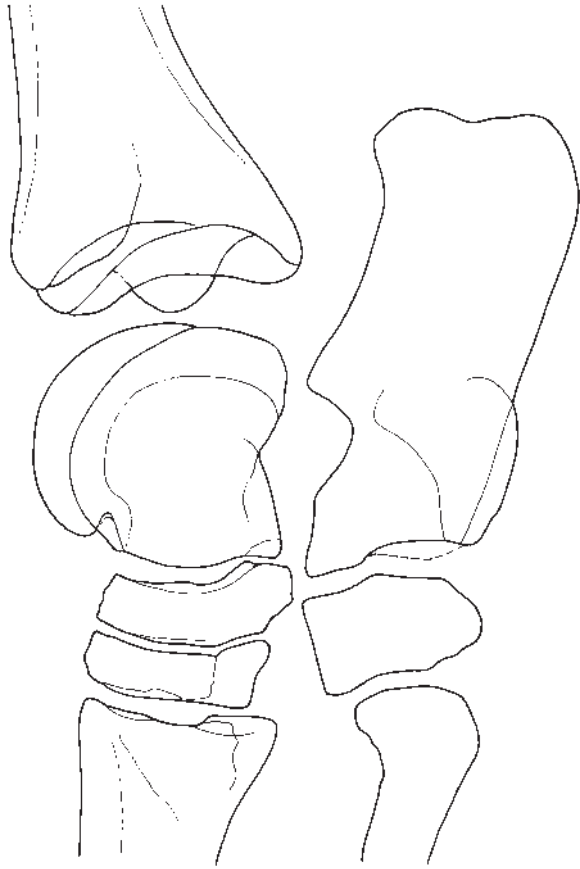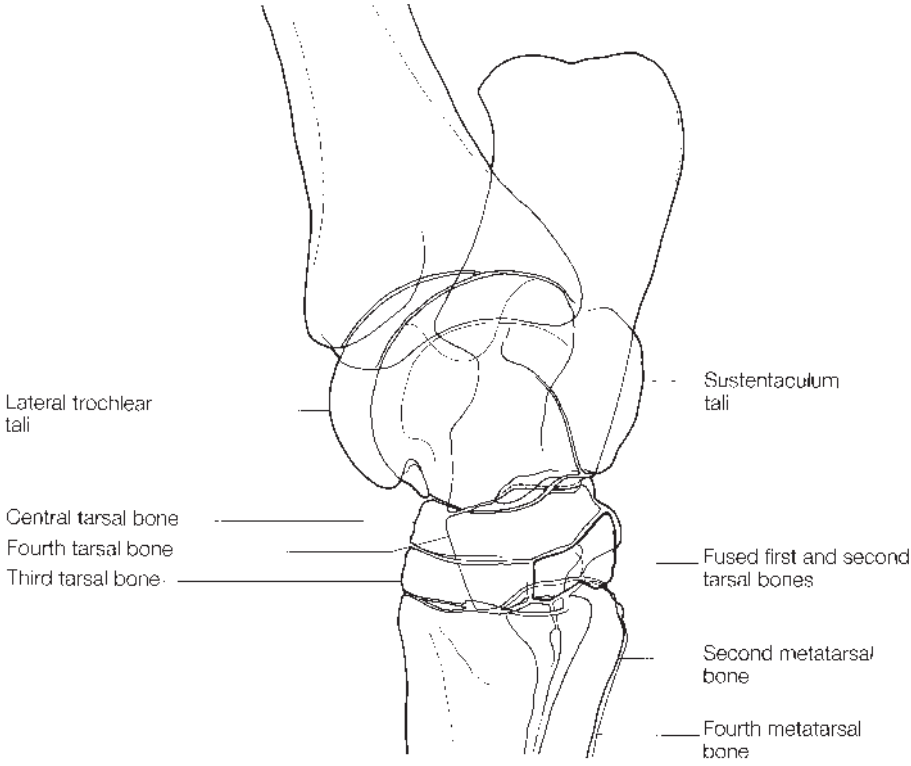
Figure 6.8 *Cont'd*
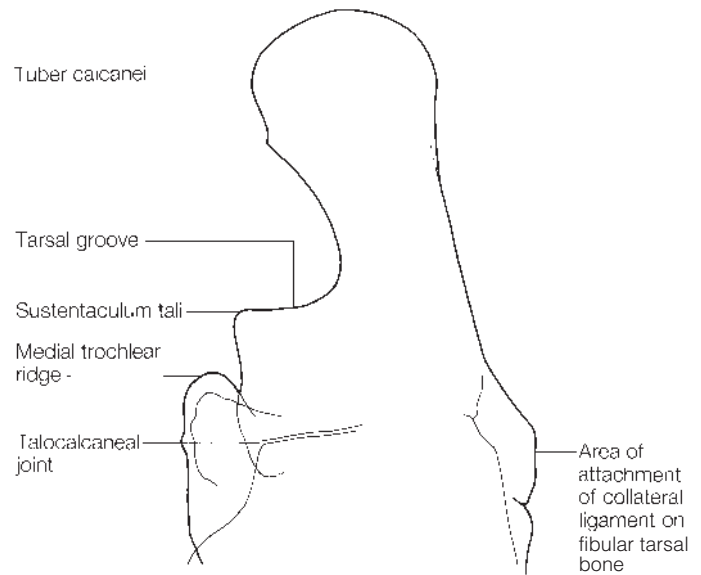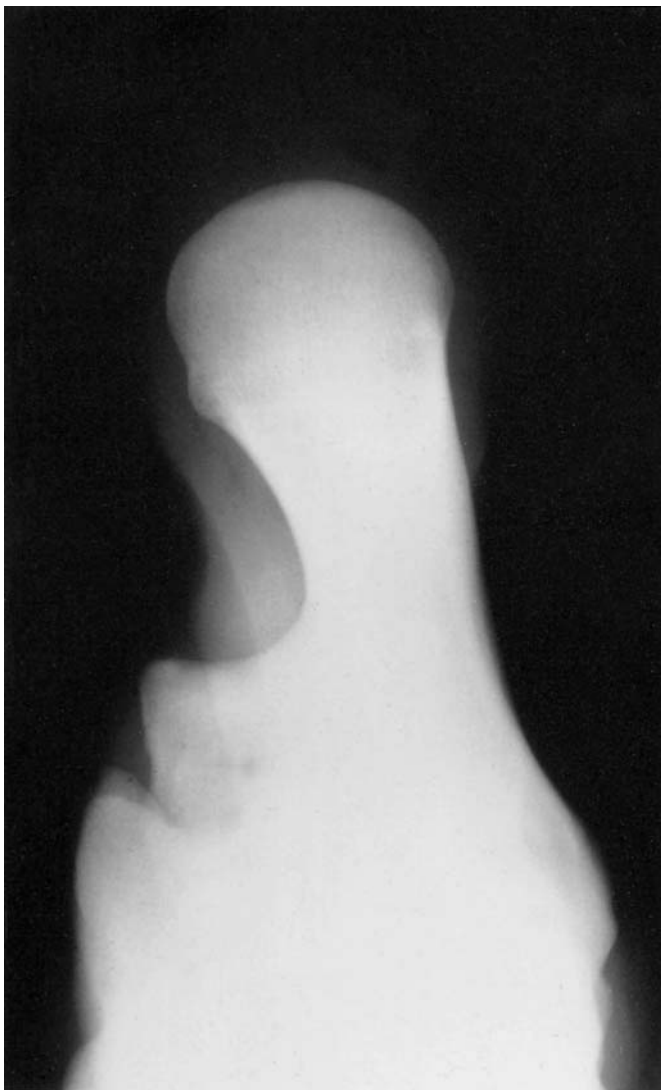
Figure 6.9 Dorsoplantar (flexed) view and diagram of a normal hock.

Diagram labels:
Tuber calcanei
Tarsal groove
Sustentaculum tali
Medial trochlear ridge
Talocalcaneal joint
Area of attachment of collateral ligament on fibular tarsal bone

SIGNIFICANT RADIOLOGICAL ABNORMALITIES

Congenital abnormalities

Congenital malformation of the sustentaculum tali of the fibular tarsal bone occurs in Saddlebreds and occasionally in Thoroughbreds (Figure 6.10). Flattening of the proximal aspect of the sustentaculum tali results in the deep digital flexor tendon slipping dorsally and medially. Clinically the plantar aspect of the tarsal region appears broader than usual and there is tarsal valgus. Radiographic abnormalities are detectable only in the dorsoplantar (flexed) view, in which the contour of the sustentaculum tali appears flattened.

Tarsal bone collapse

Tarsal bone collapse may be recognized radiographically in neonatal foals, in older foals or young adults. In a neonate the tarsal bones appear relatively immature; they are smaller and more rounded than usual due to

[264]

Figure 6.10 Dorsoplantar (flexed) oblique view of the hock of a 3-week-old Thoroughbred foal with a malformed hock. There is flattening of the sustentaculum tali (arrow).

incomplete ossification (Figure 6.11a). They may have a granular opacity (the bone is comprised of opaque granules). Clinically the neonatal foal shows excessive flexion of the hocks (sickled and curby hock conformation) and/or tarsal valgus deformities. The condition is most common in premature foals or those born one of a twin. Unless the limbs are supported in cylinder tube casts until ossification has progressed further, normal weight bearing will result in compression of either or both the central and third tarsal bones. The compressed bones appear wedge shaped in both lateromedial and dorsoplantar views, and may show fragmentation with narrowing of the joint spaces. This condition has also been seen in association with osteomyelitis of the third and central tarsal bones, in which case the bone may have a mottled opacity due to lucent areas within the bone. Since tarsal collapse is often bilateral, both hocks should be examined radiographically.

Tarsal collapse may pass unrecognized until the horse starts work, when there may be an acute onset of unilateral or bilateral hindlimb lameness or stiffness. Radiographic examination reveals wedge-shaped central and/or third tarsal bones (Figure 6.11b, page 267) and evidence of secondary joint disease (e.g. collapse of the joint spaces and periarticular new bone). In less

[265]

(i)   (ii)

Figure 6.11(a) Lateromedial views of a premature Thoroughbred foal born at a gestational age of 318 days. The radiographs were obtained (i) 6 days and (ii) 12 days post partum, i.e. at 324 and 330 days' gestation. Note the rounded edges of the incompletely ossified tarsal bones and the progressive enlargement of the bones.

severe cases there may only be a slight wedge-shaped appearance of the third tarsal bone. Compare the height of the bone dorsally with the plantar aspect.

In the neonate, provision of external support to the limb permits endochondral ossification to proceed without deformation of the bones and, provided that treatment is started early, prognosis is fair to good. In the adult, the prognosis is usually poor, although ankylosis of the bones may occur ultimately.

Osteochondrosis

Radiographic abnormalities which are thought to be a manifestation of osteochondrosis include: (a) separation of a bony fragment at either the medial (Figure 6.12, page 268) or the lateral malleolus of the tibia or the distal intermediate ridge of the tibia (Figure 6.13, page 269); (b) bony fragments at the distal end of the medial trochlear ridge of the talus (see Figure 6.4, page 254); (c) separation of a bony fragment from the medial

[266]

Figure 6.11(b) Plantarolateral-dorsomedial oblique view of a 2-year-old Thoroughbred. The third tarsal bone is wedge shaped with the dorsal part fractured. The horse was born prematurely and demonstrated bilateral hindlimb lameness when training commenced.

proximal tubercle of the talus, and (d) an irregular, flattened contour of the medial and/or lateral ridges of the talus with or without radiolucent zones in the underlying subchondral bone (Figure 6.14, page 270). Bony fragments of the medial and lateral malleoli of the tibia must be differentiated from avulsion fractures. Some medial malleolar articular fragments are not detectable in a dorsoplantar projection; a dorsal 15° lateral-plantaromedial oblique view may be required. Fragments distal to the distal end of the trochlear ridges may have originated from the distal tibia and have fallen distally. Lesions frequently occur bilaterally. Fragments at the distal intermediate ridge of the tibia are most common and can be detected at less than 3 months of age. They vary considerably in size, but are often bilaterally symmetrical. There may be an obvious lucent defect in the adjacent subchondral bone.

The incidence of osteochondrosis in the tarsus is particularly high in certain breeds (e.g. Standardbreds, Warmbloods and some heavy horse breeds) and there may be a hereditary predisposition to the condition. In Dutch Warmbloods it has been shown that fragments at the distal intermediate ridge of the tibia are frequent (>65%) at 1 month of age, but in the majority (80%) the radiographic appearance is normal at 1 year of age. Lesions of the lateral trochlear ridge of the talus are less frequent (30%) at 1 month of age, but the majority (97%) are normal at 1 year of age. A lesion present at 5 months of age in either location is likely to persist.

[267]

Figure 6.12 Dorsolateral-plantaromedial oblique view of a yearling Thoroughbred. There is a discrete osseous opacity distal to the medial malleolus of the tibia, a manifestation of osteochondrosis.

Lameness may or may not be present, or may develop at a later stage. Lameness is more likely in association with large or mobile fragments. Chronic distension of the tarsocrural joint capsule may lead to degenerative joint disease and ultimately lameness. In Standardbreds, these lesions have been associated with subtle hindlimb gait abnormalities at high speeds and, in Warmbloods, performance at high levels may be compromised. Lesions of the trochlear ridges of the talus are more often associated with mild to moderate lameness, but not invariably so. The potential significance of osteochondritic lesions as a cause of lameness must be assessed carefully. Surgical treatment may be indicated and although the bog spavin may resolve, a good cosmetic result cannot be guaranteed, despite good functional results.

Physitis or physeal dysplasia

Physitis or physeal dysplasia, which is possibly related to osteochondrosis, can cause enlargement of the distal end of the tibia, stiffness and sometimes an angular limb deformity. Radiographically the metaphysis of the bone is broadened and asymmetrical. There is sclerosis of the metaphysis adjacent to the physis, which may be more irregular in appearance than normal. The

[268]
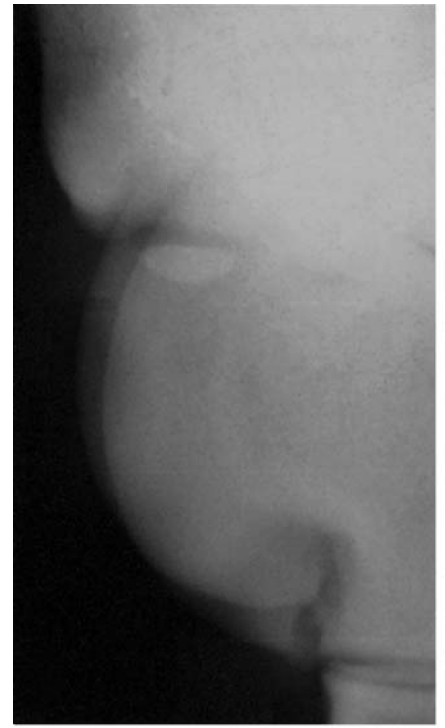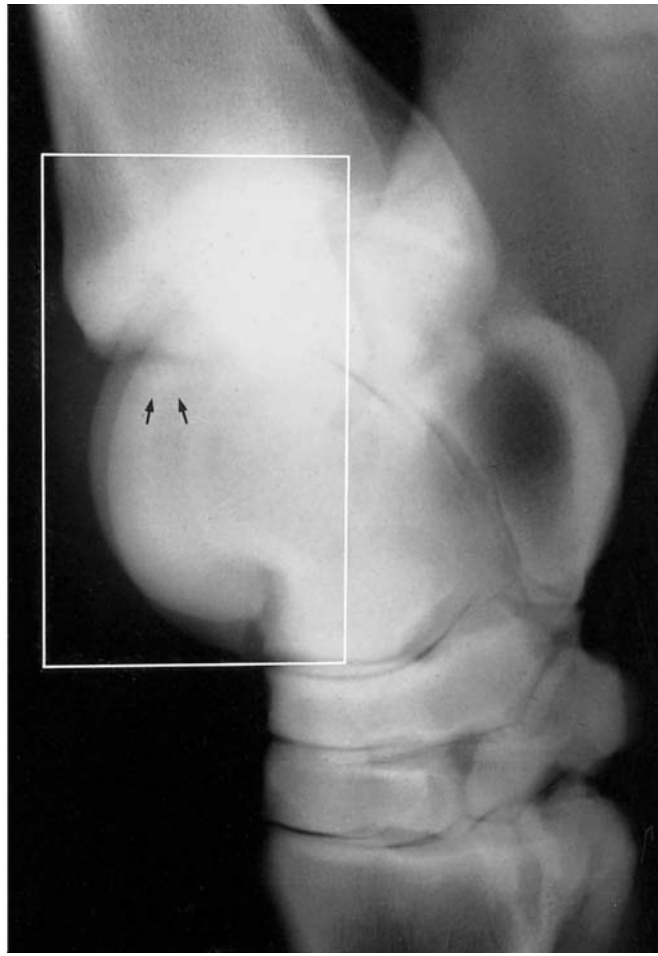
Figure 6.13 Slightly oblique lateromedial view of a 3-year-old Warmblood. There is a large discrete osseous opacity (arrows) separated from the distal intermediate ridge of the tibia. There was marked distension of the tarsocrural joint capsule but no lameness.

cortices of the metaphysis may be abnormally thick. Most cases resolve spontaneously with appropriate management of diet and exercise, although an angular limb deformity may persist in severe cases.

Degenerative joint disease

In many horses there is a poor correlation between pain associated with the distal joints of the hock and the radiographic abnormalities. There may be lameness and no detectable radiographic changes; alternatively there may be extensive radiographic changes and no associated lameness. In some horses the radiographic changes are quite advanced when clinical signs are first recognized. Radiographic examination of horses with obvious enlargements on the medial aspects of the distal joints of the hocks often reveals that this is caused primarily by soft-tissue swelling. Perineural and intra-articular anaesthesia are helpful to establish the significance of radiographic abnormalities and to define the source of pain if no lesions are detectable. This may be combined with anaesthesia of the cunean bursa in selected cases.

The centrodistal (distal intertarsal) and tarsometatarsal joints are

[269]

Figure 6.14 Plantarolateral-dorsomedial oblique view of a hock of a yearling Shire horse. There is a large osteochondritic lesion of the distal aspect of the lateral trochlear tali.

affected most frequently, either alone or in combination. The condition often occurs bilaterally. The talocalcaneal-centroquatral (proximal inter-tarsal) joint is less commonly involved, but there is often associated distension of the tarsocrural joint capsule because of the communication between these two joints. Degenerative joint disease of the talocalcaneal joint occurs rarely.

There is considerable variation between horses in the type, extent and progression of radiographic abnormalities which develop. These changes include periarticular osteophytes (Figures 6.15a–c), periosteal new bone (Figure 6.16, page 272), subchondral bone lysis (Figures 6.17a–c, pages 273 and 274) and/or sclerosis, decreased corticomedullary demarcation and narrowing or loss of the joint space (spaces) (Figures 6.18a and 6.18b, page 275). In the early stages of the disease the lesions may be subtle and only detectable in a single radiographic view; thus a complete radiographic examination is important. Even in more advanced cases the radiographic abnormalities are occasionally visible on only one of the four standard projections. Since small osteophytes and periosteal new bone are less opaque than the parent bone, they are easily overlooked. The radiographs should always be viewed over high-intensity illumination to study the bone margins. Both hocks should be examined radiographically if changes are found in one limb.

Figure 6.15(a) Slightly oblique lateromedial view of a hock of a 2-year-old Thoroughbred. There is a large, active osteophyte on the dorsoproximal aspect of the third metatarsal bone. Lameness was alleviated by intra-articular analgesia of the tarsometatarsal joint.

Figure 6.15(b) Lateromedial view of a hock of a mature horse with osteophyte formation involving the centrodistal and tarsometatarsal joints.

It may be necessary to repeat a view at different exposures in order both to evaluate corticomedullary demarcation and trabecular pattern properly and to identify marginal osteophytes.

Spur formation on the dorsoproximal aspect of the third metatarsal bone (see Figures 6.5a and 6.5b, page 255) may not reflect significant intra-articular disease and its significance must be interpreted with care. This may be an entheseophyte associated with the insertion of the cranial tibial tendon, fibularis tertius, or the dorsal tarsometatarsal ligament; however, an osteophyte may reflect degeneratiue joint disease. Osteophyte formation may also be associated with an incomplete or complete articular fracture of

Figure 6.15(c) Plantarolateral-dorsomedial oblique view of a hock of a mature horse with osteophyte formation involving the centrodistal and tarsometatarsal joints. Note also the modelling of the dorsal aspect of the third tarsal bone and the irregular opacity of the proximodorsal aspect of the third metatarsal bone.

Figure 6.16 Dorsoplantar view of a hock of a mature riding pony with degenerative joint disease of the tarsometatarsal joint. The radiograph is underexposed to highlight the extensive periosteal new bone on the medial aspect of the joint. There are ill-defined subchondral lucent zones adjacent to the narrowed tarsometatarsal joint.

Figure 6.17(a) Lateromedial view of a hock of a 2-year-old Thoroughbred. There are small subchondral lucent zones adjacent to the dorsal aspect of the centrodistal joint.
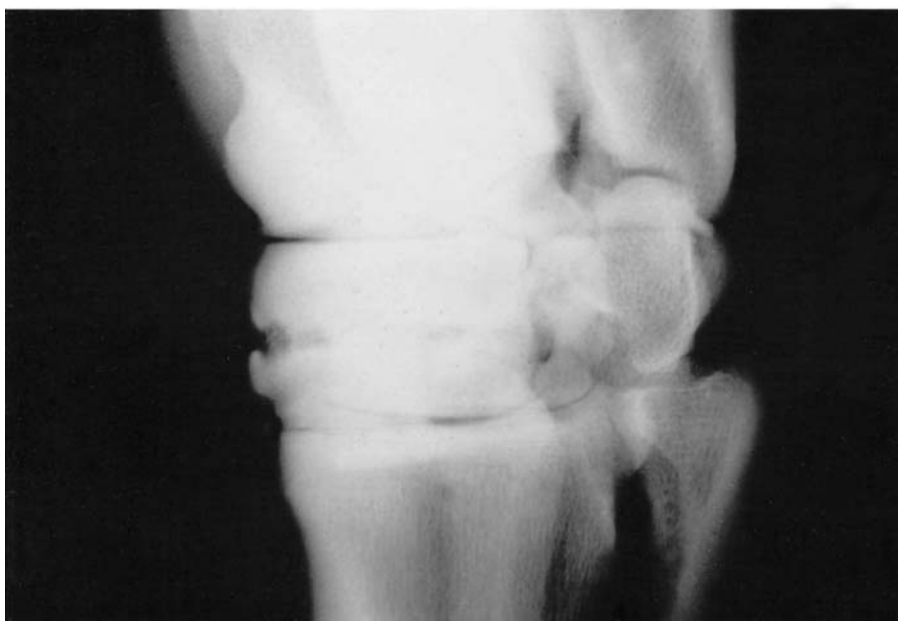
Figure 6.17(b) Dorsolateral-plantaromedial oblique view of a mature show-jumping pony. There are subchondral lucent areas adjacent to the centrodistal joint. The joint space is narrowed elsewhere, and there is loss of trabecular pattern in the central and third tarsal bones.

the dorsoproximal aspect of the third metatarsal bone (see Chapter 3, page 164). Osteophyte formation involving the dorsal aspects of the centrodistal joint (Figures 6.15b and 6.15c) or the lateral aspect of this joint (Figure 6.18a, page 275) is often associated with lameness. Osteophytes on the lateral aspect of the centrodistal joint are best seen in dorsoplantar and dorsolateral-plantaromedial oblique views, encroaching upon the tarsal canal (Figure 6.18a). Large osteophytes on the proximal aspect of the third metatarsal bone do occasionally fracture; a fracture piece (see Figure 6.5f, page 256) should not be confused with dystrophic mineralization in the cranial tibial tendon (see Figure 6.5e, page 256).

Irregular periosteal new bone occurs most commonly on the
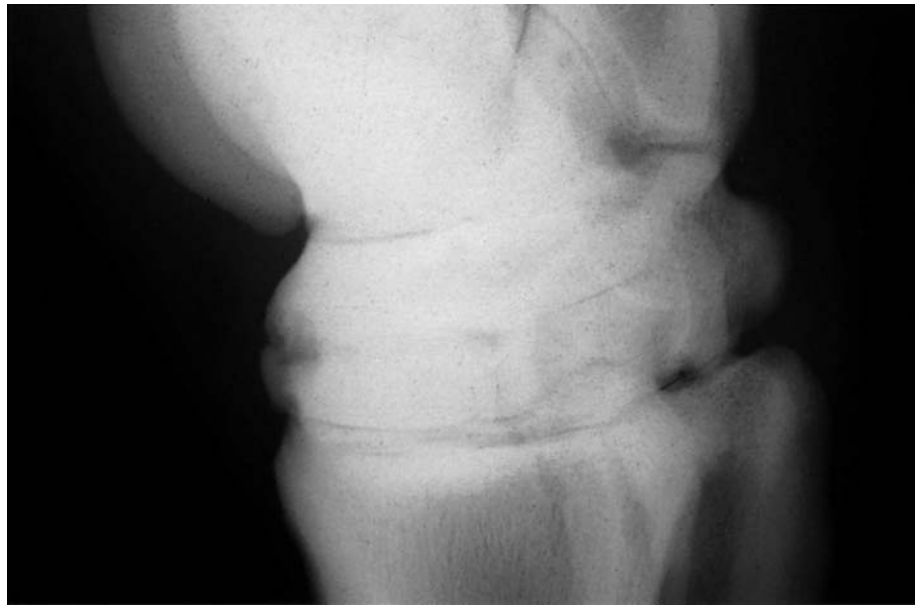
Figure 6.17(c) Slightly oblique view of the same hock as in Figure 16.7b. Note the modelled contour of the dorsal aspect of the centrodistal joint.

dorsomedial aspects of the joints, and usually signifies degenerative joint disease. It may be seen alone or in combination with destructive lesions of bone. Destructive lesions may result in irregular margins of the central and third tarsal bones and the third metatarsal bone and/or lucent zones in the subchondral bone. If there are extensive lucent areas in the subchondral bone, lameness is usually persistent. There are sometimes discrete osseous cyst-like lesions in the subchondral bone.

Narrowing of the joint spaces (Figures 6.18a and 6.18b) can occur with any of these changes. Occasionally, narrowing of the joint space is the only radiographic abnormality detectable. Conventional radiographs may underestimate the degree of functional ankylosis. The joint spaces may become obliterated completely, resulting in ankylosis of the bones and resolution of lameness. Persistence of lameness may be due to continued subchondral bone pain, or to early changes in more proximal or distal joints. Nuclear scintigraphy is useful in determining active bone modelling. In other cases there is extensive extra-articular inactive bone bridging the joints with some loss of joint space.

The shape of the central and third tarsal bones should be assessed carefully, in order to detect cases in which degenerative joint disease has developed secondary to tarsal bone collapse (see page 264).

The speed of progression of changes is both variable and unpredictable, and it is unusual to be able to monitor progressive fusion of the joints radiographically. Some horses may be treated conservatively either by intra-articular medication or by administration of anti-inflammatory analgesics and corrective shoeing. Surgical or chemical arthrodesis of the affected joints can be an effective treatment, particularly for those with extensive lytic lesions. Involvement of the talocalcaneal-centroquatral (proximal intertarsal) joint (Figures 6.19a and 6.19b, page 276) or the talocalcaneal joint (Figure 6.19c, page 276) warrants a guarded prognosis.
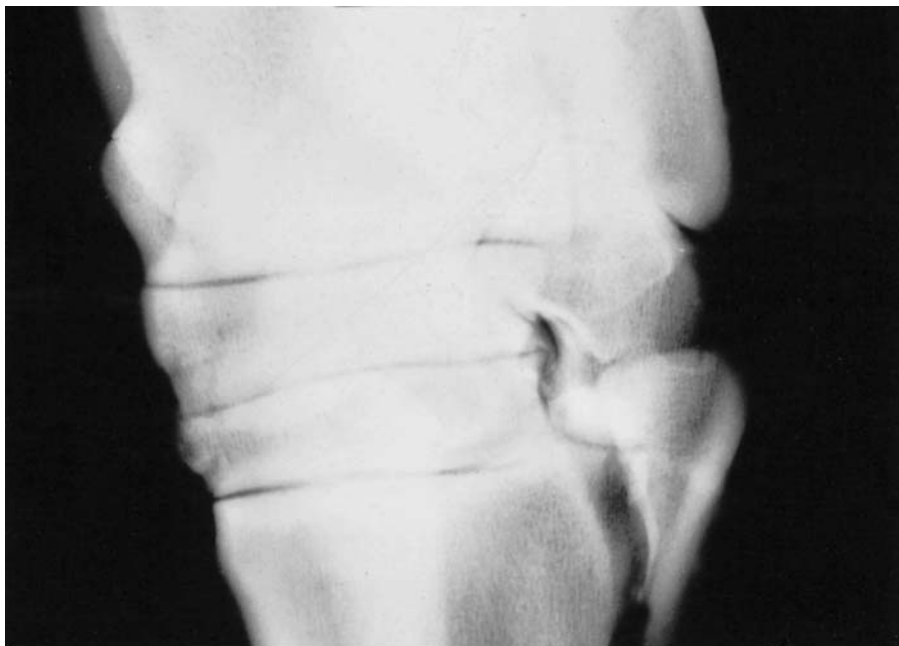
Figure 6.18(a) Dorsolateral-plantaromedial oblique view of a hock of a 3-year-old Thoroughbred. There is narrowing of the centrodistal joint space and osteophyte formation on its lateral aspect encroaching upon the tarsal canal.
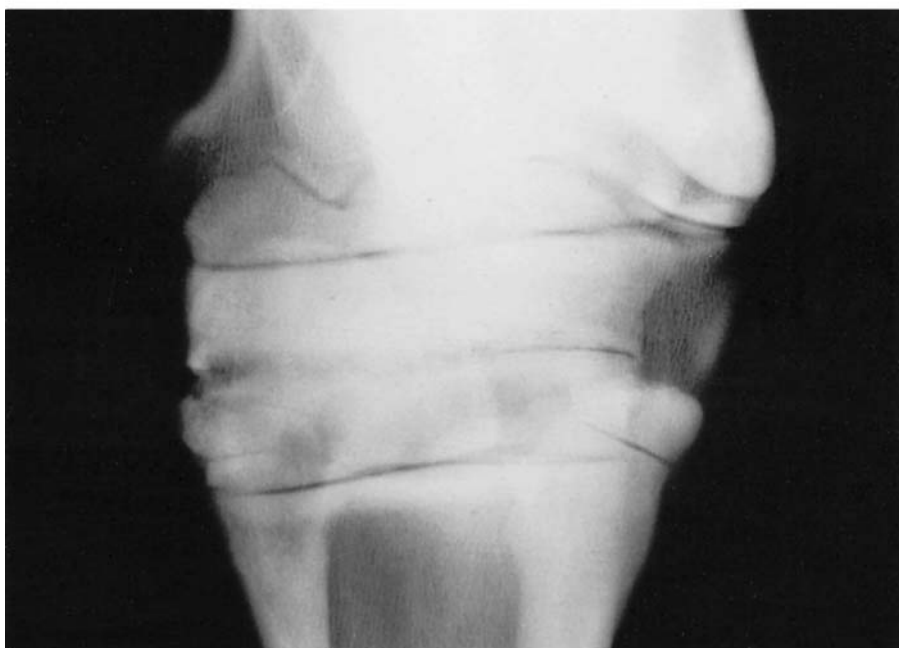
Figure 6.18(b) Dorsoplantar view of a hock of a mature riding horse. There is narrowing and partial obliteration of the centrodistal joint with subchondral bone lysis medially.

Periosteal proliferative reactions at the sites of attachment of ligaments and joint capsules

Twisting or wrenching the hock may result in a sprain of the soft-tissue structures of the hock and severe lameness. Radiographic examination is often unrewarding initially, but may be important to rule out a fracture. Diagnostic ultrasonography may be useful to evaluate the collateral ligaments of the tarsocrural joint. Nuclear scintigraphy may help to identify areas of increased bone metabolism or blood supply. After approximately 3–6 weeks,

(a)

(b)
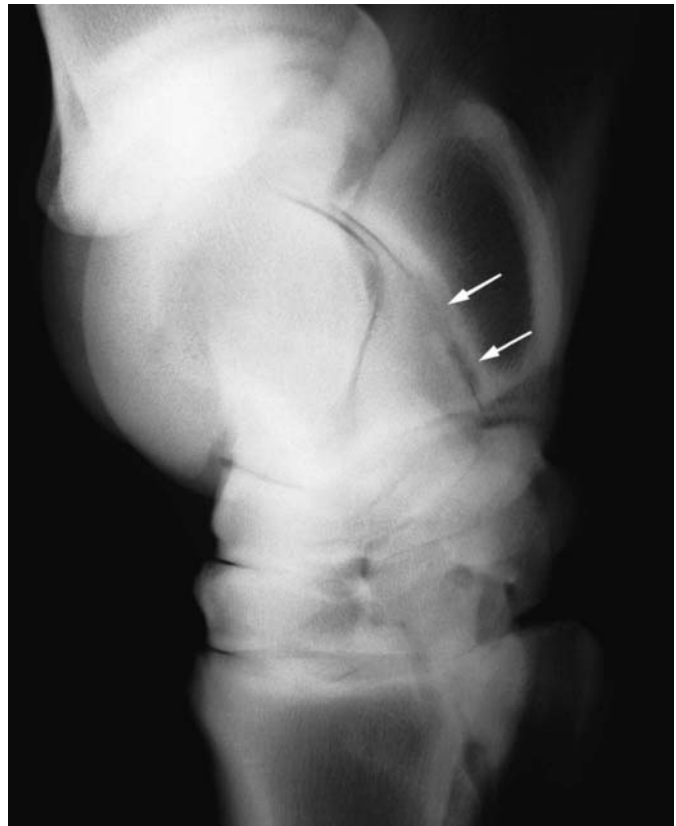
(c)

Figure 6.19(a) Dorsolateral-plantaromedial oblique view of a hock of a mature riding horse (contralateral limb to Figure 6.18b). There is narrowing of the talocalcaneal-centroquatral joint with subchondral bone destruction medially. There was distension of the tarsocrural joint capsule in this limb only.

Figure 6.19(b) Dorsolateral-plantaromedial oblique view of a hock of a mature riding horse. There is modelling of the distal medial tuberosity of the talus and of the medial aspect of the talocalcaneal-centroquatral joint with osteophyte formation (barely discernible because it is relatively less opaque). The central and third tarsal bones are fused.

Figure 6.19(c) Lateromedial view of a hock of a mature riding horse. There is narrowing of the talocalcaneal joint with subchondral lysis (arrows).

[276]

Figure 6.20 Dorsoplantar view of a hock of a 6-year-old steeplechaser several weeks after a severe fall. There is extensive periosteal new bone (arrows) at the sites of insertion of the medial and lateral collateral ligaments of the tarsocrural joint.

extensive periosteal reactions may develop at the sites of attachment of the joint capsules, collateral ligaments and intertarsal ligaments (Figure 6.20). The sites of periosteal reactions should be correlated carefully with the sites of soft tissue attachments to confirm which structures may have been damaged. These changes may be progressive and follow-up examination after a further 6–8 weeks may give a better indication of the extent of the damage. Lameness often takes a considerable time to resolve and, if new bone involves the articulations of the hock, or if there is extensive fibrosis of the ligaments involved, may be persistent.

An avulsion fracture of either the medial or, more commonly, the lateral malleolus of the tibia (Figure 6.21) may occur in association with sprain of

Figure 6.21 Dorsoplantar view of a hock of a steeplechaser. There is a displaced fracture of the lateral malleolus of the tibia.

the collateral ligaments of the tarsocrural joint. The fracture may be simple or comminuted. Fracture fragments may be displaced and rotated. It may be helpful to obtain a dorsal 15° medial-plantarolateral oblique view to highlight the fragment(s). In contrast to the osteochondral fragments of osteochondrosis, a recent fracture is more irregular in shape. Ultrasonography can be useful to identify the precise location of a fracture in the frontal plane, and to assess the collateral ligaments. Periosteal new bone may develop on the distal cranial tibia, and entheseous new bone at the insertion of the collateral ligaments on the talus. Conservative treatment offers a moderate prognosis. However, surgical removal may facilitate recovery, especially if the fracture has a large articular component, or is considerably displaced.

[278]

Luxation

Luxation of the tarsus is not common but may occur at any of the joints. The horse shows a severe, non-weight-bearing lameness, a variable degree of soft-tissue swelling and obvious instability of the tarsus. Radiographic examination is performed to establish which joint is involved and the extent of concurrent damage. 'Stressed' views may be helpful (see page 21). The majority of luxations are associated with fractures of one or more tarsal bones. The prognosis for luxation of the tarsocrural joint is poor, but closed reduction and external immobilization has been successful in treating luxations of the talocalcaneal-centroquatral (proximal intertarsal) or tarsometatarsal joints in horses which resumed light work, or were used for breeding.

Thoroughpin

Persistent lameness and swelling of the digital flexor tendon sheath (tarsal sheath) proximal to the hock (thoroughpin) may be associated with lesions of the sustentaculum tali of the calcaneus and/or mineralization in the soft tissues (Figure 6.22a). Although the latter may be identified in the standard radiographic views (particularly the plantarolateral-dorsomedial oblique view), lesions of the sustentaculum tali are often only visible in the dorsoplantar (flexed) view (Figure 6.22b). Contrast radiography and ultrasonography are additional techniques useful in the assessment of this condition. The presence of radiographic changes (e.g. lesions of the sustentaculum tali, mineralization within the sheath or filling defects in the sheath) associated with thoroughpin warrants a guarded prognosis.

Infectious arthritis and osteomyelitis

Infectious arthritis occurs most commonly in young foals, but may be a sequel to trauma in an adult, and occasionally develops without an apparent cause. The tarsocrural joint is most commonly affected, resulting in distension of the joint capsule and lameness. The lower joints may be involved alone or in combination and, especially in young foals, the central and third tarsal bones must be inspected carefully for evidence of lucent zones indicative of concurrent osteomyelitis (type T osteomyelitis, see page 23). In foals the distal tibial physis and epiphysis should also be evaluated with care, since in the majority of cases type P osteomyelitis is present.

Trauma in the region of the calcaneus may result in a chronically draining wound and severe lameness. Osteomyelitis of the tuber calcanei may be a sequel, but radiographic abnormalities may only be detectable in a dorsoplantar (flexed) view. Sinography may be helpful to establish if a draining sinus communicates with the bone. A guarded prognosis is warranted even with surgical treatment.

[279]
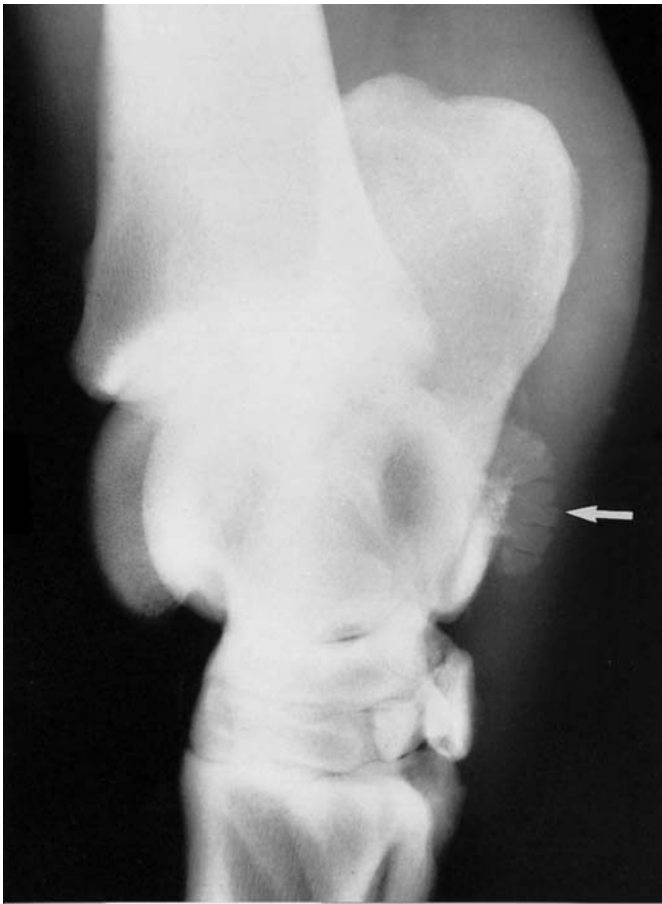
(a)
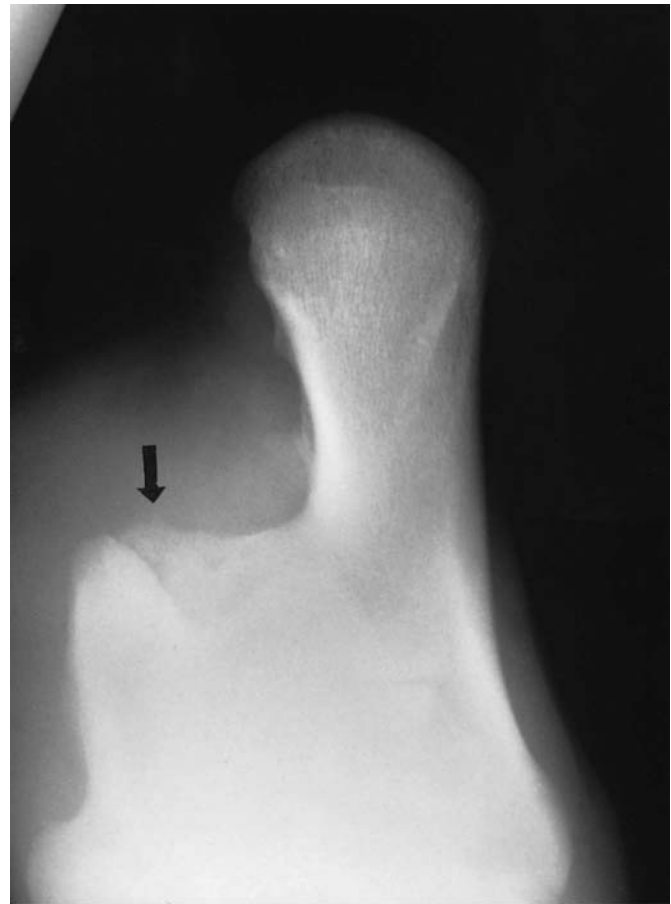
(b)

Figure 6.22(a) Plantarolateral-dorsomedial oblique view of a hock. There is considerable modelling of the sustentaculum tali (arrow) which was associated with distension of the tarsal sheath and severe lameness.

Figure 6.22(b) Dorsoplantar (flexed) view of the same hock as Figure 6.22a. Note the irregular contour of the surface of the sustentaculum tali (arrow) over which the deep digital flexor tendon passes, and the poorly defined opacities in the soft tissues medial to the calcaneus.

Osseous cyst-like lesions

Single osseous cyst-like lesions occur occasionally, most commonly in the distal tibia, the talus, the calcaneus and the third metatarsal bone. They are generally, but not always, associated with lameness. They may occur either unilaterally or bilaterally. Osseous cyst-like lesions may also occur in the central and third tarsal bones in association with degenerative joint disease (see page 269).

Hypertrophic osteopathy

See Chapter 1 (page 15).

[280]
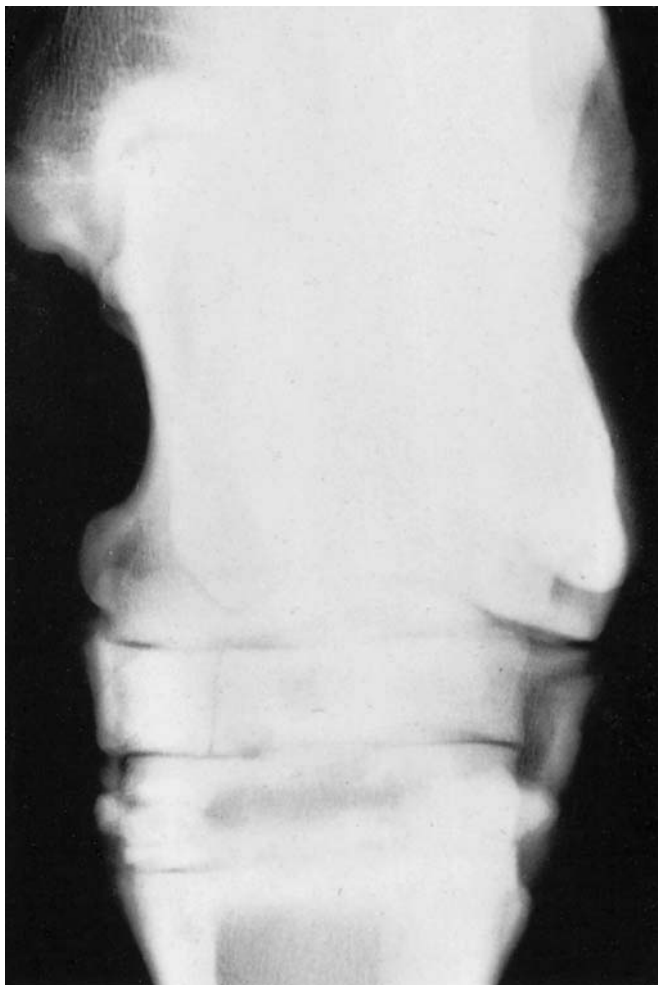
Figure 6.23 Dorsoplantar view of a hock of a mature horse. There is a complete fracture of the central tarsal bone.

Fractures

Because of the complex radiographic anatomy of the tarsus, detection of fractures is sometimes difficult. The support afforded by the intertarsal ligaments and collateral ligaments often results in minimal distraction of the fracture fragments. A slab fracture of the central or the third tarsal bone may be completely overlooked unless follow-up radiographs are obtained 7–10 days after the onset of lameness, when rarefaction along the fracture line will make it more obvious (Figure 6.23). Many oblique views may be required in order to identify the fracture. Nuclear scintigraphy may be useful in acute cases in which a fracture is suspected. Increased uptake of technetium may demonstrate results of trauma to the central and third tarsal bones, but in some cases a fracture is not subsequently identifiable. Treatment of slab fractures by internal fixation offers the best prognosis for future soundness, although secondary degenerative joint disease may be a sequel.

There are many types of fractures within the tarsus (Figure 6.24). The prognosis depends on the site of the fracture and its configuration, but is

[281]
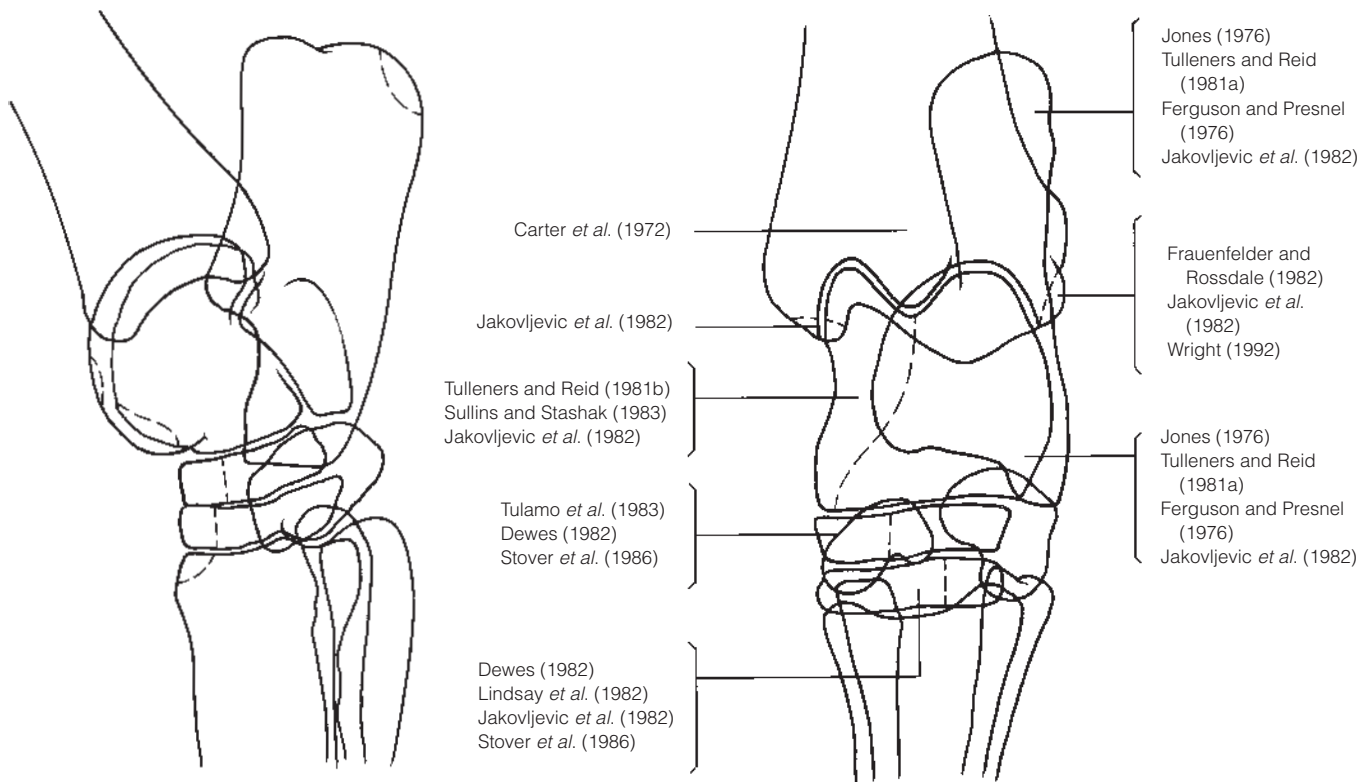
Figure 6.24 Location of common fracture sites in the hock, and suggested references (see 'Further reading').

The following reference labels appear in the figure:

Jones (1976)
Tulleners and Reid (1981a)
Ferguson and Presnel (1976)
Jakovljevic *et al.* (1982)

Carter *et al.* (1972)

Frauenfelder and Rossdale (1982)
Jakovljevic *et al.* (1982)
Wright (1992)

Jakovljevic *et al.* (1982)

Tulleners and Reid (1981b)
Sullins and Stashak (1983)
Jakovljevic *et al.* (1982)

Jones (1976)
Tulleners and Reid (1981a)
Ferguson and Presnel (1976)
Jakovljevic *et al.* (1982)

Tulamo *et al.* (1983)
Dewes (1982)
Stover *et al.* (1986)

Dewes (1982)
Lindsay *et al.* (1982)
Jakovljevic *et al.* (1982)
Stover *et al.* (1986)

generally guarded. The dorsoplantar (flexed) view may be necessary to identify fractures of the sustentaculum tali. Readers are advised to consult the references given under 'Further reading' for additional information about specific fracture types (Figure 6.24).

Fractures of the distal tibial physis are quite common in foals and yearlings, Salter-Harris type II (see Chapter 1, page 17) occurring most frequently. Treatment either by immobilization in a cast or by internal fixation has been successful in some cases. Malleolar fractures of the distal tibia are discussed on page 277.

FURTHER READING

Barneveld, A. (1983) Equine bone spavin. *PhD Thesis*, University of Utrecht

Boero, M., Kneller, S., Baker, G., Metcalf, M. and Twardock, A. (1988) Clinical, radiographic and scintigraphic findings associated with enthesitis of the lateral collateral ligaments of the tarsocrural joint in Standardbred racehorses. *Equine Vet. J.*, Suppl. **6**, 53–59

Carter, E., Horney, F. and Pennock, P. (1972) Distal tibial fractures in the horse. *Mod. Vet. Pract.*, Jan., 41–43

De Moor, A., Verschooten, F., Desmet, P., Steenhaut, M., Hooreens, J. and Wolf, G. (1972) Osteochondritis dissecans of the tibiotarsal joint in the horse. *Equine Vet. J.*, **4**, 139–143

Dewes, H. (1982) The onset and consequence of tarsal bone fractures in foals. *N.Z. Vet. J.*, **30**, 129–135

Dik, K. (1980) Bone spavin – a radiographic grading system. *Abstr. Br. Vet. Radiol. Ass.*, **2**, 46

Dik, K. and Merkens, H. (1987) Unilateral distension of the tarsal sheath in the horse: a report of 11 cases. *Equine Vet. J.*, **19**, 307–313

Dik, K. and Enzerink, E. (1998) The radiographic development of osteochondral abnormalities in the hock and stifle of Dutch Warmblood foals from 1 to 11 months of age. *Equine Vet. J.*, Suppl., in press

Edwards, G. (1978) Changes in the sustentaculum tali associated with distension of the tarsal sheath (thoroughpin). *Equine Vet. J.*, **10**, 97–100

Farrow, C., McNeel, S., Morgan, J. and Resch, R. (1976) Visualisation of the tuber calcis and sustentaculum in the horse. *Calif. Vet.*, **30**, 14–15

Ferguson, J. and Presnel, K. (1976) Tension band plating of a fractured equine fibular tarsal bone. *Can. Vet. J.*, **17**, 314–317

Firth, E., Dik, K., Goedegebuure, S., Hagens, F., Verberne, L., Merkens, H. and Kersjes, A. (1980) Polyarthritis and bone infection in foals. *Vet. Med.*, **B27**, 102–124

Firth, E., Goedegebuure, S., Dik, K. and Poulos, P. (1985) Tarsal osteomyelitis in foals. *Vet. Rec.*, **116**, 261–266

Frauenfelder, H. and Rossdale, P. (1982) What is your diagnosis? *J. Am. Vet. Med. Ass.*, **180**, 1109–1110

Fretz, P. (1980) Angular limb deformities in foals. *Vet. Clin. N. Am. Large Anim. Pract.*, **2**, 125–150

Gabel, A. (1980) Lameness caused by inflammation in the distal hock. *Vet. Clin. N. Am. Large Anim. Pract.*, **2**, 101–124

Grondahl, A., Jansen, J. and Terge, J. (1996) Accessory ossification centres associated with osteochondral fragments in the extremities of horses. *J. Comp. Path.* **114**, 385–398

Gross, D. (1984) Tarsal luxation and fracture in a pony. *Mod. Vet. Pract.*, **45**, 68–69

Haakenstaad, L. and Birkeland, R. (1974) Osteochondritis in the hock joint of the horse: surgical and conservative treatment. *Proc. 12th Nordic Vet. Congress*, Reykjavik, pp. 7–10

Hartung, K., Munzer, B. and Keller, H. (1983) Radiologic evaluation of spavin in young trotters. *Vet. Radiol.*, **24**, 153–155

Hoppe, F. (1984) Osteochondrosis in Swedish horses. *Thesis*, Sveriges Lantbruksuniversitet, Uppsala

Jakovljevic, S., Gibbs, C. and Yeats, J. (1982) Traumatic fractures of the equine hock: a report of 13 cases. *Equine Vet. J.*, **14**, 62–68

Jones, R. (1976) The diagnosis and treatment of avulsion fractures of the sustentaculum tali in a horse. *Can. Vet. J.*, **17**, 287–290

Lindsey, W., McMartin, R. and McClure, J. (1982) Management of slab fractures of the third tarsal bone in 5 horses. *Equine Vet. J.*, **14**, 55–58

MacDonald, M., Honnas, C. and Meagher, D. (1989) Osteomyelitis of the calcaneus in horses: 28 cases (1972–1987) *J. Am. Vet. Med. Ass.*, **194**, 1317–1320

Martens, R. and Auer, J. (1980) Haematogenous septic arthritis and osteomyelitis in the foal. *Proc. Am. Ass. Equine Pract.*, **26**, 47–63

Moll, H., Slane, D., Humburg, J. and Jagar, J. (1987) Traumatic tarsal luxation repaired without internal fixation in three horses and three ponies. *J. Am. Vet. Med. Ass.*, **190**, 297–300

Morgan, J. (1967) Necrosis of the third tarsal bone of the horse. *J. Am. Vet. Med. Ass.*, **151**, 1334–1342

Moyer, W. (1987) Bone spavin: a clinical review. *J. Equine Med. Surg.*, **2**, 362–371

O'Brien, T. (1974) Radiographic interpretation of the equine tarsus. *Proc. Am. Ass. Equine Pract.*, **19**, 257–262

Philips, T. (1986) Unusual hock problems. *Proc. Am. Ass. Equine Pract.*, **32**, 663–667

Pilsworth, R. (1992) Incomplete fracture of the dorsal aspect of the third metatarsal bone as a cause of hindlimb lameness in racing Thoroughbreds: a review of three cases. *Equine Vet. J.*, **24**, 147–150

Raker, C. (1974) Orthopaedic surgery: errors in surgical evaluation and management. *Proc. Am. Ass. Equine Pract.*, **19**, 205–210

Rooney, J. (1973) Bog spavin and tibiotarsal joint lesions in the horse. *Mod. Vet. Pract.*, **54**, 12

Ross, M., Sponseller, M., Gill, H. and Moyer, W. (1993) Articular fracture of the dorsoproximal aspect of the third metatarsal bone in five Standardbred racehorses. *J. Am. Vet. Med. Ass.*, **203**, 698–700

Sandgren, B. (1993) Osteochondrosis in the tarsocrural joint and osteochondral fragments in the metacarpo/metatarsophalangeal joints in young Standardbreds. *PhD Thesis*, University of Uppsala

Shaver, J., Fretz, P., Doige, C. and Williams, D. (1979) Skeletal manifestations of suspected hypothyroidism in two foals. *J. Equine Med. Surg.*, **3**., 269–275

Shively, M. (1982) Correct anatomic nomenclature for the joints of the equine tarsus. *Equine Pract.*, **4**(4), 9–13

Shively, M. and Smallwood, J. (1980) Radiographic and xeroradiographic anatomy of the equine tarsus. *Equine Pract.*, **2**(4), 19–34

Stover, S., Hornhof, W., Richardson, G. and Meagher, D. (1986) Bone scintigraphy as an aid to diagnosis of occult distal tarsal bone trauma in 3 horses. *J. Am. Vet. Med. Ass.*, **182**, 624–627

Stromberg, B. and Rejno, S. (1978) Osteochondritis in the horse: a clinical and radiological investigation of the knee and hock joints. *Acta Vet. Scand.*, Suppl. **358**, 139–152

Sullins, K. and Stashak, T. (1983) An unusual fracture of the tibiotarsal bone in a mare. *J. Am. Vet. Med. Ass.*, **182**, 1395–1396

Tulamo, R., Bramlage, L. and Gabel, A. (1983) Fractures of the central and third tarsal bones in horses. *J. Am. Vet. Med. Ass.*, **182**, 1234–1238

Tulleners, E. and Reid, C. (1981a) Osteomyelitis of the sustentaculum talus in a pony. *J. Am. Vet. Med. Ass.*, **178**, 290–291

Tulleners, E. and Reid, C. (1981b) An unusual fracture of the tarsus in two horses. *J. Am. Vet. Med. Ass.*, **178**, 291–294

Wheat, J. (1963) Trochlear fractures of the tibiotarsal bone. *Proc. Am. Ass. Equine Pract.*, **9**, 86–87

Wheat, J. and Rhode, E. (1964) Luxation and fracture of the hock of the horse. *J. Am. Vet. Med. Ass.*, **145**, 341–344

White, N. and Turner, T. (1980) Hock lameness associated with degeneration of the talocalcaneal articulation. *Vet. Med. Small Anim. Clin.*, **75**(4), 678–681

Wright, I. (1992) Fractures of the lateral malleolus of the tibia in 16 horses. *Equine Vet. J.*, **24**, 424–429

Chapter 7
The Stifle and Tibia

Stifle

RADIOGRAPHIC TECHNIQUE

Four radiographic views are necessary for complete evaluation of the stifle joint:

1. Lateromedial and/or flexed lateromedial.
2. Caudal 60° lateral-craniomedial oblique.
3. Caudocranial.
4. Cranioproximal-craniodistal oblique.

In many cases sufficient information can be obtained using views (2) and (3). If low-output portable equipment is used, all four views may be best obtained with the horse under general anaesthesia.

Equipment

For caudocranial views of the stifle in mature horses, an x-ray machine with a minimum output of 90 kV and 20 mAs is required. Radiography should only be attempted with the horse standing if it is co-operative. A fractious horse may inflict serious damage to personnel and equipment, and will result in unacceptably high radiation hazards. If the horse cannot be calmed using sedation and/or a twitch, general anaesthesia should be used.

Fast rare earth screens and films are recommended. Large cassettes (35 cm × 43 cm) are advised in order to visualize an adequate length of femur and tibia. A cassette holder should ideally be used; however, holders of this size are cumbersome and difficult to hold still. For this reason the cassette is often hand held. Using these large cassettes, and with adequate collimation of the x-ray beam, the holder's gloved hands should be well away from the primary beam. The difficulty in aligning the cassette and x-ray beam in the standing horse makes it advisable to dispense with the use of a grid. Under general anaesthesia, the quality of the radiographs can be enhanced by using a parallel grid.

The use of an aluminium wedge filter greatly improves the quality of the radiographs and enables the stifle joint to be examined using fewer exposures.

[285]

Positioning

Lateromedial view

A true lateromedial view may be required if osseous irregularities near the distal insertion of the cranial cruciate ligament are suspected. The limb to be examined should be positioned caudal to the contralateral limb, fully weight-bearing. This facilitates positioning of the cassette on the medial aspect of the stifle. The cassette usually has to be hand held, as high in the groin region as possible. The x-ray beam should be centred on the femorotibial joint. Palpate the tibial crest, and centre immediately proximal to it, approximately 10 cm caudal to the cranial aspect of the limb. To obtain lateromedial alignment, the beam should initially be aligned parallel to a tangent to the bulbs of the heel, but this may require alteration on subsequent films.

Flexion of the stifle, either with the limb lifted and retracted or with the horse resting the toe on the ground, 'drops' the stifle and facilitates obtaining a true lateromedial radiograph. Some horses will not tolerate a cassette on the medial aspect of the hind limb with the limb weight-bearing, but will accept it if the limb is flexed. This view requires an extra person to flex the limb.

A flexed lateromedial view also potentially gives extra room in which to position the cassette. Other advantages of the flexed lateromedial view include better visualization of the proximal tibia in the region of the inter-condylar eminences, assessment of the proximal aspect of the trochlear ridges of the femur, without superimposition of the patella, and a clearer view of the apex of the patella.

Caudolateral-craniomedial oblique view

A caudal 60° lateral-craniomedial oblique view is generally preferable to a straight lateromedial view for two reasons. Firstly, an oblique view prevents superimposition of the images of the trochlear ridges and the condyles of the femur. Secondly, the large adductor muscle mass on the medial aspect of the horse's thigh, together with the testicles in entire males, make accurate positioning of the cassette for a true lateromedial view difficult. With a caudal 60° lateral-craniomedial oblique view, the cassette can be positioned slightly more cranial to the joint (Figure 7.1).

Angling the x-ray beam 10–15° proximodistally (downwards) further facilitates alignment of the beam and the cassette. The x-ray beam should be centred approximately 10 cm caudal to the cranial aspect of the limb, at the level of the femorotibial joint, which is readily palpable immediately proximal to the tibial crest.

An alternative technique is to position the cassette lateral to the stifle, with the x-ray machine medial. The x-ray beam passes under the ventral aspect of the abdomen to obtain a cranial 60° medial 15° distal-caudolateral proximal oblique view of the stifle. This technique allows easier positioning of the cassette and is accepted more readily by a fractious horse. It is impracticable in a stallion or a horse with a low abdominal wall.

[286]

Further obliquity (Cd45°L-CrMO) gives better separation of the femoral condyles (Figure 7.9, page 296).

Caudocranial view

The caudocranial view is preferred to a craniocaudal view, because positioning is easier. It does put the equipment and the radiographer at risk, but with experienced handlers, correct cassette positioning and sedation, these problems can be minimized. Positioning the horse with the limb stretched caudally, and angling the x-ray beam 10–20° proximodistally, may facilitate positioning of the cassette. The cassette can be positioned without touching the flank, and this aids correct alignment of cassette and x-ray beam (Figure 7.2). The cassette should be slowly advanced medially until the radiographer can see the edge of the cassette between the hind limbs. Care should be taken not to touch the sheath in male horses. The x-ray beam should be centred on a line bisecting the limb, i.e. approximately between the semimembranosus and semitendinosus muscles, at the level of the distal third of these muscles. Alternatively the exit point of the beam from the cranial aspect of the joint should be at the level of the tibial crest.

An aluminium wedge filter is useful to attenuate the x-ray beam laterally and medially, to avoid overexposure of the edges of the joint, particularly if changes involving the periarticular structures are suspected. Overexposure of the fibula almost inevitably occurs, particularly in younger animals in which the fibula is predominantly cartilaginous.
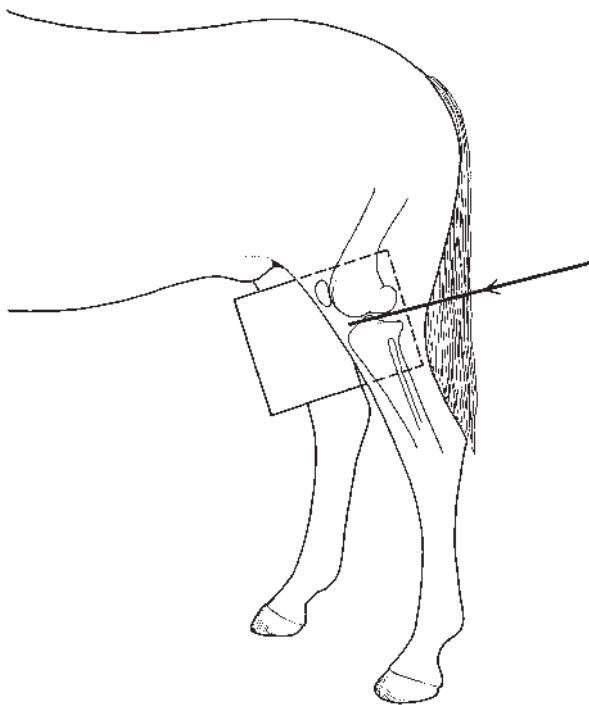
Figure 7.1 Positioning of the limb, cassette and x-ray beam to obtain a caudal 60° lateral-craniomedial oblique view of the stifle.
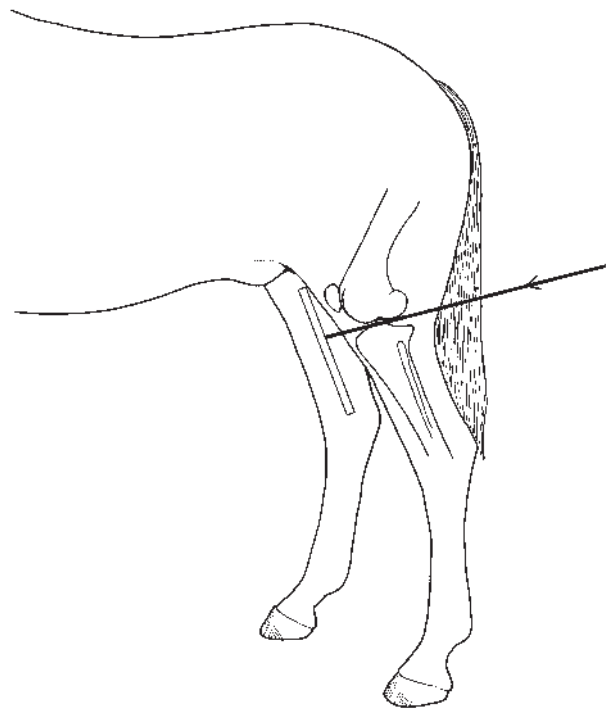
Figure 7.2 Positioning of the limb, cassette and x-ray beam to obtain a caudoproximal-craniodistal oblique view of the stifle.

(a)

(b)
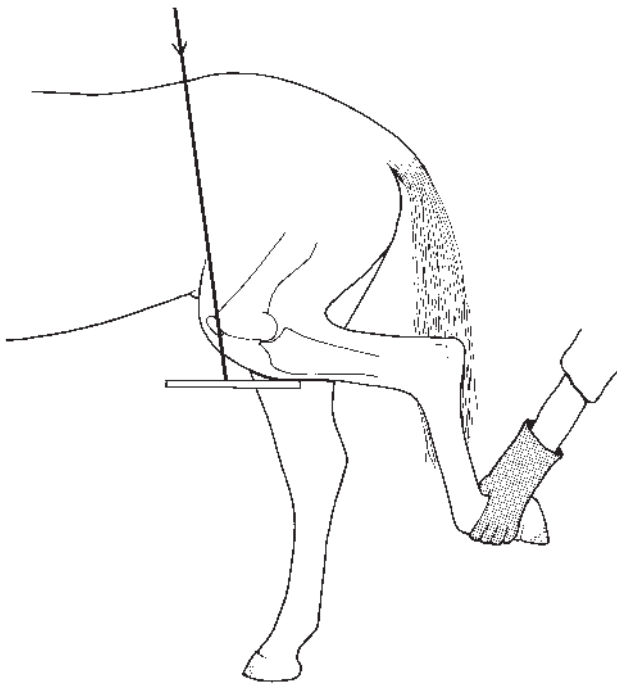
Figure 7.3(a) Positioning of the limb, cassette and x-ray beam to obtain a cranioproximal-craniodistal oblique view of the patella with the horse standing. It may be necessary to angle the x-ray beam slightly from lateral to medial.
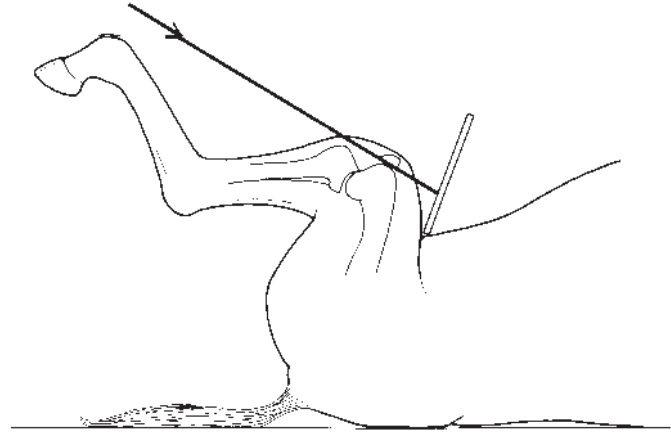
Figure 7.3(b) Positioning of the limb, cassette and x-ray beam to obtain a craniodistal-cranioproximal oblique view of the patella with the horse in dorsal recumbency.

Cranioproximal-craniodistal oblique view

This view is primarily employed to assess the patella, and the trochleas and intertrochlear groove of the femur. It is indispensable in cases of patellar fractures.

With a standing horse, the limb should be held semi-flexed behind the horse (as if for shoeing). The cassette is held approximately horizontal, with its caudal edge against the cranial aspect of the tibia, centred just proximal to the tibial crest (Figure 7.3a). It is not possible to align the x-ray beam perpendicular to the cassette, but satisfactory views are obtained by angling the x-ray beam in a proximal 10° lateral-distal medial oblique direction to avoid the abdominal wall. Adducting the flexed lame limb may facilitate positioning by rotating the stifle outwards.

The above view is sometimes more easily obtained with the horse under general anaesthesia. The horse is placed in dorsal recumbency with the limb fully flexed. The x-ray beam is directed in a craniodistal-cranioproximal direction, and is centred on the femoropatellar articulation, i.e. approximately 8 cm distal to the profile of the flexed joint. The cassette is positioned along the cranial aspect of the femur (Figure 7.3b). An aluminium wedge filter is useful to avoid overexposure of the cranial aspect of the patella.

NORMAL ANATOMY, VARIATIONS AND INCIDENTAL FINDINGS

Immature horse

Important radiographic changes occur in the stifle during growth. Six centres of ossification are present at birth (Figures 7.4a and 7.4b): the

[288]
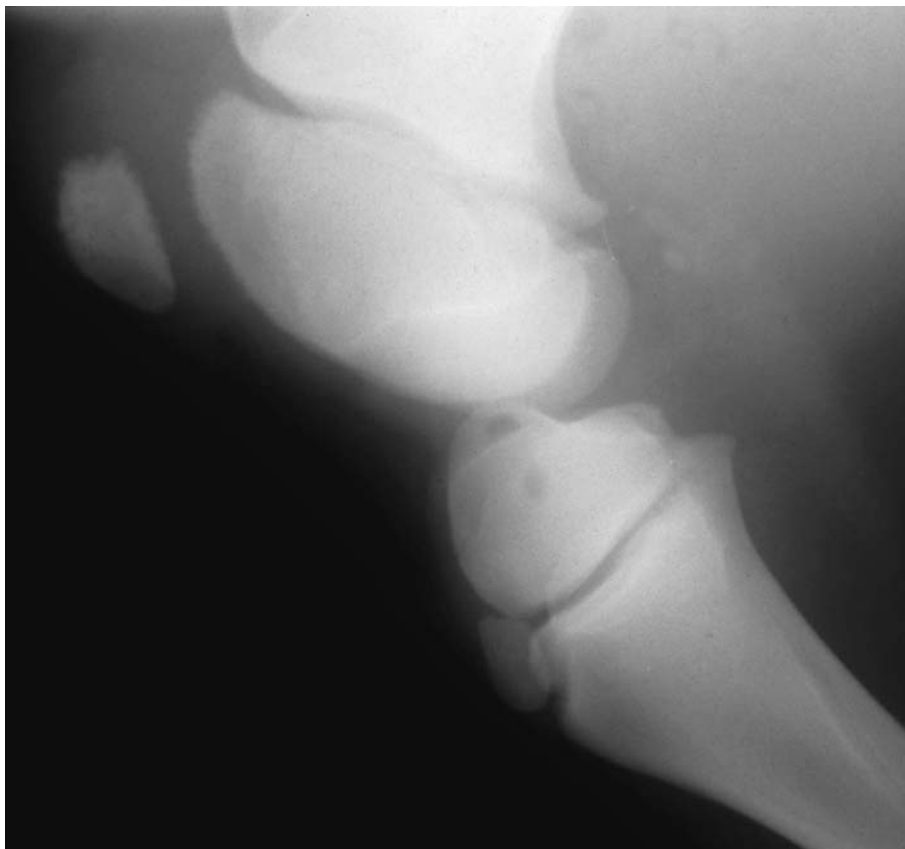
Figure 7.4(a) Flexed lateromedial view of a stifle of a normal 15-day-old foal. Note the irregular contour and granular subchondral opacity of the proximal part of the femoral trochlear and of the patella. The physes are relatively wide. The lateral and medial trochlear ridges of the femur are of similar size. There is an approximately triangular lucent area cranial to the femoropatellar joint representing fat. Note also the separate centre of ossification of the tibial crest (the tibial apophysis).
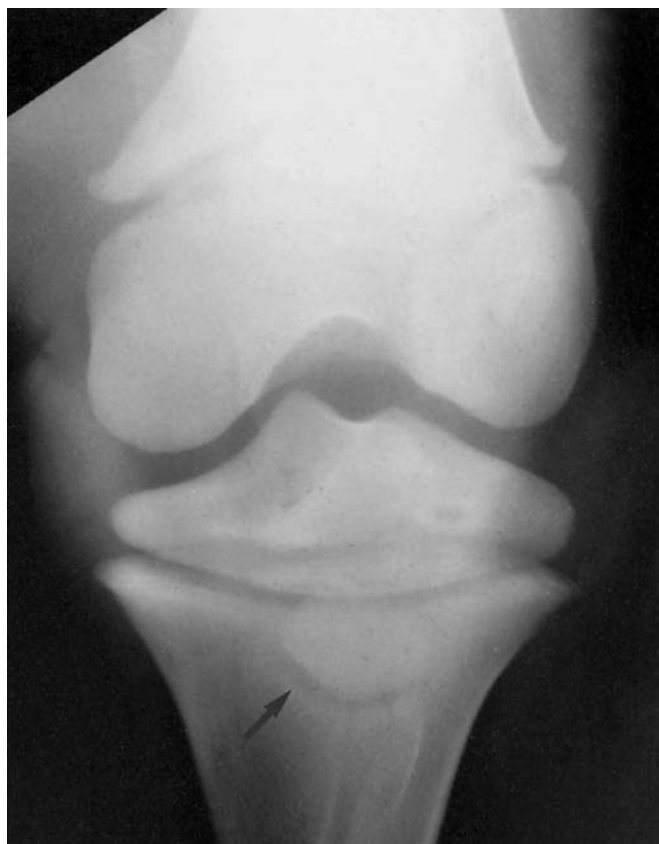
Figure 7.4(b) Caudocranial view of the stifle of a normal 3-week-old foal. Incomplete ossification of the proximal tibial epiphysis gives the impression of slanting of the tibial condyles. The femorotibial joint space is wide compared with the adult. The tibial apophysis and its physis can be identified superimposed on the tibial metaphysis (arrow).
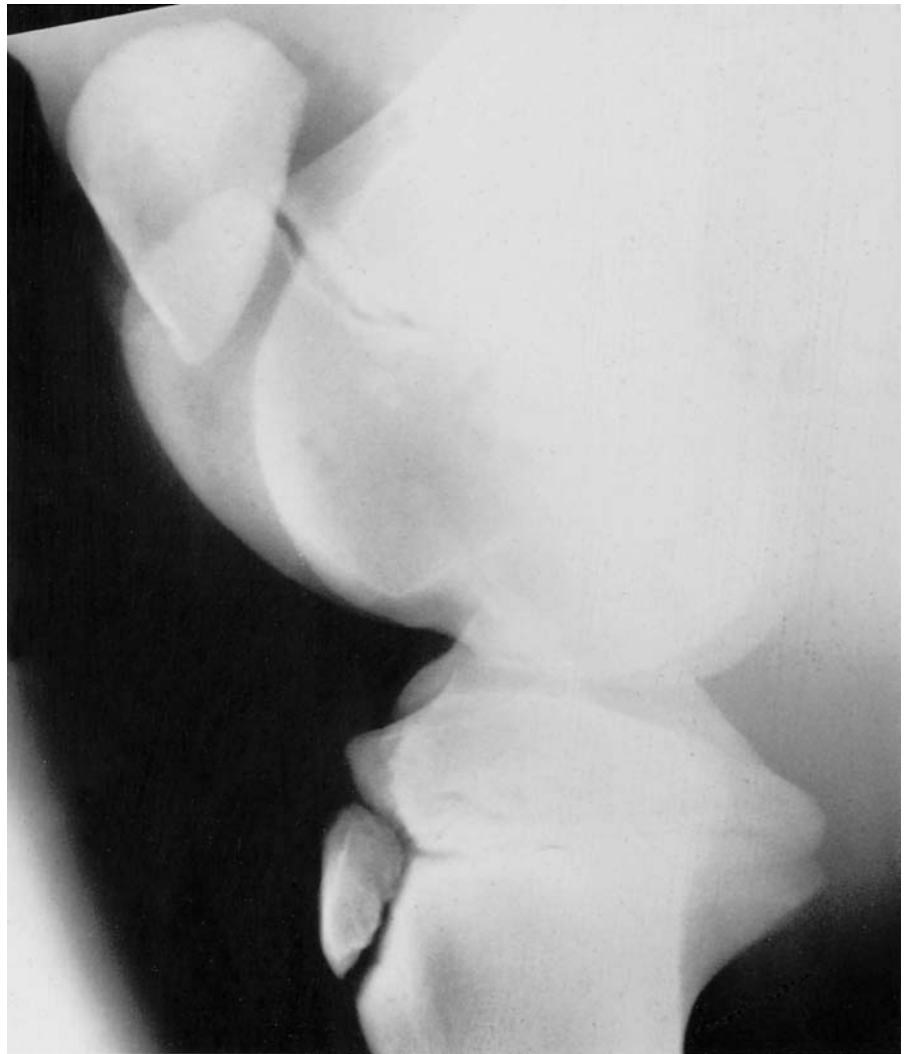
Figure 7.5 Lateromedial view of the stifle of a normal 2-month-old foal. The proximal part of the medial trochlear ridge of the femur and the patella are still incompletely ossified and therefore have an irregular outline. The shape of the trochlea of the femur and the patella, however, is more similar to an adult than to the neonatal foal (compare with Figure 7.4a).

metaphysis and distal epiphysis of the femur; the proximal epiphysis and metaphysis of the tibia; the tibial tuberosity (apophysis) and the patella.

At birth, the patella is a triangular shape, which becomes more complex with age. Initially it has an irregular contour and granular subchondral bone opacity due to incomplete ossification. The articular surface is concave. The patella is usually fully ossified by 4 months of age.

At birth, the lateral and the medial trochlear ridges of the femur are similar in size. The proximal parts of these ridges have an irregular contour and granular subchondral bone opacity. This appearance is normally present until 3 months of age, but may persist until 5 months. It is caused by irregular subchondral ossification and should be differentiated from infectious arthritis (joint-ill), which can have a similar radiographic appearance (see Figure 7.22b, page 311). At approximately 2 months of age, the medial trochlear ridge becomes more prominent than the lateral ridge at its proximal part, where it becomes wider and rounder with a smoothly contoured shoulder (Figure 7.5).

The distal femoral physis is wavy and irregular in outline. It closes at 24–30 months of age. The femoral condyles are smoothly outlined. Irregu-

larity of the condyles should be interpreted as pathological at any age. The femorotibial joint space appears wide at birth, due to incomplete ossification of the epiphyses. This incomplete ossification results in apparent sloping of the tibial condyles (Figure 7.4b, page 289), which later become more horizontal. The intercondylar eminences (lateral and medial) of the tibia are also incompletely developed, appearing small and blunted. The corresponding intercondylar fossa is shallow.

At birth, the apophysis (centre of ossification of the tibial tuberosity) is separated from the proximal tibial epiphysis as well as from the proximal tibial metaphysis. The apophyseal-metaphyseal physis is seen on lateromedial views as an oblique lucent line of irregular width, and on craniocaudal views as a V-shaped lucent line overlying the proximal tibial metaphysis. The apophyseal-epiphyseal physis closes between 9 and 12 months of age, and the apophyseal-metaphyseal physis closes at 30–36 months. The proximal tibial physis (epiphyseal-metaphyseal physis) closes at 24–30 months of age.

The fibula shows very little ossification until 1–2 months of age, at which time ossification occurs from one or more centres (Figures 7.6a–d). This ossification may remain incomplete, resulting in horizontal or oblique radiolucent lines in the fibula (Figures 7.6e–g). These should not be confused with fractures.

Skeletally mature horse

Lateromedial view

With the exception of a slight degree of obliquity, the principal radiographic features of the lateromedial view are the same as those described in detail below for the caudal 60° lateral-craniomedial oblique view.

Caudal 60° lateral-craniomedial oblique view

The large medial trochlear ridge of the femur is positioned proximal and cranial to the smaller lateral trochlear ridge (Figure 7.7, page 294). The trochlear ridges are smoothly curved in outline. Proximally the medial trochlear ridge has a small flattened area at its junction with the metaphysis of the femur. The distal two-thirds of the medial ridge are flatter than the lateral. There is a small notch where the medial trochlear ridge merges with the medial femoral condyle. From this notch an irregular sclerotic line traverses the condyles in a caudal and slightly proximal direction. This is the intercondylar fossa. Immediately above the notch, the convergence of two sclerotic lines indicates the extensor fossa. There is a sclerotic line parallel to the trochlear ridges which represents the base of the intertrochlear groove. On the lateral trochlear ridge there is a flattened area at its transition into the lateral condyle. Neither this, nor the poorly developed area of decreased opacity immediately proximal to this area should be interpreted as an osteochondral defect. If the x-ray beam is angled from too far cranially, the lateral trochlear ridge may appear flattened. The most

[291]

(a)   (b)   (c)   (d)

Figure 7.6 Caudomedial-craniolateral oblique views of the fibulas of seven horses of variable age: (a)–(d) are skeletally immature horses, and show progressive ossification occurring with increasing age; (e)–(g) are skeletally mature horses. Ossification often occurs from more than one centre of ossification which may never fuse, resulting in persistent lucent lines traversing the fibula (f and g).

proximal part of the ridge may have an indistinct margin (Figure 7.8, page 295) which should not be confused with a manifestation of osteochondrosis. The femoral condyles have a smooth convex outline. On the 60° oblique view the condyles are partly superimposed, the medial condyle being projected slightly caudal to the lateral condyle. Fabellae occasionally occur proximal to the caudal aspect of the femoral condyles.

[292]
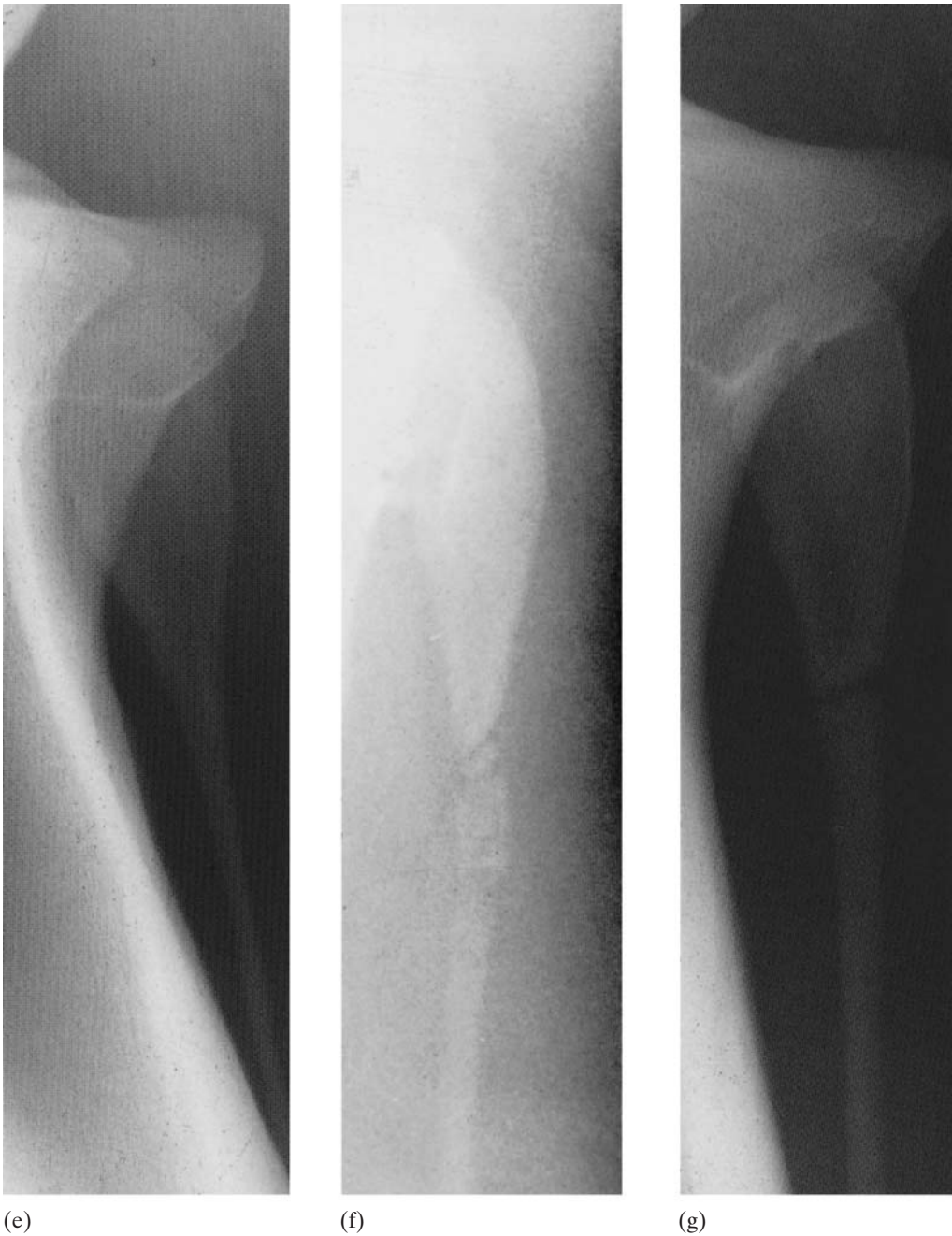
(e)   (f)   (g)

Figure 7.6 *Cont'd*

The position of the patella in relation to the distal femur changes with the degree of flexion/extension of the femorotibial joint. When the horse is bearing weight, the patella is positioned over the proximal aspect of the medial trochlear ridge. With flexion of the femorotibial joint, the patella moves distally which aids visualization of the proximal aspect of the trochlea. Softly exposed radiographs may demonstrate the patellar ligaments.

The femoral condyles and the intercondylar eminences of the tibia are
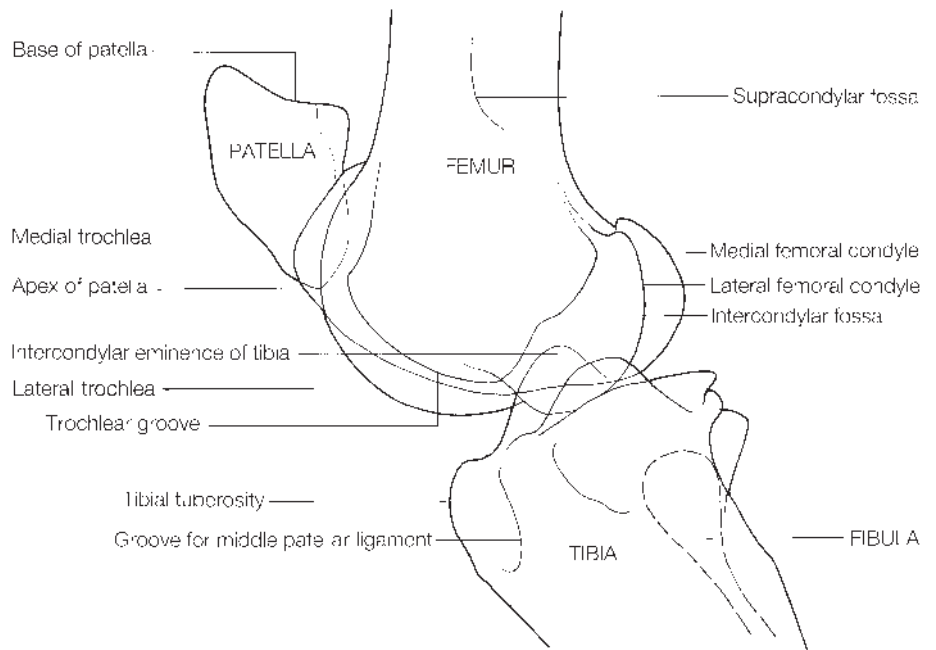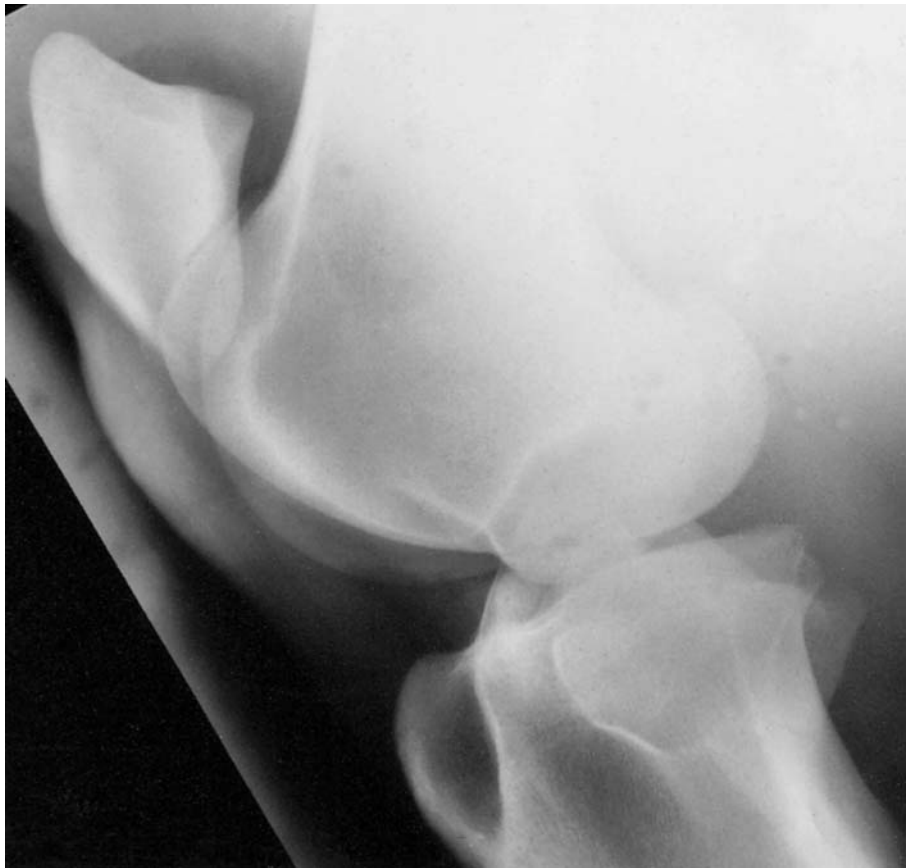
Figure 7.7 Caudal 60° lateral-craniomedial oblique view and diagram of a normal adult stifle. Note the smooth curved contour of the lateral and medial trochlear ridges of the femur. The medial trochlea is larger than the lateral. Compare with Figure 7.9, page 296.

[294]

Figure 7.8 Lateromedial (flexed) view of the stifle of a normal adult horse. The contour of the proximal aspect of the lateral trochlea of the femur is slightly flattened and ill-defined (arrow). This is the result of angulation of the x-ray beam from too far cranially and does not represent a pathological abnormality. Compare with Figures 7.7 (normal) and 7.12, page 301 (osteochondrosis).

superimposed on this view. The tibial tuberosity and tibial crest are recognized cranially.

A soft-tissue opacity is often seen at the cranial aspect of the femorotibial joint, cranial to the site of insertion of the cranial cruciate ligament.

Caudal 45° lateral-craniomedial oblique view

The femoral condyles are further separated in the caudal 45° lateral-craniomedial oblique view (Figure 7.9), compared to a Cd 60° L-CrMO view.

Caudocranial view

The patella is seen partly superimposed upon the lateral cortex of the diaphysis of the femur (Figure 7.10a, page 297). The medial ridge of the

Figure 7.9 Caudal 45° lateral-craniomedial oblique view of the stifle of a normal mature horse. Compare with Figure 7.7.

supracondylar fossa, and the border of the extensor fossa on the lateral surface of the lateral femoral condyle, can also be evaluated.

Deviations from a true caudocranial view may outline slight osseous irregularities along either the medial or the lateral femoral epicondyles. An oval area of decreased opacity is frequently seen at the proximolateral aspect of the intercondylar fossa of the femur, as is a flask-shaped lucent area distal and slightly lateral to the intercondylar eminences of the tibia. They occur as the result of superimposition, and should not be interpreted as cystic lesions in the bone. The border of the intercondylar fossa is relatively opaque.

The medial femoral condyle is rounder than the lateral, but slight flattening of the medial femoral condyle is acceptable if the trabecular pattern of the subchondral bone is normal. The shape of the femoral condyles and the width of the femorotibial joint change with the angle of projection of the radiograph.

[296]

Figure 7.10(a) Caudoproximal-craniodistal oblique view and diagram of a normal adult stifle. Note the different shapes of lateral and medial femoral condyles. The intercondylar fossa has a well-defined margin. The medial intercondylar eminence is larger than the lateral, and more sharply pointed. Note the poorly defined lucent area distal to it. The fibula is relatively overexposed and therefore barely discernible (M = medial).
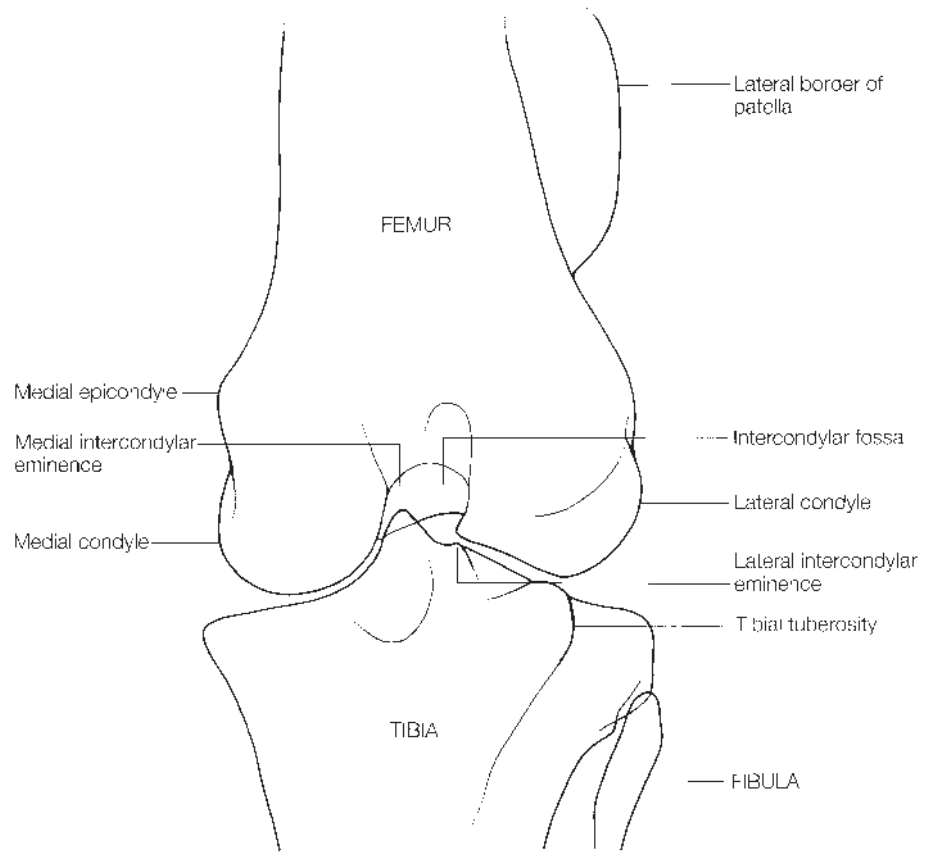
Figure 7.10(a) *Cont'd*

The lateral condyle of the femur has a proximomedial-distolateral inclination. The lateral joint space of the femorotibial joint is narrower than the medial space; this does not indicate collapse of the lateral meniscus.

The medial intercondylar eminence of the tibia is larger and more pointed than the lateral eminence (Figures 7.10a and 7.10b). The lateral condyle of the tibia has a proximomedial-distolateral inclination to mirror the outline of the lateral femoral condyle. Superimposed on the lateral condyle and metaphysis are the tibial tuberosity and tibial crest. There are focal areas of reduced opacity distal to the intercondylar eminences and proximal to the tuberosity of the tibia. The fibula articulates with the lateral aspect of the tibia.

Cranioproximal-craniodistal oblique view

The medial trochlear ridge is larger than the lateral and is separated from it by the trochlear groove (Figure 7.11, page 300). The patella is approximately triangular, and its medial angle is blunter than the lateral. The patella has a uniform opacity with a distinct subchondral bone plate and a smooth articular outline.

Other structures are poorly defined on this view.

[298]

Figure 7.10(b) High detail caudocranial radiographic view and diagram of the central region of the femorotibial joint of a normal adult horse.

SIGNIFICANT FINDINGS

Osteochondrosis

In this text, subchondral bone cysts (osseous cyst-like lesions) are regarded as a separate entity from osteochondrosis, although they are considered by some workers to be part of the same syndrome (see 'Osseous cyst-like lesions', page 24).

In the stifle, osteochondrosis is most commonly recognized radiographically involving the lateral trochlear ridge of the femur. Lesions are also seen restricted to the articular surface of the patella. Less commonly, lesions may also involve the medial trochlear ridge and the trochlear groove. Osteochondrosis frequently occurs bilaterally, and both stifles should be radiographed.

Radiographic indications of osteochondrosis of the lateral trochlear ridge are most easily detected on the caudal 60° lateral-craniomedial oblique view, and may include:

Intercondylar fossa

Axial margins of
intercondylar fossa

Medial eminence
of tibia

Distal aspect of
lateral trochlear ridge

Lateral eminence
of tibia

Normal depression cranial
to the intercondylar
eminence

M
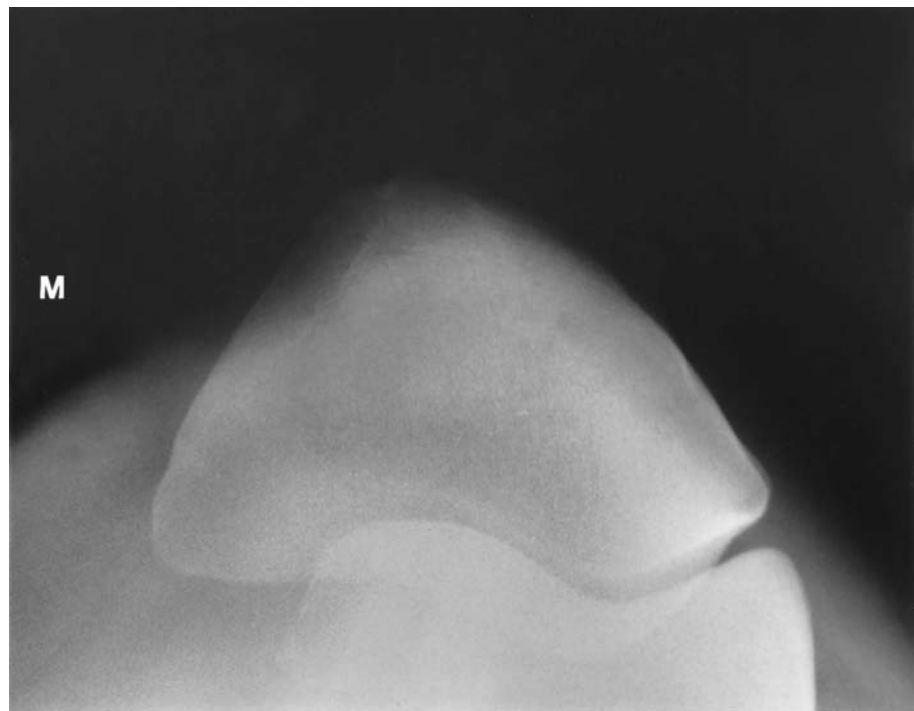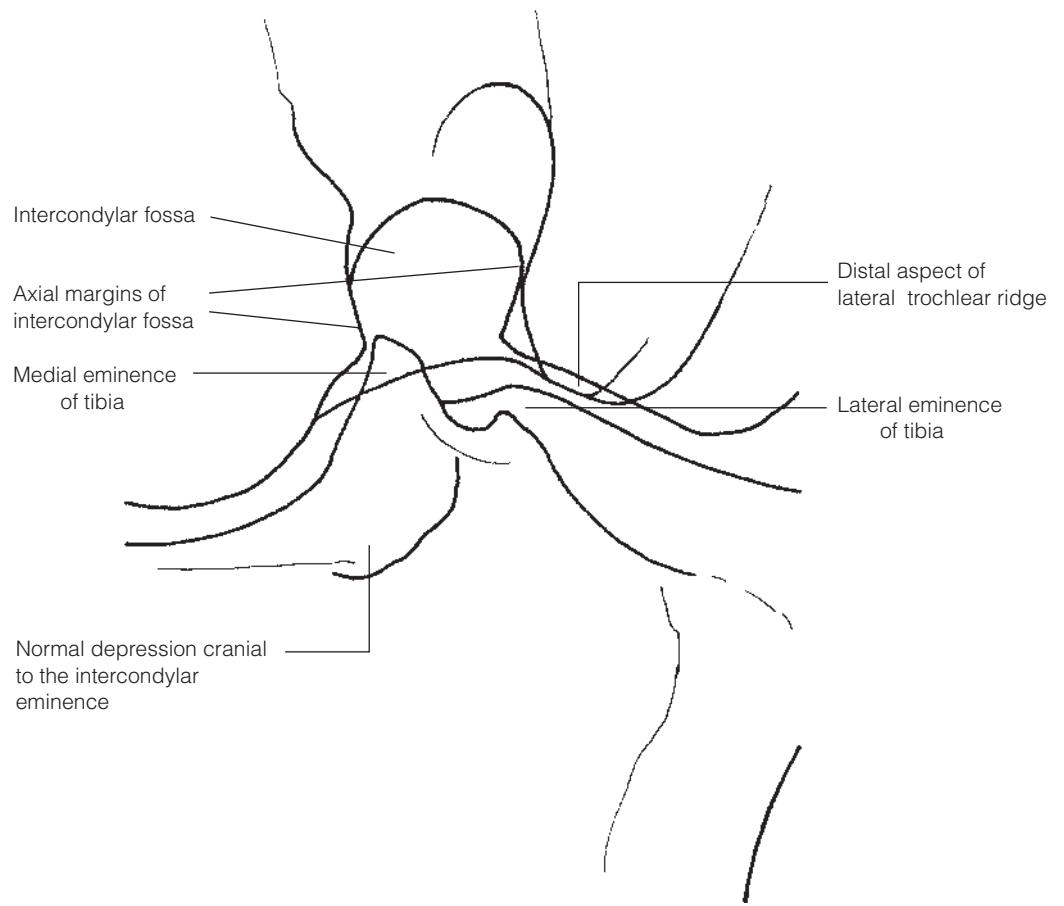
Figure 7.11 Cranioproximal-craniodistal oblique view of a patella and femoral trochleas of a normal adult horse. Note the larger medial trochlea of the femur (M = medial).

[300]

Figure 7.12 Lateromedial view of an adult horse. There is flattening of the middle one-third of the lateral trochlear ridge of the femur (arrows) (compare with Figure 7.7). There is sclerosis of the underlying subchondral bone. There were no associated clinical signs in this Grand Prix Showjumper.

1   Flattening, especially of the middle third of the ridge (Figure 7.12).

2   An irregular contour of the ridge, usually limited to the middle third, but occasionally involving as much as two-thirds of the ridge. There may be one or more subchondral lucent defects extending for up to 2 cm into the ridge (Figures 7.13, page 302 and 7.14b, page 303). These may have a sclerotic margin, and are easily demonstrated on slightly more oblique views.

3   Radiopaque fragments may be present within a defect in the ridge (Figure 7.14a, page 303).

4   In long-standing cases, the lateral trochlear ridge may be grossly undersized but have a regular outline (Figure 7.15, page 304). This is normally due to fragmentation and remodelling. There may be one or more rounded, radiopaque fragments within the femoropatellar joint, or attached to the joint capsule. Occasionally similar changes are identified in the medial trochlea of the femur.

5   The articular surface of the patella may be irregular (Figure 7.16, page 304), most commonly near the apex. Other patellar changes include subchondral lucent zones, with or without surrounding sclerosis. These changes

[301]

Figure 7.13 Lateromedial view of a stifle of an 8-month-old Thoroughbred foal. There is loss of the distinct osteochondral outline of the middle one-third of the lateral trochlear ridge of the femur (arrows). In the underlying subchondral bone there is an oval-shaped area of decreased opacity. In addition, there is a subtle depression in the outline of the middle of the medial trochlear ridge (open arrow). Similar changes were present in the contralateral limb. The foal showed only slight hindlimb stiffness, but experienced great difficulty in getting up. Grossly and histologically, the abnormalities extended into the subchondral bone. Note also the separate ossification centre of the apophysis of the tibia.

are rare, and may occur alone or in association with lesions of the lateral trochlear ridge. A fragment occasionally occurs in isolation at the base of the patella at its articular margin. It is important to ensure that the whole of the patella is visualized on radiographs, and the proximal part is not missed. The aetiology of these fragments has not been confirmed. Lesions of the patella may warrant a more guarded prognosis.

Simultaneous involvement of more than one structure in the joint has been suggested as indicative of a poor prognosis. Radiography tends to under-estimate the degree of pathological abnormality which may be detected arthroscopically.

Osteochondrosis cannot be detected radiographically until a moderate degree of subchondral bone change is present. It is important that oblique views are included, and care should be taken not to overlook subchondral

(a)

(b)

Figure 7.14(a) Caudal 60° lateral-craniomedial oblique view of a stifle of a 9-year-old horse. There is distension of the femoropatellar joint capsule and an irregularly outlined defect in the subchondral bone of the middle of the lateral trochlear ridge of the femur, within which are a number of radiopaque fragments. These represent mineralized cartilage and/or bone. The radiograph is exposed to highlight the lesions.

Figure 7.14(b) Caudal 60° lateral-craniomedial oblique view of a stifle of a 15-month-old Thoroughbred. There is distension of the femoropatellar joint capsule and marked irregularity of the contour of the lateral trochlear of the femur due to fragmentation of the articular cartilage and resorption of the underlying bone. Mineralized debris is present in the femoropatellar joint and within the defect. There is also modelling of the apex of the patella.

lucencies on overexposed films. Slight flattening of the lateral trochlear ridge need not be accompanied by clinical symptoms, and is occasionally seen with sclerosis of the subcortical bone as an incidental finding in older horses.

In early and mild cases, conservative management may be adequate. Once distension of the joint capsule and lameness are present, surgical intervention is recommended. Post-operatively, there will be some modelling of the defect, but even in clinically successful cases the radiographic appearance will remain abnormal.

The disease may remain asymptomatic throughout the horse's life, or may become symptomatic late in life. In older horses there are usually

Figure 7.15 Caudal 60° lateral-craniomedial oblique view of a distal femur of an 8-year-old horse. There is considerable distension of the femoropatellar joint capsule. The lateral trochlear ridge, although relatively smoothly outlined, is undersized (compare with Figure 7.7). There are several large, rounded mineralized fragments (arrow heads) within the femoropatellar joint ('joint mice'). Extensive modelling of the apex (white arrow) and base (open arrow) of the patella and the proximal aspect of the lateral trochlear ridge (black arrow) indicates secondary degenerative joint disease.
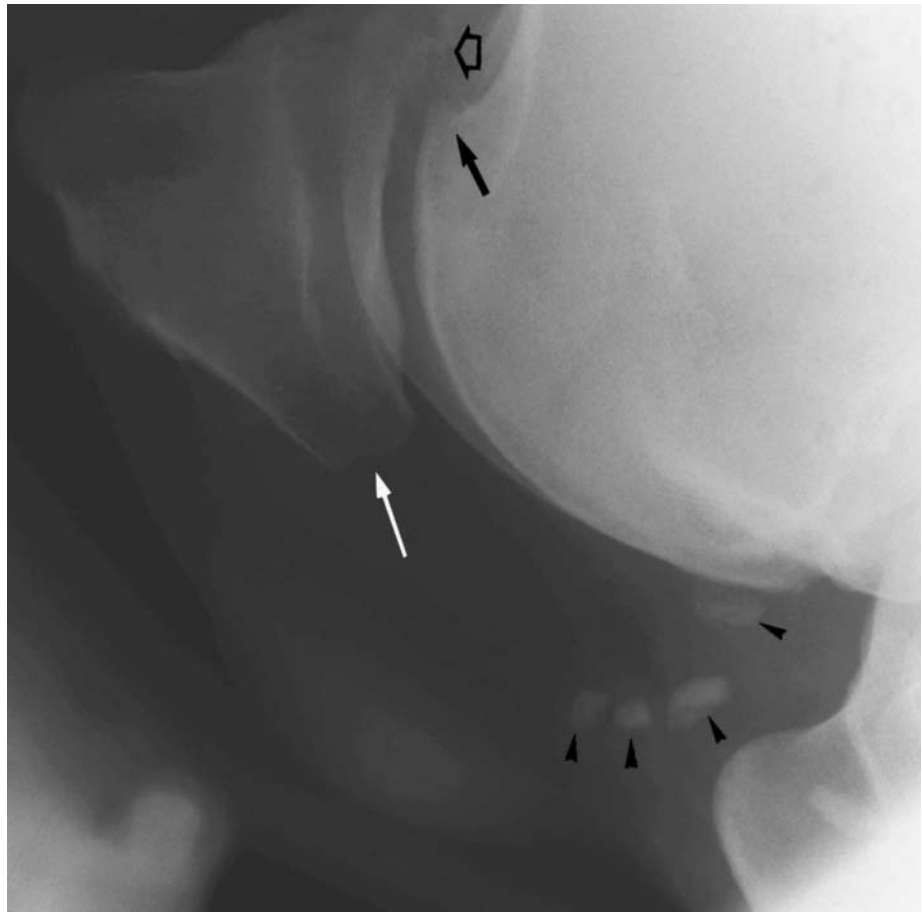
Figure 7.16 Flexed lateromedial view of a stifle of a 2-year-old Thoroughbred. The distal quarter of the articular surface of the patella is markedly irregular with extensive subchondral fragmentation towards the apex (arrows). These changes may be part of the osteochondrosis syndrome. Similar, usually less severe, changes may develop secondary to medial patellar desmotomy.

[304]

discrete bony opacities in association with a shallow defect and subchondral sclerosis. In these cases the bony fragments must be removed in order to provide a congruent articulation and prevent the development of secondary degenerative joint disease.

Osseous cyst-like lesions

Subchondral bone cysts

Although subchondral bone cysts are considered by some authors to be part of the osteochondrosis syndrome, they are referred to in this text as a separate lesion. Recent experimental evidence has shown that an elliptical full thickness cartilage plus subchondral bone defect, at the region of maximum weight bearing in the medial femoral condyle, will result in the development of an osseous cyst-like lesion within 3 weeks, which may progressively enlarge over the following 9 weeks. This supports clinical evidence of subchondral bone cysts developing in the medial femoral condyle of mature horses, following known trauma.

Subchondral bone cysts in the stifle occur almost exclusively in the medial femoral condyle. They frequently develop bilaterally, although the horse may present with a unilateral lameness; therefore both hind limbs should be examined radiographically. The fully developed subchondral bone cyst is seen as an almost circular lucent area within the subchondral bone. It is best seen on the caudocranial view, and may be difficult to see on oblique views due to superimposition of the condyles. The cyst initially develops from a saucer-shaped radiolucent area proximal to the articular cartilage (Figure 7.17a). This lucent zone gradually enlarges to become dome shaped, with a flat base in close apposition to the articular surface (Figures 7.17b,c). If a cyst develops prior to skeletal maturity, continued growth and endochondral ossification of the epiphysis gives the impression that the cyst moves proximally into the condyle. The cyst becomes more rounded (Figure 7.18a, page 307), and a communicating lucent channel develops between the cyst and the medial femorotibial joint (Figure 7.18b, page 307). This channel is formed by infolding of the subchondral bone plate. An almost complete subchondral bone plate may become re-established at the medial femorotibial articulation.

Shallow saucer-shaped radiolucent lesions proximal to the articular cartilage do not necessarily develop into subchondral bone cysts. They need not cause pain, although many are believed to cause lameness at some time. A number of caudocranial views with varying proximodistal inclination of the x-ray beam are necessary to evaluate the subchondral trabecular pattern and the depth of the lesion. When a subchondral bone cyst is present in one limb, a shallow saucer-shaped lesion is occasionally present in the contralateral limb. This may remain quiescent, or develop as discussed above.

Shallow saucer-shaped lesions when associated with lameness may respond to conservative treatment; surgical treatment has yielded inconsistent results. When well-developed subchondral bone cysts are present, the

(a)

(b)

(c)

Figure 7.17 Caudocranial views of one stifle of an Arab horse, showing the development of a dome-shaped subchondral bone cyst in the medial femoral condyle from a crescent-shaped subchondral defect: (a) 12 months of age; (b) 18 months of age; (c) 21 months of age. Note the sclerotic rim surrounding the defect.

Figure 7.18(a) Caudocranial view of a stifle of a 2-year-old horse. There is a large oval subchondral bone cyst in the medial femoral condyle. There is a thin rim of sclerosis surrounding the cyst and apparent reformation of a subchondral bone plate between the cyst and the medial femorotibial joint.

Figure 7.18(b) Caudocranial view of a stifle of an adult horse. There is a large rounded subchondral bone cyst in the medial femoral condyle which probably communicates with the medial femorotibial joint via a narrow canal through the subchondral bone plate. The outline of the subchondral bone is flattened. Considerable sclerosis surrounds the cyst. There is osteophyte formation on the medial aspect of the medial tibial condyle.

radiographs should be carefully assessed for evidence of degenerative joint disease (see page 309), which may warrant a more guarded prognosis. Conservative treatment may restore clinical soundness in approximately 20–50% of horses, but there is little radiographic change except for the formation of a sclerotic rim of bone around the periphery of the cyst. Long-standing cysts may be seen radiographically when not causing lameness, but their future clinical significance is uncertain.

Surgical treatment of subchondral bone cysts results in up to 80% of cases returning to normal work. There is little correlation between clinical progress and the postoperative radiographic appearance of a cyst, although in some cases progressive enlargement of the cyst has been noted, associated with persistent lameness. Radiographic resolution of the lesion is not
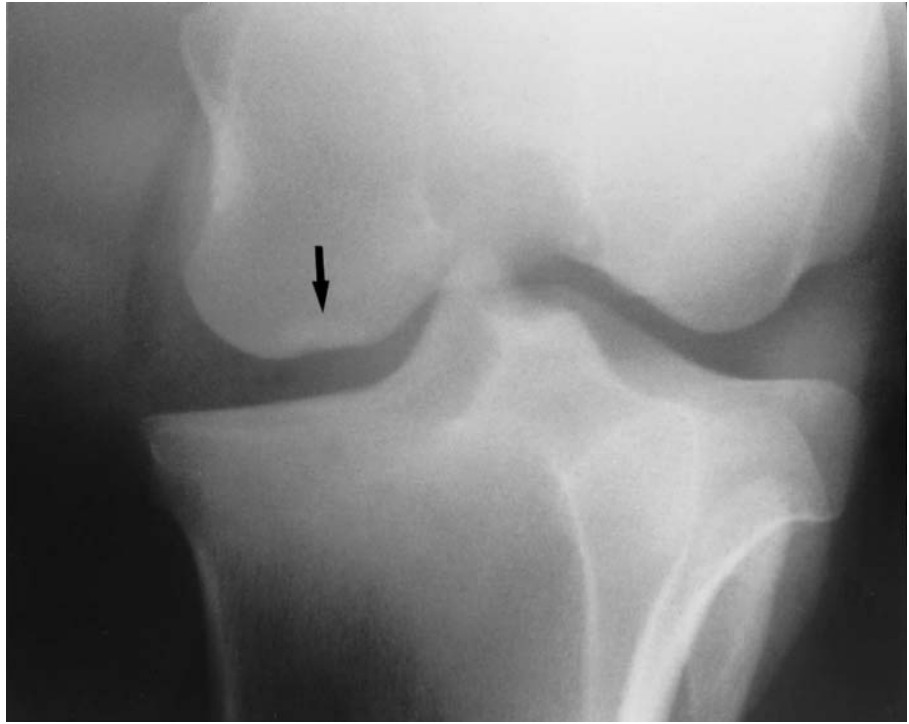
Figure 7.19 Caudocranial view of a stifle of a 7-year-old dressage horse, with pain associated with the medial femorotibial joint. There is flattening of the centre of the articular margin of the medial femoral condyle, with underlying subchondral sclerosis (arrow). The overlying articular cartilage was abnormal.

necessary for a satisfactory clinical outcome. Focal flattening of the subchondral bone of the medial femoral condyle, with an underlying semicircular sclerotic zone, has been seen in some older horses with pain associated with the medial femorotibial joint (Figure 7.19). The aetiology of these lesions and their significance are unknown. Some are associated with abnormalities in the overlying articular cartilage.

Other osseous cyst-like lesions

Osseous cyst-like lesions may occur in the lateral femoral condyle and the proximal epiphysis of the tibia (Figure 7.20). Osseous cyst-like lesions in the proximal tibia may be surrounded by a marked sclerotic rim. Osseous cyst-like lesions distal to the intercondylar eminences may be associated with cruciate ligament injuries (see Figure 7.24, page 314) or tearing of cranial meniscal ligaments.

Physitis

Physitis is associated with irregular widening of the physis, usually involving the distal femoral physis. The incidence in the stifle is very low. Bilateral physitis may result in an upright hind-limb stance and a stiff and stilted gait. The differential diagnosis should include osteochondrosis.

[308]

Figure 7.20 Caudocranial view of a stifle of a 1-year-old Thoroughbred. The osteochondral outline of the medial tibial condyle is slightly irregular (black arrow). There is a well-circumscribed osseous cyst-like lesion in the subchondral bone, surrounded by a broad rim of sclerosis (open arrow). There is also a suggestion of slight flattening of the opposing medial femoral condyle.

Degenerative joint disease

Degenerative joint disease of the femorotibial joint is best recognized radiographically on a caudocranial view (Figures 7.21a and 7.21b). The lateromedial view is more useful for the femoropatellar joint. Changes include:

- Periarticular osteophyte formation.
- Flattening of the articular surfaces.
- Sclerosis of the subchondral bone.
- Lucent zones in the subchondral bone.
- Narrowing of the femorotibial joint space.

Osteophytes on the tibial condyles, best seen on caudocranial views, are not necessarily a cause of lameness. They occur most often on the medial tibial condyle. It is helpful to compare the radiographs of suspected lesions with radiographs of the contralateral joint. Degenerative joint disease may develop secondarily to trauma to other structures of the stifle, and the radiographs should be inspected carefully for evidence of meniscal damage, cruciate ligament injury or collateral ligament injury (page 312). Diagnostic ultrasonography is useful for evaluating soft tissue pathology, including damage of the meniscal cartilages, the patellar ligaments and the collateral ligaments of the joint.

A poor prognosis is warranted for degenerative joint disease of the stifle.

[309]

Figure 7.21(a) Caudocranial view of a stifle of a 13-year-old Hanoverian. There is large, irregularly outlined, osteophyte formation on the medial aspect of the medial tibial condyle (white arrow). The periphery is less opaque than the parent bone, suggestive of active bone formation. The medial aspect of the medial femoral condyle is also irregular (black arrow), but there is no other evidence of degenerative joint disease. The radiograph is deliberately exposed to highlight these abnormalities.

Figure 7.21(b) Caudocranial view of a stifle of an 8-year-old horse. There is irregularity in the contour of the lateral aspect of the intercondylar fossa (black arrow) and new bone formation on the most axial aspect of the lateral femoral condyle (open arrow). There is a suggestion of a discrete mineralized opacity proximal to the medial intercondylar eminence of the tibia. The circular lucent zone with a more opaque centre, distal to the medial intercondylar eminence, is abnormal (compare with Figure 7.10). These changes are indicative of degenerative joint disease and probably result from trauma to either the cruciate ligament and/or a cranial meniscal ligament (see Figure 7.23).

Infection

Septic arthritis (type S) and osteomyelitis in foals (types E and P) frequently affect the femorotibial joint and the femoral condyles (the medial condyle being most commonly affected; see Figure 7.22a). Lateromedial radiographs may reveal patchy lucencies in the subchondral bone due to destruction and collapse of the cartilage and the subchondral bone. An irregular joint surface is therefore seen (Figure 7.22b). This should not be confused with

Figure 7.22(a) Caudoproximal-craniodistal oblique view of a stifle of a 3-month-old foal. There are poorly defined lucent zones in the medial femoral condyle, surrounded by more sclerotic bone. There is a suggestion of a discrete fragment (arrow) extending from the medial aspect of the intercondylar fossa medially, which may represent a sequestrum or a pathological fracture. These radiographic abnormalities are consistent with severe type E osteomyelitis.
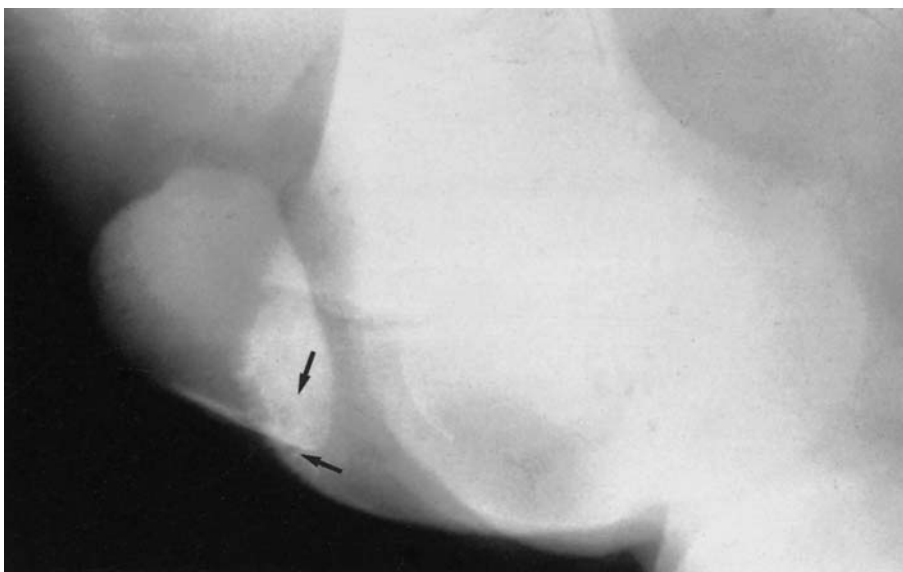
Figure 7.22(b) Flexed lateromedial view of a stifle of an approximately 4-week-old Thoroughbred foal. The foal had distension of the femoropatellar joint capsule, and synovial fluid analysis confirmed a diagnosis of septic arthritis. The apex of the patella and the trochlear ridges of the femur are incompletely ossified, as is normal for a foal of this age. There are also poorly defined lucent zones (arrows) in the subchondral bone of the medial trochlea ridge indicative of osteomyelitis.

the radiographic appearance of incomplete ossification normally seen in the trochlear ridges of the femur and the patella in young foals (see Figure 7.4, page 289). Changes may also be recognized within the tibial epiphysis and are usually best demonstrated on caudocranial views.

Osteomyelitis of the patella may occur in horses of any age. It is usually the result of direct trauma to the region, and is often associated with a draining sinus. Although radiographic changes may be seen in the

lateromedial view, a cranioproximal-craniodistal oblique view may be required. Contrast radiography of cases with a discharging sinus may be useful.

Miscellaneous soft-tissue injuries

In addition to the collateral ligaments common to most joints, the femorotibial joint includes lateral and medial menisci and associated ligaments, as well as cranial and caudal cruciate ligaments.

Collateral ligaments

The collateral ligaments of the femorotibial joint originate from the femoral epicondyles. In most normal horses, the outline of the epicondyles may be irregular on caudocranial radiographs. Sprain of these ligaments may result in increased irregularity due to new bone production. There may also be entheseophyte formation at their insertions on the proximal tibia. Occasionally avulsion fractures occur. Further information may be obtained from ultrasonographic examination. If rupture of a collateral ligament is suspected, radiographs should be obtained with the joint under latero-medial stress, in order to confirm unilateral widening of the femorotibial joint space.

Meniscal damage

The true incidence of damage to the medial or lateral meniscus, or the supporting cranial and caudal ligaments, is unknown, but with the development of exploratory arthroscopy an increasing number of injuries are being identified, frequently unassociated with any detectable radiological abnormality. Some cases of degenerative joint disease (see page 309) develop secondarily to meniscal instability or meniscal tears. Traumatic injuries severe enough to damage the menisci may also result in damage to other structures, such as the collateral and the meniscal ligaments. Plain and contrast radiographs are of limited value in outlining a meniscal tear, but meniscal damage may result in narrowing of the joint space. This is best assessed on caudocranial weight-bearing radiographs which may be difficult to obtain, as resting pain is often present. It is helpful to compare the width of the joint space with that of the contralateral stifle. Mineralization of a damaged meniscus has been recognized. Lucent zones distal to the inter-condylar eminences of the proximal tibia may be seen in association with tears of the cranial meniscal ligaments.

　　Surgical debridement of tears of the axial aspect of a meniscus may have favourable results, but prognosis for other meniscal injuries is poor.

Cruciate ligaments

Rupture of the cranial and caudal cruciate ligaments has been described, and has a poor prognosis.

　　Sprain of the cruciate ligaments with or without partial detachment of
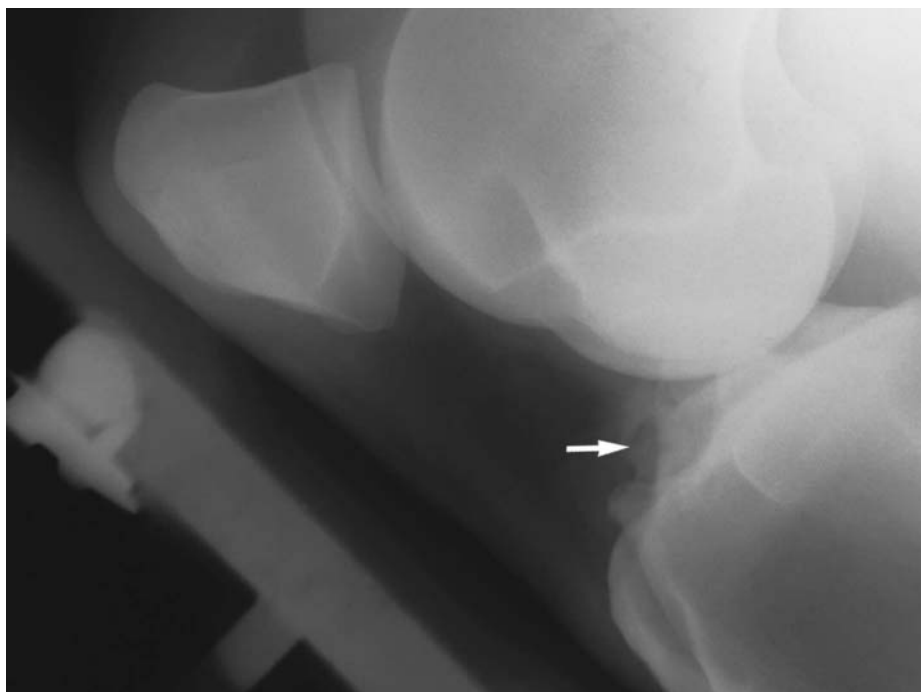
Figure 7.23 Flexed lateromedial view of a stifle of a 13-year-old horse. There is extensive, poorly defined new bone immediately cranial to the intercondylar eminences (arrow), suggesting trauma to the distal insertion of the cranial cruciate ligament and/or a cranial meniscal ligament. (This is the same case as Figure 7.21a.)

the distal insertion of the cranial cruciate ligament occurs more frequently. This ligament inserts with the cranial ligaments of the menisci immediately cranial to the intercondylar eminences. A discrete soft-tissue radiopacity immediately cranial and proximal to the site of insertion may indicate damage to the cruciate ligament. If seen on a lateromedial view, it should not be confused with the area of increased opacity seen on the cranial aspect of the normal femorotibial joint. In chronic cases there may be bony proliferative changes (Figure 7.23), often best seen on a flexed lateromedial view. Osseous cyst-like lesions may occur at the sites of origin and insertion of the cruciate ligaments. They are seen proximal to the intercondylar fossa, superimposed on the femoral condyles and/or distal to the inter-condylar eminences of the tibia (Figure 7.24). Apparently detached osseous fragments may be evident in the intercondylar fossa, often in association with irregularities in the contour of the intercondylar eminences. All of these lesions are considered to have a guarded prognosis. A fracture of the medial intercondylar eminence may be seen in association with cruciate ligament injury, but is not synonymous with it. A fracture may be seen in isolation, with surgical removal resulting in a satisfactory outcome.

Other soft-tissue injuries

Caudal 60° lateral-craniomedial oblique radiographs, obtained with low kilovoltage, may reveal increased opacity of the patellar ligaments. New bone formation near the proximal ligament insertions on the patella may

[313]

Figure 7.24 Caudocranial view of a proximal tibia of an 11-year-old Thoroughbred cross horse. There is a poorly defined area of reduced radiopacity immediately distal to the intercondylar eminences. The area is circumscribed by a thick rim of sclerosis. Osseous cyst-like lesions occurring at this site have been associated with damage to the insertion of the cruciate ligament or a cranial meniscal ligament. There is slight modelling of the medial aspect of the medial tibial condyle. The circular opacity on the lateral aspect of the femorotibial joint is a screen artefact.

also occur. These changes normally follow injury to the patella. The prognosis for this type of injury is good following rest.

Periosteal proliferation may be seen on the cranial aspect of the tibia, close to the distal aspect of the tibial crest, with or without cortical lucency. Sometimes a lucent line parallel to the cortical surface is seen, with or without a radiopaque fragment (Figure 7.25). These changes have been seen in young Thoroughbreds, with focal pain on pressure to the area, and probably reflect an insertional enthesopathy of semitendinosus.

Remodelling of the apex of the patella

Remodelling of the apex of the patella may develop within weeks of performing a medial patellar desmotomy, to treat intermittent upward fixation of the patella. Radiographic changes include spur formation at the apex of the patella, an irregular outline or fragmentation. Lameness is usually resolved by surgical debridement.

Calcinosis circumscripta

Calcinosis circumscripta (tumoral calcinosis) is a condition characterized by the formation of one or more hard, circumscribed subcutaneous swellings,

[314]

Figure 7.25 Lateromedial view of the proximal tibia of 3-year-old Thoroughbred racehorse. There is an osseous fragment (white arrow) at the tibial site of insertion of semitendinosus. The cranial cortex has a slightly irregular outline and there is a parallel lucent line in the cortical bone (black arrow).

typically formed at the lateral aspect of the femorotibial joint. Lameness is not usually present. Caudocranial radiographs demonstrate the lesion as a distinctly outlined mass of soft-tissue opacity irregularly infiltrated with small, highly opaque, amorphous granules (Figure 7.26). If lameness is present, surgery may be necessary.

Patellar luxation

Lateral luxation of the patella occurs occasionally in foals, but rarely in adults other than miniature breeds. Radiography may help to diagnose this condition. The radiographs should be inspected carefully to determine if there is primary hypoplasia of the trochlear ridges of the femur. Surgical treatment may be successful.

Upward fixation of the patella is a common condition, in which radiography is of little value. Lameness sometimes develops secondarily to

Figure 7.26 Caudocranial view of a stifle of a 1-year-old Thoroughbred. Radiopaque 'masses' extend from the lateral aspect of the femorotibial articulation distally. This is calcinosis circumscripta (tumoral calcinosis). Note that the fibula is incompletely ossified. The radiograph is deliberately softly exposed.

medial patellar desmotomy for this condition. It is associated with remodelling of the apex and cranial distal surface of the patella, best seen in caudal 60° lateral-craniomedial oblique, or flexed lateromedial views.

Infectious osteitis of the patella

Infectious osteitis of the patella usually follows known trauma and a penetrating wound. There may be a detectable radiolucent tract running from the skin surface to the cranial aspect of the patella, which develops both lytic lesions and some new bone formation. A sequestrum and involucrum may develop. Diagnostic ultrasonography may be a more sensitive diagnostic technique early in the disease process.

Fractures

The presence of bone fragments in the joint may indicate the presence of a fracture or fractures, but it is not always possible to identify where the fragments have originated from. They should not be confused with fragments associated with osteochondrosis.

[316]

Patellar fractures may be recognized or suspected on lateromedial views (Figure 7.27a), but a flexed cranioproximal-craniodistal oblique view is essential to ascertain the location and extent of a fracture and to determine if comminution is present (Figure 7.27b).

Small fragments separated from the base of the patella are often slightly displaced proximally, and are best seen on lateromedial views. They are usually avulsion fractures at the insertion of the quadriceps muscle, and seldom cause persistent lameness. Some persist radiographically, whereas others disappear.

Avulsion fractures of the medial angle of the patella (Figure 7.27b) are sometimes displaced proximally or medially. Lateromedial and cranioproximal-craniodistal oblique views are required to determine the location and extent of these fractures. Surgical removal of the avulsed fragment, sometimes together with the attached fibrocartilage, normally ensures a satisfactory clinical outcome, provided that there is no evidence of degenerative joint disease.

Patellar fractures are frequently seen in association with fractures of

Figure 7.27(a) Caudal 60° lateral-craniomedial oblique view of a 7-year-old horse which hit a fixed cross-country fence. There is a fracture of the base of the patella. A cranioproximal-craniodistal oblique view should be obtained to evaluate the patella more fully (see Figure 7.27b).
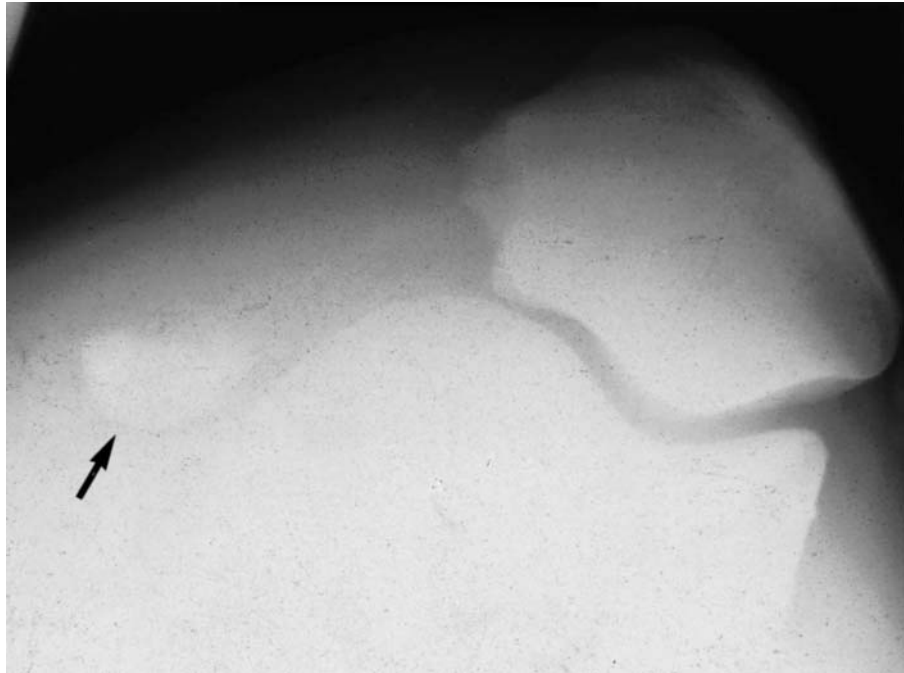
Figure 7.27(b) Cranioproximal-craniodistal oblique view of the patella of a 6-year-old eventer. There is a displaced articular fracture of the medial aspect of the patella (arrow). The horse was treated by surgical removal of the fracture and made a complete recovery.

the trochlear ridge (Figure 7.28), and this may affect the prognosis. Sagittal patellar fractures involving the medial pole are sometimes seen in association with fractures of the lateral trochlear ridge of the femur (Figure 7.28) and this may affect the prognosis, unless recognized and treated accordingly.

Sagittal fractures of the patella involving more than the medial one-third of the bone carry a much poorer prognosis. Transverse fractures of the patella occur less commonly, and are readily identifiable in lateromedial views. Treatment by internal fixation offers the best prognosis.

Femur

Fractures of the trochlear ridges and the caudal aspect of the femoral condyles can be demonstrated on caudal 60° lateral-craniomedial oblique views (Figure 7.28). They may be accompanied by fractures of the patella.

Fractures of the caudal aspect of the femoral condyles can be demonstrated on lateromedial oblique views, and usually occur with other injuries to the joint, which may seriously affect the prognosis. Care must be taken not to mistake fabellae (which are occasionally present at this location) for fractures.

Salter-Harris fractures of the distal femoral physis occur occasionally. Lateromedial and caudocranial views should be obtained. These fractures have a guarded prognosis, although internal fixation may be possible in younger animals.

[318]
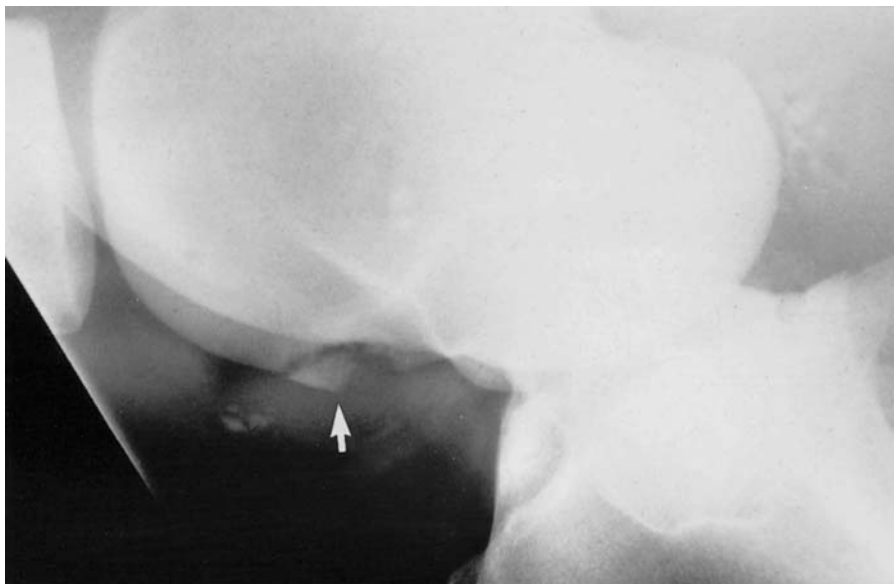
Figure 7.28 Flexed lateromedial view of a stifle of an adult horse with a fracture of the distal aspect of the lateral trochlear ridge (arrow). Note the more distal location of this fracture compared with the typical site of osteochondrosis. Cranioproximal-craniodistal oblique views also demonstrated a slightly displaced avulsion fracture of the medial aspect of the patella.

Avulsion of the origin of peroneus tertius from the lateral extensor fossa of the femur occurs occasionally, usually in foals and rarely in adult horses, resulting in loss of function of the reciprocal apparatus of the hind limb and lameness. One or more fragments may be avulsed, and are usually displaced cranially and distally. The prognosis is poor in adults, and guarded in foals, although removal of the fragments and prolonged rest have been successful in some.

Tibia

Fractures of the tibial tuberosity or fractures of the tibial crest are best seen on a caudolateral-craniomedial oblique view (Figure 7.29). They are frequently the result of direct trauma, e.g. hitting a fixed fence. Care must be taken in horses less than 3 years of age to differentiate fractures from the normal apophyseal-metaphyseal physis (see page 290). The radiographs should be inspected carefully to determine the presence of comminution, and to relate the precise fracture location to the insertion of the patellar ligaments. Conservative treatment of non-displaced fractures may be adequate, although healing may be prolonged. If there is significant separation of the fracture, surgical repair or fragment removal may be required.

Fractures of the medial intercondylar eminence may be associated with damage to the cranial cruciate ligament (see page 312) but not necessarily so. In the absence of cruciate ligament injury, surgical removal of the fragment warrants a fair prognosis.

Fractures of the proximal physis of the tibia are rare.

Figure 7.29 Caudolateral-craniomedial oblique view of the stifle of a 12-year-old Thoroughbred, 7 days after the onset of lameness. There is a slightly displaced avulsion fracture of the tibial tuberosity (arrow). The fracture is traversed by many poorly defined lucent lines. The horse was treated conservatively and made a complete recovery.

Fibula

Fractures of the fibula may give rise to lameness (Figure 7.30). Care should be taken not to interpret normal lucent lines across the fibula as fractures (see pages 292–3). Fracture lines tend to run obliquely across the fibula and are normally associated with both resorption and callus.

Tibia

RADIOGRAPHIC TECHNIQUE

Good quality radiographs of the tibia may be obtained using a portable x-ray machine and either rare earth or high-definition screens with appropriate film. Large cassettes are useful, but it may be necessary to obtain radiographs of the proximal and distal halves of the tibia separately.

These is less muscle surrounding the distal half of the tibia, so exposure factors should be reduced accordingly. A complete assessment requires four views: lateromedial, caudocranial (or craniocaudal), craniolateral-caudomedial oblique, and caudolateral-craniomedial oblique. The caudo-cranial view is best obtained by holding the cassette parallel to the cranial aspect of the bone, and directing the x-ray beam perpendicularly to the

Figure 7.30 Caudocranial view of a stifle of a 10-year-old Thoroughbred. There is a slightly displaced fracture of the head of the fibula. External callus is present (arrow). This fracture became a non-union fracture and required pulsating electromagnetic field treatment to stimulate osseous healing.

cassette, i.e. obliquely downward. This is therefore more correctly termed a caudoproximal-craniodistal oblique view.

NORMAL ANATOMY, VARIATIONS AND INCIDENTAL FINDINGS

The proximal and distal tibia are described on pages 288–99 and in Chapter 6 (pages 249–63). In the caudocranial view the tibial crest is superimposed over the lateral aspect of the proximal tibia, and in an immature horse, the lucent line of the open physis should not be confused with a fracture. Lateral to the tibial crest is an obliquely oriented narrow or broad lucent line, the nutrient canal, which extends through the metaphysis and proximal diaphysis (Figure 7.31). There is a prominent ridge on the medial aspect of the proximal tibial metaphysis and this may be outlined in a caudocranial projection as a smooth irregularity of the medial cortex. Its outline will depend upon the angle of projection.

[321]

Figure 7.31 Caudocranial view of the proximal two-thirds of a normal adult tibia and fibula. Note the oblique broad lucent line in the diaphysis of the tibia which represents the principal nutrient foramen. There is a less well-defined thin lucent line lateral to the superimposed tibial crest – an edge effect. A faint lucent line traverses the fibula. The exposure factors were selected to give optimum penetration of the tibial and fibular diaphyses; thus the proximal tibia is underexposed.

SIGNIFICANT RADIOLOGICAL ABNORMALITIES

Enostosis-like lesions and other focal opacities

Enostosis is defined as a mass of proliferating bone within a bone, and is a general term used synonymously with bone islands in man and panosteitis in the dog. Equine enostosis-like lesions have been characterized radiographically as focal or multifocal intramedullary sclerosis in the diaphyseal region of long bones, near the nutrient foramen, often along the endosteal surface of the bone. In the horse they have been recognized most

[322]
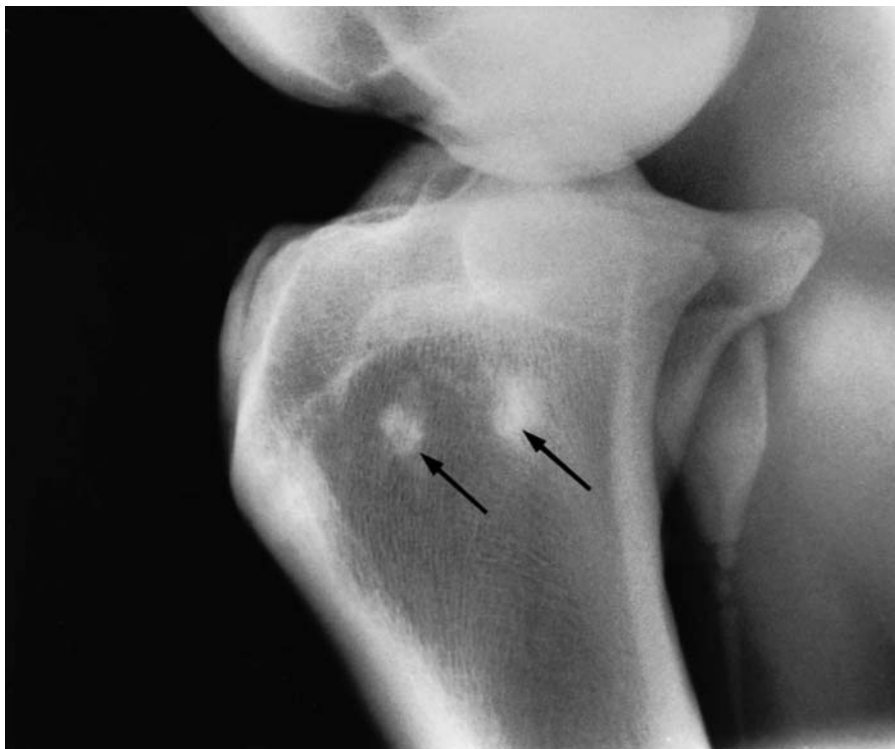
Figure 7.32 Lateromedial view of the proximal tibia of a 6-year-old Welsh Section A pony. There are two irregularly outlined opacities (arrows) in the medulla of the proximal tibia. These are enostosis-like lesions. Note also the separate centres of ossification of the fibula.

commonly in the tibia. Their clinical significance is unclear. They should not be confused with endosteal callus secondary to a fatigue fracture.

Small focal rounded radiopacities (Figure 7.32) have been seen in the proximal tibia. Their aetiology and clinical significance are unknown.

Fractures

Proximal and distal physeal fractures are considered on page 319 and in Chapter 6 (page 282).

Complete diaphyseal fractures of the tibia are usually either mid-shaft oblique fractures or spiral fractures, and result in severe, non-weight-bearing lameness, soft-tissue swelling and crepitus. A complete radiographic examination should be performed if surgical repair is contemplated, in order to determine if the fracture is single or comminuted, and to determine its precise orientation. Surgical repair may be successful in foals, but in older horses the prognosis is very poor.

Incomplete metaphyseal and diaphyseal fractures occur most commonly in young Thoroughbred horses and Standardbreds, and are associated with an acute onset of lameness. Careful palpation of the medial aspect of the tibia, where there is a minimum of overlying soft tissues, may identify a focus of pain. Swelling is often minimal, and clinical diagnosis may be extremely difficult in the acute stage. Radiographic examination in the acute stage may be similarly unrewarding. Repeat radiographic examination after 7–10 days may reveal a fracture line, and slight callus formation may be evident where the fracture passes through the cortex (Figure 7.33). In the Thoroughbred the proximolateral or proximocaudal aspects of the tibia are the most

[323]

common sites for these fractures, which may spiral distally. Fractures also occur on the distal cranial aspect of the tibia in Thoroughbreds. In Standardbreds oblique mid-diaphyseal fractures are most common, with no tendency to spiral. Nuclear scintigraphy may be a more sensitive indicator of trauma to the bone than radiography. Most incomplete fractures heal satisfactorily if treated conservatively, although internal fixation has been used in selected cases to minimize the risk of the fracture becoming complete and possibly compound.

Figure 7.33 Caudocranial view of the proximal tibia of a 2-year-old Thoroughbred colt with lameness of 13 days' duration. There is a healing, non-displaced fatigue (stress) fracture (arrow) from the lateral cortex, extending in a proximal and medial direction towards the medial condyle, with associated callus formation and apparent sclerosis of the proximal tibial metaphysis.

[324]

Adams, W.M. and Thilstead, J.P. (1985) Radiographic appearance of the equine stifle from birth to 6 months. *Vet. Radiol.*, **26**, 126–132

Baker, G., Moustafa, M., Boero, M., Foreman, J. and Wilson, O. (1987) Caudal cruciate ligament function and injury in the horse. *Vet. Rec.*, **121**, 131–321

Bassage, L. and Ross, M. (1998) Enostosis-like lesions in the long bones of 10 horses: scintigraphic and radiographic findings. *Equine Vet. J.*, **30**, 35–42

Colbern, G. and Moore, J. (1984) Surgical management of proximal articular fracture of the patella in a horse. *J. Am. Vet. Med. Ass.*, **185**(5), 543–546

De Moor, A. and Verschooten, F. (1983) Subchondrale Knochenzysten und verwandte Läsionen beim Pferd. In *Orthopädie bei Huf- und Klauentieren* (edited by P.F. Knezevic), Schlutersche, Hannover, West Germany, pp. 244–250

Dik, K.J. and Nemeth, F. (1983) Traumatic patellar fractures in the horse. *Equine Vet. J.*, **15**, 244–247

Dyson, S., Wright, I., Kold, S. and Vatistas, N. (1992) Clinical and radiographic features, treatment and outcome in 15 horses with fracture of the medial aspect of the patella. *Equine Vet. J.*, **24**, 264–268

Embertson, R., Bramlage, L. and Gabel, A. (1986a) Physeal fractures in the horse 2. Management and outcome. *Vet. Surg.*, **15**(3), 230–236

Embertson, R., Bramlage, L., Herring, W. and Gabel, A. (1986b) Physeal fractures in the horse 1. Classification and incidence. *Vet. Surg.*, **15**(3), 223–229

Firth, E.C. (1983) Studies of the morphology of the immature equine radius and metacarpus, and its relationship to chondro-osseous disease. *PhD Thesis*, University of Utrecht

Goulden, B.E. and O'Callaghan, M.K. (1980) Tumoral calcinosis in the horse. *N.Z. Vet. J.*, **27**, 217–219

Haynes, P., Watters, J., Mclure, R. and French, W. (1980) Incomplete tibial fractures in three horses. *J. Am. Vet. Med. Ass.*, **177**, 1143–1145

Hermans, P., Kersjes, A., Van der Mey, G. and Dik, K. (1987) Investigation into the heredity of congenital lateral patellar subluxation in the Shetland pony, *Vet. Qtly.*, **9**(1), 1–8

Hertsch, B. (1980) Die Ossifikationsvorgänge am Kniegelenk beim jungen Pferde. *Zbl. Vet. Med. A*, **27**, 279–289

Howard, R., McIlwraith, C.W. and Trotter, G. (1995) Arthroscopic surgery for sub-chondral cystic lesions of the medial femoral condyle in horses: 41 cases (1988–1991) *J. Am. Vet. Med. Ass.*, **206**, 842–850

Jeffcott, L.B. (1986) Equine radiography: a guide to interpretation. The stifle joint (edited by P.M. Webbon and P.D. Rossdale), *Equine Vet. J.*, Suppl. 4, pp. 15–22

Jeffcott, L.B. and Kold, S.E. (1982) Radiographic examination of the equine stifle. *Equine Vet. J.*, **14**, 25–30

Jeffcott, L.B. and Kold, S.E. (1982) Stifle lameness in the horse; a survey of 86 referred cases. *Equine Vet. J.*, **14**, 31–39

Jeffcott, L.B. and Kold, S.E. (1982) Clinical and radiological aspects of stifle bone cysts in the horse. *Equine Vet. J.*, **14**, 40–46

La Faunae, N., Lerner, D. and O'Brien T. (1971) Bilateral congenital lateral patellar luxation in a foal. *Can. Vet. J.*, **12**, 119–120

McIlwraith, C.W. (1987) *Adams' Lameness in Horses*, 4th edn (edited by T.S. Stashak), Lea and Febiger, Philadelphia, pp. 396–419

McIlwraith, C.W. and Trotter, G.W. (1981) The treatment of equine osteochondrosis. *Proc. Am. Ass. Equine Pract.*, **27**, 161–173

Mackay, V., Trout, W., Meagher, W. and Hornhof, W. (1987) Stress fractures of the humerus, radius and tibia in horses. *Vet. Radiol.*, **28**, 26–31

Mattheson, G. (1984) Die Arthographie des Kniegelenks beim Pferd. *PhD Thesis*, University of Hannover

Morgan, J.P. (1972) *Radiology in Veterinary Orthopaedics*, Lea and Febiger, Philadelphia

Nickels, F.A. and Sande, R. (1982) Radiographic and arthroscopic findings in the equine stifle. *J. Am. Vet. Med. Ass.*, **181**, 918–924

O'Brien, T.R. (1973) Radiology of the equine stifle. *Proc. Am. Ass. Equine Pract.*, **19**, 271–287

O'Brien, T., Baker, T.W. and Koblitz, P. (1986) Stifle radiography; how to perform an examination and interpret the radiographs. *Proc. Am. Ass. Equine Pract.*, **32**, 531–552

Pascoe, J.R., Pool, R.R., Wheat, J.D. and O'Brien, T.R. (1984) Osteochondral defects of the lateral trochlear ridge of the distal femur of the horse. Clinical, radiographic and pathological examination, and results of surgical treatment. *Vet. Surg.*, **13**, 99–110

Prades, M., Grant, B., Turner, T., Nixon, A. and Brown, M. (1989) Injuries to the caudal cruciate ligament and associated structures: summary of clinical, radiographic, arthroscopic and pathological findings. *Equine Vet. J.*, **21**, 354–357

Rejno, S. and Stromberg, B. (1978) Osteochondrosis in the horse II. Pathology. In *Osteochondrosis in Domestic Animals, 1* (edited by S.E. Olsson). *Acta Radiol.*, Suppl. 358, pp. 153–178

Ruggles, A., Moore, R., Bertone, A. *et al.* (1996) Tibial stress fractures in racing Standardbreds: 13 cases (1989–1993). *J. Am. Vet. Med. Ass.*, **209**, 634–637

Samy, M.T. (1977) Osteochondritis dissecans (O.D.) bei Mensch, Hund und Pferd. *Thesis*, University of Hannover

Sanders-Shamis, M., Bukowiecki, C. and Biller, D. (1988) Cruciate and collateral ligament failure in the equine stifle: seven cases. *J. Am. Vet. Med. Ass.*, **193**, 573–576

Schneider, R., Jenson, P. and Moore, R. (1997) Evaluation of cartilage lesions on the medial femoral condyle as a cause of lameness: 11 cases (1988–1994*). J. Am. Vet. Med. Ass.*, **210**, 1649–1652

Shanis, L. and Auer. J. (1985) Complete ulnas and fibulas in a pony. *J. Am. Vet. Med. Ass.*, **186**, 802–804

Smith, B., Auer, J. and Watkins, J. (1990) Surgical repair of tibial tuberosity avulsion fractures in 4 houses. *Vet. Surg.*, **19**, 117–121

Stromberg, B. (1976) Osteochondrosis dissecans of the stifle joint in the horse. A clinical, radiographic and pathological study. *J. Am. Vet. Radiol. Soc.*, **17**, 117–124

Trotter, G.W. and McIlwraith, C.W. (1981) Osteochondritis dissecans and subchondral cystic lesions and their relationship to osteochondrosis in the horse. *Equine Vet. Sci.*, **1**, 157–162

Vaden, M.F. (1977) Anatomical review of the equine stifle. *Auburn Veterinarian*, **34**(1), 12–14

Verschooten, F. and De Moor, A. (1982) Subchondral cystic and related lesions affecting the equine pedal bone and stifle. *Equine Vet. J.*, **14**, 47–54

Chapter 8
The Head

RADIOGRAPHIC TECHNIQUE

The head is a difficult area to radiograph, because it is mobile and high off the ground. A technique is described for obtaining radiographs of all parts of the head, but details on positioning, anatomy and significant findings are given under headings for individual areas. The use of tranquillizers (e.g. xylazine, romifidine or detomidine) may be beneficial, both for their sedative action and also because the head will be lowered, making the examination physically easier.

Equipment

It is quite possible to obtain satisfactory radiographs with portable equipment. Because the head is anatomically complex, large cassettes (35 cm × 43 cm) should be used in order to maintain spatial relationships when evaluating the radiograph. It is often helpful to use both right and left projections in order to take advantage of both image sharpness and magnification in the localization of a lesion.

When obtaining radiographs of the head of a standing horse it is important to recognize that the holder of the horse is potentially close to the primary x-ray beam. It is essential to cone the beam down as much as possible. The horse holder should wear lead gloves. A headcollar and its buckles may be superimposed over an area of interest. Use of a lightweight rope halter may be preferable.

The x-ray cassette must be held by some mechanical device to reduce the radiation hazard to personnel, and because movement with a hand-held cassette is almost inevitable. A plate holder can easily be fixed to a wall, using vertical runners to allow adjustment for height, or it can be hung from a drip stand. This also to some extent restricts lateral movement of the head.

Usually only straight lateral views and slightly oblique views can be obtained in the conscious patient. Occasionally a dorsoventral view of the rostral portion of the head may also be obtained. To obtain diagnostic films with correctly aligned ventrodorsal, oblique and occlusal views of the head of the horse, general anaesthesia is usually required.

A grid may be beneficial in all views of the head, except occlusal views. With portable x-ray machines, it is best to use standard rate rare earth screens and compatible film.

[327]

Positioning

Lateral view

A lateral view is normally obtained with the horse standing. The position for centring and the exposure factors depend on the area to be examined, e.g. the paranasal sinuses or the mandibular cheek teeth. If the horse is in lateral recumbency it is necessary to support the rostral end of the head to keep the midline of the head parallel with the cassette. Care must be taken that the head does not rotate along a rostral–caudal axis (i.e. turn sideways), and some support under the angle of the jaw may be required.

Ventrodorsal view

This view of the skull can only safely be obtained under general anaesthesia, and it is difficult to obtain correctly positioned views. The horse is placed in dorsal recumbency, and the head extended. It is generally not possible to bring the dorsal surface of the head to a horizontal position. For this reason, if the cassette is to be placed against the dorsal surface of the head (the preferred position), and not oblique to the head, a pad may be necessary under the cassette at the rostral end of the head to hold the cassette in position. If the cassette is to be placed far enough caudally to visualize the occipital bone, it may be necessary to raise the poll on a small radiolucent pad, or allow the head to become oblique to the cassette. The x-ray beam is aligned from the ventral aspect, in the midline, and perpendicular to the cassette. It is centred over the point of interest (Figure 8.1). The dorsoventral plane of the skull must be maintained vertical, as any degree of obliquity results in loss of information on the radiograph. It may be helpful to withdraw the endotracheal tube, if one is used, as this can mask abnormalities.

Oblique views

Oblique views are essential for evaluation of teeth roots, some fractures, and for separation of the temporomandibular joints; they are best obtained under general anaesthesia. Risk to personnel is minimized and the angle of obliquity can be more carefully controlled since the head is still. If necessary, repeat views can be obtained after readjustment of the angle. The horse is positioned in lateral recumbency and the x-ray beam is angled relative to the head. Oblique views can be obtained in a standing horse, but it is more difficult to reproduce positioning accurately. Oblique views may either be obtained by angling the x-ray beam and the cassette while keeping the head and neck of the horse straight, or by rotating the horse's head towards a vertical cassette, using a horizontal x-ray beam.

Cranium

This section covers the bony structures at the base of the skull which can all be visualized on one radiograph. It includes the cranial vault and the
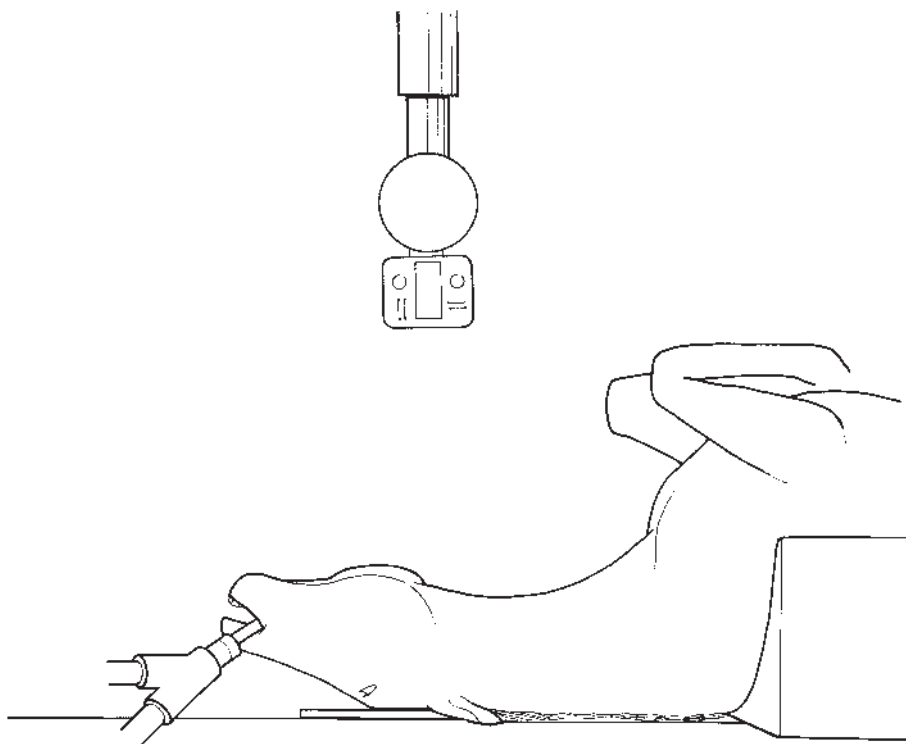
Figure 8.1 Positioning of the horse and cassette to obtain a ventrodorsal view of the head.

bony skull caudal to it. Also included are the ethmoid bones, part of the frontal bones, part of the vertical rami of the mandibles, and the atlas. The general positioning of the horse and equipment has been discussed above.

RADIOGRAPHIC TECHNIQUE

Lateral view

The x-ray beam is centred approximately 5 cm (2 in.) caudal to the orbit, and aligned at right angles to the midline of the head (and the cassette).

Ventrodorsal view

The x-ray beam is centred on the larynx, and aligned at right angles to the cassette.

Oblique views

There are no oblique views recommended as essential for examining this part of the head. They may be needed to examine the temporomandibular joints and the temporohyoid joints, as well as parts of the skull which are superimposed over the vertical ramus of the mandible, or that are masked by the very dense petrous temporal bone. They can also be used to determine on which side of the skull a lesion is present.

[329]

Immature horse

The skull is a complex structure; at birth a number of bones are not fully formed and many sutures are not fused. The ages at which these bones fuse, and sutures are obliterated, are given in Table 8.1.

At birth, the cranium is rather more domed than in the adult, and on a lateral radiograph a 'fontanelle' is evident as a radiolucency between the frontal bones at the rostral third of the cranial vault (Figure 8.2). This closes at 3–4 months. Also evident at birth is the nasofrontal suture, which becomes less evident over the first 6 months of life.

The spheno-occipital suture at the base of the cranium is seen on radiographs until about 5 years of age (Figure 8.2). It becomes a progressively less prominent feature as the foal ages.

Skeletally mature horse

Figures 8.3, page 332 and 8.4, page 334 show normal lateral and dorsoventral views of the cranium of an adult horse.

On lateral radiographs the cranial cavity is evident as a large oval structure. The dorsal aspect has a rather irregular appearance. Ventrally the base of the cranial cavity is overlain by the dense articulations of the mandibles,

Table 8.1 Fusion times for bones of skull

Bone	Ossification centres at birth	Fusion of suture	Obliteration of suture
Occipital			
Parieto-occipital	1. Squamous	2 and 3 by 4 mo	5 yr
Spheno-occipital	2. Lateral	2/3 with 1, 12–24 mo	5 yr
Occipitomastoid	3. Basilar		Aged
Sphenoid			
Spheno-occipital	1. Presphenoid	Uncertain, but as foal	5 yr
	2. Postsphenoid		
Ethmoid			
	1. Perpendicular	Uncertain, soon	
	2. Cribriform	after birth	
Parietal			
Parietal suture	One centre		4 yr
Parieto-occipital			5 yr
Premaxilla			
Left and right	One centre		4th yr
Nasal			
Left and right	One centre		Do not fuse
Nasofrontal			1 yr
Mandible			
Left and right	Two halves		3 mo

Figure 8.2 Lateral view of the cranium of a 1-month-old Thoroughbred. Note the radiolucency in the cortex of the frontal bones, an open fontanelle (open arrow). This normal feature closes by 3–4 months of age. Note also the clearly demarcated spheno-occipital suture line between the basioccipital and basisphenoid bones (black arrow). This is usually closed by approximately 5 years of age.

the coronoid processes and the zygomatic arch, and is difficult to identify. At the caudal aspect of the cranial cavity, the two petrous temporal bones are evident as very opaque, irregular, roughly spherical bony masses.

The nuchal crest is a well-defined structure on the caudal aspect of the squamous part of the occipital bone, the latter having a marked medulla and smooth opaque cortices. New bone formation at the site of attachment of the nuchal ligament may be seen as an incidental abnormality, but may be associated with clinical signs (see page 341). Ventral to the temporal bones the basilar part of the occipital bone also has a marked medulla, extending caudally to form the occipital condyles. The condyles have a smooth oval outline. Slightly oblique radiographs may reveal a small smooth depression in the caudal aspect of the condyles. This is a normal finding.

[331]
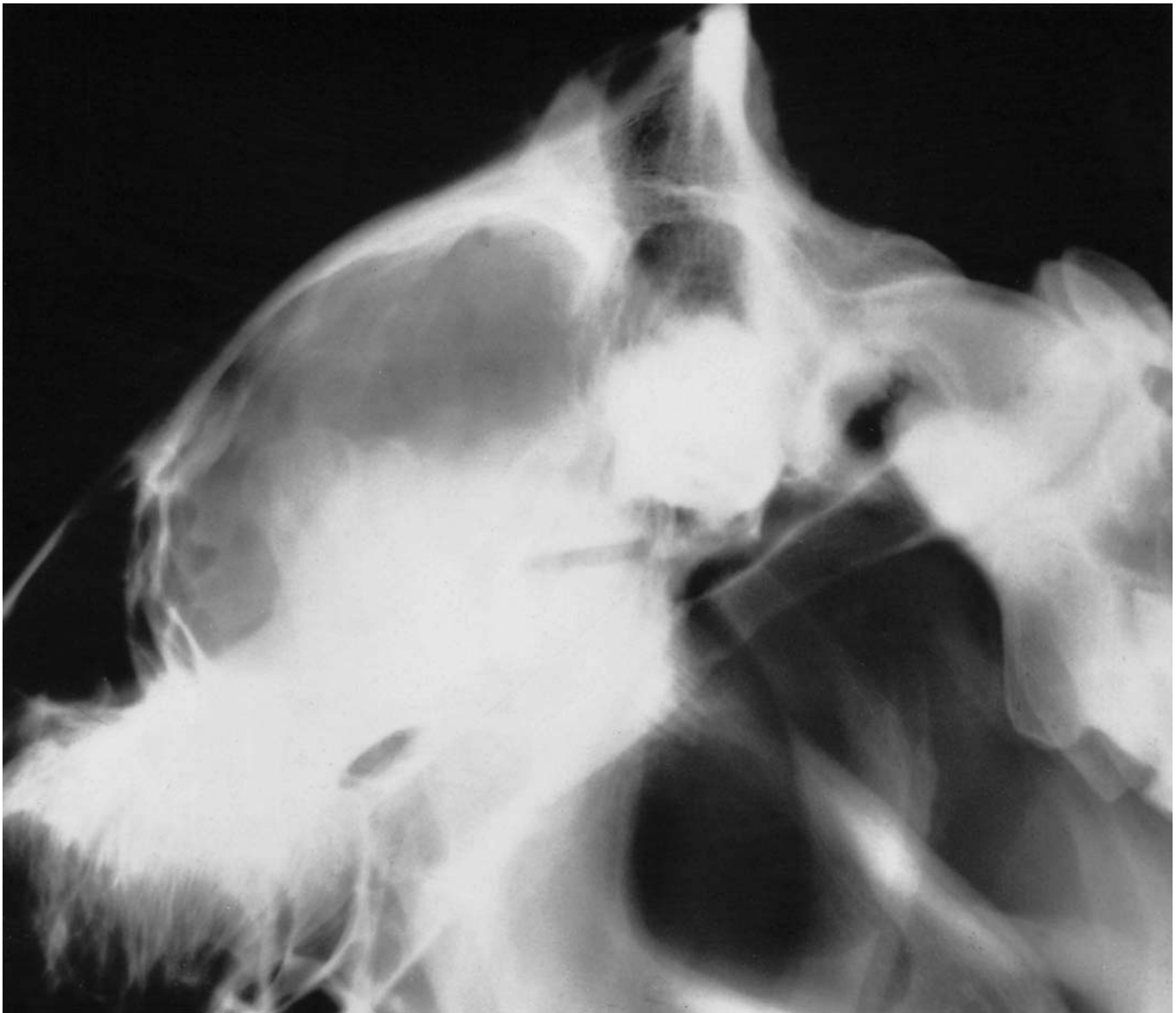
Figure 8.3 Lateral view and diagram of the cranium of a normal mature horse. There is slight rotation of the mandible resulting in separation of the right and left condylar and coronoid processes.

Rostral to the cranial cavity are the ethmoid turbinates which have a 'brush-like' appearance. Their caudal aspect is denser, roughly circular and surrounded by rather more opaque bone, the ethmoid plate. The rostral aspect of the ethmoid bones is superimposed over the maxillary sinus, and additional radiographs may be required for satisfactory visualization.

Dorsal to the ethmoid turbinates is the frontal sinus and overlying frontal bones.

Ventral to the occipital and sphenoid bones are the lucent Eustachian tube diverticula (guttural pouches, see page 384), partly superimposed on the vertical rami of the mandibles. The outline of the trachea, pharynx, larynx and hyoid apparatus may also be seen (see page 384).

[332]

Figure 8.3 *Cont'd* 1 = Coronoid process, 2 = condyloid process, 3 = stylohyoid, 4 = occipital condyle, 5 = ethmoid turbinates, 6 = hypoglossal foramen, 7 = temporomandibular articulation, 8 = petrous temporal bone, 9 = external acoustic meatus, 10 = basioccipital bone, 11 = body of basisphenoid, 12 = rami of mandibles, 13 = zygomatic process of temporal bone, 14 = zygomatic process of frontal bone, 15 = orbit, 16 = pterygoid process, 17 = cranium, 18 = frontal sinus, 19 = nuchal crest, 20 = external occipital protuberance, 21 = internal plate of frontal bone, 22 = caudal fossa of cranium, 23 = temporal process of zygomatic arch, 24 = articular tubercle of temporal bone, 25 = osseous temporal process, 26 = sphenopalatine sinus.

[333]

Figure 8.4 Ventrodorsal view and diagram of the cranium of a normal mature horse.

[334]
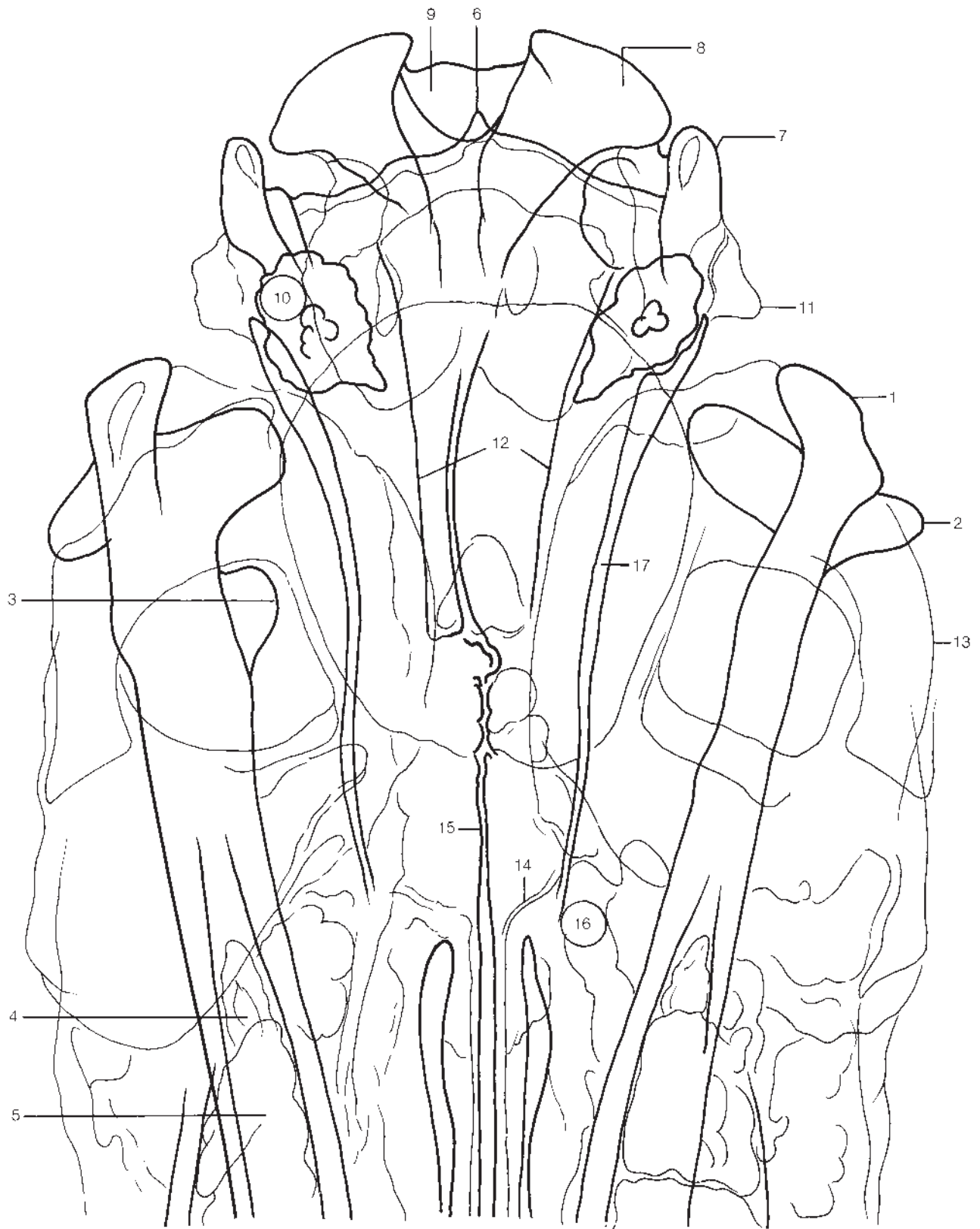
Figure 8.4 *Cont'd* 1 = Caudal border of ramus of mandible, 2 = condylar process of
mandible, 3 = coronoid process of mandible, 4 = third lower molar tooth, 5 = third
upper molar tooth, 6 = nuchal crest, 7 = jugular process, 8 = occipital condyle, 9 =
foramen magnum, 10 = tympanic bulla, 11 = mastoid process, 12 = basilar part of
occipital bone, 13 = zygomatic arch, 14 = rostral border of choanae, 15 = vomer,
16 = ethmoid turbinate region, 17 = stylohyoid.

Dentigerous cysts

Dentigerous cysts (or temporal teratomata) of variable shape and size may be found in many positions (Figure 8.5). They usually have an opaque core, composed of dental tissue, but may have less dense tissue surrounding it. They are frequently found around the base of the ear and in close apposition to the petrous temporal bones.

These cysts are usually only identified clinically after a mass is noted or a discharging sinus has formed. The introduction of a probe or contrast medium into the sinus is helpful in locating them.

Dentigerous cysts can normally be removed surgically, the difficulty of the operation depending upon their position.

Choanal restriction

The choanae form the junction between the nasal and nasopharyngeal airways. Choanal restriction is relatively uncommon. Congenital total obstruction of the choanae may occur unilaterally or bilaterally, due to a bony or membranous septum, resulting in either an abnormal respiratory noise, or severe dyspnoea or death in a neonatal foal. A bony septum may be visible in a ventrodorsal radiographic view. If an obstructive membranous septum is suspected from endoscopic examination, it can be confirmed radiographically by observing blockage of positive radiographic contrast agent placed in the nasal cavities.

Narrowing of the caudal aspect of one or both nasal airways can occur, with or without deviation of the nasal septum, resulting in respiratory noise. Carefully positioned ventrodorsal radiographic views are required to document narrowing, with comparisons made between both the two sides of the head, and horses of similar breed, age and size.

Ethmoid haematoma and diseases of the Eustachian tube diverticulum

See pages 309 and 341.

Bony proliferation at the temporohyoid joint: 'otitis media'

So-called 'otitis media' in the horse may in fact be a misnomer. Clinical signs typical of peripheral vestibular disease and facial nerve paralysis are sometimes associated with specific radiographic changes: there is an irregular increased opacity in the region of the acoustic meatus and articulation of the hyoid and petrous temporal bones, with or without fracture of the stylohyoid bone. Bony proliferation in the region of the temporohyoid joint may be visualized in an oblique projection (Figures 8.6a and 8.6b). The aetiology of these changes is not clear, although it is probably traumatic. Once the changes have developed, normal movement of the stylohyoid bone may result in haemorrhage into the middle and inner ear, giving
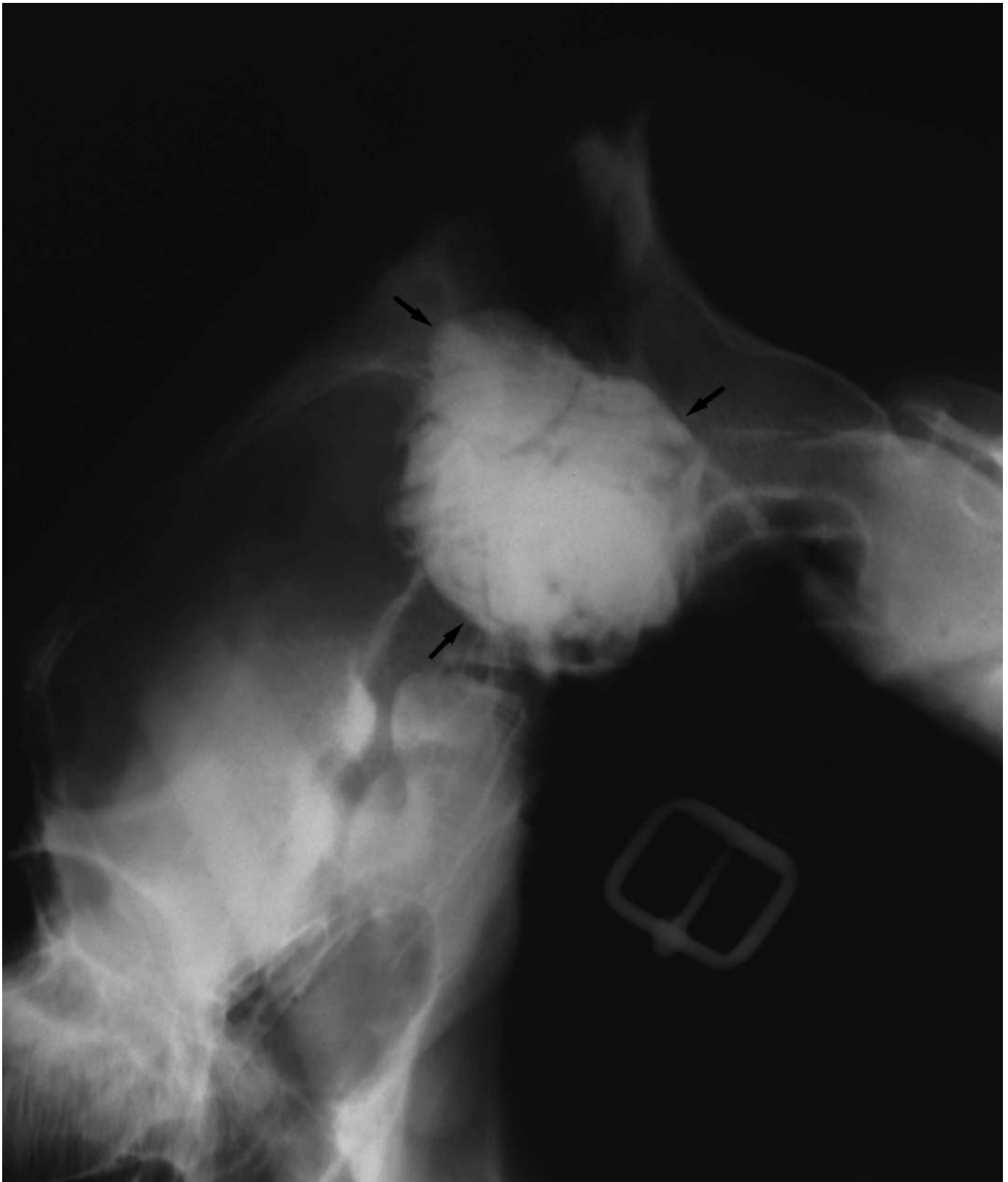
Figure 8.5 Lateral view of the occipital region of a 5-year-old Thoroughbred with a firm swelling distal to the ear. There is a large well-circumscribed opaque mass (arrows) superimposed over the petrous temporal bone. In the dorsal part of the mass, a tooth-like structure can be seen. This mass is a dentigerous cyst.

[337]

Figure 8.6(a) Lateral view of the caudal aspect of the head of an 8-year-old Warmblood with sudden onset of left-sided facial nerve paralysis, peripheral vestibular signs and keratoconjunctivitis sica. There is a poorly defined area of increased opacity (arrows) in the region of the temporohyoid joint. See also Figure 8.6(b).

Figure 8.6(b) Oblique view of the caudal aspect of the head, separating the two hyoid bones and the rami of the mandibles. The opaque mass, new bone formation (white arrows), is much more easily seen than in the lateral view (compare with Figure 8.6a), and should be differentiated from the more dorsal acoustic meatus (black arrow). A piece of the stylohyoid bones was removed surgically. The bony mass regressed considerably, and the horse made a complete functional recovery.

[339]

recurrence or exacerbation of clinical signs. Surgical resection of part of the hyoid may give resolution of clinical signs and regression of the radiological changes.

Nasal polyps

Nasal polyps are soft-tissue masses which may partially occlude the airway and result in abnormal respiratory noise and/or nasal discharge. They appear radiographically as smoothly marginated soft-tissue opacities (Figure 8.7). They should be distinguished from soft-tissue opacities within a sinus.

Hydrocephalus

Hydrocephalus in the horse is usually a clinical diagnosis, but may be confirmed by radiography. The cranial vault has a domed appearance, the

Figure 8.7 Lateral radiograph of the head of a 4-year-old horse with a 10-week history of a bilateral nasal discharge. Within the nasal cavity are several (at least three) well-circumscribed soft-tissue opacities (arrows). These are nasal polyps. The paranasal sinuses are normal.

Figure 8.8 Lateral view of the caudal aspect of the head of an 8-year-old show jumper with a history of reluctance to accept and go forward to the bit and stiffness through the back. There is entheseophyte formation on the caudal aspect of the occiput at the site of insertion of the nuchal ligament.

overlying bones being thin. The cranial cavity has a homogeneous appearance. This condition may be more common in the miniature breeds.

Entheseophyte formation on the occiput associated with the nuchal ligament

New bone formation may occur in the region of insertion of the nuchal ligament on the occiput (Figure 8.8), also extending slightly dorsal and ventral to the site of insertion. This may be seen as an incidental finding, most commonly in Warmbloods. Clinically affected horses tend to resist the reins, find difficulty in flexion at the poll and may rear or head shake. The significance of the bony abnormality is determined by local infiltration of local anaesthetic solution. Treatment by local infiltration of corticosteroids and local anaesthetic solution, combined with modification of the training programme has variable results.

Fractures

Frontal bone

Depression fractures of the frontal bone are relatively common after trauma to the head. They can be seen on lateral or slightly oblique lateral views, best visualized when exposed for the sinuses (page 334). They are evident, in an acute case, as an area of bone pushed ventral relative to the remainder of the dorsal surface of the face. It is important to check for possible sequestra in more chronic cases. These cases should also be assessed for concurrent sinusitis, and possible involvement of the bony orbit and lacrimal duct.

If treated conservatively, there is generally good functional healing, provided that sequestra do not form. It is possible to raise these fractures surgically to give more aesthetically pleasing healing.

Nasofrontal suture separation

This is a relatively common finding in young horses (Figures 8.9a and 8.9b). There is frequently no history of trauma, but a hard swelling forms across the dorsal aspect of the head, level with the rostral aspect of the orbits. On radiographs this is apparent on lateral views as a radiopaque protuberance of callus forming in the region of the nasofrontal suture. Typically the bone shows increased opacity either side of the suture, and initially a radiolucent suture line may be evident traversing the new bone. There may be concurrent involvement of the nasolacrimal suture, and occasionally bleeding into the maxillary sinus is evident as a fluid line within the sinus. This lesion is of little clinical significance, but normally results in permanent disfiguration of the head.

Occipitosphenoid suture separation

This fracture usually occurs after direct trauma, typically a horse falling over backwards and hitting its head on the ground. It is most commonly seen in young horses, when the suture is not closed, and radiological confirmation of separation may therefore be very difficult. It is generally best visualized on good lateral and oblique views.

Clinical signs may include blindness, inco-ordination and slight nasal haemorrhage. The condition carries a very guarded prognosis, depending on the degree of clinical signs seen.

Avulsion fracture of the nuchal crest

This is an unusual finding. It is associated with trauma, and results in stiffness of the neck. A small radiopaque fragment may be seen caudal to the nuchal crest on lateral radiographs.

A hopeful prognosis can be given with conservative treatment.

[342]
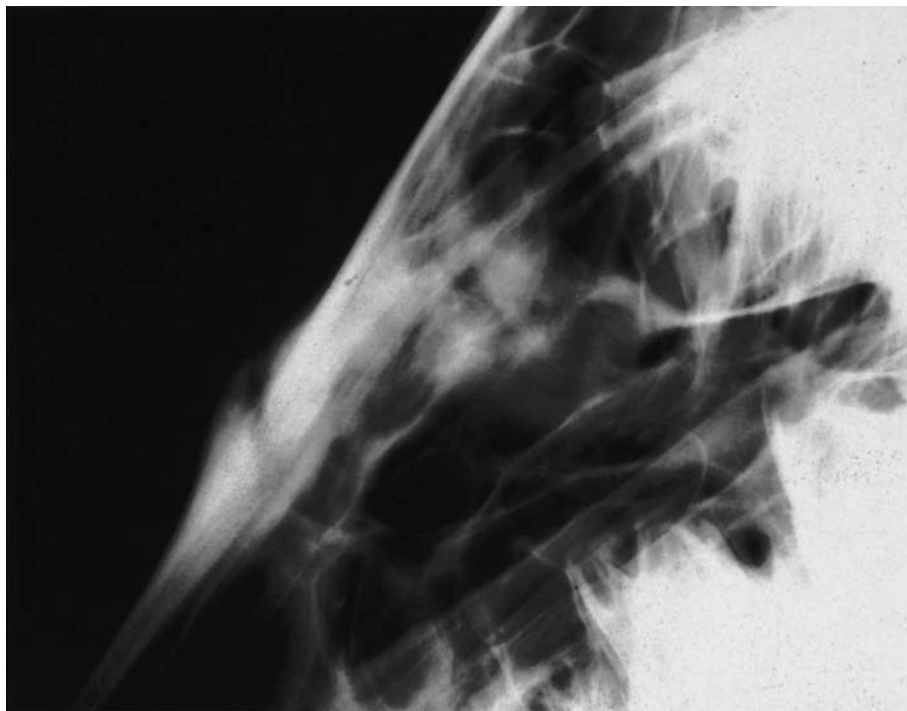
Figure 8.9(a) Oblique view of the nasofrontal region of a 6-year-old Thoroughbred. The history is of the development, over the past 2 weeks, of a firm swelling on the dorsal midline of the head, distal to the eyes. There is separation at the nasofrontal suture and associated incomplete bridging callus. The underlying sinus is of normal lucency.
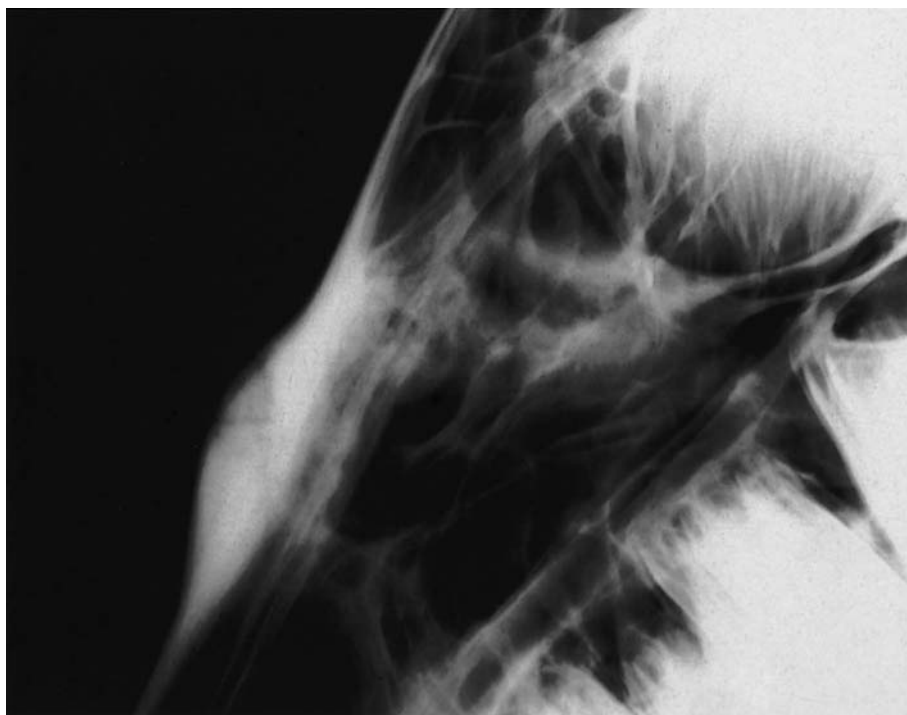
Figure 8.9(b) Oblique view of the nasofrontal region of the same horse as in Figure 8.9a, 6 weeks later. The callus is much more extensive and has a relatively smooth outline.

Fractures involving the orbit

Fractures involving the zygomatic arch occur rarely. They are generally difficult to visualize on radiographs, but are most easily seen on lateral views of the cranial region. Slight obliquity of the view, to separate the two arches, may be helpful. Fractures may be simple, or comminuted, with varying degrees of displacement. Although the prognosis for simple undisplaced fractures is quite good, displacement and comminution, causing remodelling of the orbit, often causes chronic ophthalmitis. Surgery to reduce displacement and remove sequestra may therefore be required.

Fracture of the mandible

Fractures of the vertical ramus of the mandible are usually visualized on lateral or slightly oblique lateral views. As the ramus of the mandible is relatively thin, they may be difficult to delineate, and require several different exposures for complete visualization. The prognosis varies depending on the configuration of the fracture and the age of the horse (see page 381).

Frontal and maxillary sinuses and maxilla

RADIOGRAPHIC TECHNIQUE

Lateral view

The x-ray beam is centred midway between the orbit and the lateral opening of the infraorbital canal, about 2.5 cm (1 in.) dorsal to the facial crest. It is aligned at right angles to the midline of the head and the cassette.

Ventrodorsal view

The x-ray beam is centred in the midline between the horizontal rami of the mandible, approximately one-third of the distance from the caudal aspect of the rami towards the rostral aspect of the mandible. It is aligned at right angles to the cassette.

Dorsoventral views can be obtained in a well sedated horse, but excellent collimation of the x-ray beam is essential to ensure safety of personnel. The x-ray tube is positioned in front of the head, with the beam angled obliquely downwards, perpendicular to the cassette. The cassette is held ventral to the mandible, and parallel to it. It is not possible to evaluate the more caudal structures of the head using this technique, and it is more difficult to obtain true dorsoventral views without some degree of obliquity.

Oblique views

There are no oblique views recommended as essential for examining the sinuses themselves, although they may be helpful to separate overlying

images. They are frequently required to determine the primary cause of sinusitis, especially to evaluate the teeth roots.

NORMAL ANATOMY, VARIATIONS AND INCIDENTAL FINDINGS

The lateral view allows visualization of lesions involving the frontal sinus, maxillary sinus and nasal cavity (Figure 8.10).

The frontal sinus appears triangular on lateral radiographs, and is seen dorsal to the turbinate bones and rostral to the cranial vault. There are normally two distinct septa positioned in a dorsoventral direction across the sinus.

The maxillary sinus is immediately dorsal to the cheek teeth, which form the ventral border of the sinus. The appearance of this varies with the stage of development of the teeth. The sinus extends from the orbit caudally to include the last three or four cheek teeth rostrally (depending partly on the age of the animal). The dorsal border of the sinus is difficult to visualize on radiographs, but runs parallel to the facial crest, along a line roughly level with the infraorbital foramen. The sinus is divided into rostral and caudal parts by a septum lying obliquely across the centre of the sinus.

Medial and dorsal to the maxillary sinus are the nasal cavities.

On ventrodorsal views, the two horizontal rami of the mandible and the cheek teeth are the dominant features. The narrow nasal septum runs a straight course in the midline, between the two rami. The nasal cavity and turbinates are located on either side of the septum. Lateral to the mandible and cheek teeth, a small portion of the maxillary sinus can be seen.

SIGNIFICANT FINDINGS

Sinusitis

Sinusitis in the maxillary or frontal sinuses will usually give rise to increased opacity of the sinus on lateral radiographs. The radiograph must be correctly exposed, otherwise this increase in opacity may be missed. On standing radiographs, one or more horizontal fluid lines are generally visible in the sinuses (Figure 8.11a). When viewing the radiographs they should be positioned at the same angle as when exposed, if the fluid lines are to be horizontal. The radiograph should be carefully evaluated to determine if there is more than one fluid line, reflecting involvement of more than one sinus cavity. The fluid is generally of uniform opacity, unless there is inspissated pus, when it may be heterogeneous. The increased opacity should be distinguished from other causes such as a maxillary cyst or dental tumour (see page 371).

It should be remembered that sinusitis in the horse is frequently secondary to other conditions, e.g. tooth root abscess, ethmoid haematoma, maxillary sinus cysts, or fracture. The radiographs should be carefully examined for possible causative conditions. It may be necessary to drain the sinus and obtain further radiographs before the primary cause can be identified.
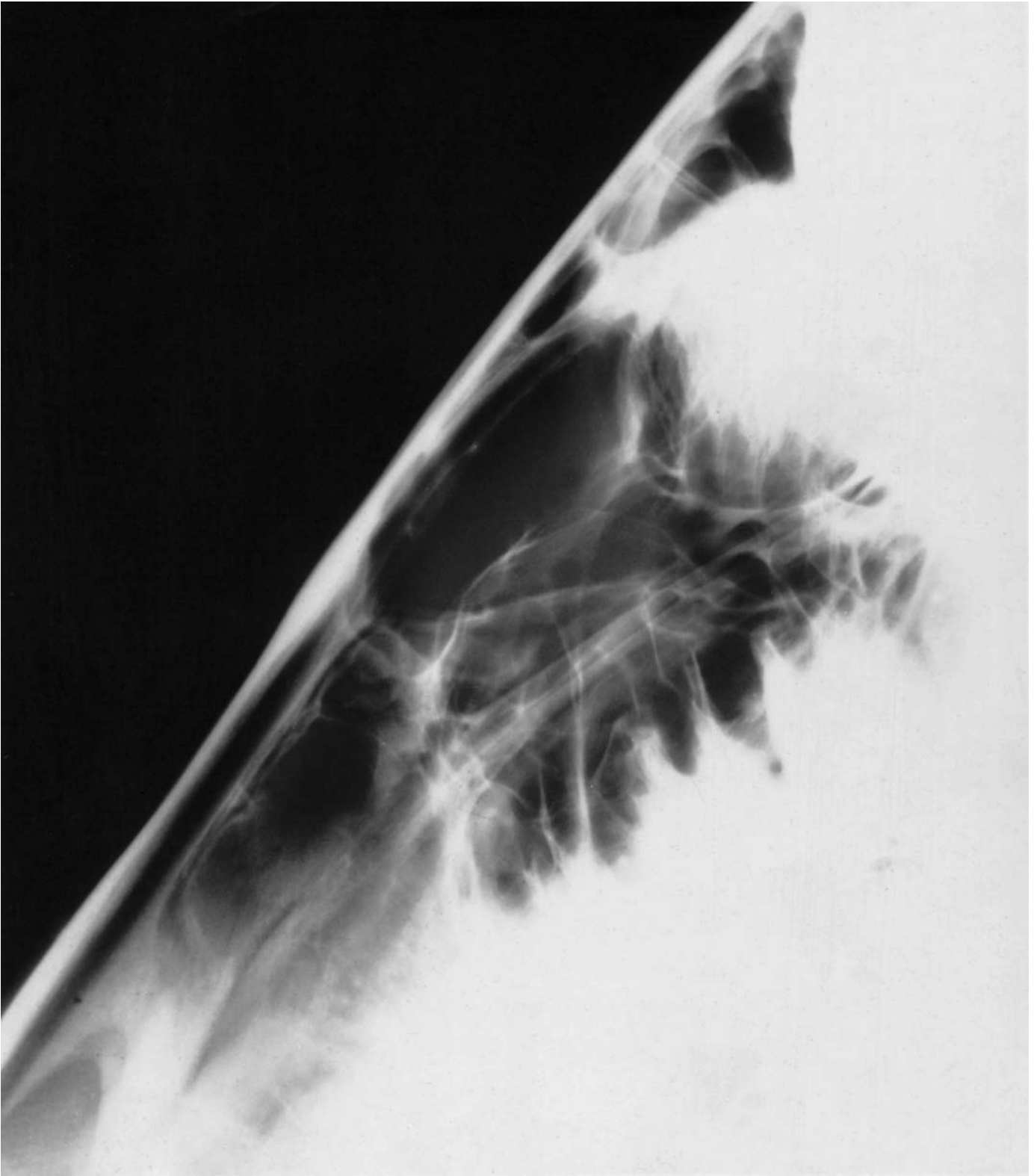
Figure 8.10 Lateral view and diagram of the nasofrontal region of a normal adult horse, exposed to evaluate the paranasal sinuses rather than the tooth roots.

[346]
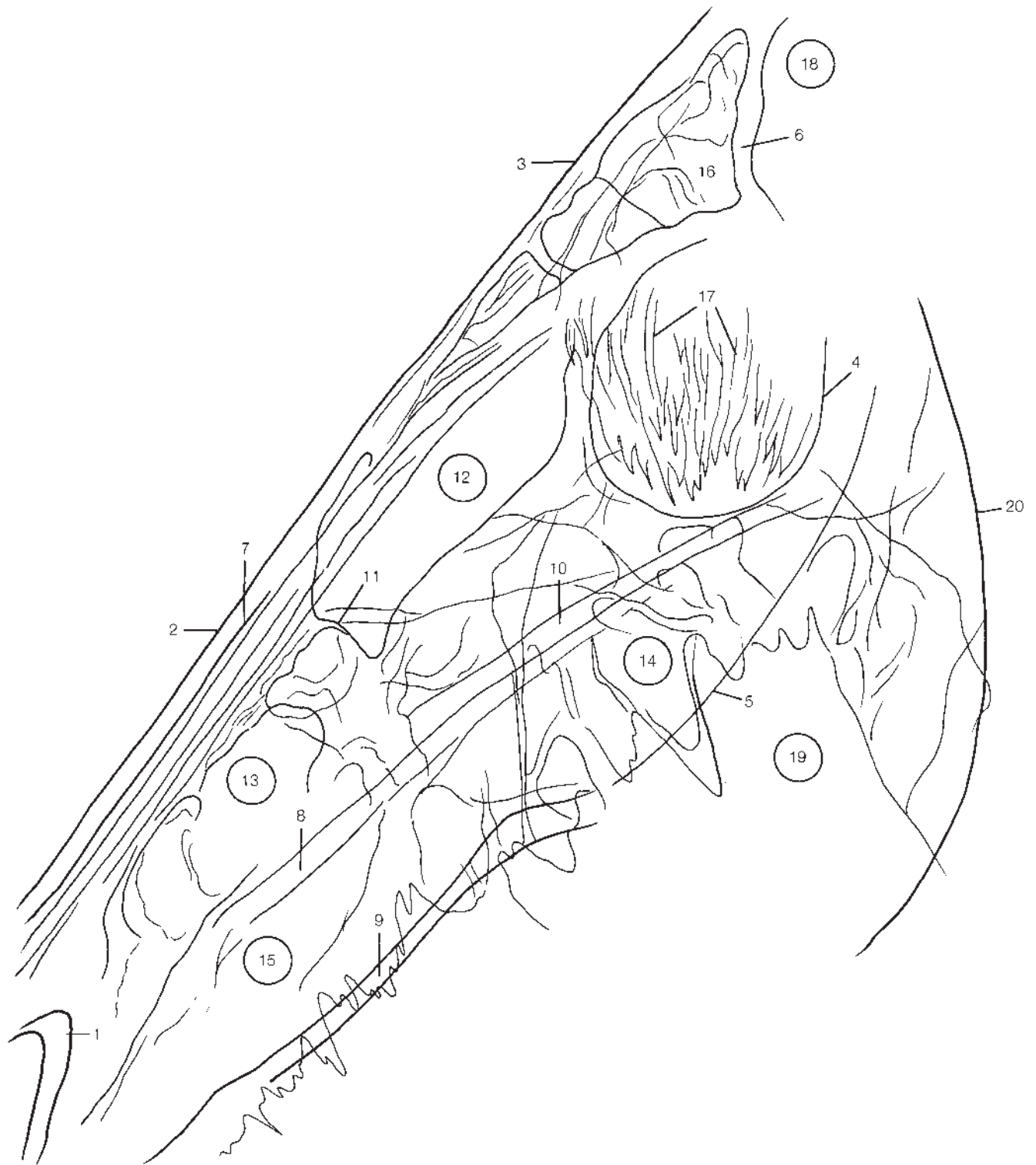
Figure 8.10 *Cont'd* 1 = Nasomaxillary notch, 2 = nasal bone, 3 = frontal bone, 4 = orbit, 5 = facial crest, 6 = internal plate of frontal bone, 7 = dorsal nasal meatus, 8 = middle nasal meatus, 9 = ventral nasal meatus, 10 = infraorbital canal, 11 = conchal sinus septum, 12 = conchofrontal sinus, 13 = recess of dorsal nasal concha, 14 = sinus of ventral nasal concha, 15 = recess of ventral nasal concha, 16 = frontal sinus, 17 = ethmoid turbinates, 18 = cranial cavity, 19 = third upper molar tooth, 20 = cranial aspect of ramus of mandible.

[347]
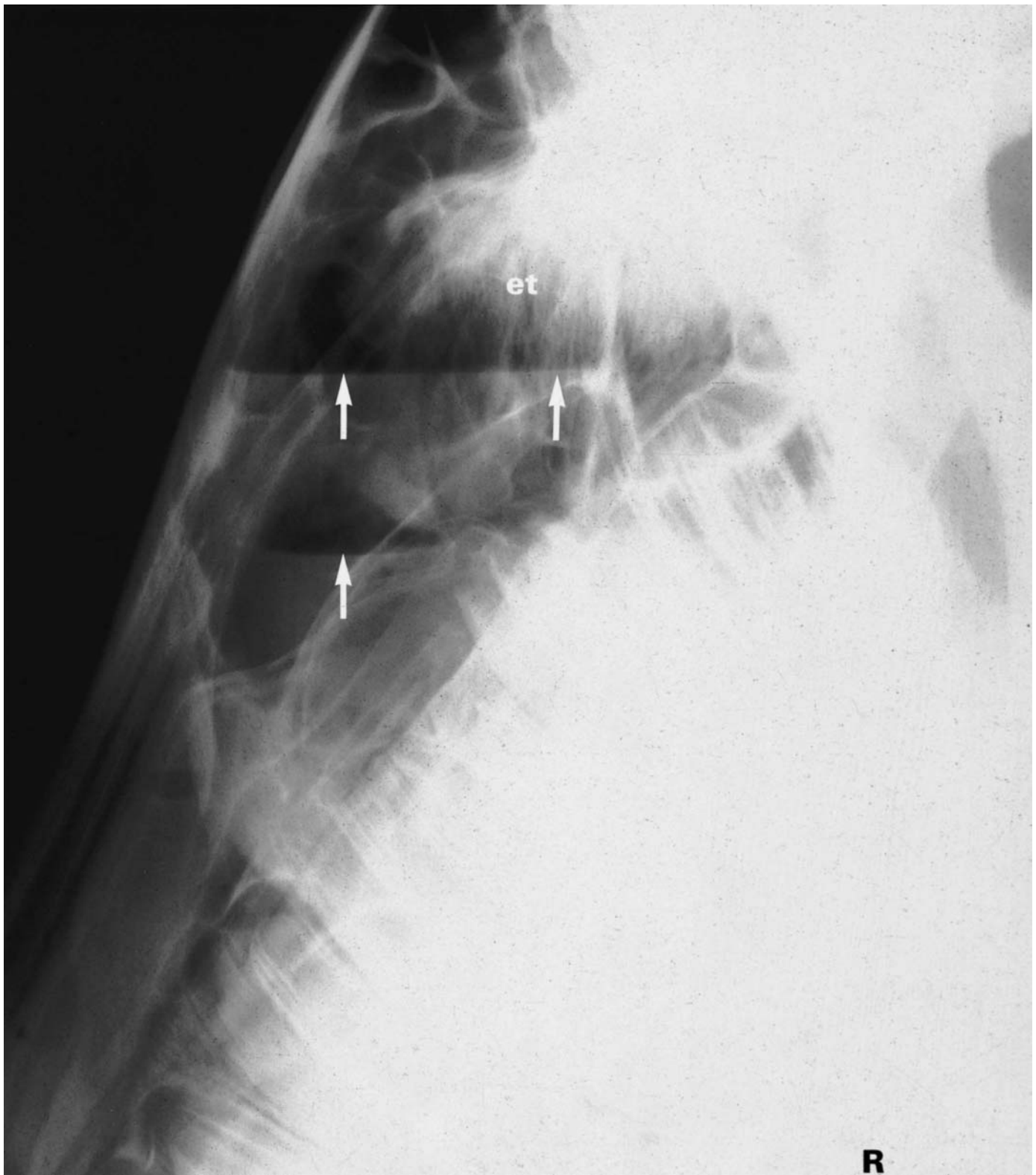
Figure 8.11(a) Right lateral projection of the head of a 2-year-old Thoroughbred with a history of sinusitis for approximately 12 months. There are fluid lines (arrows) in both the frontal and maxillary sinuses. In the right lateral projection the fluid lines were smaller and sharper than in the left lateral projection, indicating right-sided involvement. Note the position of the proximal fluid line relative to the ethmoid turbinates (et). See also Figure 8.11(b).

[348]
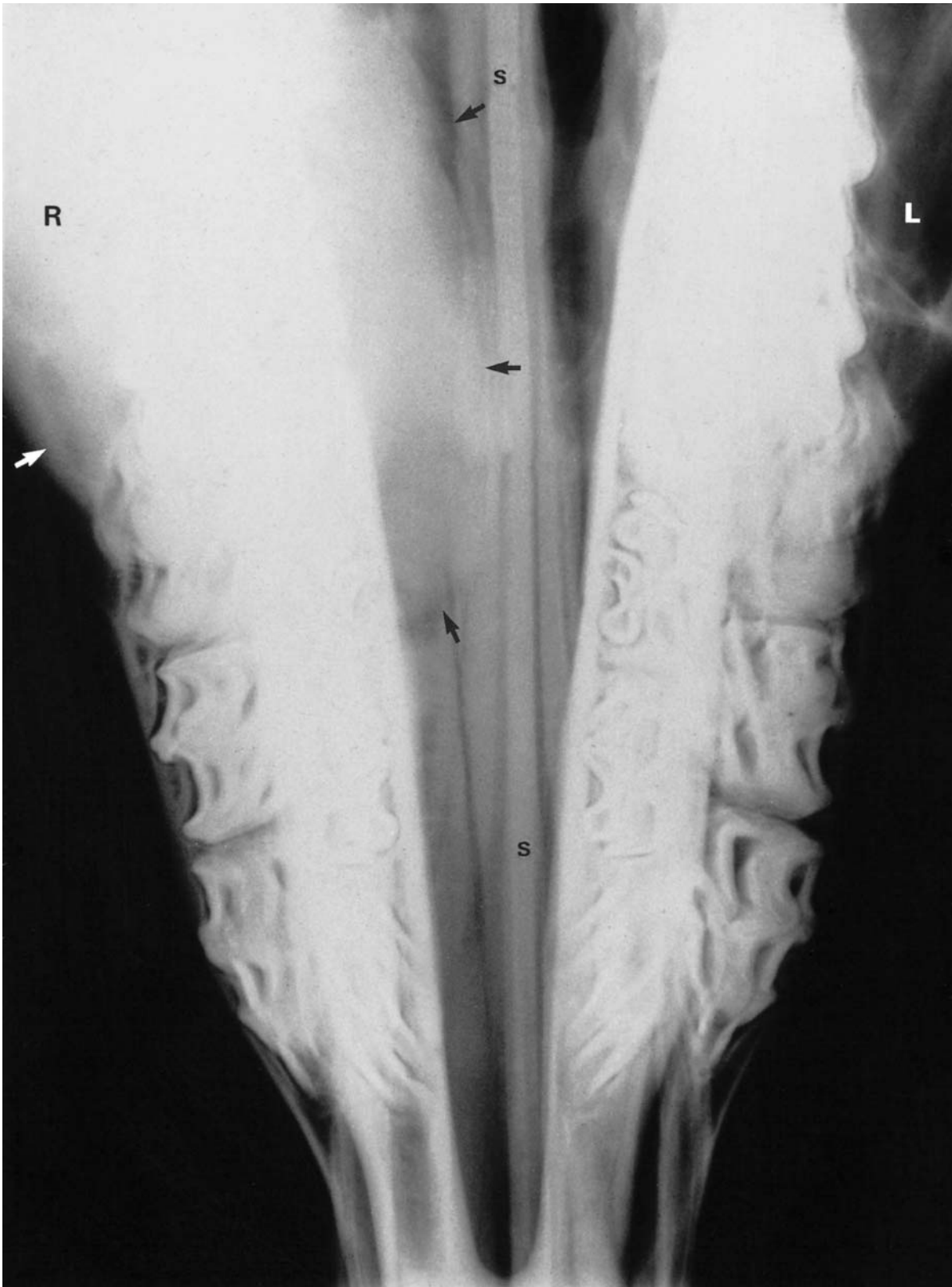
Figure 8.11(b) Ventrodorsal view of the same horse as Figure 8.11(a), confirming that the right side is involved. Note the diffuse soft-tissue opacity (arrows) in the right maxillary sinus (R) and the relatively more lucent left maxillary sinus (L). There is minimal deviation of the nasal septum (s).

Clinically, sinusitis is usually associated with a unilateral nasal discharge, frequently of a purulent and malodorous nature.

Although some cases of sinusitis will respond to treatment with antibiotics, surgical drainage and correction of the underlying cause is often required.

Submucosal cyst

A submucosal cyst may result in deformity of the facial bones and new bone production. A soft-tissue mass is identifiable radiographically (Figure 8.12). Clinically the facial deformity should be differentiated from that due to a previous fracture, a sinus cyst or a tumour. The soft-tissue opacity should be distinguished from an ethmoid haematoma, sinusitis, or other causes of sinus opacity. In contrast to sinusitis a horizontal fluid line cannot usually be identified.

Maxillary sinus cyst

This condition is not uncommon, but can be difficult to diagnose with certainty, especially in the early stages. It usually occurs in young horses (up to 5 years old), but is occasionally seen in older animals. The presenting signs are usually facial swelling, respiratory noise, or unilateral nasal discharge. A secretory lining is present in the sinus and this is fluid filled. In the early stages this may pass undetected on lateral radiographs, causing only a slight increase in the opacity of the sinus. The cyst may be loculated, facilitating differentiation from sinusitis, and may completely fill the sinus. The cyst may gradually enlarge, and may cause distortion of the surrounding bone. Usually the medial wall of the sinus is gradually pushed mesially, and this may cause gradual progressive obstruction of the nasal passages and obstruction of the airway – this can be seen on ventrodorsal views (Figure 8.13, page 352). This view will also allow the opacity of the parts of the sinus seen lateral to the mandibular rami to be compared. In more advanced cases, there may also be dorsolateral displacement of the maxilla, causing a gradual 'swelling' of the face of the horse. Treatment is by surgical resection of the cyst, including its lining.

Maxillary cysts

Multiple cystic lesions of the maxilla, usually involving the tooth roots, sometimes occur in young foals. Their origin is uncertain.

This lesion may be seen on lateromedial views, but ventrodorsal views are also useful to visualize the extent of involvement of the maxilla hidden radiographically by the superimposition of the very opaque outline of the teeth. Multiple radiolucent, sometimes lobulate cystic lesions are present, often with enlargement in size of the maxilla. In extensive cases, there may be little bone surrounding the cysts.

Treatment is by surgical drainage, but the prognosis is guarded, depending on the extent of the lesion.
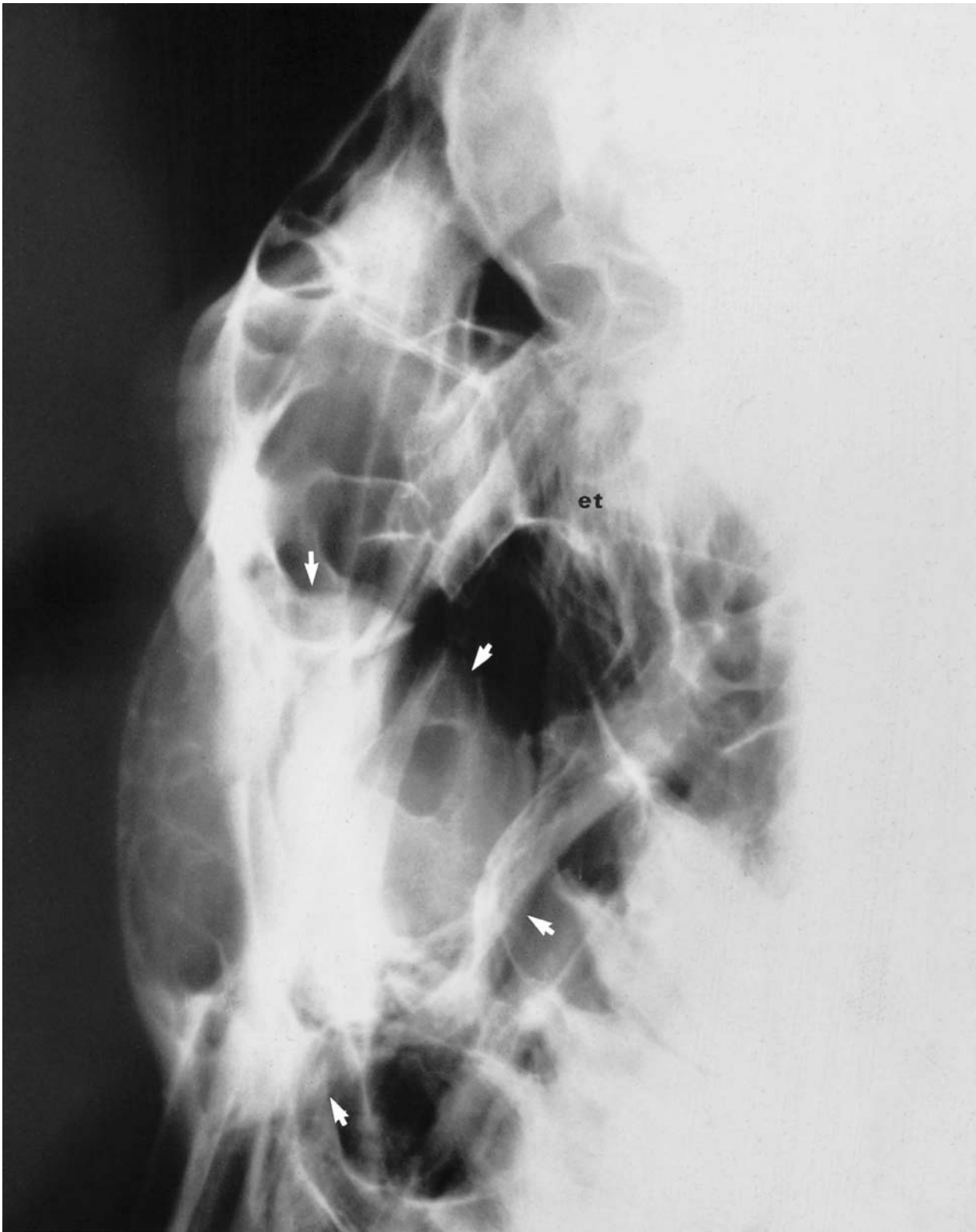
Figure 8.12 Right oblique view of the frontal area of a 10-year-old Quarterhorse with a history of a slowly progressive deformity of the facial bones on the right side. There is a well-circumscribed soft-tissue mass (arrows) rostral to the ethmoid turbinates (et), extending dorsally and deforming the nasal and maxillary bones. This soft-tissue mass is a submucosal cyst. The sinuses appear otherwise normal.

Figure 8.13 Ventrodorsal view of the head of a yearling Thoroughbred with stertorous breathing and an intermittent right sided nasal discharge. There is a large, well-circumscribed radiopacity in the right maxillary sinus (arrows), axial to the molar teeth. Note the deviation of the nasal septum to the left. There is also an ill-defined opacity (open arrows) abaxial to the molar teeth (compare with the left side). Diagnosis: maxillary sinus cyst.

[352]

Ethmoid haematoma

This condition is usually characterized clinically by intermittent nasal haemorrhage, usually unilateral. Strictly speaking it is a condition of the nasal chamber, and will only affect the sinuses in advanced cases. It is most easily diagnosed endoscopically, but it may be visualized on radiographs, and these may help ascertain the size and involvement of the lesion (Figures 8.14a and 8.14b). The lesion is of soft tissues and is therefore only seen as a slight increase in radiopacity. In early cases the lesion is seen on lateral views overlying the maxillary sinus immediately rostral to the ethmoid bone. It may be more easily seen on ventrodorsal views, where the opacity of the two sides of the head can be compared. In advanced cases there may be remodelling of the turbinate bones and nasal septum. The lesion may also invade the sinuses in some cases.

The condition is treated by surgical resection of the lesion, and carries a fair to guarded prognosis. More recently, treatment by repeated injection of formaldehyde into the lesion has shown promising results.

Other causes of opacity of the maxillary sinus

The most common cause of opacity of the maxillary sinus is undoubtedly sinusitis. Frequently this is associated with tooth disease. In some cases, however, the tooth root may become surrounded by fibrous tissue, and this has been seen to extend into the maxillary sinus and may completely fill the sinus on one side. In rare cases this fibrous reaction may mineralize, giving discrete areas of radiopaque material within the sinus (Figure 8.15, page 356). These changes can be seen on lateral radiographs, but ventrodorsal views are needed to determine the extent of the lesion.

These lesions require surgical treatment.

Although neoplasia is rare in the horse, tumours are more common in the head than elsewhere in the horse. Squamous cell carcinoma, osteosarcoma (Figure 8.16, page 357) and melanoma may occur in this region, and have the characteristic appearance of neoplasia, as described in Chapter 1 (page 14).

Adamantinomas and ameloblastic odontomas are tumours derived from the enamel organ (the embryological precursor of a tooth), and are seen in young horses. Radiographically they appear as lesions of the maxilla or mandible, and have a variable appearance. An adamantinoma remains as primarily soft tissue, and has a septate configuration, resulting in a 'foamy' appearance. An odontoma is derived from dental residues, and tends to have a more opaque tooth-like structure (Figures 8.17a and 8.17b, pages 358 and 359).

Osteomas are benign, smoothly outlined, opaque tumours. They may become very large before being detected, as they grow slowly and cause few clinical signs. They have been associated with head shaking.

Adenocarcinomas occur in the frontal sinus and the nasal cavity. They occur in older animals and are very destructive. They are rapid growing and tend to be ill-defined. There is usually an associated unilateral nasal discharge.

[353]

Figure 8.14(a) A left lateral view of the nasofrontal region of a yearling. There is a soft-tissue opacity (arrows) dorsal to the most caudal upper cheek tooth, adjacent to, and summating with, the ethmoid turbinates. The mass is an ethmoid haematoma (see also Figure 8.14b). Note that this projection is slightly oblique: the cheek teeth are at different levels.

[354]

Figure 8.14(b) Ventrodorsal view of the same horse as in Figure 8.14(a) demonstrating much more clearly the soft-tissue opacity (arrows) axial to the most caudal left cheek tooth. There is slight deviation of the nasal septum towards the right (R). The mass is an ethmoid haematoma.

Figure 8.15 Right lateral oblique view of the maxillary region of a 10-year-old Standardbred. The horse had previously had the bulk of the fourth upper right cheek tooth removed, but a piece remains. There is periapical lysis (rarefaction) around the caudal root of the third upper cheek tooth. Dorsal to the first upper right cheek tooth is an area of dystrophic mineralization within the conchal sinus. The rostral maxillary sinus and the ventral conchal sinus communicate via the conchomaxillary opening. Such dystrophic mineralization ('coral') is invariably the result of chronic infection (usually dental in origin).

Increased lucency of the maxillary sinus

Increased lucency of the bone surrounding the maxillary sinus has been seen associated with neoplasia (see page 353) and maxillary cysts (see page 350).

Cyst-like lesions on the incisive bone (premaxilla)

Cyst-like lesions occasionally develop in the incisive bone (premaxilla). These are expansile lesions which usually result in distortion of the facial contour and thinning of the overlying cortex (Figures 8.18a and 8.18b, pages 360 and 361).

[356]

Figure 8.16 Lateral view of the nasofrontal region of an aged Thoroughbred with facial swelling. There is a large opaque mass occupying the region of the frontal and maxillary sinuses and distorting the frontal and nasal bones. The mass was identified as an osteosarcoma at post-mortem examination.

Teeth and mandible

RADIOGRAPHIC TECHNIQUE

Mandible

The views described below for the teeth, and on page 329 for the cranium, are also used to visualize the mandible. The exposure factors required for teeth and bone, however, are very different, and several radiographs may need to be obtained of each area to acquire all the available information.

Cheek teeth

Lateral view

Satisfactory lateral views can usually be obtained with the horse standing. The x-ray beam is centred at the point where the first molars (fourth cheek
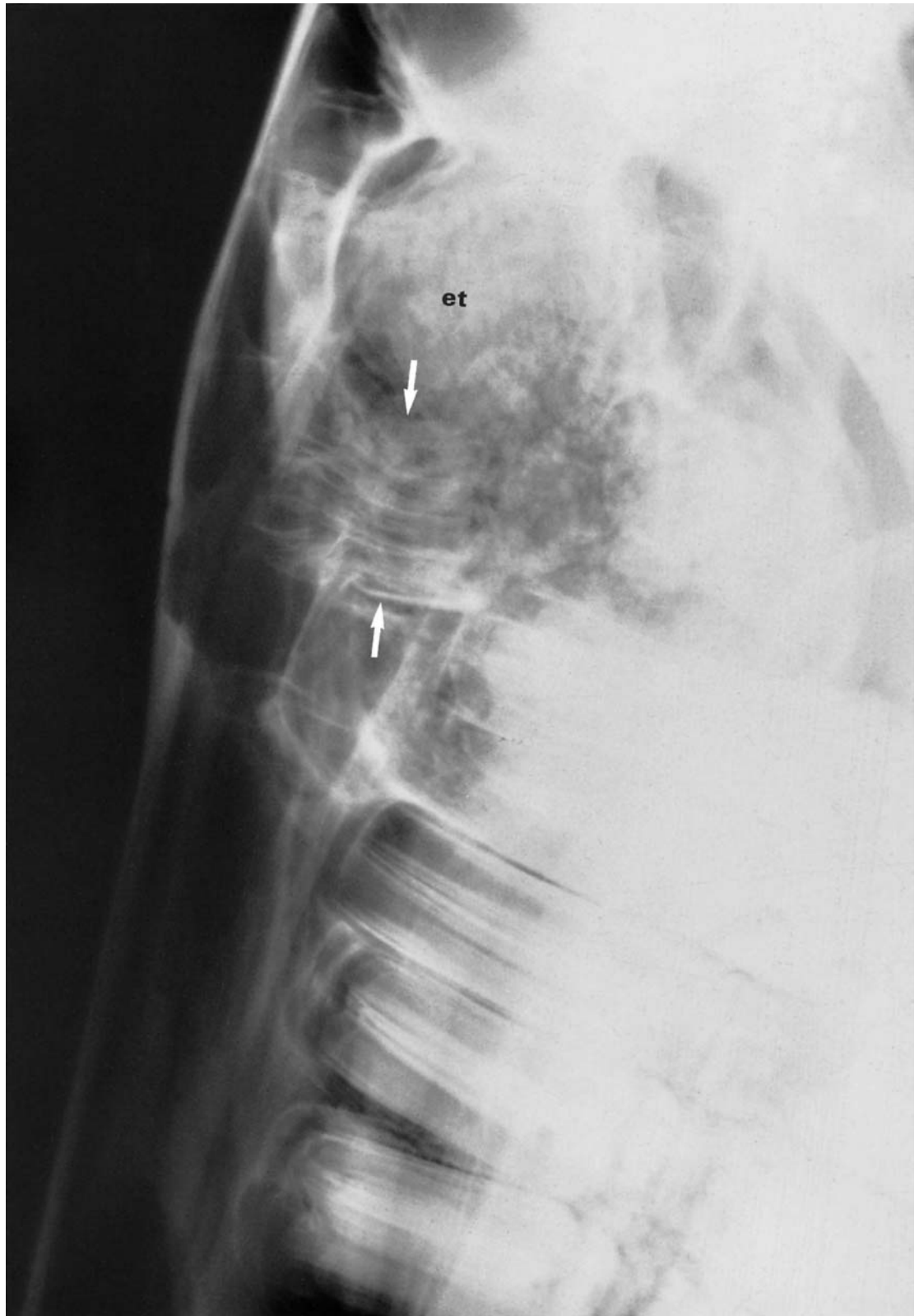
Figure 8.17(a) Slightly oblique left lateral view of the nasofrontal region of a 3-year-old Thoroughbred with a recent history of swelling below the left eye, left-sided mucoid nasal discharge and dyspnoea. There is a large mass of irregular opacity in the region of the most caudal upper cheek tooth. Within the mass are several opacities resembling teeth (arrows); et = ethmoid turbinates. See also Figure 8.17(b).

[358]
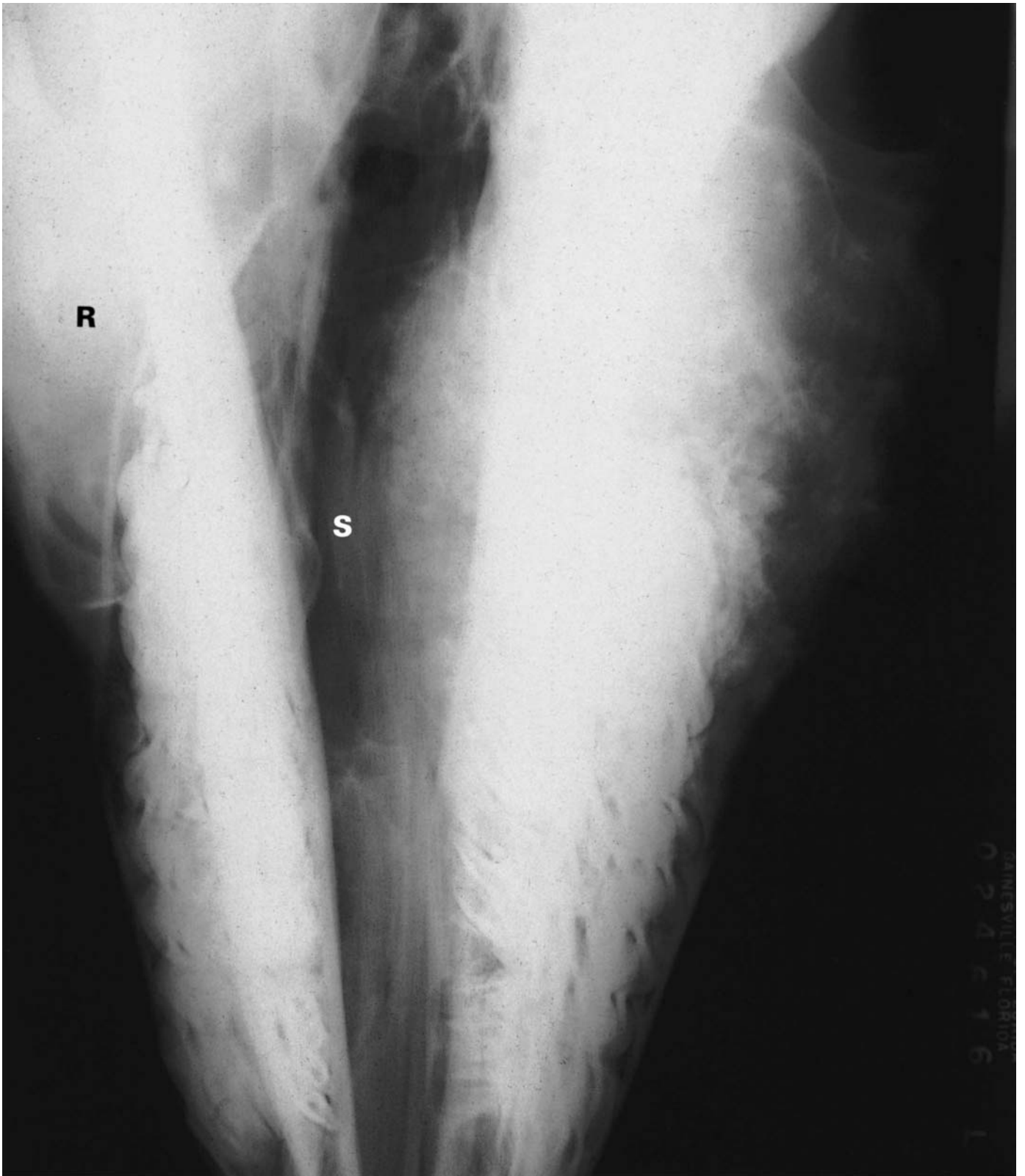
Figure 8.17(b) Ventrodorsal view, clearly demonstrating the mass and showing marked distortion of the nasal septum (S) towards the right (R) and narrowing of the nasal passage. Post-mortem examination confirmed that the mass was an ameloblastic odontoma. See also Figure 8.17(a).

Figure 8.18(a) Right oblique view of the rostral head region of an aged pony with a slowly enlarging facial swelling. There is a cyst-like lesion in the incisive bone (premaxilla), distorting its dorsal contour. The overlying cortex is thinned and has a slightly scalloped appearance caudally. See also Figure 8.18(b).

teeth) of the upper and lower jaws meet. The x-ray beam is aligned at right angles to the midline of the head and the cassette.

Ventrodorsal view

A ventrodorsal view is best and most safely obtained with the horse in dorsal recumbency under general anaesthesia. It is important to ensure that the midline of the head is positioned vertically, to avoid oblique views. The x-ray beam is centred in the midline between the horizontal rami of the two mandibles, at the level of the first molars. Dorsoventral radiographic views of adequate quality can be obtained in a co-operative patient, using the technique described on page 344. It is more difficult to evaluate the most caudal cheek teeth using this method.

Oblique views

Oblique views are essential to view the roots of the teeth satisfactorily, since their density precludes examination of one tooth superimposed over another. Radiographs are most easily obtained with the horse in lateral

[360]

Figure 8.18(b) Slightly oblique dorsoventral, occlusal view of the incisive region (the same horse as in Figure 8.18a). The cyst-like lesion is well defined. There are ill-defined opacities within it. The right canine tooth is partially superimposed over the axial aspect of the cyst-like lesion.

recumbency, with the head resting on the cassette, but can also be obtained in a standing horse (see page 362). The best radiographs are obtained with the teeth of interest against the cassette, although for clinical reasons it is often more practicable to have these teeth uppermost. To view the teeth against the cassette, the x-ray beam is then angled dorsally 30° to visualize the maxillary roots or ventrally 30° to visualize the mandibular roots (Figure 8.19). The x-ray beam should be centred on the root to be examined. If the tooth of interest is uppermost, then the angulation of the x-ray beam is reversed.
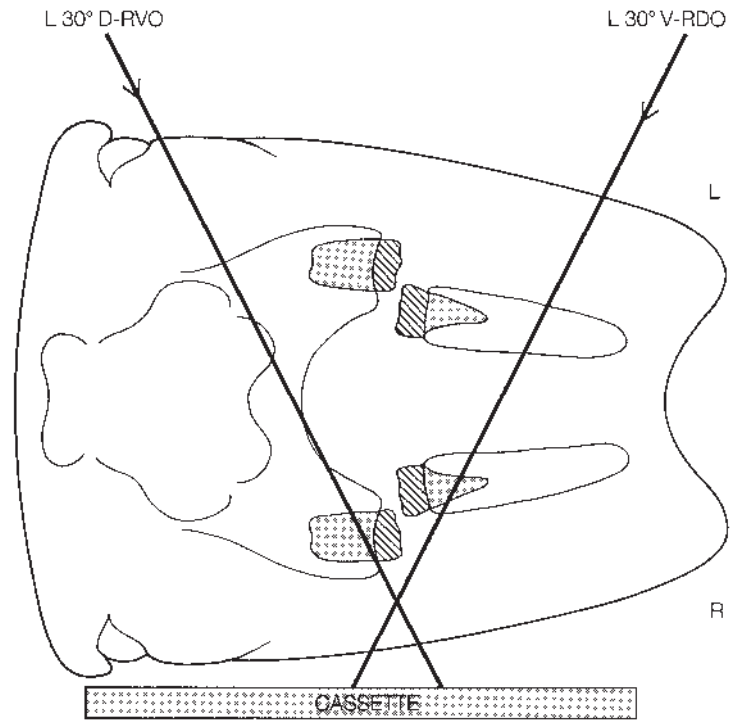
L 30° D-RVO   L 30° V-RDO

Figure 8.19 Diagrammatic transverse section of head to show angulation of the x-ray beam to obtain views of the right maxillary (L30°D-RVO) and mandibular (L30°V-RDO) cheek teeth roots with the horse in right lateral recumbency under general anaesthesia.

It is possible to separate the left and right tooth arcades with the horse standing. For maximum safety the x-ray beam should be collimated as tightly as possible. It is usually easiest to rotate the horse's head towards or away from the cassette, which is positioned vertically, using a horizontal x-ray beam. If the head is turned towards the cassette, the maxillary cheek teeth nearest the x-ray tube and the mandibular cheek teeth roots nearest the cassette will be visualized.

Alternatively, the head can be maintained in a neutral position. The tooth roots to be examined are positioned closest to the cassette, which is held perpendicular to the angle of the x-ray beam. To examine the maxillary cheek teeth roots the x-ray beam is angled obliquely, dorsal 60° on the side away from the cassette, 30° proximal towards the cassette (Figure 8.20). For the mandibular cheek teeth roots the obliquity of the x-ray beam is reversed. Using this second technique it is easier to reproduce accurately the angle of projection.

Incisors

Lateral view

The x-ray beam is centred at the rostral aspect of the head, on the occlusal surfaces of the incisor teeth. It is aligned at right angles to the midline of the head and the cassette.

[362]
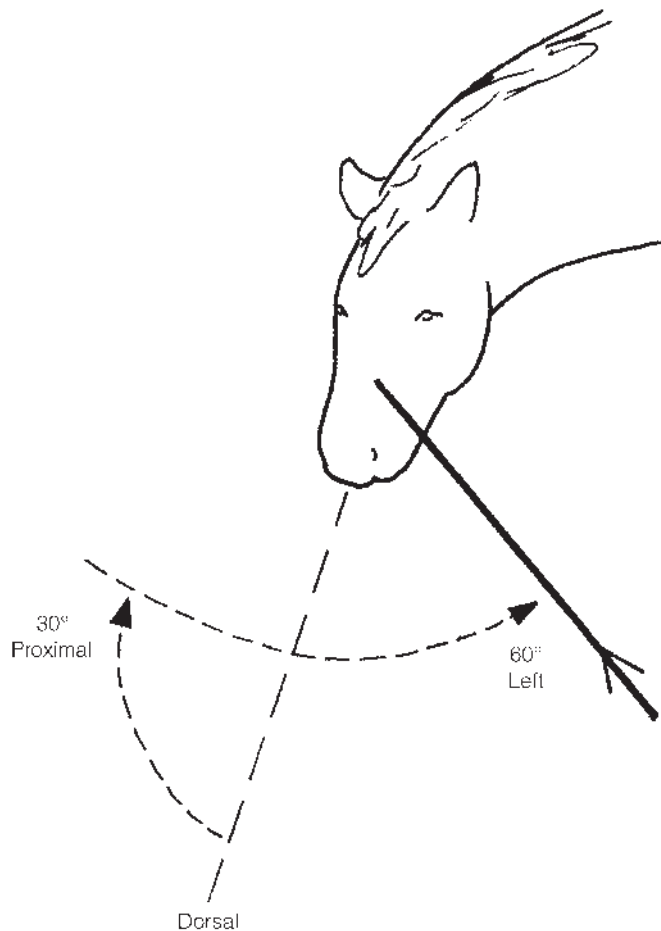
Figure 8.20 Positioning to obtain oblique views of the upper cheek teeth in a standing horse, with the head in a neutral position. The teeth to be examined are closest to the cassette. The x-ray beam must be tightly collimated to ensure safety of personnel.

Ventrodorsal view

This view is obtained with the x-ray beam centred on the ventral aspect of the muzzle of the horse, and the x-ray cassette against the dorsal aspect of the head. It is also possible to obtain occlusal films of the incisor teeth, placing the cassette in the oral cavity, so that only the upper or lower teeth are visualized on the film.

Oblique views

Oblique views are not essential for routine examination of the incisor teeth, because the occlusal films give excellent visualization. They are, however, sometimes beneficial for specific lesions.

NORMAL ANATOMY AND VARIATIONS

In the rostral part of the rostral mandible there is an oval shaped relatively lucent area, at the caudal aspect of which is an irregular opacity (Figure 8.21a). This region of the mandibular symphysis is rather variable in
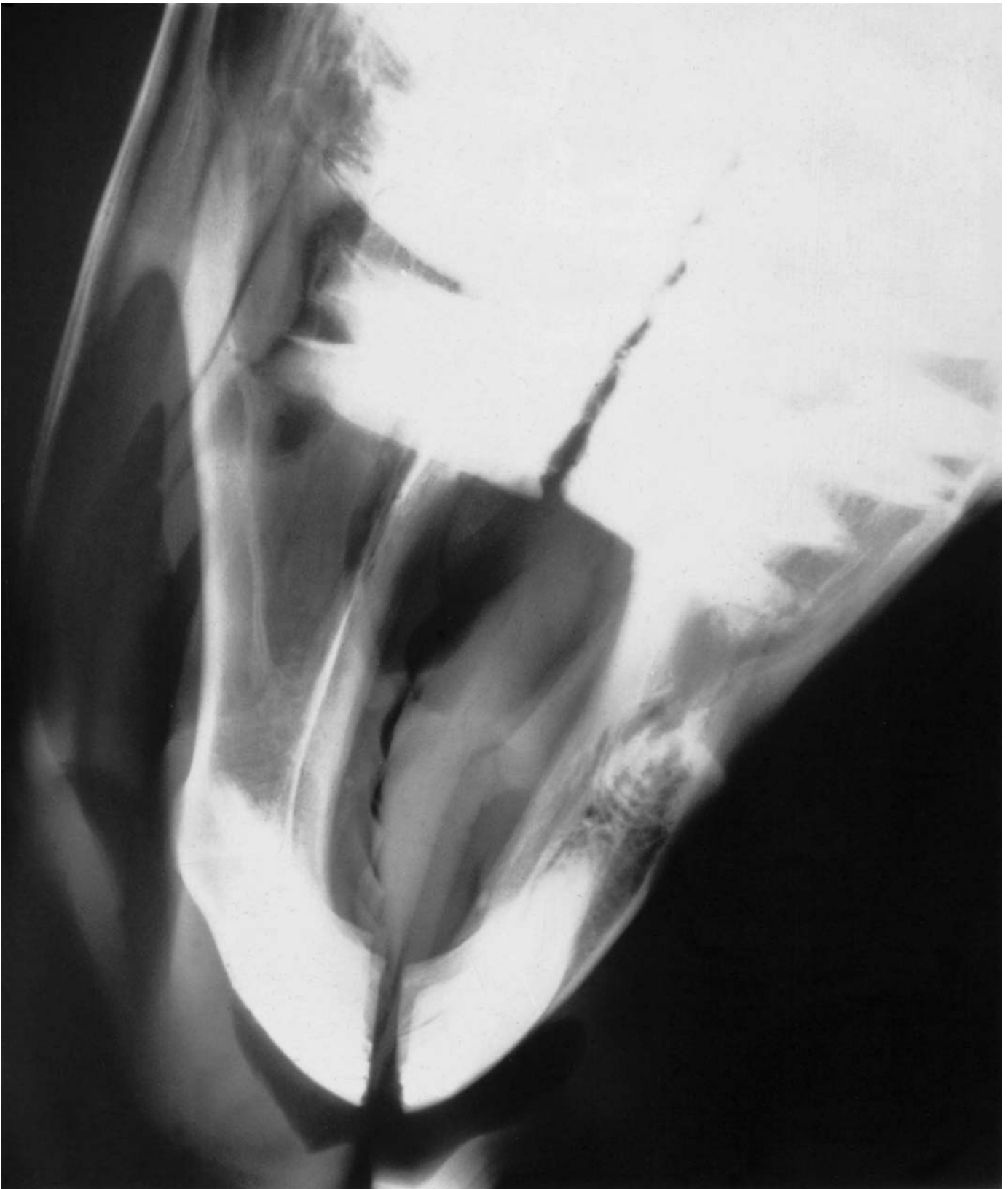
Figure 8.21(a) Lateral view and diagram of the rostral head of a normal mature horse.

[364]
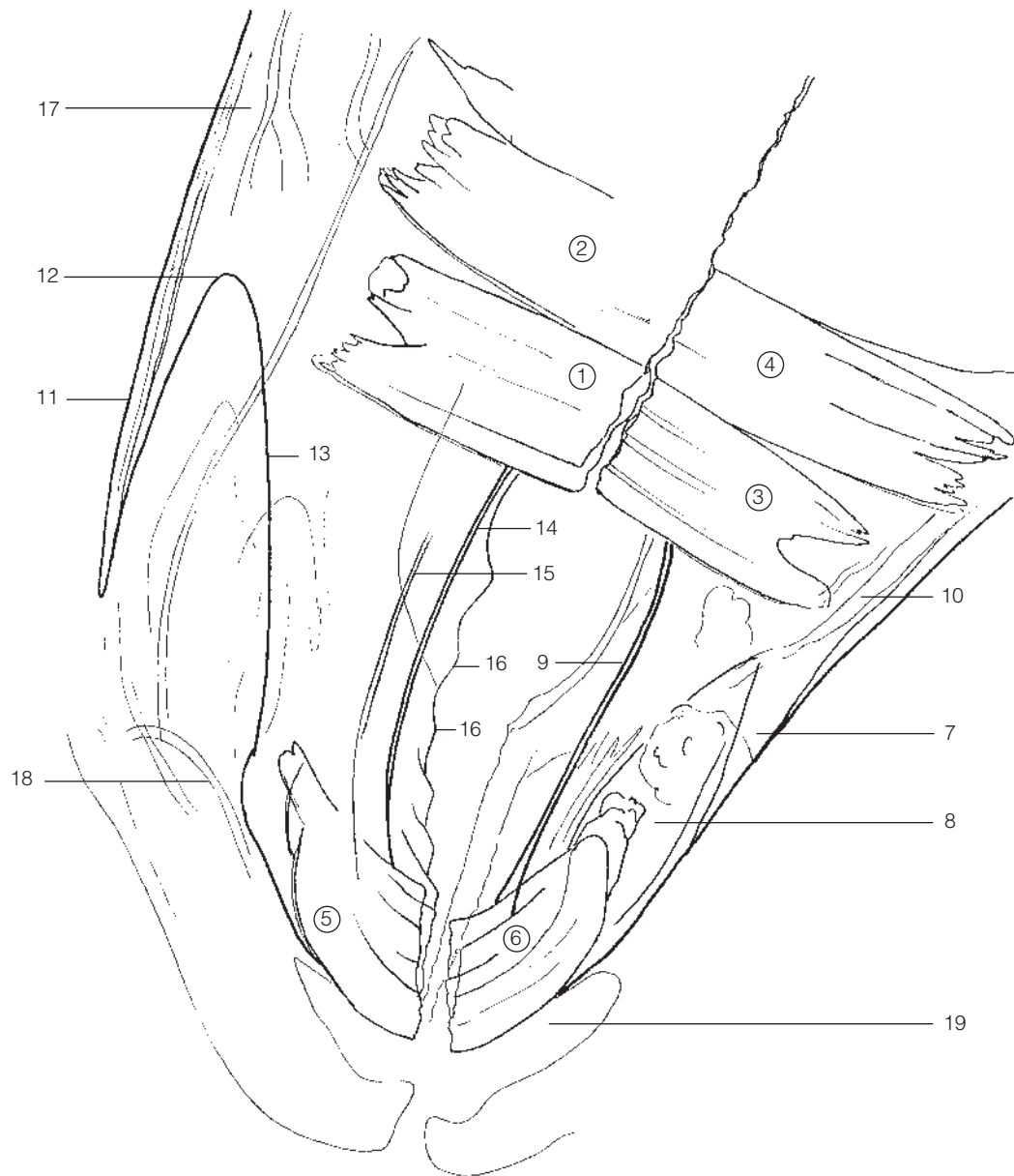
Figure 8.21(a) *Cont'd* 1 = Second upper premolars, 2 = third upper premolars, 3 = second lower premolars, 4 = third lower premolars, 5 = upper incisor teeth, 6 = lower incisor teeth, 7 = body of mandible, 8 = area of mandibular symphysis, 9 = interalveolar margin of mandible, 10 = mandibular canal, 11 = nasal process, 12 = nasomaxillary notch, 13 = dorsal border of nasal process of incisive bone, 14 = interalveolar border of incisive bone, 15 = palatine process of incisive bone, 16 = ridge of hard palate, 17 = dorsal nasal meatus, 18 = nostril, 19 = vestibulum oris.
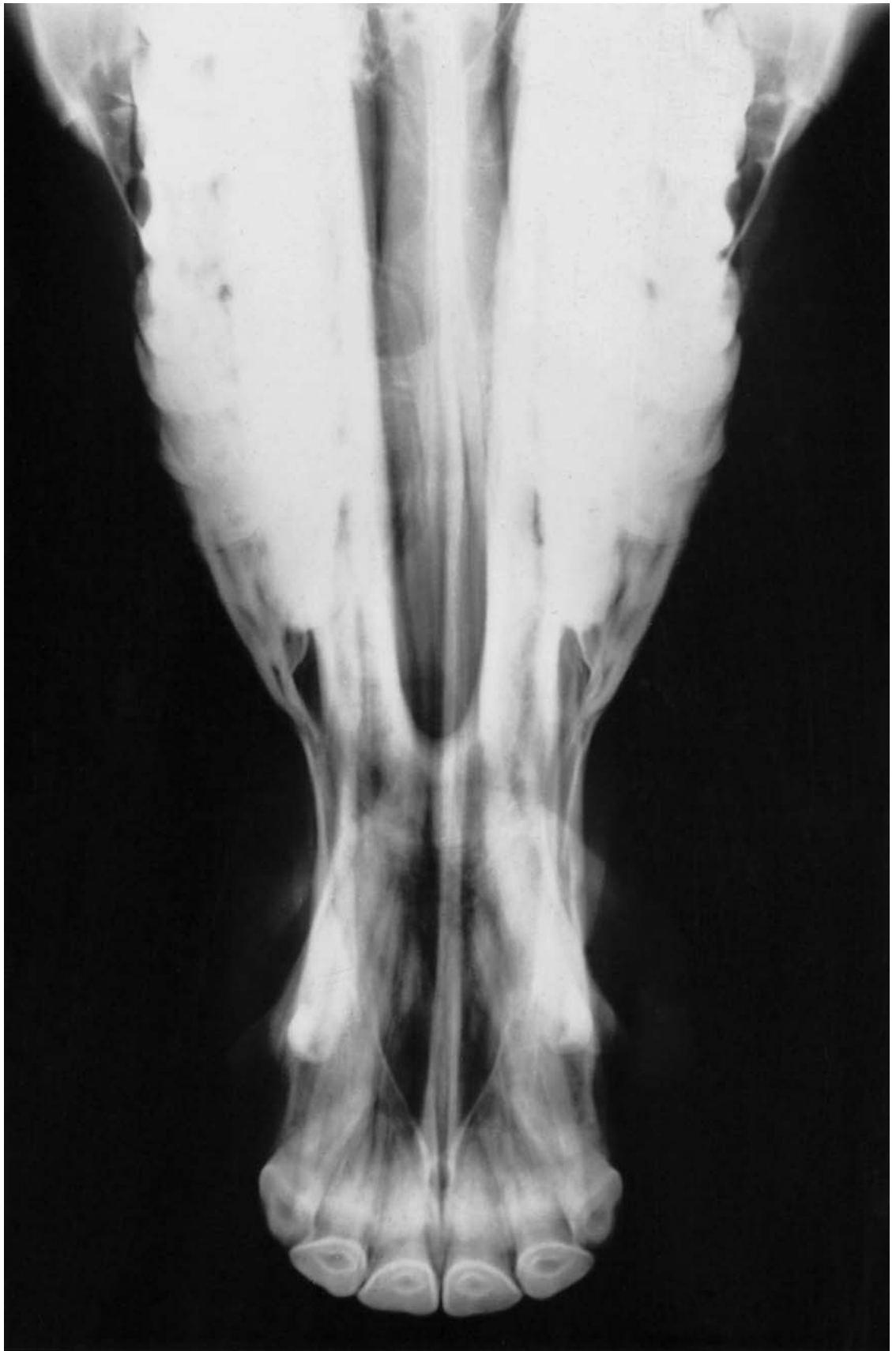
Figure 8.21(b) Ventrodorsal view and diagram of the rostral head of a normal mature horse.

[366]
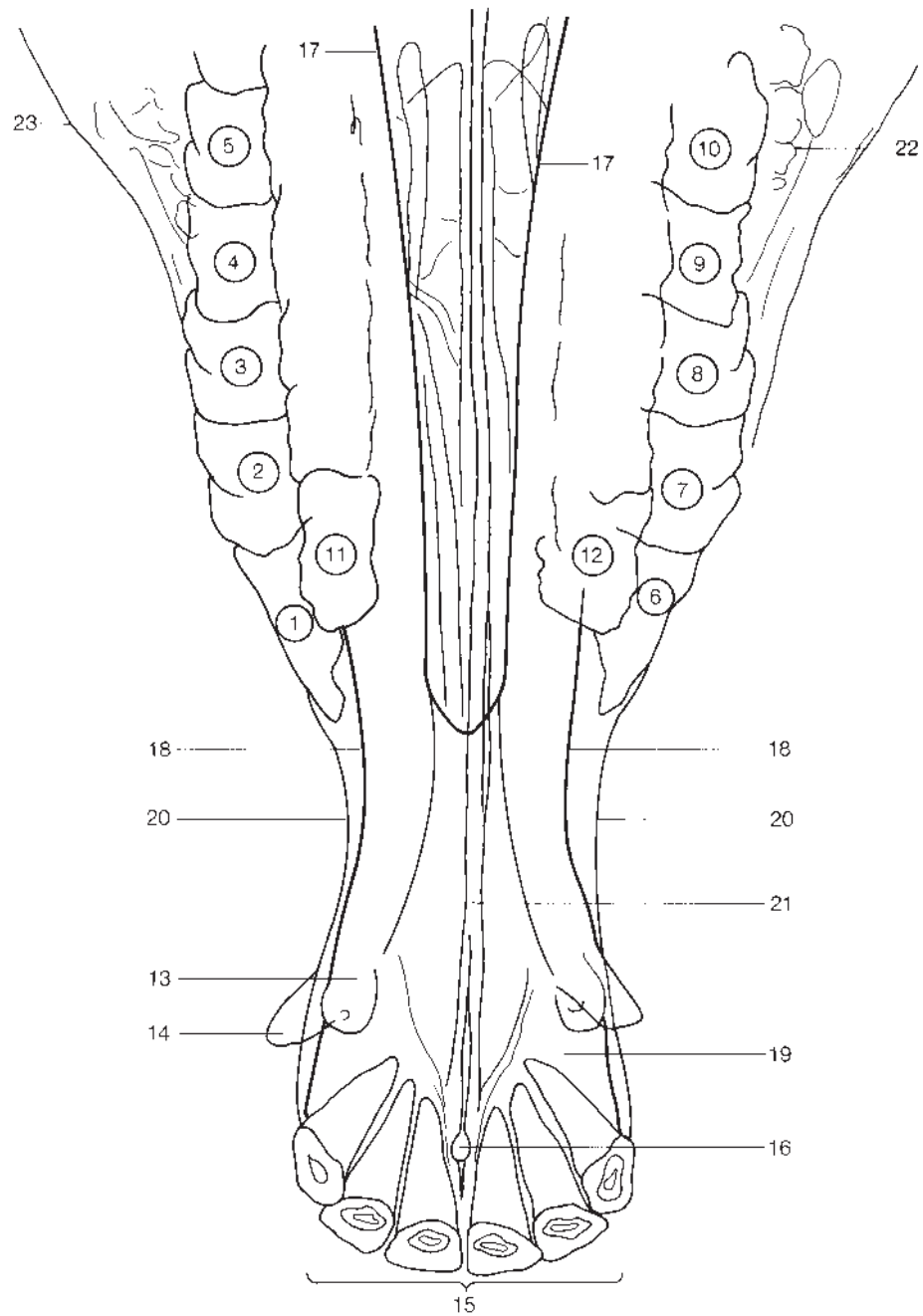
Figure 8.21(b) *Cont'd* 1 = Second right upper premolar, 2 = third right upper premolar, 3 = fourth right upper premolar, 4 = first right upper molar, 5 = second right upper molar, 6 = second left upper premolar, 7 = third left upper premolar, 8 = fourth left upper premolar, 9 = first left upper molar, 10 = second left upper molar, 11 = second right lower premolar, 12 = second left lower premolar, 13 = incisive canine tooth, 14 = mandibular canine tooth, 15 = incisor teeth, 16 = interincisive canal, 17 = medial border of molar part of mandible, 18 = lateral border of body of mandible, 19 = body of incisive bone, 20 = lateral border of nasal process of incisive bone, 21 = vomer, 22 = maxillary sinus, 23 = facial crest.

appearance and should not be confused with a lesion. The horse has four premolars and three molars (Figures 8.22a, 8.22b and 8.22c). The first premolar (the wolf tooth) is frequently absent or is vestigial. Enamel is the most radiodense material in the body, making examination of the structure within the teeth impossible. The teeth develop and erupt from the gums as shown in Table 8.2. The developing tooth is first seen as a lucent area within the mandible or maxilla. As the enamel is laid down, the tooth itself becomes evident, the enamel gradually becoming folded, so that the tooth has its typical structure by the time it erupts from the gum. As the tooth erupts, the lamina dura develops a cystic and distended appearance. This should not be confused with a tooth root abscess, which has a similar appearance (see page 372). The lamina dura of the erupting tooth is more regular in outline, and is not associated with any periosteal reaction or sclerosis of the surrounding bone. Anatomically the roots do not form until the tooth has erupted, when the base of the tooth becomes narrowed and more distinctly outlined. The roots of the premolars are aligned roughly at right angles to the long axis of the horizontal ramus of the mandible. The molars show progressive angulation, the roots being more caudal than the crowns towards the caudal aspect of the jaw.

As the teeth develop, the appearance of the mandible changes considerably. In the young horse the teeth are deeply embedded in the bone, which

Table 8.2 Tooth development

Tooth	Precursor present	Erupt from gum	Come into wear	Tooth lost
DECIDUOUS				
1st incisor	N/A	1st wk	1 mo	$2^1/_2$ yr
2nd incisor	At birth	4–6 wk	By 3 mo	$3^1/_2$ yr
3rd incisor	?	6–9 mo	By 1 yr	$4^1/_2$ yr
Canine: inconsistent and do not erupt				
1st cheek tooth	N/A	0–2 wk	By 1 yr	$2^1/_2$ yr
2nd cheek tooth	N/A	0–2 wk	By 1 yr	3 yr
3rd cheek tooth	N/A	0–2 wk	By 1 yr	4 yr
PERMANENT				
1st incisor	Approx. 20 mo	$2^1/_2$ yr	3 yr	
2nd incisor	Approx. 30 mo	$3^1/_2$ yr	4 yr	
3rd incisor	Approx. 42 mo	$4^1/_2$ yr	5 yr	
Canine?	4–5 yr – inconsistent			
1st premolar (wolf tooth) – inconsistent				
2nd premolar	Approx. 15 mo	$2^1/_2$ yr		
3rd premolar				
Upper	Approx. 17 mo	3 yr		
Lower	Approx. 15 mo	$2^1/_2$ yr		
4th premolar				
Upper	Approx. 25 mo	4 yr		
Lower	Approx. 25 mo	$3^1/_2$ yr		
1st molar	Approx. 3 mo	9–12 mo		
2nd molar	Approx. 10 mo	2 yr		
3rd molar	Approx. 30 mo	4 yr		

is accordingly rather thick. At about 2 years of age the ventral aspect is often somewhat irregular, as the roots of the cheek teeth cause 'swellings' along the horizontal ramus. In the adult horse the ventral surface of the mandible is smooth and the bone is somewhat thinner, as the teeth are extruded from the bone.

The incisor teeth gradually change their angle throughout life, the occlusal surfaces becoming more rostral with age (Figures 8.21a and 8.21b, pages 365 and 366).

The canine teeth (tushes or false wolf teeth) may be vestigial or absent, but are more common in geldings and stallions than in mares. They generally erupt at about 4–5 years of age, approximately in the middle of the interdental space (the gap between the incisors and premolars).

'Wolf teeth' are vestigial remnants of the first premolars. They are frequently absent, or there may be up to four present. They tend to be placed close to the rostral aspect of the second premolar, and generally have a roughly conical crown. There may be little or no apparent root to these
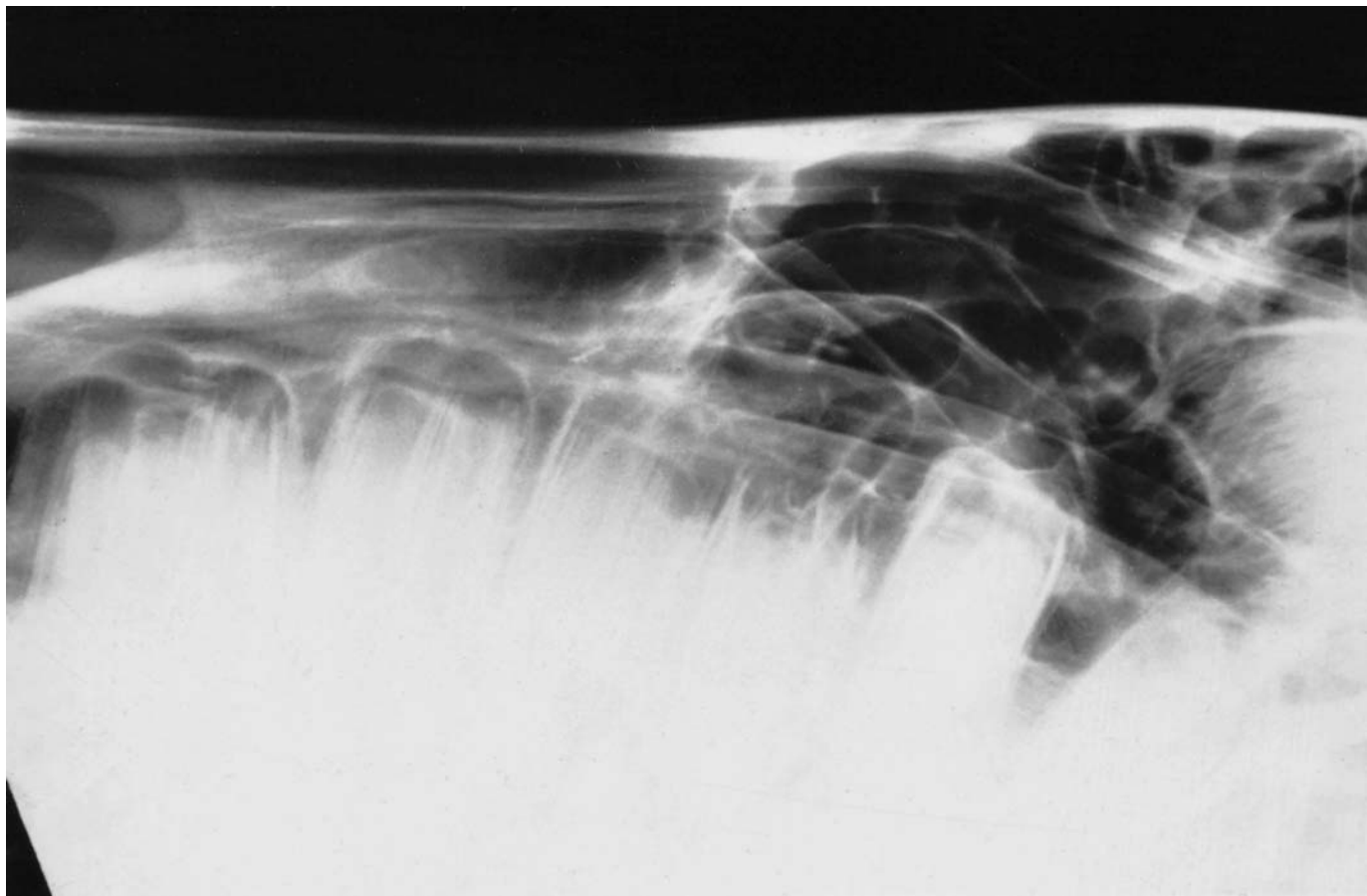
Figure 8.22(a) Right oblique view of the maxillary region of a normal 3-year-old Thoroughbred. Note the well-defined periapical lucent zones which represent the normal dental sacs. The lamina dura are well delineated (compare with Figures 8.14a and 8.24).
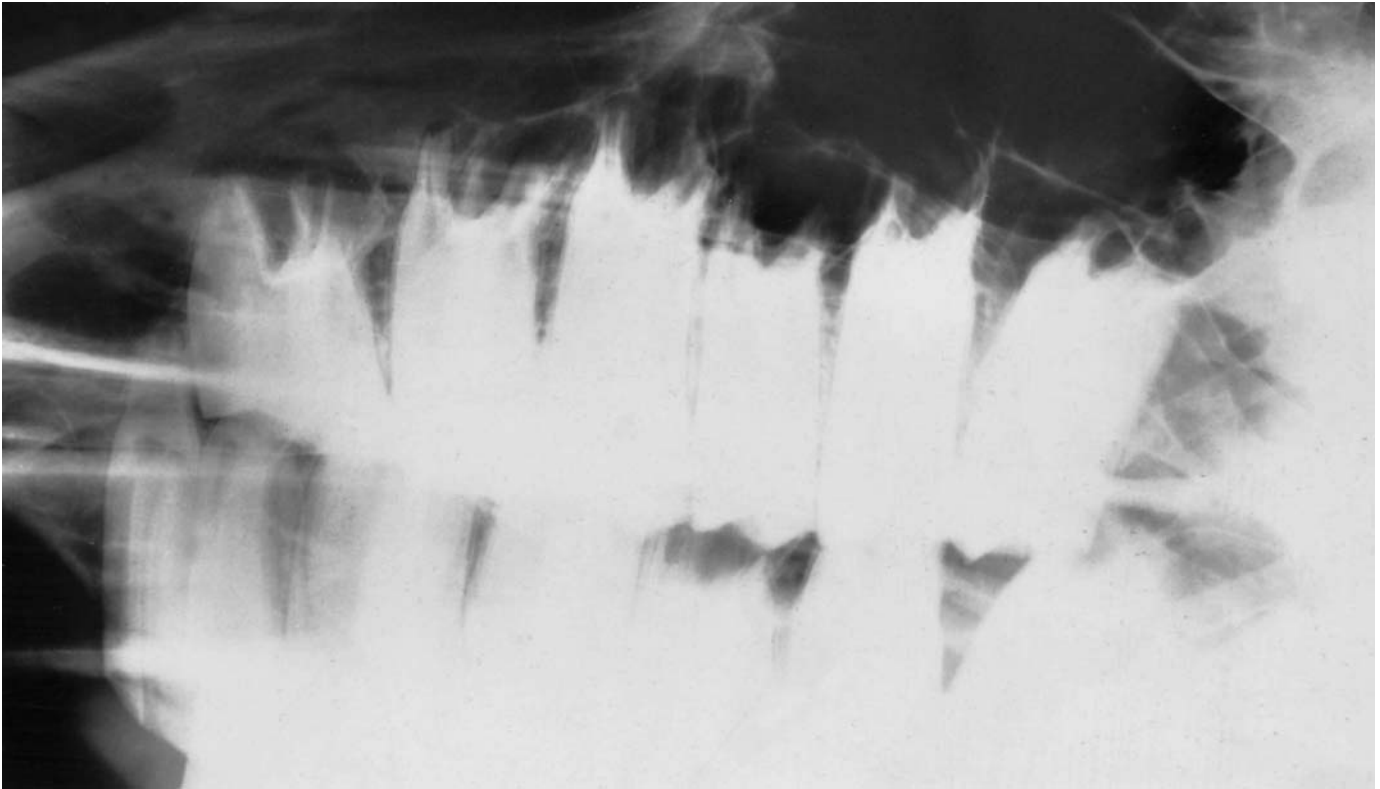
Figure 8.22(b) Right oblique view and diagram of the maxillary region of a normal 10-year-old Thoroughbred. The exposure was selected to highlight the detail of the tooth roots.

teeth, or they may have a root penetrating variable depths into the bone. In many cases the teeth never penetrate the gum, and can only be detected on x-ray or by palpation.

SIGNIFICANT FINDINGS

Brachygnathia and prognathia

These conditions are generally congenital, and can be seen on lateral radiographs. While it is not necessary to radiograph patients to make this diagnosis, radiographs of the cheek teeth may be valuable to check for sharp points where there is irregular wear, e.g. in brachygnathia the lower jaw is shorter than the upper, and there tend to be sharp points on the rostral aspect of the upper second premolar and caudal aspect of the lower third molar teeth.

Polydontia

Polydontia is the presence of teeth in excess of the normal dental formula. It most commonly results from persistence of the temporary dentition, particularly in the incisors. Incisors are usually displaced labially or lingually, and cause little trouble, although they may result in ulceration of the

[370]
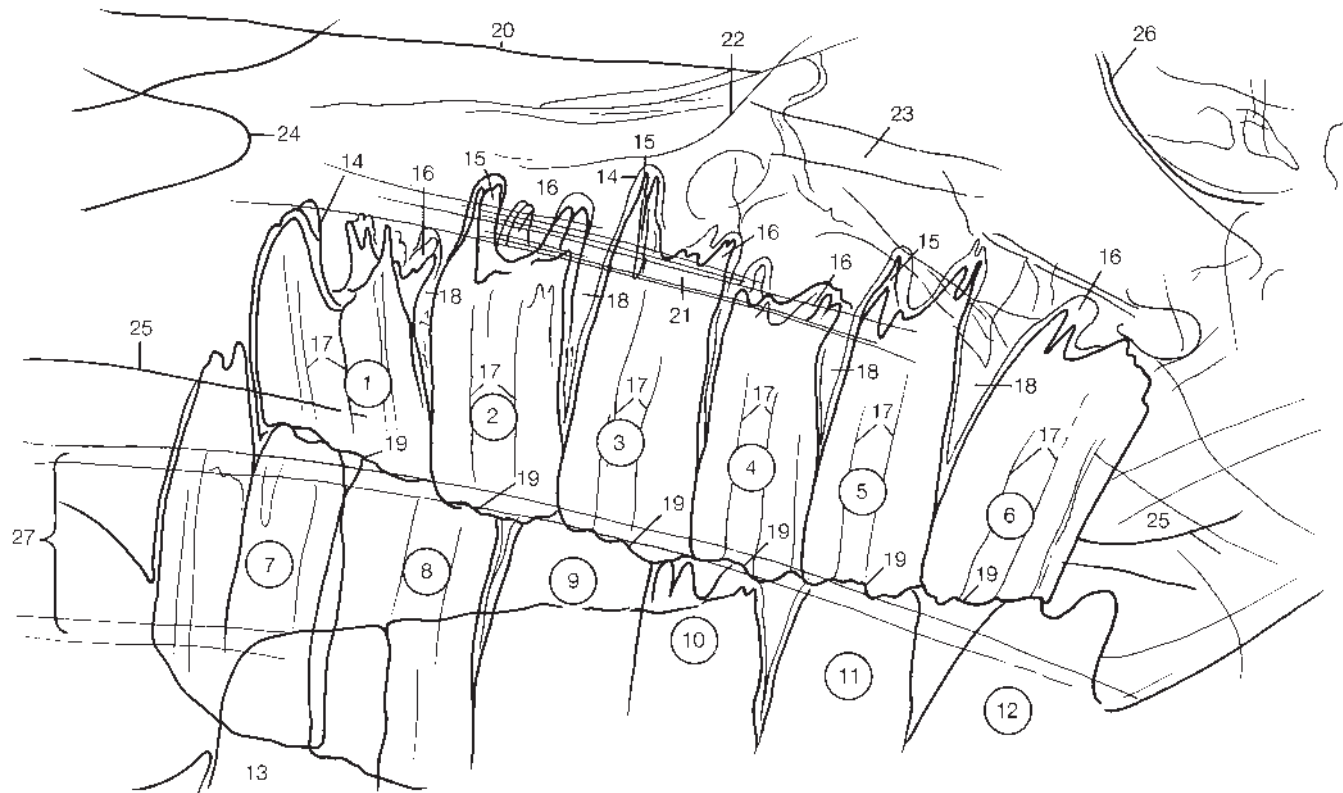
Figure 8.22(b) *Cont'd* 1 = Second right upper premolar, 2 = third right upper premolar, 3 = fourth right upper premolar, 4 = first right upper molar, 5 = second right upper molar, 6 = third right upper molar, 7 = second left upper premolar, 8 = third left upper premolar, 9 = fourth left upper premolar, 10 = first left upper molar, 11 = second left upper molar, 12 = third left upper molar, 13 = second right lower premolar, 14 = socket, 15 = buccal root, 16 = lingual root, 17 = buccal longitudinal crest and folds of peripheral enamel, 18 = interalveolar septum, 19 = masticatory surface, 20 = dorsal nasal meatus, 21 = middle nasal meatus, 22 = sinus of nasal turbinate, 23 = infraorbital canal, 24 = nasomaxillary notch, 25 = hard palate, 26 = orbit, 27 = endotracheal tube.

gum or lip. With the cheek teeth, the demand made for additional space by supernumerary teeth tends to result in teeth being rotated or adjacent teeth being displaced. This results in disturbance of the wear patterns, resulting in sharp spikes on the teeth and resultant damage to soft tissues.

Radiography is not really necessary to diagnose this condition, but it may be helpful in differentiating between deciduous and permanent teeth, the permanent teeth having longer roots.

Oligodontia

The congenital absence of a tooth is of little clinical significance, although it may lead to sharp points on teeth, caused by uneven wear.

Tumours of dental origin

Adamantinomas and ameloblastic odontomas are tumours derived from the enamel organ (the embryological precursor of a tooth). They are generally recognized in young horses. They may occur in the maxilla or the mandible

[371]
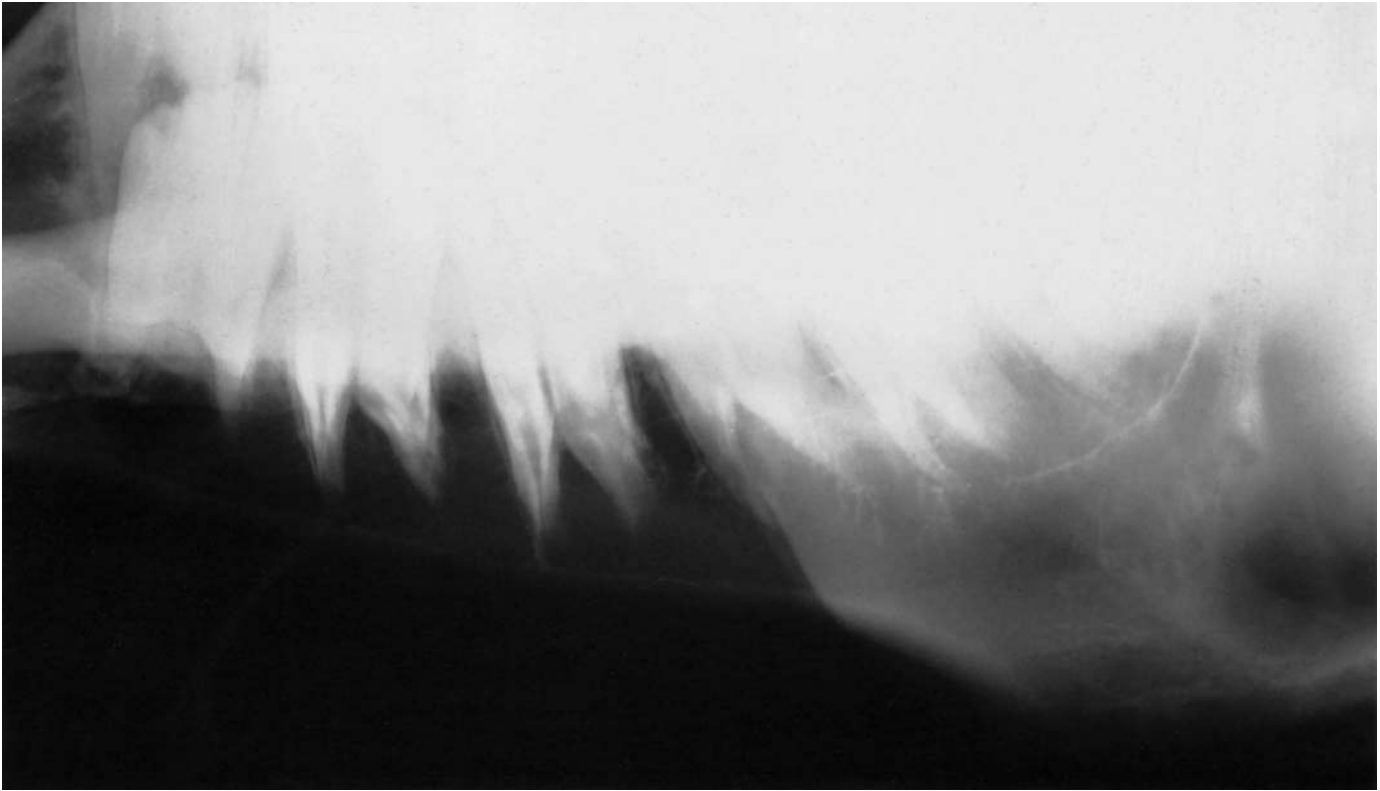
Figure 8.22(c) Right oblique view of the mandible of a normal 10-year-old Thoroughbred, to show the tooth roots.

and have a variable appearance. An adamantinoma remains primarily of soft tissue, and has a septate, 'foamy' appearance. An odontoma usually has a more opaque tooth-like structure (Figures 8.17a, page 358 and 8.17b, page 359).

Tooth root infection

Infections of the tooth roots vary in their appearance, and can be difficult to distinguish on radiographs. They show a number of changes progressing through: loss of detail of the lamina dura; lysis of the periapical bone, possibly with sclerosis of the surrounding bone; destruction of the apex of the tooth root, giving it an irregular margin or marked change in shape.

Infections of the teeth in the mandible tend to present clinically as swellings on the lower jaw (Figure 8.23). These may be very slow to develop, and eventually a discharging sinus may occur at the ventral aspect of the swelling.

Infections of the upper teeth may develop similarly (Figures 8.24a to 8.24d, pages 374–7), with swelling and discharge from the maxilla or peri-orbital area. More usually, if the upper molars (and occasionally fourth pre-molar) are involved, there will be either a nasal discharge or a purulent sinusitis (see 'Sinusitis', page 345). Infection of the maxillary teeth is some-times accompanied by quite extensive fibrous reactions in the maxillary sinus, possibly including areas of local mineralization. If such changes are
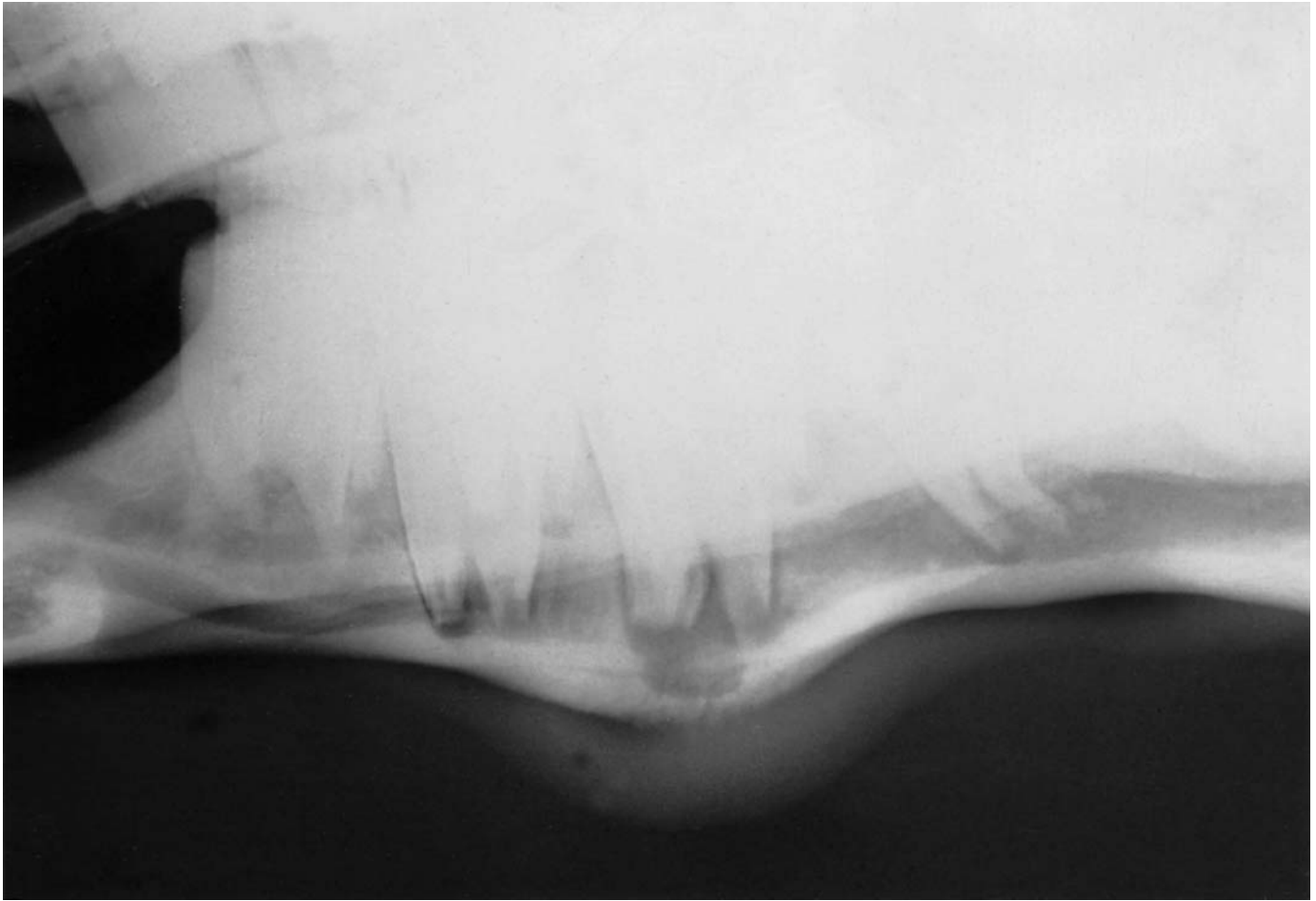
Figure 8.23 Left oblique view of the mandible of an 8-year-old Thoroughbred with a history of a swelling developing in the left mandibular region over the previous 4 weeks. There is distortion of the cortex of the mandible with overlying soft-tissue swelling. Note the radiating poorly bordered, active periosteal new bone formation covering the ventral aspect of the alveolus. There is loss of detail of the lamina dura and a suggestion of blunting of the tooth roots of the third lower cheek tooth with considerable lysis of the periapical bone. There is a suggestion of slight sclerosis of the surrounding bone rostrally and caudally. These abnormalities are typical of tooth root infection.

found in the maxillary sinus, tooth root infection or periodontal disease should always be considered a likely cause (see Figure 8.15, page 356).

In the horse, by the time these infections have been diagnosed it is usually necessary to extract the affected teeth. Although attempts have been made to drain these infections, and operate on or fill the tooth roots, this is generally unsuccessful, uneconomic and, in view of the reasonable prognosis for conventional treatment, unnecessary.

Periodontal disease

Periodontal disease is more common in the maxillary teeth than in the mandibular teeth.

[373]

Figure 8.24(a) Lateral view of the upper cheek teeth of a 7-year-old Thoroughbred with head-shaking behaviour of several months' duration and recent onset of left-sided, foul-smelling nasal discharge. The tooth roots of one of the fourth upper cheek teeth are poorly defined. There is a reticular radiopacity superimposed over some of the tooth roots which represents a rope halter. See also Figure 8.24(b).

Figure 8.24(b) Left oblique view of the upper tooth arcade of the same horse as in Figure 8.24(a). The abnormalities of the left fourth upper cheek tooth are much more clearly defined. There is loss of the lamina dura and the tooth roots are reduced in opacity. The roots also have an abnormal shape.

Figure 8.24(c) Oblique view of the right upper cheek tooth arcade. There is loss of definition of the lamina dura of the second upper cheek tooth, with a nodular opacity dorsal to it within an area of increased opacity. This is a more unusual finding associated with chronic tooth root infection. Compare with Figures 8.24(a) and 8.24(b).
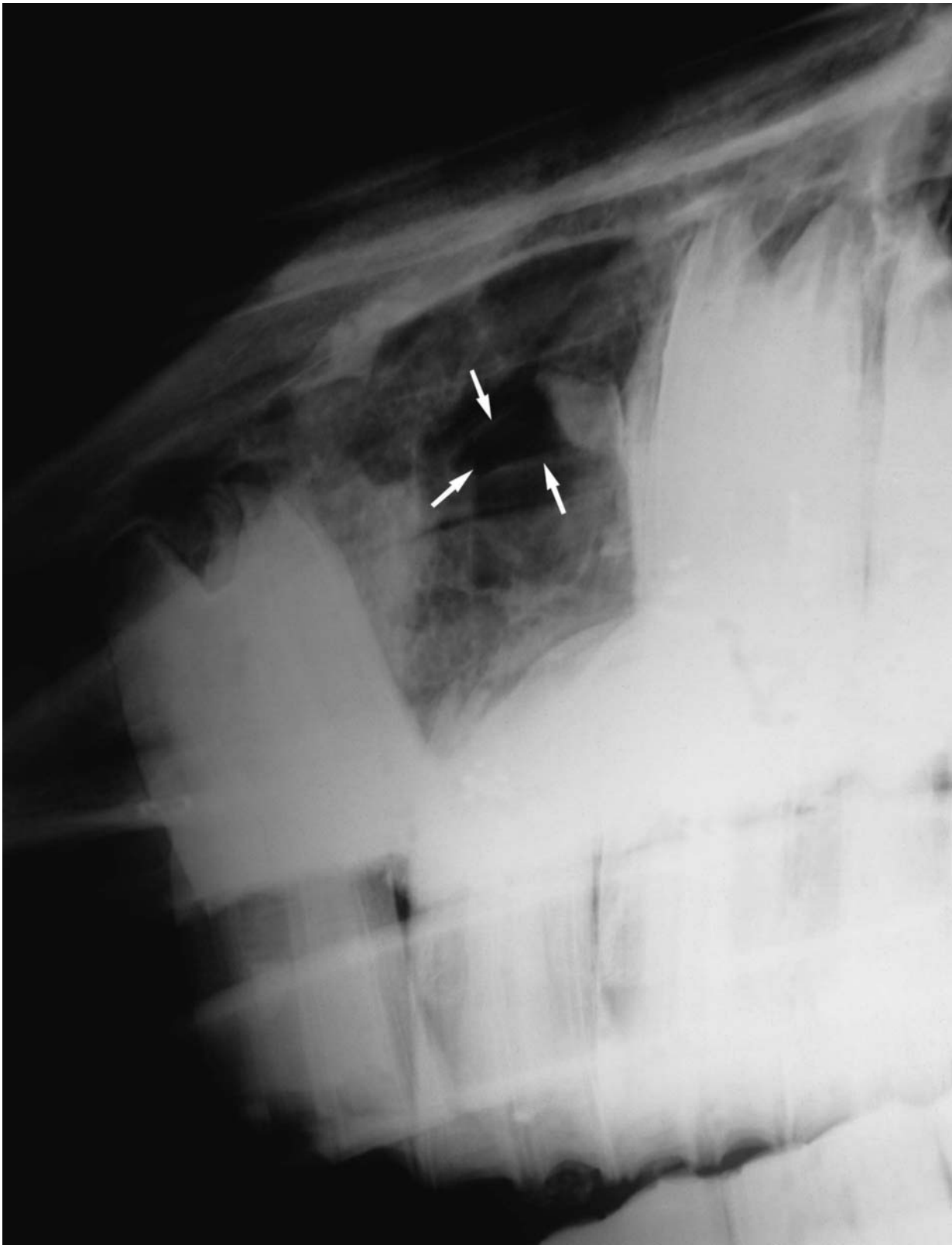
Figure 8.24(d) Left oblique view of the rostral upper cheek teeth 2 months after removal of the left third upper premolar. A chronic nasal discharge has persisted. There is a fragment of tooth, rostral to which is a radiolucent area, surrounded by a more opaque rim (arrows). This is a sequestrum. Note also the diffuse, somewhat reticular opacity in the remainder of the space formerly occupied by the tooth.

The radiological signs are similar to those for root infections, but there tends to be more reaction on the alveolar bone. Although periodontal disease is frequently accompanied by food material packing around the teeth, and even passing up into the maxillary sinus, it may be accompanied by little detectable oral discomfort.

Mandibular periostitis

Periostitis of the mandible is characterized radiologically as periosteal new bone formation, usually on the ventral surface of the mandible. It is seen subsequent to chronic bruising, e.g. as a result of tight-fitting tack, or repeated contusion from looking over a high door.

The soreness will resolve once the inciting factor is removed, although some change in contour of the mandible is likely to remain. This condition should be differentiated from tooth root abscess, and tumour of the mandible.

Osteomyelitis

Osteomyelitis of the mandible is not uncommon and is characterized radiographically by destruction of bone with or without new bone formation (Figure 8.25). It is sometimes difficult to distinguish radiographically widespread infection from a tumour. Small lesions may be treated surgically, but widespread lesions carry a guarded prognosis.

Mandibular cysts

Multiple cystic lesions of the mandible, usually involving the tooth roots, are not uncommon in young foals (Figure 8.26, page 380). They generally involve the rostral half or two-thirds of the horizontal ramus. Their origin is uncertain.

This lesion is easily recognized on lateral radiographs as multiple radiolucent cystic lesions in the mandible, often with enlargement in size of the mandible. In extensive cases there may be little bone surrounding the cysts.

Clinically there is swelling of the mandible, often with a rather bulbous or even lobulate appearance. The teeth may be loose in the jaw in extensive cases, and the horse may have difficulty eating. Differential diagnosis includes ameloblastoma, cystic fibrosis and infection. Treatment is by surgical drainage, but the prognosis is guarded, depending on the extent of the lesion.

Craniomandibular osteopathy

A condition resembling craniomandibular osteopathy in the dog has been recognized in the horse, resulting in large firm non-painful swellings on the ventral aspect of the rami of the mandibles of a young horse. Radiographically this is due to extensive periosteal new bone formation

[378]

Figure 8.25 Slightly oblique left lateral view of the mandible of a weanling Morgan with a history of a small mass developing on the mandible 6 weeks previously and enlarging progressively despite antimicrobial therapy. There is a large expansile lesion of the mandible that has a reticulate or 'foamy' appearance. Post-mortem examination confirmed that this was the result of osteomyelitis, although its radiographic appearance was similar to that of an odontoma, a reparative granuloma or an aneurysmal bone cyst.

extending from the ventral cortices of the bones (Figure 8.27, page 381). Bone biopsies show similar histological changes to craniomandibular osteopathy in the dog. There is some degree of spontaneous regression of the lesions over 1 year. The lesions do not interfere with mastication.

Tumours

The mandible is one of the more common sites for a tumour in bone in the horse. Most tumours result in widespread destruction of bone (Figures 8.28, page 382 and 8.29, page 383) and carry a poor prognosis. It is usually not possible to identify a specific tumour type by its radiographic appearance. Tumours must be differentiated from osteomyelitis (see Figure 8.25).

Temporomandibular joint arthritis

This is a rare condition, and may be infectious or more usually traumatic in origin. The radiographic changes seen are similar to those seen in any other

[379]
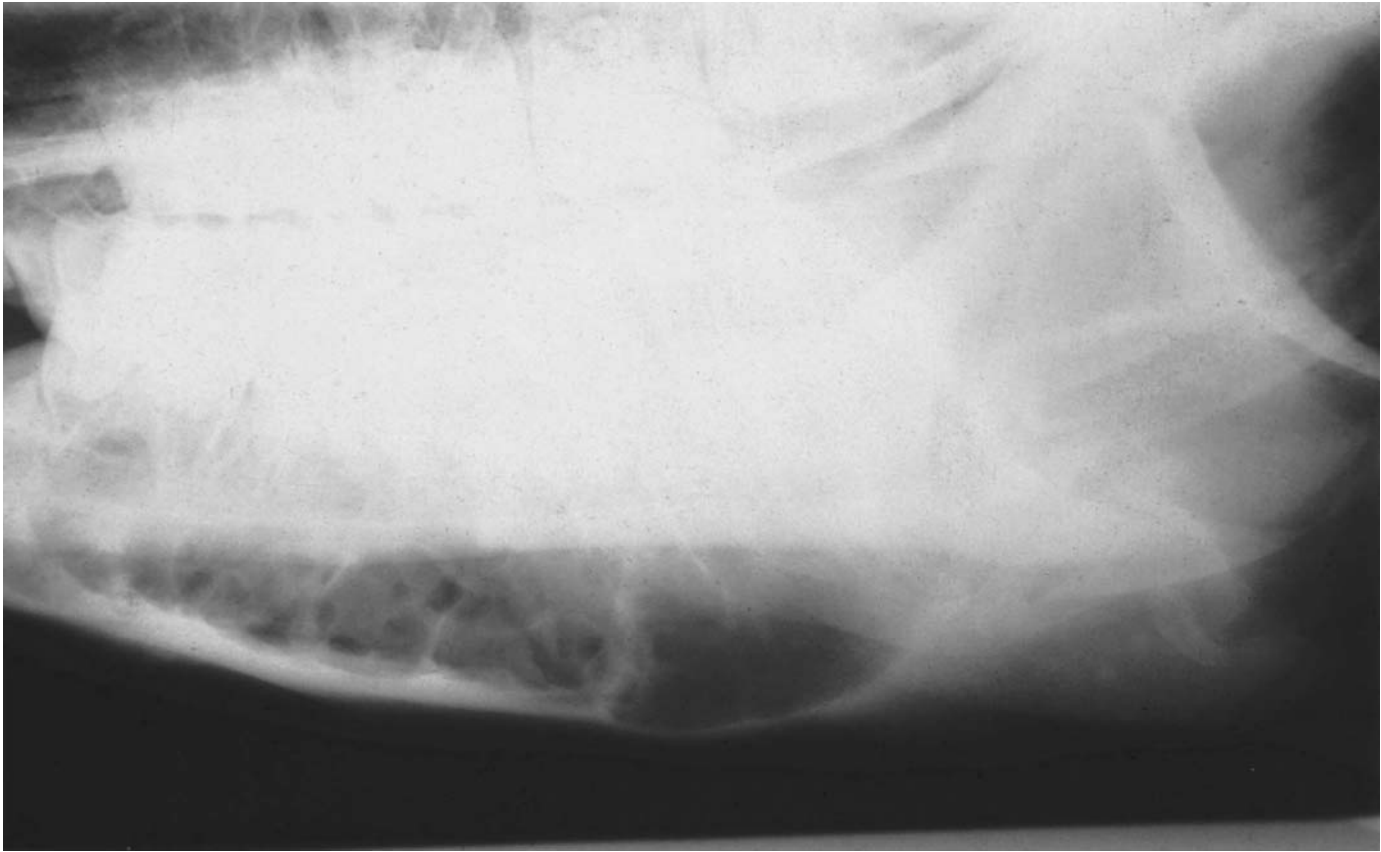
Figure 8.26 Left oblique view of the mandible of a 3-month-old Thoroughbred with diffuse swelling in the left mandibular region. There is a multiloculated cyst-like lesion involving the rostral half of the left mandible. The cortex of the bone is smoothly irregular and appears to be of variable width. The cyst-like structures extend as far as the tooth roots. The swelling resolved following surgical curettage.

joint (see Chapter 1, page 25); for example, radiographs show proliferative new bone around the joint, accompanied in infectious cases by some bone lysis. The condition is very painful, resulting in dysphagia and weight loss. The prognosis is poor, although condylectomy has been described and may be beneficial.

Luxation of the temporomandibular joint

Temporomandibular joint luxation is usually the result of trauma and may occur unilaterally or bilaterally. There may be associated fractures. Oblique radiographic views may be required to separate the two joints. There is usually associated malocclusion of the molars. The radiographs should be inspected carefully for the presence of concurrent fractures.

Fractures

Fractures of the rostral aspect of the mandible are common, especially in foals and young horses. They frequently involve a fracture at, or

[380]

Figure 8.27 Lateral view of the head of a 3-year-old Thoroughbred colt with a rapidly expanding mass on the cranial aspect of the ramus of the left and right mandibles. There is extensive new bone on the ventral aspect of the mandible and loss of the cortex. The rami of the mandible have a heterogeneous radiopacity. The lesions progressively resolved with time and non-steroidal anti-inflammatory treatment. Diagnosis: craniomandibular osteopathy.

immediately caudal to, the third incisor (Figure 8.30, page 384). They may result in one or more teeth being broken or torn from the body of the mandible, usually with some associated bone. Injuries may involve only one side, or both mandibles may be fractured.

These fractures generally require surgical intervention, either to remove loose fragments or to stabilize the fracture by internal fixation. They carry a good prognosis with surgical treatment, although some brachygnathia may result or develop with growth.

Fractures of the horizontal ramus occur at any point, although frequently involve the diastema. They may respond to conservative treatment if unilateral, or may benefit from internal fixation. Internal fixation may be impracticable if the tooth roots are too closely involved with the fracture line, and in some cases in young horses the tooth roots may involve too much of the bone for fixation to be possible. Fractures of the horizontal ramus of the mandible often open into the oral cavity, with a high risk of developing osteomyelitis.

Fractures of the vertical ramus of the mandible are often best visualized

Figure 8.28 Slightly oblique left lateral radiograph of the skull of a 7-year-old Quarterhorse with a 3-month history of swelling in the region of the left mandible and difficulty in chewing. There is a large lucent area (arrows) in the cranial angle of the left mandible. The bone adjacent to the margins of the defect appears lytic and irregular. The left stylohyoid bone (h) cannot be evaluated totally, but appears to be involved in the process. The approximate location of the normal cranial angle of the mandible is marked with a dotted line. The epiglottis (e) is normal. Post-mortem examination confirmed the presence of a squamous cell carcinoma.

[382]

Figure 8.29 Left lateral view of the rostral maxilla and mandible of a yearling Thoroughbred. A firm lump was noted on the left rostral mandible 2 months previously. There is a large multiloculated expansile mass in the left mandible which is displacing the incisor teeth. The mass was excised surgically and histological examination revealed that this was fibrous dysplasia with reactive new bone but no evidence of malignancy.

on the view described on page 329 for examination of the cranium. They are usually unilateral, and may be difficult to delineate. They may require several different exposures for complete evaluation. Internal fixation is not generally practicable, but if the horse can feed adequately the fractures may heal with conservative treatment. The prognosis is good, provided that the fracture does not enter the temporomandibular joint.

The radiographs should be carefully examined to ensure that concurrent dislocation of the temporomandibular joint has not also occurred.

Sequestrum of the interdental space

The mandibular interdental space is relatively poorly covered by soft tissues, and is potentially at risk to trauma from the bit. This may predispose it to sequestrum formation.

Radiographically there are typical signs of sequestrum formation (see Chapter 1, page 15), usually immediately rostral to the first premolar.

Figure 8.30 Intra-oral ventrodorsal view of the rostral mandible of a show pony. There is a displaced fracture of the mandible involving the tooth roots of the corner and intermediate incisors. Note that the root of the corner incisor is fractured.

Oblique views are necessary to separate the two horizontal rami of the mandible. This can be achieved by turning the horse's head slightly towards or away from the x-ray machine.

Clinical signs include depressed appetite, oral discomfort, slight swelling on the ventral and lateral aspects of the mandible, and sometimes a draining sinus. Surgical treatment carries a good prognosis.

Pharynx, larynx and Eustachian tube diverticulum

This area includes structures that are an integral part of the respiratory system, and the reader may also want to refer to Chapter 11.

Radiographs of this area give visualization of the soft palate, epiglottis, hyoid apparatus, nasopharynx and Eustachian tube diverticulum (guttural pouch).

[384]

Lateral view

Evaluation of this area is almost always limited to lateral views, normally obtained with the horse standing. The x-ray beam is centred between the base of the ear and the angle of the mandible, and aligned at right angles to the midline of the head and the cassette. When the Eustachian tube diverticulum (guttural pouch) is being evaluated, it is often advantageous to obtain both right and left lateral radiographs in order to determine the side of involvement (see page 327). Exposures appropriate for soft tissues should be used.

Ventrodorsal view

This view is obtained under general anaesthesia, and is difficult to obtain without some degree of rotation. The horse is placed in dorsal recumbency and the head extended. The poll is placed on a small pad, so that the x-ray cassette can be placed in contact with the dorsal aspect of the skull, and be placed far enough caudally to visualize the Eustachian tube diverticulum and pharynx. The dorsoventral plane of the skull must be maintained vertical, in order that diagnostic radiographs are obtained. It may be necessary to reposition the head to obtain straight ventrodorsal views, as any obliquity results in loss of information on the radiograph. It may also be helpful in some cases to withdraw the endotracheal tube, if one is used, as this can mask abnormalities.

NORMAL ANATOMY, VARIATIONS AND INCIDENTAL FINDINGS

When examining radiographs of this area it is important to remember that the soft-tissue structures are constantly moving. Radiographs only indicate the position of the structure for a fraction of a second in the life of the patient, and must be interpreted on this basis. For this reason, assessment of the relationship of structures such as the soft palate or epiglottis to other structures must be interpreted with care (Figure 8.31a).

The most obvious structures on this view are the radiolucent Eustachian tube diverticula (guttural pouches) (Figure 8.31b). The dorsal aspect is in contact with the base of the skull and the atlas. The caudal border lies roughly below the articulation of the atlas and axis. The ventral border forms the roof of the pharynx, and lies roughly level with the dorsal aspect of the arytenoid cartilages and the rostral aspect of the ethmoid bone. The ventral cranial third of the Eustachian tube diverticulum lies between the vertical rami of the mandible. The caudal and ventral borders of each Eustachian tube diverticulum are apparent as double lines, as the two pouches seldom lie exactly over one another. The greater cornua of the stylohyoid bones cross the diverticulum between the medial and lateral compartments.

The soft palate is at the rostral aspect of the pharynx. Rostrally it is seen
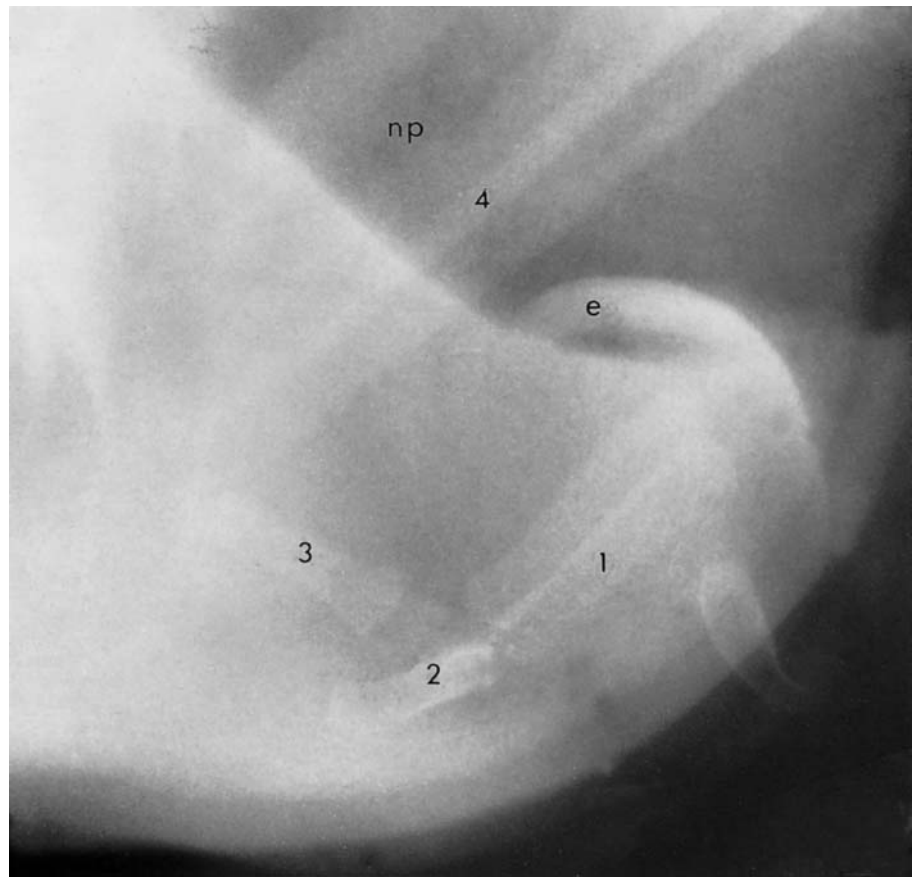
Figure 8.31(a) Well-collimated slightly oblique lateral view of a normal pharynx of an immature horse. The nasopharynx (np) contains air. Note the epiglottis (e), thyrohyoid (1), basihyoid (2), ceratohyoid (3) and stylohyoid (4).

caudal to the last upper molars, generally positioned about midway between the crown and root of the tooth. It follows a smooth S-shaped course over the back of the tongue, to lie under the epiglottis caudally. There is sometimes a small triangular area of air betwen the soft palate and the base of the tongue.

The epiglottis is clearly seen caudal to the last lower molar, the opening formed by the epiglottis and arytenoid cartilages forming a smooth continuation of the tracheal lumen into the nasopharynx. The epiglottis is markedly curved (dorsally convex), nearly forming a complete semicircle. Its base is approximately vertical, while the tip lies nearly at a right angle to the dorsal surface of the soft palate.

A small lucent gas shadow may be seen at the base of the epiglottis, in the trachea (the middle ventricle of the larynx), and two further lucent crescents are seen below the base of the arytenoid cartilages (the lateral ventricles).

The tracheal rings are clearly delineated. Dorsal to the trachea, immediately caudal to the tip of the arytenoid cartilage, a small lucent linear air shadow may occasionally be seen in the cranial part of the oesophagus. This should not extend more than 2–5 cm in length in a normal horse.

Mineralization of the laryngeal cartilages, hyoid apparatus and tracheal rings may occur as a normal variation in some older horses.

[386]
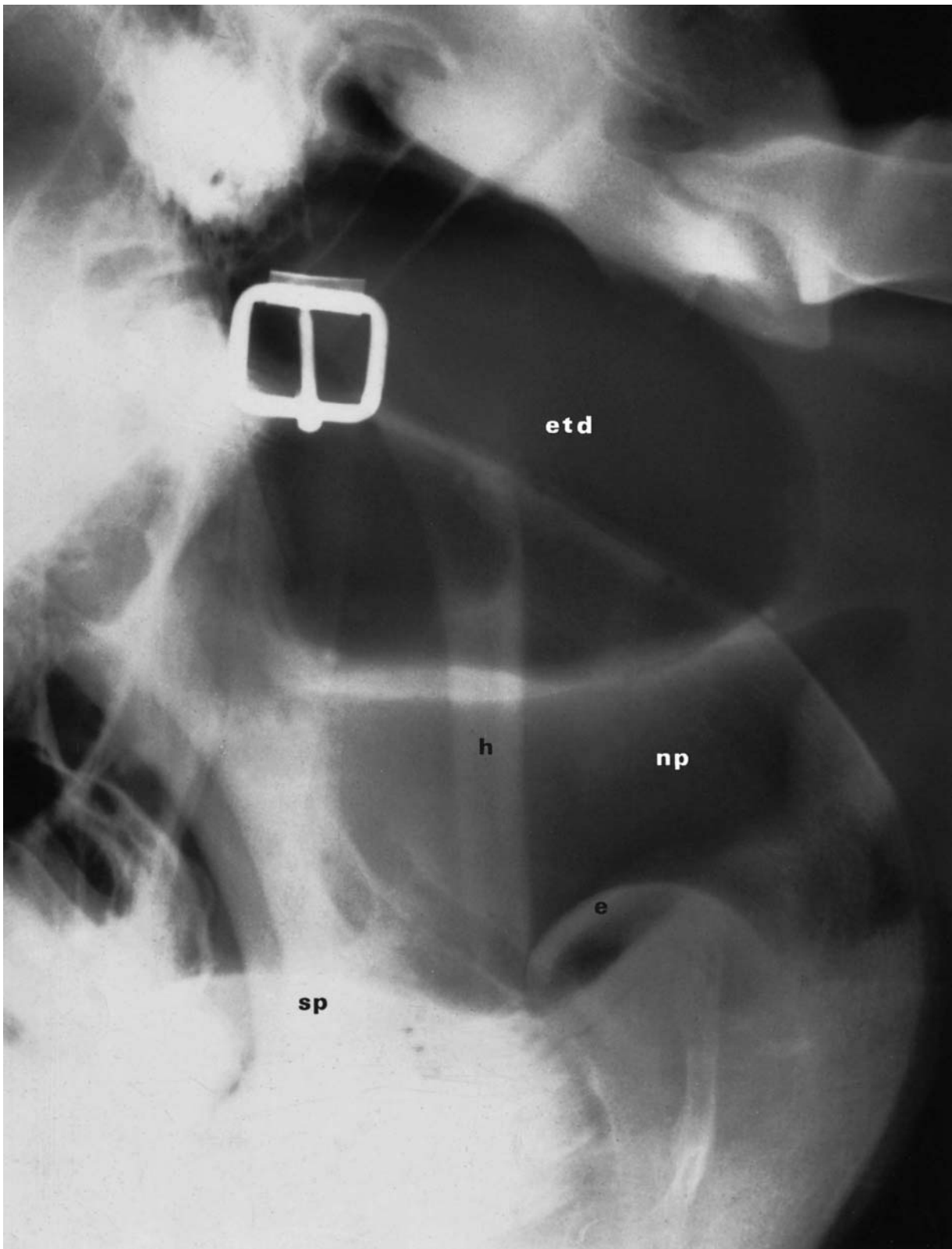
Figure 8.31(b) Slightly oblique view and diagram of the pharyngeal region of a normal adult horse. Note that the cranial angles of the left and right mandibles are slightly separated, indicating slight obliquity. There is gas in the Eustachian tube diverticulum (etd) and the nasopharynx (np). The epiglottis (e), soft palate (sp) and stylohyoid bones (h) are clearly demarcated.
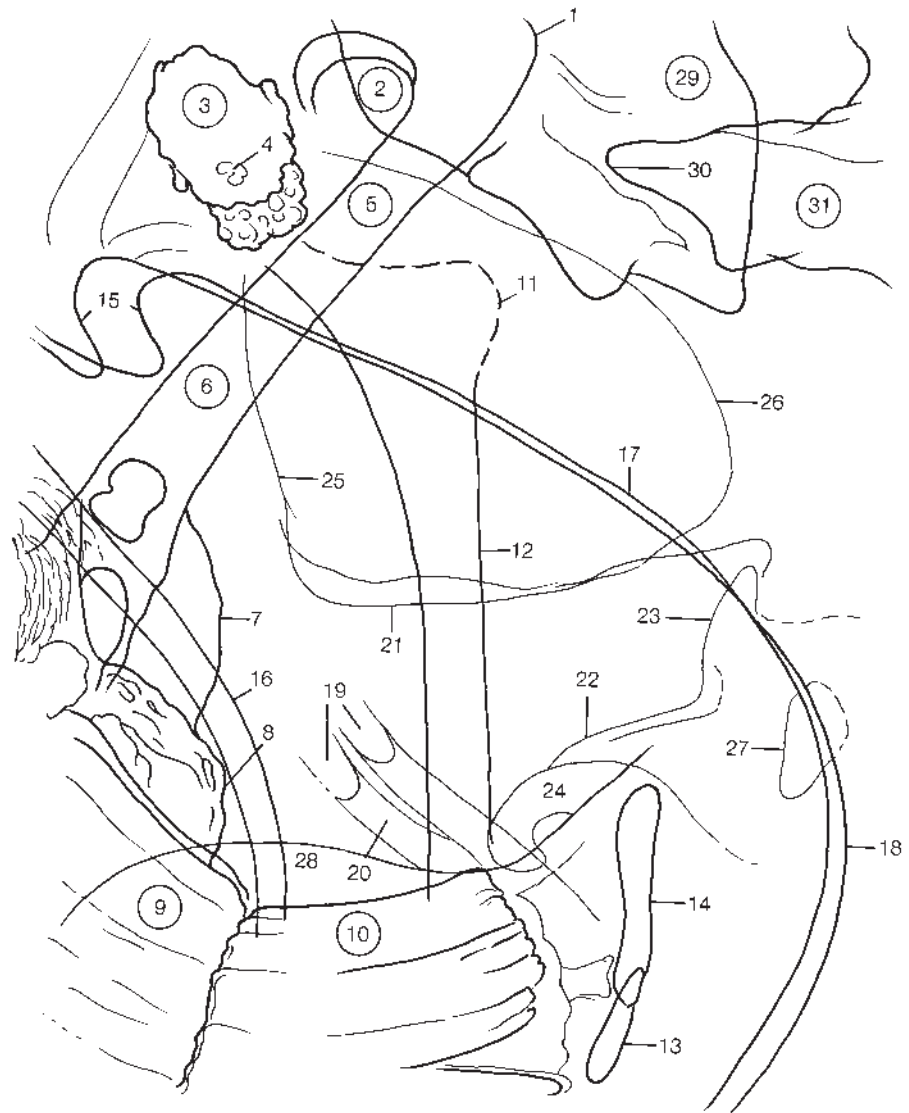
Figure 8.31(b) *Cont'd* 1 = Occipital condyle, 2 = hypoglossal foramen, 3 = petrous temporal bone, 4 = external acoustic meatus, 5 = basioccipital bone, 6 = body of basisphenoid bone, 7 = pterygoid process, 8 = maxillary tuberosity, 9 = third upper molar tooth, 10 = third lower molar tooth, 11 = stylohyoid angle, 12 = stylohyoid, 13 = basihyoid, 14 = thyrohyoid, 15 = condyloid process of mandible, 16 = ramus of mandible, cranial edge, 17 = ramus of mandible, caudal edge, 18 = angle of mandible, 19 = mandibular foramen, 20 = mandibular canal, 21 = dorsal wall of pharynx, 22 = aryepiglottic fold, 23 = arytenoid cartilage, 24 = epiglottis, 25 = cranial wall of Eustachian tube diverticulum (guttural pouch), 26 = caudal wall of Eustachian tube diverticulum (guttural pouch), 27 = laryngeal ventricles, 28 = soft palate, 29 = axis (first cervical vertebra), 30 = dens, 31 = atlas (second cervical vertebra).

SIGNIFICANT FINDINGS

Eustachian tube diverticulum empyema

Although probably becoming a less common condition, this may be seen in areas with a large population of horses. It usually follows a streptococcal infection, particularly *Streptococcus equi*. Clinically there is usually a unilateral offensive purulent nasal discharge.

[388]
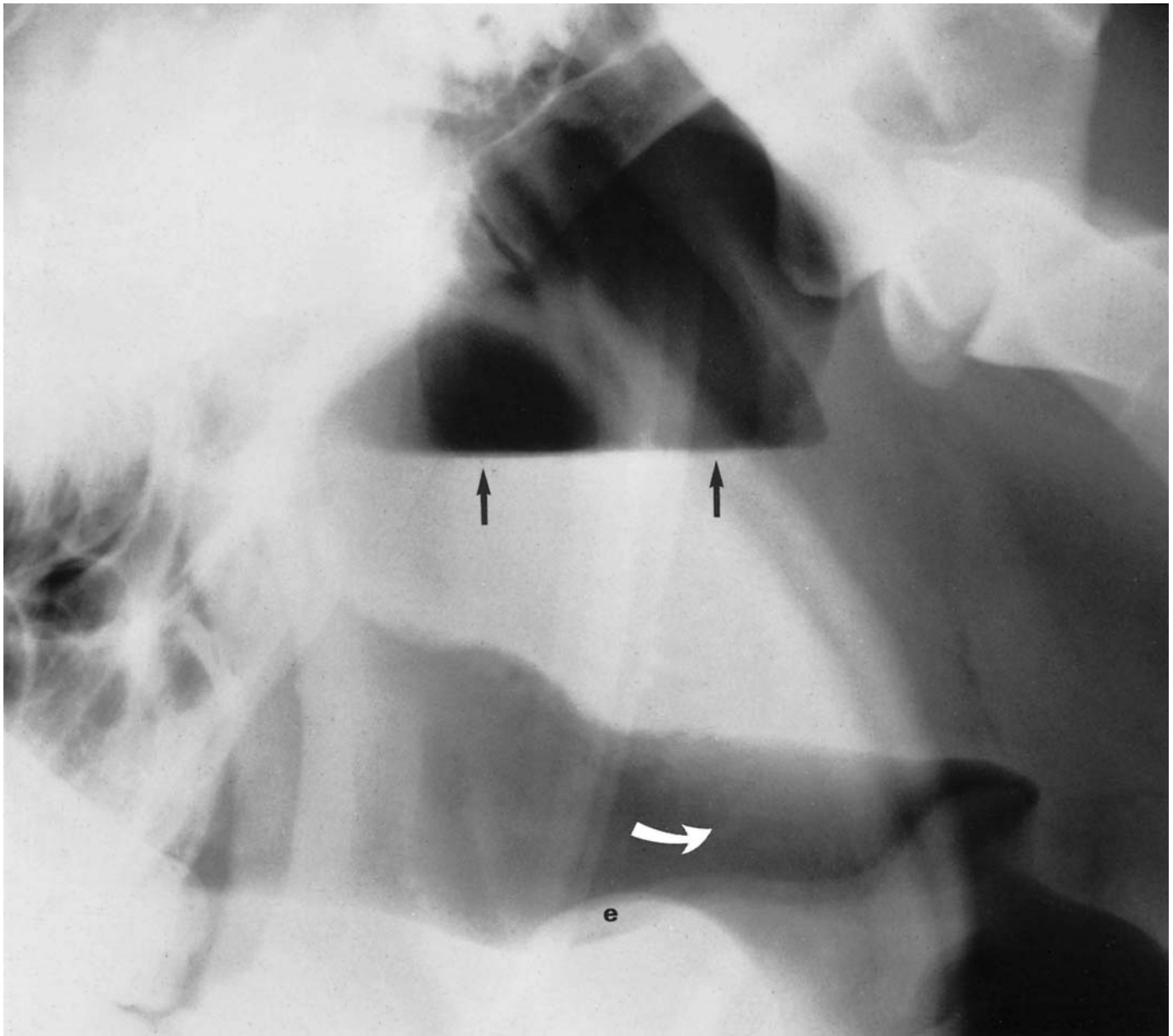
Figure 8.32 Lateral view of the pharyngeal region of a 2-year-old Thoroughbred with a history of nasal discharge and an occasional cough. There is a fluid line (straight arrows) in one or both Eustachian tube diverticula. The ventral half of the diverticulum is uniformly opaque due to the accumulation of pus, i.e. empyema. Note also the irregular outline of the dorsal pharyngeal wall, and the fine mottled opacities (curved arrow) in the dorsal nasal pharynx. This represents pharyngeal lymphoid hyperplasia. The epiglottis (e) is normal.

Empyema may fill one or both pouches (Figure 8.32), giving an increase in radiopacity of the diverticulum. There is normally a fluid line in the diverticulum, which aids differentiation from a soft-tissue mass. It is possible to determine if the condition involves one or both pouches by obtaining ventrodorsal views. It may be easier, however, to obtain radiographs from the left and right sides. The radiographs are compared for magnification and sharpness of the fluid line. The air cap appears larger and less sharp when

[389]

Figure 8.33 Lateral view of the pharyngeal region of an 8-year-old pony. There are many well-circumscribed opaque masses within the Eustachian tube diverticulum. These are chondroids, a sequel to *Streptococcus equi* infection.

away from the cassette. It is often possible to obtain a further radiograph with the nose of the horse elevated. This moves the fluid within the diverticulum, and allows assessment of the thickness of the cranial ventral margins. The thickness of the diverticular walls at this point gives some indication of the nature of the fluid and the chronicity of the condition.

The condition should initially be treated conservatively, but surgical drainage may be needed. A reasonable prognosis can be given for early cases, but if surgery is required the prognosis is guarded.

Eustachian tube diverticulum chondrosis

This condition is now unusual. It normally results from chronic empyema that has been inadequately treated. If it occurs as a sequel to strangles the horse may be a permanent carrier and potential shedder of *Streptococcus equi*. The chondroids seen on radiographs are smooth, irregularly shaped radiopaque masses within the diverticula (Figure 8.33). Although some

[390]
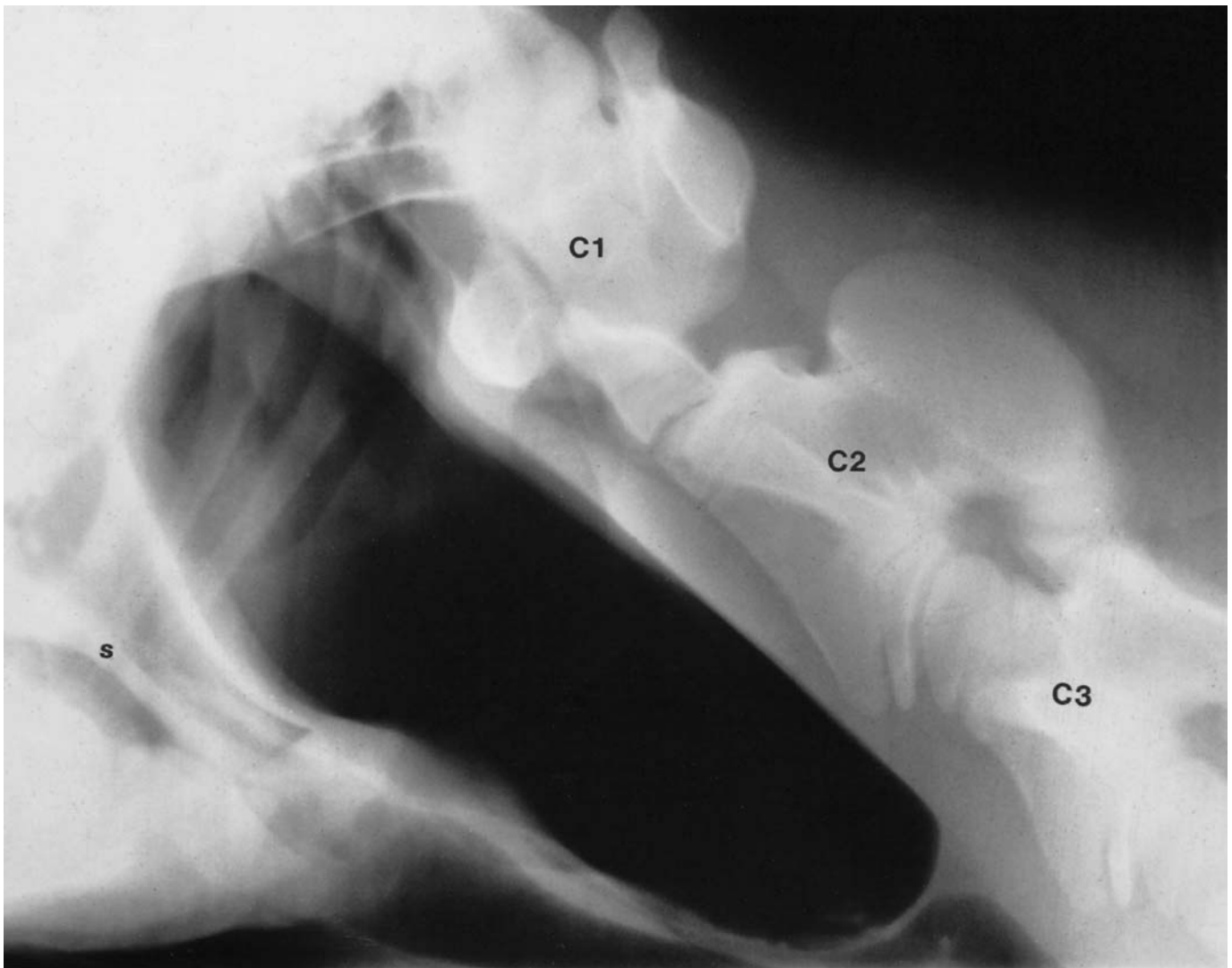
Figure 8.34 Right lateral view of the pharyngeal region of a 1-month-old Arab. The soft tissues in the parotid region were noted to be enlarged soon after birth and progressively enlarged and became more fluctuant. Both Eustachian tube diverticula are markedly distended with gas (air), and extend caudally to the level of the middle of the third cervical vertebra. This is consistent with bilateral Eustachian tube diverticula tympany. Note also gas in the oesophagus just caudal to the distended diverticula. The soft palate (s) is delineated by air in the oropharynx. The epiglottis is flat against the soft palate.

cases are asymptomatic, removal of the chondroids may be indicated, especially if *Streptococcus equi* is cultured.

Eustachian tube diverticulum tympany

Tympany of the Eustachian tube diverticulum is most commonly seen in young animals. It generally presents clinically as a soft fluctuant swelling in the parotid area. In severe cases it may cause respiratory distress.

Radiographically it presents as a grossly enlarged Eustachian tube diverticulum, extending caudal to the atlas (Figure 8.34). There is some

rounding of the outline of the diverticulum, and often narrowing of the nasopharynx. Generally the condition is unilateral so that two distinct diverticular outlines can be seen. Occasionally bilateral cases occur.

The condition may arise from the presence of excessive soft tissue at the pharyngeal orifice, which acts as a valve and allows air into the pouch during deglutition but does not allow for the exit of air. As a sequel to the condition, there may be respiratory distress due to narrowing of the pharynx, and in some cases aspiration pneumonia. For this reason, radiographs of the thorax should also be obtained.

Cases may resolve spontaneously as the horse ages, but usually require surgical treatment.

Eustachian tube diverticulum mycosis

Radiographically this is an unrewarding condition. Fluid lines may be seen in the Eustachian tube diverticulum, or there may be no radiological abnormality on plain radiographs. This is a life-threatening condition, and angiography of the carotid tree may be useful in diagnosis and treatment (see page 565).

The condition can present as slight or massive spontaneous epistaxis, usually when at rest. In a minority of cases it may present as difficulty in deglutition, Horner's syndrome, or as other signs of damage to the cranial nerves. The condition is thought to result from mycotic infection of an aneurysm, generally but not always involving the internal carotid artery.

Eustachian tube diverticulum masses

A number of masses are seen in association with the Eustachian tube diverticulum. The most common is enlargement of the parotid or retropharyngeal lymph nodes (Figure 8.35), which may impinge on the wall of the diverticulum and give the appearance of a mass involving the Eustachian tube diverticulum. Similarly, cysts and abscesses may give this appearance.

Tumours of the pouch have been recorded, the most common being a squamous cell carcinoma.

Pharyngeal lymphoid hyperplasia

This condition is seen radiographically as a diffuse mottled increase in soft-tissue opacity of the pharyngeal wall (see Figure 8.32, page 389). This is frequently recognized in the racing Thoroughbred, but may be a normal phenomenon in the development of all young horses. It may cause some respiratory noise and respiratory obstruction, but its effect on performance is uncertain. Treatment is by conservative management, and it has a good long-term prognosis.

[392]
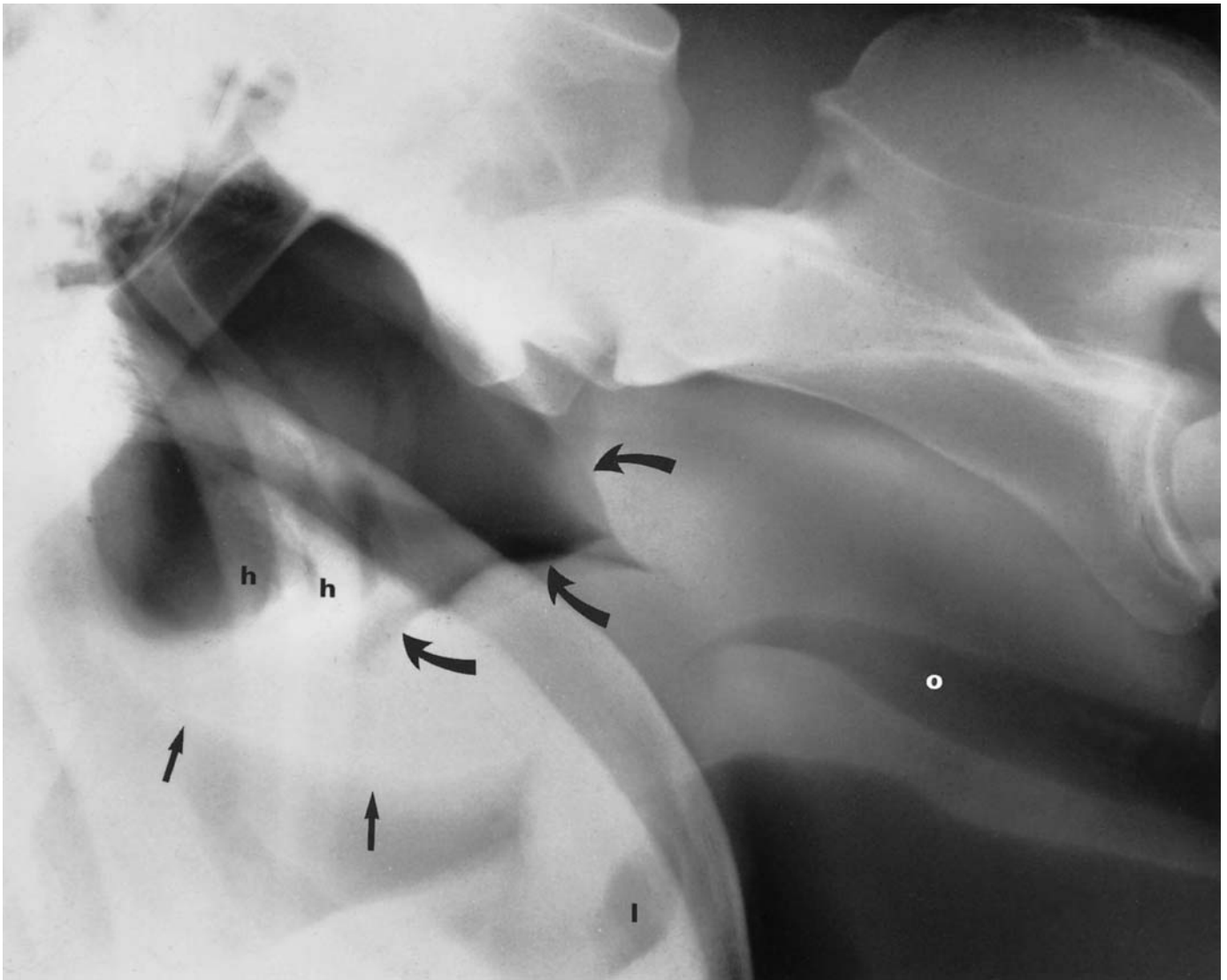
Figure 8.35 Lateral view of the pharyngeal region of a 4-year-old Quarterhorse with a 3-day history of dysphagia. Clinical examination revealed eighth and ninth cranial nerve deficits and bilateral nasal discharge containing food. The ventral margins of the Eustachian tube diverticula (ETD) are irregular (straight arrows) and there is soft-tissue swelling in the retropharyngeal area impinging on the ventral caudal aspect of the ETD (curved arrows). There is air in the oesophagus (o) and the lateral saccules (l). The stylohyoid bones (h) are normal. The caudal ventral soft-tissue mass is due to retropharyngeal lymphadenopathy and local inflammation, caused by infection with *Streptococcus equi*. Compare with Figure 8.33.

Fracture and osteomyelitis of the stylohyoid bone

It is thought that osteomyelitis of the stylohyoid bone may be followed by pathological fracture, and for this reason these two apparently separate conditions are treated here as one.

The condition can be seen on lateral radiographs, although slightly oblique views may be necessary to determine whether the left or right bone is involved. Fracture of the stylohyoid bone can also be seen in isolation (Figure 8.36).

[393]
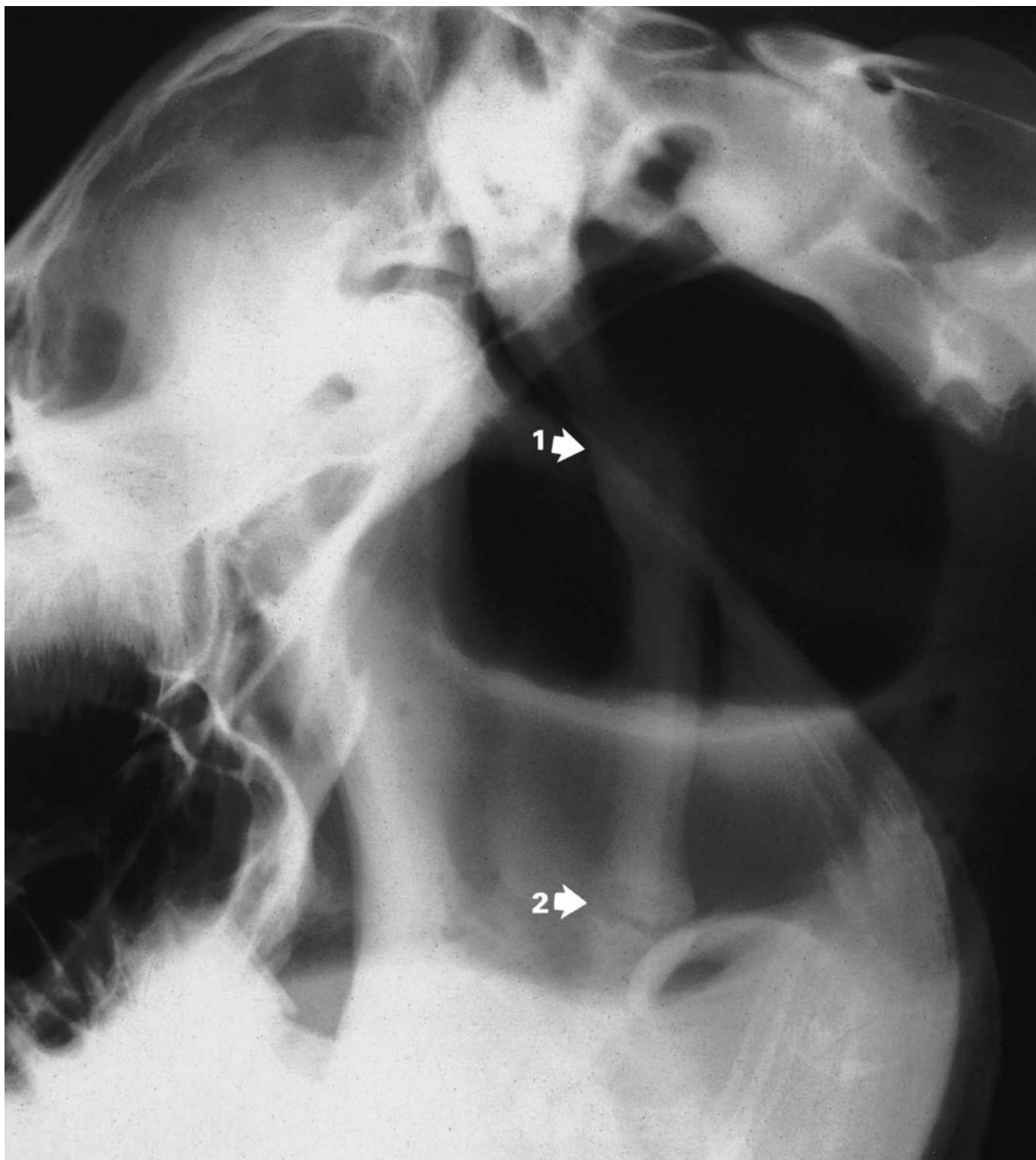
Figure 8.36 Lateral radiograph of the pharyngeal region of a 15-year-old Quarterhorse. The mare had exhibited transient facial nerve paralysis 12 months previously, which had recently recurred. There is an old healed fracture of the stylohyoid (arrow 1) and a delayed union fracture further distally (arrow 2). Note the flaring of the ends of the bone at the fracture site (2), and slight sclerosis along the fracture margins, typical of a delayed union. A normal epiglottis is partially superimposed over the distal fracture piece.

[394]

Epiglottic entrapment

In this condition the apex and lateral margins of the epiglottis become enveloped by the ventral mucosa and aryepiglottic folds (Figure 8.37). The radiographic appearance is somewhat varied, but the epiglottis always appears blunted and shortened. It should be confirmed by endoscopy, and must be differentiated from epiglottic shortening (see below). There may be concurrent dorsal displacement of the soft palate, but this is inconsistent.

Clinically the horse shows exercise intolerance and abnormal respiratory sounds at high speeds, but is asymptomatic at rest. Treatment is surgical and carries a reasonable prognosis.

Epiglottic shortening

Abnormal shortness of the epiglottis may predispose to dorsal displacement of the soft palate or entrapment of the epiglottis by the aryepiglottic folds. The length of the epiglottis can only be objectively radiographically assessed by taking into account magnification. Radiopaque markers of known length (Al and Ar) must be taped to the right and left sides of the horse's neck. The length of these markers on a lateral radiograph should be measured (Rl and Rr), together with the distance between the tip of the epiglottis and the thyroid cartilage (Re). The formula for correction for magnification to determine the actual epiglottic length (Ae) is as follows:

$$Ae/Re = (Al/Rl + Ar/Rr)/2$$

Normal values have been recorded for the Thoroughbred (8.76 ± 0.44 cm) and Standardbred (8.74 ± 0.38 cm).

A horse with an abnormally short epiglottis is usually asymptomatic at rest, but may show exercise intolerance and make an abnormal respiratory noise at high speed exercise.

Subepiglottic cysts

Subepiglottic cysts are believed to arise from remnants of the thyroglossal duct (Figure 8.38, page 397). They are visualized as well-circumscribed radiopaque (soft-tissue) masses under the ventral aspect of the base of the epiglottis. They displace the epiglottis in a caudodorsal direction. Treatment is surgical and carries a reasonable prognosis.

Arytenoid chondritis

Arytenoid chondritis causes exercise intolerance and abnormal respiratory noise. The arytenoid cartilages may have a mottled increase in opacity or an irregular outline, particularly of the cranial margin of the cartilage (Figure 8.39, page 398). They may also have some mineralization, which may occasionally be seen incidentally in old animals, where there is more generalized involvement throughout the laryngeal cartilages (Figure 8.40, page 399). If

[395]
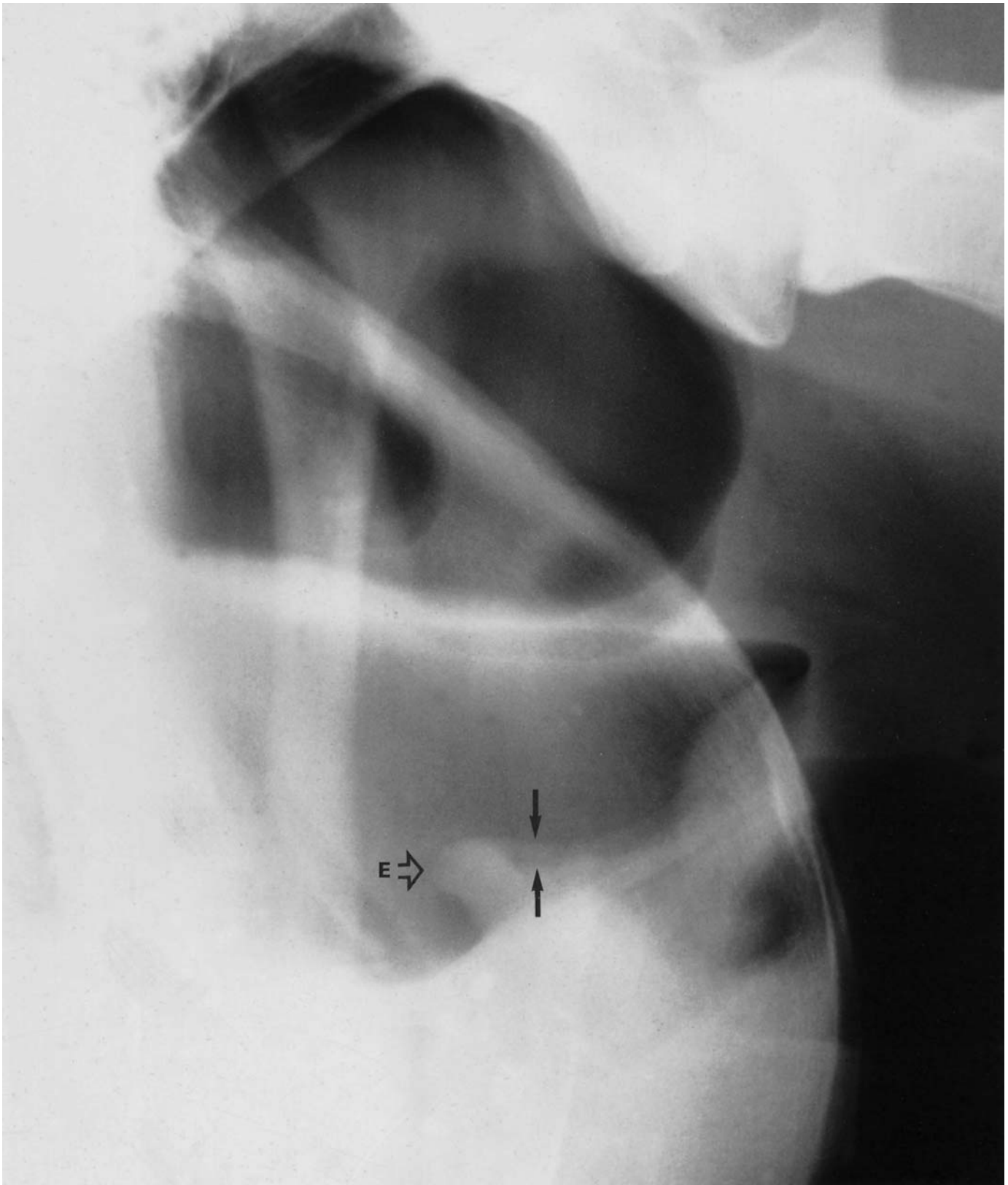
Figure 8.37 Lateral view of the pharyngeal region of a 4-year-old Quarterhorse. Note the blunted appearance of the epiglottis (E, open arrow), which does not have a normal curvature. The epiglottis is entrapped by the aryepiglottic folds (arrows). There is gas in the nasopharynx and in the Eustachian tube diverticula.

[396]

Figure 8.38 Lateral view of the pharyngeal region of a 1-month-old Standardbred colt, with a history of dyspnoea following suckling or strenuous exercise. There is a smoothly outlined soft-tissue opacity (arrows), ventral to the epiglottis (e), in the oropharynx. The mass, a subepiglottic cyst, appears to displace the soft palate (sp) dorsally above the epiglottis, but the area between the soft palate, epiglottis and subepiglottic cyst cannot be defined. Note air in the oesophagus (o) and the trachea (t).

the condition is unilateral a breeding horse may be treated conservatively, but surgery is usually required to return a horse to athletic function or if the condition is bilateral.

Dorsal displacement of the soft palate

Dorsal displacement of the soft palate may be intermittent or persistent, with the soft palate located dorsal to the epiglottis (Figure 8.41, page 400). The presence of air between the tongue and soft palate is usually the first radiographic abnormality noticed. Careful examination of the radiograph may show the caudal part of the soft palate lying over the epiglottis. This is a dynamic condition, and so may not be seen on plain radiographs. It is

Figure 8.39 Lateral view of the pharyngeal region of an 11-year-old hunter with a history of exercise intolerance and an abnormal respiratory noise. Endoscopic examination of the larynx revealed distortion in shape of the arytenoid cartilages, i.e. arytenoid chondropathy (chondritis). Radiographically there is extensive well-defined soft-tissue swelling (arrows) on the craniodorsal aspect of the larynx (in some cases there may also be ill-defined mineralization within the arytenoid cartilages).

most likely to be demonstrated immediately after the horse swallows, and may be more easily confirmed by endoscopy or radiographic screening. This condition has been reported in horses that have shown no clinical signs of exercise intolerance.

Cleft palate

This condition is most commonly seen in foals, but may not be diagnosed in some animals until quite late in life. Careful evaluation of lateral radiographs may reveal the presence of a double soft palate shadow.

[398]

Figure 8.40 Lateral view of the pharyngeal region of an aged Thoroughbred. The head is slightly extended to improve visualization of this area. There is partial mineralization of the laryngeal cartilages. This was an incidental radiological finding.

Positive contrast studies (barium swallows, see page 536) may reveal the presence of contrast agent dorsal to the soft palate. If clinically significant, these cases frequently develop aspiration pneumonia, and so assessment of the thorax should be carried out.

Confirmation of the diagnosis by endoscopy is necessary to determine the extent of the cleft. In mild cases, conservative treatment is often sufficient. In more extensive cases, surgery may be necessary, but does carry a very guarded prognosis.

Multilobular osteoma (chondroma rodens)

Multilobular osteoma is not common, but has a characteristic radiographic appearance. It is a well-defined mass with clearly demarcated undulating
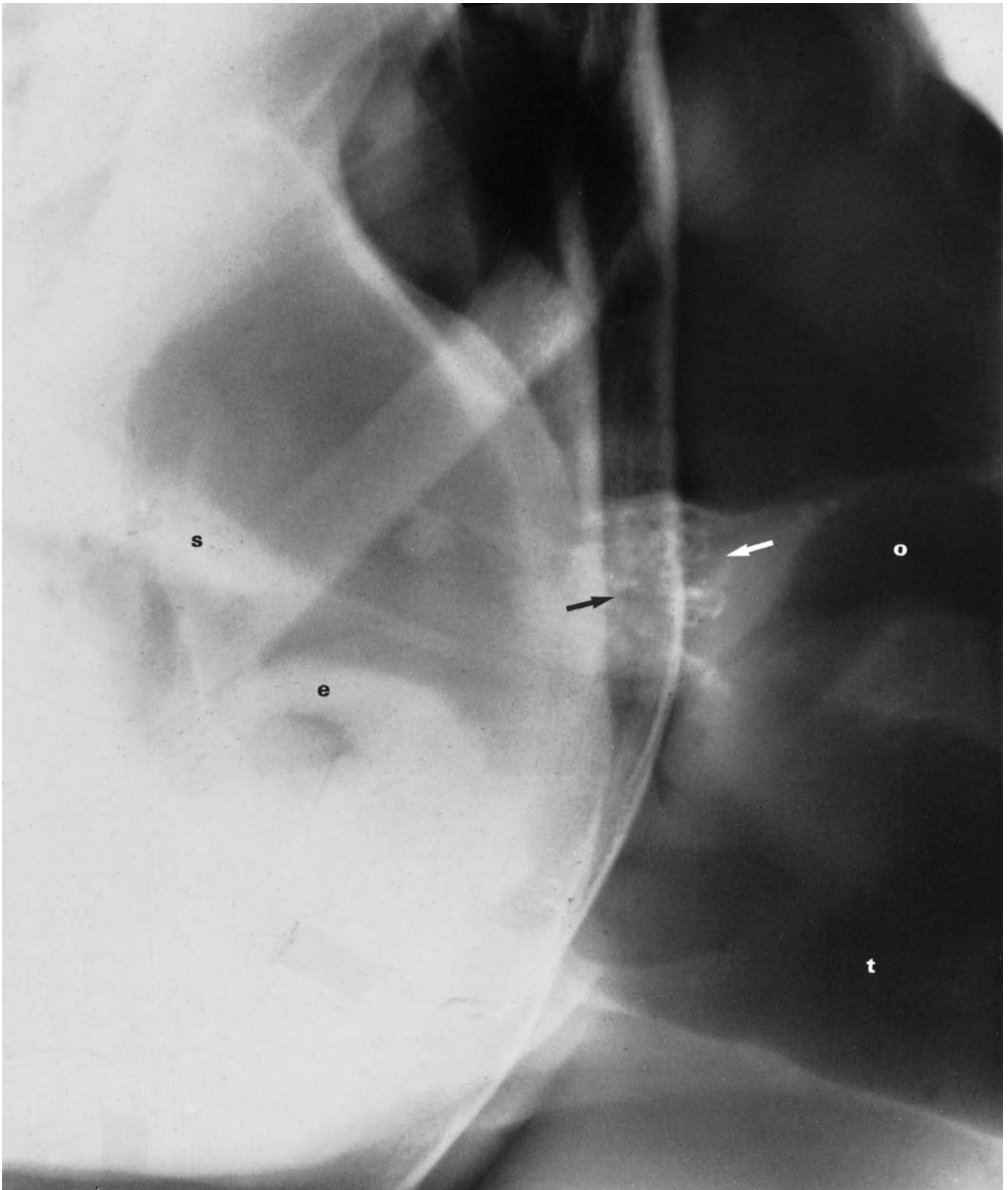
Figure 8.41 Lateral view of the pharyngeal region of an aged Thoroughbred. The soft palate (s) is displaced dorsally to the epiglottis (e). There is an area of diffuse mineralization (arrows) in the dorsocaudal nasopharynx. Note gas in both the trachea (t) and the oesophagus (o).

[400]

borders and a homogeneous stippled internal radiopacity. Clinical signs depend on the location of the mass in the skull. The mass usually enlarges slowly. Surgical removal is indicated.

Aneurysmal bone cyst

Aneurysmal bone cysts are rare in the horse, but have been reported in the mandible and the long bones. The lesion is characterized radiographically by an expansile relatively lucent lesion, traversed by opaque incomplete septa. The overlying cortex is thinned and there is usually extensive periosteal new bone formation.

Luxation of the temporomandibular joint

Temporomandibular joint luxation is usually the result of trauma, and may occur unilaterally or bilaterally. There may be associated fractures. Oblique radiographic views may be required to separate the two joints. There is usually associated malocclusion of the molars. The radiographs should be inspected carefully for the presence of concurrent fractures.

FURTHER READING

Ackerman, N., Coffman, J. and Corley, E.A. (1974) The spheno-occipital suture of the horse: its normal radiographic appearance. *J. Am. Vet. Rad. Soc.*, **15**, 79–81

Acland, H.M., Orsini, J.A., Elkins, S., Lee, J.W., Lein, D.H. and Morris, D.D. (1984) Congenital ethmoid carcinoma in a foal. *J. Am. Vet. Med. Ass.*, **184**, 979–981

Baker, G.J. (1971) Some aspects of equine dental radiology. *Equine Vet. J.*, **3**, 46–51

Boles, C.L. (1975) Epiglottic entrapment and follicular pharyngitis: diagnosis and treatment. *Proc. Am. Ass. Equine Pract.*, **21**, 29–34

Boles, C.L., Raker, C.W. and Wheat, J.D. (1978) Epiglottic entrapment by arytenoepiglottic folds in the horse. *J. Am. Vet. Med. Ass.*, **172**, 338–342

Cook, W.R. (1970) Skeletal radiology of the equine head. *J. Am. Vet. Rad. Soc.*, **11**, 35

Cook, W.R. (1973) The auditory tube diverticulum (guttural pouch) in the horse. Its radiographic examination. *J. Am. Vet. Rad. Soc.*, **14**, 51–71

Evans, L.H. (1981) Entrapment of the epiglottis. *Proc. Am. Ass. Equine Pract.*, **27**, 61–62

Ferraro, G.L. (1981) Equine follicular pharyngitis. *Proc. Am. Ass. Equine Pract.*, **27**, 55–56

Gibbs, C. (1974) The equine skull: its radiological investigation. *J. Am. Vet. Rad. Soc.*, **15**, 70–78

Gibbs, C. and Lane, J.G. (1987) Radiographic examinations of the facial, nasal and paranasal sinus regions of the horse. (ii) Radiological findings. *Equine Vet J.*, **19**, 474–482

Gibbs, C., Lane, J.G., Meynink, S.E. and Steele, F.C. (1987) Radiographic examinations of the facial, nasal and paranasal sinus regions of the horse. (i) Indications and procedures in 235 cases. *Equine Vet. J.*, **19**, 466–473

Haynes, P.F. (1981) Persistent dorsal displacement of the soft palate associated with epiglottic shortening in two horses. *J. Am. Vet. Med. Ass.*, **197**, 677–681

Haynes, P.F., Snider, T.G., McClure, J.R. and McClure, J.J. (1980) Chronic chondritis of the equine arytenoid cartilage. *J. Am. Vet. Med. Ass.*, **177**, 1135–1142

Jubb, K.V.F., Kennedy, P.C. and Palmer, N. (1985) *Pathology of Domestic Animals*, 3rd edn, Academic Press, Orlando

Lane, J.G. (1989) The management of guttural pouch mycosis. *Equine Vet. J.*, **21**, 321–324

Lavach, J.D. and Severin, G. A. (1977) Neoplasia of the equine eye, adnexa and orbit: a review of 68 cases. *J. Am. Vet. Med. Ass.*, **170**, 202–203

Linford, R., O'Brien, T., Wheat, J., *et al.* (1983) Radiographic assessment of epiglottic length and pharyngeal and laryngeal diameters in the Thoroughbred. *Am. J. Vet. Res.*, **44**, 1660–1666

Morgan, J.P. and Silverman, S. (1984) *Techniques of Veterinary Radiography*, 4th edn, Veterinary Radiology Associates, Davis, California

Richardson, J., Lane, J.G. and Day, M. (1994) Congenital choanal restriction in 3 horses. *Equine Vet. J.*, **26**, 162–165

Robert, M.C., Groenendyk, S.L. and Kelly, W.R. (1978) Ameloblastic odontoma in a foal. *Equine Vet. J.*, **10**, 91–93

Schmotzer, W.B., Haltgren, B.D., Watrous, B.J., Wagner, P.C. and Kaneps, A.J. (1987) Nasomaxillary fibrosarcomas in three young horses. *J. Am. Vet. Med. Ass.*, **191**, 437–439

Stilson, A.E., Hening, D.S. and Robertson, J.T. (1985) Contribution of the nasal septum to the radiographic anatomy of the equine nasal cavity. *J. Am. Vet. Med. Ass.*, **186**, 590–592

Theilen, G.H. and Madewell, B.R. (1979) *Veterinary Cancer Medicine*, Lea and Febiger, Philadelphia

Thrall, D.E. (1936) *Textbook of Veterinary Diagnostic Radiology*, W.B. Saunders, Philadelphia

Tulleners, E. (1991) Correlation of performance with endoscopic and radiographic assessment of epiglottic hypoplasia in racehorses with epiglottic entrapment corrected by use of contact neodymium: ytrium aluminum laser. *J. Am. Vet. Med. Ass.*, **198**, 621–626

Chapter 9
The Spine

Cervical spine

Indications for radiographic examination of the cervical vertebrae include abnormal head and or neck posture, swelling, stiffness or pain of the neck, trauma to the neck, ataxia, inability to stand and, occasionally, forelimb lameness. Radiographic assessment of such cases requires at least lateral radiographs of the occipital bone, all cervical vertebrae, and the first thoracic vertebra. Lateral radiographs are best obtained with the horse standing, but can be obtained with the horse in lateral recumbency, under general anaesthesia. Ventrodorsal views can only be obtained in the recumbent horse.

RADIOGRAPHIC TECHNIQUE

Equipment

Good quality views of the cranial and mid-neck regions are within the capability of portable x-ray machines, but views of the seventh cervical (C7) and first thoracic (T1) vertebrae require more powerful equipment in all but the smallest horses. Fast rare earth screens and appropriate film are recommended. A grid, although beneficial, is not essential for the cranial part of the neck, but is necessary for the caudal one-third.

In order to assess the relative alignment of the cervical vertebrae it is helpful to use large cassettes (35 cm × 43 cm) so that part of at least three vertebrae is projected on each film. The cassette should be supported in a cassette holder, which is mounted on a wall or mobile stand. If the cassette holder is not linked to the x-ray machine, alignment can be difficult, and it is helpful to mark the neck on both sides at the sites where the x-ray beam is to be centred. This is easily done using sticky tape.

Positioning

Radiography of the head and neck in the standing horse renders the handler particularly at risk to exposure to radiation, and appropriate precautions including wearing lead gloves are important. If the area to be radiographed involves the occipito-atlantal articulation, a rope halter should be used rather than a head collar with metal buckles, in order to avoid artefacts.

The standing horse

Slightly oblique radiographic views are difficult to interpret, and in most circumstances true lateral views are essential. Many horses are apprehensive of the x-ray machine and the cassette, especially when these are close to the head. To minimize movement of the horse it may be helpful to restrain it in stocks; sedation with either xylazine romifidine or detomidine is useful as it causes the horse to lower its head and neck. The horse usually moves less and it is more likely to hold the head and neck in the sagittal plane. It has the disadvantage that the neck may be flexed relative to the normal standing position; thus the alignment of the vertebrae is altered. In some horses it is not possible to obtain true lateral projections of all the cervical vertebrae, despite appropriate positioning. This usually reflects abnormal modelling of the caudal synovial facet joints, which results in a permanent slight rotation of the more cranial vertebrae. Occasionally it is the result of abnormal muscle spasm due to pain.

Lead markers placed on the skin of the neck above the level of the vertebrae can be helpful for orientation when taking and interpreting radiographs. Complete radiographic assessment of the cervical vertebrae (C1–C7) of an adult horse usually requires at least four views: the occiput and C1 (atlas); C1–C3; C3–C5; and C5–C7.

In many cases a fifth view is required to evaluate the seventh cervical vertebra and its articulation with the first thoracic vertebra. Radiographs are obtained with the horse standing with its head and neck in the sagittal plane. The x-ray beam is aligned perpendicular to the neck. In the caudal half of the neck the cervical vertebrae are situated ventrally, and the x-ray beam should be centred accordingly. It is usually easiest to radiograph the mid-neck region first, and then the more caudal area, before examining the cranial part. This allows the horse to become familiar with the equipment before it is placed close to the head.

It is sometimes helpful to obtain both left to right and right to left projections in order to establish on which side of the neck a lesion is situated. The lesion is smaller and more clearly defined when closer to the cassette.

The anaesthetized horse

In order to obtain true lateral projections when the horse is in lateral recumbency, it is necessary to support the head and neck, using radiolucent cushions, so that it lies horizontally from the shoulder to the head. Aligning the x-ray machine and the cassette with the horse in this position may be difficult, but longer exposure times can be used than when the horse is standing. The neck may be flexed passively in order to accentuate a subluxation seen in a lateral view, but care must be taken neither to kink the endotracheal tube nor to exacerbate a potential spinal cord compression.

Ventrodorsal views can only be obtained safely in a recumbent horse. Even with high-output x-ray machines it is difficult to get good-quality

radiographs caudal to the fifth cervical vertebra because of the surrounding muscle mass. Myelography is discussed in Chapter 13 (page 570).

NORMAL ANATOMY, VARIATIONS AND INCIDENTAL FINDINGS

There are seven cervical vertebrae (C1–C7). In the resting position the neck is S-shaped with a smooth transition of angulation between the vertebrae, from slight flexion (dorsal convexity) cranially, to slight extension (dorsal concavity) caudally. This is particularly obvious in foals and small ponies. Apparent hyperflexion/subluxation at the articulation between the second and third (see Figure 9.13, page 418) or third and fourth vertebrae may occur without clinical signs, in horses with a wide dorsoventral diameter of the vertebral foramen (minimum sagittal diameter).

The cervical vertebrae, other than the atlas, have a similar basic shape. The two sides of the vertebral arch (pedicles), its roof (lamina) and the body of each vertebra form the vertebral foramen in which lies the spinal cord (Figure 9.1). The series of vertebral foramina together constitute the vertebral canal. Within each vertebra the vertebral foramen appears approximately rectangular in shape (Figure 9.2). The minimum sagittal diameter (MSD) can be measured directly from a radiograph (Figure 9.2b). This is useful for comparison between vertebrae, but comparison between horses can be unreliable due to variable magnification. Comparison should only be made between horses of similar size (Table 9.1).
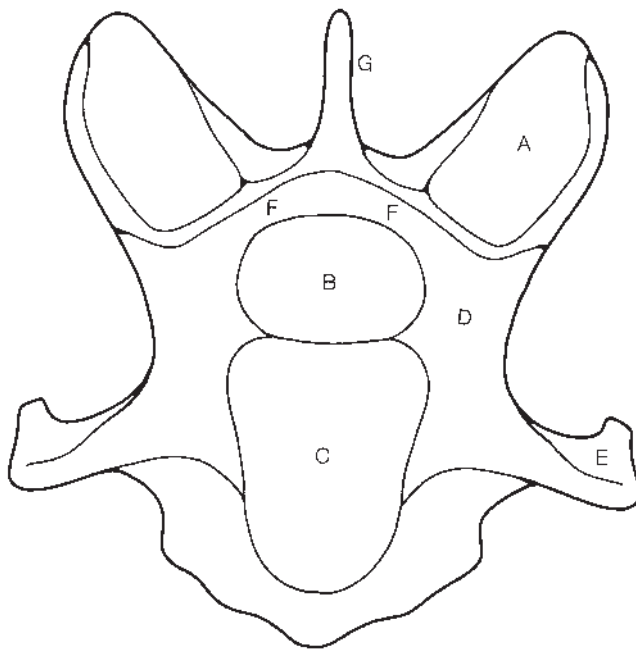
Figure 9.1 Craniocaudal view of the seventh cervical vertebrae of an adult horse. A = facet of cranial articular process, B = vertebral foramen, C = head of vertebral body, D = lateral vertebral arch or pedicle, E = transverse process, F = dorsal laminae, forming dorsal arch, G = spinous process.

Figure 9.2(a) Lateral view of the fourth to sixth cervical vertebrae of a normal adult horse.

In horses with severe stenosis of the vertebral canal, MSD measurements are sufficiently accurate to differentiate between normal and affected horses, but in less severe cases diagnosis can be difficult.

The problem of variable magnification between horses, due to differences in object–film distance, can be eliminated by use of a sagittal ratio method, rather than absolute measurements, which thereby standardizes the assessment of MSD between horses. The sagittal ratio is obtained by dividing the MSD value by the dorsoventral height of the corresponding vertebral body at the cranial aspect of its widest point (Figure 9.3a). Alternatively a corrected MSD can be used: the absolute MSD is divided by the length of the vertebral body (Figure 9.3b, page 408) (Table 9.2, page 408). Although these techniques are more objective methods of assessment of horses with generalized narrowing of the vertebral canal (see page 415), they are not reliable for identification of potential sites of spinal cord compression, giving false positive diagnoses. The sagittal diameter of the vertebral canal tends to be slightly smaller in the mid-cervical region compared with more cranial and caudal levels. The third, fourth and fifth cervical vertebrae are similar in shape (Figure 9.2), but the rest have distinctive characteristics.

[406]
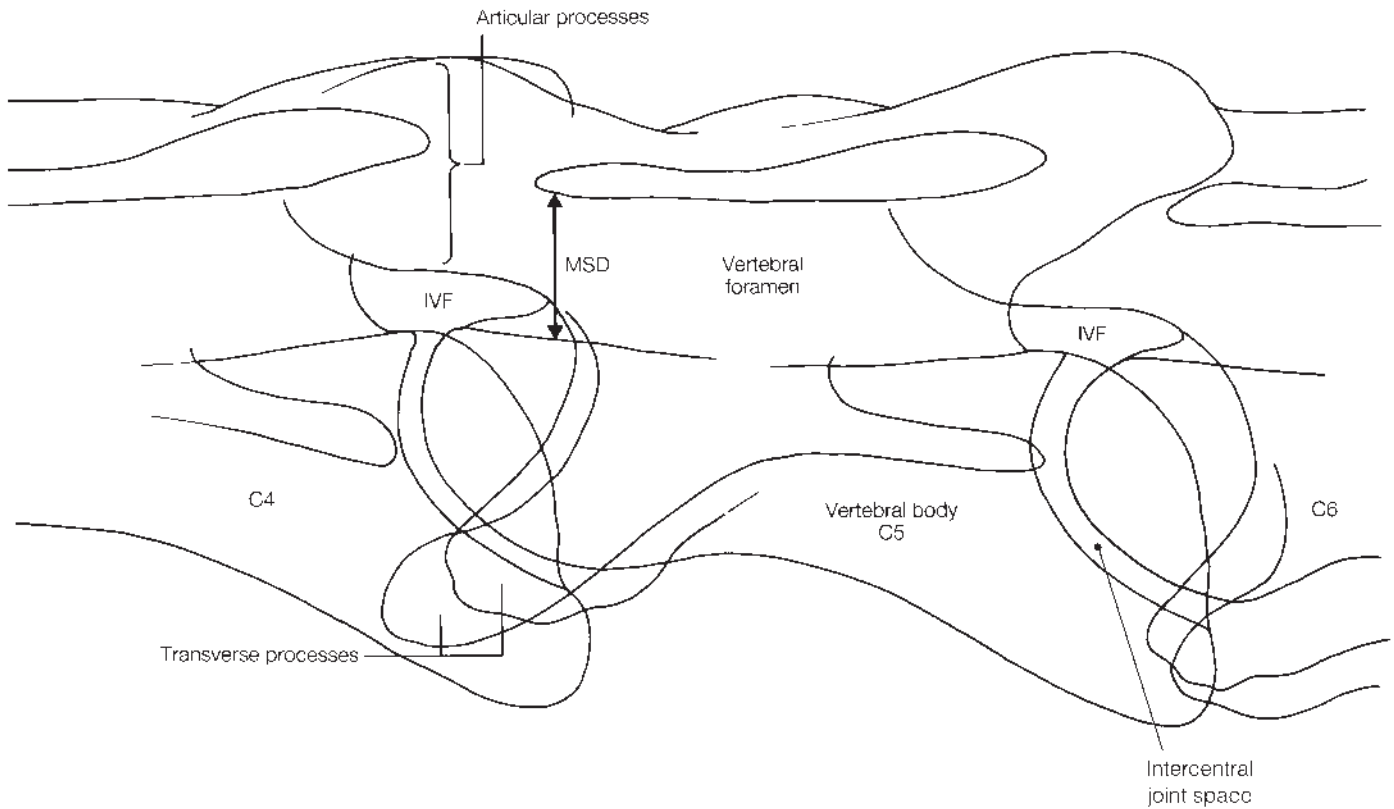
Figure 9.2(b) Diagram of Figure 9.2(a). IVF = intervertebral foramen, MSD = minimum sagittal diameter, C4 = fourth cervical vertebra, C5 = fifth cervical vertebra, C6 = sixth cervical vertebra.

Table 9.1 Minimum sagittal diameter (mm) of the vertebral foramen, measured from radiographs of clinically normal horses. (From Mayhew, Whitlock and de Lahunta, 1978, by permission)

| | Less than 320 kg body weight | | | | | |
	C2	C3	C4	C5	C6	C7
Mean	23.8	19.8	18.7	19.7	21.1	22.9
Standard deviation	1.5	0.9	1.0	1.2	1.5	1.6
Reference limits*	20.8	18.1	16.7	17.3	18.3	19.8
	26.8	21.5	20.7	22.1	23.9	26.1

| | More than 320 kg body weight | | | | | |
	C2	C3	C4	C5	C6	C7
Mean	26.7	22.2	21.3	22.4	24.1	27.4
Standard deviation	2.3	1.8	1.8	1.8	2.5	2.6
Reference limits	22.1	18.5	17.7	18.7	19.0	22.6
	31.3	25.9	24.9	26.1	29.1	32.6

*Maximum and minimum sagittal diameter which can be considered normal.

[407]

Table 9.2 Normal values for radiographic minimum sagittal diameter (MSD) (mm) and corrected MSD (cMSD) (%) for Thoroughbred foals, 3–7 months of age (From Mayhew *et al.*, 1993, by permission)

	C2	C2–C3	C3	C3–C4	C4	C4–C5	C5	C5–C6	C6	C6–C7	C7
						Cervical vertebral site					
MSD	23	28	20	25	20	25	21	26	21	31	23
Standard deviation	1	4	1	2	1	2	1	3	1	5	1
cMSD	18	33	24	30	24	31	25	34	27	46	35
Standard deviation	1	2	2	2	2	2	2	3	2	5	2
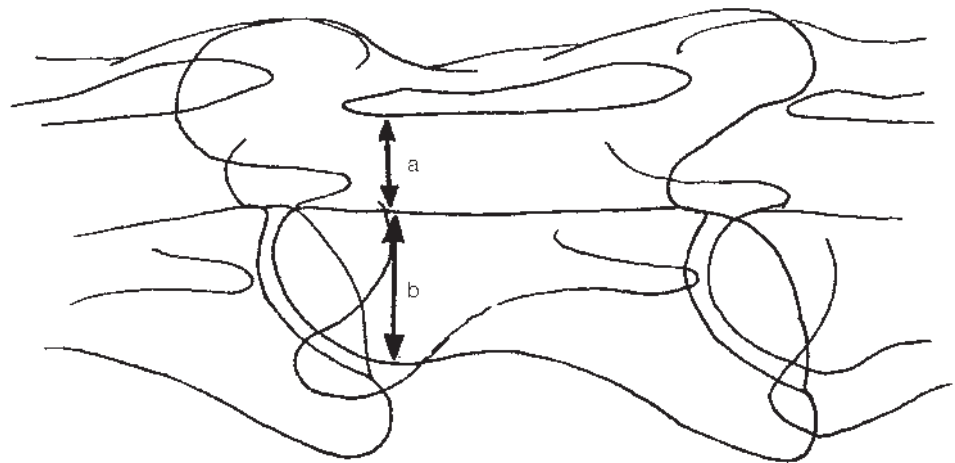
Figure 9.3(a) Method to obtain the sagittal ratio of the vertebral foramen. Divide the minimum sagittal diameter (MSD) (a) by the dorsoventral height (b) of the corresponding vertebral body at biggest point of its cranial aspect.
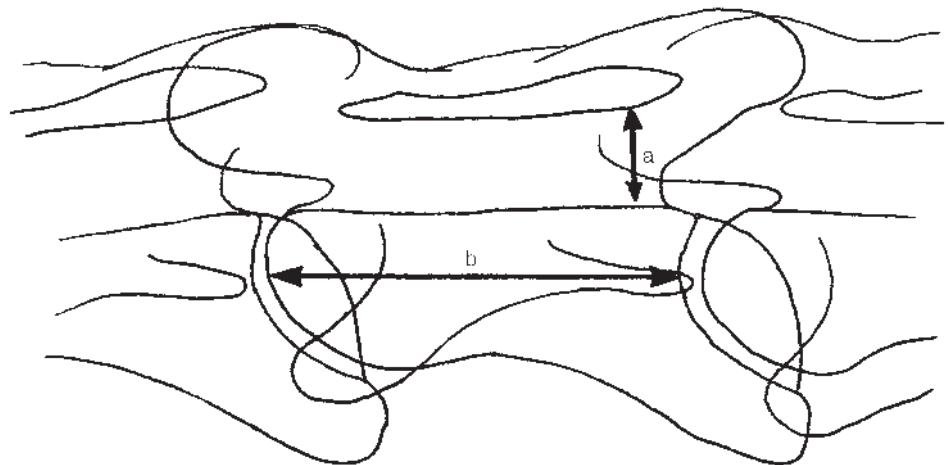
Figure 9.3(b) Method to obtain a corrected minimum sagittal diameter (cMSD). The absolute (measured) MSD (a) is divided by the length (b) of the corresponding vertebral body.

[408]

Figure 9.4 Lateral view of the cranial cervical vertebrae (C1–C3) of a 6-week-old Thoroughbred foal. Note the separate centre of ossification (arrowed) of the dens of the axis (C2). The cranial and caudal physes of C2 and C3 are open.

The atlas (C1) has no body or articular process. It develops in two lateral halves which gradually ossify. In a ventrodorsal view of a neonate, there is a longitudinal lucent line between the two halves.

The axis (C2) has separate centres of ossification for the dens (odontoid peg), head, body and caudal epiphysis (Figure 9.4). The dens fuses with the head at approximately 7 months (Figure 9.5). The cranial arch of C2 bears lateral vertebral foramina, the cranial borders of which are incomplete in young horses (Figure 9.7, page 412), and may remain as a notch in the adult. The dorsal spine usually has a smooth contour, but its cranial and caudal edges may be slightly irregular. Occasionally a small bony spur is seen on the dorsal aspect of the caudal epiphysis (Figure 9.6, page 411), projecting into the vertebral canal.

The vertebral bodies of the third to seventh vertebrae have cranial and caudal epiphyses. Closure of the physes occurs gradually, the time varying between individuals. Closure of the cranial physes starts ventrally (Figure 9.7, page 412) and is complete by approximately 2 years after birth. The caudal physes remain open until 4–5 years of age, closure starting

Figure 9.5 Lateral view of the occiput and cranial cervical vertebrae (C1 and C2) of a normal adult horse. Note the complete foramina in the cranial aspect of the axis (compare with Figure 9.7).

dorsally (Figure 9.7, page 412). The ventral processes of C6, and occasionally of other vertebrae, have small centres of ossification at their caudal limits which should not be confused with fractures (see Figure 9.12, page 417). The convex cranial articular surface of each vertebral body is usually smoothly curved or slightly flattened, and reasonably congruous with the concave caudal articular surface of the adjacent vertebra. The latter has a relatively sclerotic subchondral bone plate. Flattening of the joint surfaces or irregularity in width of an intercentral articulation should be regarded as abnormal (see page 423). It is helpful to compare the shape of adjacent vertebrae.

The third to seventh cervical vertebrae each have pairs of cranial and caudal articular processes projecting from the borders of the vertebral arch. The extremities of these processes carry articular surfaces (facets) which articulate with those of adjacent vertebrae, forming the cervical synovial articulations. The sixth cervical vertebra is different from C5; it is slightly shorter and it has a trifid transverse process. An extra ventral lamina or

[410]
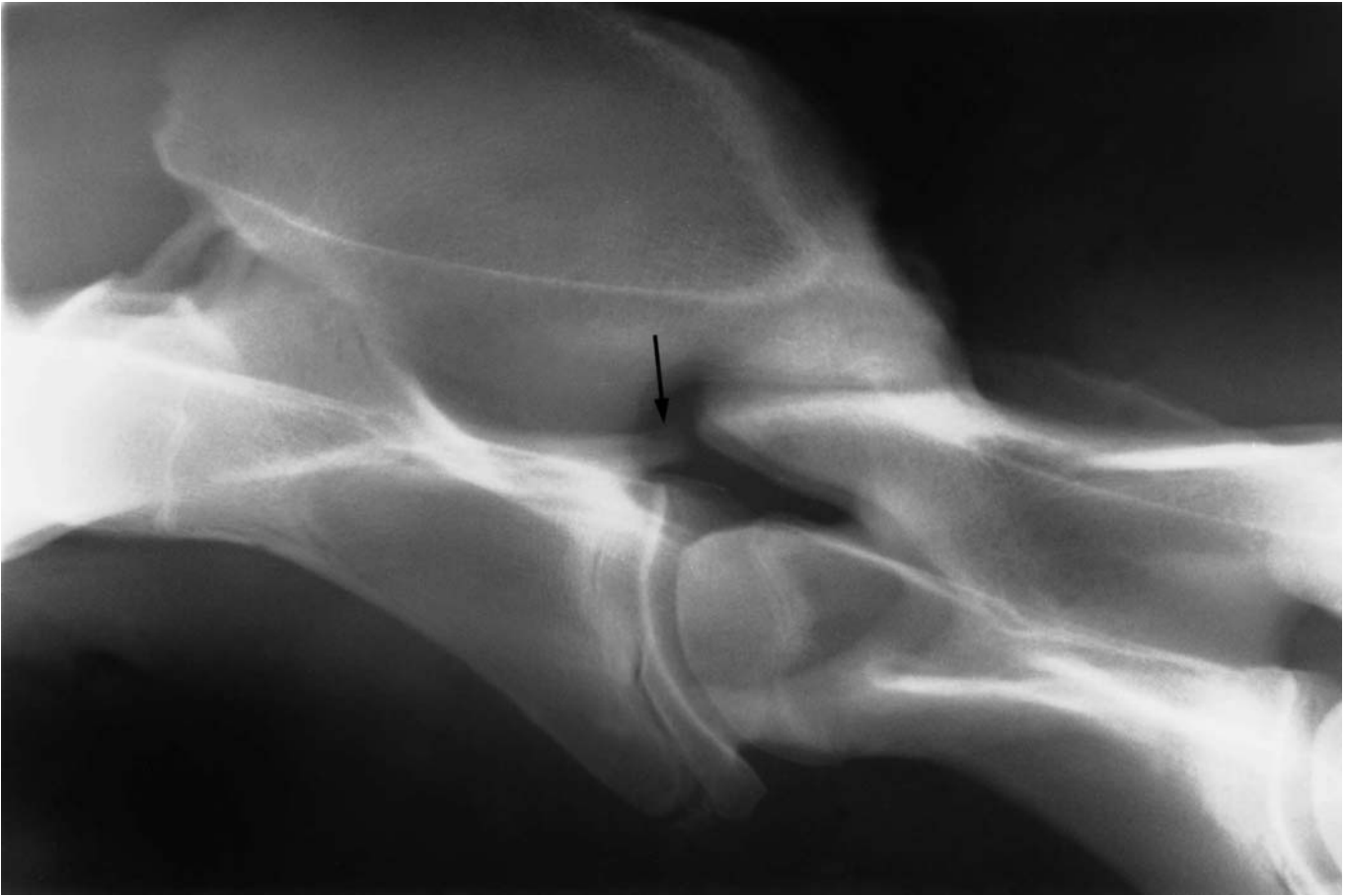
Figure 9.6 Lateral view of the cranial cervical vertebrae of a normal adult horse. There is a large spur (arrow) on the dorsocaudal aspect of the vertebral body of the axis (C2), protruding into the vertebral canal. This is a common incidental radiological finding. The large vertebral canal at this level makes it unlikely that the spur will impinge on the spinal cord.

process projects caudally and ventrally (Figure 9.8). Sometimes one or both of these processes may be transposed onto the ventral surface of C7 (see Figures 9.15–9.17, pages 420–22) or very rarely onto C5. When this transposition onto C7 occurs bilaterally, the ventral aspect of C6 has the same profile as C5. C7 is shorter than C6 and has a small dorsal spinous process. This may be superimposed over the synovial articulation between C6 and C7, and should not be confused with new bone associated with degenerative joint disease. The first thoracic vertebra has a larger dorsal spinous process (Figure 9.9, page 414).

In older horses, small spondylitic spurs are sometimes seen as incidental findings on the ventral surface of the vertebral bodies adjacent to one or more intercentral articulations (Figure 9.8, page 413). Modelling of the synovial joints of the dorsal articular process of the fifth and sixth and the sixth and seventh cervical vertebrae occurs commonly (see Figure 9.15, page 420) and is considered in more detail below ('Modelling of the cervical synovial articulations', page 418).
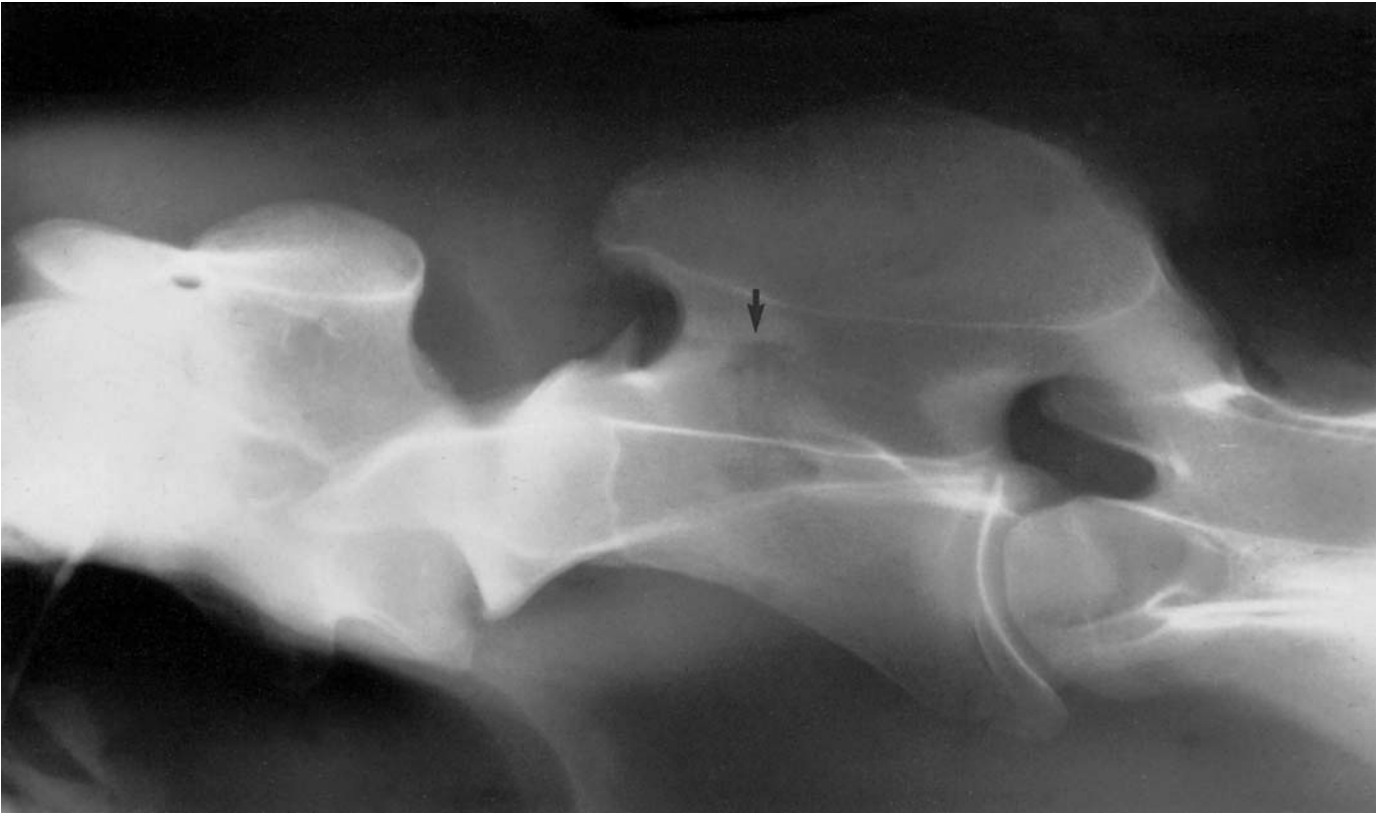
Figure 9.7 Lateral view of the cranial cervical vertebrae (C1–C3) of a normal Thoroughbred yearling. The cranial borders of the vertebral foramina of the axis (C2) are incomplete. The physes of C2 and C3 are not fully closed. The star-shaped lucent area (arrowed) in the vertebral arch of C2 is normal.

SIGNIFICANT RADIOGRAPHIC ABNORMALITIES

When assessing radiographs of the neck it is important not only to examine each vertebra, but also to consider the neck as a whole and to evaluate the shape of the vertebral canal, the alignment of the vertebral bodies, the shape and size of the epiphyses, the regularity of both the intercentral and synovial articulations, and the size of the intervertebral foramina. Comparison with radiographs of a normal horse of similar age, and with bone specimens, is often helpful. When the results of lateral survey radiographs are negative or equivocal it may be necessary to obtain dorsoventral views and/or to perform myelography (see Chapter 13, page 570).

Congenital abnormalities

Vertebral malformations are rare, and although neck stiffness, distortion of the neck and/or ataxia may be seen soon after birth, some lesions are not clinically apparent until the spinal cord becomes compromised.

Occipito-atlanto-axial malformation (OAAM)

This is the most common congenital abnormality, and is most often seen in Arab horses, in which it is thought to be familial. The vertebral defects may

[412]

Figure 9.8 Lateral view of the caudal cervical vertebrae (C5–C7) of a normal adult horse. The sixth cervical vertebra, which is slightly rotated, has ventral processes and is therefore different from both C5 and C7. Note the small spondylitic spur (arrowed) on the ventral aspect of C7. The articular processes of C6/C7 are larger than C5/C6 but are within the normal range (compare with Figure 9.15).

be symmetrical or asymmetrical and include fusion and a variety of distorted shapes (Figure 9.10). Lateral and ventrodorsal radiographic views are needed for proper assessment of this abnormality.

Vertebral fusion

Vertebral fusion may involve two or more vertebrae (Figure 9.11, page 416). Absence of irregular bony callus helps to distinguish congenital fusion from fusion following a fracture in a foal, but in an older horse the two may be indistinguishable once the callus has modelled.

Developmental abnormalities

The cervical vertebrae can undergo modelling during growth, influenced by the biomechanical stresses placed upon them and the rate of bone turnover. The cause and time of onset of these changes are uncertain, but they result in one or more of a variety of cervical abnormalities, considered together

[413]

Figure 9.9 Lateral radiographic view of the cervicothoracic junction of a normal adult horse. Note the smooth ventral aspect of the vertebral body of the seventh cervical vertebra, and the large dorsal spinous process of the first thoracic vertebra.

as developmental abnormalities. These may predispose to, or cause, compression of the spinal cord and thus ataxia. Some of the changes described may be related to osteochondrosis. These changes may in part be reversed in foals by restriction of feed intake and exercise. It should be noted that any of these variants, alone or in combination, can be seen in clinically normal horses. The greater both the number of abnormal variants and their severity, the more likely there are to be associated clinical signs. Vertebral stenosis and vertebral angulation are most likely to be associated with spinal cord compression, followed by enlargement of a caudal epiphysis and caudal extension of the arch of the vertebral canal over the cranial aspect of the next vertebra.

Enlargement of the caudal epiphyses

The caudal epiphyses of C2–C7 form the most caudal part of the floor of each vertebral foramen. Dorsal enlargement of one or more of the caudal epiphyses (a 'ski jump') can reduce the sagittal diameter of the vertebral foramen (see Figure 9.14, page 419), resulting in compression of the spinal cord and ataxia. This usually develops within the first year of life.

[414]
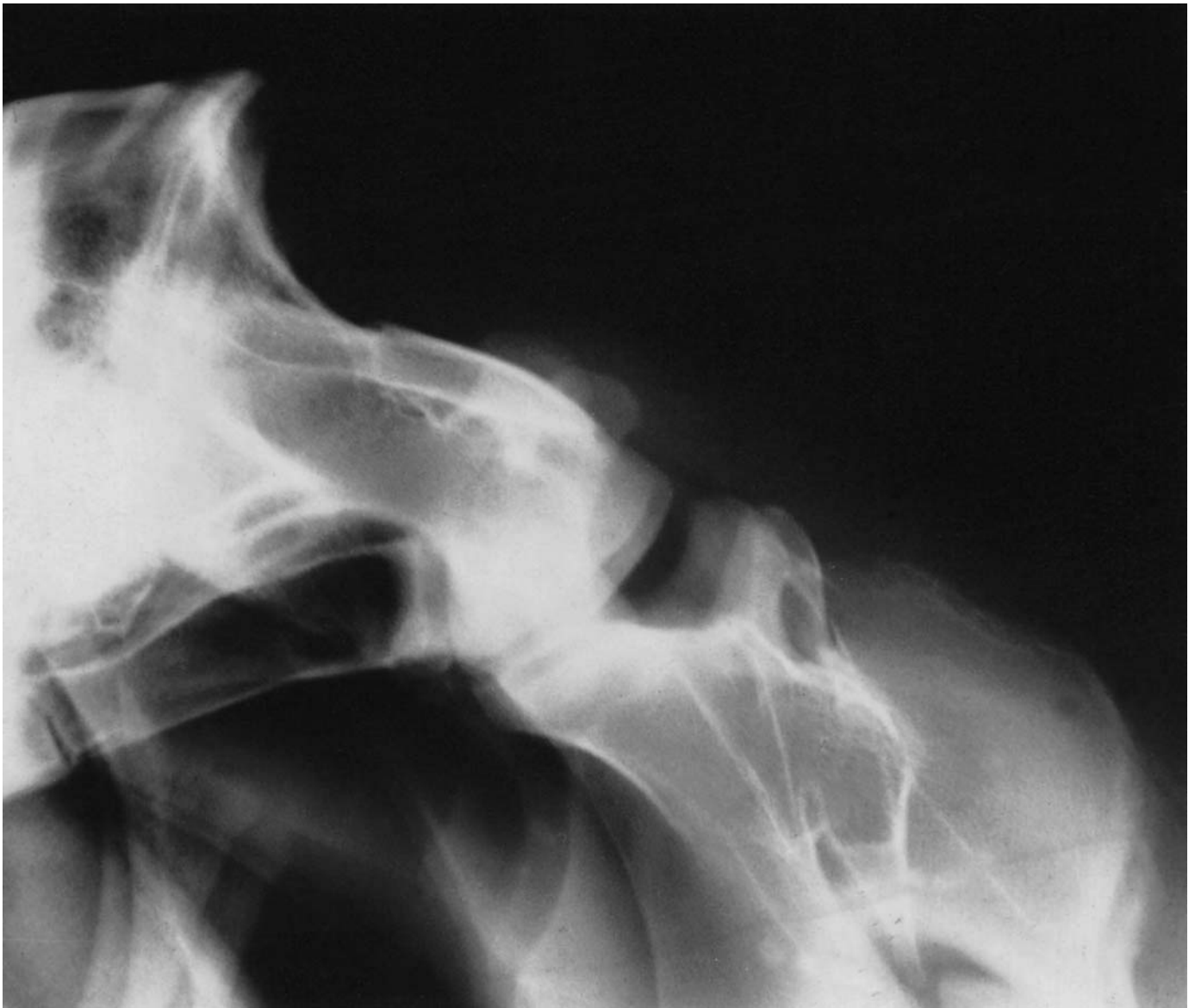
Figure 9.10 Lateral view of the occiput and the cranial cervical vertebrae (C1 and C2) of a yearling Arab filly exhibiting ataxia and abnormal prominence of the wings of the atlas. The atlas (C1) is fused to the occiput and the axis (C2) is misshapen – an occipito-atlanto-axial malformation. Note that the axis is slightly rotated. Compare with Figure 9.5.

Vertebral stenosis

Short vertebral pedicles (the lateral walls of the vertebral foramen) result in reduction of the sagittal diameter of the vertebral foramen. The articular processes show only marginal clearance of the intervertebral foramina (Figure 9.12, page 417), which therefore appear reduced in size. The stenosis is usually more pronounced towards the cranial aspect of the vertebra, resulting in a triangular vertebral foramen. The condition is the basis for many cases of spinal cord compression and occurs most commonly in young male Thoroughbreds. Sagittal ratio measurements or corrected MSD values

[415]

Figure 9.11 Lateral view of the caudal neck (C5–T1) of a 5-month-old Thoroughbred colt with forelimb and hind limb ataxia. The sixth and seventh cervical and first thoracic vertebrae are misshapen and fused (a synostosis). This was a congenital abnormality. Note the absence of callus. Post-mortem examination revealed a small ventral meningomyelocele passing into a cleft in the vertebral bodies of C7 and T1.

may be more accurate than absolute MSD values for detection of generalized vertebral stenosis (see page 406).

Vertebral instability, subluxation or angulation

Vertebral instability, subluxation or angulation occurs most commonly at the C3–C4 articulation (Figure 9.13, page 418). The apparent subluxation is often present in the resting position, and is exaggerated by flexion. Other developmental abnormalities (see 'OAAM', page 412, 'Vertebral stenosis', page 415, and 'Modelling of the cervical synovial articulations', page 418) are often present concurrently, resulting in narrowing of the sagittal diameter of the vertebral foramen and spinal cord compression, possibly at more than one site. Occasionally there is reciprocal hyperextension at a more caudal articulation, resulting in a 'zig-zag' orientation of the cervical vertebrae. Slight malalignment of two adjacent vertebrae occurs commonly and

[416]

Figure 9.12 Lateral view of the caudal cervical vertebrae (C5–C7) of an ataxic yearling Thoroughbred colt. There is stenosis of the cranial orifice of C6 (black arrow) due to short vertebral pedicles. This causes the vertebral foramen to assume a triangular shape (compare with Figure 9.8), and causes a reduction in size of the intervertebral foramina. Note the separate centres of ossification (white arrow) on the caudal aspect of the ventral processes of C6. This is normal and should not be confused with a fracture.

may have no clinical significance. If the minimum sagittal diameter of the vertebral canal is relatively wide, malalignment is often of no significance (Figure 9.14, page 419). The radiographs must be examined and interpreted in the light of the clinical signs, and if there is any doubt about the potential significance of a lesion it is helpful to obtain flexed lateral views, and to perform myelography.

Caudal extension of the arch of the vertebral canal

In a normal vertebra the dorsal aspect of the arch of the vertebral canal (the dorsal lamina) reaches, but does not extend over, the cranial epiphysis of the next caudal vertebra. Caudal extension of the arch of the vertebral canal is identified by drawing a line perpendicular to the longitudinal aspect of

[417]
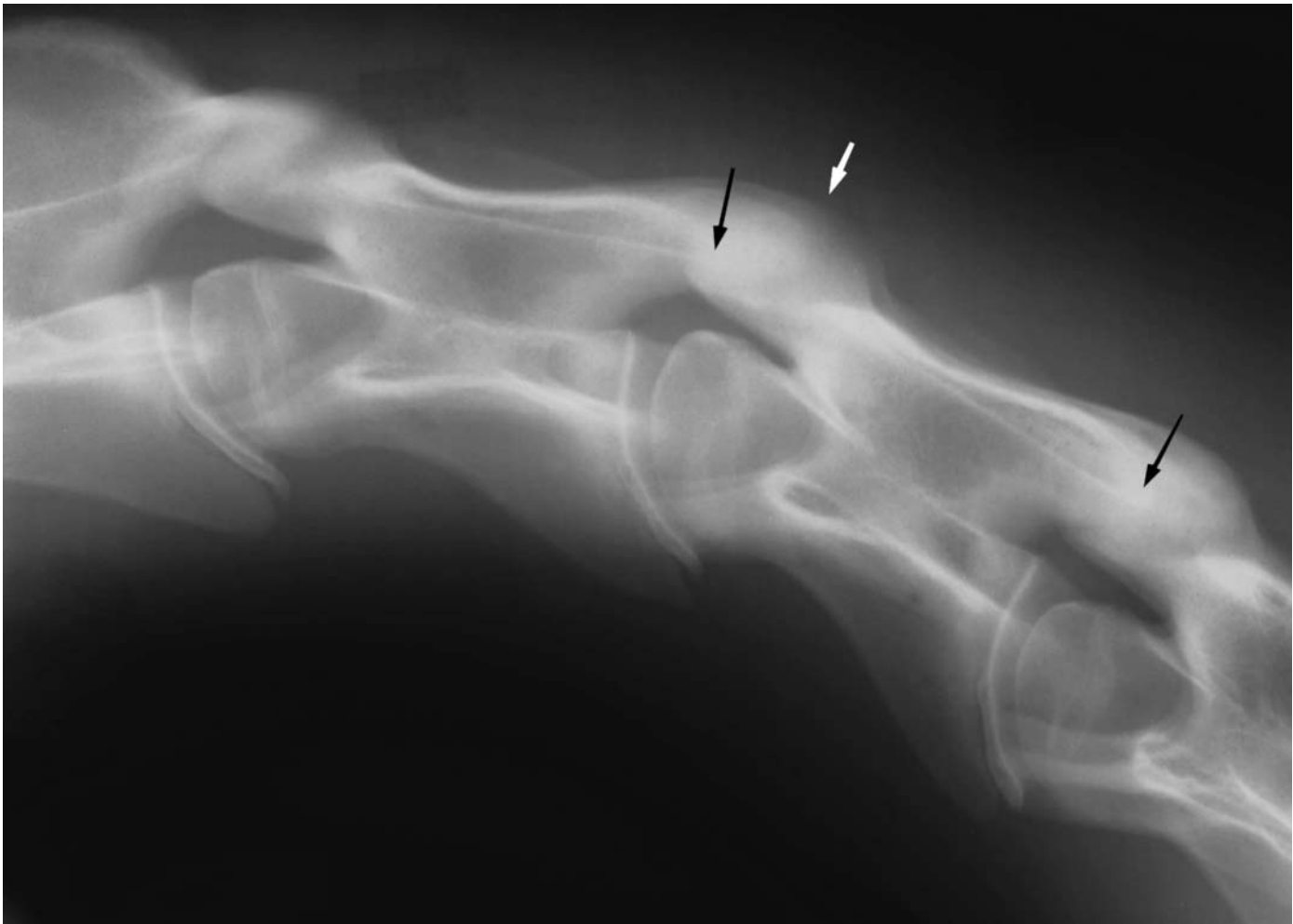
Figure 9.13 Lateral view of the second to fifth cervical vertebrae of an ataxic yearling Thoroughbred colt, obtained with the colt standing normally. There is subluxation of the third and fourth cervical vertebrae (white arrow) with narrowing of the minimal sagittal diameter of the vertebral canal. Spinal cord compression was confirmed at this level. Note also the caudal extension of the vertebral arch of the third and fourth cervical vertebrae (black arrows).

the vertebral canal from the caudal tip of the vertebral arch (dorsal lamina) (Figure 9.13). If this line extends onto the dorsal aspect of the cranial epiphysis of the next caudal vertebra, this is defined as mild caudal extension. Severe caudal extension is present if the line reaches the cranial physis of the vertebra.

Modelling of the cervical synovial articulations

Rooney (1963) described two distinct lesions of the synovial articulations (see 'Further reading'). Type 1 occurs at the C2–C3 articulation, associated with malalignment of the articular processes. It results in hyperflexion and stenosis of the vertebral foramen and causes ataxia. In a Rooney type 2 lesion there is medial enlargement of the articular processes of C4, or

[418]

Figure 9.14 Lateral view of the second to fourth cervical vertebrae of an ataxic yearling Thoroughbred filly, obtained with the filly standing normally. There is apparent subluxation at C2–C3 (white arrow), but the dorsoventral diameter of the vertebral canal was not significantly narrowed. Spinal cord compression was confirmed at the C6–C7 level, in association with a severe arthropathy. Note the moderate enlargement of the caudal epiphysis of C3 (black arrow).

occasionally C5, and this may cause spinal compression, especially in foals. This lesion cannot be detected radiographically on a plain lateral view and is difficult to identify on a ventrodorsal view.

The articular facets of C5–C6 and C6–C7 are frequently enlarged and modelled in mature horses, resulting in blurring of the normally smooth contours of the articulations (Figure 9.15). This is usually of no clinical significance, but these modelling changes are the prerequisite for development of an epidural synovial bursa or 'cyst', which can compress the spinal cord and cause ataxia.

Periarticular new bone can be produced in association with articular cartilage lesions and this may be of clinical significance in a horse with neck stiffness or ataxia. Small lucent zones in the region of the articular

Figure 9.15 Lateral view of the sixth and seventh cervical vertebrae of a clinically normal adult horse. There is modelling and enlargement of the synovial articular facets, a common incidental finding. Note the absence of buttresses (compare with Figure 9.17). C6 is slightly rotated. There is transposition of one ventral process from C6 to C7.

processes represent deep pits in the vertebral pedicles (Figure 9.16). These are usually indicative of a clinically significant lesion.

A bony 'knob' may be seen on the ventral aspect of one or both cranial articular processes, in normal and ataxic horses. If well developed this 'buttress' impinges on to the body or arch of the more cranial vertebra and forms a false joint. Radiographically the buttress partially obliterates the intervertebral foramen (Figure 9.17, page 422). This may be of no clinical significance unless the joint capsule balloons axially and compresses the spinal cord.

Massive enlargement of the synovial articular facet joints of C4–C5 and C6–C7 has been seen in association with unilateral forelimb lameness (Figure 9.18, page 423). Nerve root impingement associated with atrophy of the caudal cervical musculature has been documented by contrast-enhanced

[420]
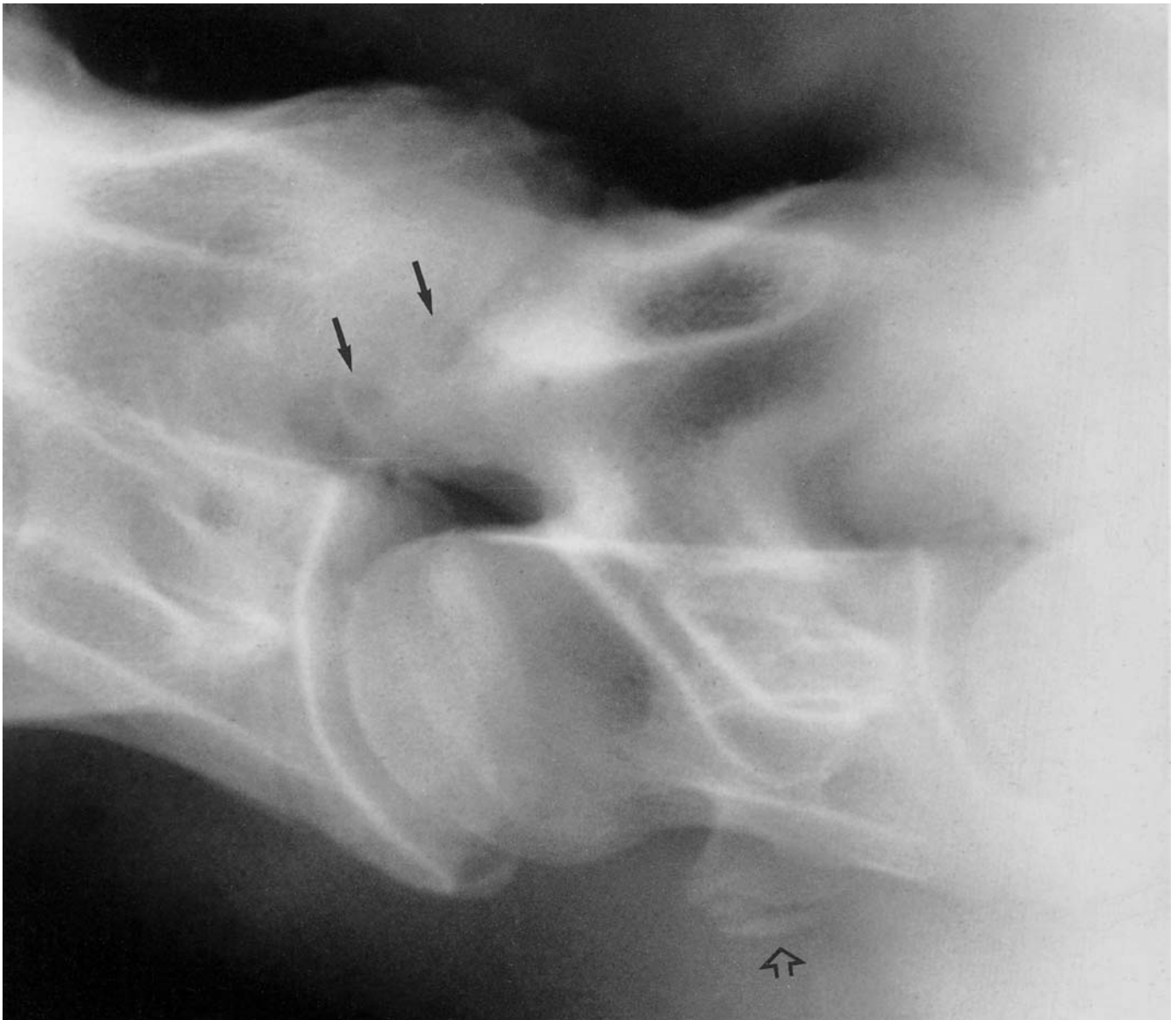
Figure 9.16 Lateral view of the caudal cervical vertebrae (C6 and C7) of an ataxic yearling Thoroughbred filly. There is extensive modelling of the articular facets of C6–C7 and an irregular joint contour. Radiolucent areas (black arrows) represent pits in the vertebral pedicles. Spinal cord compression was confirmed at C6–C7, associated with a synovial cyst. One ventral process, with separate centre of ossification, was transposed from C6 to C7 (open arrow).

computed tomography at C4–C5 and C5–C6, associated with severe degenerative joint disease of the synovial articular facet joints.

A pathological fracture may develop secondarily to modelling of a cervical synovial articulation. There is usually minimal displacement of the fracture fragments, but a lucent line is detectable radiographically (Figure 9.19, page 424). Fractures may occur unilaterally or bilaterally, but this is difficult to assess on lateral radiographs. An associated ataxia warrants a poor prognosis.
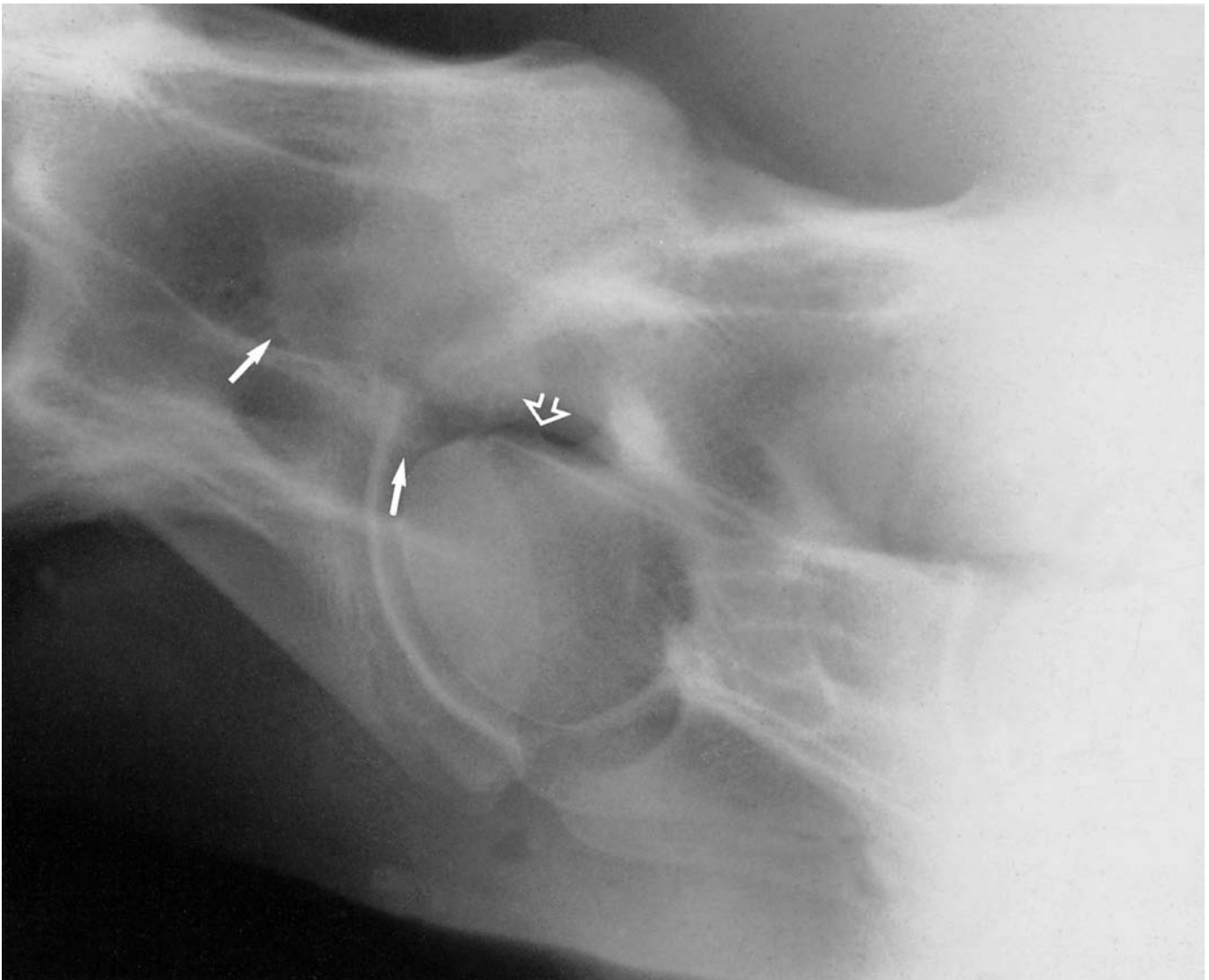
Figure 9.17 Lateral view of the caudal neck vertebrae (C6–T1) of a 7-year-old hunter gelding, with ataxia of 4 weeks' duration. Large buttresses (white arrows) on the cranial articular processes of C7 partially obliterate the C6–C7 intervertebral foramina (open arrow). Spinal cord compression was confirmed at this level, caused by a bulging joint capsule. Note the transposition of both ventral processes of C6 to C7 (compare with Figure 9.8).

Subluxation

Subluxation of the atlanto-axial joint may occur in foals or less commonly in an adult horse, associated with damage of the ventral ligaments of the dens. It results in an abnormal neck posture, with or without ataxia. The abnormal position of the vertebra is easily seen on a lateral radiographic view (Figure 9.20, page 425), which should be scrutinized carefully for a concurrent fracture. The distance between the dorsal lamina of the first cervical vertebra and the dorsal aspect of the dens should be measured and compared with normal values. The prognosis is poor.

[422]

Figure 9.18 Lateral view of the caudal cervical region (C5–C7) of a 9-year-old riding horse, with right forelimb lameness and low grade neck pain. The synovial articulations between the C5 and C6, and C6 and C7 are massively enlarged. There is obliteration of the intervertebral foramen between the fifth and sixth cervical vertebrae.

Entheseophyte formation on the occiput associated with the nuchal ligament

New bone formation may occur in the region of insertion of the nuchal ligament on the occiput, also extending slightly dorsal and ventral to the site of insertion (Figure 8.8, page 341). It can be seen as an incidental finding, especially in Warmbloods. Clinically affected horses tend to resist the reins, find difficulty in flexion at the poll and may rear or head-shake. The significance of the bony abnormality may be determined by local infiltration of local anaesthetic solution. Treatment by local infiltration of corticosteroids and local anaesthetic solution, combined with modification of the training programme has variable results.

Degenerative changes of the intercentral articulations

Narrowing of an intercentral articulation due to primary degeneration of an intervertebral fibrocartilage (disc) is rarely seen, but degenerative changes

[423]
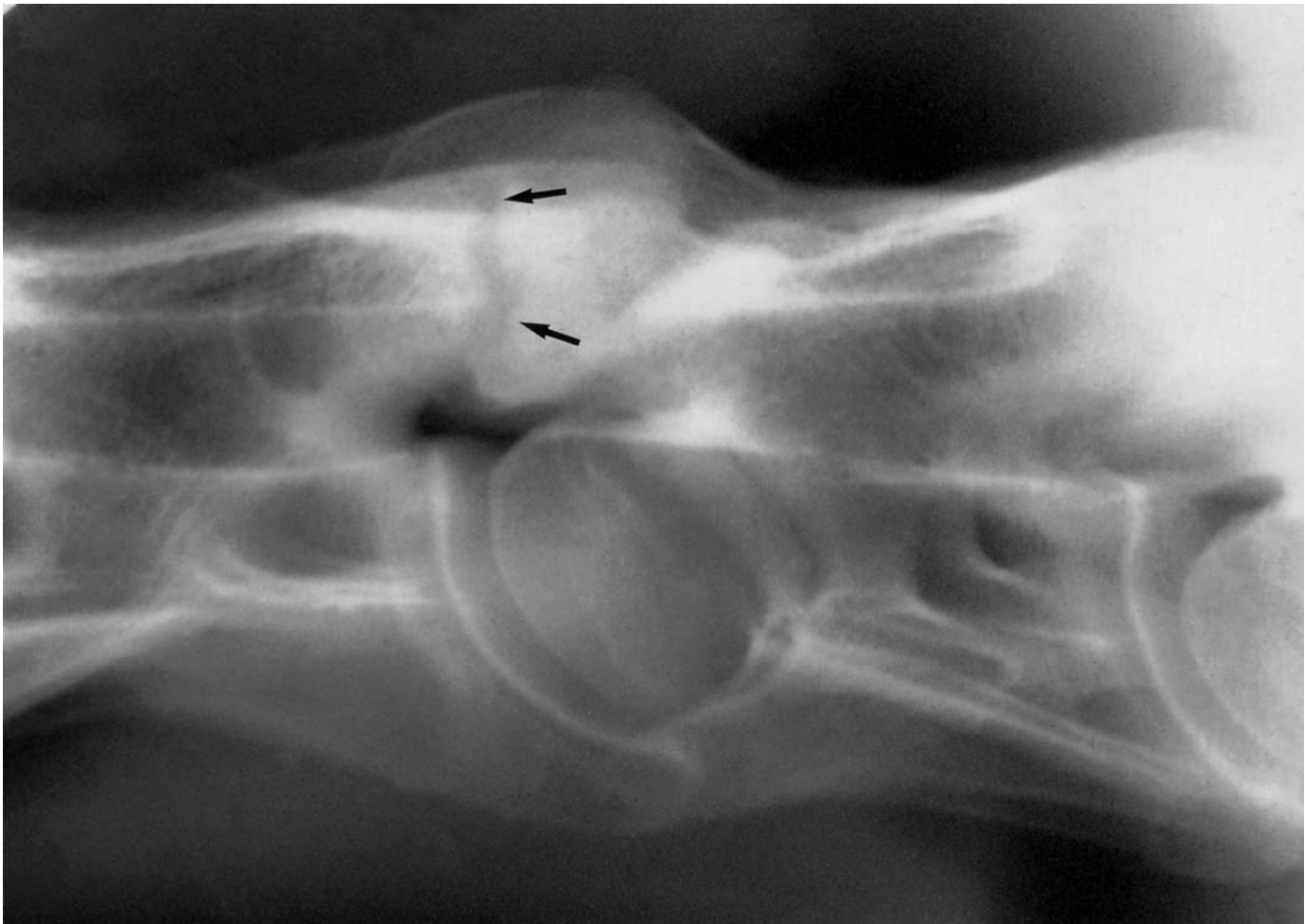
Figure 9.19 Slightly rotated lateral view of the fifth and sixth cervical vertebrae of an ataxic 2-year-old Thoroughbred colt. There is a fracture involving the articular process of C5–C6 (arrows). The cranial orifice of C6 was stenotic and this was considered to contribute to spinal cord compression.

of the joint may occur secondary to trauma. Radiographic abnormalities include narrowing of the intercentral joint space, change in shape of the joint surfaces, and change in the subchondral bone opacity.

Osteomyelitis

In foals, systemic infections may localize in cancellous bone, often in the vetebral bodies. This usually results in neck stiffness and recurrent pyrexia. Focal lucent areas are the first identifiable radiographic change, but if the foal survives, sclerotic bony changes may develop. In older horses local extension of a chronic soft-tissue infection (e.g. avian tuberculosis) can result in osteomyelitis and neck stiffness. Radiolucent areas which are usually surrounded by more sclerotic margins are seen within the vertebral bodies (Figure 9.21, page 426).

[424]

Figure 9.20 Lateral view of the cranial cervical vertebrae (C1–C2) of a 9-year-old advanced event horse with severe neck stiffness and an audible click associated with these vertebrae. There is subluxation of the atlantoaxial joint. Note the narrowed space between the dorsal aspect of the odontoid peg of the axis and the ventral aspect of the dorsal lamina of the atlas (arrowed). Compare with Figure 9.5.

Discospondylitis

Discospondylitis (inflammation of the vertebral body and associated inter-vertebral disc) was described, in association with infection, by Adams *et al.* (1985) (see 'Further reading'). The horses showed neck pain with or without ataxia. Radiolucent zones and some sclerosis were seen in the bone adjacent to the disc space. The prognosis for this condition is poor.

Neoplasia

Neoplastic invasion of cervical vertebrae is rare, but may present clinically as neck stiffness, neck pain or ataxia. Pressure caused by an expanding soft-tissue mass may cause smooth modelling of the bone. Neurofibromatosis can cause enlargement of the transverse and intervertebral foramina and cavitation of the vertebral arch, resulting in a large well-defined radiolucent zone (Figure 9.22, page 427). A mottled opacity of the vertebral bodies may
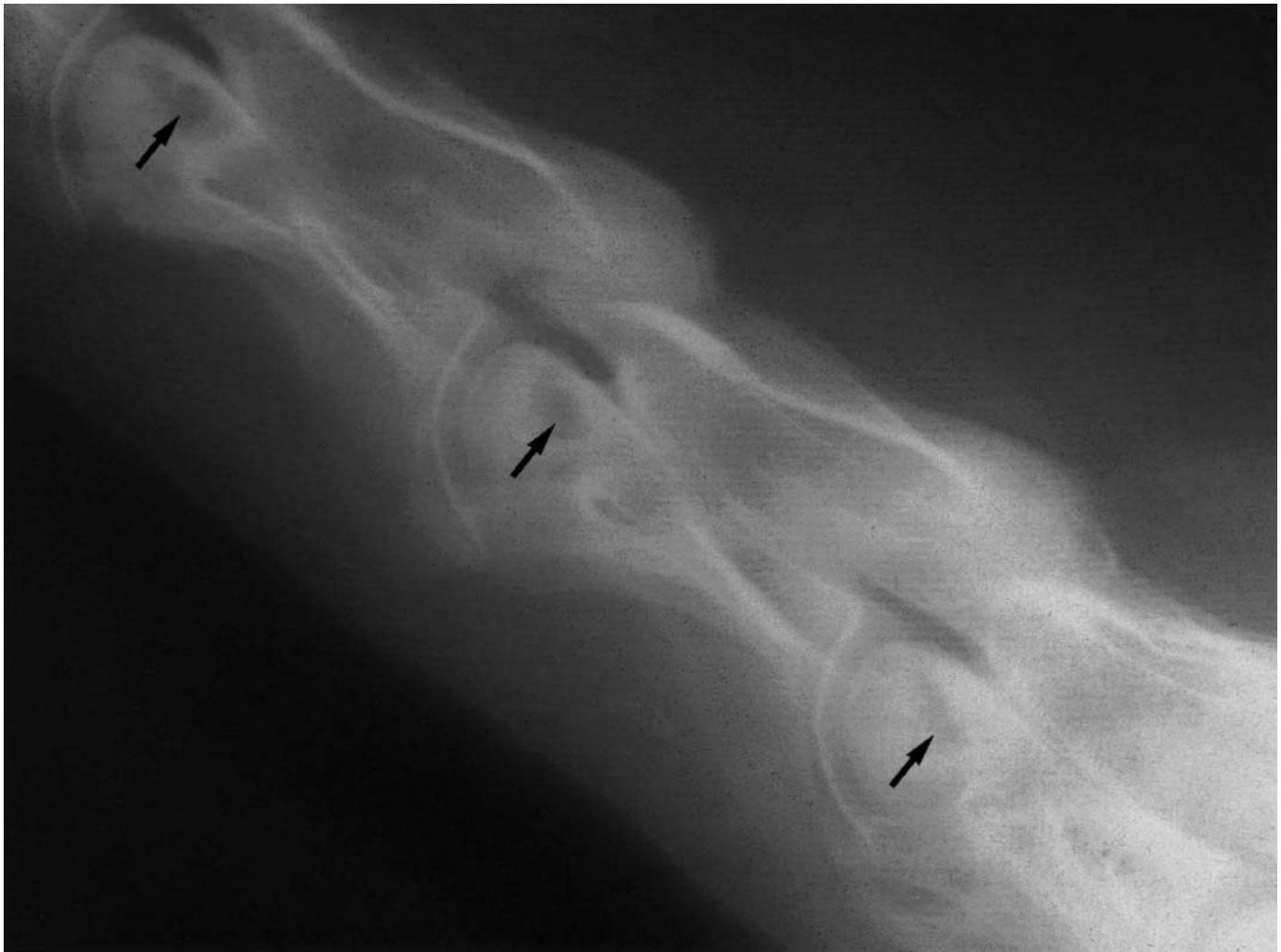
Figure 9.21 Lateral view of the fourth to sixth cervical vertebrae of a 5-year-old Thoroughbred mare with severe neck stiffness, persistent leucocytosis and neutrophilia, and an increase in β_2 globulins. There are irregular radiolucent areas in the vertebral bodies (arrowed) surrounded by sclerotic bone. Tuberculous osteomyelitis was confirmed post mortem.

be suggestive of neoplastic invasion of the bone marrow (e.g. lymphosarcoma, plasma cell myeloma), which may result in osteomalacia and pathological fractures. It may be difficult to differentiate radiographically between the effects of neoplasia, infection and trauma.

Soft-tissue lesions

Mineralization in the soft tissue should not be confused with lesions involving the vertebrae. This may occur secondary to an intramuscular injection (Figure 9.23, page 428) or as the result of previous trauma. A common site is in the ligamentum nuchae, caudal to the occiput. This dystrophic mineralization is readily identifiable radiographically, but may not be of long-term clinical significance.

[426]

Figure 9.22 Lateral view of the fifth to seventh cervical vertebrae of a 2-year-old Thoroughbred colt with neck stiffness, patchy sweating on the left side of the neck, atrophy of left supraspinatus, and left forelimb lameness. There are radiolucent areas in the vertebral body (white arrows) and in one of the pedicles of C6 (open arrows), secondary to invasion by neurofibromatous tissue. The horse died suddenly due to total collapse of the weakened C6 and laceration of the spinal cord.

Tearing of muscle and ligamentous insertions on the ventral aspect of the vertebral bodies may result in entheseophyte formation, readily identifiable radiographically on a lateral projection. This may be of no long-term clinical significance.

Fractures

Fractures are usually the result of trauma (e.g. a fall) or occur secondarily to a pre-existing lesion (e.g. modelling of a cervical synovial articulation). They result in neck pain and stiffness, and may cause ataxia. In young

[427]

Figure 9.23 Slightly oblique lateral view of the mid-cervical region of a mature horse. There is diffuse mineralization in the soft tissues secondary to an intramuscular injection. This radiopacity is partially superimposed on the articulation between C4 and C5 and should not be confused with a lesion involving the vertebrae.

horses, separation frequently occurs along unfused physes and this occurs most often in the axis. The prognosis depends on the site of the fracture, particularly with reference to the vertebral foramen, the degree of fracture displacement and the amount of callus which develops subsequently.

In the acute stage it is often difficult to make an accurate prognosis based on the clinical signs or the radiographic appearance of the fracture (Figures 9.24, page 429 and 9.25, page 430). Initial ataxia may resolve, only to recur when callus impinges on the spinal cord. Fusion of adjacent vertebrae may develop and cause neck stiffness. Generally, fractures involving the bone surrounding the vertebral foramen or the articular process warrant a guarded prognosis.

Occasionally a fracture of a caudal cervical vertebra may be associated with unilateral forelimb lameness.

[428]
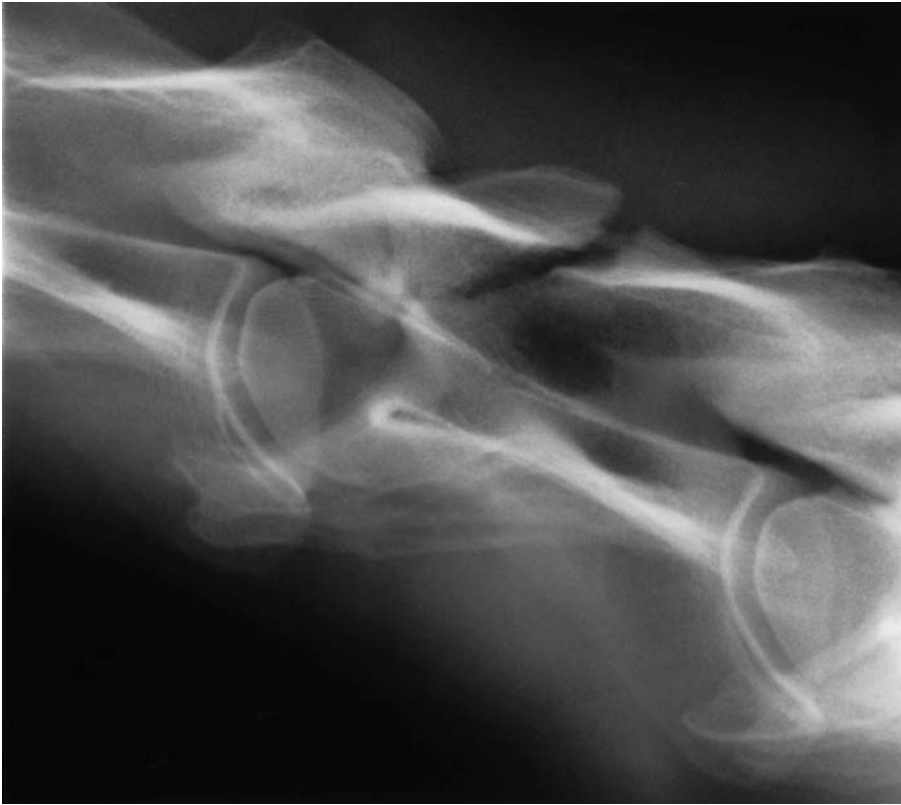
Figure 9.24(a) Lateral view of the third and fourth cervical vertebrae of a 9-year-old Dutch Warmblood dressage horse with severe neck pain and stiffness, and inco-ordination following a fall in a field 12 days previously. There is a comminuted, slightly displaced fracture of the dorsal arch of the fourth cervical vertebra. See also Figure 9.24(b).
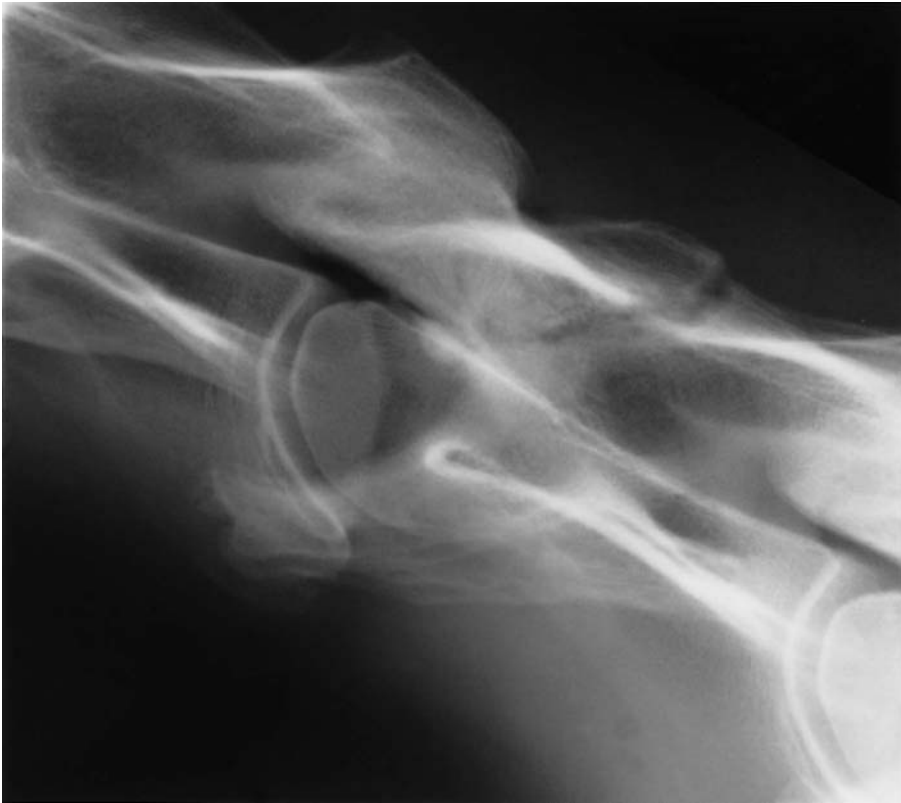
Figure 9.24(b) Lateral view of the third and fourth cervical vertebrae of the same horse as in Figure 9.24(a), obtained 6 weeks later. There is evidence of some bony union. The horse made a complete functional recovery.

[429]

Figure 9.25(a) Lateral view of the cervicothoracic junction (C6–T1) of a 6-year-old Thoroughbred cross, which had fallen while jumping a hedge 10 days previously. There is a slightly displaced fracture through the dorsal arch and vertical pedicle of the seventh cervical vertebra. There is evidence of pre-existing enlargement of the synovial articulations between the sixth and seventh cervical vertebrae. See also Figure 9.25(b).

Thoracolumbar spine

RADIOGRAPHIC TECHNIQUE

Equipment

Radiography of the thoracolumbar spine in adult horses poses a number of technical problems. The thickness of the back requires radiographic equipment with an output of 75–120kV and 100–250mAs, and the large mass of soft tissues causes considerable scattered radiation which must be controlled to obtain diagnostic radiographs.

Figure 9.25(b) Lateral view of the cervicothoracic junction of the same horse as Figure 9.25(a) obtained 4 months later. There is some osseous union, but the fracture line is still evident. The horse had shown some clinical improvement but developed severe ataxia 1 month later.

Ideally the x-ray tube is mounted on an overhead gantry with a linked cassette holder to ensure alignment of the x-ray beam and the film. Diagnostic radiographs of limited areas of the spine can be obtained using a mobile unit. The cassette holder is best mounted on the horizontal beam of a set of stocks, or directly on a wall. This will improve safety, as well as help to reduce movement. Stocks are recommended not only to restrain the horse, but to ensure that it is standing straight, so that true lateral views are obtained.

Rare earth screens and appropriate film are necessary. The effect of scattered radiation must be controlled, and the use of a 10:1 ratio focused grid is recommended. In addition, a lead sheet (at least 0.01 mm lead equivalent) should be placed behind the cassette to prevent backscatter. These

[431]

measures are particularly important for radiographs of the lumbar spine. To compensate for the differences in tissue density, an aluminium wedge filter is useful (see page 5) to prevent overexposure of the summits of the dorsal spinous processes.

With the above equipment, it is technically possible to obtain radiographs of the thoracolumbar spine from the first thoracic (T1) to approximately the third or fourth lumbar vertebrae (L3/L4), depending on the size and thickness of the horse. Further caudally, the lumbosacral spine and iliac wings are superimposed, making interpretation impossible (except in foals and small thin ponies). In the lumbar region, the mass of soft tissues results in a lot of scattered radiation, so that without the use of an appropriate grid, detail and contrast is lost.

To minimize movement of the patient, tranquillization is sometimes necessary. Radiographs are best obtained at end expiration. Only lateral radiographs of the thoracolumbar spine can be obtained with the horse standing. Ventrodorsal radiographs of the caudal thoracic spine may be obtained under general anaesthesia. Ventrodorsal views of the lumbar region are discussed elsewhere (see Chapter 10, page 458).

To evaluate the thoracolumbar spine (T2–L3) adequately, it is necessary to use large cassettes (35 cm × 43 cm), and to obtain at least four to six radiographs. To help identify individual vertebrae on successive radiographs, it is helpful to tape small radiodense markers (e.g. lead arrows) to the skin on the midline of the back. Four or five of these should be evenly spaced between the withers and the croup.

Positioning

The horse should stand squarely taking weight evenly on all four limbs, with the head and neck straight. Resting a limb causes rotation of the vertebrae, resulting in radiographic images that are difficult to interpret. The first radiograph is normally obtained in the mid-thoracic region (approximately T9–T15). For routine radiographs, the x-ray beam is centred at the level of the vertebral canal (approximately 15–20 cm below the dorsal midline of the back in an adult Thoroughbred horse), and aligned at right angles to the long axis of the trunk. Successive radiographs are similarly aligned, centring cranial or caudal to the previous view. Adjacent radiographic images should overlap, as this greatly aids identification of vertebrae. At the withers, the x-ray beam needs to be centred so that the top of the cassette is just above the highest point of the withers.

For all areas of the thoracolumbar spine, at least two differently exposed films will be needed: one to examine the summits of the dorsal spinous processes, and a second to examine the vertebral bodies and their articulations. Visualization of the articular processes and their articulations (facet joints) requires high-quality, well-collimated radiographs. It is important to be able to assess the entire length of the dorsal spinous processes, the articular facet joints and the vertebral bodies for complete evaluation. Assessment of the summits of the dorsal spinous processes may be enhanced by the use of exposures at reduced kilovoltage, without a grid.

If linked equipment is not available, it is often helpful to mark the horse on each side with an adhesive label where each radiograph is centred, to aid alignment of the cassette.

NORMAL ANATOMY, VARIATIONS AND INCIDENTAL FINDINGS

Immature horse

At birth the thoracolumbar spine is dorsally convex, and remains so until it becomes straight at about 6 months of age. All the vertebral bodies have cranial and caudal physes, the cranial physes closing at about 6–12 months and the caudal physes between 2 and 4 years of age (Figure 9.26).

At approximately 12 months of age the cranial thoracic dorsal spinous processes (T2–T8) develop separate centres of ossification within their cartilaginous summits. This ossification is gradual. These centres of ossification have an irregular outline and mottled opacity, and usually remain separate from the parent bone and incompletely ossified throughout life (Figure 9.27).

Skeletally mature horse

The horse normally has 18 thoracic vertebrae. The number of lumbar and sacral vertebrae varies between horses. Most horses have 6 lumbar vertebrae and 5 sacral vertebrae, but a significant number of horses have only 5 lumbar vetebrae, or may have 6 sacral vertebrae. The donkey has only 5 lumbar vertebrae and 4–6 sacral vertebrae. The vertebral bodies are approximately rectangular in shape, cranially convex and caudally concave. They articulate at the intercentral joints which are uniform in width. Care should be taken not to interpret overlying lung opacities as modelling of the vertebral bodies. The vertebral canal is of similar height throughout the thoracolumbar spine. The synovial or facet joints are difficult to evaluate and higher exposures may be required (see Figure 9.35a, page 447). Large well-muscled horses are easier to examine than smaller, fatter horses. These articulations are identified as oblique radiolucent lines dorsal to the vertebral canal. The articular facets in the lumbar region are larger than in the thoracic region; they appear more radiopaque and have a more irregular outline (see Figure 9.31, page 441). There are marked variations in shape of the articular facet joints from the cranial thoracic region to the caudal lumbar region, and comparison with articulated bone specimens is invaluable. The ribs articulate dorsal to the intercentral articulations and initially course dorsally and caudally, but then turn ventrally (see Figure 9.35a, page 447). If the ribs are 'highly sprung' they will be superimposed over the articular facet joints, prohibiting evaluation of the joints.

The dorsal spinous process of T1 has a triangular shape and is considerably shorter than that of T2. The dorsal spinous process of T2 is noticeably shorter than T3 and more rectangular than T1. It shows marked variation in width between individuals. T1 has no separate dorsal ossification
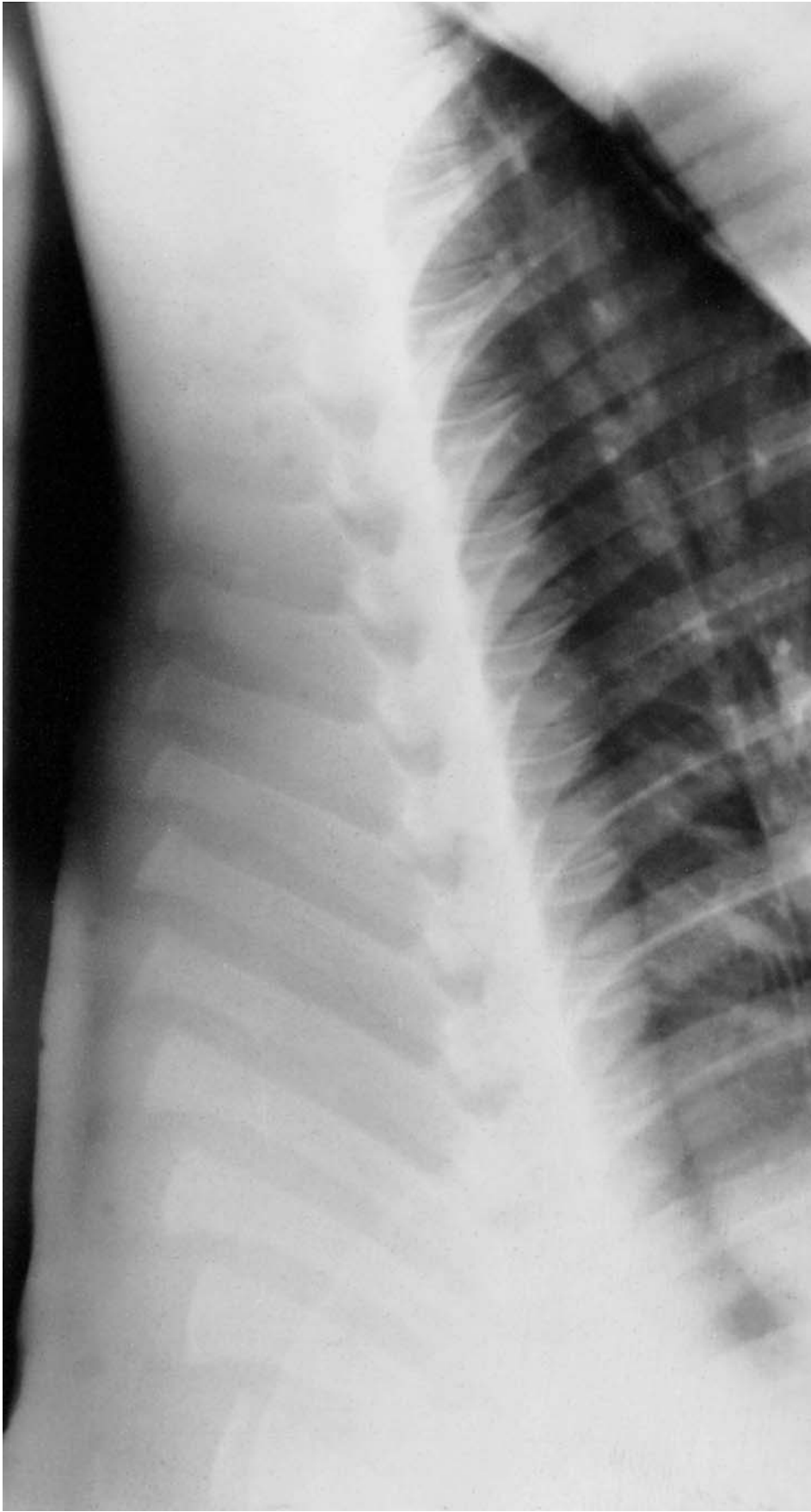
Figure 9.26 Lateral view of the thoracic vertebrae of a 10-day-old Thoroughbred foal. Note the absence of mineralization of the separate centres of ossification of the dorsal spinous processes of the more cranial vertebrae compared with an adult horse (Figure 9.27). The cranial and caudal physes of the vertebral bodies are clearly seen.
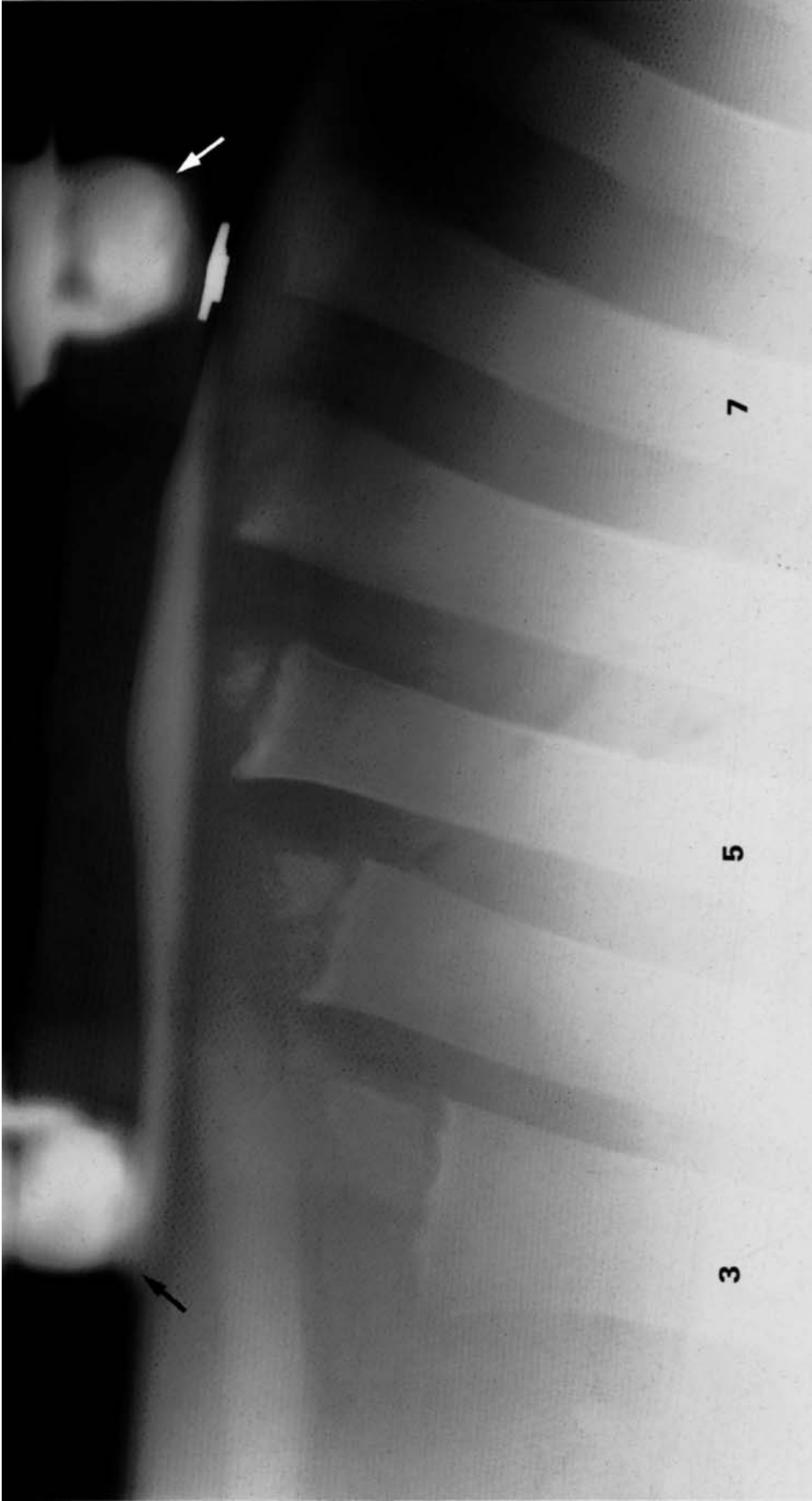
Figure 9.27 Lateral view of the cranial region (withers) of a normal adult Thoroughbred. Note the uneven opacity of the separate centres of ossification of the summits of the dorsal spinous processes. This appearance persists throughout life. The broad horizontal, more opaque band on the top left represents part of the nuchal ligament. Use of an aluminium wedge filter (arrows) prevents overexposure of the summits of the dorsal spinous processes. The numbers represent the number of each thoracic vertebra.

centre, but there are separate ossification centres from T2 to T7 or T8. These are usually single centres, but occasionally two are present. Further caudally the summit of each dorsal spinous process is smoothly rounded. Smoothly outlined, irregular new bone formation may reflect previous supraspinous enthesopathy.

The dorsal spinous processes at the withers (approximately T2–T10) are long and slender and slope caudally (Figure 9.27). Their cranial aspects frequently have a smoothly outlined irregular border. Caudal to the seventh thoracic vertebra, the processes become shorter, more upright and broader (Figure 9.28). The dorsal spinous processes are approximately parallel, and any marked deviation from this indicates that the vertebral bodies and inter-vertebral facets should be examined carefully. The anticlinal vertebra (which has a vertical dorsal spinous process) is usually T15. Caudal to this the dorsal spinous processes slope cranially and the interspinous spaces are con-siderably narrowed. There is considerable variation between horses in the spacing of the dorsal spinous processes in the mid to caudal thoracic region (Figures 9.29a and 9.29b, pages 438 and 439). On either side of the anticli-nal vertebra the dorsal spinous processes tend to be closer together (Figure 9.34a, page 445). The dorsal spinous processes may be in apposition, espe-cially in short coupled horses. Normally they have a smooth, relatively straight cranial and caudal cortex, throughout their length. Smoothly irreg-ular new bone is frequently seen on the cranial and caudal aspects of the dorsal spinous processes of the second to tenth thoracic vertebrae, unasso-ciated with clinical signs. It is less common to see new bone formation on more caudal thoracic dorsal spinous processes in clinically normal horses. There is sometimes a cranially directed 'beak' on the summits of dorsal spinous processes in the caudal thoracic region. The spinous processes of the lumbar vertebrae resemble those of the caudal thoracic region (Figure 9.30, page 440). However, their orientation varies. In horses with 5 lumbar vertebrae, the dorsal spinous processes tend to be parallel, whereas in horses with 6 lumbar vertebrae there may be divergence of the two most caudal dorsal spinous processes.

The thoracic vertebrae have relatively small transverse processes compared with the lumbar vertebrae where the transverse processes are large and flattened, and can be identified on lateral radiographs (Figure 9.31, page 441).

Identification of individual vertebrae is most easily made by identifying the dorsal spinous processes of T1, and numbering caudally. As a rough guide, the following structures can be used:

1 The separate centre of ossification on the dorsal spinous process of T3 is broad and triangular shaped.

2 Separate centres of ossification are present on the dorsal spinous processes of T2–T8.

3 The dorsal spinous process of T6 (or T7) normally forms the highest point of the withers.

4 T15 is normally the anticlinal vertebra.

5 Except in full inspiration, the image of the diaphragm normally lies over the vertebral body of T16 or T17.

[436]

Figure 9.28 Lateral view of the mid-thoracic region (T9–T16) of a normal adult Thoroughbred. The radiograph was obtained using an aluminium wedge filter and there are lead markers on the skin. The dorsal spinous processes in this region are completely ossified (compare with Figure 9.27). Note the rather irregular outline of the cranial and caudal aspects of the more cranial dorsal spinous processes. There is slight sclerosis (arrows) of the subcortical bone of the adjacent surfaces of the most caudal dorsal spinous processes, which has developed due to their closeness. The facet joints are underexposed and cannot be evaluated.

[437]
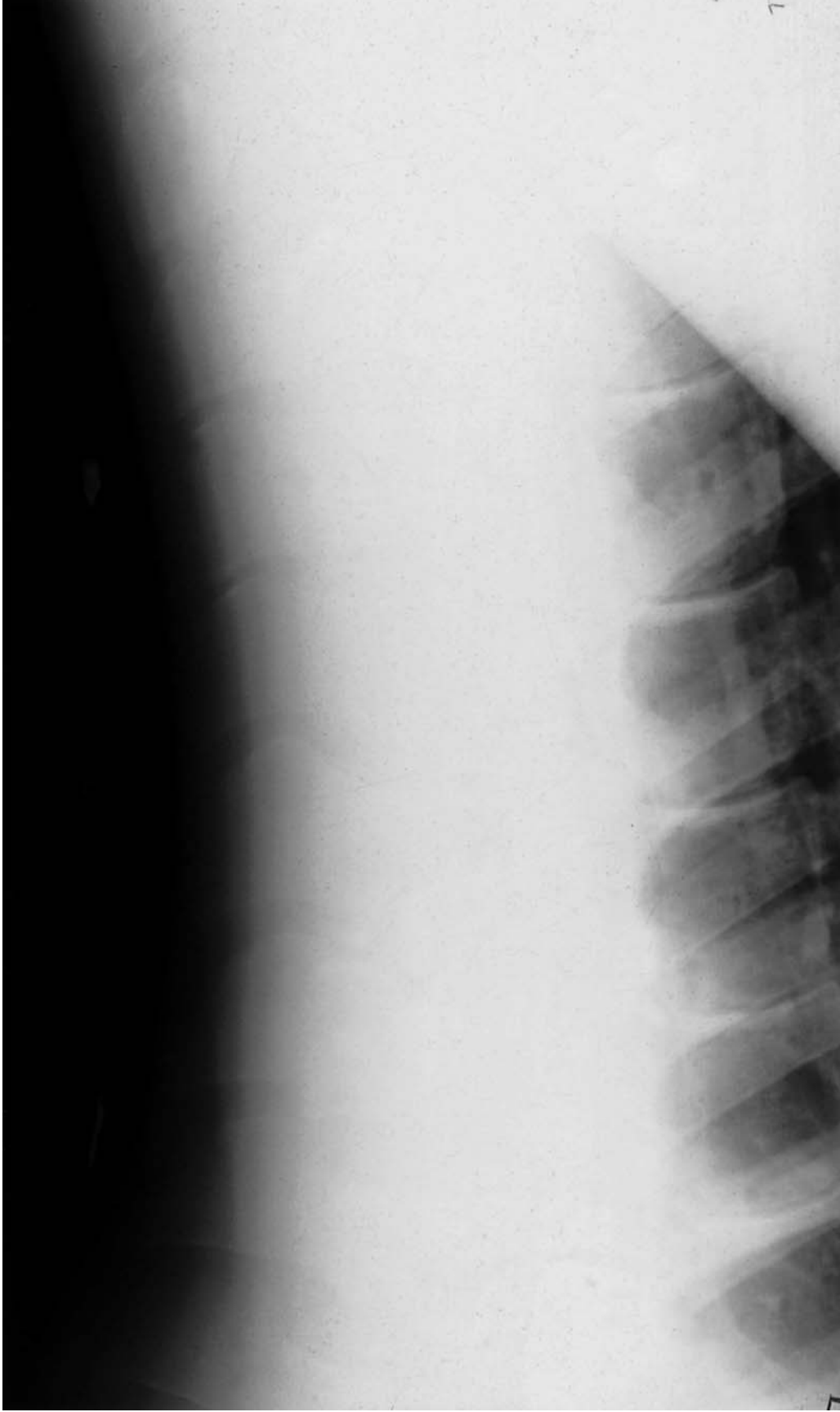
Figure 9.29(a) Lateral view of the caudal thoracic region (T11–T17) of a normal adult horse. The summits of the dorsal spinous processes are overexposed and the articular facets underexposed. The dorsal spinous processes are particularly well spaced; they are closer in many normal horses (compare with Figure 9.29b). The line of the diaphragm crosses the body of the sixteenth thoracic vertebra. There are lead markers on the skin.
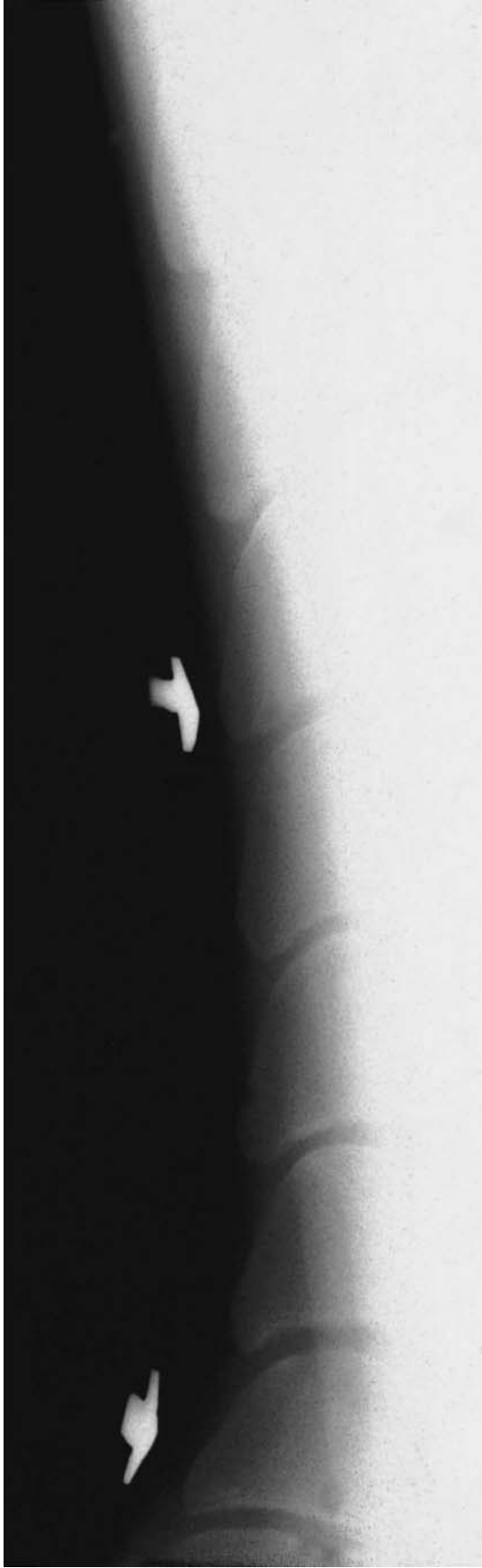
Figure 9.29(b) Summits of the dorsal spinous processes of the caudal thoracic region (T12–T18) of a normal adult horse. This is a different animal from Figure 9.29(a) and the dorsal spinous processes are closer together. Note the even opacity of the subcortical bone in the more cranial dorsal spinous processes. It is not possible to determine whether or not the more caudal dorsal spinous processes impinge since they are underexposed. There are lead markers on the skin. The radiograph was obtained using an aluminium wedge filter.

Figure 9.30 Summits of the dorsal spinous processes of the cranial lumbar vertebrae (T18–L4) of a normal adult horse. They are well spaced. It is not possible to assess the more ventral part of the dorsal spinous processes and the vertebral bodies without overexposing the summits.
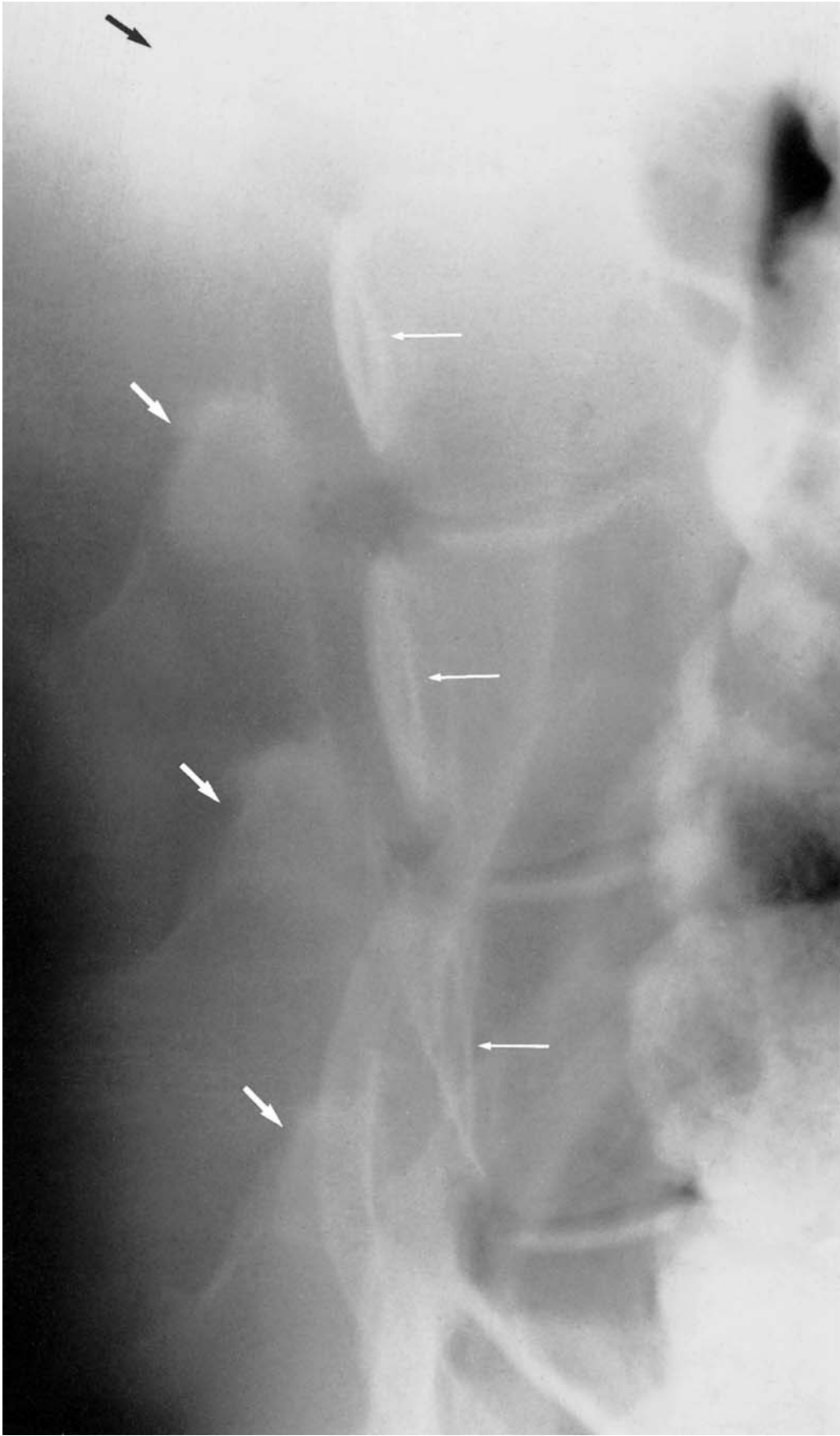
Figure 9.31 Articular facet joints and vertebral bodies of the cranial lumbar vertebrae. Superimposed over the more cranial vertebrae are the caudal ribs and abdominal viscera. Note the relatively sclerotic appearance of the facet joints (large arrows), through which a faint lucent line courses from caudodorsal to cranioventral. The oval-shaped sclerotic area (small arrows) on the dorsal aspect of each vertebral body represents the transverse processes. Note the opaque caudal subchondral bone plate of each vertebral body.
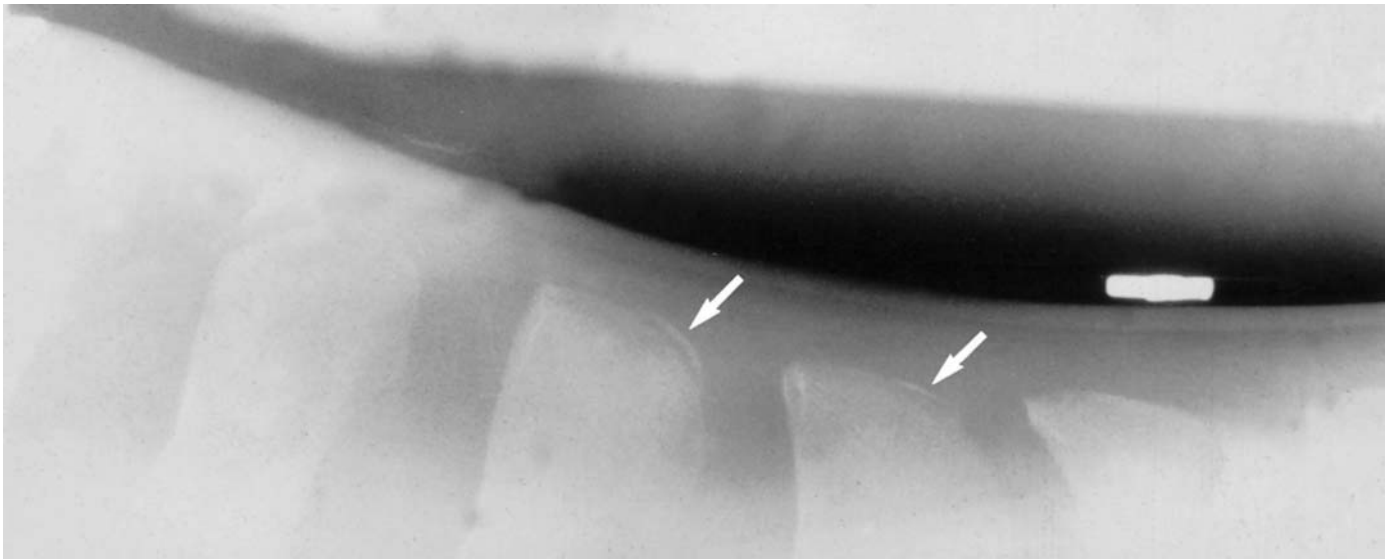
Figure 9.32 Lateral view of the summits of the dorsal spinous processes in the mid to caudal thoracic region of a 9-year-old Thoroughbred. There is separation of a thin radiopaque 'flake' on the dorsocaudal aspect of two processes (arrows), which is believed to reflect elevation of the periosteum following damage to the supraspinous ligament.

SIGNIFICANT FINDINGS

It is important to recognise that several radiographic abnormalities of the thoracolumbar vertebrae may occur concurrently, which may influence treatment and prognosis. It is therefore important to evaluate the vertebrae in their entirety, not just for example the dorsal spinous processes. Radiographic abnormalities are not always of clinical significance and must be interpreted in the light of clinical findings. Nuclear scintigraphic evaluation can be helpful in identifying which radiographic abnormalities are likely to be of clinical significance, although a negative result does not preclude the existence of back pain.

Sprain of the supraspinous ligament

The supraspinous ligament is a functional continuation of the nuchal ligament of the neck. It attaches to the periosteum of the summits of the dorsal spinous processes from T10/T11, caudally to the last lumbar vertebra. If these attachments are sprained following severe trauma such as a fall, there may be 'lifting' of the periosteum at the dorsal aspect of successive processes. This may be seen on softly exposed radiographs as a small radiopaque 'flake' dorsal and in close proximity to the summit of the dorsal spinous process (Figure 9.32). Alternatively entheseous new bone may develop on the summit of the dorsal spinous process. The condition is most frequently seen in the T10–T13 or L1–L3 regions. Ultrasonographic evaluation of the supraspinous ligament may be helpful. The condition may be accompanied by inflammation of other soft-tissue structures, and can

Figure 9.33 Lateral view of the dorsal spinous processes of the caudal thoracic vertebrae of a 4-year-old Hanoverian/Thoroughbred, which had become trapped under a horse box partition 10 weeks previously. There is extensive entheseous new bone on the caudal aspect of the dorsal spinous process of T15 (arrows), due to tearing of the interspinous ligament. The articular facet joint between T15 and T16 is also enlarged (arrow heads). The horse also damaged the supraspinous ligament and the summits of the dorsal spinous processes in the mid to caudal thoracic regions.

cause symptoms of back pain for several months. Satisfactory improvement with rest normally occurs, but the radiographic appearance does not necessarily alter, and these changes may therefore be an incidental radiographic finding. Nuclear scintigraphic evaluation may help to determine the presence of active bone modelling, and thus the likely clinical significance.

Interspinous ligament enthesopathy

Smoothly irregular new bone formation on the cranial and caudal aspects of the dorsal spinous processes of the first 8–10 thoracic vertebrae is a common incidental finding (Figure 9.27), but new bone formation on the dorsal spinous processes of more caudal vertebrae is more likely to be of clinical significance (Figure 9.33), reflecting interspinous ligament enthesopathy. It may be seen alone, or together with either impinging dorsal spinous processes, or degenerative joint disease of the articular facet joints.

[443]

Impingement and overriding of the dorsal spinous processes

It is important to be aware that impingement and overriding of the summits of the thoracic dorsal spinous processes is a fairly common radiological observation, even in clinically normal horses (Figure 9.34a). In one study involving 110 normal horses, approximately 30% revealed radiographic evidence of impingement of the dorsal spinous processes. Radiographic changes should be looked upon with some caution and must be interpreted in the light of a comprehensive clinical examination of the horse at rest and at work. It is not possible to relate the radiographic changes to the degree of clinical signs exhibited. Radiographic changes may simply be evidence of previous impingement, and no longer of clinical significance.

Impingement may result in discrete lucent zones in the subcortical bone, and periosteal reaction with new bone formation. This may be followed by sclerosis and modelling of the opposing surfaces of the spinous processes (Figure 9.34b). The cranial aspect of the summit of one dorsal spinous process may model to envelop the caudal aspect of the adjacent cranial dorsal spinous process. Closeness or impingement of the summits of successive processes is frequently seen, but need not be of clinical significance. Active periosteal proliferative reactions are more likely to be of significance. Significance can also be determined by infiltration of local anaesthetic solution, and by nuclear scintigraphic evaluation. In some cases where overt back pain is absent, 'overcrowding' of the processes (reduced interspinous spaces, without marked reaction of the opposing bone surfaces) may reduce the flexibility of the back, and hence reduce performance at the highest levels of competition. The greater the number of dorsal spinous processes involved, the higher the likelihood of associated clinical signs.

Conservative management frequently results in clinical improvement, although there is generally little or no change in the radiographic appearance. Surgical treatment by resection of the summits of one or more dorsal spinous processes should be contemplated in severe or intractable cases. It is important to evaluate the vertebrae in their entirety, to preclude other co-existing pathological changes of likely significance, which will adversely influence the prognosis.

Vertebral fusion

Vertebral fusion may involve two or more vertebrae, but is rare in the thoracolumbar spine. The absence of irregular bony callus helps to distinguish a congenital abnormality from fusion following a recent fracture. A fracture which occurred a year or more previously may be indistinguishable from a congenital fusion, due to modelling of the callus.

Lordosis, kyphosis and scoliosis

Varying degrees of lordosis, kyphosis and, occasionally, scoliosis occur.

Lordosis may be the result of congenital hypoplastic articular processes, but may also be an acquired defect. Marked lordosis of the thoracolumbar
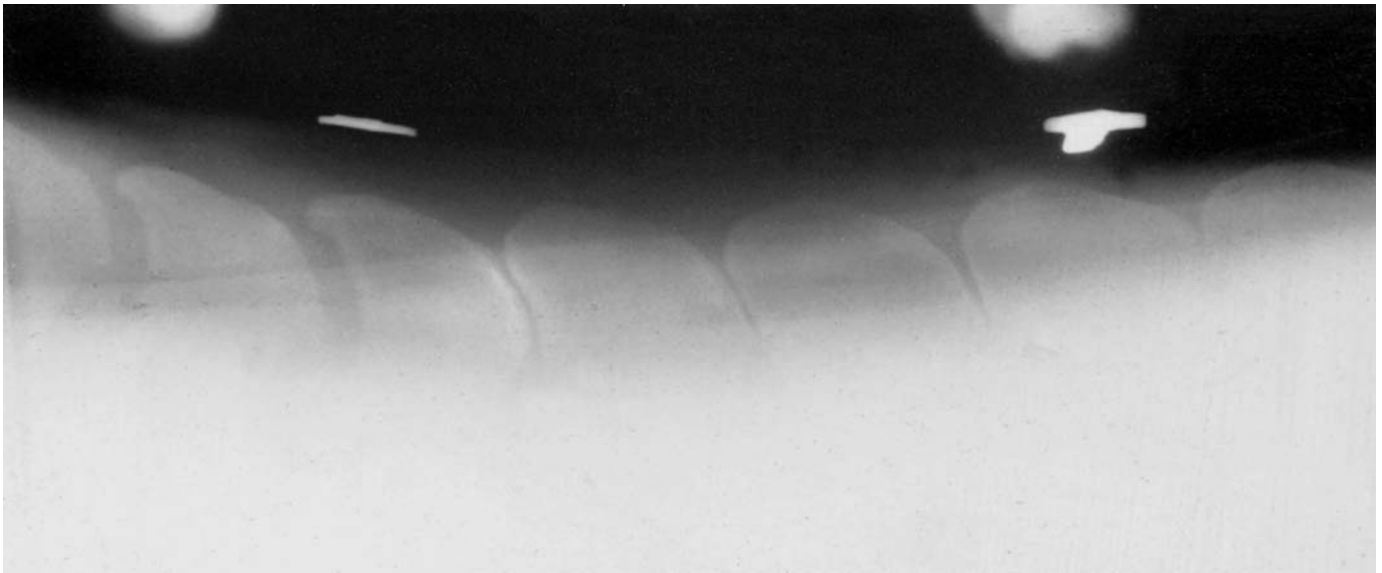
Figure 9.34(a) Lateral view of the summits of the dorsal spinous processes in the caudal thoracic region. The dorsal spinous processes are close together and there is slight cortical sclerosis and poorly defined subcortical lucent areas at the points where they are in closest apposition. This may be an incidental finding of no clinical significance.
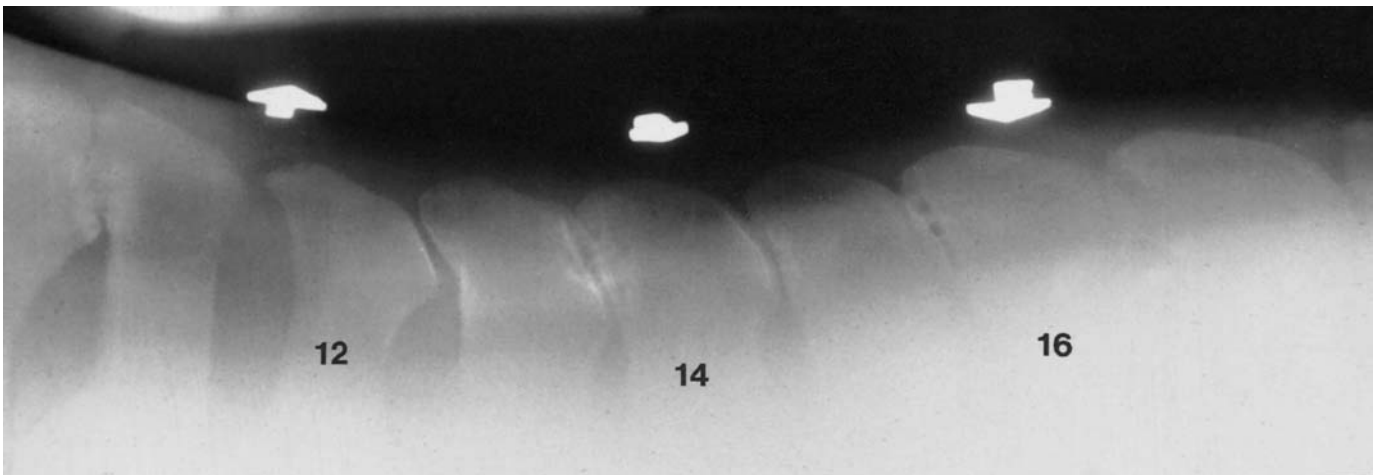
Figure 9.34(b) Lateral view of the tenth to seventeenth thoracic vertebrae of a 4-year-old Thoroughbred steeplechaser with a history of chronic back pain. There is impingement of the dorsal spinous processes of T10 and T11, and T13–T17 inclusive. Compare the irregular poorly defined margins of the dorsal spinous processes of T13 and T14 (which show ill-defined lucent zones in the subcortical bone, and diffuse sclerosis) with the well-demarcated margins between T15 and T16. The latter reflects long-standing impingement with remodelling. The horse was treated by surgical resection of the summits of the spinous processes of T11, T14 and T16 with a favourable outcome.

spine is recognized radiographically as a ventral convexity (dipping) of the thoracolumbar spine, and may adversely affect performance, although it does not necessarily do so.

Kyphosis may also be congenital or acquired. It is recognized radiographically as a dorsal convexity (arching) of the thoracolumbar spine. A similar posture may be adopted by young horses with bilateral osteochondrosis of the femoropatellar articulations, and this must be considered in the differential diagnosis.

Congenital scoliosis may occur (possibly due to uterine malpositioning). On lateral radiographs, twisting of the spine results in asymmetry of the positioning of the ribs, and an apparent variation in the length of the vertebral bodies. Wedge-shaped vertebral bodies may be seen on lateral or dorsoventral radiographs.

Mild degrees of lordosis and kyphosis are frequently seen and are not necessarily associated with poor performance, although they may be of significance in horses undertaking particular athletic activities. Scoliosis is often of sufficient severity to interfere with any type of performance.

Degenerative joint disease

The articular processes (facet joints) in the thoracic region form simple arthrodial joints with small and flat articular surfaces (Figure 9.35a). In the lumbar region, the articular processes are hinge-like and have a slightly different radiographic appearance (see Figure 9.31, page 441). True lateral projections are essential for assessment of any abnormality involving these structures. The joints under suspicion must be in the middle of the radiograph, and it may be helpful to compare the size and shape of the adjacent facet joints. Evaluation of the joints can be extremely difficult if the ribs are 'highly sprung'.

Degenerative joint disease of the articulations of the articular processes (facet joints) (Figure 9.35b) is difficult to diagnose and requires high quality radiographs, with good definition. Coning down may markedly enhance radiographic quality. The condition was formerly thought to be a rare cause of back pain, but with improved radiographic technique, and also the use of nuclear scintigraphy, is now being recognized more frequently. Degenerative joint disease of the articular facet joints most often affects the caudal thoracic and cranial lumbar vertebrae.

Radiographic abnormalities include:
● Asymmetry: no clear joint space is visible, or there is a double joint space.
● Reduced joint space, with or without osteolysis.
● Sclerosis: the subchondral bone plate is thickened and of increased opacity.
● Osteolysis or subchondral bone stress fracture.
● Dorsal periarticular proliferation, resulting in increased size of the joint. This is most easily recognized in the lumbar region. There may be reduced space between the dorsal spinous processes, especially in the caudal thoracic region.

[446]

Figure 9.35(a) Lateral view of the vertebral bodies and facet joints in the mid to caudal thoracic region of a normal adult horse. Note the relatively opaque articular facets (arrows) crossed by a lucent line (the joints) coursing from caudodorsally to cranioventrally. The vertebral canal is obscured by superimposition of the ribs. In some horses with very highly curved ribs, the facet joints may also be obscured. The intercentral articulations are well defined. Note the relatively broad caudal subchondral bone plate of each vertebral body.
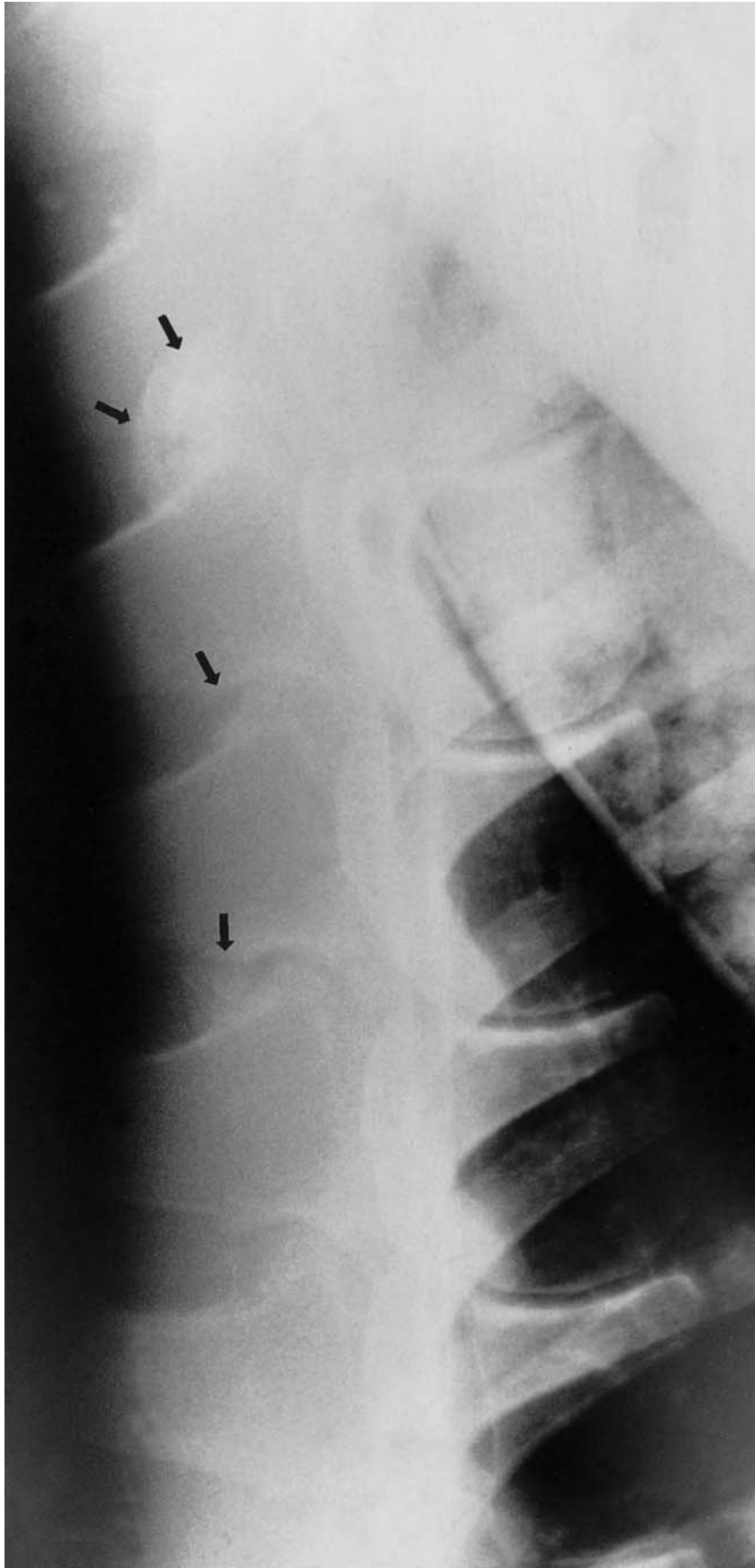
Figure 9.35(b) Lateral view of the caudal thoracic vertebrae of an 8-year-old horse with chronic back pain. There is degenerative joint disease of the facet joints characterized by periarticular new bone formation (arrows) and loss of joint spaces. These changes are most advanced caudally.

[448]
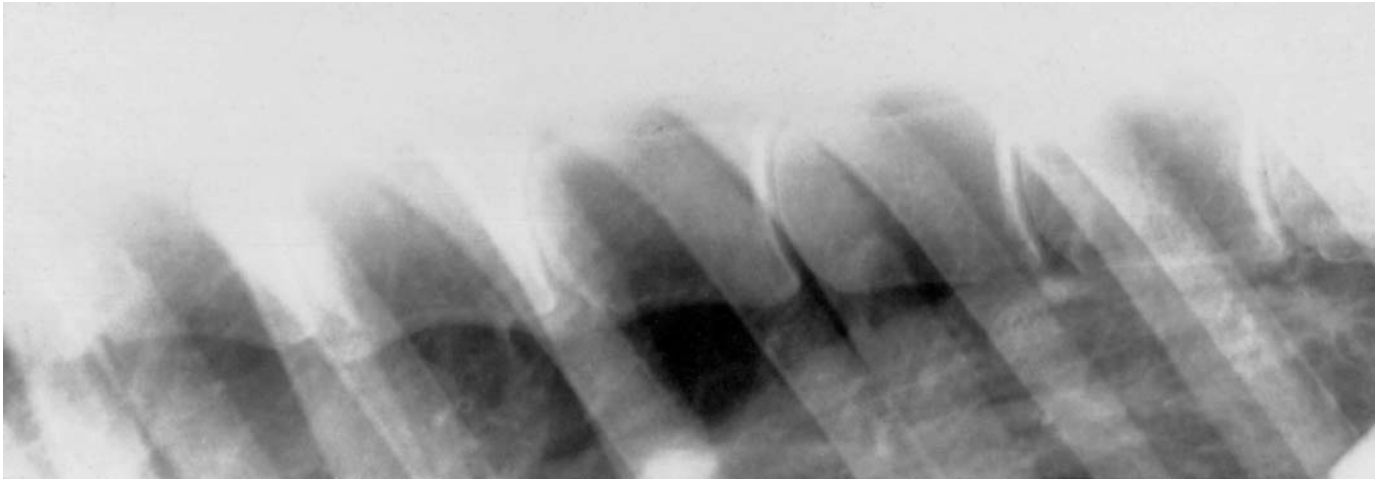
Figure 9.36(a) Lateral view of the tenth to sixteenth thoracic vertebrae of a 10-year-old Thoroughbred used for pleasure purposes. She had poor hindlimb action and clinical evidence of pain in the thoracolumbar region. There is new bone formation on the cranioventral and caudoventral aspects of T12 and the cranioventral aspect of T13. This is vertebral spondylosis. The intercentral joints appear normal. Care must always be taken to differentiate genuine new bone formation from superimposed lung opacities.

- Ventral periarticular proliferation. This can only be recognized in the lumbar region, due to the superimposition of the ribs in the thoracic region.

Occasionally concurrent abnormalities of the intercentral articulations are identified, which probably reflect previous trauma, or new bone may extend proximally between the dorsal spinous processes, reflecting interspinous enthesopathy.

Ossifying spondylosis (spondylosis deformans)

This is a relatively uncommon condition in the horse, the aetiology of which is not known. It is consistently found in the caudal half of the thoracic region (T10–T16). It may be multifocal and in some horses reflects ventral ligament enthesopathy.

Osteophytes (spondyles) arise from the ventral borders of the vertebral bodies near the intercentral articulations. The osteophytes usually extend across the intercentral joint towards similar osteophytes on adjacent vertebrae (Figure 9.36a). Frequently a radiolucent line of varying width remains between the opposing spondyles as an apparent continuation of the intercentral joint (Figure 9.36b), but complete bridging between adjacent vertebrae may occur (Figure 9.36c). There is considerable variation in the degree of spondylosis which develops, and the clinical significance of the changes has not yet been well established.

Once spondylosis has started to form, it will frequently progress in caudal and cranial directions. Spondylosis may occur without obvious clinical signs. This may depend on the athletic demands placed on the horse.

[449]
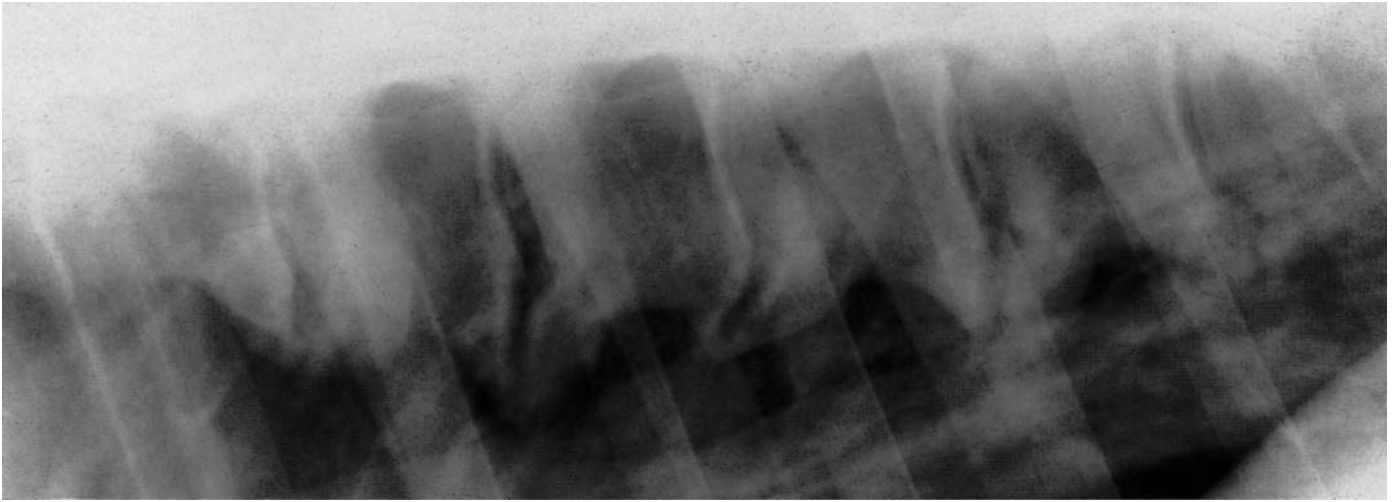
Figure 9.36(b) Lateral view of the tenth to sixteenth thoracic vertebrae of a 9-year-old part Thoroughbred. The horse was used for general riding purposes and showed no clinical signs referable to the thoracolumbar region, either when radiographed or in the succeeding 4 years. There is extensive new bone formation on the ventral and ventrolateral aspects of the eleventh to sixteenth thoracic vertebrae. Note the lucent spaces between adjacent spondyles, resulting in apparent continuation of the intercentral articulations. The opposing surfaces of the spondyles are relatively sclerotic.
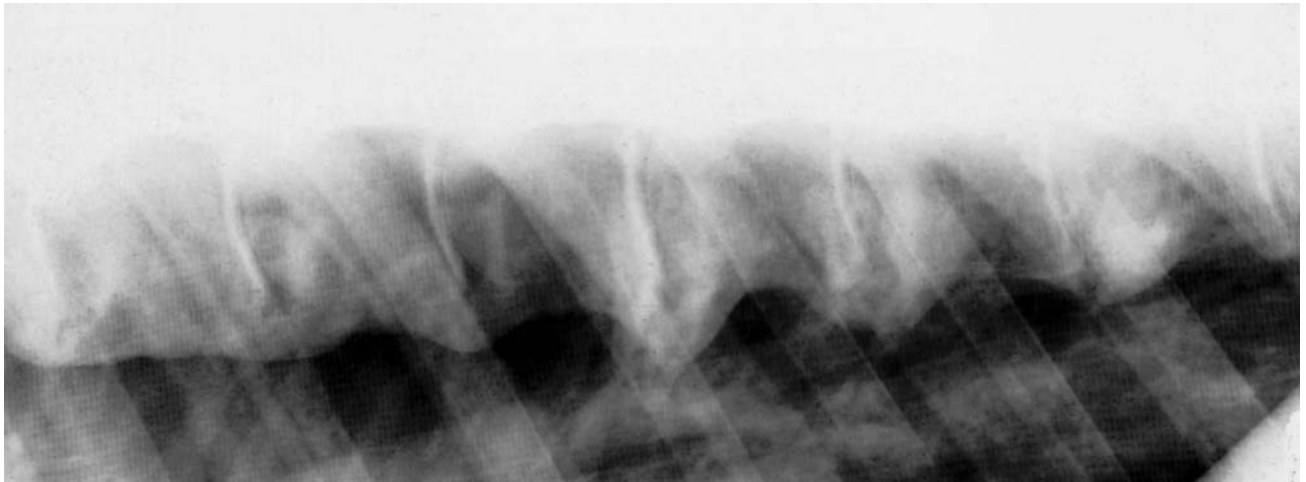
Figure 9.36(c) Lateral view of the eighth to fourteenth thoracic vertebrae of a 10-year-old horse presented due to poor performance and difficulty in going uphill or downhill. There was clinical evidence of thoracolumbar pain. There is advanced spondylosis with complete bridging of new bone on the ventral aspects of many of the vertebral bodies. The intercentral articulations are normal but are less well defined ventrally because new bone arising on the lateral aspects of the vertebral bodies is superimposed.

[450]

Some horses with associated back pain have been able to perform acceptably with controlled medication, although only limited athletic pursuits are possible.

Spondylosis has also been seen concurrent with other abnormalities, such as impinging dorsal spinous processes.

Osteomyelitis

Systemic infections may localize in the vertebral bodies. This may result in some stiffness of the back, and intermittent pyrexia. Radiographically, focal lucent areas, sometimes surrounded by a sclerotic rim, are seen. While a number of systemic infections may cause this condition in foals, including *Rhodococcus equi*, the most common cause in the adult horse is tuberculosis. Neoplastic metastases may give a similar radiographic appearance. Negative radiographic findings do not preclude the possibility of vertebral infection. Nuclear scintigraphy may be more sensitive.

Infection in the withers region (fistulous withers) may involve the dorsal spinous processes. This may appear as lucency in the subcortical bone, and periosteal new bone formation. It should not be confused with the normal radiographic appearance of the dorsal spinous processes in this region (see Figure 9.27, page 453). Diagnostic ultrasonography may be helpful to determine if a draining tract is associated with osteomyelitis. This condition has become less common in the United Kingdom in recent years, probably due to the reduced incidence of brucellosis, with which it was commonly associated. Topical treatment with metronidazole has been found helpful in some cases. Surgery may be required, but some cases remain refractory to treatment.

Discospondylitis

Discospondylitis (inflammation of the vertebral body and associated intervertebral disc) has been seen rarely in association with infection, characterized by back stiffness and an abnormal stance and gait. Blood fibrinogen may be elevated. Radiographically there is narrowing or obliteration of the intervertebral joint space, with new bone on the ventral aspect of the vertebral bodies. Successful treatment with antimicrobial drugs has been reported.

Fractures

Fractures involving the bodies of the thoracolumbar vertebrae are relatively uncommon. They normally cause or are accompanied by damage to the spinal cord, which often results in immediate paraplegia.

Hairline fractures with minimal displacement may prove impossible to detect radiographically, but may be detected using nuclear scintigraphy. Stress fractures are now thought to occur more commonly than previously

Figure 9.37 Lateral view of the dorsal spinous processes of the second to ninth thoracic vertebrae of an advanced event horse with acute onset of pain in the withers region following a fall in water, and subsequently becoming cast in a stable within 24 hours. There are displaced comminuted fractures of the dorsal spinous processes of T3–T9. The horse was treated conservatively and made a complete functional recovery, although slight malformation of the withers region persisted. The radiograph was obtained using an aluminium wedge filter.
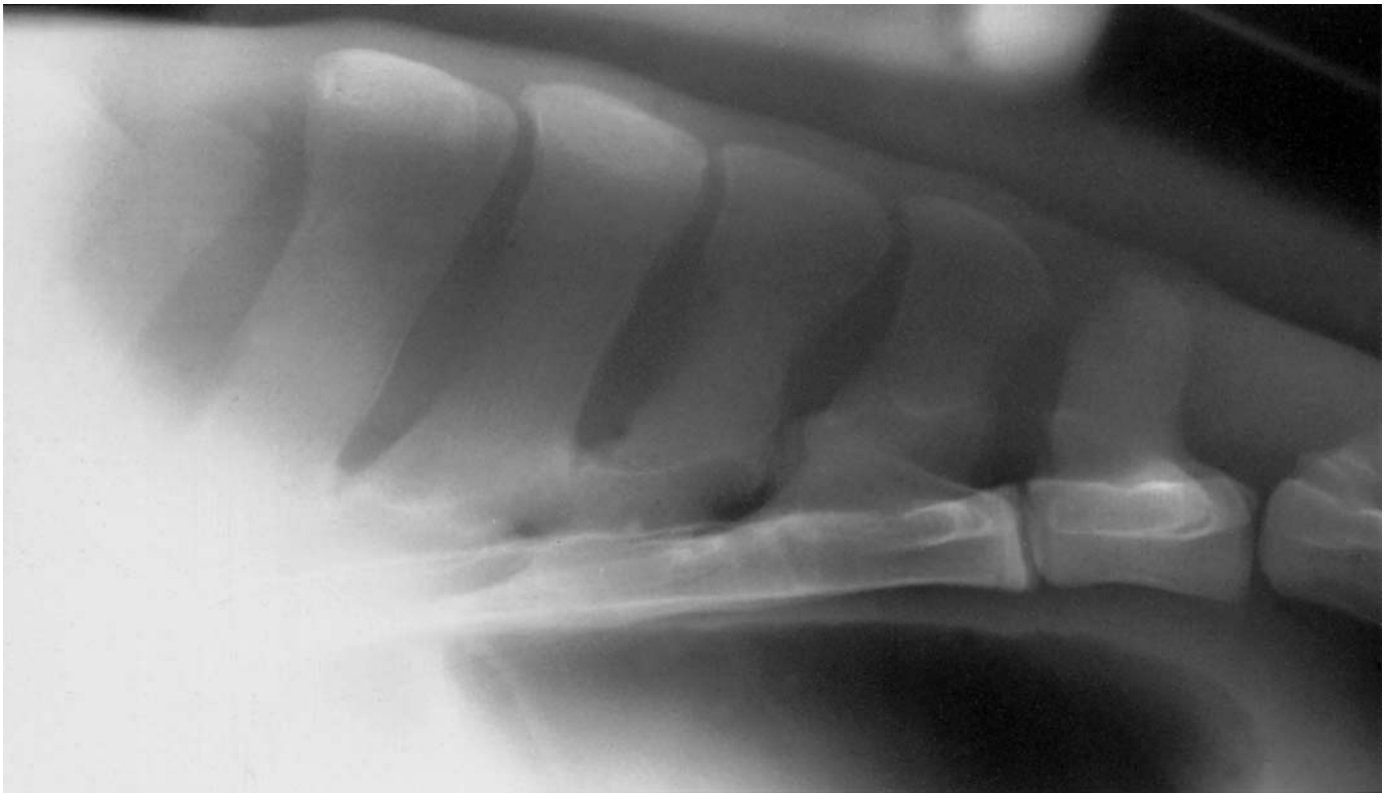
Figure 9.38 Lateral view of the sacrum and cranial coccygeal vertebrae of a normal adult horse. The horse was poorly muscled over its dorsal midline and the sacrum is defined better than in the majority of horses. The radiograph was obtained using an aluminium wedge filter.

recognized in young Thoroughbreds in training. Significant radiological signs of a vertebral fracture include: (a) apparent shortening of the length of the vertebral body; (b) a change in shape of the intercentral articulations, possibly with upward displacement of the vertebra; (c) callus formation.

In young animals, pathological fractures of vertebrae may occur secondarily to osteomyelitis following destructive and resorptive changes in the vertebral body.

Fracture of a vertebral body generally has a grave prognosis.

Fractures of the dorsal spinous processes usually occur at the withers as the result of a fall. Displacement of the fragments is often present (Figure 9.37). Complete osseous healing frequently does not occur, and there is often deformation of the dorsal spinous processes. A good prognosis for future performance can be given, although a special saddle may be required.

Other fractures occur, but may be difficult to identify on radiographs.

Fracture of the ribs may present clinically as back pain. Fracture of the first rib may result in forelimb lameness or a neurological gait deficit (see Chapter 11, page 524).

[453]
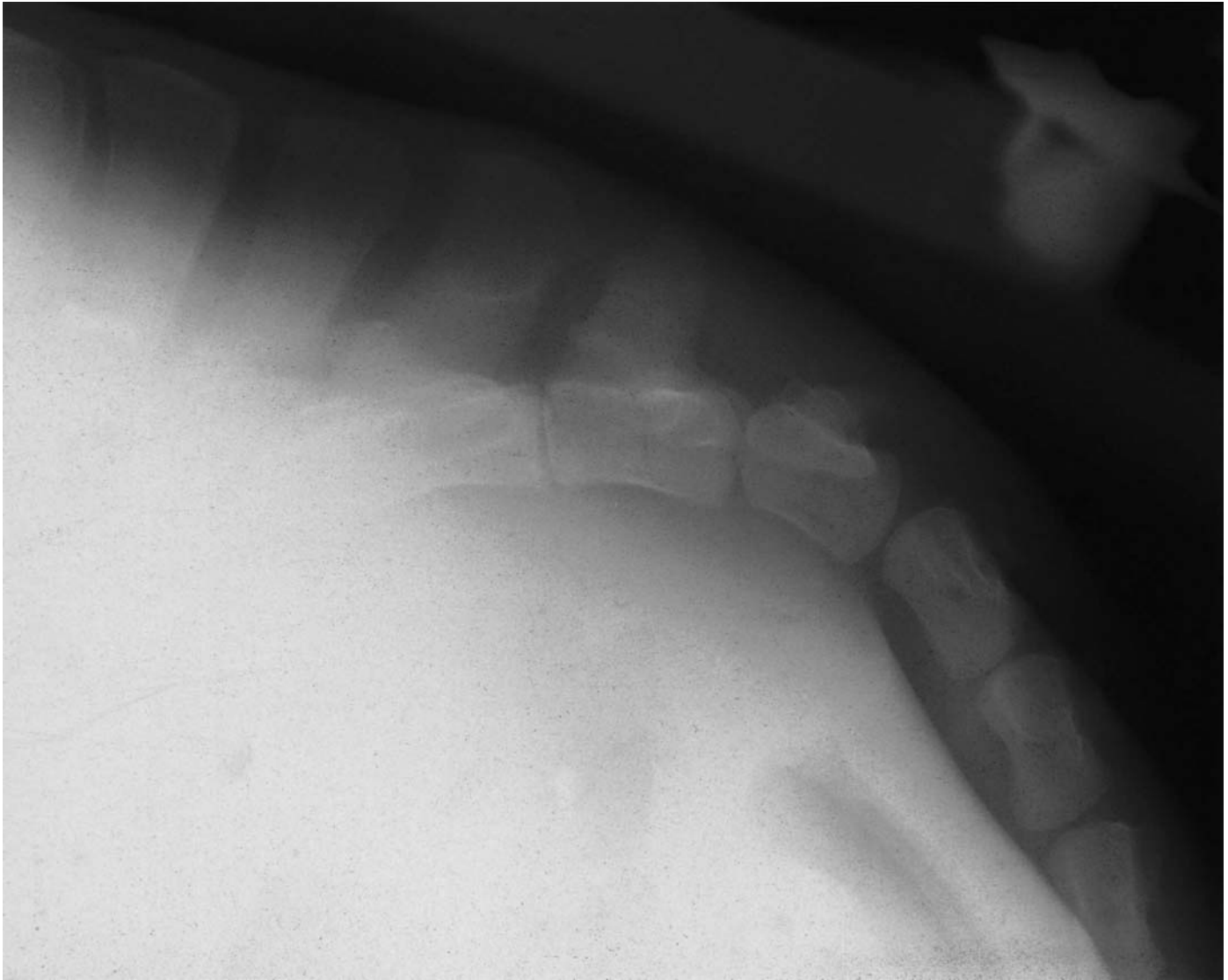
Figure 9.39 Lateral view of the caudal aspect of the sacrum and the cranial coccygeal vertebrae (C1–C5) of a normal adult horse. Note the different shape of each coccygeal vertebra. The radiograph was obtained using an aluminium wedge filter.

Sacrum and coccygeal vertebrae

Lateral radiographs of the sacrum and coccygeal vertebrae are obtained similarly to those of the thoracolumbar spine. Definition is often poor due to the overlying soft tissues and the resulting scattered radiation. Ventrodorsal views can be obtained with the horse in dorsal recumbency under general anaesthesia (see Chapter 10, under 'Pelvis', page 458).

On a lateral view of a normal horse, the sacrum is poorly defined, but its ventral border is seen as a linear opacity (Figure 9.38). The coccygeal vertebrae are aligned in a curvilinear manner (Figure 9.39).

Sacral fractures are often displaced in a dorsoventral direction, and thus are best identified in a lateral projection. Clinically these fractures may

[454]

result in a change in conformation of the hindquarters and neurological abnormalities.

FURTHER READING

Adams, A., Steckel, R. and Blevins, W. (1985) Diskospondylitis in five horses. *J. Am. Vet. Med. Ass.*, **186**, 270–272

Alitalio, I. and Karkkainen, M. (1983) Osteochondrotic changes in the vertebrae of four ataxic horses suffering from cervical vertebral malformation. *Nord. Vet. Med.*, **35**, 468–474

Funk, K. and Erickson, E. (1968) A case of atlanto-axial subluxation in a horse. *Can. Vet. J.*, **9**, 120–123

Giguere, S. and Lavoie, J. (1994) *Rhodococcus equi* vertebral osteomyelitis in 3 Quarter Horses. *Equine Vet. J.*, **26**, 74–78

Greet, T.R.C., Jeffcott, L.B., Whitwell, K.E. and Cook, W.R. (1980) The slap test for laryngeal adduction function in horses with suspected cervical spinal cord damage. *Equine Vet. J.*, **12**, 127–131

Guffy, M., Coffman, J. and Strafuss, A. (1969) Atlantoaxial luxation in a foal. *J. Am. Vet. Med. Ass.*, **155**, 754–757

Haussler, K. and Stover, S. (1998) Stress fractures of the vertebral lamina and pelvis in Thoroughbred racehorses. *Equine Vet. J.*, **30**, 374–383

Haussler, K., Stover, S. and Willits, N. (1997) Developmental variation in lumbosacropelvic anatomy of Thoroughbred horses. *Am. J. Vet. Res.*, **58**, 1083–1091

Jeffcott, L.B. (1975) The diagnosis of diseases of the horse's back. *Equine Vet. J.*, **7**, 67–78

Jeffcott, L.B. (1979) Radiographic examination of the equine vertebral column. *Vet. Radiol.*, **20**, 135–139

Jeffcott, L.B. (1979) Radiographic features of the normal equine thoracolumbar spine. *Vet. Radiol.*, **20**, 140–147

Jeffcott, L.B. (1979) Back problems in the horse – a look at past, present and future progress. *Equine Vet. J.*, **11**, 129–136

Jeffcott, L.B. (1980) Disorders of the thoracolumbar spine of the horse – a survey of 443 cases. *Equine Vet. J.*, **12**, 197–210

Jeffcott, L.B. and Dalin, G. (1980) Natural rigidity of the horse's backbone. *Equine Vet. J.*, **12**, 101–108

Jeffcott, L.B. and Hickman, J. (1975) The treatment of horses with chronic back pain by resecting the summits of the impinging dorsal spinous processes. *Equine Vet. J.*, **7**, 115–119

Leipold, H., Brandt, G., Guffy, M. and Blauch, B. (1974) Congenital atlanto-occipital fusion in a foal. *Vet. Med./Small Anim. Clin.*, **69**, 1312–1316

McCoy, D., Shires, P. and Beadle, R. (1974) Ventral approach for stabilisation of atlantoaxial subluxation secondary to odontoid fracture in a foal. *J. Am. Vet. Med. Ass.*, **185**, 545–549

Mayhew, I. (1978) Congenital occipitoatlantoaxial malformations in the horse. *Equine Vet. J.*, **10**, 103–113

Mayhew I, Whitlock, R. and de Lahunta, A. (1978) Spinal cord disease in the horse. *Cornell Vet.*, **68**, Suppl. 6, 44–68

Mayhew, I., Donawick, W., Green, S. *et al.* (1993) Diagnosis and prediction of cervical vertebral malformation in Thoroughbred foals based on semi-quantitative radiographic indicators. *Equine Vet. J.*, **25**, 435–440

Moore, B., Holbrook, T., Stefanacci, J. *et al.* (1992) Contrast-enhanced computed tomography in six horses with cervical stenotic myelopathy. *Equine Vet. J.*, **24**, 197–202

Moore, B., Reed, S., Biller, D. *et al.* (1994) Assessment of vertebral canal diameter and bony malformations of the spine in horses with cervical sclerotic myelopathy. *Am. J. Vet. Res.*, **55**, 5–13

Olchowy, T. (1994) Vertebral body osteomyelitis due to *Rhodococcus equi* in 2 Arabian foals. *Equine Vet. J.*, **26**, 79–80

Owen, R. ap R. and Smith-Maxie, L. (1978) Repair of a dens of the axis in a foal. *J. Am. Vet. Med. Ass.*, **173**, 854–856

Rantanen, N., Gavin, P., Barbee, S. and Sande, R. (1981) Ataxia and paresis in horses,

Part 2: Radiographic and myelographic examination of the cervical vertebral column. *Comp. Cont. Educ.*, **3**, 161–171

Ricardi, G. and Dyson, S. (1993) Forelimb lameness associated with radiographic abnormalities of the cervical vertebrae. *Equine Vet. J.*, **25**, 422–426

Richardson, D. (1986) *Eikenella corrodens* osteomyelitis of the axis in a foal. *J. Am. Vet. Med. Ass.*, **188**, 298–299

Rooney, J.R. (1963) Equine incoordination 1. Gross morphology. *Cornell Vet.*, **53**, 411–422

Rooney, J.R. and Prickett, M.E. (1966). Congenital lordosis of the horse. *Cornell Vet.*, **57**, 417–428

Smythe, R.H. (1962) Ankylosis of the equine spine; pathologic or biologic? *Mod. Vet. Pract.*, **43**, 50–51

Vaughan, L. and Mason, B. (1975) *A Clinicopathological Study of Racing Accidents in Horses*, Adlard and Son, Bartholomew Press, Dorking, Surrey

Whitwell, K. (1980) Causes of ataxia in horses. *Vet. Rec. Suppl. In Practice*, **2**, 17–24

Whitwell, K. and Dyson, S. (1987) Interpreting radiographs 8: Equine cervical vertebrae. *Equine Vet. J.*, **19**, 8–14

Wilson, W., Hughes, S., Ghoshal, N. and McNeel, S. (1985) Occipitoatlantoaxial malformation in two non Arabian horses. *J. Am. Vet. Med. Ass.*, **187**, 36–40

Chapter 10
The Pelvis and Femur

Pelvis

The primary indications for radiography of the pelvis are:

1 Asymmetry of the pelvis, assessed by comparison of the tubera coxae and sacrale.

2 Hindlimb lameness in the absence of clinical and radiographic abnormalities of the lower limb.

3 Audible or palpable crepitus in the pelvic region associated with hindlimb lameness (radiography performed with the horse under general anaesthesia should be postponed in these circumstances for at least 6 weeks – see 'Fractures', page 474). It should be noted that diagnostic ultrasonography can be useful to identify fractures, especially those of the ilial wing.

4 Positive nuclear scintigraphic findings.

RADIOGRAPHIC TECHNIQUE

Equipment

Radiographs of the pelvis require radiographic equipment with an output in excess of 100 kV and 200 mA s. Rare earth screens and films are required. Large (35 cm × 43 cm) cassettes are recommended. Lateral views of the pelvis are only practical in foals and thin small horses, and have very limited diagnostic value. Standing ventrodorsal oblique radiographs can be obtained, and may be useful to diagnose obvious lesions of the coxofemoral joint and the ischium, particularly when general anaesthesia is clinically undesirable. Strict control of personnel is essential to minimize the radiation hazard. Such radiographs may underestimate the degree of pathological abnormality. It is not possible to assess the ilia or sacroiliac joints using this technique. Much more detailed, high quality radiographs of the entire pelvic region are obtained with the horse in dorsal recumbency under general anaesthesia. Because of the large exposures required, no personnel should be in the x-ray room during radiography.

It is preferable to have an x-ray table that incorporates a cassette tunnel, since accurate positioning of the cassettes directly under a recumbent horse is difficult (Figure 10.1).

Because of the large amount of soft tissue present, scattered radiation is a serious problem. It must be carefully controlled using one or more of the following:

• precise collimation of the primary x-ray beam, using a light beam diaphragm;

[457]
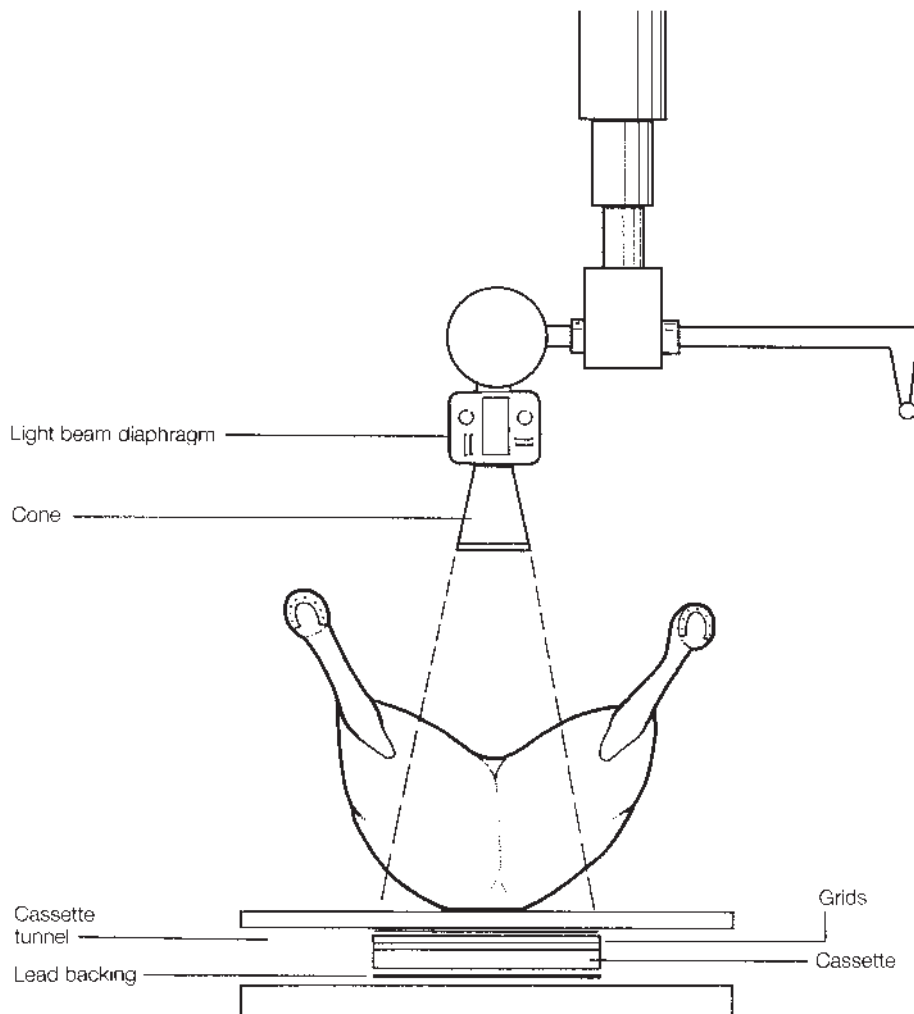
Figure 10.1 Positioning of the x-ray machine, horse and cassette to obtain ventrodorsal radiographic views of the pelvis and lumbar vertebrae (not to scale).

- a focused grid (12:1 ratio), or ideally two focused grids with grid lines at right angles to each other (this will markedly increase the exposure required);
- a lead intensifying screen (lead equivalent 0.002 cm) placed in front of the grid(s) to absorb low-energy radiation;
- a sheet of lead (0.01 mm lead equivalent) placed behind the cassette in order to reduce backscatter;
- a lead cone in addition to a light beam diaphragm is helpful to collimate the primary beam fully.

Positioning

Ventrodorsal views of the pelvis with the horse in dorsal recumbency

For accurate assessment of pelvic radiographs it is important that the horse is positioned symmetrically in dorsal recumbency in the so-called 'frog leg' position, i.e. with the caudal lumbar spine and the sacrum in a straight line, and the hindlimbs flexed and abducted. In horses with unilateral atrophy of the muscles of the hindquarters and/or severe asymmetry of the pelvis,

[458]

positioning can be difficult. The best guide to ensure that positioning is correct is to assess the linea alba, which should be straight and lie vertically above the spine. The position of the flexed hind limbs, and in particular the points of the hocks, can be deceptive. All the radiographs are obtained with the x-ray beam aligned perpendicular to the table on which the horse is supported.

For complete assessment of the pelvis of an adult horse, at least seven standard overlapping radiographic views are recommended (using 35 cm × 43 cm cassettes) (Figure 10.2).
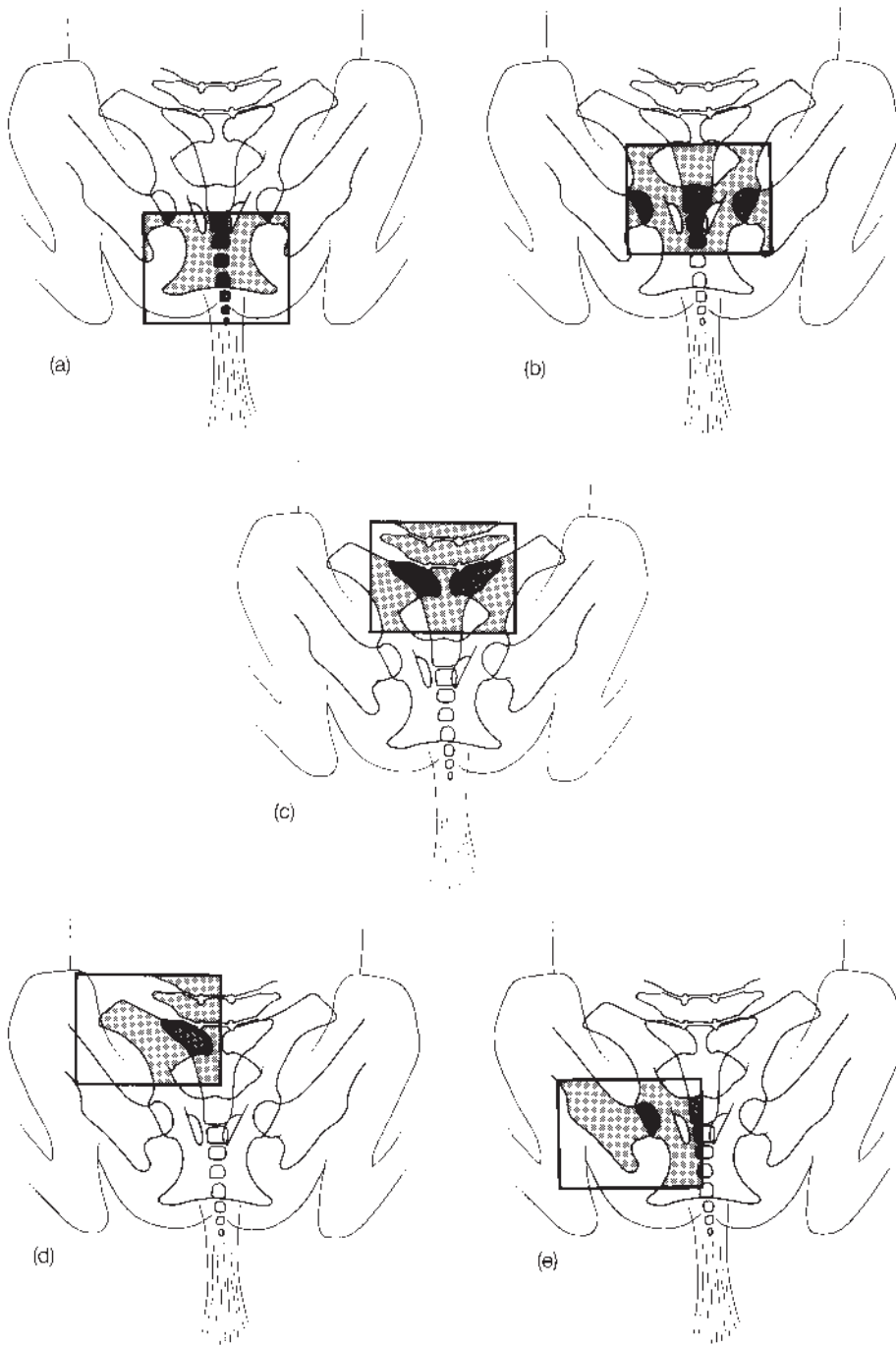
Figure 10.2 Positioning the cassette relative to the horse to obtain ventrodorsal views of (a) the tubera ischia, (b) the pelvic canal, (c) the sacroiliac joints, (d) an iliac wing and (e) a coxofemoral joint. The latter is obtained with the horse rocked towards the side to be examined.

[459]

Three views are obtained along the midline of the pelvis. The x-ray beam in each case is centred on the linea alba.

1 To examine the tubera ischii, the caudal edge of the cassette is positioned immediately caudal to the tubera ischii.

2 To examine the region of the coxofemoral joints and obturator foramina, the cassette is moved cranially, so that the two radiographic images overlap by about 5 cm. This also gives visualization of the caudal part of the sacrum.

3 To examine the sacroiliac and lumbosacral joints and the cranial part of the sacrum, the cassette is moved cranially, to overlap the previous position by about 5 cm.

Separate views are obtained of each tuber coxae. The cassette is positioned 5–10 cm cranial to the most cranial view of the pelvic canal, but is centred approximately 20 cm to the right or left of the midline. This view may aid definition of the individual sacroiliac joints.

For examination of the left and right coxofemoral joints, the horse should be rolled slightly so that the limb on the side to be radiographed is tilted nearer to the table, forming an angle of 10–15° with the horizontal. The cassette is positioned about 10 cm cranial to the position for the caudal pelvic view, and the x-ray beam is centred 5–10 cm lateral to the linea alba. This view will also give good visualization of the proximal femur.

Demonstration of specific lesions may require non-standard views. Oblique views are best obtained by rolling the horse, rather than angling the x-ray beam, in order to avoid grid cut-off.

Superimposition of gas- and ingesta-filled viscera over the pelvis is a problem. Routine starvation prior to general anaesthesia and radiography unfortunately has little effect upon this. During radiography rectal manipulation of the viscera and manual emptying of the rectum can be tried, but tend to be ineffective in moving the intestinal contents significantly.

Ventrodorsal views of the pelvis in the standing horse

It is essential that the horse is adequately sedated. It should stand with the hind limbs abducted as far as is compatible with standing both comfortably and still. A cassette and cross-hatch grid are placed dorsal to the pelvic region, angled so that they will be perpendicular to the x-ray beam. The x-ray tube is then positioned ventral to the horse's abdomen, cranial to the hind limbs, and the beam is angled dorsally 10–25° caudad. The cassette and cross-hatch grid are positioned over the hindquarter to be examined, or over the dorsal midline to examine both sides simultaneously (Figure 10.3). The cassette and the x-ray tube can be moved caudally, cranially or laterally to visualize the coxofemoral joints, the caudal pelvic canal and the tubera ischii. It is important to recognize the potential risk to personnel in the room, with the large exposure factors required (up to 150 kV, 400 mA s for a 500 kg horse). The use of a vertically mounted Bucky and cassette holder is highly recommended. The cassette should never be hand held.
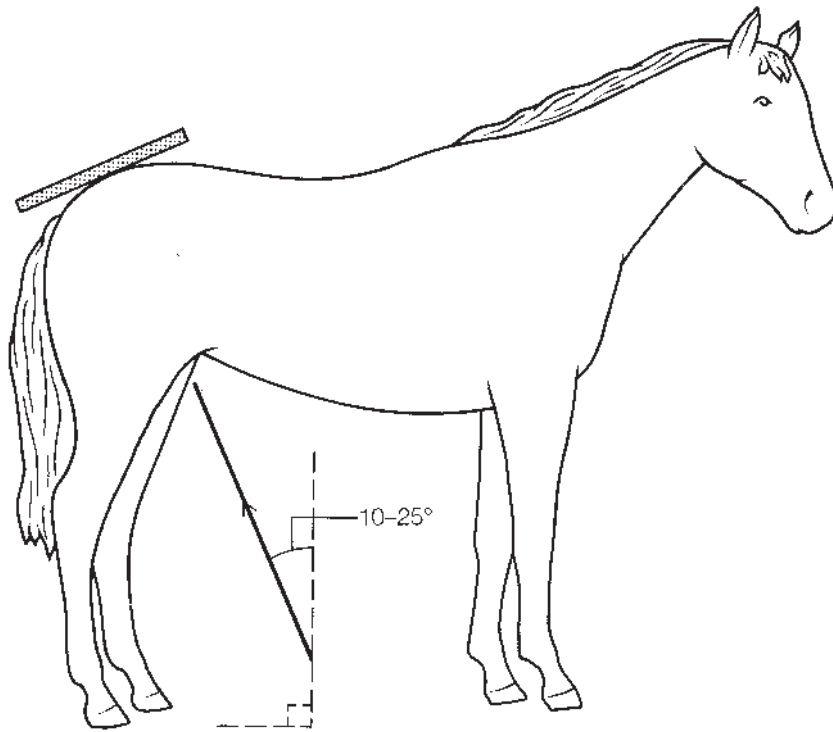
Figure 10.3 Positioning to obtain ventrodorsal views of the pelvis in the standing horse.

NORMAL ANATOMY, VARIATIONS AND INCIDENTAL FINDINGS

Immature horse

The pelvis consists of three paired bones (left and right): the ilium, pubis and ischium (Figure 10.4). At birth the symphyseal branches of the pubis and ischium are fused to each other, but ossification of their shafts, and fusion with the ilium to complete the acetabulum, does not occur until about 1 year of age (see page 587). In foals and yearlings the points of the tubera ischii are irregular and bluntly outlined due to incomplete ossification.

Separate ossification centres occur in each of the bones: ilium – iliac crest and tuber coxae; pubis – acetabular portion of the shaft; ischium – caudal portion of the bone and tubera ischii.

The separate centres of ossification of the pelvis fuse by about 10–12 months, but the symphysis pubis remains unfused throughout life.

The proximal femur has separate centres of ossification for the femoral head, the trochanter major, and the trochanter minor. The physis of the femoral head closes between 24 and 36 months, and the trochanter major fuses with the femoral shaft between 18 and 30 months. Fusion of the trochanter minor is less consistent, usually occurring at about 2 years.

[461]
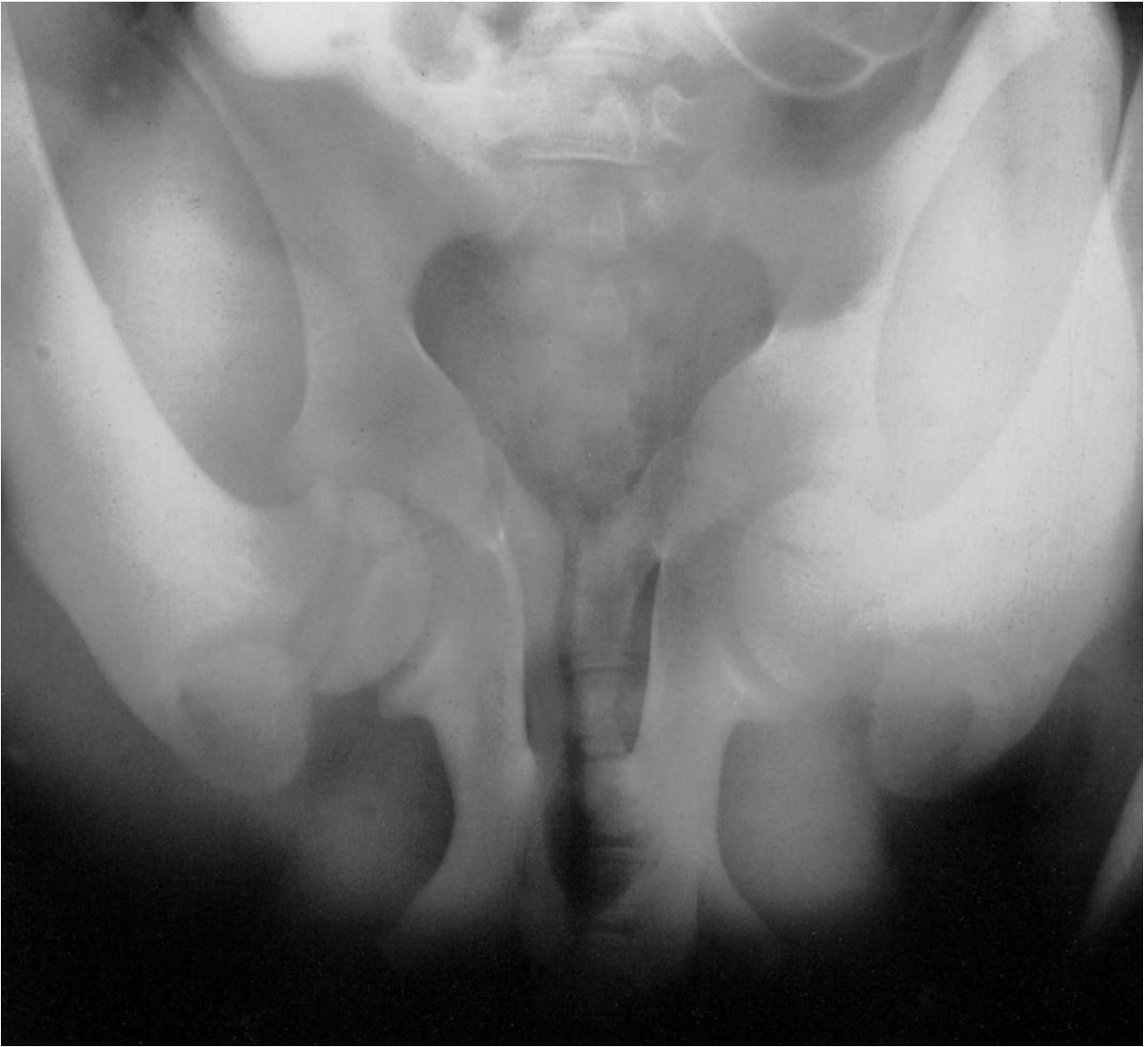
Figure 10.4 Ventrodorsal view of the pelvis, caudal lumbar vertebrae and sacrum of a normal foal of 11 days of age (compare with Figures 10.5a–c). Note the position of the symphyses between the ilium and pubis, and the ischium and the ilium, the wide pubic symphysis and the physis of the femoral head.

Skeletally mature horse

When examining radiographs of the pelvis it is useful to start by assessing the obturator foramina (Figure 10.5b, page 464). If the horse is correctly positioned, these should appear symmetrical. If the foramina appear asymmetrical, this may be due to poor positioning or to traumatic damage to the pelvis. Asymmetry of the foramina is frequently seen in combination with pubic, ischial or acetabular fractures.

The symphysis pubis remains evident throughout life (Figure 10.5a). It is relatively straight. Occasionally a bony protuberance is evident at the

Figure 10.5(a) Ventrodorsal view of the caudal aspect of the pelvis of a normal adult horse. The cranial coccygeal vertebrae are superimposed over the pubic symphysis. Note the slight irregularity in outline of the cranial edge of each tuber ischium (arrows).

[463]
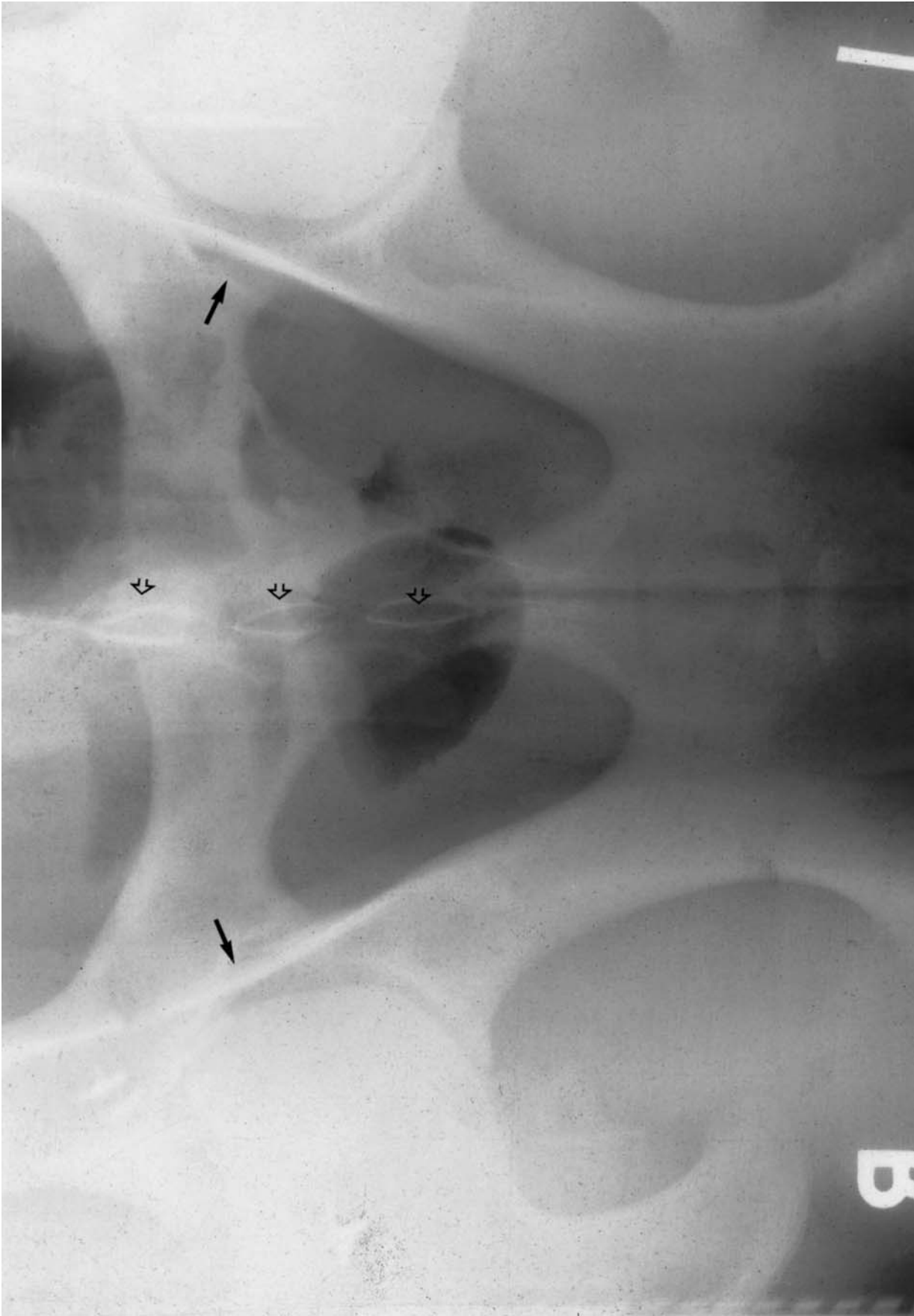
Figure 10.5(b) Ventrodorsal view of the pelvic canal of a normal adult horse. The oval-shaped opacities in the midline (open arrows) represent the dorsal spinous processes of the sacrum. Superimposed abdominal viscera cause the gas shadows. Note the symmetry of the obturator foramina, apparent widening of each coxofemoral joint in the region of the insertion of the teres ligament (closed arrows) and the flat appearance of the outline of the opposing femoral heads.

[464]

cranial aspect of the pubic symphysis. The pubic bones should be aligned, with no step at the pelvic brim. Roughening on the cranial aspect of the pubis in the region of the pubic tubercle and iliopubic eminence may be seen.

The outline of the tubera ischii varies slightly between individuals, but should always be regular (Figure 10.5a, page 463).

The shaft of the ilium is smooth, with some roughening of the psoas tubercle. The ilium broadens cranially to form the body of the ilium and tuber coxae laterally, and the tuber sacrale medially (Figure 10.5d, page 468).

To compare the left and right coxofemoral joints, it is important that the pelvis is symmetrically positioned with similar rotation and abduction of the femurs. This can be evaluated on radiographs by comparing the angle formed between the trochanter major and the acetabular branch of the ischium.

The acetabulum is formed by fusion of the ilium, ischium and pubis. The dorsal rim has a smooth outline (Figure 10.5e, page 469). The ventral rim has, at its deepest point, a depression – the acetabular fossa – for attachment of the ligament of the femoral head (teres ligament). At the site of attachment of this ligament on the femoral head, a small focal lucent area – the fovea capitis – can sometimes be seen, opposite the acetabular fossa.

The sacroiliac joints (left and right) provide the only articulation between the pelvis and the spine, and have little movement (Figure 10.5c, pages 466 and 467). They are diarthrodial joints with flattened joint surfaces which are angled at approximately 30° to the horizontal plane. The size and contour of the joints vary between individual animals. The joints are difficult to identify on a ventrodorsal projection, due to their angle and superimposition of abdominal viscera. It may be helpful to locate the narrowest (caudal) part of the sacrum between the shafts of the ilia and follow the diverging outlines of the sacrum cranially towards the external angle of the lumbosacral joint (Figure 10.5c, pages 466 and 467). The sacroiliac joints are located where these lines are superimposed upon the wings of the ilia.

The five sacral vertebrae are fused, but have separate dorsal spinous processes which are seen as oval-shaped opacities in the midline, superimposed on the body of the sacrum (Figure 10.5c). The body of the sacrum broadens cranially. The first sacral vertebra has transverse processes which articulate with the transverse processes of the most caudal (the sixth) lumbar vertebra. The lumbosacral joints are easily recognized on dorsoventral radiographs (Figure 10.5c). The sacral body has intervertebral foramina between the adjacent vertebrae, but these can be difficult to identify radiographically. The intervertebral foramina between the sacrum and the most caudal lumbar vertebra and adjacent lumbar vertebrae are clearly seen as approximately circular lucent zones on the left and right sides of the intercentral articulations. The intercentral articulations are slightly variable in width and often appear wider in the sagittal midline than at the periphery of the joints, because the caudal articular surfaces are more curved than the cranial articular surface of the adjacent vertebra. The caudal subchondral bone plate of each lumbar vertebra is relatively sclerotic.

[465]

[466]
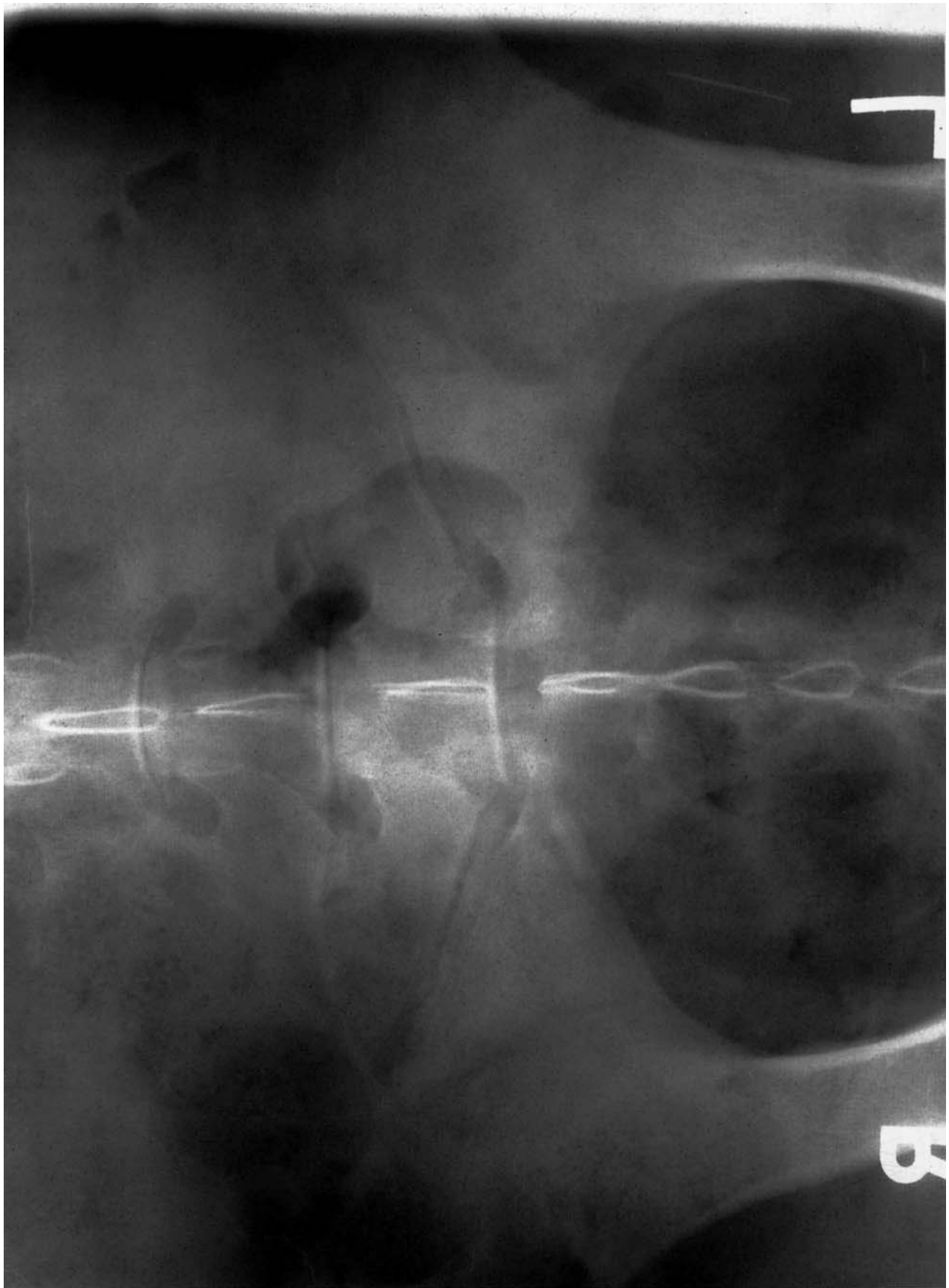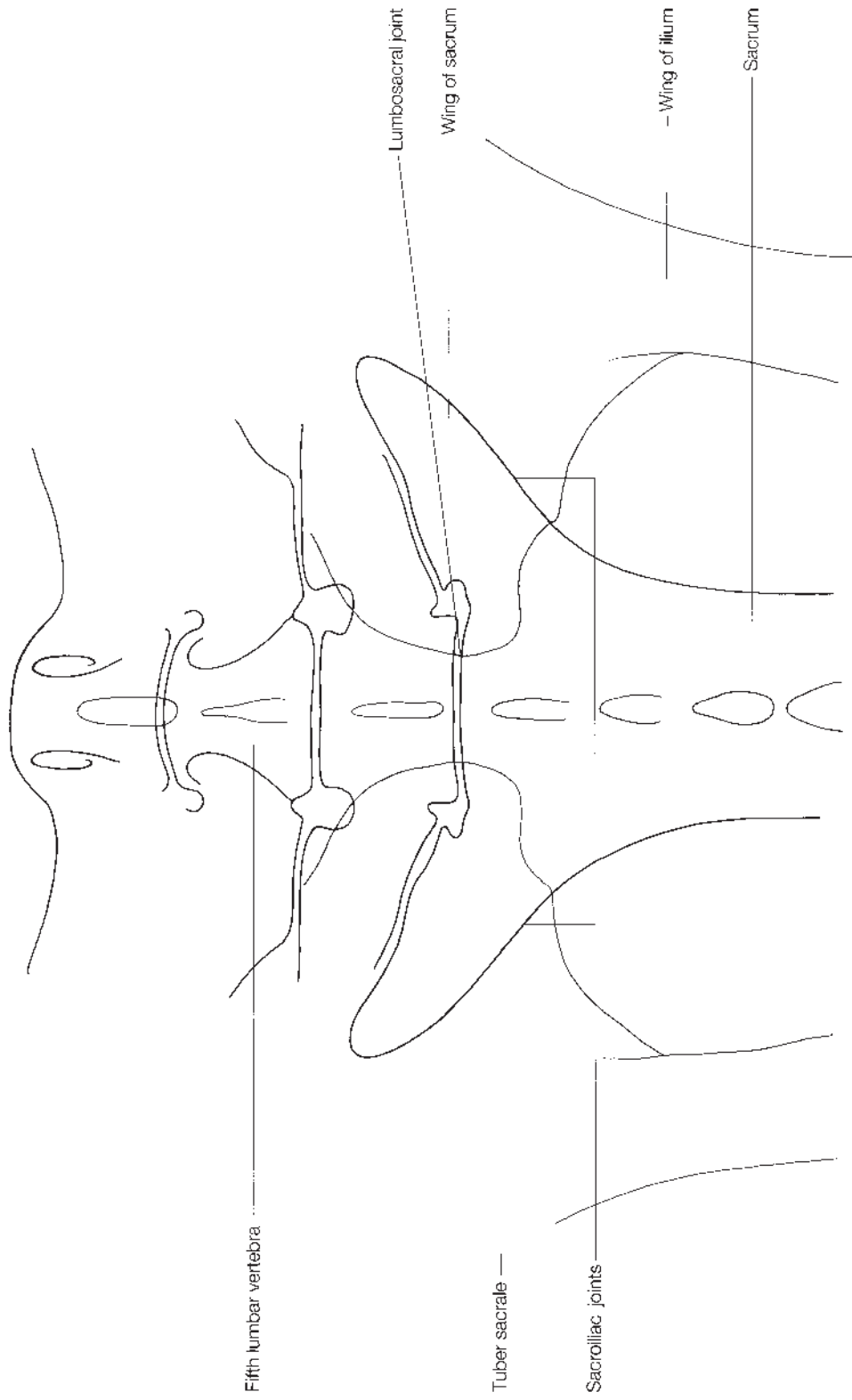
Figure 10.5(c) Radiograph (above) and diagram of a ventrodorsal view of the lumbosacral region of a normal adult horse. Note the changing shape of the intercentral articulations of the lumbar vertebrae from cranially to caudally and the wider lumbosacral joint. The articulations between the transverse processes of the caudal lumbar vertebrae and the sacrum are well defined. The sacroiliac joint is less well defined on the left side due to superimposition of abdominal viscera.

Figure 10.5(d) Ventrodorsal view of the right iliac wing and shaft of a normal 4-year-old horse. Note the incomplete fusion of the separate centre of ossification of the tuber coxae (arrow). The right sacroiliac joint is underexposed and therefore poorly defined.

[468]

Figure 10.5(e) Ventrodorsal view of a coxofemoral joint of a normal adult horse. Note the slightly irregular margin of the cranial aspect of the proximal femur (arrow) which should not be confused with new bone formation.

[469]

Articulations between the transverse processes of the lumbar vertebrae are variable and may be asymmetrical. There is no relationship between age and the number of articulations, or the presence of ankylosis. The size and width of intertransverse articulations tends to be greatest at the lumbosacral joint and decreases craniad. The articulations between the transverse processes of adjacent lumbar vertebrae are often slightly irregular in outline. Occasionally irregular lucent zones and areas of sclerosis are seen in the cortical bone opposing the joints.

Less commonly there may be fusion of the intercentral joints between the most caudal lumbar vertebrae and between the sixth lumbar vertebra and the sacrum, but this usually cannot be detected in a dorsoventral radiograph unless associated spondyles project laterally. The clinical significance of these changes is uncertain.

In the standing horse acceptable images of the caudal ilium and ischium, the acetabulum and femoral head and neck can be obtained. Views of the obturator foramen are obliqued compared to views obtained with the horse under general anaesthesia, resulting in foreshortening. Caudal abdominal contents are superimposed over the pubis, making evaluation difficult. Evaluation of the ilia and sacroiliac joints is impossible.

SIGNIFICANT FINDINGS

Hip dysplasia

This condition occurs very infrequently. Radiographic evidence includes flattening of the acetabulum, deformation of the femoral head and neck, subluxation, and secondary degenerative changes in the joint. Such changes can only be appreciated on radiographs obtained with the horse under general anaesthesia. Even then care must be taken when evaluating radiographs, since relatively small changes in the position of the horse, or angle of the x-ray beam, can cause artefacts, especially in the region of attachment of the round ligament.

Subluxation of the coxofemoral joint

Subluxation of the coxofemoral joint has been described in association with malformation of the acetabulum and femoral head. Although the latter may be developmental in origin, it is also thought to occur secondarily to trauma and hip dysplasia (see above). The condition is characterized radiographically by flattening of the contour of the acetabulum and the femoral head, and an increase in the width of the joint space.

Luxation of the coxofemoral joint

Luxation of the coxofemoral joint is rare and is usually the result of trauma with craniodorsal displacement of the femoral head. Radiographically there is superimposition of the acetabulum and the femoral head. The

[470]

radiographs should be inspected carefully for evidence of concurrent fractures of the femoral head and acetabulum. The condition is characterized clinically by moderately severe to non-weight-bearing lameness, a tendency to abduct the stifle and foot, and dorsal displacement of the trochanter major of the femur. There is often audible and palpable crepitus. Surgical treatment has been successful in some cases, but the prognosis is otherwise poor.

Septic arthritis/osteomyelitis

Septic arthritis and osteomyelitis complex occurs occasionally in the coxofemoral joint of young horses and is characterized radiographically by widening of the joint space and productive and destructive bone changes involving both the acetabulum and the femoral head. The proximal femoral physis may also be involved in type P osteomyelitis (see Chapter 1, page 21).

Degenerative joint disease

Degenerative joint disease of the coxofemoral joint is an unusual cause of lameness in the horse. In some cases it is secondary to hip dysplasia, an acetabular fracture or damage to the teres ligament. Radiographic changes include: (a) modelling of the acetabulum, with osteophyte formation on the cranial and caudal margins (Figure 10.6); (b) flattening of the femoral head; (c) irregular width of joint space; (d) changes in subchondral bone opacity; (e) new bone formation on the neck of the femur.

    The prognosis for future athletic function is hopeless in mature animals, but some horses may be sound enough to be retired for breeding purposes.

Sacroiliac joint disease

The radiographic features associated with a chronic sacroiliac lesion are usually minimal or absent. Occasionally there may be increase of the width of the joint space, or asymmetry of the two joints. The relative positions of the tubera sacrale and the summits of the sacral dorsal spinous processes may be altered. In a few advanced cases, peripheral osteophytes near the most caudal margin of the joint can be seen, disrupting the relatively smooth caudal outline of the medial aspect of the wing of the ilium (Figure 10.7, page 473). It is not possible to demonstrate radiographic abnormalities in the majority of cases where clinical signs are suggestive of lameness associated with the sacroiliac joints.

    Linear tomography has shown potential for examining the lumbosacral region, including abnormalities of the sacroiliac joint. This equipment is only available at a very small number of clinics, and therefore is not discussed further.

    Nuclear scintigraphic examination may also be valuable in acute cases.
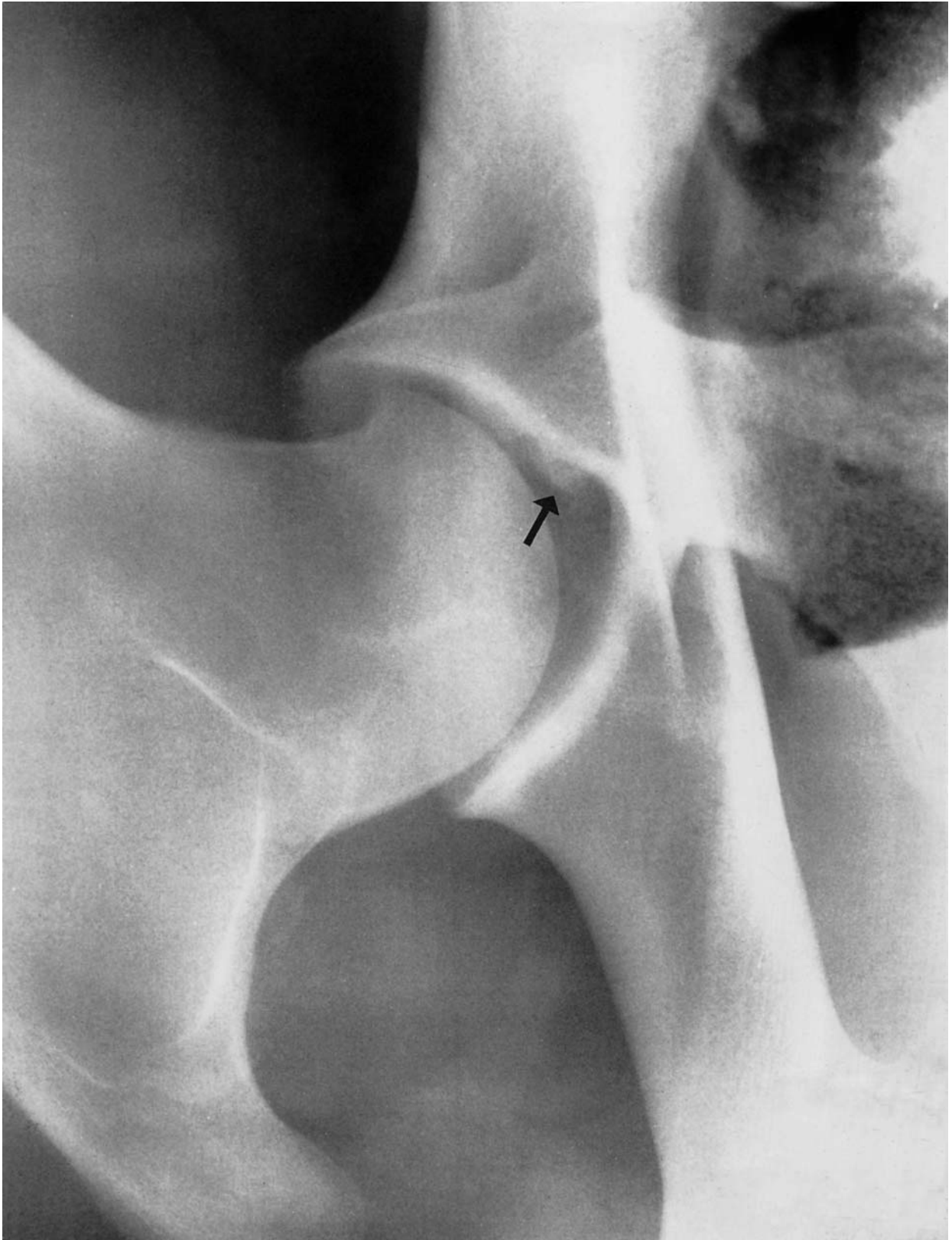
Figure 10.6 Ventrodorsal view of the right coxofemoral joint of a 14-year-old part Thoroughbred with evidence of degenerative joint disease. The cranial half of the acetabulum is poorly defined due to osteophyte formation (arrow) (compare with Figure 10.5e); there is also slight loss of definition of the caudal half of the acetabulum.

[472]

Figure 10.7 Ventrodorsal view of the sacrum and right iliac wing of a 5-year-old Arab with asymmetry of the tubera sacrale and right hindlimb lameness. The right sacroiliac joint is abnormal in shape and widened irregularly. There is no evidence of new bone formation on the caudal aspect of the joint.

[473]

Osseous cyst-like lesions

Osseous cyst-like lesions have been recorded in the femoral head and the acetabulum. There is insufficient information for any prognosis or treatment to be recommended.

Osteochondrosis

The coxofemoral joint is an unusual site for osteochondrosis. Radiographic abnormalities have been described in both the acetabulum and the femoral head, and include poorly defined lucent zones in the subchondral bone, with or without a surrounding sclerotic rim. Circular lucent zones in the subchondral bone have been referred to as subchondral bone cysts, but there is little evidence to show whether these are true subchondral bone cysts. Modelling of the caudal aspect of the acetabulum without associated lucent zones in the subchondral bone has also been described. The prognosis for further athletic soundness is generally considered to be poor.

Fractures

If a fracture of the pelvis is suspected, standing radiography may be useful in some cases. If radiographs are to be obtained with the horse in dorsal recumbency, it is recommended that anaesthesia should be delayed for at least 6 weeks in order to avoid further displacement of the fracture during induction and recovery.

Although severe direct trauma is normally required to fracture the pelvis, 'spontaneous' fracture (often of the shaft or wing of the ilium) does occasionally occur during exercise in young Thoroughbreds in training. Spontaneous fractures are more common in females. These fractures probably initiate as incomplete stress fractures. With the more routine use of nuclear scintigraphic evaluation combined with diagnostic ultrasonography, fatigue fractures have been detected earlier, and the incidence of complete fractures has decreased.

The most common sites of fractures are the ilium, acetabulum and ischium (Figure 10.8). As a general rule the prognosis is considerably worse if there is an articular component to the fracture (coxofemoral or sacroiliac), due to subsequent secondary degenerative joint disease.

Fractures of the ilium

Fractures of the tuber coxae alone are recognized by a slight palpable irregularity of the external angle of the ilium, and seldom require radiography for diagnosis. On radiographs the tuber coxae appears blunted, but the displaced fragment may not be visible. These fractures carry a good prognosis.

Fractures of the iliac wing frequently extend obliquely in a craniocaudal
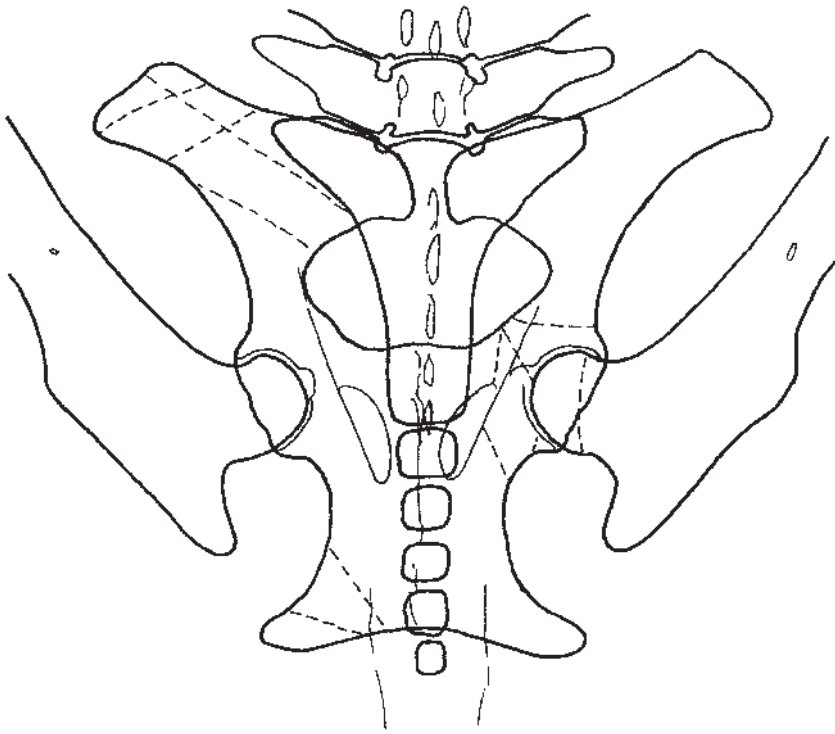
Figure 10.8 Common fracture sites of the pelvis. Compare with the position of the symphyses of the immature horse in Figure 10.4. See also Little and Hilbert (1987), Rutowski and Richardson (1989) and Pilsworth *et al.* (1994).

direction. There is often displacement due to the action of the muscle masses which attach to the tuber coxae. Large fissures which frequently ramify towards the centre of the wing (Figure 10.9) can occur with minimal displacement of the ilium. These may extend towards and sometimes involve the sacroiliac joint. Such fractures can usually be demonstrated using diagnostic ultrasonography.

Fractures of the iliac wing alone carry a fair prognosis if there is osseous union, but fibrous union accompanied by continual lameness may occur. If the fractures involve either the sacroiliac or (less frequently) the lumbosacral joints, the prognosis is guarded to poor.

Fractures of the shaft of the ilium are often articular (see below). The prognosis is poor.

Fractures involving the coxofemoral joint

Fractures of the bones comprising the acetabulum are frequently accompanied by deformation of the ipsilateral side of the pelvis due to the severity of the initiating trauma. The most common site is at or close to the symphysis between the ilium and pubis. If the fracture involves only a small part of the acetabulum in a skeletally immature horse, satisfactory modelling of the joint may occur without radiographic evidence of degenerative joint disease. Such an animal may be capable of an athletic career. If large

Figure 10.9 Ventrodorsal view of the right ilium of a 2-year-old Thoroughbred mare with a history of acute onset severe right hindlimb lameness after work 6 weeks previously. There is a displaced fracture of the right iliac wing, ramifying towards the iliac shaft. There is no bony union. The right sacroiliac joint is obscured by superimposed abdominal viscera. The radiograph was obtained using an aluminium wedge filter.

parts of the acetabular surface are involved, particularly in a skeletally mature animal, and/or articular incongruity exists, secondary degenerative joint disease is inevitable. This may be recognized radiographically within 4–5 weeks.

Fractures of the proximal femoral physis occasionally occur in foals. If a complete Salter-Harris type 1 fracture occurs, this may result in displacement of the femoral head (Figure 10.10). Internal fixation may be

[476]

Figure 10.10 Ventrodorsal view of a coxofemoral joint of a yearling Thoroughbred with lameness of approximately $2^1/_2$ months' duration. There is a displaced fracture of the femoral head through the physis (Salter-Harris type 1) with secondary changes in the femoral head and degenerative joint disease. Note the sclerosis of the femoral head adjacent to the physis.

[477]

attempted, but with a very guarded prognosis. Secondary degenerative changes may ensue. Fracture of the femoral head may follow severe trauma in the adult. The prognosis is hopeless.

If there is marked deformation of the pelvis, even without articular involvement, changes in apposition of the joint surfaces of the coxofemoral or sacroiliac joints may result in a change in gait or lameness.

Fracture of the ischium

The acetabular branch of the ischium is frequently involved in fractures of the acetabulum (see above). Fractures of the tuber ischii occur separately and are often related either to direct trauma or to the distracting effect of the semitendinosus and semimembranosus muscles, which originate on the ventral surface of this bone. There is often slight displacement of the most peripheral 5–7 cm of the tuber ischii. The prognosis for this fracture is usually good, the majority responding satisfactorily to 3–6 months of rest. Osseous healing with slight deformation of the tuber usually occurs, although occasionally lameness resolves despite lack of bony union. Non-union fractures with continual lameness rarely occur.

Femur

RADIOGRAPHIC TECHNIQUE

Equipment

The proximal two-thirds of the femur are best radiographed with the horse under general anaesthesia. It is not easy to obtain more than one view with the horse in a single position. High output x-ray equipment and fast rare earth screens are essential, and a grid is beneficial, because of the large muscle mass which must be penetrated.

Positioning

A craniolateral-caudomedial oblique view is the easiest to obtain. The horse is positioned in dorsal recumbency, tipped towards the limb to be examined, as described for radiography of the coxofemoral joint (see page 460). It is usually necessary in an adult horse to obtain more than one radiograph in order to assess the entire length of the femur. It is difficult to obtain other projections, but this can be done by adjusting the position of the horse and limb.

An alternative technique is to place the horse in lateral recumbency, lying on the limb to be examined. This limb is then extended caudally and the contralateral limb extended cranially. This technique does not give such good results for the most proximal aspect of the femur.

The distal one-third of the femur may be radiographed using the

same techniques as for the stifle joint (see page 286) and caudocranial, lateromedial and oblique views are readily obtained either with the horse standing or under general anaesthesia.

RADIOGRAPHIC ANATOMY

For details of the anatomy of the proximal and distal aspects of the femur, the reader is referred to the coxofemoral joint (pages 461–5) and the stifle joint (pages 288–98).

The proximal femur has separate centres of ossification for the femoral head, the trochanter major and the trochanter minor. The physis of the femoral head closes between 24 and 36 months, and the trochanter major fuses with the femoral shaft between 18 and 30 months. Fusion of the trochanter minor is less consistent, usually occurring at about 2 years of age.

The distal femoral physis is wavy and irregular in outline, closing at 24–30 months of age.

The greater and lesser trochanters and the third trochanter of the femur are readily seen in a craniolateral-caudomedial oblique view.

RADIOGRAPHIC ABNORMALITIES

Fractures of the femur

Fractures involving the proximal and distal epiphyses are discussed in conjunction with the coxofemoral joint (page 475) and the stifle joint (page 318).

Diaphyseal fractures of the femur

Diaphyseal fractures are relatively uncommon and result in a non-weight-bearing lameness. In immature or small horses it may be possible to detect crepitus, but in adult horses this may be concealed by the large muscle mass and soft-tissue swelling. In young horses the fractures are usually simple and oblique, but in adults the fractures are generally comminuted. There is often considerable overriding of the fracture fragments. Surgical repair of simple diaphyseal fractures may be attempted in foals, provided that the nutrient foramen is not involved. In older horses the prognosis is extremely bad.

Fracture of the third trochanter

Fracture of the third trochanter of the femur occasionally occurs (Figure 10.11). The horse shows moderate lameness and there may be palpable crepitus, although this may be difficult to detect in a well muscled horse. Nuclear scintigraphic examination may help to identify such fractures. Although the fracture may heal only by fibrous union, the horse may return to full athletic function.

[479]

Figure 10.11 Caudocranial view of a femur of an 8-year-old advanced event horse, with acute onset hindlimb lameness of 2 weeks' duration, after being cast. There is a fracture of the third trochanter of the femur (arrows). The horse made a complete recovery.

FURTHER READING

Bennet, D., Campbell, J. and Rawlinson, J. (1977) Coxofemoral luxation complicated by upward fixation of the patella in the pony. *Equine Vet. J.*, **9**, 192–194

Davison, P. (1967) A case of coxofemoral subluxation in a Welsh pony. *Vet. Rec.*, **80**, 441–443

Hance, S.R., Bramlage, L.R., Schneider, R.K. and Embertson, R.M. (1992) Retrospective study of 38 cases of femur fractures in horses less than one year of age. *Equine Vet. J.*, **24**, 357–363

Haussler, K., Stover, S. and Willits, N. (1997) Developmental variation in lumbosacro-pelvic anatomy of Thoroughbred horses. *Am. J. Vet. Res.*, **58**, 1083–1091

Haussler, K. and Stover, S. (1998) Stress fractures of the vertebral lamina and pelvis in Thoroughbred racehorses. *Equine Vet. J.*, **30**, 374–383

[480]

Jeffcott, L.B. (1979) Radiographic examination of the equine vertebral column. *Vet. Radiol.*, **20**, 135–139

Jeffcott, L.B. (1979) Radiographic features of the normal equine thoracolumbar spine. *Vet. Radiol.*, **20**, 140–147

Jeffcott, L.B. (1982) Pelvic lameness in the horse. *Equine Pract.*, **4**, 21–47

Jeffcott, L.B. (1983) Technique of linear tomography for the pelvic region of the horse. *Vet. Radiol.*, **24**, 194–200

Jeffcott, L.B. (1983) Radiographic appearance of equine lumbosacral and pelvic abnormalities by linear tomography. *Vet. Radiol.*, **24**, 201–213

Lewis, R.E. and Heinze, C.D. (1971) Radiographic examination of the equine pelvis – technique. *J. Am. Vet. Med. Ass.*, **159**, 1387–1390

Little, C. and Hilbert, B. (1987) Pelvic fractures in horses: 19 cases. *J. Am. Vet. Med. Ass.*, **190**, 1203–1205

May, S., Patterson, J., Peacock, J. and Edwards, G. (1991) Radiographic technique for the pelvis in the standing horse. *Equine Vet. J.*, **23**, 312–314

Miller, C. and Todhunter, R. (1987) Acetabular osteochondrosis dissecans in a foal. *Cornell Vet.*, **77**, 75–83

Nixon, A., Adams, R. and Teigland, M. (1988) Subchondral cystic lesions (osteochondrosis) of the femoral heads in a horse. *J. Am. Vet. Med. Ass.*, **192**, 360–362

Pilsworth, R.C., Shepherd, M.C., Herinckx, B.M.B. and Holmes, M.A. (1994) Fracture of the wing of the ilium, adjacent to the sacroiliac joint in Thoroughbred racehorses. *Equine Vet. J.*, **26**, 94–99

Roneus, B., Svanholm, R. and Carlson, J. (1987) Diagnostik, etiologi och prognos vid skadar i backenregionen hos häster. *Svensk Veterinärtidning*, **39**, 315–323

Rose, J., Rose, E. and Smylie, D. (1981) Case history: acetabular osteochondrosis in a yearling thoroughbred. *Equine Vet. Surg.*, **1**, 173–174

Rutowski, J. and Richardson, D. (1989) A retrospective study of 100 pelvic fractures in horses. *Equine Vet. J.*, **21**, 256–259

Skidell, J. (1987) Backenfractur hos häst – en litteratursammanstallning och beskrivning av 33 fall. *Svensk Veterinärtidning*, **39**, 326–333

Speitz, V.C. and Wrigley, R. (1979) A case of bilateral hip dysplasia in a foal. *Equine Vet. J.*, **11**, 202–204

Stecher, R. and Goss, L. (1961) Ankylosing lesions of the spine of the horse. *J. Am. Vet. Med. Ass.*, **138**, 248–255

Chapter 11
The Thorax

RADIOGRAPHIC TECHNIQUE

Equipment

Complete radiographic examination of the thorax of adult horses is only possible with large stationary x-ray units and a grid (10:1 ratio) or moveable Bucky. If a grid is not available the effects of scatter radiation can be reduced by leaving an air gap between the patient and the cassette. This technique should be avoided whenever possible because of the increased parallax and magnification that occurs.

A short exposure time is required to eliminate motion unsharpness; therefore it is best to use fast rare earth screens and compatible film. Large cassettes (35 cm × 42 cm) are recommended. Foals can occasionally be radiographed in lateral and ventrodorsal recumbency by placing the cassette and grid on the floor or by using a machine with an x-ray table incorporating a Bucky grid.

Positioning

The adult or standing horse should be positioned with the forelimbs slightly forward in order to decrease the amount of muscle mass over the cranial thorax. The radiographs should be obtained at full inspiration (see pages 494 and 495). Expiratory radiographs are of value for comparison with inspiratory radiographs in two instances: to evaluate the effect of respiration on tracheal diameter or for evaluation of restrictive lung disease (see 'Chronic obstructive pulmonary disease', page 507). It is recommended that four 35 cm × 42 cm radiographs of the thorax be obtained with overlap of the fields (Figure 11.1): (a) dorsocaudal, (b) ventrocaudal, (c) dorsocranial and (d) ventrocranial (Figures 11.1a–11.1d, pages 485–8). Fields (a) and (b) are possible to radiograph with large mobile units, but fields (c) and (d) usually require larger equipment in order to penetrate the greater muscle mass in this area. The entire thorax can often be evaluated on one or two radiographs in foals (Figure 11.2, page 489), ponies and small horses (Figures 11.3a and 11.3b, pages 490 and 491).

In order to compensate for parallax and magnification, views (a) and (b) should be obtained with the right side (right lateral projection) and then the left side (left lateral projection) of the thorax next to the cassette. Parallax and magnification are major problems in evaluation of the equine thorax, but they can be used to advantage by utilizing the changes in position, size and image sharpness to determine the location of the lesion
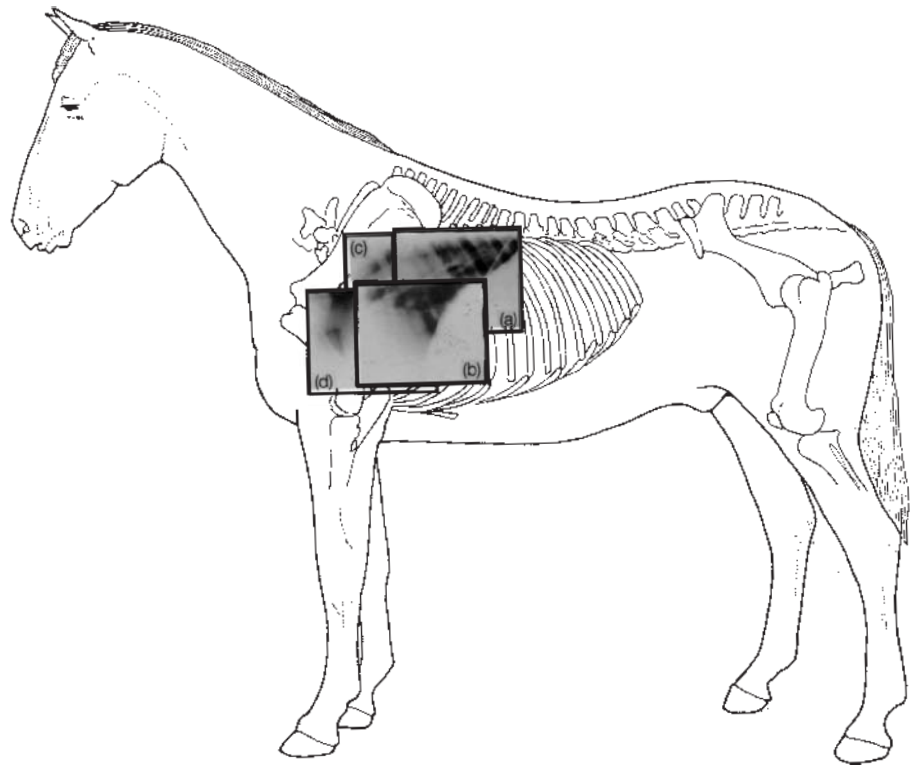
Figure 11.1 Placement of cassettes for the four overlapping views of the thorax.

(left side versus right side). Structures close to the cassette will be well visualized and have sharp margins, whereas those away from the cassette will be magnified and less distinct due to the large film focal distance (Figures 11.4a, page 492 and 11.4b, page 493).

Examination of neonates or miniature horses in lateral recumbency should include both right and left lateral recumbent views. Ventrodorsal views should be obtained when possible. When obtaining recumbent lateral radiographs, care must be exercised not to extend the forelimbs excessively as this will cause the chest to rotate and a true lateral radiograph will not be obtained.

It is recommended that thoracic radiographs be obtained using a film focal distance of 100–120 cm.

Other imaging techniques

Nuclear scintigraphy

Nuclear scintigraphy, when coupled with radiography, offers advantages in evaluation of intrathoracic disease and is particularly helpful in the investigation of chronic obstructive pulmonary disease (COPD) and exercise-induced pulmonary haemorrhage (EIPH) (see pages 507 and 520).

[484]
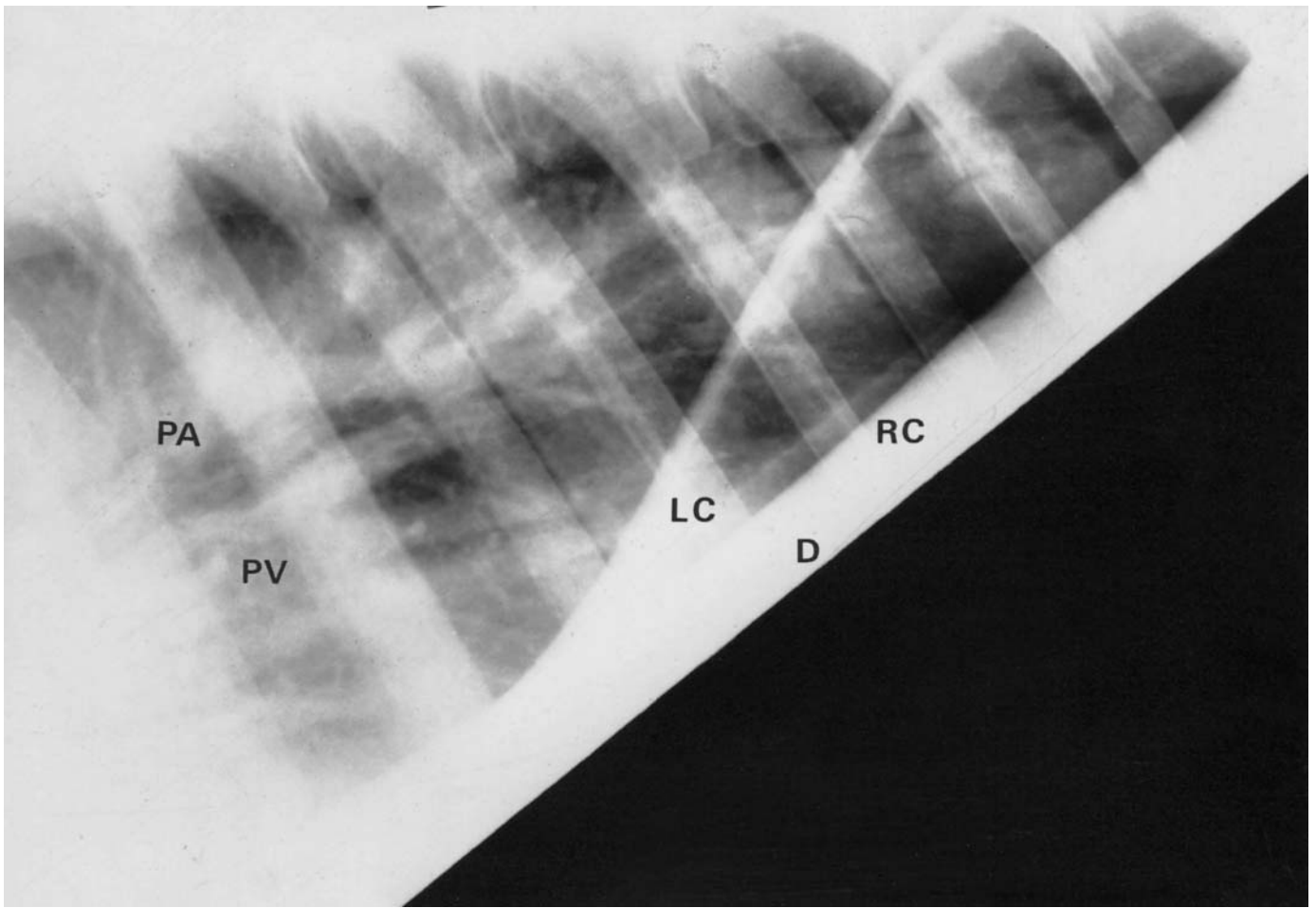
Figure 11.1(a) Dorsocaudal portion of the thorax of a normal adult horse. The branching pulmonary arteries (PA) and pulmonary veins (PV) pass dorsocaudad. The diaphragm (D) is separated into the left crus (LC) which overlies the major portion of the gastric gas cap which is also partially seen below the right crus (RC).

Ultrasound

The greater availability, economy and safety of ultrasonography make it more desirable for the evaluation of cardiac and pleural disease.

Diagnostic ultrasound is more reliable than survey radiography for the documentation of heart chamber enlargement, for the evaluation of the contractility of the myocardium and for the diagnosis of pericardial disease, pericardial effusion and valvular disease. Diagnostic ultrasound is the most valuable imaging modality for evaluation of intrathoracic disease in the presence of pleural fluid, and is an invaluable adjunct to the evaluation and differentiation of pulmonary abscesses, granulomas and tumour masses.

Monitoring pulmonary and/or pleural disease

It should be borne in mind that radiography may be much more informative then auscultation of the thorax. For example, a neonatal foal may have minimal or no abnormalities detectable by auscultation, but there may be significant abnormalities detectable radiographically. In the adult,

[485]
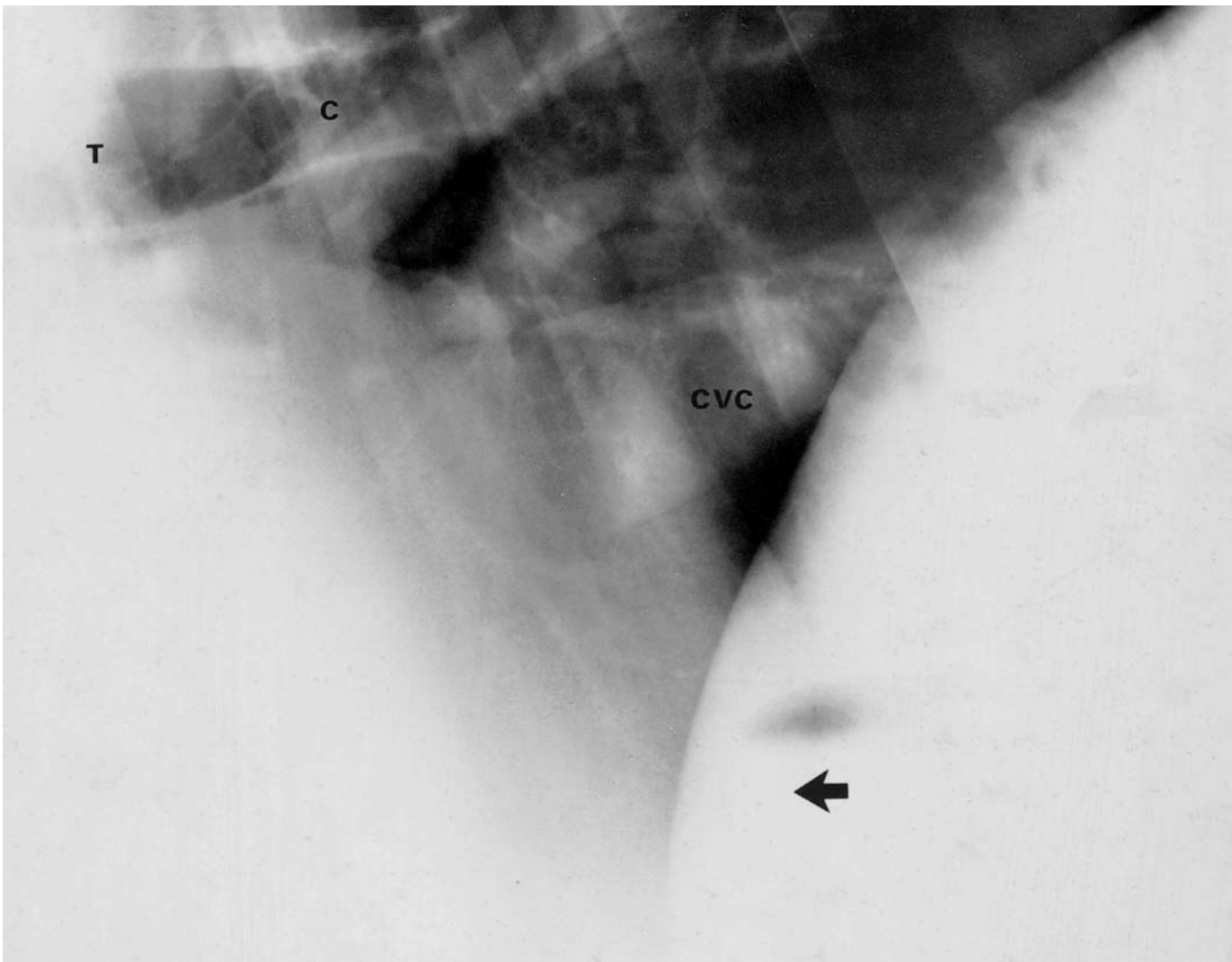
Figure 11.1(b) Ventrocaudal portion of the thorax of a normal adult horse. The caudal border of the heart overlaps the right diaphragmatic crus and is marked by the large black arrow. The pulmonary vessels overlie the caudal margin of the cardiac silhouette. The cranial portion of the cardiac silhouette is obscured by muscle mass which is not penetrated on this film. The caudal vena cava (CVC) is clearly delineated below the pulmonary arteries and veins as they exit and enter the heart, respectively. The trachea (T) passes caudally over the base of the heart and bifurcates at the carina (C). There is a lucent gas shadow in the cranial ventral abdomen adjacent to the diaphragm and the cardiac silhouette.

however, development of radiographic abnormalities may lag behind clinical signs. It should also be recognized that radiographic signs of improvement may lag behind clinical improvement in both the immature and mature horse.

NORMAL ANATOMY

It should be noted that the age of the horse, its size, the width of the thorax, the phase of respiration at which exposures are made, and the exposure factors will all influence the radiographic appearance of the lungs. High

[486]
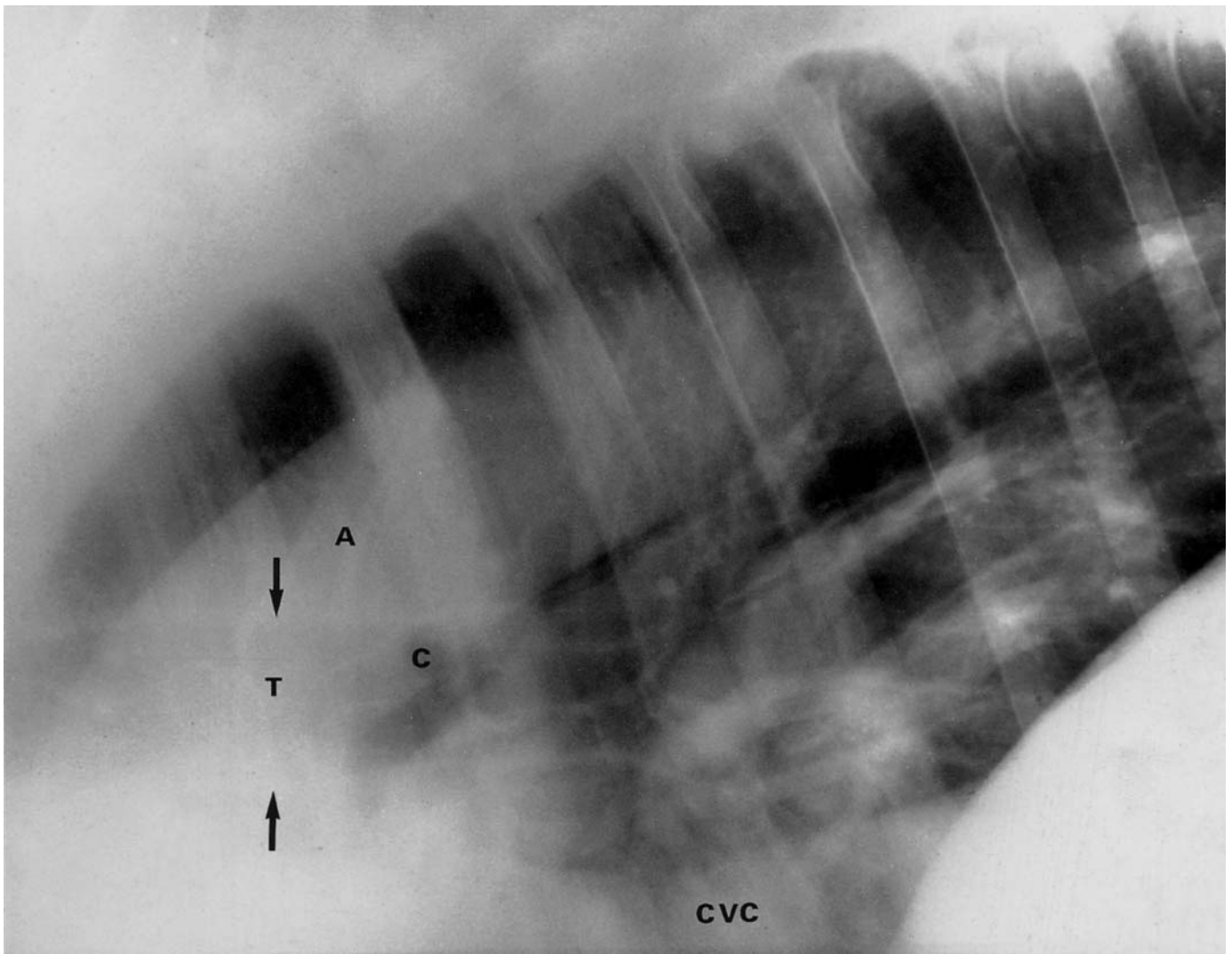
Figure 11.1(c) Dorsocranial portion of the thorax of a normal adult horse. The aorta (A) arises from the base of the heart and passes dorsocaudad, where it is lost from view due to over-penetration of the radiograph. The great pulmonary vessels arise from and enter the heart between the aorta and the caudal vena cava (CVC). The trachea (T) lies between the black arrows as it passes caudad and ends at the carina (C) where the main stem bronchi branch.

speed film–screen combinations are required, but this means some loss of resolution. Scatter radiation also reduces contrast and resolution, especially in the ventral lung fields. Thoracic wall, visceral and parietal pleura and mediastinal structures all contribute to the overall radiographic density. Interpretation of pulmonary patterns is therefore not easy. Underexposure may create artefactual lung opacities, whereas overexposure may mask lesions. It is therefore not surprising that even experienced radiologists may interpret radiographs of the thorax differently. Using a high kV, low mA technique will help to reduce artefacts created by exposure factors. For comparison of radiographs between horses, or for serial examinations of the same horse, it can be helpful to try to achieve a constant radiopacity of the vertebral bodies as a guide to exposure.

[487]
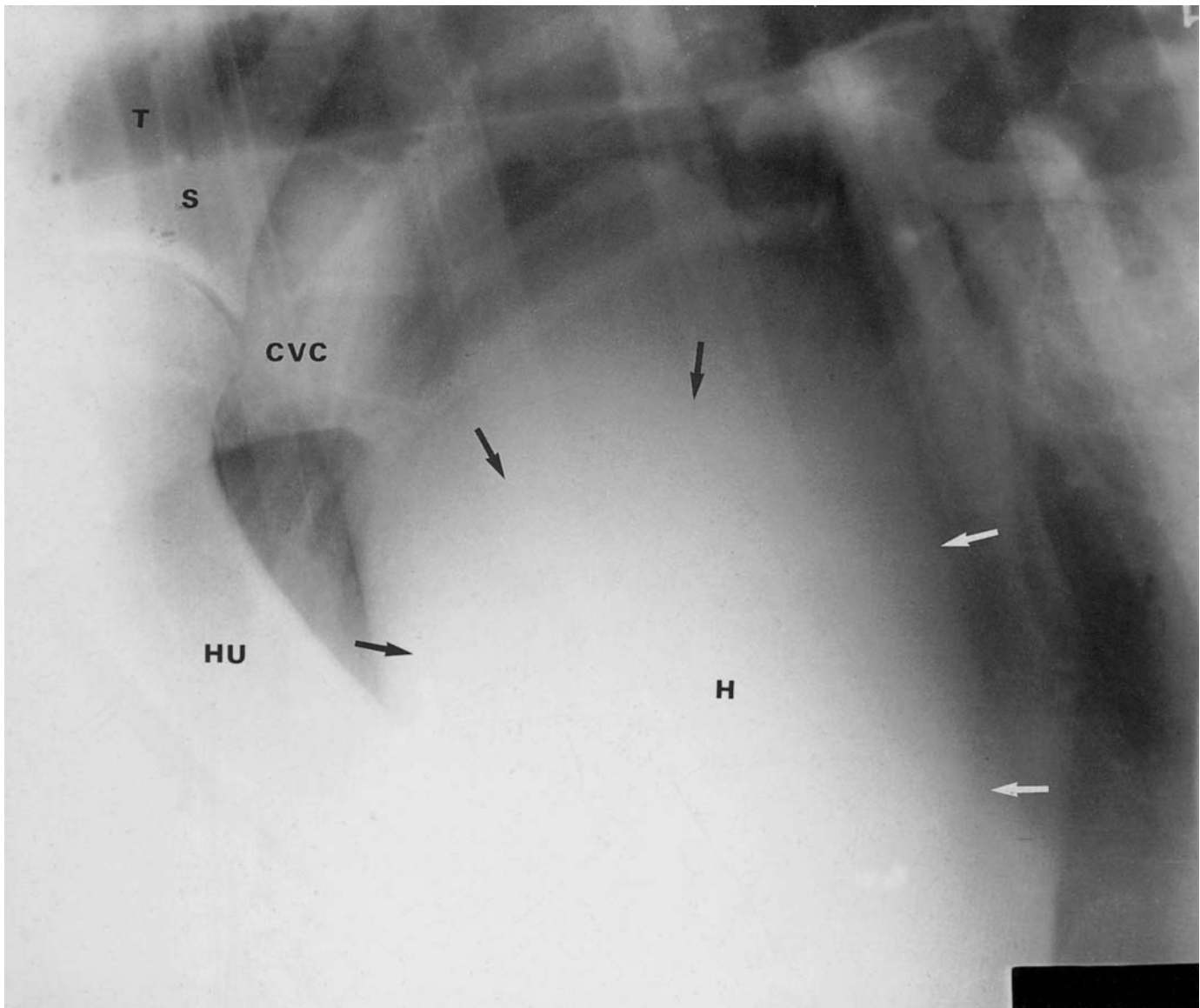
Figure 11.1(d) Ventrocranial portion of the thorax of a normal adult horse. High exposure factors are required to penetrate the muscle mass, humerus (HU) and scapula (S). The cranial vena cava (CVC) lies between the trachea (T) and the oesophagus in the cranial mediastinum. The cranial and caudal margins of the heart (H) are clearly visible and vessels arch over the top of the cardiac silhouette. The approximate border of the cardiac notch of the lungs is indicated by arrows (black and white).

Immature horse

The cardiac silhouette occupies a greater proportion of the thoracic cavity in the neonate than in the adult (compare Figures 11.1, 11.2 and 11.3). In the normal foal the craniocaudal dimension should be between 5.6 and 6.3 times the length of a mid-thoracic vertebra, and the apicobasilar dimension should be 6.7–7.8 times the length of a mid-thoracic vertebra. Radiographs of the thorax of foals obtained within the first few hours of birth usually have a generalized interstitial opacity due to incomplete inflation. Within 12

[488]
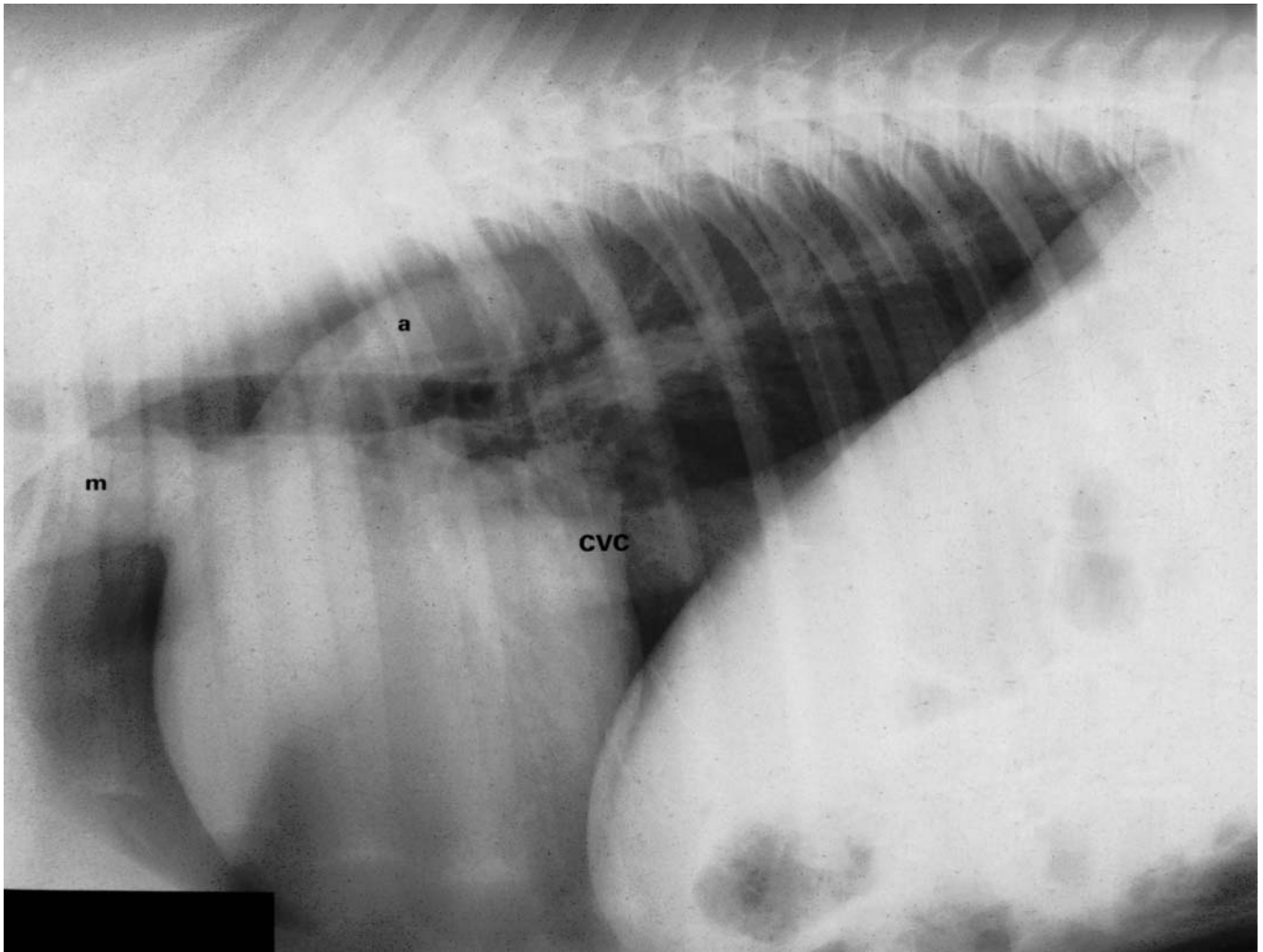
Figure 11.2 A normal 1-day-old Arabian colt. The portions of the abdomen which are seen on this film are also normal. Note the position of the trachea and its slightly ventral course, and the inability to visualize the margins of the aorta (a) beyond the caudal cardiac margin. The caudal vena cava (CVC) is well visualized. The great vessels in the cranial mediastinum are masked by other soft tissues in the mediastinum (m). Note how the fine vascular structures can be seen over the cardiac silhouette and extending to the periphery.

hours the lungs become more lucent as the foal becomes active and the lungs are more completely inflated. The initial increased opacity leads to some diagnostic challenges during the first few days of life, as premature (see Figure 11.18, page 516) and septicaemic foals will also have increased interstitial opacity. Foals with questionable abnormalities should therefore be re-evaluated in 24 and 48 hours.

Mature horse

Normal lung should appear lucent with well-defined vascular structures that are largest at the heart base and taper gradually to the periphery of the
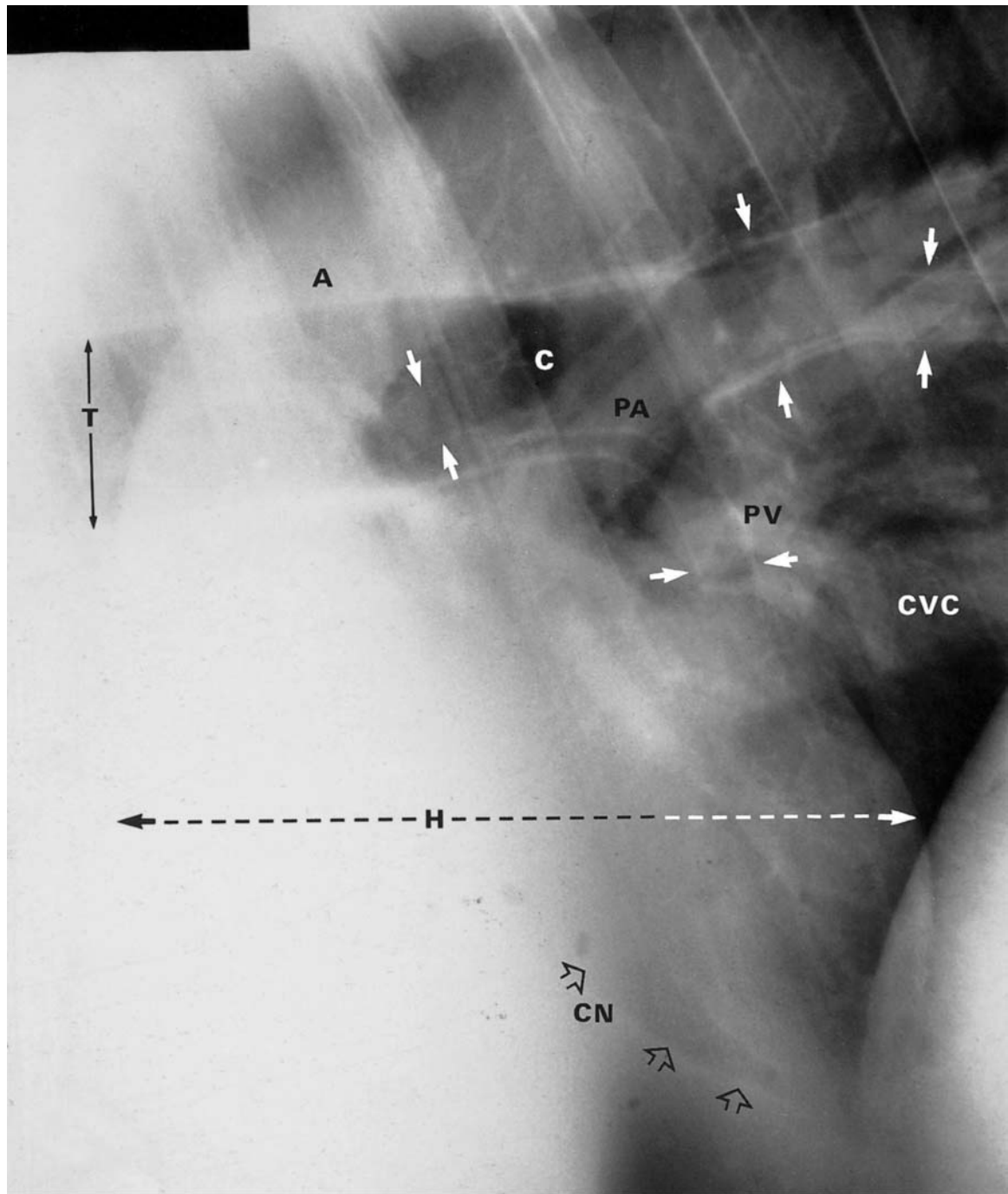
(a)

Figure 11.3 Normal adult thorax. Due to the small size of the patient, the entire thorax was obtained on two radiographs, both right lateral projections. Portions of the dorsocranial and ventrocranial thorax as well as a portion of the ventrocaudal thorax are demonstrated in (a), whereas (b) demonstrates the normal dorsocaudal thorax and a portion of the ventrocaudal thorax.

(a) The tracheal diameter (T) is marked by arrows. The trachea bifurcates at the carina (C). Some of the major bronchi are marked between short white arrows. The cranial to caudal dimension of the cardiac silhouette is defined by (H) and arrows. Major pulmonary vessels can be seen and include the aorta (A), pulmonary arteries (PA), pulmonary vein (PV) and the caudal vena cava (CVC). The caudal ventral lung margin can be seen over the cardiac notch (CN) and is marked by open arrows. Fine vascular structures are readily identified over the caudal margin of the heart, aorta and vertebral bodies.

[490]
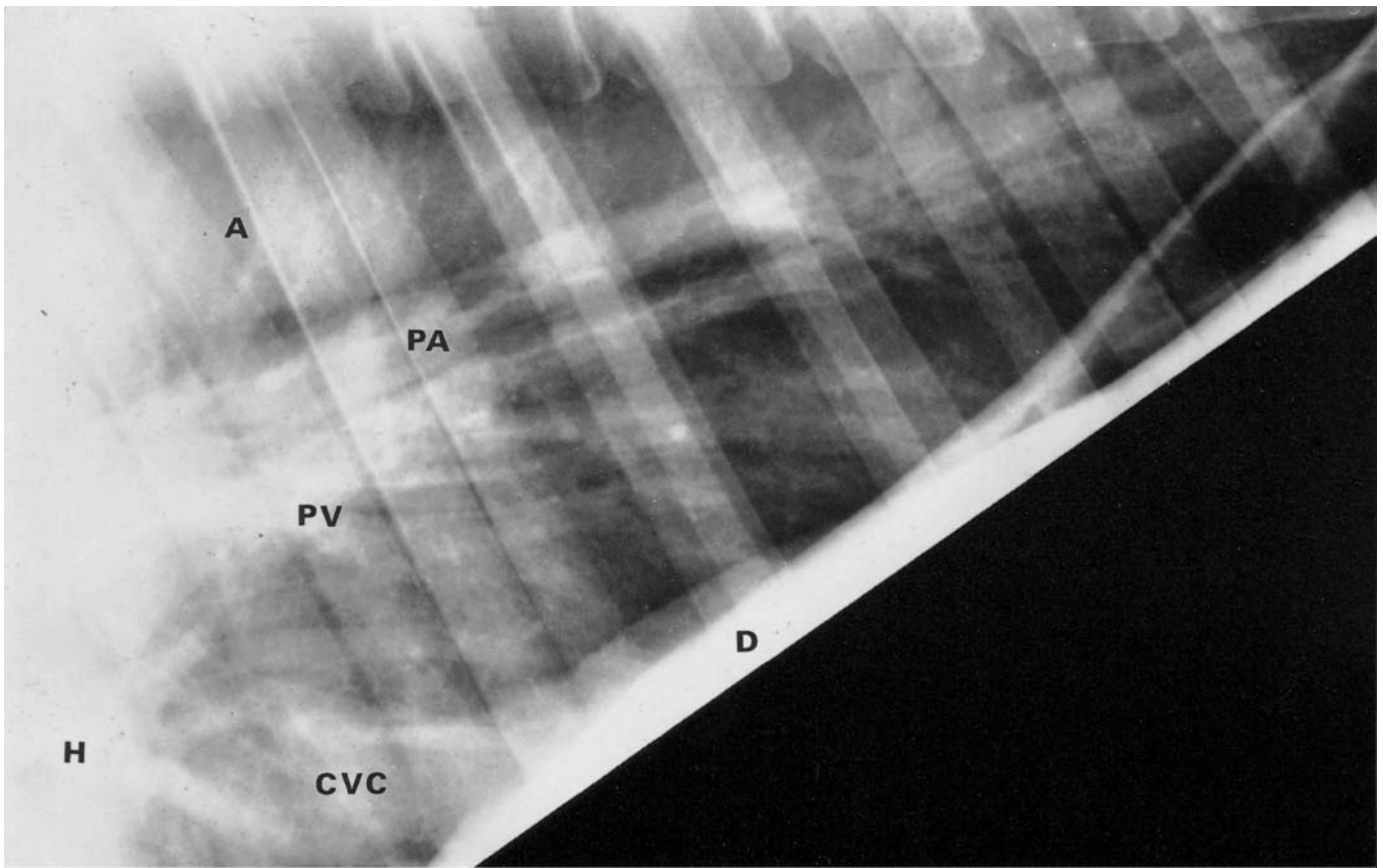
(b)

Figure 11.3 *Cont'd* (b) The caudodorsal lung fields are clear, and close inspection allows visualization of fine bronchial structures with parallel walls. Fine vascular structures can be seen over the vertebral bodies and ribs where the x-ray beam is attenuated. The margins of the aorta (A) are no longer visualized caudally. The pulmonary arteries (PA) and pulmonary veins (PV) can be seen exiting and entering the heart (H) above the caudal vena cava (CVC) which can be seen passing from the heart to the diaphragm (D). Dorsocaudally the gas in the stomach can be seen against the left diaphragmatic crus, while the right crus is flatter and lies over the hepatic shadow. Many pulmonary vascular structures can be seen centrally, but are lost caudodorsally due to beam penetration. The lungs are clear and normal.

lungs. These vessels should be most opaque over their greatest dimension and gradually decrease in opacity as they progress peripherally. The trachea enters the thoracic inlet as a lucent tubular structure that has well-defined tracheal cartilages within the wall. The outer wall cannot be differentiated from other mediastinal soft tissues. The tracheal cartilages are not usually seen in young animals because they lack mineral content which develops with age. The trachea terminates at the carina (point of bifurcation) at the base of the heart (Figure 11.1b, page 486) where it becomes the right and left mainstem bronchi. The mainstem bronchi if seen end-on are round, well-demarcated structures at the base of the heart; in longitudinal plane their linear, opaque, well-defined walls are seen. Bronchi are not normally seen much beyond the bifurcation (carina) (Figure 11.1c, page 487 and 11.3a, page 490). The left mainstem bronchus is more dorsal than the right because of the close association of the left bronchus with the left atrium.
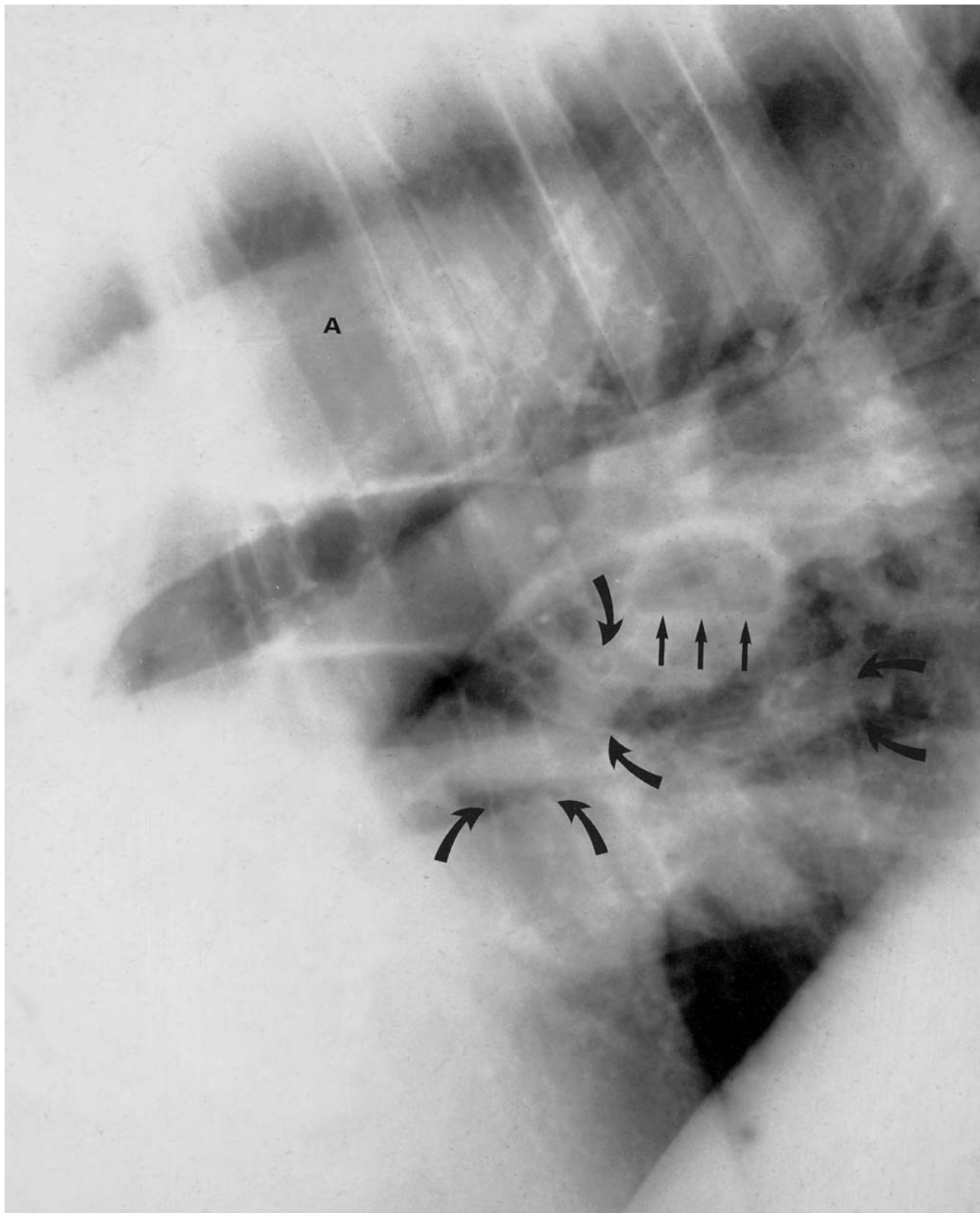
Figure 11.4(a) Right lateral radiograph of a 10-year-old Standardbred stallion with a history of pulmonary disease. There was mucus and pus in the trachea. This figure demonstrates a solitary cavitary pulmonary lesion. There is a well-circumscribed mass containing both air and fluid. The air fluid interface (straight arrows) is demonstrated on both views. The lungs are normal and fine vascular structures can be seen in the dorsal lung fields and over the aorta (A). Bronchial walls and end-on bronchi (curved arrows) are also seen.

[492]
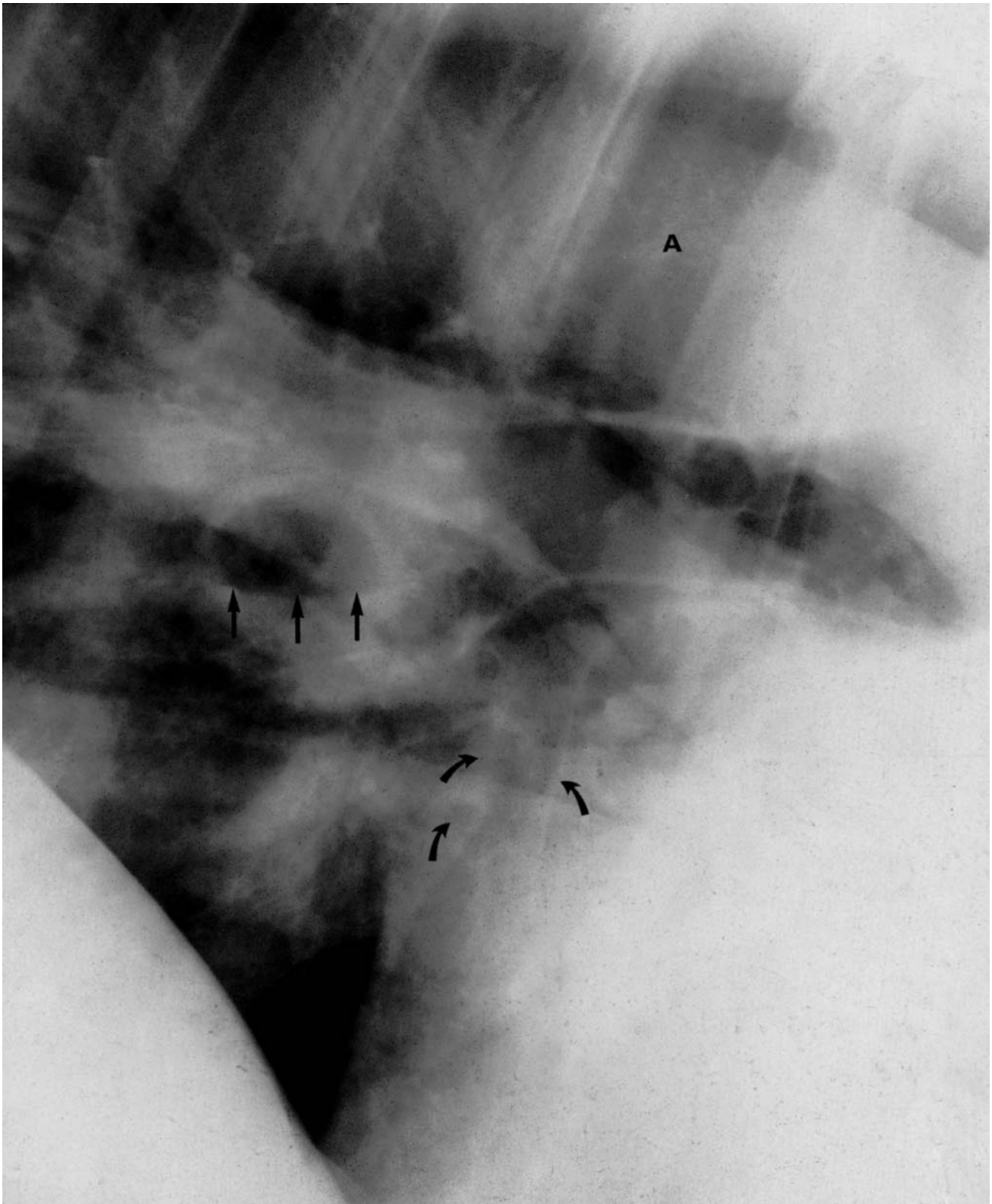
Figure 11.4(b) Left lateral projection of the same area also demonstrates the cavitary pulmonary lesion; however, the margins of the fluid line and mass are less well defined and slightly magnified, indicating that the lesion is in the right hemithorax. On both views, bronchial walls and end-on bronchi are also identifiable (curved arrows).

A lucent triangle of normal lung tissue is usually identifiable caudoventrally in radiographs obtained at full inspiration. The sides of the triangle are made up of the caudal vena cava dorsally, the cardiac silhouette cranially and the diaphragm caudally. This triangle should be evaluated to determine the degree of inspiration. At peak inspiration, the apex of the triangle may be slightly blunted as the diaphragm and the cardiac silhouette separate, and the apex is formed by the sternum.

The cardiac notch in both the right and left lung leaves an area overlying the mid-ventral heart which is not covered by lung tissue; thus this area over the cardiac silhouette is devoid of pulmonary vessels. Care must be taken not to confuse the lack of vessels in this area with consolidated lung which might, in another location, have a similar appearance.

Dorsocaudal lung field

A portion of the aorta is usually observed just below or slightly overlapping the bodies of the thoracic vertebrae. The caudal portion of the aortic silhouette is only seen when the radiograph is obtained at peak inspiration. This is because the aortic silhouette becomes incorporated in the increasing lung opacity in the dorsocaudal lung, when the lungs contain less air (expiration). The pulmonary artery and vein extend from the base of the heart towards the vertebral bodies. Small pulmonary vessels are seen at the periphery of the lungs and can best be evaluated over the vertebral bodies, the cardiac silhouette and the diaphragm (Figure 11.1a, page 485).

Ventrocaudal lung field

The dorsal portion of this radiographic view should overlap field (a). The caudal edge is defined by the silhouette of the diaphragm while the ventral side is defined by the diaphragm, sternum and the caudal aspect of the heart. The caudal vena cava is best evaluated in the right lateral projection as it lies on the right side of the thorax (Figure 11.1b, page 486).

Dorsocranial lung field

The dorsocranial region overlaps portions of fields (a) and (b) but extends craniad. The aortic arch is the most prominent structure in this view and only a small amount of lung tissue, which is not obscured by the base of the heart and the muscle mass over the shoulders, is seen. A part of the trachea and the carina can be seen just above the cardiac silhouette. The great vessels can be evaluated as they leave the base of the heart (Figure 11.1c, page 487).

Ventrocranial lung field

In this view the ventrocranial thorax can be evaluated, but the lungs are often obscured by the forelimbs cranially and by the cardiac silhouette caudally. This can be improved by extending and pulling forward the limb that is closest to the x-ray tube. There is some overlap with the other three fields

[494]

at the dorsocaudal portion of this view. This is usually the least useful of the four views (Figure 11.1d, page 488).

NORMAL VARIATIONS AND INCIDENTAL FINDINGS

An increase in lung opacity (interstitial density) may be noted as horses age, resulting in an inability to visualize the fine vascular structures and in loss of structural detail. This change in appearance is due to chronic pulmonary fibrosis. With age, the mainstem bronchi and tracheal rings may be more prominent due to cartilage mineralization.

Factors influencing interpretation

A single set of radiographs of the equine thorax represents the status at the time the radiographs are obtained. Many diseases will pass through similar stages during progression or regression, and radiographic findings will often, but not always, lag behind the clinical signs. Underexposed thoracic radiographs give the appearance of increased lung opacity while overexposure results in apparent decreased opacity. If an error is to be made, overexposure is preferable because information can be retrieved by the use of high-intensity illumination. Expiratory radiographs (radiographs obtained at end expiration) give the appearance of increased lung opacity because the air to tissue ratio is decreased; thus the soft tissues summate and result in a false interstitial pattern. The same phenomenon occurs when there is a large amount of intra-abdominal fluid or an abdominal mass, both of which interfere with normal diaphragmatic excursion and thus prevent peak inspiration.

Interpretation of thoracic radiographs is based on a thorough understanding of the patterns that make up the various thoracic diseases as well as their pathophysiology and the effect of positioning.

When evaluating lateral recumbent thoracic radiographs of young or small horses, it is important to understand that the image and its interpretation have been slightly altered by position. The sharpest image will be in the upper lung because the dependent lung will partially collapse. This partial collapse obscures opacities within the lung because of the lack of adjacent air to contrast with them. Concurrently the well-aerated upper lung will allow for better definition of structures despite parallax and magnification artefacts. Therefore, both lateral projections should be obtained in the recumbent as well as standing patients.

SIGNIFICANT FINDINGS

Patterns of lung disease

Interstitial

Within the connective tissue framework of the lungs are the arteries, veins, lymphatics, nerves and the bronchi. The walls of the bronchi and the alveoli

[495]

separate the interstitium from the air space. Thus, any inflammatory or infiltrative disease that affects any of these structures will result in what is referred to as an interstitial pattern (Figures 11.5 and 11.6, page 498). Although the pattern may vary to some degree depending upon the pathogenesis of the disease process, its hallmark is an increase in background opacity that results in the loss of visualization of the fine vascular structure that typifies a normal, well-inflated (aerated) lung. Because of the varied tissues involved, this is the predominant pattern noted in the early stages of most pulmonary disease, including: viral, bacterial, mycotic, parasitic, hypersensitive, haemorrhagic, neoplastic, and cardiogenic. In the foal an interstitial pattern is seen in both septicaemic and immature patients, and has recently been described in proliferative interstitial lung disease.

A generalized interstitial pattern may indicate the presence of pulmonary interstitial oedema from cardiac origin, an early phase of viral or bacterial pneumonia, or chronic pulmonary fibrosis due to age and chronic irritation. Expiration also decreases the proportion of air to tissue density and can thus create the impression of an interstitial opacity; this is undoubtedly the most common cause of misdiagnosis of pathology in normal lung. A granular or fine nodular interstitial pattern suggests a cellular infiltrate in the interstitium. This would lead to consideration of metastatic or mycotic disease in the differential diagnosis, as well as other causes of cellular infiltrates.

Vessels are within the interstitium and as such can only be differentiated prior to the accumulation of interstitial fluid (oedema) or infiltrate. These mask the underlying fine vascular structures or give them an indistinct outline. An increase in pulmonary vasculature may be associated with congenital or acquired heart disease or early stages of inflammatory lung disease. Radiographically there appears to be an increase in the number and size of vessels. These are most easily recognized as round to ovoid fluid densities of varying size that lie over the other vessels as they are seen end-on in the peripheral lung tissue. Many pulmonary diseases start within the interstitium, before involving the air spaces, so the presence of this pattern alone is not pathognomonic for any disease. Follow-up radiographs are always advisable.

Bronchial

Although the bronchi are part of the interstitial complex, diseases of the conducting system are often considered separately. The linear pattern can be differentiated on the basis of whether the bronchi appear sharply defined (bronchial pattern, Figure 11.6, page 498) or ill defined with apparently thickened walls (peribronchial pattern). A bronchial pattern is more indicative of chronic disease with changes in the bronchi themselves such as mineralization or bronchiectasis (see Figure 11.14, page 509). A peribronchial pattern is indicative of an infiltrate around the bronchi and therefore of acute or chronic inflammatory disease such as allergic pneumonitis or early bronchopneumonia.

The radiographic signs of bronchial disease include:

[496]
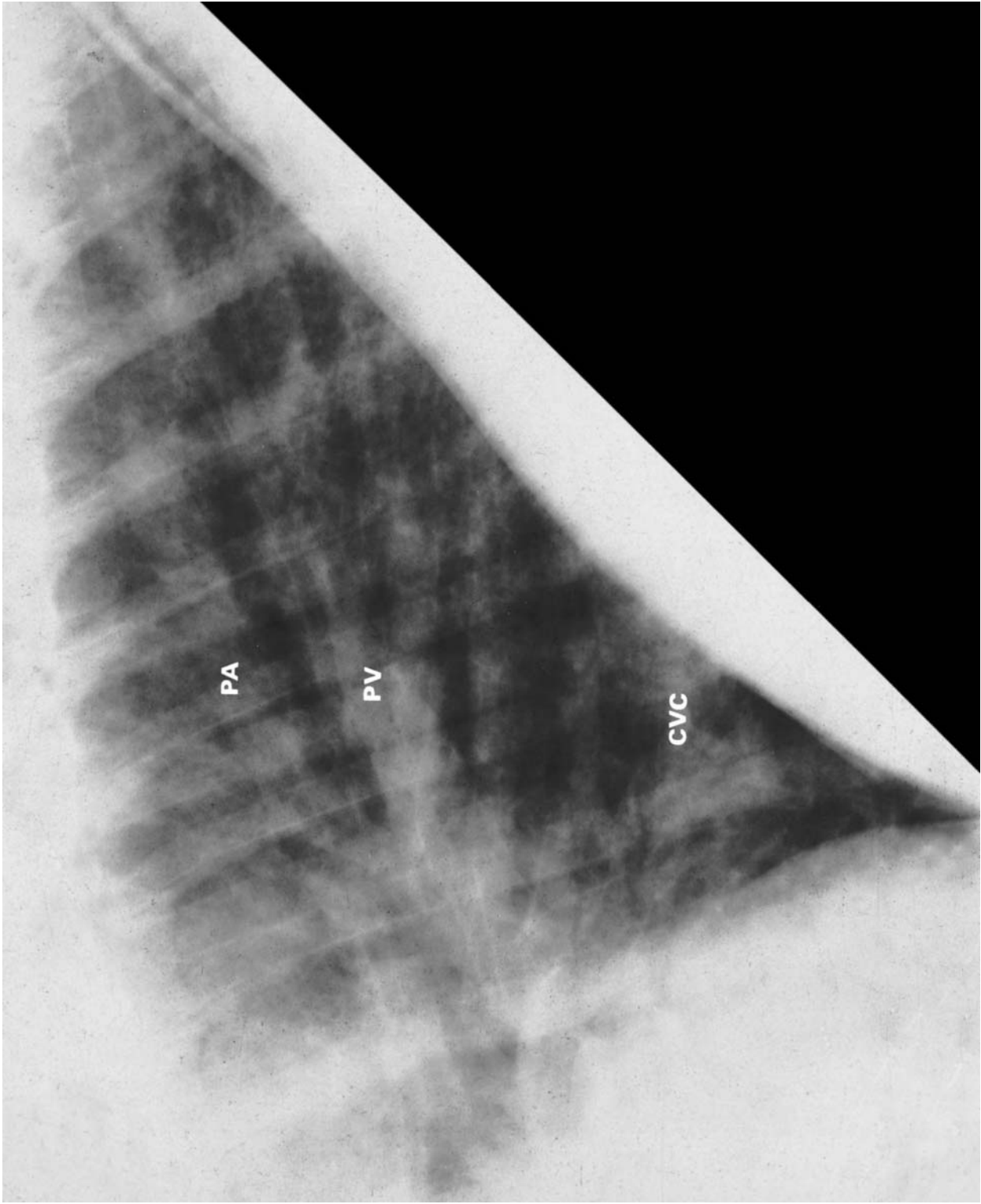
Figure 11.5 Five-month-old Thoroughbred colt admitted with severe acute dyspnoea. The radiograph demonstrates pulmonary interstitial infiltrates, characterized by a generalized increased lung opacity and the inability to visualize the fine vascular markings. The right pulmonary artery (PA) and the right pulmonary vein (PV) are still visible but poorly marginated, as is the caudal vena cava (CVC) and other vessels.
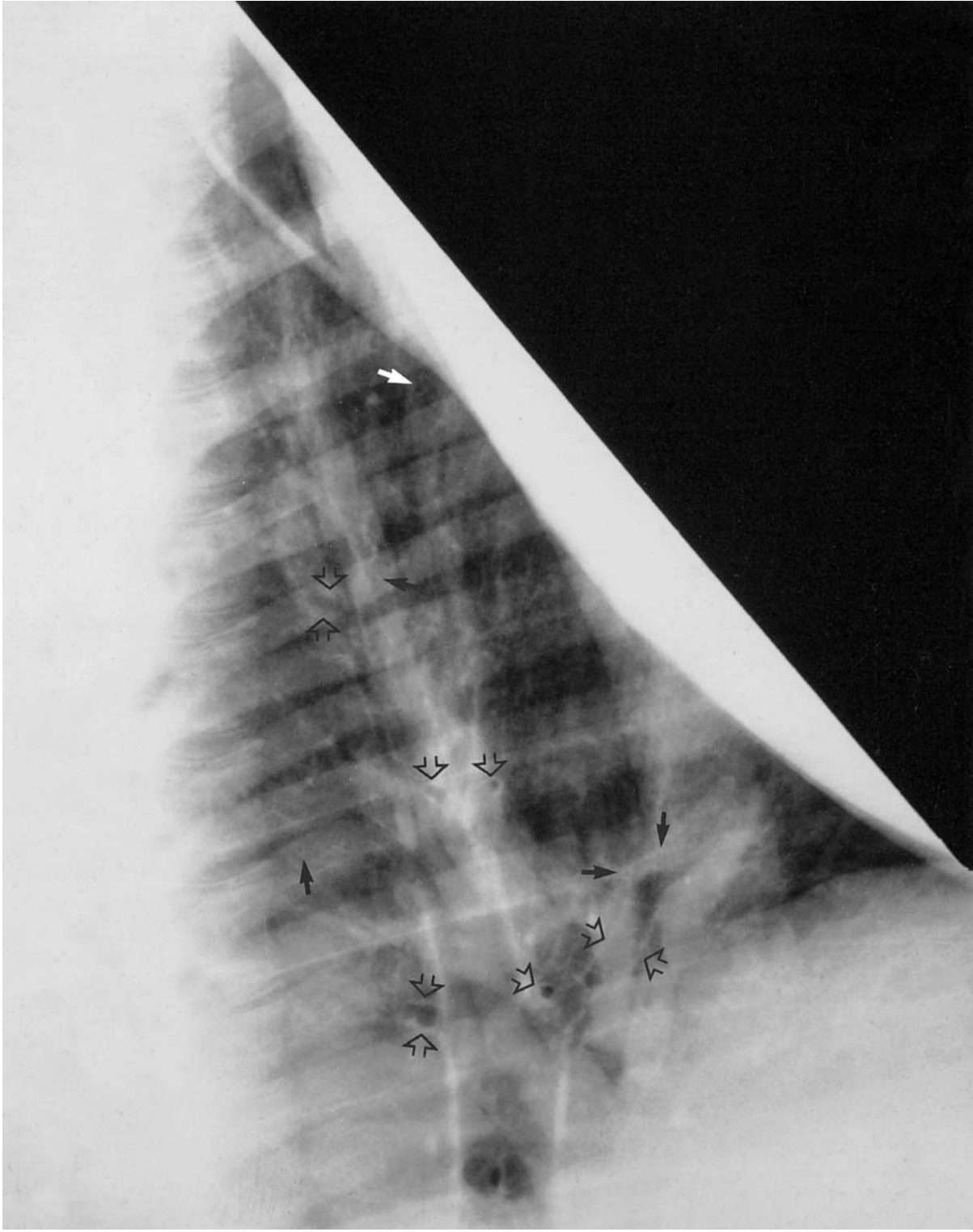
Figure 11.6 Three-month-old Thoroughbred colt which had previously had guttural pouch empyema with a recent 2-week history of pneumonia and nasal discharge. The nasal discharge had improved within the last 3–4 days. The radiograph demonstrates interstitial and bronchial pattern due to bacterial pneumonia. There is a generalized increase in interstitial density of which a major component is a bronchial pattern, increased visualization of bronchial markings and well-circumscribed end-on bronchi. Some of the larger bronchi are marked with open arrows. Note the width of the bronchus and prominent bronchial walls. Solid arrows mark small bronchi in the periphery.

[498]

1 Increased thickness of bronchial structures due to peribronchial infiltrates; this is often referred to as peribronchial cuffing. Apparent thickening of the bronchi by material which lines the inside of the airways, such as a diphtheritic membrane, may cause the bronchial walls to appear thicker than normal and also to have a decreased luminal clarity. This aids differentiation of these two causes of apparent wall thickening.

2 Increased diameter or change in shape of bronchi as seen in tubular or saccular bronchiectasis.

3 Apparent increased numbers because previously invisible bronchi are now more easily seen due to changes in opacity of the bronchi themselves or due to the enhanced lucency of surrounding air spaces.

Alveolar

When the terminal air spaces become involved in any disease process, the alveoli begin to fill with fluid (transudate, exudate or blood) or tissue and thus assume a soft-tissue opacity rather than normal lucency of air. In the early stages when few alveoli are involved, the structures that are normally visualized will be obscured by fluffy or cloudy fluid opacities. With the involvement of more and more alveoli there is a progressive coalescence and summation of these opacities, which eventually results in the formation of air bronchograms. These appear as lucent branching structures within an opaque lung field (Figures 11.7 and 11.16, page 512). The finding of air bronchograms is an indication of nearly complete alveolar filling; thus the only remaining air space is the bronchi which are then visible as dark branching structures in a background of grey. At this stage the distribution of the air bronchograms will aid in the differentiation between various causes of alveolar filling. The differential diagnosis includes: bacterial, mycotic, and aspiration pneumonia, and pulmonary oedema of both cardiogenic and non-cardiogenic origin (see 'Diseases of the lung', page 507).

Diseases of the pleural space and mediastinum

Hydrothorax (pleural effusion, free pleural fluid)

Small amounts of fluid in the pleural space may be seen as fluid opacities which occupy the pleural fissures (Figure 11.8). With increased amounts of fluid there is a diffuse fluid opacity in the ventrocaudal thorax of the standing patient. The presence of large amounts of fluid results in a loss of definition between the heart and the diaphragm (Figure 11.9). This fluid line is poorly demarcated because of the capillary action of the pleural space and is only sharply delineated when there is concurrent pneumothorax. The loss of definition progresses dorsally with increasing amounts of fluid, which may at times be defined by the lung margins as they begin to retract dorsally. This results in an undulating fluid–lung interface, which indicates that the lungs are near normal. Abnormal (pneumonic) tissue tends to remain more ventral and summate with the fluid.

All fluids appear similar and cannot be differentiated radiographically

[499]
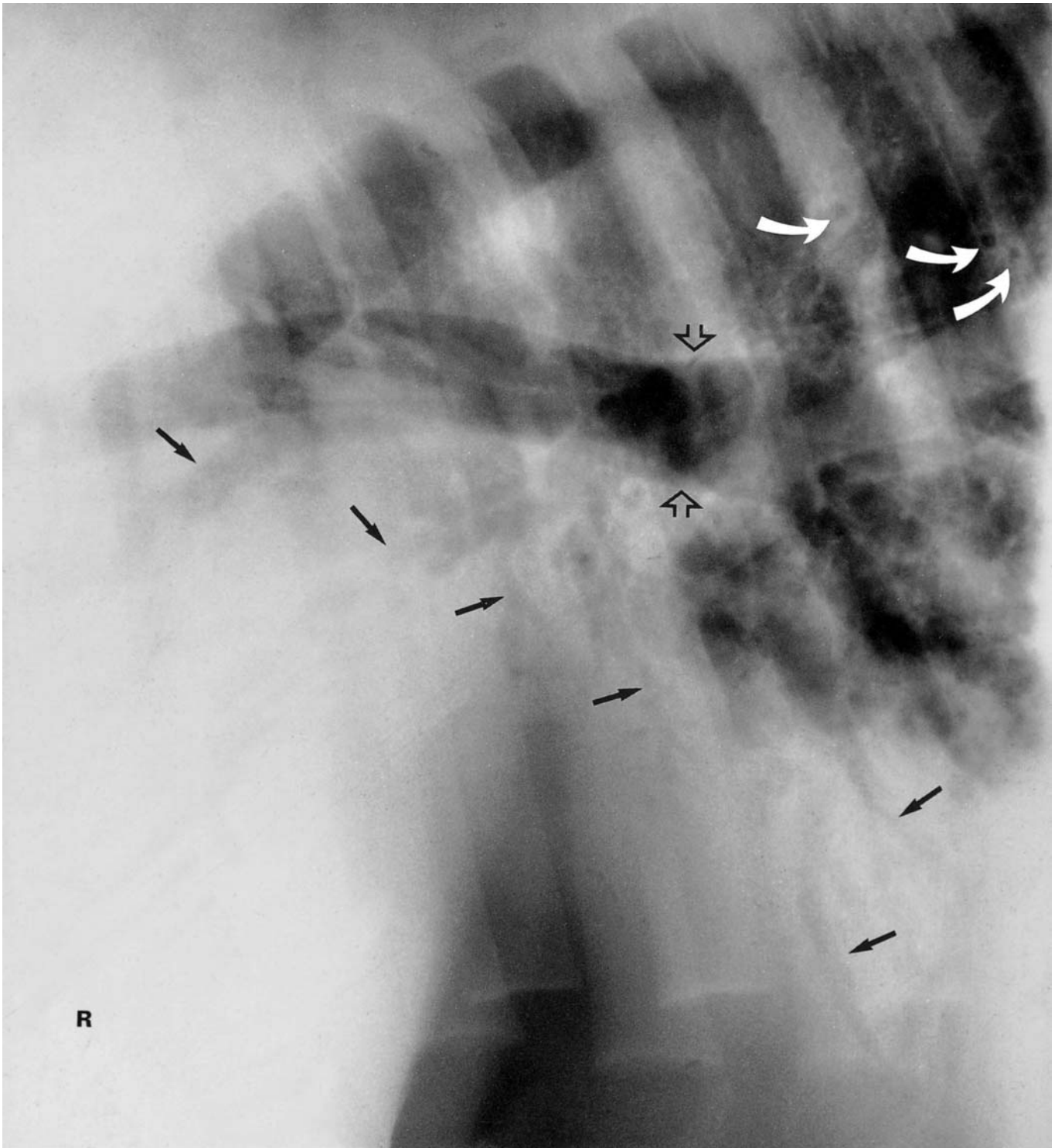
Figure 11.7 Three-month-old Thoroughbred filly with a history of acute onset of respiratory distress. There is an irregular fluid opacity which involves the entire ventrocaudal thorax and obscures the cardiac silhouette. Air bronchograms (black arrows) are readily visible. Dilatation of the caudal trachea at the carina (open arrows) is indicative of maximal inspiratory effort and dyspnoea. Peribronchial changes are noted dorsal to the carina (white curved arrows). These changes are typical of either severe aspiration or bacterial pneumonia. The air bronchograms branch as they extend towards the periphery and are indicative of alveolar infiltrate and consolidation. Diagnosis: bacterial and aspiration pneumonia.

[500]
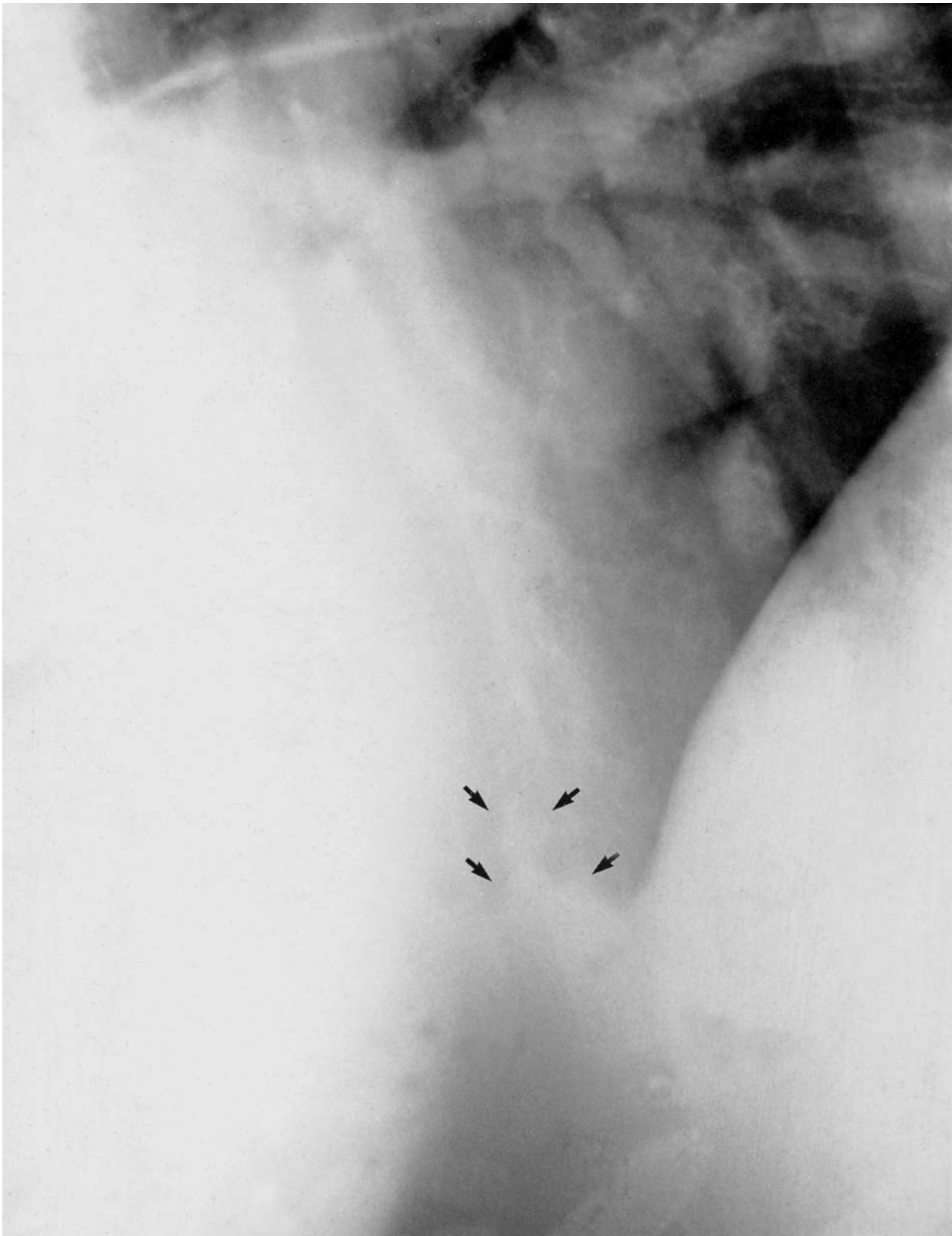
Figure 11.8 Yearling Thoroughbred colt with a history of thoracic disease. There is a small irregular fluid opacity in the ventrocaudal thorax over the cardiac silhouette (arrows). The remainder of the thorax is normal. This opacity represents a small amount of free pleural fluid at the base of the ventrocaudal lung adjacent to the cardiac notch.
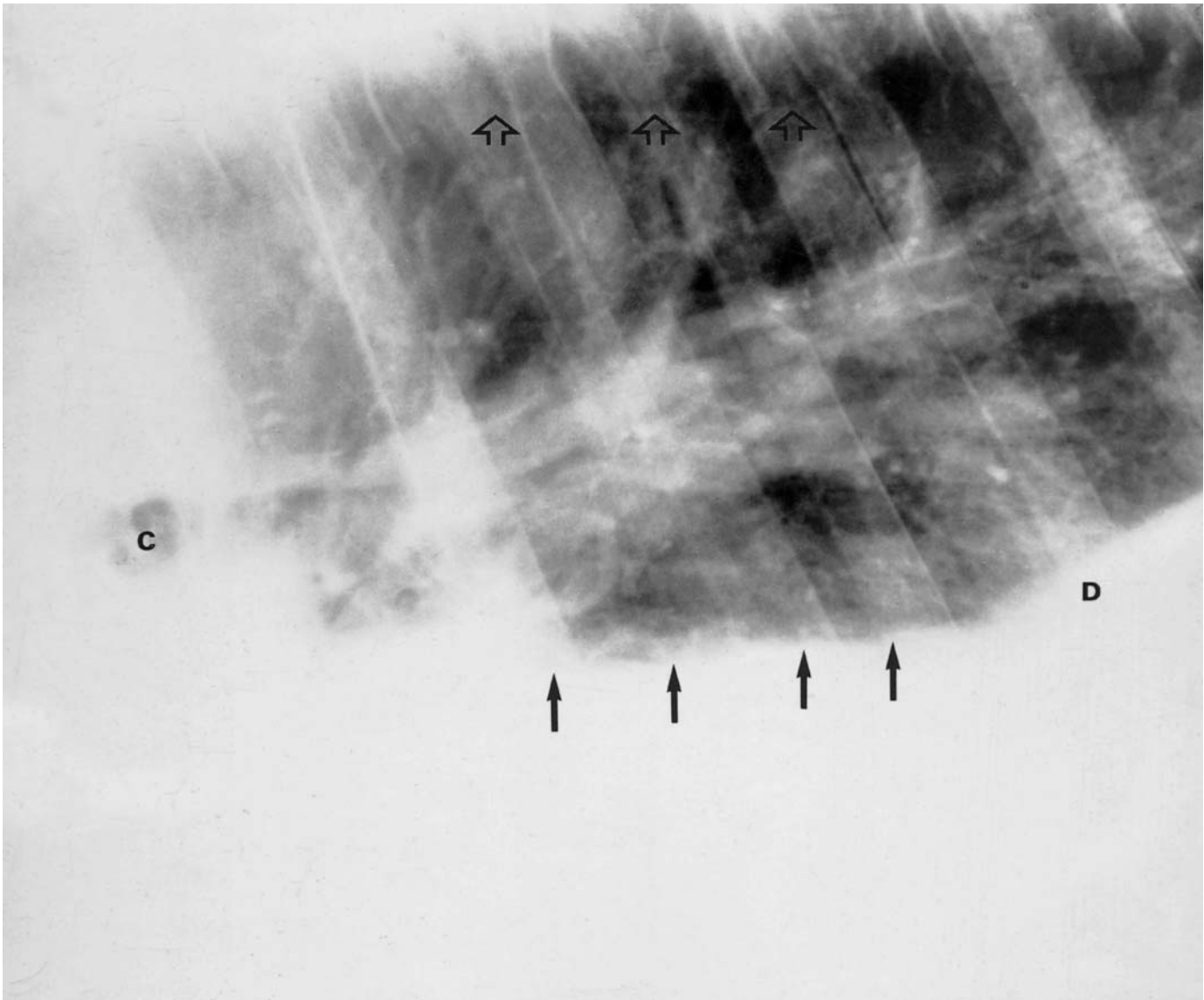
Figure 11.9 Six-year-old Thoroughbred stallion with an 8-week history of respiratory distress. Thirty-two litres of fluid were removed the day prior to radiographic evaluation. There is an irregular fluid level (black arrows) ventral to the carina (C) and extending to the diaphragm (D). The cardiac silhouette and ventral thorax are completely obscured by the fluid opacity. The lung cannot expand normally which has resulted in increased interstitial pattern in all lung lobes. The margin of one lung is just visible dorsally (open arrows) indicating a small amount of pneumothorax which probably resulted from the drainage procedure on the previous day.

as transudate, modified transudate, exudate, haemorrhage and lymph (chyle). They have a uniform ground glass appearance similar to the cardiac silhouette or the diaphragm and underlying liver. Malignant mesothelioma must be considered in the differential diagnosis when pleural fluid is present. In these cases the pericardial sac may also be involved and result in pericardial effusion. A final diagnosis must rely on additional techniques such as ultrasound and pleurocentesis. Diagnostic ultrasound adds to the study of pleural disease by occasionally defining the character of the fluid

and often allowing identification of fibrin, adhesions or concurrent cardiac disease, pericardial disease, pericardial effusion, lung consolidation and occasionally masses or abscesses within the consolidated lung.

It is advisable to re-radiograph the thorax after the removal of pleural fluid in order to evaluate the lungs both for possible causes and for involvement of areas which could not be evaluated in the presence of the fluid.

Pneumothorax

Free air in the pleural space rapidly collects dorsally, in the paraspinal recess and the dorsal caudal reflection of the pleura adjacent to the diaphragm at the highest portion of the paraspinal recess. The dorsocaudal area of the thorax is, therefore, the most important area to evaluate when small amounts of gas are expected. Radiographically the lung margins are retracted both from the diaphragm caudally and the vertebral bodies dorsally, thus allowing the pleural surface of the lung to be visualized (Figure 11.10). Unilateral pneumothorax may occur, and in these cases it is possible to see one lung margin retracted and to visualize the vessels in the contralateral lung. In cases of bilateral pneumothorax, both lung lobes are retracted.

Pneumothorax can arise as a result of a penetrating wound, which allows air to enter the pleural space either from the lung itself or from the outside, or from the rupture of a bulla, bleb or abscess.

Pneumothorax can also arise secondary to pneumomediastinum, or tearing of a pleural adhesion. The entire thorax should be scrutinized for signs of concurrent pathology such as rib fractures and foreign bodies.

Pneumomediastinum

Radiographically, pneumomediastinum is seen as air outlining mediastinal structures. Both sides of the trachea are clearly defined together with other structures which cannot normally be seen within the mediastinum, such as the oesophagus and the great vessels at the base of the heart (Figure 11.11, page 505).

Pneumomediastinum may be progressive, extending into the pleural space and resulting in a pneumothorax. The converse is never true; an increase in intrathoracic pressure compresses the mediastinum, thus preventing the entrance of air into the potential mediastinal space. Pneumothorax and pneumomediastinum can exist concurrently, usually as the result of trauma.

Free air in the mediastinum may result from rupture of a tracheal ring, a penetrating wound or an abscess, or may be iatrogenic following techniques such as a transtracheal wash or intravenous fluid administration.

Mediastinal masses

Mediastinal masses may be seen as areas of increased soft-tissue opacity that summate with or displace other structures in the mediastinum such as

[503]
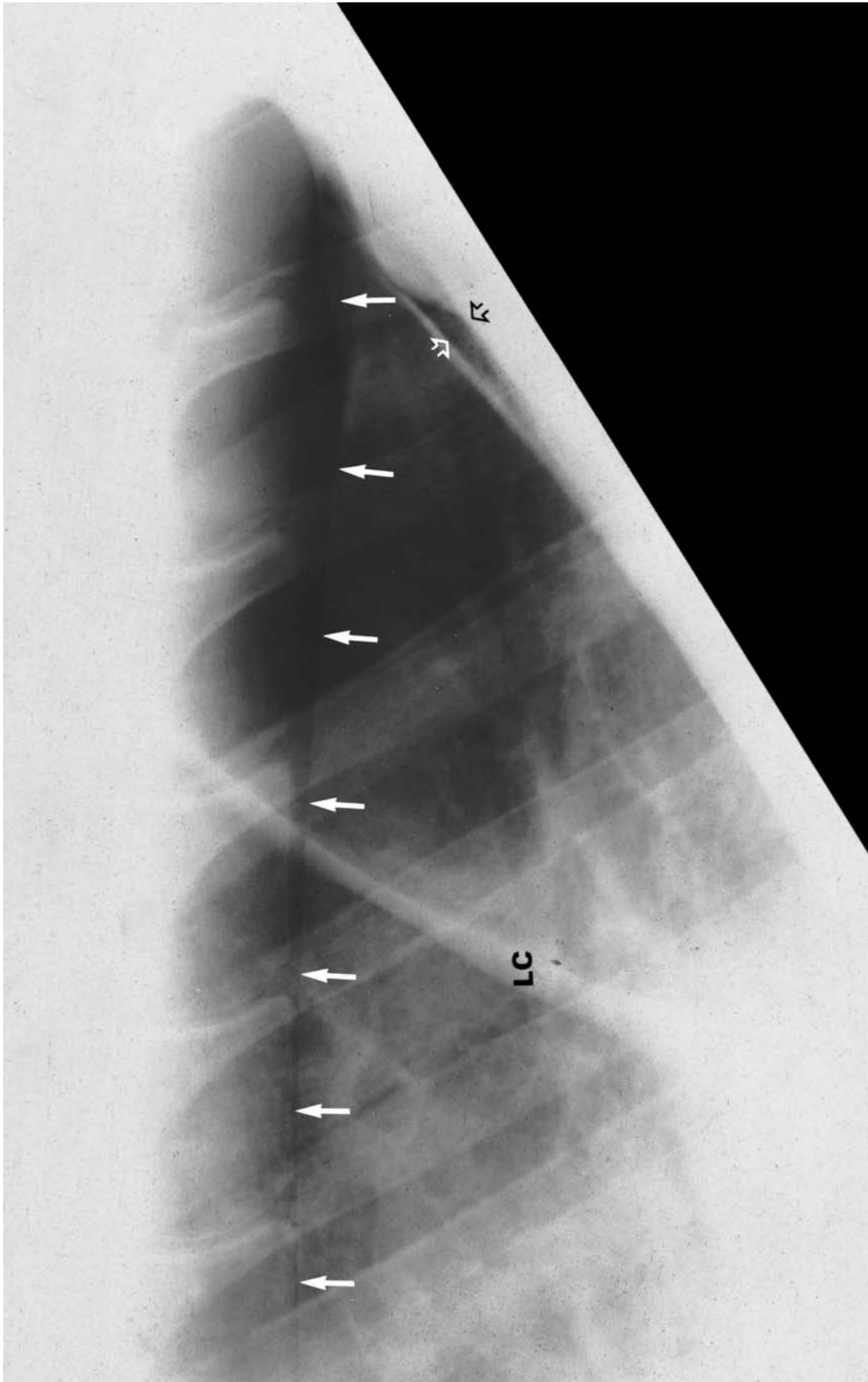
Figure 11.10 Eight-year-old Thoroughbred gelding with a 10-day history of lower respiratory tract disease. The right lung is retracted ventrally and cranially from the thoracic margins and the diaphragm, respectively. Free air is seen between the right diaphragmatic crus and the lung margin (open arrows). The dorsum of the right lung is identified by white arrows. The left diaphragmatic crus (LC) is cranial to the gas-distended stomach which is displacing the left lung lobe cranially. Note that vessels can be seen over the three more cranial vertebral bodies and not over the caudal three. Diagnosis: pneumothorax.

[504]
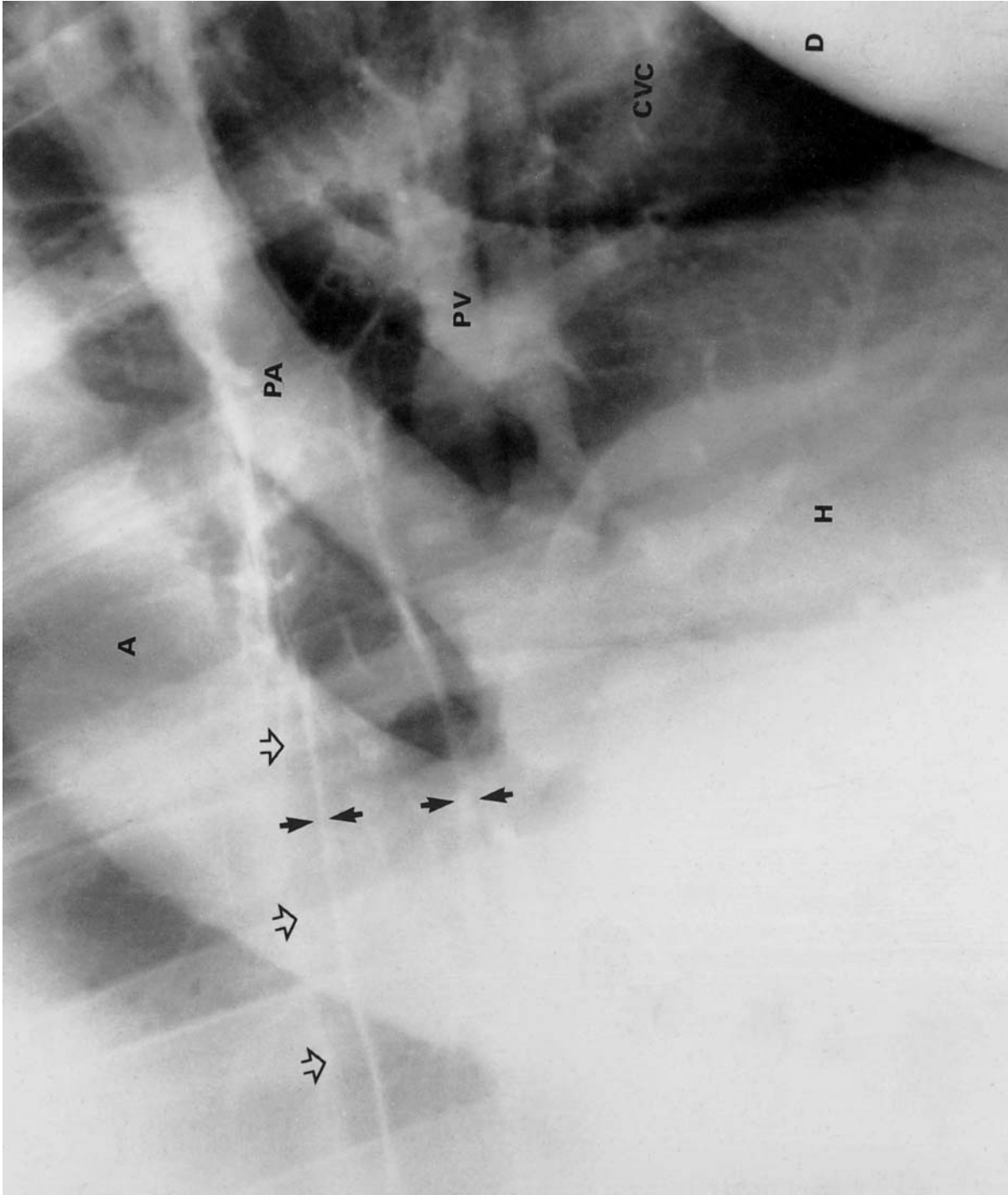
Figure 11.11 Yearling female Quarterhorse which was in a trailer accident and had multiple head and neck lacerations, resulting in pneumomediastinum. There is free air in the mediastinum which outlines both sides of the tracheal wall (between solid black arrows). Air in the mediastinum is seen between the dorsal tracheal wall and the open black arrows. Air in the mediastinum also allows for visualization of the major pulmonary vascular structures. The aorta (A), pulmonary arteries (PA) and the pulmonary veins (PV) are easily visualized. The pulmonary arteries and veins to the caudal ventral lung lobes are visualized over the heart (H). The diaphragm is identified (D). The caudal vena cava (CVC) is poorly visualized.

Figure 11.12 Fourteen-year-old miniature horse with a history of chronic inspiratory stridor and, when exercised, a 'honking' sound on expiration. There is severe collapse of the cervical and thoracic trachea. The cardiac silhouette appears to be slightly enlarged. Diagnosis: hypoplastic trachea.

the trachea, great vessels or the heart. Although rare they are often associated with free pleural fluid and are therefore obscured by the fluid which has the same opacity as the mass. The most common mediastinal disease in the horse is lymphosarcoma. Diagnosis and differentiation are aided by diagnostic ultrasound and/or drainage of the pleural fluid, followed by radiographic re-evaluation.

Tracheal collapse and stenosis

When tracheal collapse or tracheal stenosis is suspected, comparison of inspiratory and expiratory films may show a change in intratracheal dimension which will aid in the interpretation.

Congenital abnormalities of the trachea such as hypoplastic trachea are occasionally seen and are most common in miniature horses (see Figure 11.12). Occasionally focal narrowing of the tracheal lumen is seen. True

[506]

tracheal masses must be differentiated from material being expectorated. With the latter there is usually an associated pneumonia and the mass will move with continued coughing (Figure 11.13).

Diseases of the lung

Bronchitis and bronchiolitis

These diseases may result in only minor increases in lung opacity associated with the bronchial walls and therefore do not have pathognomonic radiographic signs. Bronchiectasis due to chronic bronchitis has the pathognomonic changes of large well-delineated and/or irregularly shaped bronchi (see Figure 11.14, page 509).

Chronic obstructive pulmonary disease (COPD)

Radiographic abnormalities are only detectable in relatively advanced cases of COPD. In the case of emphysema there is air trapping, the lung is more lucent than normal, and local contrast is improved. The lung parenchyma will have the same appearance on both inspiratory and expiratory radiographs, and although the lungs appear well aerated they may have a slightly reticulated interstitial pattern. This is often referred to as a honeycomb appearance and results from over-expanded terminal airways and consolidation of tissue and/or interstitial fibrosis. Redistribution of vascular flow has also been shown to contribute to this pattern. Late in the disease, bronchiectasis may be seen (see Figure 11.14, page 509).

Bacterial pneumonia

This disease is usually bilateral and often associated with abscess or granuloma formation (see pages 513–4 and Figure 11.4, pages 492 and 493). Although bacterial pneumonia may be generalized it often has a ventral distribution (see Figures 11.7, page 500 and 11.16, page 512). With abscessation there is often cavitation (see 'CPL', page 513) and evidence of an air–fluid interface with a 'fluid line' in the cavity. With thick material in the abscess the dorsal margins may curve upwards, forming a meniscus. Although most bacterial pneumonias cannot be differentiated on the basis of radiographic signs, chronic *Rhodococcus* pneumonia of young horses usually has a cottonball appearance (Figures 11.15a and 11.15b, pages 510 and 511) which may later cavitate or consolidate.

Aspiration pneumonia

This disease is almost always ventral in distribution due to the aspiration of particulate matter, and is often associated with severe consolidation. This results in a generalized increase in lung opacity and loss of all lung detail except for air bronchogram formation (see Figures 11.7, page 500 and 11.16, page 512). If aspiration occurs when the patient is in dorsal or lateral
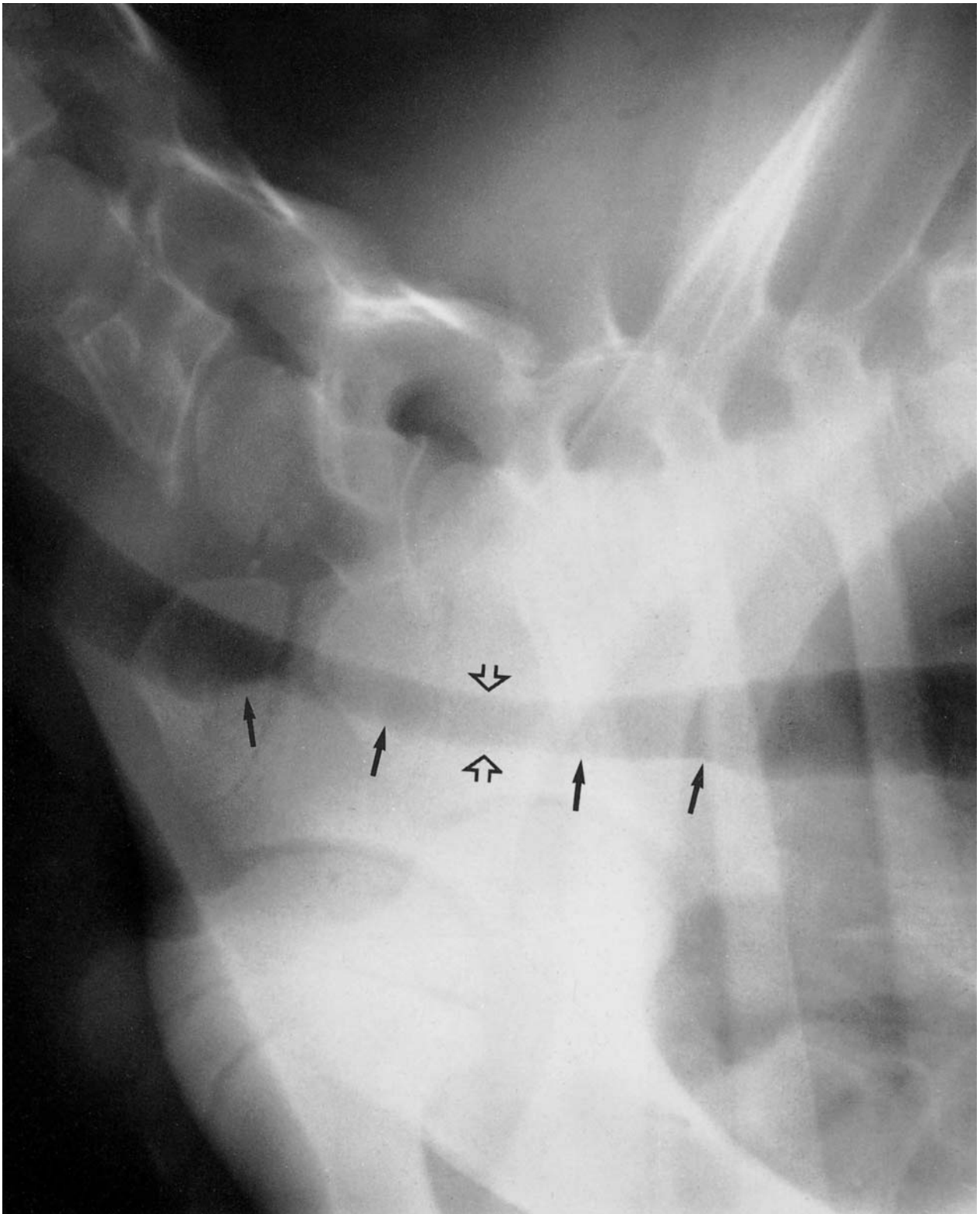
Figure 11.13 Three-month-old Arab colt with chronic pneumonia. There is narrowing of the trachea to approximately 50% of its diameter (open arrows). A tracheal mass is demonstrated on the ventral tracheal wall (black arrows). This mass may represent either a true intraluminal mass or material that is being expectorated. Note the open physes of the scapulae and humeri. Diagnosis: material in the trachea that is being expectorated from the lungs.

[508]

Figure 11.14 A 23-year-old Friesian mare with bronchiectasis and emphysema. The lungs are markedly overinflated and demonstrate large tortuous bronchi, between straight arrows (black and white). Thin-walled end-on bronchial structures are marked with open arrows. Only a few of the bronchi are marked. The aorta (A) and the pulmonary arteries (PA) are readily visualized extending caudal to the periphery.

[509]

Figure 11.15(a) Lateral view of dorsocaudal lung field of a foal. There are multiple large circular opacities, in many of which are fluid lines. The caudal vena cava is obscured by 'cottonball' opacities. This is typical of the radiographic appearance of *Rhodococcus equi* pneumonia.
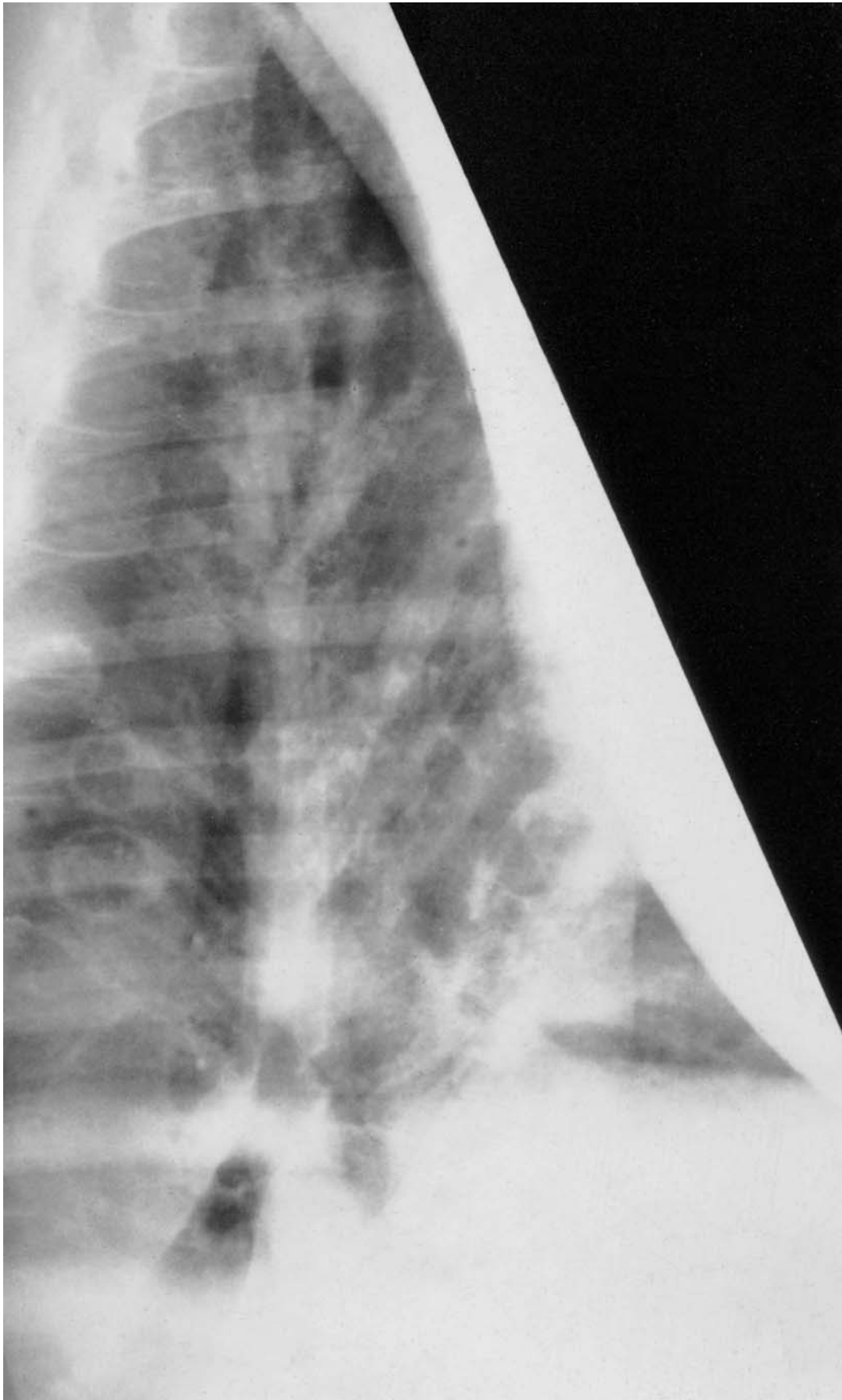
Figure 11.15(b) The same foal as in Figure 11.15(a), 19 days later, following treatment with erythromycin and rifampin. Although several round cavitated abscesses persist, many of the 'cottonball' opacities are no longer detectable and the caudal vena cava is now visible. An increase in interstitial density persists.
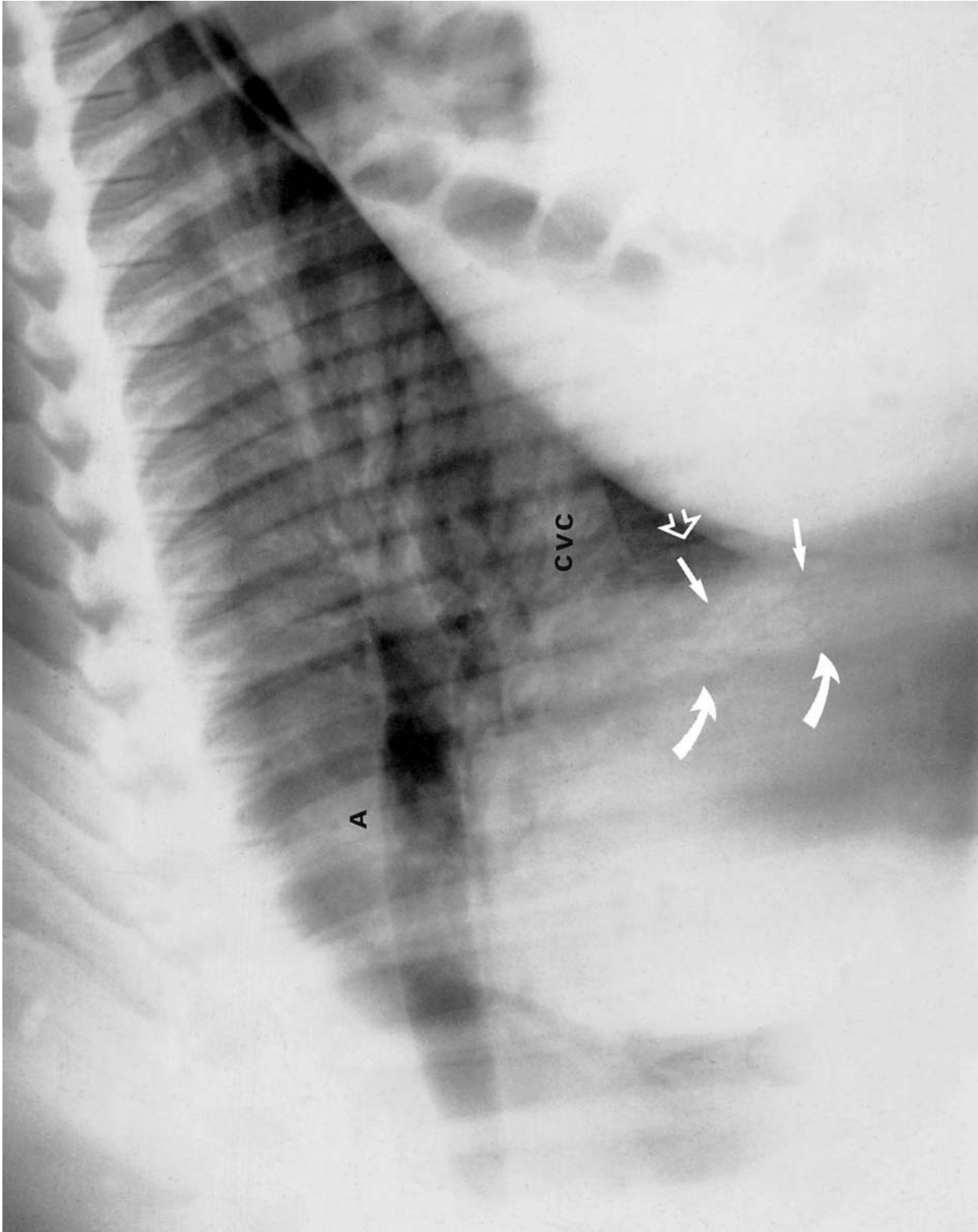
Figure 11.16 Right lateral recumbent view of the thorax of a newborn foal. There is an interstitial pattern in all lung lobes and an alveolar pattern over the cardiac silhouette extending from the curved white arrows to the caudal aspect of the heart (open arrow), below the caudal vena cava (CVC). Straight white arrows demonstrate air bronchograms. The interstitial density obscures the aortic root (A). The bowel pattern is normal. Because of the ventral distribution and the air bronchogram formation, both aspiration and bacterial pneumonia should be considered.

recumbency the distribution will be dorsal or to the downside lung, dependent upon the position of the patient at the time of aspiration.

Inhalation pneumonia

This disease usually has a more dorsocaudal distribution due to the non-particulate nature of the inhalant. In general, inhalation pneumonia is less consolidative than aspiration pneumonia and results in a more generalized interstitial pattern. If the inhalant is very irritating (smoke or toxic fumes), the lining of the air spaces may become so damaged that it results in oedema and alveolar flooding. Air bronchograms may then be seen in the consolidated lung.

Cavitary pulmonary lesion(s) (CPL)

This term is used to describe a cavity that occurs in the lung. In the horse the most common form is the result of abscess formation, liquefaction and loss of the fluid centre through a communicating bronchus (see Figures 11.4, pages 492 and 493, and 11.17). These are usually seen in young horses and have a thick opaque wall. Other abscesses or granulomas may also be seen. Air fluid levels are often present. The lesions usually resolve with the associated pneumonia, but may be the last radiographic sign to disappear. The effect of geometric distortion is substantial and therefore positioning, phase of respiration and change due to growth of the patient must be taken into consideration when evaluating the size, progression and resolution of a CPL.

Other forms of CPL exist, but are rare in the horse. They include neoplastic, traumatic and congenital cavitary lesions (Figures 11.18 and 11.19, pages 516 and 517). Neoplastic cavitary lesions have not been described in the horse, but might be difficult to distinguish from infective CPLs because both infectious and neoplastic CPLs have thick walls. Traumatic cavitary lesions (in other species) have walls that vary in thickness and usually resolve spontaneously. They may remain as thin-walled ring shadows, which in the horse might be hard to distinguish from an end-on bronchus, without a history of known thoracic trauma. Congenital CPLs in other species are usually thin walled and may contain some fluid. Any cavity lesion may rupture and result in pneumothorax (see page 503), pneumomediastinum (see page 503) or other complications, depending on their content.

Pulmonary masses

ABSCESSES

In the horse the most common form of pulmonary masses are abscesses which appear as opaque masses with or without a lucent gas cap dorsally (see Figure 11.4, pages 492 and 493). Solitary abscesses may be quite large (see Figure 11.20) and if cavitated may be confused with a hollow viscus from a diaphragmatic hernia (see Figure 11.22, page 522). Abscesses are
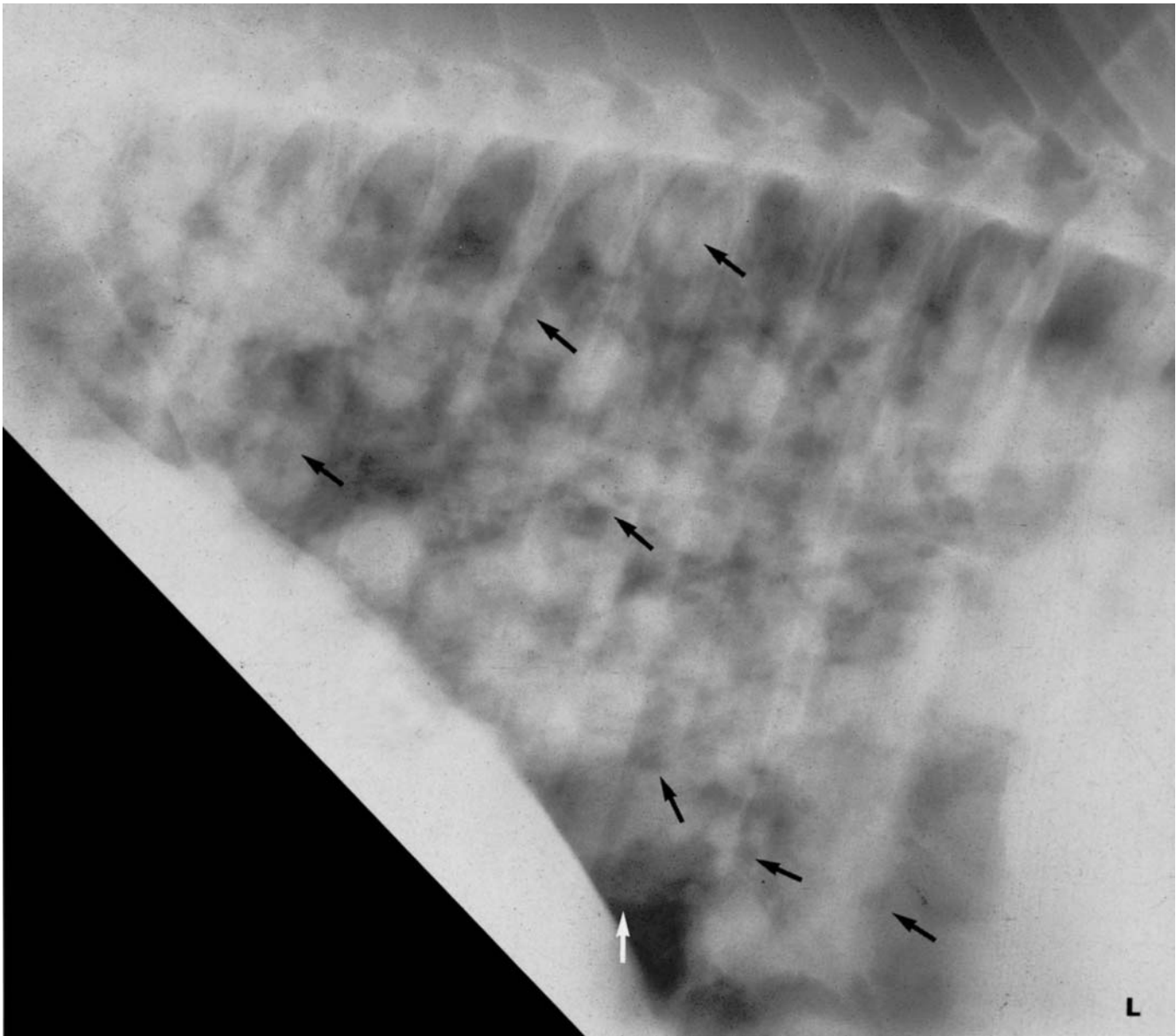
Figure 11.17 Six-week-old colt with a 2-week history of coughing. Right (this page) and left (opposite) lateral thoracic films are characterized by generalized nodular opacities through all lung lobes. The cardiac silhouette is obscured by the coalescing opacities. Some of the opacities have lucent centres indicating cavitation (white and black arrows). Cavitation is more obvious in the left (L) lateral radiograph, indicating that most of the cavitation is on that side. Diagnosis: granulomatous pneumonia with cavitation. Compare with Figures 11.4a, 11.4b, 11.18 and 11.19.

always associated with other signs of infection including interstitial and usually alveolar infiltrates. In general they have irregular indistinct margins and may form CPLs (see 'Inhalation pneumonia', page 513).

GRANULOMAS

Like abscesses, granulomas may be associated with other intrapulmonary disease, but may also be the only remnants of a previous more active disease.

[514]
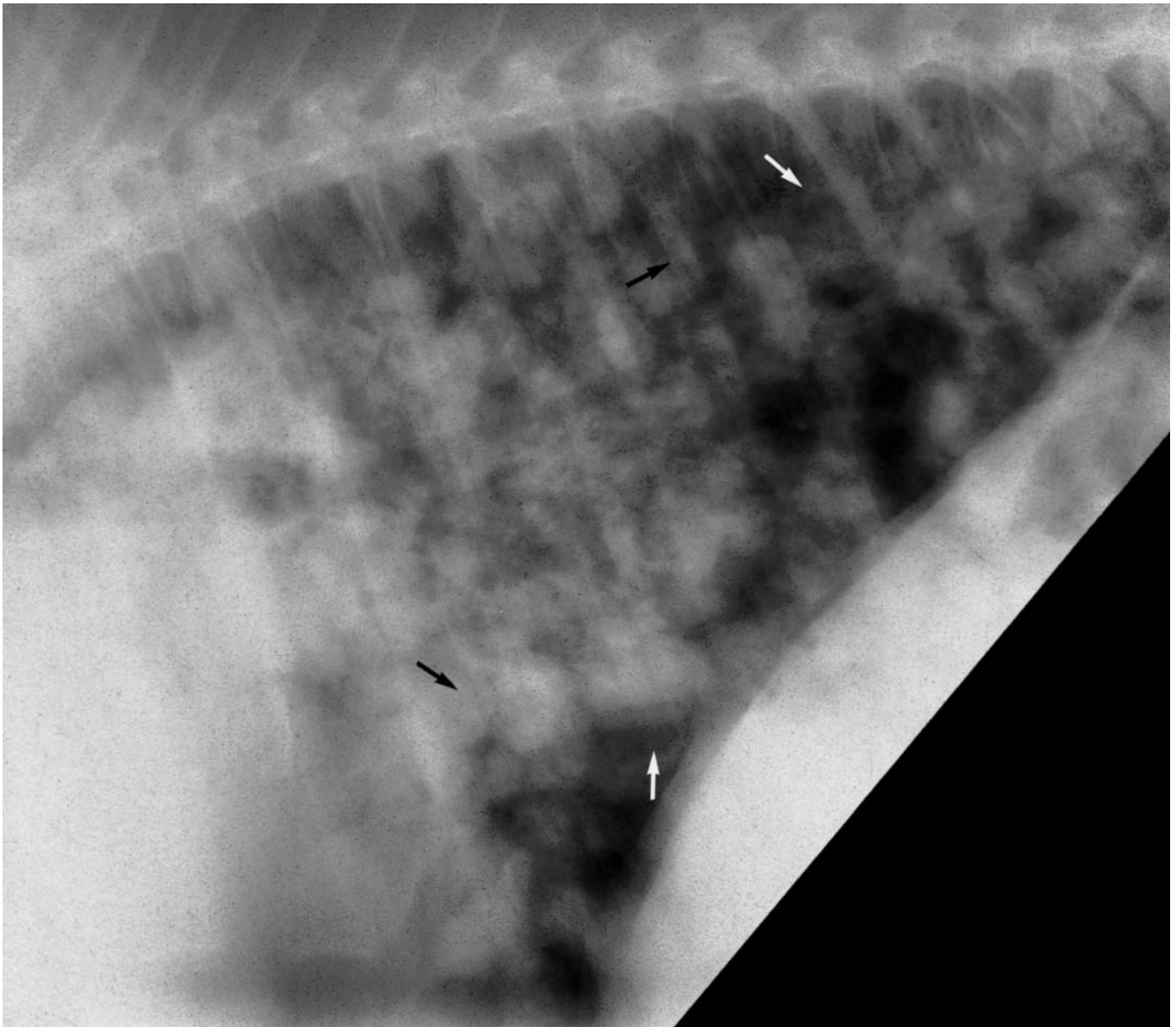
Figure 11.17 *Cont'd*

Granulomas are opaque and their margins may be more distinct than abscesses. Mycetomas have a tendency to have indistinct margins and are multi-compartmented.

INFARCTS AND EMBOLISM

These occur occasionally, especially in the caudal dorsal lung lobes. They usually have a somewhat triangular shape with a sharply defined cranial margin and an indistinct periphery (Figure 11.21, page 520). Infarcts and exercise-induced pulmonary haemorrhage (EIPH) appear similar radiographically, but may be differentiated by obtaining serial radiographs. Infarcts persist, whereas EIPH resolves rapidly.
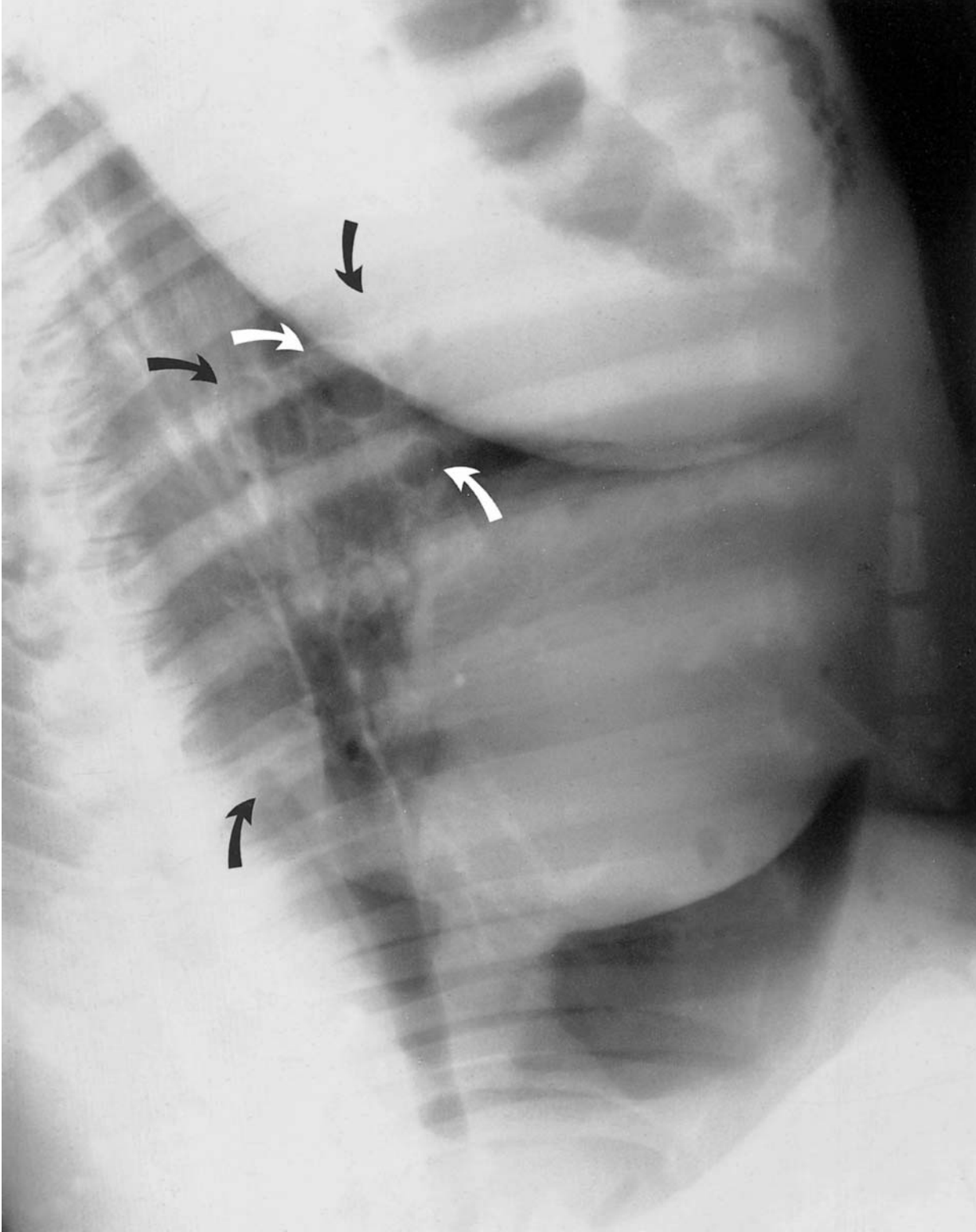
Figure 11.18 A foal 2 weeks premature, with a profuse watery diarrhoea. There are multiple, various sized, thin-walled cavitary pulmonary lesions (white and black arrows). The cranial lung lobes are normal. The caudal lung lobes have an increase in both interstitial and bronchial markings which are felt to be age related. Diagnosis: multiple cavitary pulmonary lesions. The cavitary pulmonary lesions may represent a congenital cyst, resolving haematomas from a difficult parturition or, less likely, abscessation. Compare with Figures 11.4a, 11.4b, 11.17 and 11.19.
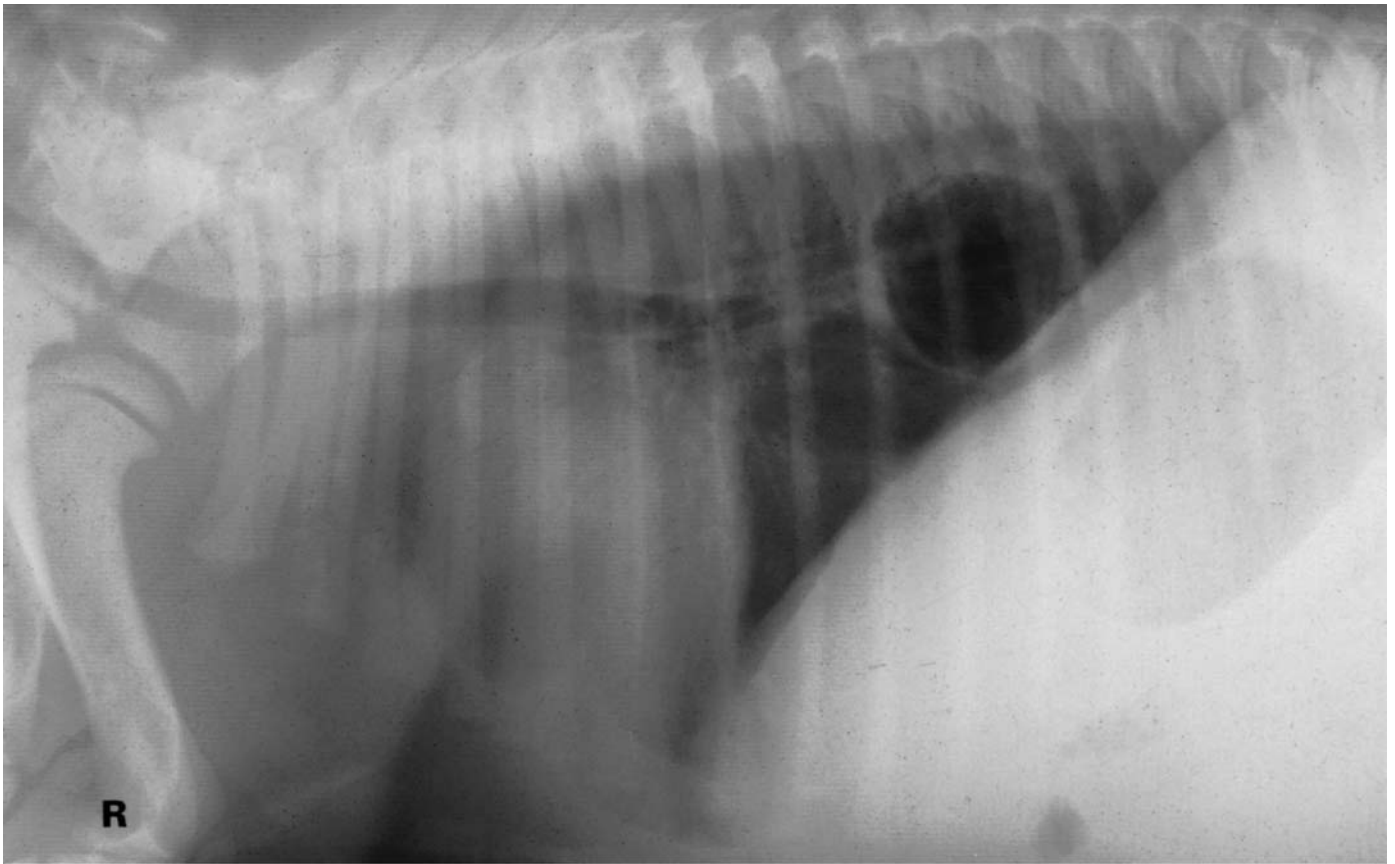
(a)

Figure 11.19 Six-day-old miniature horse born prematurely, with salmonella diarrhoea but no clinical signs of respiratory disease. A lateral radiograph (a) shows a large, thick-walled air-filled bulla which can be seen in the caudal right lung lobe. The inner wall of the bulla is irregular. The remainder of the thorax is normal. A dorsoventral radiograph (b) also demonstrates the lesion. Differential diagnosis should include a congenital bulla or a pneumatocele secondary to haematoma or infarct. Abscessation is felt to be less likely because of the lack of associated pulmonary disease. Compare this case with Figures 11.4a, 11.4b, 11.17 and 11.18. Diagnosis: congenital cavitary pulmonary lesion.

METASTATIC LUNG DISEASE

This is occasionally seen as multiple circular opacities which vary in size and in the sharpness of their margins. The appearance of the metastatic lesion will be dependent on the cell type of the original tumour, the tumour doubling time, the location of the nodule in the lung, and whether there have been single or multiple showers of neoplastic cells. Solitary masses of 0.5 cm, or less, in diameter will usually be missed, and masses as large as 2 cm in diameter may be overlooked. However, superimposition of multiple nodules of 1 cm or larger will usually be identified after careful examination.

[517]

R
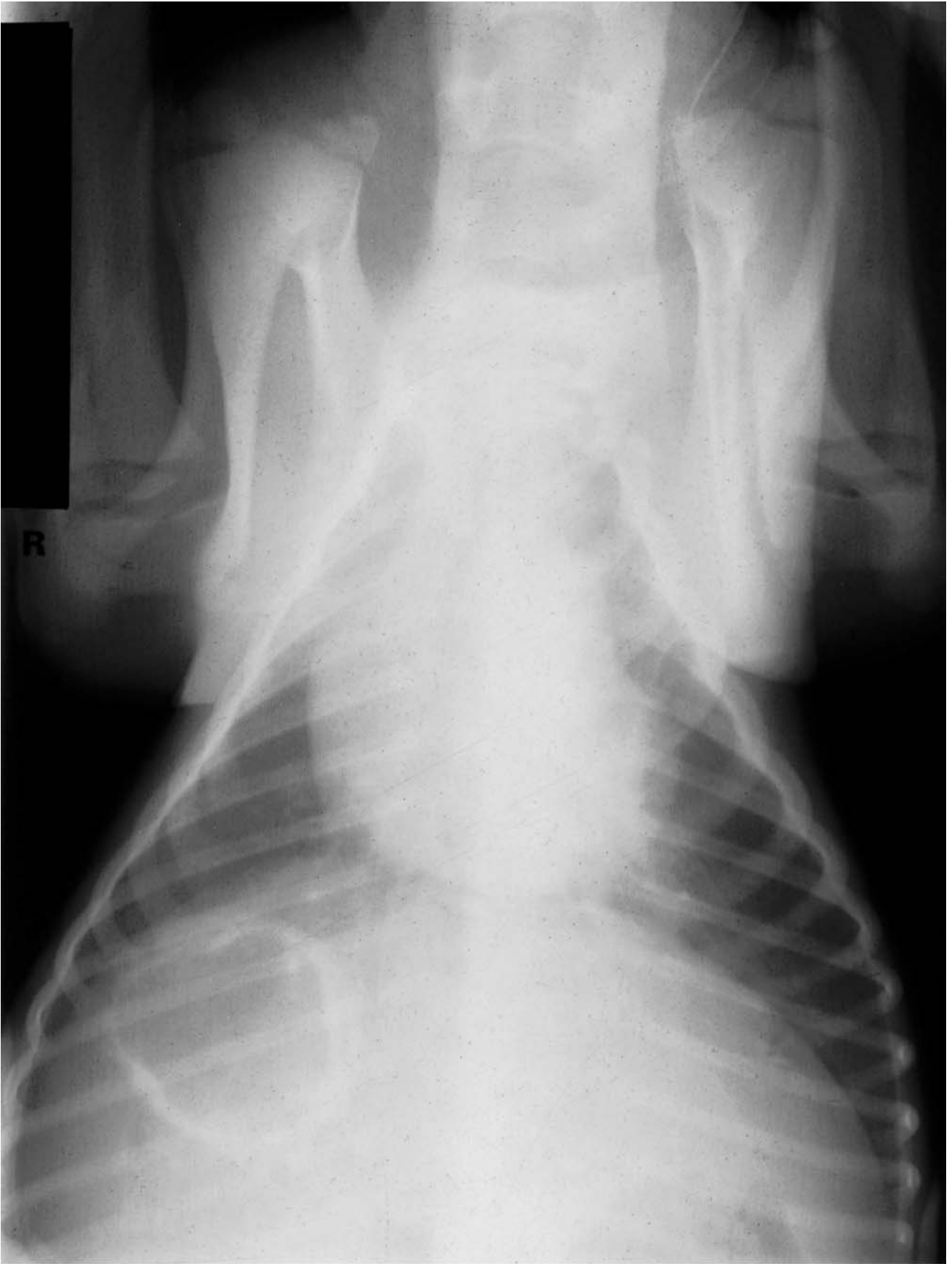
(b)

Figure 11.19 *Cont'd*

[518]
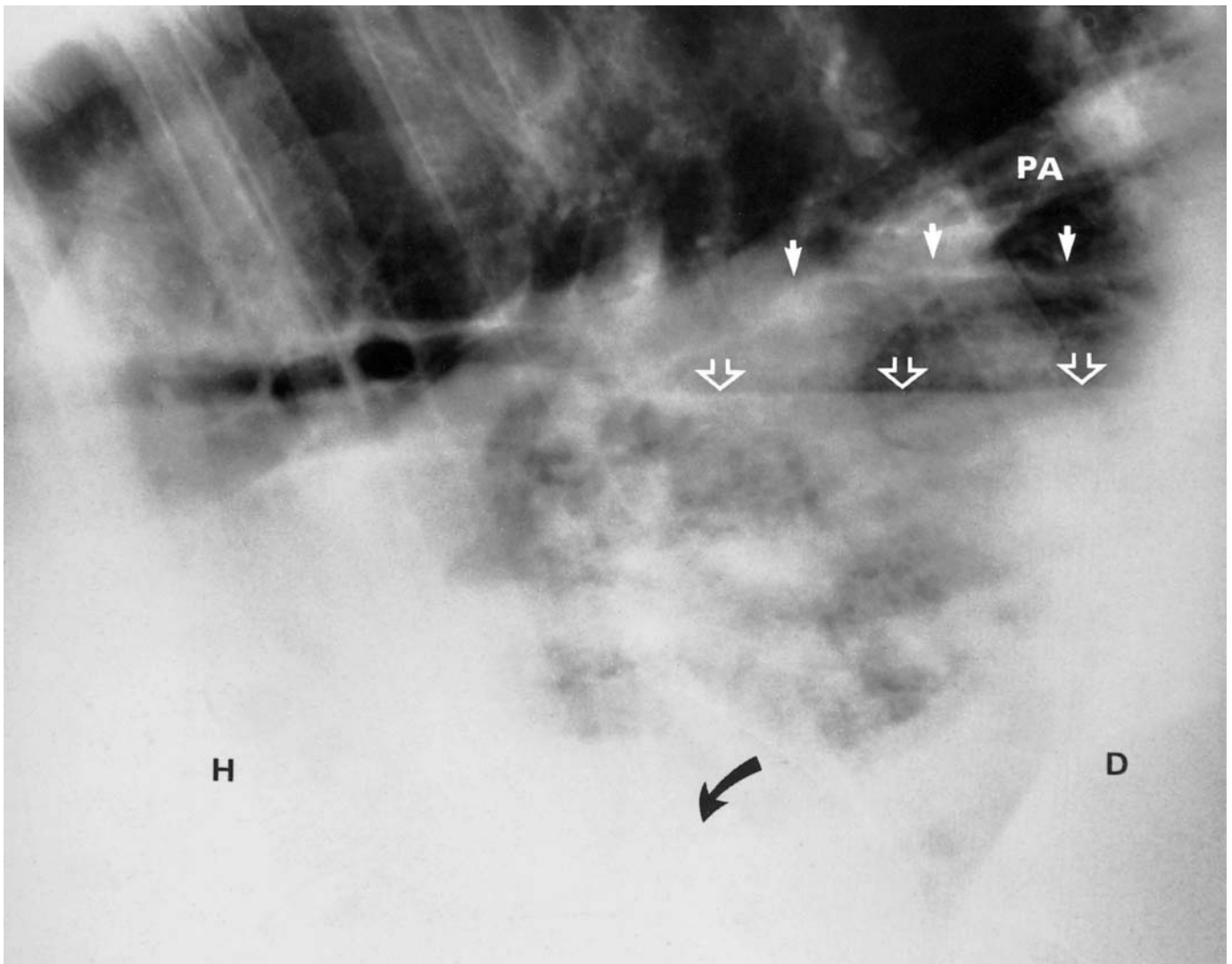
Figure 11.20 Two-year-old Thoroughbred stallion with a 3-week history of pleuropneumonia. Twenty-two litres of fluid were drained from the left hemithorax the day before these radiographs were obtained. There is a large pulmonary abscess in the caudal ventral thorax between the heart (H) and the diaphragm (D), ventral to the solid white arrows. There is a fluid line below the open arrows and an air space between the open arrows and the wall of the abscess (solid white arrows). The pulmonary arteries (PA) are marked. There is a generalized interstitial and bronchial pattern in the remainder of the thorax. Other smaller and less well-defined abscesses can be seen above the heart. They are poorly defined because they are in the right hemithorax and this radiograph is a left lateral projection in order to demonstrate the size and character of the larger abscess. A chest tube is in place in the thoracic cavity: the curved black arrow denotes the position of a metallic marker on the chest drain. Diagnosis: multiple pulmonary abscesses with a large cavitating abscess in the left hemithorax; hydrothorax.

PRIMARY LUNG TUMOURS

These are rare but, when they occur, tend to be well circumscribed and solitary. The most common lung tumour in the horse is adenocarcinoma. When present a tumour usually appears as singular masses which vary in size depending on the tumour doubling rate and the length of time that they have been present. They are usually quite large when found and may

[519]
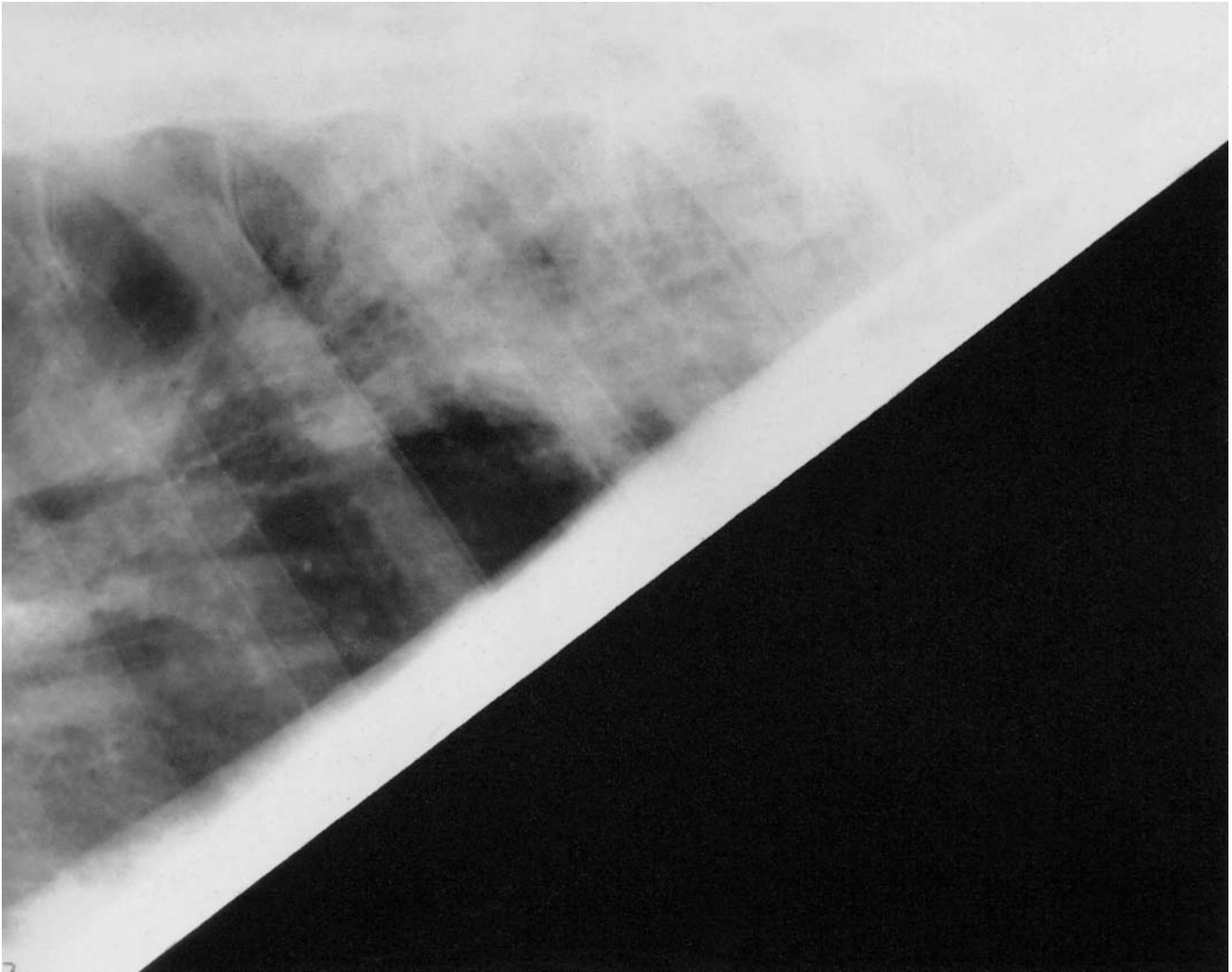
Figure 11.21 Three-year-old Thoroughbred filly with a history of chronic pleuritis and weight loss. There is a caudodorsal lung mass of mixed interstitial and alveolar infiltrates. The cranial margins of the mass are well circumscribed. The findings are suggestive of infarct or pulmonary haemorrhage. The possibility of bacterial pneumonia cannot be ruled out. The smooth margins cranially, the triangular shape and less distinct peripheral margins are more characteristic of infarct. Diagnosis: caudal thoracic mass, probably an infarct.

be seen as incidental findings when examining the lung for other diseases. They must be differentiated from abscesses, granulomas and resolving EIPH.

Exercise-induced pulmonary haemorrhage (EIPH)

The diagnosis of EIPH is usually based on the presence of haemorrhage from the nostrils and on endoscopic examination immediately following strenuous exercise. Radiographic findings when present are limited to the caudodorsal lungs and consist of interstitial opacities with a wispy appearance that often obliterate the thoracophrenic angle and summate

with the diaphragmatic shadow. The opacities are usually more circum-scribed toward the hilus and less well defined toward the periphery. Reso-lution of the opacity has been reported as early as 10 days, but may last for several months with a gradual decrease in size and increase in mar-gination. Cavitation and pleural fluid accumulation have both been reported as sequelae to this condition. A pre-existing abscess may predispose to haemorrhage.

Diaphragmatic hernia

Diaphragmatic hernias may be either congenital or acquired. Congenital diaphragmatic hernias may occur dorsally, in the mid-diaphragm on the left side, or ventrally, where they are usually larger. Although congenital hernias are reported to have smooth well-rounded margins, this change is not seen radiographically. Large defects have been reported in foals with arthrogryphosis and scoliosis.

Acquired diaphragmatic hernias are usually associated with trauma or violent exercise (jumping) or increased intra-abdominal pressure (par-turition, a fall or colic). When signs of trauma are absent consideration must be given to the existence of a congenital defect that has been exacerbated by exercise or increased intra-abdominal pressure.

There may be no clinical signs which relate to the diaphragmatic rupture immediately after the initial trauma. However, the acute signs of abdomi-nal distress (colic) or respiratory distress may be noted later on.

The radiographic signs of diaphragmatic rupture include gas-capped fluid levels and bowel patterns in the ventral thorax with or without free fluid (Figure 11.22). Fluid opacities may be present when liver, spleen or omentum are in the thoracic cavity without accompanying bowel structures. Striations or crescent-shaped lines through gas-containing structures may indicate haustra of the large bowel. Normal structures such as the pulmonary vessels and the heart may be displaced by the presence of abdominal viscera in the thoracic cavity.

Laterality may be determined by obtaining both right and left lateral projections of the thorax and comparing the image sharpness and magnification. Lesions or structures will be on the side in which they appear small and sharply delineated. If laterality cannot be determined by this method, the defect may be near the midline.

Cardiac diseases

In general, cardiac disease in the large equine patient does not lend itself to radiographic diagnosis, but congenital cardiac disease may occasionally be diagnosed in the foal (Figure 11.23, page 523). The use of diagnostic ultra-sound is usually much more valuable in the diagnosis of cardiac disease in the horse. Occasionally other radiographic signs may lead to the inclusion of cardiac disease in the differential diagnosis. Decreased number and diminished size of pulmonary vessels, although quite subjective, should lead to the consideration of diseases that cause hypoperfusion. Increasing size of
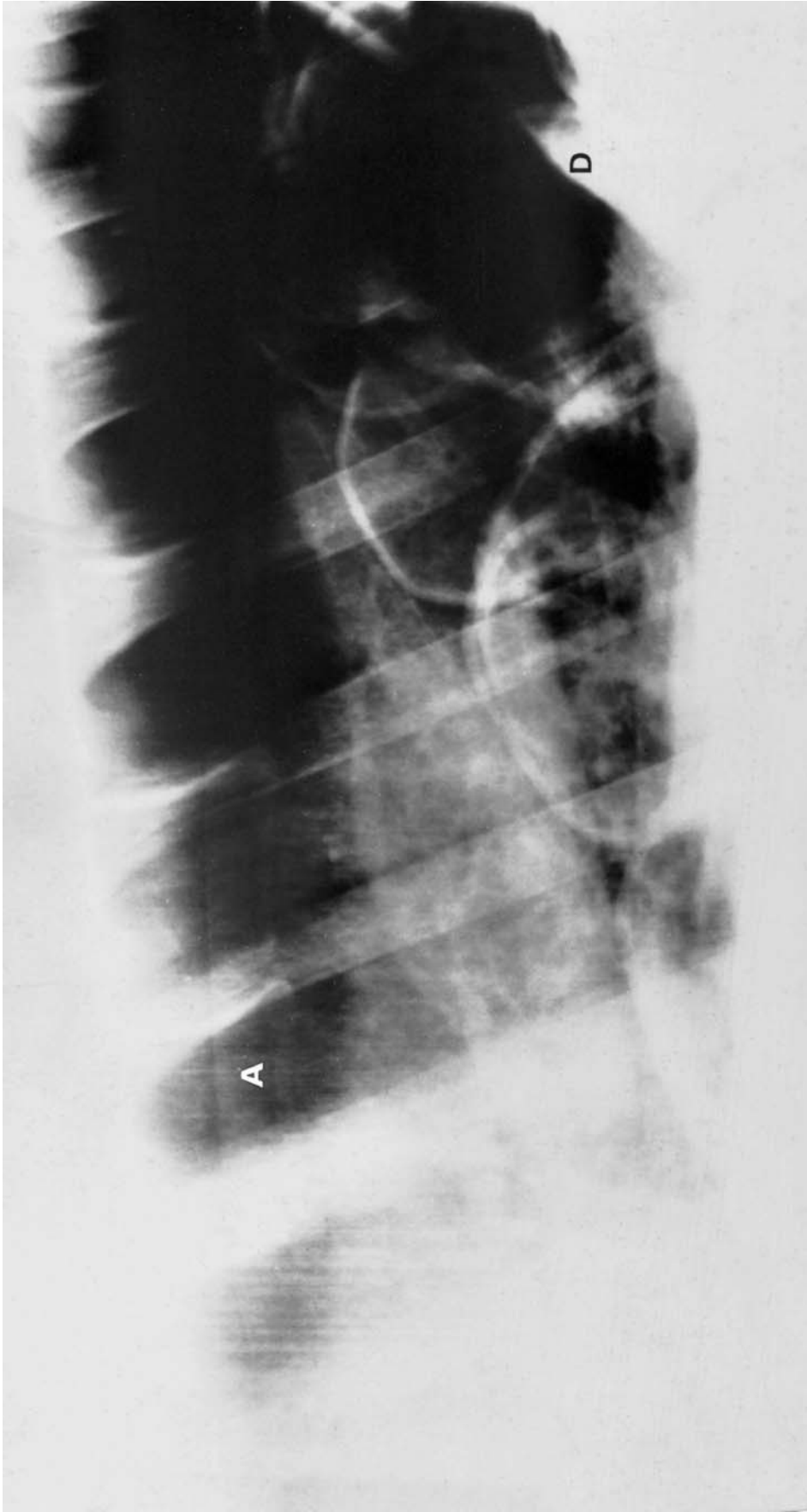
Figure 11.22 Radiographic abnormalities characteristic of a diaphragmatic hernia. There are gas-filled bowel loops cranial to the diaphragm (D), containing gas and fluid at various levels. The dorsal margin of the aorta (A) passes over the vertebral bodies. The lungs are displaced ventrally from the paraspinal gutter by pneumothorax. The lungs appear opaque due to the atelectasis caused by the fluid and pneumothorax.
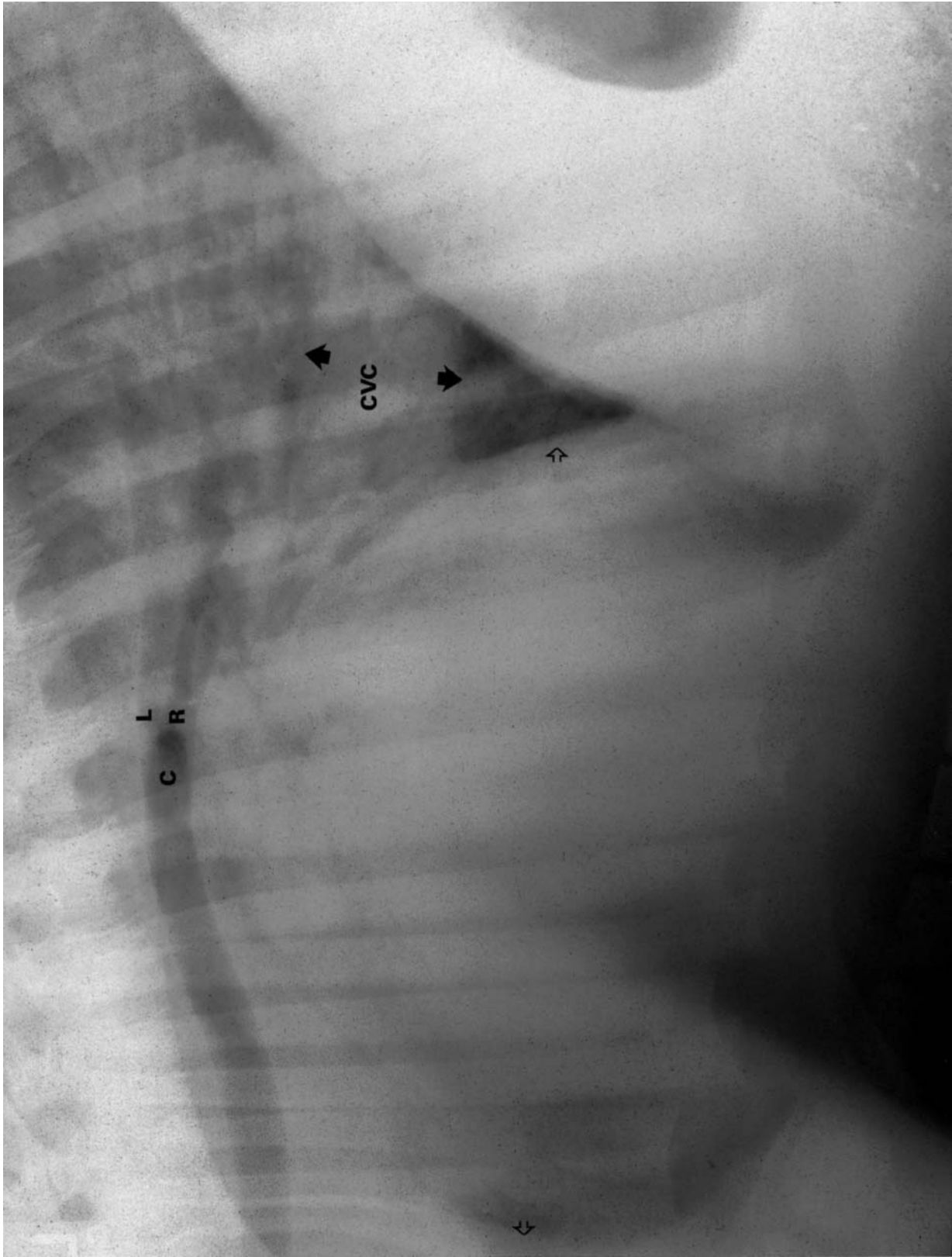
Figure 11.23 A 45-day-old Thoroughbred colt with harsh lung sounds and poor growth. There is cardiac enlargement with dorsal displacement of the trachea just cranial to the carina (C). The left main stem bronchus (L) is slightly elevated over the right (R). The caudal vena cava (CVC) is markedly dilated (black arrows). There is a generalized increase in pulmonary interstitial infiltrates in all lung lobes. This results in an overall opacification of the lungs. The cranial and caudal margins of the cardiac silhouette are marked with open arrows. Diagnosis: congenital right and left heart enlargement with congestive heart failure.

these structures should lead to the consideration of overperfusion, which might lead to other signs such as progression from interstitial to alveolar oedema. Marked enlargement of the cardiac silhouette may be indicated by dorsal displacement of the carina or a rounded appearance, and points to cardiac or pericardial disease.

Rib lesions

TUMOURS

When productive lesions are noted on the ribs or when a pleural mass appears to be associated with a rib, chondrosarcoma must be considered. These tumours may appear as a mass lesion and it may be difficult to define either bone destruction or production, although both components are usually present.

RIB FRACTURES

Such fractures may lead to pneumothorax, lung contusion or pleural haemorrhage. A fracture of a more cranial rib may result in abnormal behaviour when the horse is tacked-up or mounted. Rib fractures are often hard to find radiographically and may be defined by centring the x-ray beam over an area of suspected trauma. Fractures may persist as chronic non-union fractures due to motion. The ends of the opposing ribs may appear slightly flared adjacent to the lucent fibrous union. A fracture of the first rib may result in forelimb lameness and muscle atrophy; the fracture may best be identified by using the technique described for radiography of the shoulder (see page 205).

MULTIPLE OSTEOCHONDROMAS

Multiple hereditary osteochondromatosis has been reported in the horse and should be suspected when smoothly marginated bone protrusions are noted on flat bones. Other osteochondromas may be found on long bones (see pages 192 and 238). Osteochondromas are not usually of any clinical significance, but they may be considered to be potentially pre-cancerous growths.

Abnormalities of the oesophagus are dealt with in Chapter 12 (page 537).
    Also see 'Hypertrophic osteopathy', Chapter 1, page 15.

Sternum

Lateral views of the sternum can be obtained using portable x-ray equipment. Rare earth screens and appropriate film are recommended. The sternum is best radiographed with one forelimb protracted to minimize the amount of soft-tissues which the x-ray beam has to penetrate. An aluminium
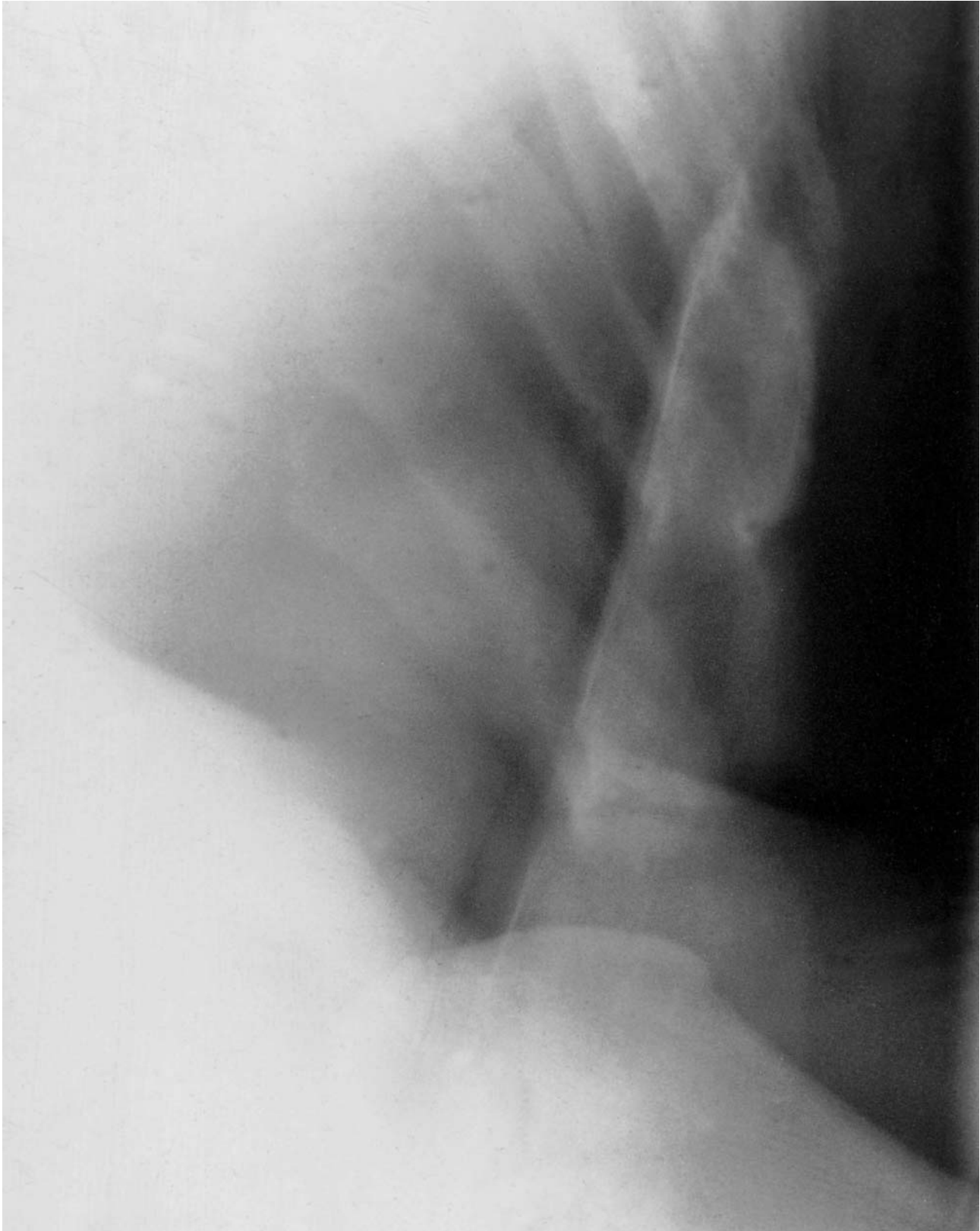
Figure 11.24(a) Lateral view of the caudal one-third of the sternum and the costal cartilages of a normal adult horse. Note the indentations ventrally at the intersternebral articulations.

Figure 11.24(b) Lateral view of the caudal sternum of a mature polo pony. There is fragmentation at the most caudal aspect of the sternum (compare with Figure 11.24a). The pony had shown a sudden onset of violent bucking behaviour when tacked-up or when mounted. When re-examined 6 weeks later, the sternum had modelled considerably; the pony resumed full work without recurrence of abnormal behaviour.

[526]

wedge filter can be useful. The x-ray beam is centred caudal to the elbow approximately 10 cm proximal to the ventral aspect of the thorax.

At birth the sternum consists of seven bony segments, sternebrae, which are united by intersternebral cartilages. The two most caudal sternebrae fuse by approximately 3 months of age, but the remainder only partially fuse. Only the caudal one-third to one-half of the sternum can easily be seen radiographically because of the overlying structures of the forelimb cranially. The sternum inclines ventrally from cranial to caudal (Figure 11.24a). The dorsal border is straight, whereas the ventral border is smoothly curved with indentations at the site of the intersternebral articulations. The most caudal aspect of the sternum is rather variable in shape between horses, being pointed or somewhat rounded. The so-called costal cartilages are mineralized and are seen radiographically. They articulate with the ribs dorsally.

Radiographic abnormalities of the sternum, costal cartilages or ribs are not common, but have been identified in horses demonstrating abnormal behaviour when tacked up or mounted. Abnormalities include a fracture of a costal cartilage and fragmentation of the most caudal aspect of the sternum (Figure 11.24b).

FURTHER READING

Buergelt, C.D., Hines, S.A., Cantor, G., Stirk, A. and Wilson, J.H. (1986) A retrospective study of proliferative interstitial lung disease of horses in Florida. *Vet. Pathol.*, **23**, 750–756

Carlsten, J. (1986) Imaging of the equine heart. An angiographic and echocardiographic investigation. *Thesis*, Uppsala, Sweden, Merkantil-Tryckeriet AB, Uppsala

Carlsten, J., Kvart, C. and Jeffcott, L.B. (1984) Method of selective and non-selective angiocardiography for the horse. *Equine Vet. J.*, **12**, 47–52

Farrow, C.S. (1981) Equine thoracic radiology. *J. Am. Vet. Med. Ass.*, **179**, 776–781

Farrow, C.S. (1981) Radiography of the equine thorax: anatomy and technique. *Vet. Radiol.*, **22**, 62–78

Farrow, C.S. (1981) Radiographic aspects of inflammatory lung disease in the horse. *Vet. Radiol.*, **22**, 107–114

Farrow, C.S. (1976) Pneumomediastinum in the horse: a complication of transtracheal aspiration. *Vet. Radiol.*, **17**, 192–195

Farrow, C.S. (1982) Inhalation pneumonia in a horse. *Can. Vet. J.*, **23**, 340–341

Hillidge, C.J. (1986) Review of *Corynebacterium* (*Rhodococcus*) *equi* lung abscess in foals: pathogenesis, diagnosis and treatment. *Vet. Rec.*, **119**, 261–264; *Vet. Radiol.*, **9**, 80–88

Kangstrom, L.E. (1968) The radiological diagnosis of equine pneumonia. *Vet. Radiol.*, **9**, 80–88

Kohn, C.W. (1981) Recognition and management of equine viral respiratory disease. *Compend. Contin. Educ.*, **3**(3), 73–81

Kosch, P.C., Koterba, A.M., Coons, T.J. and Webb, A.I. (1984) Developments in management of the newborn foal in respiratory distress 1: Evaluation. *Equine Vet. J.*, **16**, 312–318

Koterba, A.M., Brewer, B.D. and Tarplee, F.A. (1984) Clinical and clinicopathological characteristics of the septicaemic neonatal foal: review of 38 cases. *Equine Vet. J.*, **16**, 376–383

Kvart, C., Carlsten, J., Jeffcott, L.B. and Nilsfors, L. (1985) Diagnostic value of contrast echocardiography in the horse. *Equine Vet. J.*, **17**, 357–360

Lamb, C.R., O'Callaghan, M.W. and Pradis, M.R. (1990) Thoracic radiography in the neonatal foal: a preliminary report. *Vet. Radiol.*, **31**, 11–16

Martens, R.J., Martens, J.G. and Fiske, R.A. (1989) *Rhodococcus equi* foal pneumonia: pathogenesis and immunoprophylaxis. *Proc. Am. Ass. Equine Prac.*, **35**, 199–213

Martens, R.J. and Renshaw H.W. (1982) Foal pneumonia. A practical approach to diagnosis and therapy. *Compend. Contin. Educ.*, **4**(9), 217–228

Morris, D.D. and Beech, J. (1983) Disseminated intravascular coagulation in six horse. *J. Am. Vet. Med. Ass.*, **183**, 1067–1072

O'Callaghan, M.W. and Seehermans, H.J. (1989) New ways of looking at lung disease in the horse using radiography and scintigraphy. *Proc. Am. Ass. Equine Prac.*, **35**, 221–232

Pascoe, J.R., O'Brien, T.R., Wheat, J.D. and Meagher, D.M. (1983) Radiographic aspects of exercise-induced pulmonary hemorrhage in racing horses. *Vet. Radiol.*, **24**, 85–92

Rantanen, N.W. (1986) Diagnostic ultrasound. *Veterinary Clinics of North America. Equine Practice*, Vol. 2, No. 1, W.B. Saunders, Philadelphia

Shively, J.F., Dellers, R.W., Buergelt, C.D. *et al.* (1973) *Pneumocystis carinii* pneumonia in two foals. *J. Am. Vet. Med. Ass.*, **162**, 648–652

Silverman, S., Poulos, P.W. and Suter, P.F. (1976) Cavitary pulmonary lesions in animals. *J. Am. Vet. Radiol. Soc.*, **17**, 134–146

Toal, R.L. and Cudd, T. (1986) Equine neonatal thoracic radiography: a radiographic-pathologic correlation. *Proc. Am. Ass. Equine Pract.*, **32**, 117–128

Verschooten, F., Oyaert, W., Muylle, E., DeMoor, A., Steenhaut, M. and Moens, Y. (1977) Diaphragmatic hernia in the horse: Four case reports. *J. Vet. Radiol.* **18**(2), 45–50

Walker, M. and Goble, D. (1980) Barium sulphate bronchography in horses. *Vet. Radiol.*, **21**, 85–90

Wisner, E., O'Brien, T., Lakritz, J. *et al.* (1993) Radiographic and microscopic correlation of diffuse interstitial and broncho-interstitial pulmonary patterns in the caudodorsal lung of adult Thoroughbred horses in race training. *Equine Vet. J.*, **25**, 293–298

Chapter 12
The Alimentary and Urinary Systems

Although the oesophagus could be discussed in a regional manner, we have chosen to include it in its entirety with the alimentary system. Diseases of the diaphragm are discussed with the thorax (see Chapter 11, page 521). Abdominal radiography in the adult horse is difficult and only limited information can be obtained. Therefore emphasis is placed on those conditions in which abdominal radiography is of real value: abdominal radiography of the foal and on the use of contrast studies for the diagnosis of abdominal diseases.

RADIOGRAPHIC TECHNIQUE

Equipment

With the exception of the cervical oesophagus, the radiographic evaluation of the alimentary system of adult horses cannot be accomplished with portable equipment. High-output portable units can be used in small horses and foals, and small animal x-ray units can be used for young foals and miniature horses. Radiography of the abdomen of adult horses is of little value except for the diagnosis of enterolithiasis, diaphragmatic hernia (see page 521), bowel obstruction, sand impaction in the large colon, and urinary calculi. These studies in adult horses can only be performed with large stationary equipment and exposures in the range 90–120 kVp and 180–600 mAs. It is difficult, if not impossible, to obtain diagnostic radiographs from horses with an abdominal width greater than 70 cm. Fast rare earth screens are recommended and a focused grid (140 cm focus, 103 lines per cm and a 10:1 ratio) is essential.

Abdominal radiography in the adult horse is usually performed standing using four views with overlapping fields: (a) cranioventral, (b) midventral, (c) mid-dorsal, and (d) dorsocaudal. In young foals and miniature horses one or two views are usually sufficient to evaluate the entire abdomen (Figures 12.1, 12.2a, page 532 and 12.2b, page 533). Recumbent radiographs may be obtained, but standing lateral films are preferred (Figures 12.3a and 12.3b, pages 534 and 535). The radiographs should be obtained with the side with the area of interest next to the cassette. Regardless of positioning for the initial radiograph, a second one should be obtained in the opposite lateral position, centred over the area of concern. Evaluation of the stomach should always be performed with the left side against the cassette. In a recumbent foal both lateral and ventrodorsal views are recommended, especially when contrast material is used.

Figure 12.1 Lateral radiograph of a normal abdomen of a 6-day-old Thoroughbred filly, obtained with the foal recumbent. There is gas, fluid and food material within the stomach. The lack of abdominal visceral detail is due to the age of the patient. There is gas in the large and small bowel.

The oesophagus

Examination of the oesophagus of adult horses should be performed with the patient standing with its left side next to the cassette. If recumbent radiographs are obtained, the patient should be in left lateral recumbency. If contrast material is to be used in the conscious recumbent animal, it should be limited to barium paste which is easier to swallow and less likely to be aspirated than barium suspension.

The abdomen

Abdominal radiography in young and adult horses is always performed in the standing position, whereas abdominal radiography of the neonatal equine patient or a miniature horse may be carried out either standing or in lateral recumbency, with the cassette placed on the floor or using a standard x-ray table. Standing and recumbent abdominal radiographs differ in the distribution of gas and fluid. Gas-capped fluid levels can only be evaluated on radiographs obtained in the upright (standing) position (Figure 12.3b, page 535). Ventrodorsal radiographs of adult horses are seldom used because of the need for general anaesthesia and the paucity of information gained; however, they can be obtained in neonates and miniature horses using minimal chemical restraint.

Contrast examinations

Contrast examinations are covered in detail with each specific area to be examined, but the clinician must be aware of the basic principle that proper evaluation of a hollow viscus requires that the viscus must be distended. The distension can be obtained with either positive contrast (barium- or iodine-containing compounds), negative contrast (air) or a combination of the two. In general, micropulverized barium sulphate should be administered as a 30% (weight per volume) suspension. In foals and young horses, a dosage of 5 ml/kg body weight may be used, whereas in adult horses a dosage of 3 ml/kg body weight is recommended. When a barium paste is used the dosage is quite variable, depending on the tolerance of the patient; usually half a tube of esophotrast is adequate. The paste is placed in the mouth and the patient is allowed to swallow in a normal manner. For contrast studies of the abdomen the patient should be starved for 12 hours prior to the examination to enhance detail.

Oesophagus

RADIOGRAPHIC TECHNIQUE

The appropriate technique is discussed on page 529, and contrast studies on page 536.
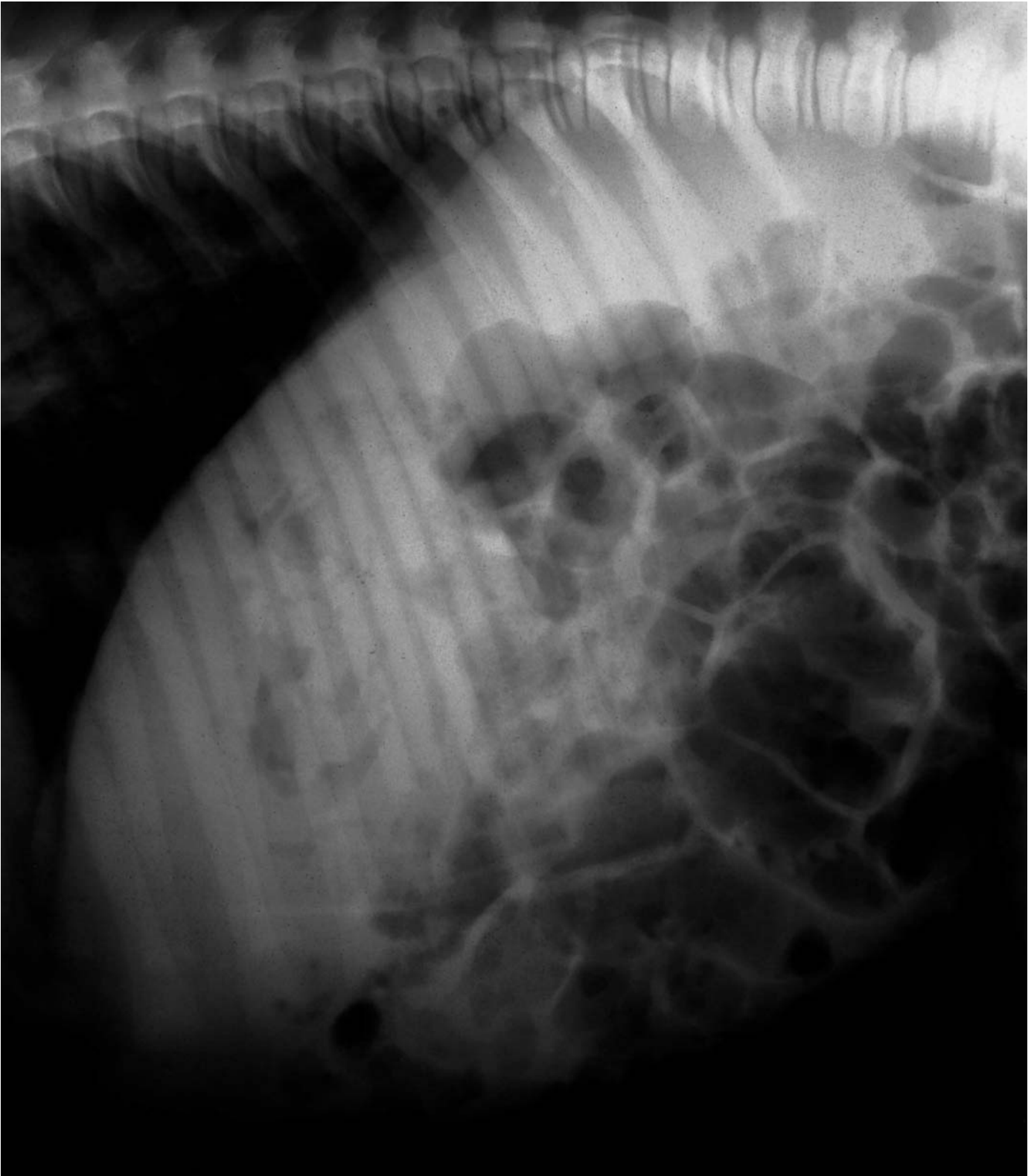
Figure 12.2(a) Lateral recumbent radiograph of the normal cranial abdomen of a 3-day-old foal. There is food and gas within the stomach. The large and small bowel are mostly gas-filled loops without evidence of overdistension.
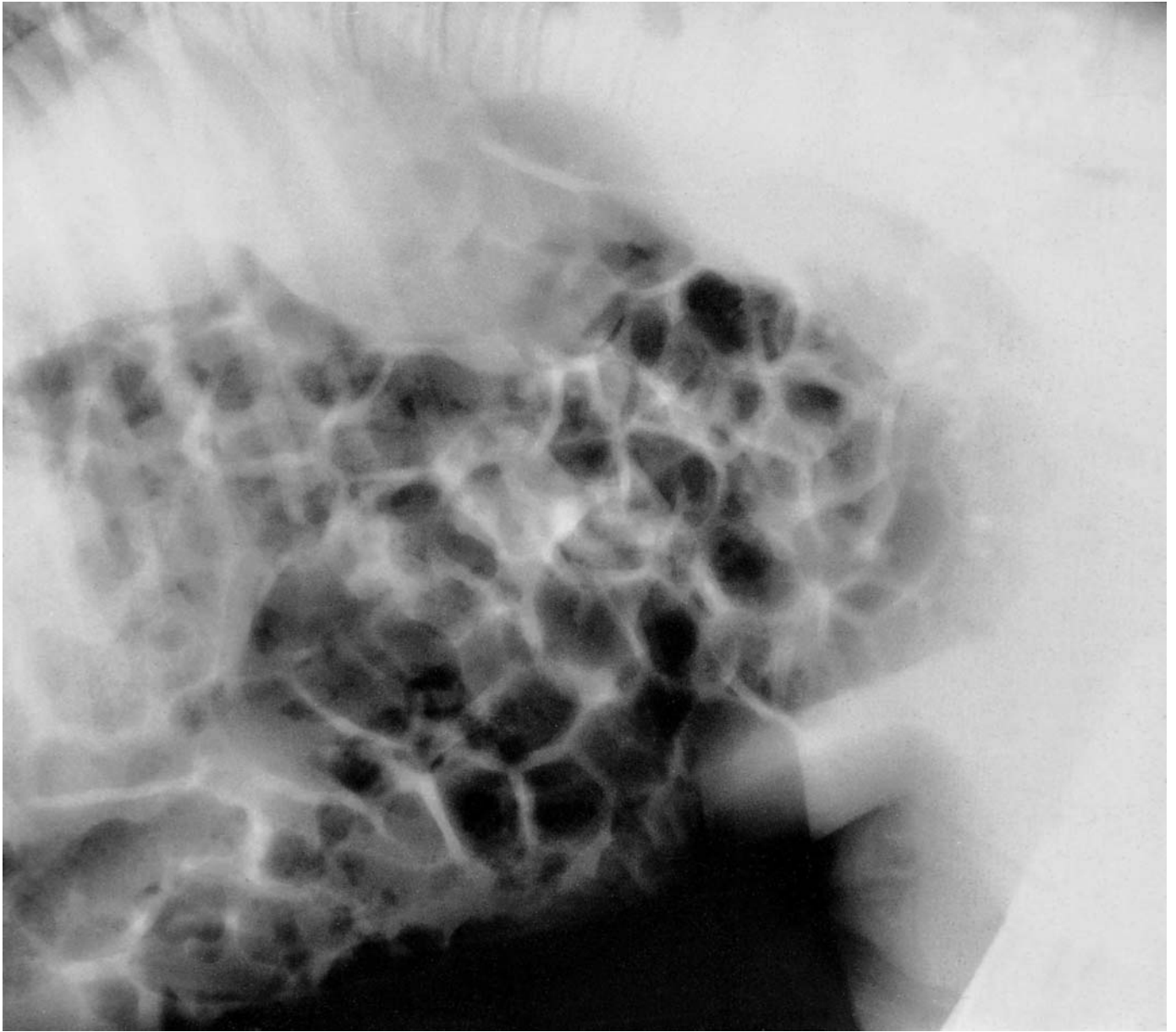
Figure 12.2(b) Lateral recumbent radiograph of the normal caudal abdomen of a 3-day-old foal, demonstrating gas- and fluid-filled large and small bowel loops. The urinary bladder can be seen adjacent to the caudoventral abdominal wall.
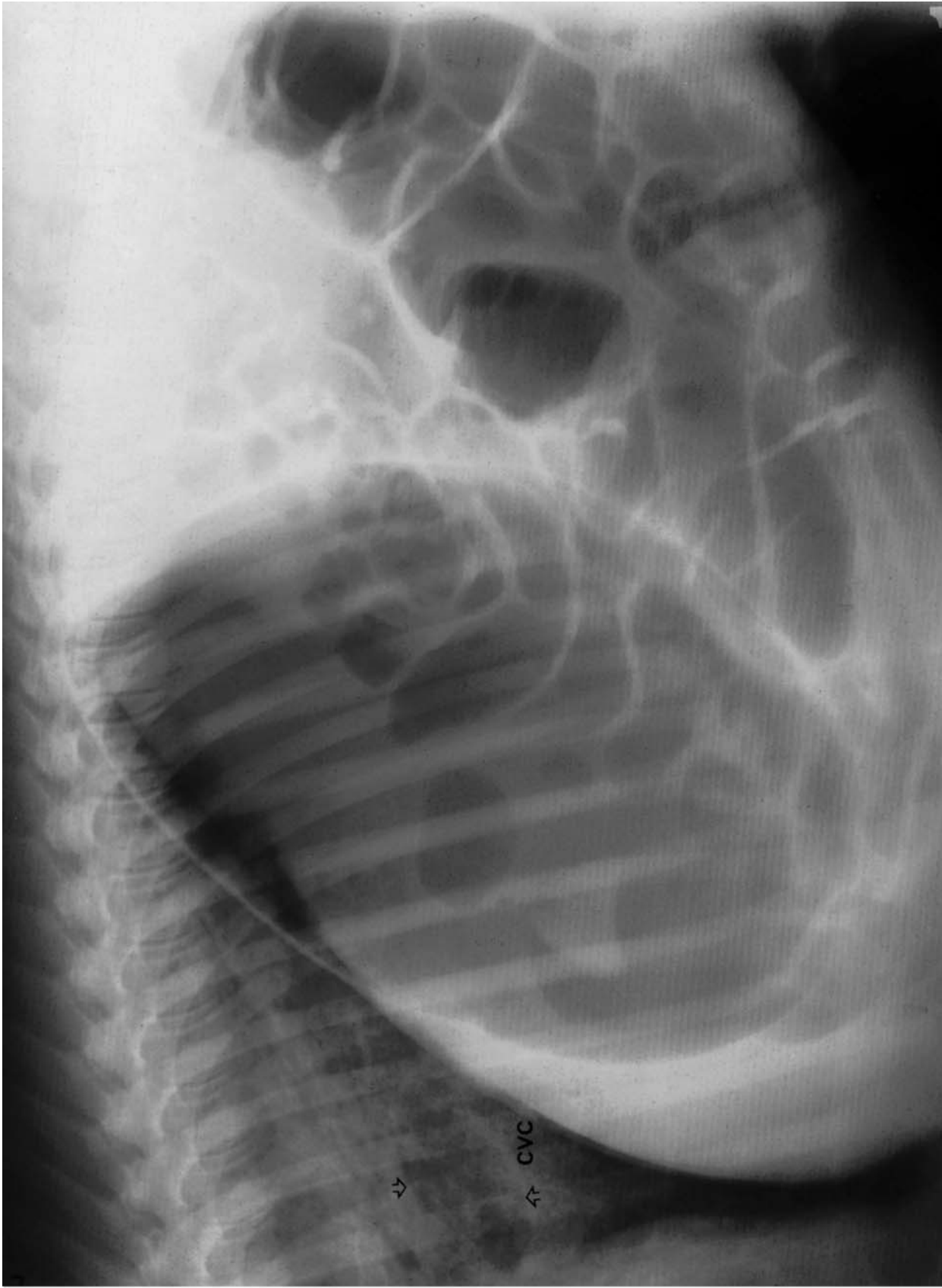
Figure 12.3 Recumbent lateral (a) and standing lateral (b) views of a normal abdomen of a 3-day-old Thoroughbred colt. (a) There is a well-circumscribed gas lucency noted in the caudal oesophagus (arrows) overlying the caudal vena cava (CVC). There is gas and fluid distension of the stomach. The large and small bowel contain both gas and fluid, but there is no indication of overdistension or obstruction. There is a generalized increase in interstitial markings in the portions of the lung that are visible. This is probably due to age and pressure from the distended stomach, preventing complete inflation.

(a)
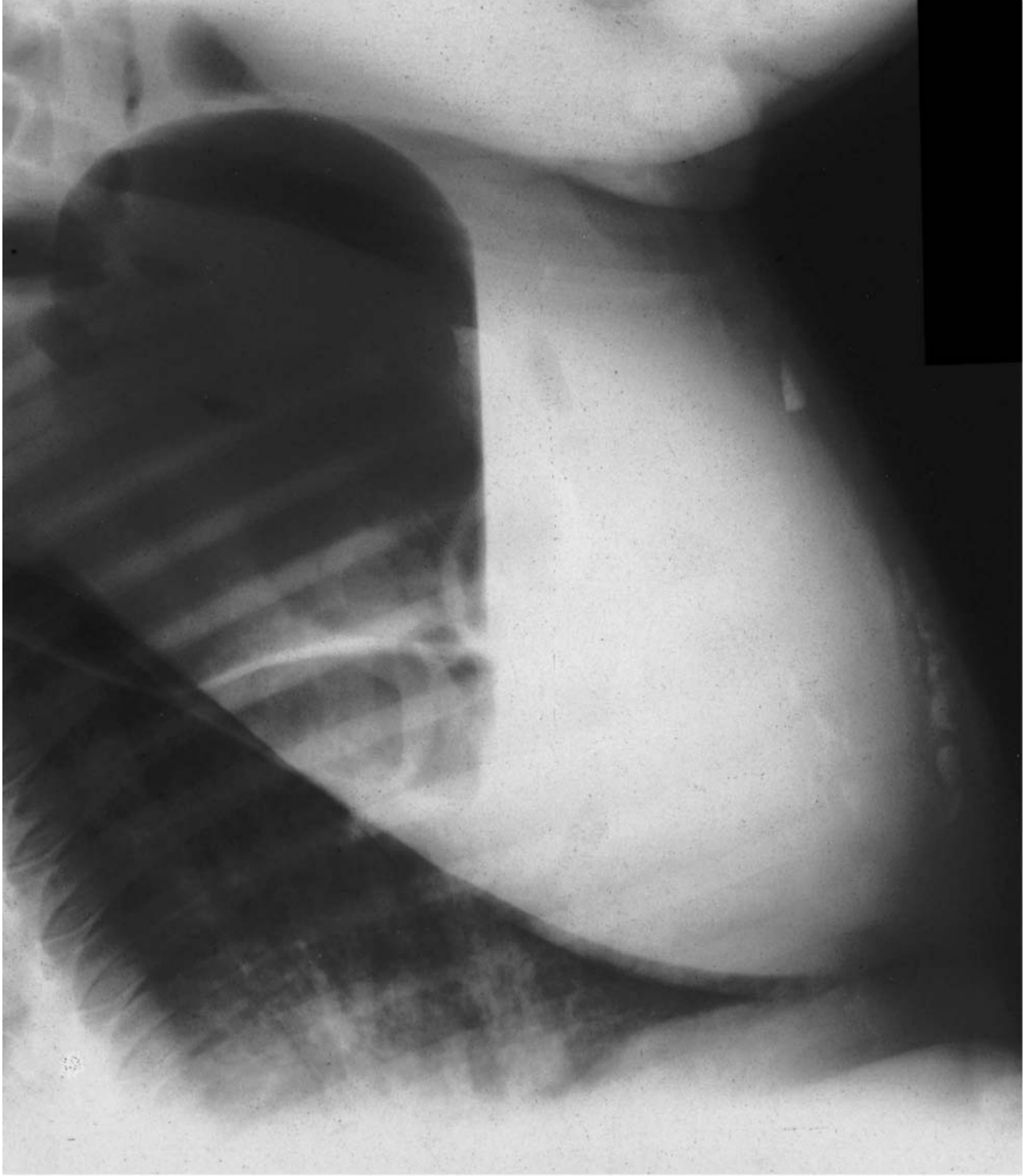
(b)

Figure 12.3 *Cont'd* (b) This standing lateral projection of the abdomen was obtained several hours after (a). Note that the gas and fluid now form a fluid line. The caudal abdomen cannot be as well visualized in the standing lateral film due to the position of the limbs which cover the caudal abdomen. Gas and fluid can be seen in both the large and small bowel. Opaque material in the ventral colon is sand.

NORMAL ANATOMY AND ACTION OF THE OESOPHAGUS

In the normal horse there is no air in the oesophagus. As the oesophagus passes through the thoracic inlet it may drape over, and partially obscure, the dorsum of the trachea. The oesophagus then elevates slightly as it passes over the heart and caudally through the cardia into the stomach.

A bolus of food (or contrast material) collects rostral to the epiglottis at the base of the tongue. When the horse swallows, the bolus passes into the retropharyngeal area and into the oesophagus. It is carried rapidly down the oesophagus by the stripping motion of the oesophageal contractions. The passage of a bolus takes between 4 and 10 seconds. Although the act of deglutition can only be followed with fluoroscopy, the results can often be noted on serial radiographs obtained after the administration of contrast material.

Contrast examination of the oesophagus

When there is a history of dysphagia, oesophageal obstruction or recurrent oesophageal disease and survey radiographs are normal, a contrast examination of the oesophagus should be performed. Barium paste is used to evaluate the oesophageal mucosa. The paste coats the mucosa and has the advantage of outlining structures for several minutes. In the normal oesophagus the contrast medium is seen as fine radiopaque linear streaking outlining the longitudinal oesophageal mucosal folds after the passage of the bolus. A bolus may be seen on a single radiograph, but will normally pass on gradually, or be carried away with the next bolus. The bolus should not be in the same location in subsequent radiographs.

Barium suspension is the contrast medium of choice when diverticuli or mega-oesophagus are suspected, because of the greater volume of contrast material required to demonstrate such changes. Liquid barium given per os or by stomach tube into the cranial oesophagus is passed in a similar manner to barium paste, but does not coat the oesophageal mucosa as well. Occasionally a small amount of contrast material is held momentarily at the thoracic inlet or just cranial to the cardiac silhouette. Contrast medium may also remain momentarily at the cardia, but will pass gradually into the stomach. Barium-coated food such as pellets or hay can also be used to demonstrate strictures which may not be demonstrated by the use of liquid barium alone.

Delayed oesophageal emptying and distension with air and contrast material has been reported as a sequel to recent passage of a nasogastric tube and has been associated with the use of tranquillizers.

If liquid barium is administered by mouth, in some cases traces will be seen dorsal to the soft palate, or in the larynx or trachea. This is abnormal and indicative of abnormal pharyngeal function. A clinical evaluation of the nasophraynx and larynx should be performed to differentiate conditions

[536]

such as cleft palate, a foreign body and Eustachian tube diverticulum mycosis, from primary oesophageal diseases.

DISEASES OF THE OESOPHAGUS

Diseases of the oesophagus can be divided into three main categories:

Diseases that decrease the diameter

Stricture from scar tissue

Scar tissue results from damage due to previous trauma such as choke, a foreign body, a penetrating wound, previous surgery or over-zealous attempts to relieve a choke. The stricture can usually be demonstrated with barium paste, but may require a mixture of food and barium. The wall is normally smooth at the point of stricture and barium and/or food will be retained cranial to the stricture (Figure 12.4).

Abscessation

Abscessation of the oesophageal wall may result from penetration from inside or outside. Soft-tissue swelling and irregularity of the mucosal surface may be noted when an abscess originates from internal trauma. The mucosal surface may be smooth if the abscessed wall has not yet ruptured into the lumen. Wounds to the oesophagus may result in fistula formation as well as scarring and abscessation as noted above. Following rupture of the oesophagus, food and gas may be seen in the peri-oesophageal tissues (Figure 12.5, page 539).

Spasm

Spasm is usually a temporary condition and may not be found on subsequent radiographs. The mucosal surface is smooth and a second examination is often necessary to differentiate spasm from stricture.

External masses

Pressure from adjacent tissue such as a tumour, goitre or external abscess may be identified by noting that the oesophagus, dilated by contrast material, appears to deviate around a soft-tissue mass rather than being completely encircled by the mass. Ultrasonographic examination may be very helpful in these cases.

Neoplasia

Oesophageal neoplasia is extremely rare in the horse, but must be considered in cases where there is a mass and irregularity of the mucosal surface of the oesophagus. The differential diagnosis includes abscessation.
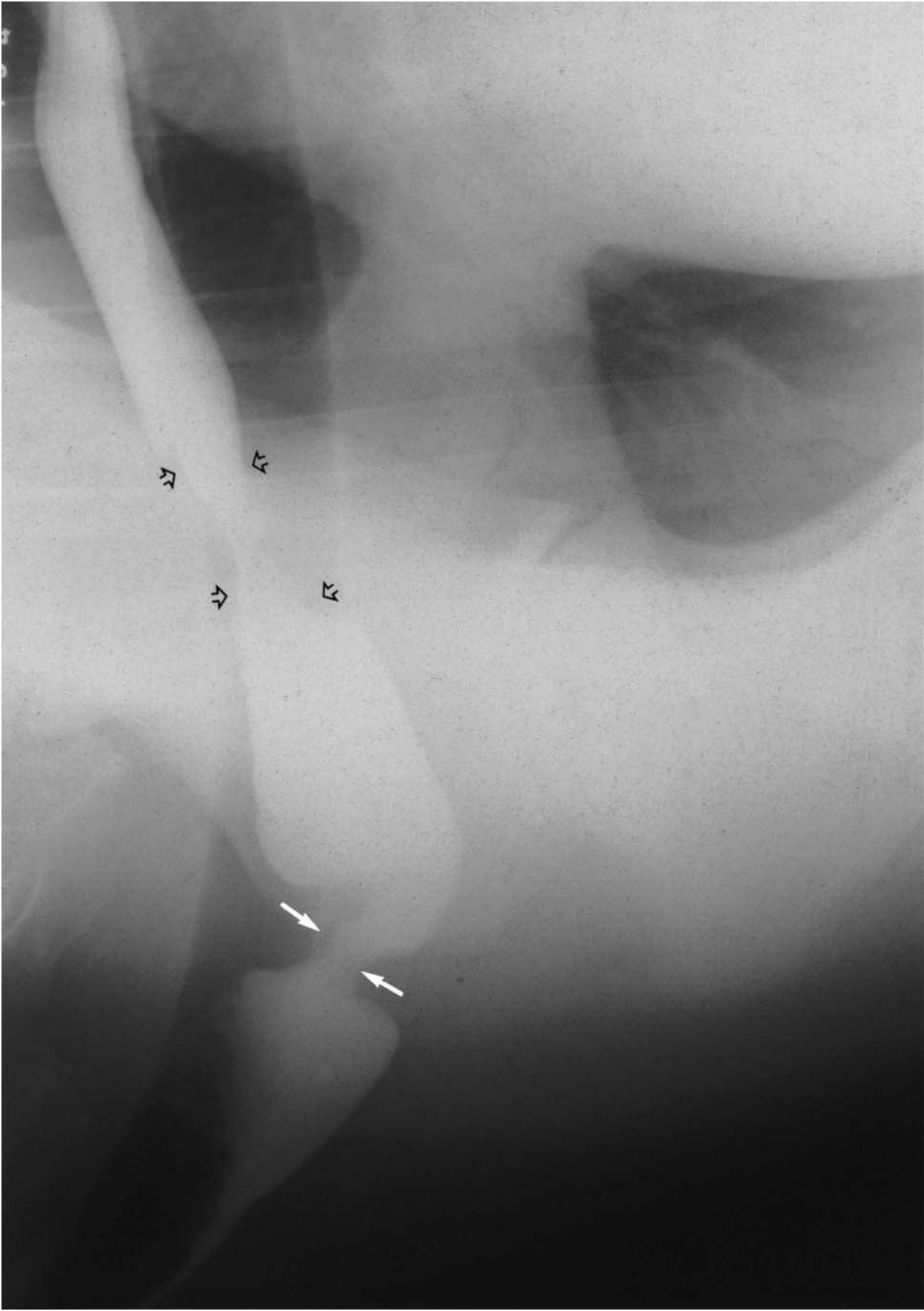
Figure 12.4 This 4-year-old Standardbred filly was presented with a history of having had choke 28 days previously. The horse is now having difficulty swallowing. Survey radiographs of the cervical oesophagus did not demonstrate any abnormality. Fifty millilitres of micronized barium sulphate diluted in a similar volume of water was administered via stomach tube in the cranial oesophagus. There is a stricture of the oesophagus at the thoracic inlet (solid arrows), with pre- and post-stenotic dilatation. A second area of stenosis is noted caudal to the first (open arrows). The remainder of the oesophagus is normal. Diagnosis: oesophageal stricture at two locations.
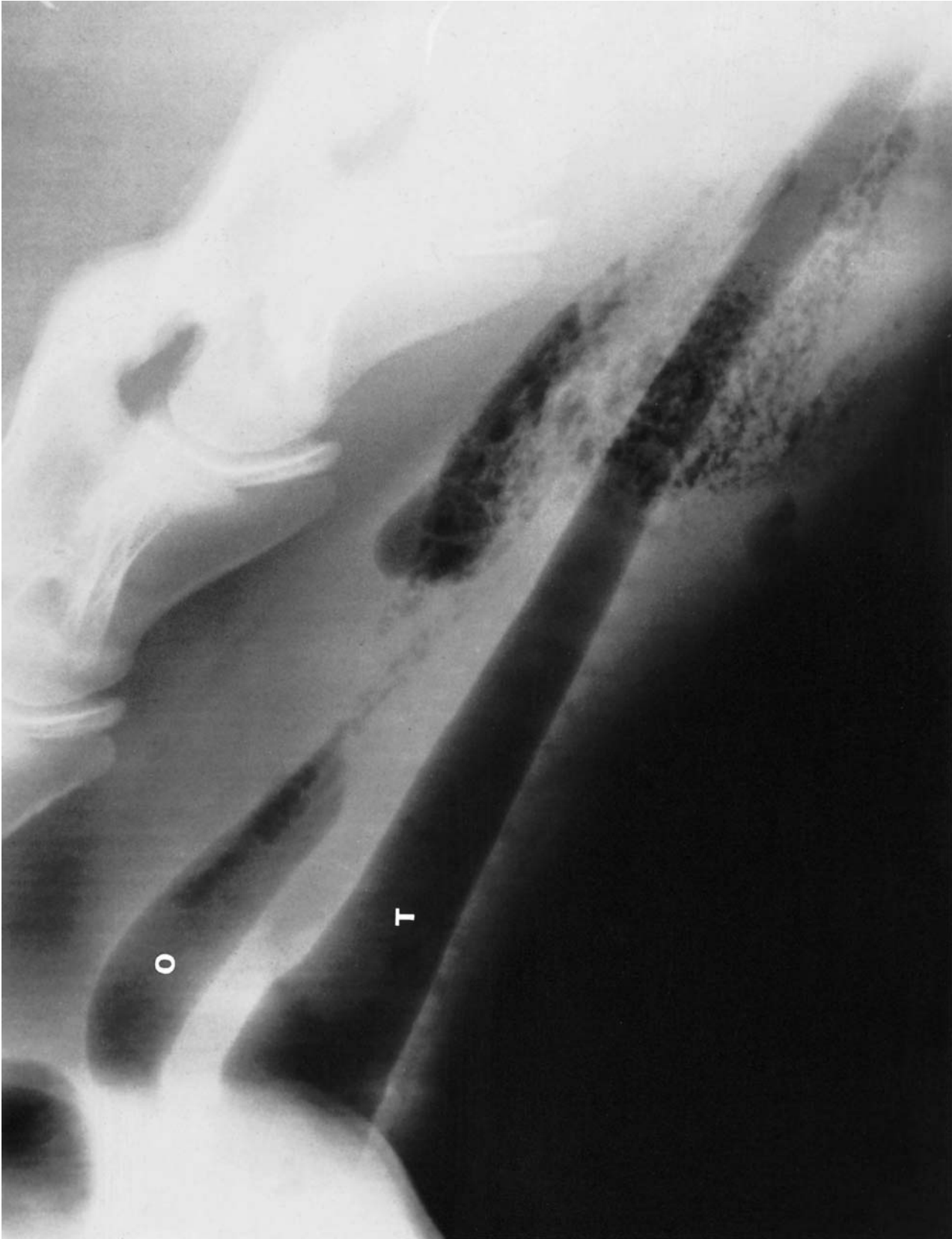
Figure 12.5 This yearling Thoroughbred filly was presented with a swollen neck. There was no evidence of a skin wound. A lateral radiograph of the cervical area demonstrates the soft-tissue swelling which appears to compress the trachea (T) and narrow the tracheal lumen. There is gas in the cranial oesophagus (O) and a mottled irregular appearance representing both gas and food material in the soft tissues. Diagnosis: ruptured oesophagus with food and gas in the peri-oesophageal soft tissues.

Diseases which increase the diameter

Mega-oesophagus – dilatation of the oesophagus

The affected segment of the oesophagus may be dilated with gas (Figure 12.6, page 542), fluid or food, either alone or in combination (Figure 12.7, page 543).

Mega-oesophagus may be focal, resulting from a stricture, a foreign body or an annular ring anomaly or may involve the entire oesophagus due to neuromuscular dysfunction or abnormality of the cardiac sphincter. Generalized mega-oesophagus has been reported in chronic grass sickness in the United Kingdom. In foals, generalized mega-oesophagus may be seen in gastroduodenal ulcer disease (Figure 12.7, page 543) (see page 552). Focal mega-oesophagus with accumulation of food is usually considered to be the result of oesophageal obstruction (see below). Lack of oesophageal motility can be demonstrated using liquid barium and obtaining several exposures without moving the patient. If oesophageal motility is present, the contrast – column or contrast – air interface will change. A common sequel to mega-oesophagus is aspiration pneumonia (see page 507).

Diverticuli

Horses with a diverticulum may have either a history of spontaneous occurrence or of previous injury or choke. Diverticula may be classified as either pulsion or traction. A pulsion diverticulum is the result of mucosal herniation through an acquired defect in the muscularis, due to over-dilatation at an impaction site which causes separation of the muscularis. These diverticuli may be large. Regardless of size or cause, a diverticulum appears as a rounded outpouching of the oesophagus rather than the linear appearance of the normal oesophagus cranial and caudal to the diverticulum (Figures 12.8a–12.8c, pages 544–5 and 12.9a–12.9c, pages 546–7). A traction diverticulum is usually small and of little significance. It may have a pointed rather than rounded appearance because it results from peri-oesophageal scarring which exerts traction on a segment of the wall.

Oesophageal dysfunction and obstruction (choke)

Choke

Although oesophageal obstruction is often related to the rapid ingestion of food, it may also occur secondarily to scar formation or diverticula (Figure 12.8, pages 544 and 545) within the oesophagus or as a result of impingement upon the oesophagus from masses or annular ring anomalies, or for no discernible reason.

The radiographic appearance varies depending upon the cause of the obstruction, but most often has a mottled gas and soft-tissue opacity resulting from the mixture of gas and food material (Figure 12.9, page 546). The mass is most commonly oval in shape. Air may be seen at one or both ends of the mass and conforms to the shape of the mass and then

tapers sharply to a point. The obstruction may occur at any location within the oesophagus, but the thoracic inlet, base of the heart and the cardia are the most common sites when there is no underlying pathology as the cause of the obstruction.

Contrast material will aid in the definition of the obstruction, but care must be taken that reflux of the contrast into the trachea does not occur. Aspiration pneumonia may be seen as a sequel to oesophageal obstruction (see page 507). A post-treatment control study, using barium sulphate paste, is helpful in the evaluation of the oesophagus after the obstruction has been relieved (Figure 12.9, pages 546 and 547).

Grass sickness

In some cases of grass sickness (in the United Kingdom) a bolus of food (or contrast medium) passes down the oesophagus more slowly than normal and may oscillate to and fro, particularly at the thoracic inlet or at the diaphragm. A bolus may remain stationary at the diaphragm for several minutes before passing into the stomach.

Abdomen and gastrointestinal tract

RADIOGRAPHIC ANATOMY

Foal abdomen

The most common reason for abdominal radiography in the foal is acute abdominal discomfort. In young foals, abdominal structures may be poorly visualized due to the lack of abdominal fat which usually helps differentiation of structures (Figure 12.10, page 550). A normal standing lateral abdominal radiograph has the appearance of a mixture of gas, fluid and ingesta with occasional bowel loops with gas-capped fluid levels. There is often a large amount of gas in the terminal bowel. Distension of small bowel loops is considered to be present when their diameter is slightly greater than the length of the body of the first lumbar vertebra. This measurement can only be made when there is enough gas distension for the small bowel loops to be identified.

Right lateral standing position

The fundus of the stomach is located adjacent to the left crus of the diaphragm, with the body of the stomach inclining slightly forward against the liver. When both air and fluid are present in the stomach, there is a gas cap dorsally in the fundus and against the diaphragm. Fluid and/or food are located ventrally in the pyloric area. Gastric size is considered normal when the width is approximately half the length. The duodenum exits the pylorus near the mid to ventral third of the abdomen. The diaphragmatic flexure of the colon is found ventral to the stomach and in contact with the liver. The
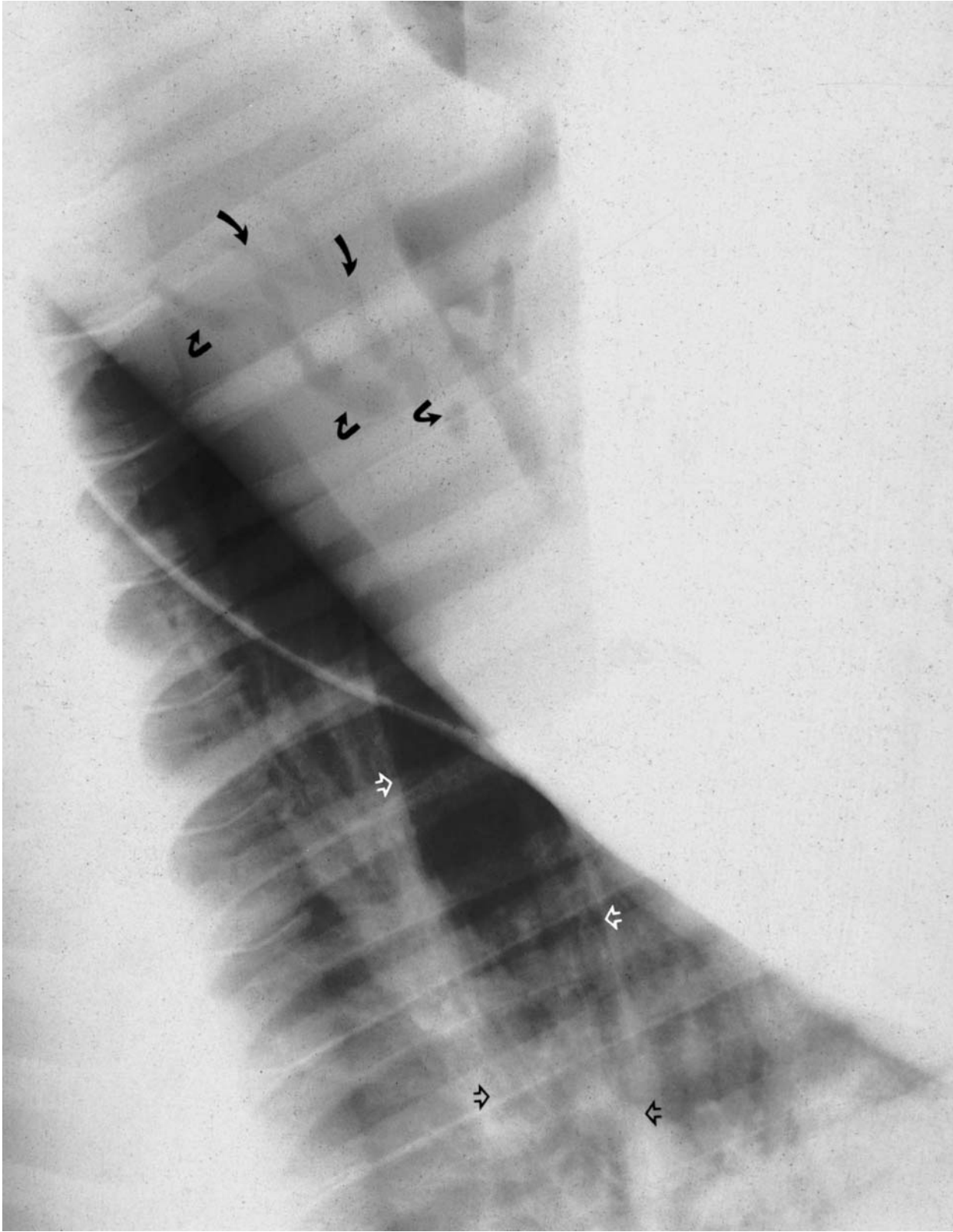
Figure 12.6 This 4-month-old Thoroughbred colt was presented with a history of black tarry diarrhoea. The tentative diagnosis was gastroduodenal ulcer disease. The gas-distended oesophagus is seen in the caudal dorsal thorax, between open arrows. The increased opacity in the caudal dorsal lung lobes is due to pulmonary interstitial infiltrates. A fluid line can be seen in the gas- and fluid-distended stomach. Gas is seen in the biliary tree (curved arrows). Radiographic diagnosis: gastric dilatation with air and fluid, mega-oesophagus, pulmonary interstitial infiltrates and gas in the biliary tree. These findings are indicative of gastroduodenal ulcer disease of the foal.
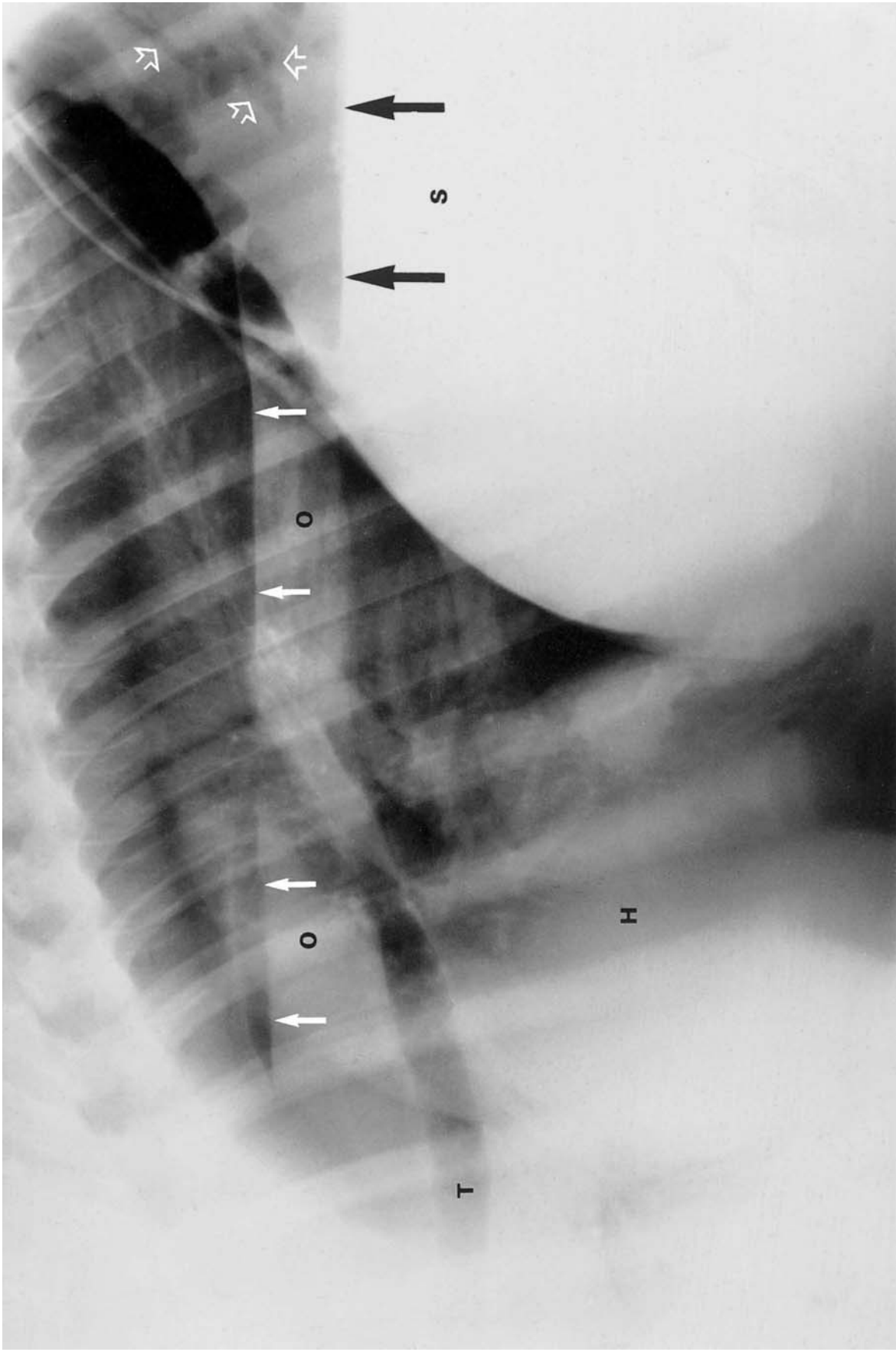
Figure 12.7 This 1-month old Thoroughbred colt was presented depressed and with a painful abdomen, with a 3-week history of signs compatible with gastric ulcer disease. The lateral radiograph demonstrates mega-oesophagus (T) over the base of the heart (H). There is a mixed alveolar and interstitial pattern in the caudal ventral lungs which is best seen over the caudal margin of the cardiac silhouette. The stomach (S) is distended with fluid and air, resulting in a gas-capped fluid level (large black arrows). Gas can also be seen in the biliary tree as branching lucencies (open white arrows) over the opaque liver. Diagnosis: gastroduodenal ulcer disease with mega-oesophagus, aspiration pneumonia and gas in the biliary tree.
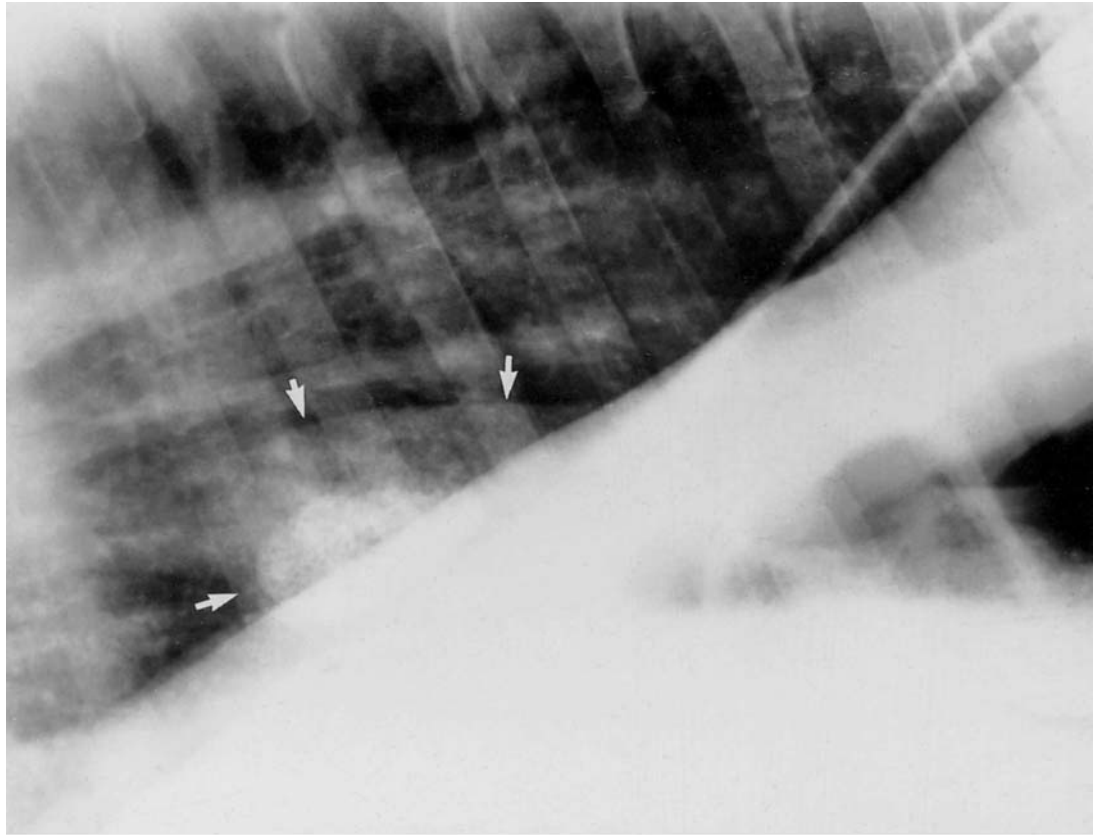
(a)

Figure 12.8 This 14-year-old Quarterhorse mare had a history of four episodes of nasal regurgitation in the previous 6 months.
(a) Survey radiograph of the caudal thorax demonstrates focal dilatation of the caudal oesophageal hiatus (arrows). There is dense granular food material within the mass. Tentative diagnosis: oesophageal diverticulum or gastro-oesophageal invagination.
(b) Approximately 50 ml of micropulverized barium sulphate was administered via stomach tube and a radiograph of the suspected diverticulum was obtained immediately. Contrast material is seen in the normal oesophagus to the level of the mass, where it passes over the mass and delineates the dorsal border. Increased interstitial markings in the lungs probably represent chronic fibrosis secondary to regurgitation.
(c) Administration of additional barium sulphate and air dilates the oesophagus and demonstrates the extent of the diverticulum (curved white and black arrows). A fluid line can be seen in the oesophagus due to the air–fluid interface. The dorsal oesophageal margins are marked (open white and black arrows). Diagnosis: oesophageal diverticulum and secondary pulmonary fibrosis.

[544]

(b)

(c)

[545]
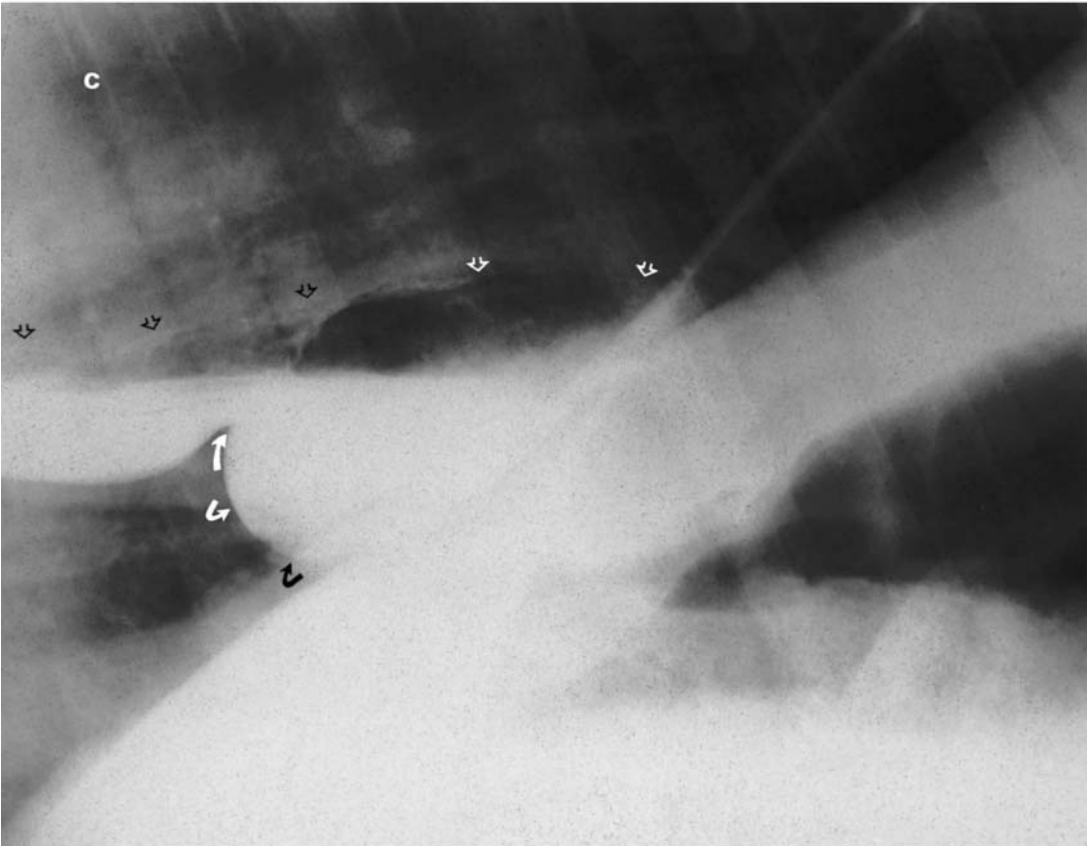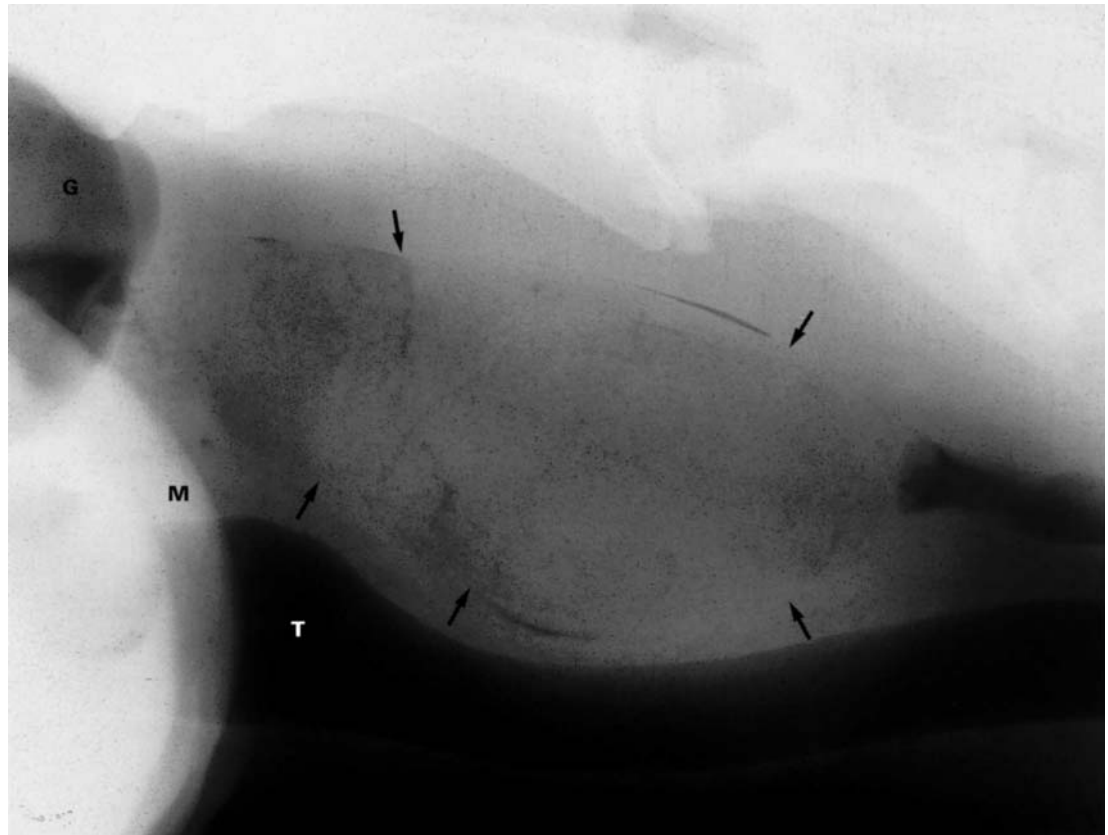
(a)

Figure 12.9(a) A lateral radiograph of the cranial cervical oesophagus demonstrates a large granular gas- and fluid-containing mass within the oesophagus (arrows), compressing the trachea ventrally. There is gas caudal to the mass within the oesophageal lumen. The guttural pouches are identified (G). The right and left rami of the mandible (M) can be seen over the guttural pouches, a portion of the oesophagus and the trachea (T). Diagnosis: oesophageal obstruction 'choke' of the cervical oesophagus.

Figure 12.9(b) Six days after relief of the 'choke' the oesophagus remains dilated and somewhat irregular. There appears to be mucosal folding at several locations (curved arrows). The trachea remains compressed beneath the gas-containing mass. Gas can also be noted in the lateral ventricle (L).

Figure 12.9(c) Barium sulphate paste was administered immediately following the survey radiographs (b). The contrast examination demonstrates mucosal irregularity and contrast material in the wall of the oesophagus. The thickened oesophageal wall can be seen between the contrast column and the trachea. The trachea is depressed by the mass. Aspirated contrast material lines the tracheal wall. The oesophagus is normal beyond the developing diverticulum. Diagnosis: oesophageal obstruction due to chronic oesophageal wall disease and developing diverticulum.

[546]

(b)

(c)

[547]
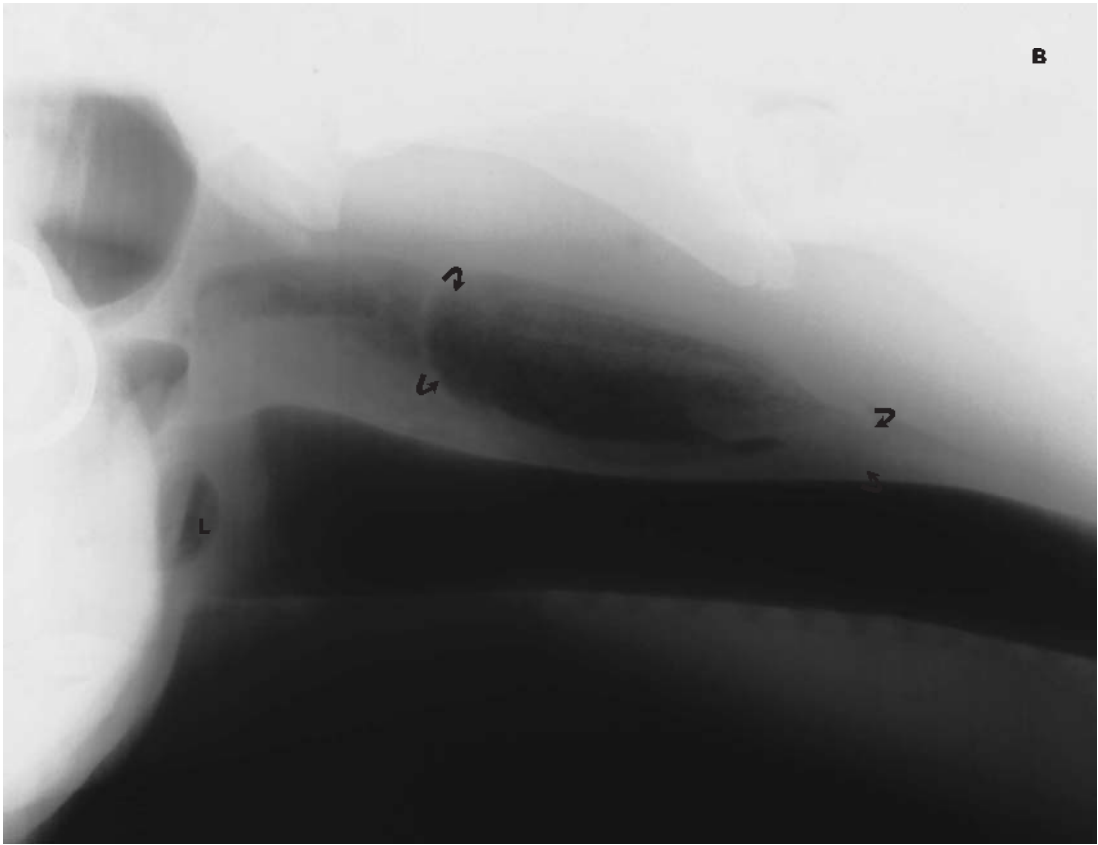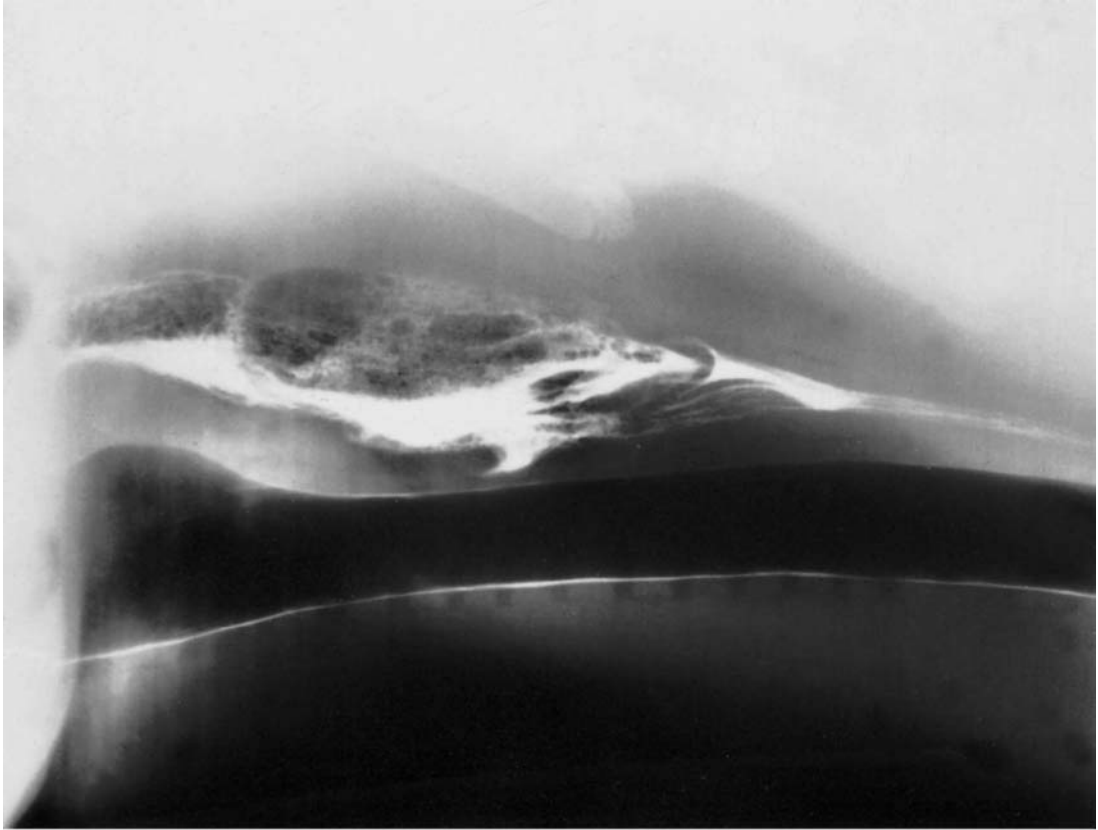
ventral colon is just caudal to the diaphragmatic flexure against the ventral abdominal wall. Crescent-shaped folds may be identified between the haustra of the ventral colon when the content is more or less dense than soft tissue. The caecum is located in the mid abdomen and often has a gas cap. The colon lies ventrally with the sternal flexure, beneath the diaphragmatic flexure. The dorsal and ventral flexures of the colon cannot usually be separated. The pelvic flexure is found ventrally adjacent to the urinary bladder. The small colon and rectum are located dorsocaudally. The kidneys are rarely seen radiographically.

Right and left lateral recumbent positions

There is little change in the anatomical location of structures, but they may become more or less visible due to the shifting of air and fluid contents or, in the case of contrast examination, the passage of contrast material silhouetted against soft tissue or a gas-filled viscus.

Ventrodorsal position

The stomach is located to the left of the midline, with the diaphragmatic flexure of the colon crossing over against the liver and occupying the right cranial abdomen. The duodenum exits the pyloric antrum caudal to the main body of the stomach and the sigmoid loop extends approximately two-thirds of the way to the right body wall, just caudal to the ventral colon, before passing caudally as the descending loop. The descending loop passes caudally to about the level of the last rib before changing course medially and cranially to form the caudal flexure. The jejunum is caudal to the stomach and lies mostly on the left side. The base of the caecum is located in the right caudal abdomen, with the apex near the xiphoid cartilage. The small colon is located on the left side. The right and left ventral and dorsal large colon lie on both sides ventrally.

Adult abdomen

The liver lies adjacent to the diaphragm and separates the stomach from the sternum in the cranioventral abdomen. The stomach is craniodorsal on the left side, but is not fixed in position.

ANATOMICAL VARIATIONS

The main difference in the anatomy of the foal and the adult horse is the relative change in size of the stomach, the caecum and large colon. In the foal the stomach is larger in proportion, but this decreases with age as the caecum and colon increase in size.

[548]

Contrast studies in the foal

Survey radiographs should always be obtained before the administration of contrast material in order to have baseline information regarding the size, shape and position of organs prior to contrast administration.

The foal cannot be fasted for the same time interval as the adult because fluid and electrolyte balance must be maintained. Therefore, fasting should not be more than 4 hours in foals that are still on fluid diet and 12 hours for foals which are eating solid food. Fasting should be limited to solid matter and not fluids. Contrast material should be administered by nasogastric tube at the rate of 5 ml of barium sulphate suspension (30% w/v) per kilogram. Radiographs should be obtained immediately and at 30 minutes, 1 hour and then at hourly intervals thereafter until the contrast reaches the small colon. Additional radiographs can be obtained as required. When possible, standing right lateral and ventrodorsal radiographs should be obtained. Normal transit time is approximately 8 hours.

The stomach is best evaluated using a double contrast technique following a 4–12 hour fast (see above). Barium sulphate suspension 30% w/v is then administered via stomach tube at a rate of 5 ml/kg. Normally there is adequate air in the stomach, but if not it should be slightly distended by administration of air. Care must be taken not to overdistend the stomach. The standing patient is placed with the left side to the cassette and radiographed. In a recumbent foal, right and left lateral recumbent and ventrodorsal radiographs should be obtained immediately following administration of the contrast and air. These radiographs should be repeated at 30 minutes, 1 hour and 2 hours post-administration. Contrast material may begin to exit the stomach as early as 10 minutes after administration, but emptying may vary greatly depending on the gastric content. The pylorus and the duodenum may not be recognized as distinct features, but contrast material may be defined in the descending duodenum within the first 10 minutes as it exits the pylorus in the mid to lower third of the abdomen and passes over the gas-filled stomach. The remainder of the small bowel then fills and contrast usually reaches the caecum in 4–5 hours.

DISEASES OF THE GASTROINTESTINAL TRACT

Small intestinal obstruction

Multiple small intestinal loops are distended with gas and fluid (Figures 12.10, 12.11, page 551 and 12.13a, page 554). Hairpin curves are often noted as well as many gas-capped fluid levels. The stomach may also be gas distended. Mechanical or functional obstruction cannot be differentiated.

Large intestinal obstruction

Meconium retention or large intestinal obstruction may be visualized on lateral standing or recumbent radiographs as an ileus (Figures 12.11, page

Figure 12.10 A standing lateral radiograph of a 3-week-old foal demonstrates lack of abdominal visceral detail ventrally with some granular material which is apparently within the large intestinal structures. The very opaque material is sand within a bowel segment. The moderately dilated small intestinal loops with unequal fluid levels (inverted Us) are suggestive of mechanical ileus.
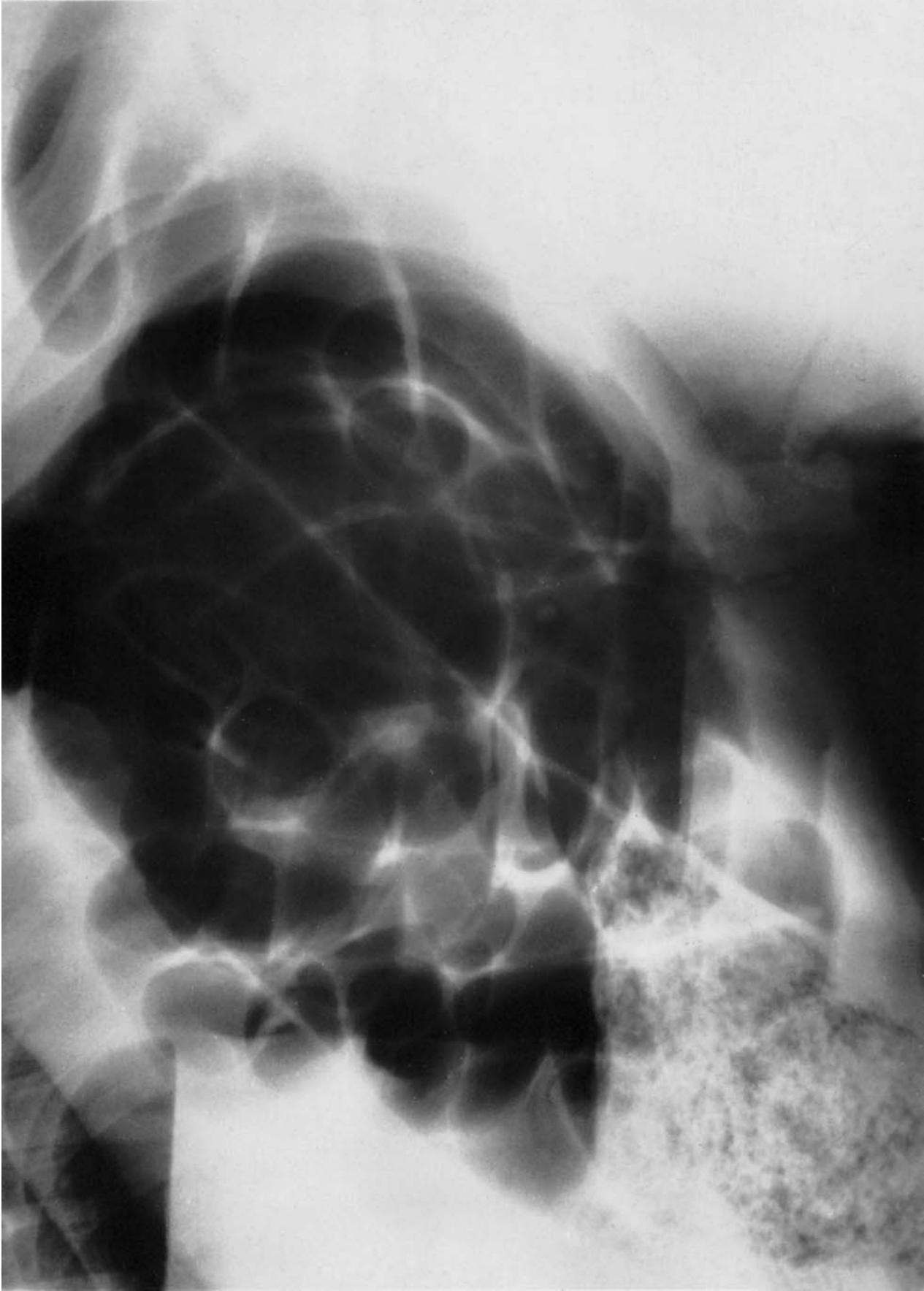
Figure 12.11 Thoroughbred foal with suspected meconium impaction. There are gas-distended large and small intestines. Cranioventrally there is granular appearing material in the large bowel which probably represents retained meconium. Gas in the rectum is thought to be secondary to enemas. Radiographic diagnosis: obstructive ileus, probably due to meconium in the mid large bowel.

[551]

551 and 12.12). Gas-distended bowel may outline the meconium retention. If the meconium is not visualized on a survey radiograph, barium or air may be placed in the rectum with the aid of either a stomach tube and gravity flow or a rubber syringe, thus demonstrating the area of blockage. With a barium or air enema care must be exercised. Stop immediately if pressure is encountered.

Atresia coli

Atresia coli has been reported in the foal and must be differentiated from other causes of ileus and colic. The lesion can be demonstrated by injection of contrast into the rectum, showing a lack of communication with the remainder of the large intestine (Figure 12.13b, page 555).

Ileocolonic aganglionosis

Ileocolonic aganglionosis occurs in white progeny of Overo Spotted Horses – 'lethal white foal'. These foals are normal at birth but do not defaecate. They develop signs of colic in the first day of life and must be differentiated from meconium retention, atresia coli (which may also occur in these foals) and atresia ani as well as other causes of colic. Radiographic diagnosis in these cases is based on ruling out other causes of colic and on the presence of distension of the stomach, small intestines and large bowel. A barium enema will not be expelled due to lack of contractility.

Gastroenteritis

There is a decrease in the granular appearance of the bowel content which appears to be more uniformly fluid filled than normal. Gas-capped fluid levels may be common, but there is no distension and hairpin loops are seldom seen. The gas caps do not stay in the same location on subsequent films, indicating that there is intestinal motility. Transit time is usually much shorter than the expected 8 hours.

Gastroduodenal ulcer disease in foals

Standing lateral radiographs demonstrate gastric distension which does not diminish with fasting. A gas cap is usually noted and air is often seen in the hepatic ducts (see Figures 12.6, page 542 and 12.7, page 543). Double contrast gastrography, performed with the foal in right lateral recumbency, demonstrates delayed gastric emptying for up to 4 hours and the contrast fills the pylorus and duodenal ampulla. Ulcers in the non-glandular portion of the stomach may be demonstrated as round to elliptically shaped lucent (black) filling defects with well-marginated walls of increased opacity (white). Ulcers can best be demonstrated by obtaining both right and left lateral recumbent and ventrodorsal radiographs which allow for double contrast coating of the mucosal surfaces. Standing thoracic radiographs may demonstrate mega-oesophagus with fluid and/or air. Contrast studies may
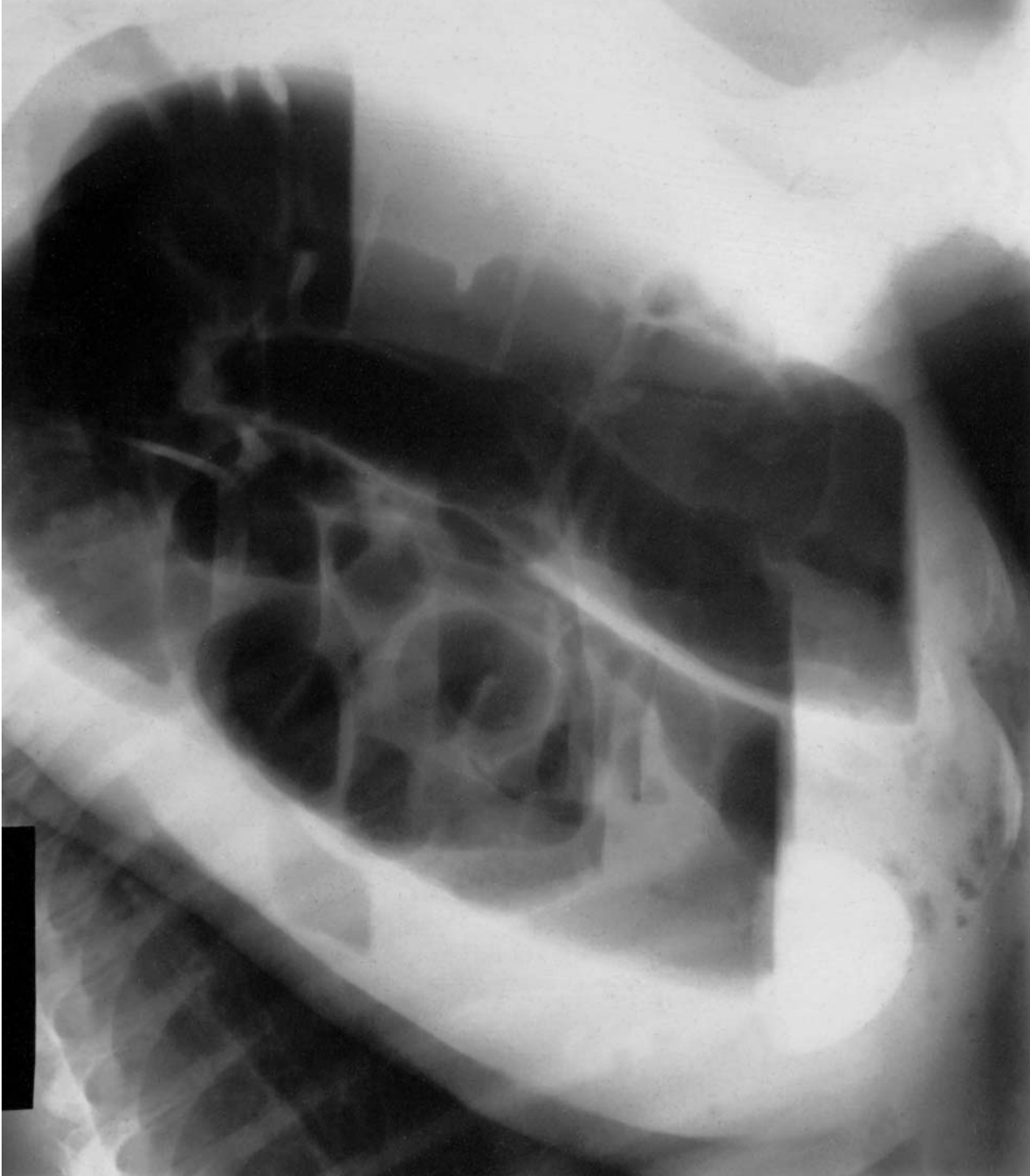
Figure 12.12 This 1-week-old Quarterhorse filly was presented because of recurrent colic. Meconium has passed normally, but there has been no faecal matter noted since then. Radiographs of the abdomen demonstrated markedly dilated large bowel structures with variable fluid lines. The small bowel appears normal. There is sand in the stomach. Radiographic diagnosis: large bowel obstruction.

[553]
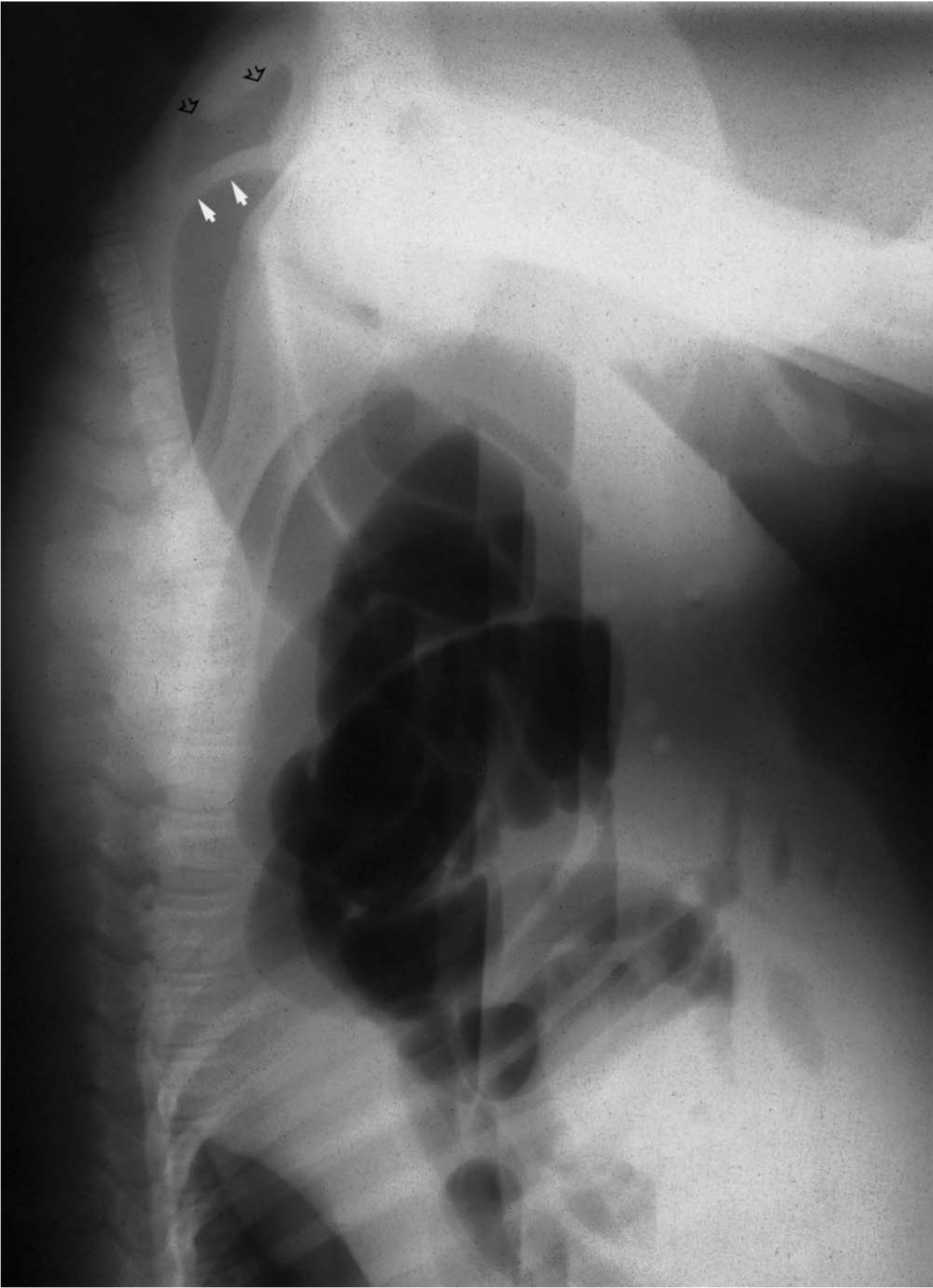
Figure 12.13 This 12-hour-old Arabian foal was born 3 weeks prematurely and had not passed meconium. (a) A survey radiograph shows fluid- and gas-distended bowel loops with varying fluid levels indicative of obstructive ileus. The large bowel appears to terminate at a soft-tissue wall (solid white arrows). Gas in the rectum (open arrows) does not appear to communicate with the remainder of the bowel.

Figure 12.13 *Cont'd* (b) Barium sulphate injected into the rectum does not communicate with the terminal large bowel. The soft-tissue wall is again noted. Radiographic diagnosis: atresia coli.

demonstrate gastro-oesophageal reflux or retention of contrast in the oesophagus. These foals often have increased interstitial lung markings which are in part due to an inability to make a maximal inspiratory effort due to the abdominal distension. Inhalation pneumonia may be a complication of this disease (see Chapter 11, page 513).

Rupture of a hollow viscus

A hallmark of rupture of a hollow viscus is free abdominal gas (Figure 12.14) which allows for visualization of the poles of the kidneys and is often seen between the stomach and the diaphragm. Gas-filled bowel loops appear to be elevated in the abdomen or to float due to free abdominal fluid, which also causes loss of abdominal visceral detail. The abdomen may appear pendulous and there may be a generalized increase in opacity of the abdomen.

Enterolithiasis of adult horses

Enterolithiasis should be suspected in patients with moderate, recurrent abdominal pain which is refractory to conservative therapy and when there is evidence of bowel obstruction. Enterolithiasis has been described in both the small intestine and the rectum, but the majority of cases occur in the colon.

   When enteroliths are suspected, radiographs should be obtained with the right side of the horse against the cassette. Left lateral radiographs should be obtained if further information is needed. Radiographic diagnosis is made by defining single or multiple opaque enteroliths. The diagnosis is sometimes aided by the presence of air adjacent to an enterolith. Absence of radiographic findings does not preclude the presence of enteroliths nor does the presence of an enterolith alone signify the presence of obstructive bowel disease.

Sand impaction

Sand impaction occurs most often in the ventral colon and results in occlusion of the lumen by an opaque mass.

Urinary system

In the adult horse, abdominal radiography for the diagnosis of urinary tract disease is primarily of use for identification of calculi. The use of ultrasound is generally superior for the evaluation of the kidneys.

CONTRAST EXAMINATION

Intravenous pyelography is of limited value, but can be used to visualize the kidneys and ureters (see page 581). Cystography (positive or double
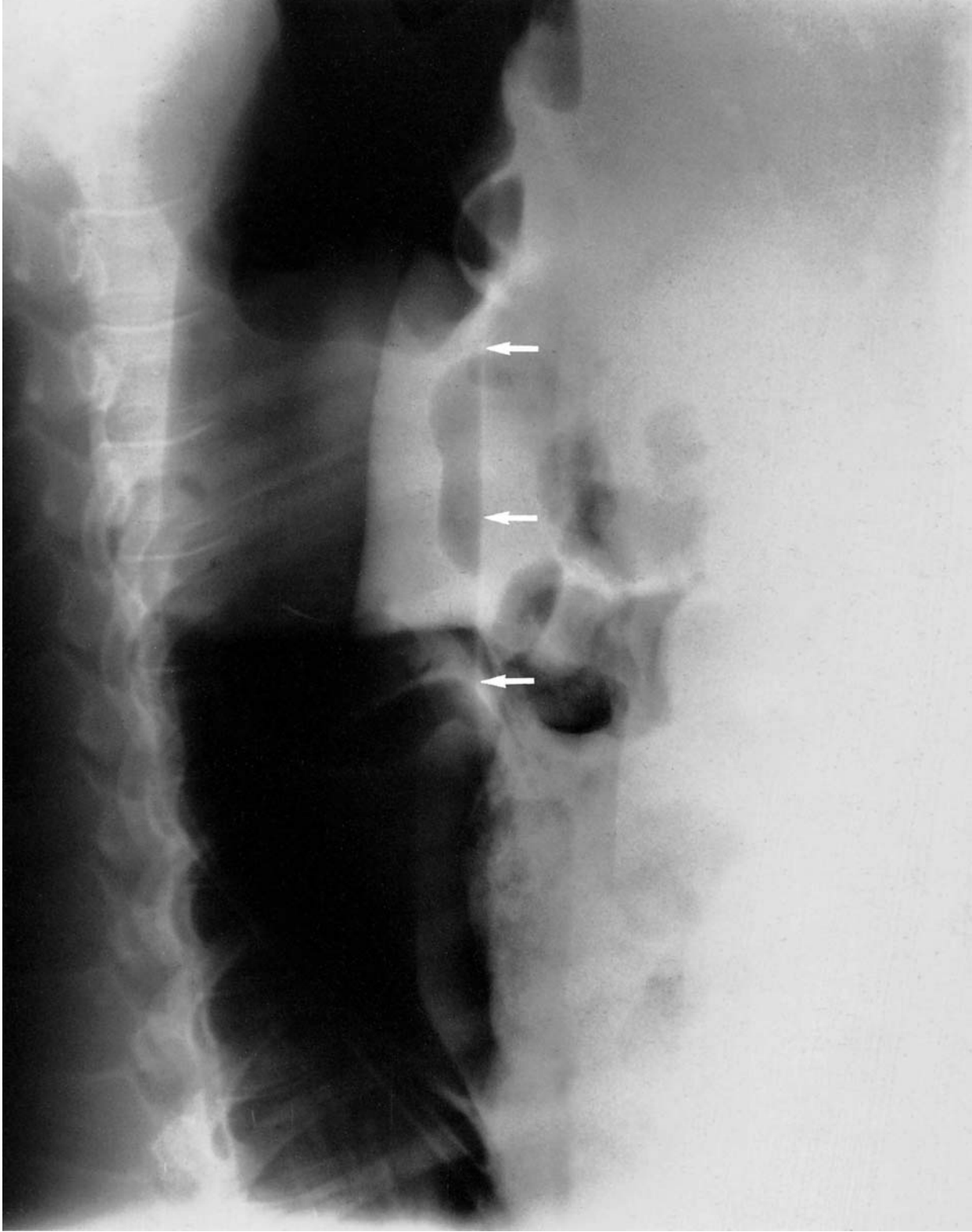
Figure 12.14 This 5-week-old Thoroughbred filly was presented with a history of prolonged diarrhoea. The patient had acute abdominal pain. The standing lateral radiograph reveals a lack of abdominal visceral detail ventrally. In the mid-portion of the radiograph, gas can be seen in bowel loops and multiple fluid levels are noted. Centrally in the mid-abdominal area there is a fluid line (arrows) which is not within a hollow viscus. This finding is indicative of free peritoneal air. Radiographic diagnosis: lack of abdominal visceral detail with free peritoneal air indicative of peritonitis and ruptured hollow viscus.

[557]

contrast) is useful for evaluating the bladder of the foal (see below and page 577).

Positive contrast cystography should be preceded by survey radiography of the caudal abdomen to assess bladder size and position. A flexible catheter is then placed in the urinary bladder and urine withdrawn. This allows for evaluation of the urine as well as giving some idea of the volume of urine present. Since the catheter is now filled with fluid, air will not be injected into the bladder, causing artefacts at the beginning of the examination. Between 2 and 5 ml of local anaesthetic is injected through the catheter into the urinary bladder so that the bladder may be distended without causing discomfort. A solution of equal volumes of any water-soluble contrast material, which is recommended for intravenous use, and sterile saline is then injected. The total volume of contrast mixture which will adequately distend the urinary bladder can be calculated at the rate of 12 ml/kg of body weight.

If no urine is retrieved after catheterization, half of the calculated amount of contrast can be infused and a radiograph obtained to evaluate the urinary bladder for content and placement. Additional contrast material, over the amount of urine withdrawn, or 50% of the calculated dose should be given slowly by syringe or by gravity flow. When resistance is noted, the filling should stop. Lateral and two ventrodorsal oblique radiographs are then obtained. These three views allow for visualization of the entire urinary bladder and assessment of the bladder wall. The positive contrast is then removed and an equal volume of air placed in the urinary bladder and the three radiographic views are repeated.

DISEASES OF THE URINARY BLADDER OF THE FOAL

Patent urachus

Although the diagnosis of congenital patent urachus does not require radiography, cystography and/or catheterization of the urachal remnant, these techniques may be of value in assessing the degree of the defect and the condition of the urinary bladder. Ultrasonographic examination of the urachus is often helpful in defining associated abscesses, free fluid and to monitor patency. A patent urachus (Figure 12.15) or urachal remnant (Figure 12.16, page 560) often result in cystitis (see below) and may be the nidus for recurrent cystitis as well as for the development of polyarthritis/polyosteomyelitis (see page 23). Patency may be demonstrated radiographically either by placing contrast material in the urinary bladder or by injection of the urachal remnant. Umbilical cord infection is often present without the presence of a patent urachus. Acquired patent urachus is caused by extension of inflammation and necrosis from the umbilical artery, vein or urachal remnant causing the urachus to reopen.

[558]

Figure 12.15 This 1-day-old Thoroughbred colt was presented because of a swollen prepuce and umbilicus. A patent urachus was suspected and a cystogram was performed by the placement of a catheter into the urinary bladder. Distension of the urinary bladder with contrast material demonstrates a patent urachus in the cranial ventral bladder wall and accumulation of contrast material in the subcutaneous tissues of the abdominal wall.

Figure 12.16 This 10-day-old Arabian colt presented because he did not exteriorize his penis and had urine scalds. Cystitis was suspected and a cystogram was performed by injection of contrast material through a urethral catheter. The standing lateral radiograph demonstrates a normal foal abdomen. The urinary bladder is in a normal position, but there is a urachal remnant noted in the mid ventral portion of the urinary bladder. The bladder wall is thickened adjacent to the diverticulum. Radiographic diagnosis: urachal diverticulum with concurrent cystitis.

[560]

Cystitis

Cystitis, regardless of cause, is evident radiographically by the appearance of a thickened and irregular bladder wall. The cranial ventral portion of the bladder is often more severely affected. In severe cases the entire bladder wall may be involved. Thickness and irregularity of the bladder wall can only be assessed when the urinary bladder has been adequately distended.

Rupture

Rupture of the urinary bladder is most common in the foal. The most consistent radiographic sign is the presence of free abdominal fluid, but an ileus may result and signs of ileus as well as the presence of fluid may be noted (see page 556).

The area of rupture may be demonstrated by cystography but demonstration may require that radiographs are obtained while contrast material is being instilled into the urinary bladder.

Free contrast material in the abdominal cavity does not present a problem so long as a sterile solution of water-soluble contrast is used and the patient is well hydrated. Barium should never be placed in the urinary bladder.

Ultrasonographic examination can demonstrate free fluid in the abdomen but will not demonstrate a tear.

FURTHER READING

Aanes, W.A. (1975) The diagnosis and surgical repair of a diverticulum of the oesophagus. *Proc. Am. Ass. Equine Pract.*, **21**, 211–222

Adams, S.B. and Fessler, J.F. (1987) Umbilical cord remnant infections in foals: 16 cases (1975–1985) *J. Am. Vet. Med. Ass.*, **190**, 316–318

Barga. U. (1972) The radiological examination of the digestive system of the horse. *Acta Rad. Suppl.*, **319**, 59–61

Bowman, K.F., Vaughan, J., Quick, C., Hankes, G., Redding, R., Purohit, R., Rumph, P., Powers, R. and Harper, N. (1978) Mega-oesophagus in a colt. *J. Am. Vet. Med. Ass.*, **172**, 334–337

Campbell, M.L., Ackerman, N. and Peyton, L.C. (1984) Radiographic gastrointestinal anatomy of the foal. *Vet. Radiol.*, **25**, 194–204

Campbell-Thompson, M.L., Brown, M., Slone, D., Merritt, M., Moll, H. and Levy, M. (1986) Gastroenterostomy for treatment of gastroduodenal ulcer disease in 14 foals. *J. Am. Vet. Med. Ass.*, **188**, 840–844

Dik, K.J. and Kalsbeek, H.C. (1985) Radiography of the equine stomach. *Vet. Radiol.*, **26**, 48–52

Fischer, A.T., Kerr, L.Y. and O'Brien, T.R. (1987) Radiographic diagnosis of gastrointestinal disorders in the foal. *Vet. Radiol.*, **28**, 42–48

Greet, T.R.C. (1982) Observations on the potential role of oesophageal radiography in the horse. *Equine Vet. J.*, **14**, 73–79

Greet, T.R.C. and Whitwell, K.E. (1986) Barium swallow as an aid to the diagnosis of grass sickness. *Equine Vet. J.*, **18**, 294–297

Hultgren, B.D. (1982) Ileocolonic aganglionosis in white progeny of Overo Spotted Horses. *J. Am. Vet. Med. Ass.*, **180**, 289–292

Pankowski, R.L. and Fubini, S.L. (1987) Urinary bladder rupture in a two-year-old horse: Sequel to a surgically repaired neonatal injury. *J. Am. Vet. Med. Ass.*, **191**, 560–562

Pearson, H., Pinsent, P.J.N., Polley, L.R. and Waterman, A. (1977) Rupture of the diaphragm in the horse. *Equine Vet. J.*, **9**, 32–36

Peterson, F.B., Donawick, W., Merritt, A., Raker, C., Reid, C. and Rooney, J. (1972) Gastric stenosis in a horse. *J. Am. Vet. Med. Ass.*, **160**, 328–332

Rose, J.A., Rose, E.M. and Sande, R.D. (1980) Radiography in the diagnosis of equine enterolithiasis. *Proc. Am. Ass. Equine Pract.*, **26**, 211–220

Schneider, J.E. and Leipold, H.W. (1978) Recessive lethal white in two foals. *J. Equine Med. Surg.*, **2**, 479–482

Traub, J.L., Gallina, A., Grant. B., Reed S., Gavin, P. and Paulsen, L. (1983) Phenylbutazone toxicosis in the foal. *Am. J. Vet. Res.*, **44**, 1410–1418

Verschooten, F., Oyaert, W., Muylle, E., De Moor, A., Steenhaut, M. and Moens, Y. (1977) Diaphragmatic hernia in the horse: four case reports. *Vet. Rec.*, **18**, 45–50

West, H.J. and Kelly, D.F. (1987) Renal carcinomatosis in a horse. *Equine Vet. J.*, **19**, 548–551

Wimberly, H.C., Andrews, E.J. and Haschek, W.M. (1977) Diaphragmatic hernias in the horse: a review of the literature and analysis of six additional cases. *J. Am. Vet. Med. Ass.*, **170**, 1404–1407

Yarsborough, T., Langer, D., Snyder, J. *et al.* (1994) Abdominal radiography for diagnosis of enterolithiasis: 141 cases (1990–1992). *J. Am. Vet. Med. Ass.*, **205**, 592–595

Chapter 13
Miscellaneous Techniques

ARTHROGRAPHY

Arthrography is the technique of introducing a contrast medium into a joint prior to obtaining radiographs. It has been used to aid evaluation of articular cartilage, meniscal damage, subchondral bone, and synovial membrane. It may be indicated in cases showing chronic joint distension, without apparent radiological abnormality on plain radiographs, radiographic findings incompatible with the clinical signs, or suspected joint capsule or articular cartilage damage. More specific indications include: evaluation of joint capsule ruptures or penetration, evaluation of cartilage flaps in osteochondrosis, to look for a cartilaginous joint mouse, and to differentiate between intra-articular and extra-articular bone fragments. Diagnostic ultrasonography can also be useful in assessment of some of these problems. Contraindications for arthrography may include infections of the joint or adjacent tissues, inflammation, and patients known to be allergic to contrast media.

For positive (or radio-opaque) contrast studies, any media approved for intravenous use may be used. Concentrated contrast media may obscure the joint surface, and thus obscure the lesions it is intended to outline, and so dilution of the media may be required. Approximately 25% tri-iodinated water-soluble contrast material is recommended. Some radiologists recommend the use of negative (or radiolucent) contrast (air, nitrogen or carbon dioxide), or double contrast, i.e. the use of negative and positive agents together. Negative contrast techniques may cause artefacts, due to gas bubbles forming in the synovial fluid during injection, and for this reason negative and double contrast studies are not often carried out. The formation of bubbles can be reduced by injecting the gas prior to the positive medium, and by using a positive medium with a low viscosity.

Technique

The patient may require sedation or general anaesthesia. The skin overlying the joint is prepared aseptically. Plain survey radiographs should be obtained immediately prior to the contrast study in order to re-evaluate the joint, as the contrast agent may remain in the joint or adjacent tissues for some time, making subsequent plain radiography impracticable.

A needle is introduced into the joint using aseptic technique. A volume of synovial fluid is then withdrawn and the equivalent volume of contrast agent introduced. The volumes will vary from 2 to 20 ml, depending on the size of the joint concerned. For double contrast studies, as much fluid as possible is withdrawn initially, and after injection of positive contrast as

much fluid as possible is again withdrawn. The joint is then distended with gas in order to outline the structures of the joint. (Although this is the normal technique, allowing radiographs to be made with positive contrast only if desired, it has been suggested that introduction of the gas first results in fewer artefacts from the formation of bubbles.)

After the injection of contrast agents, the joint should be extended and flexed, in order to spread the agents evenly throughout the joint. The study should be completed as soon as possible, and certainly within 20 min, or the contrast material will begin to be absorbed through the synovial membrane and the sharp appearance of the structures will be lost (see Figure 2.65b, page 117, and Figure 5.8, page 217).

Diagnostic criteria

Positive contrast medium will fill the joint, mixing with the synovial fluid. It will thus outline the joint pouches and will lie as a thin layer over the cartilage surfaces. The radiograph should be carefully examined, initially to ensure that areas of contrast conform with the normal anatomical shape of the joint. Subsequently the areas of contrast should be searched for any lucent areas (filling defects). These may represent radiolucent tissue masses (e.g. in chronic proliferative synovitis – Figure 2.65b, page 117), or simply be areas of the joint to which contrast has failed to be dispersed for some other reason. The differentiation between the two may be difficult, but further passive movement of the joint may help ensure even filling. The cartilage surfaces should be carefully examined for irregularity of the contrast film adherent to the cartilage surface. This may be particularly useful for detection of cartilage flaps, where contrast medium will be seen between the flap and the underlying bone, resulting in a visible cartilage irregularity and a lucent area in the contrast medium overlying the defect.

If double contrast studies are used, care must be taken that bubbles of gas are not misdiagnosed as tissue masses.

TENDONOGRAPHY

The term 'tendonography' includes any radiographic study of tendons. However, plain radiography of tendons is generally not very rewarding and so this section only describes studies involving the use of contrast agents. The tendons and ligaments on the palmar and plantar aspects of the third metacarpal and metatarsal bones may be visualized using contrast agents. This can be useful in the diagnosis of tendonitis, tendovaginitis, and contracture of the palmar/plantar annular ligaments of the metacarpophalangeal and metatarsophalangeal joints. The techniques have been largely superseded by the use of the diagnostic ultrasound.

Technique

Radiological examination of the tendon sheaths and bursae can be made in a manner similar to that described above for arthrography, using similar

techniques and concentrations of contrast medium. For evaluation of soft-tissue structures, however, the use of air as the contrast agent is often preferable.

Air tendograms can be made of the tendons between the tendon sheaths. The technique is normally carried out under mild sedation with the horse standing, although general anaesthesia may improve the results. An area of skin is clipped over the centre of the flexor tendons of the metacarpus/metatarsus, on the palmar or plantar surface. The skin is then prepared aseptically. Local anaesthetic is infiltrated at the site where the contrast is to be injected, to desensitize the area of injection. A needle is passed through the skin, and air injected subcutaneously and between the flexor tendons and ligaments. One hundred millilitres of air is usually sufficient. In order to separate the tendons and peritendinous tissues, considerable pressure may be required. Most of the air will be resorbed in 24 hours, and no adverse reactions have been reported. Standard radiographic views are made, using approximately half the mAs normally required.

Diagnostic criteria

The radiographic anatomy of the tendon sheaths is relatively complex, and the reader is referred to specific papers in the 'Further reading' list if they wish to embark upon this technique. Contrast studies permit the assessment of sheath or dorsal wall thickness, integrity of the synovial wall, and adhesion formation.

Air tendograms of the flexor structures of the limb aid assessment of the thickness of the flexor tendons, and allow accurate measurement and comparison. Enlargements are normally indicative of tendon strain. If peritendinous swelling is present, the outlines of the tendons lose sharpness. Adhesions will result in failure of the structures to separate. Rupture of ligaments and tendons can also be confirmed.

ANGIOGRAPHY

Angiography is the technique whereby blood vessels are visualized by the injection of positive contrast agent at the time of radiography. It is used to gain information about the anatomical position of blood vessels, to gain evidence of vascular disease, and in some circumstances to study the flow of blood through the vessels. Although it has been largely used for experimental purposes in equine veterinary medicine, it has an important role to play in the investigation and treatment of certain diseases, such as auditory tube diverticulum mycosis and suspected vascular abnormalities. It has also been used extensively in studies of the distal limb of the horse.

The technique is normally (but not invariably) carried out under general anaesthesia. For examination of the arteries, a positive contrast agent is injected into a major artery supplying the area. For venous studies, however, contrast may be injected via a major artery, allowing normal flow to carry it into the veins, or it may be injected directly into a suspected venous abnormality. It is also possible to stop venous outflow from an area with a

tourniquet, and inject contrast into a vein filling the veins 'against the flow', i.e. a retrograde injection. Although it is advantageous to obtain a series of radiographs after injection in order to visualize flow through the blood vessels, it may be adequate for many clinical cases to obtain a single radiograph, the timing depending on the area to be examined, but generally being about 2–5 seconds after the end of the injection.

Technique

The skin over the vessel to be injected is prepared as for surgery. Subcutaneous vessels may be injected directly with a percutaneous injection, but deeper vessels such as the carotid or common digital arteries are best approached surgically. It is important that arteries are handled with care, as trauma may cause spasm and give false results. It is recommended that the Seldinger technique be used to catheterize arteries, as this permits the introduction of a catheter of relatively large diameter with the minimum of trauma. After the study is completed, the catheter may be withdrawn, and haemorrhage controlled by applying finger pressure to the vessel for at least 2 minutes. For deeper injection sites, it is recommended that the tissues should be sutured and the incision closed prior to the withdrawal of the catheter, unless the patient is suspected to have clotting defects. Subsequent to withdrawal, pressure applied to the area with fingers, or a pressure pad and bandage, is normally adequate to stem haemorrhage. If a very large diameter catheter is used, then a purse string suture should be placed in the vessel wall prior to removal of the catheter, and pulled tight and tied after catheter withdrawal. Once a catheter has been introduced into a blood vessel, it may be passed on through the vessel, and manipulated to follow branches of the vessel (e.g. the internal carotid artery may be catheterized by passing a catheter with a curved tip along the common carotid artery). When injections of contrast are made, the tip of the catheter should be positioned at least 5 cm to the cardiac side of any branches of the vessel that are to be examined as part of the study.

A pressure injector is recommended if flow studies are required, or for adequate visualization of large vessels where a large volume of contrast is required. Hand injections are adequate in many practice situations, although they may require the use of a larger diameter catheter to allow injection of adequate volumes of contrast medium. There are many contrast media available for use in angiography, and there are no special requirements for the horse. The volume of contrast agent required should be just sufficient so that when the injection is completed, it fills the arterial vessels only, with no contrast evident in the capillary bed or veins. This varies with the area involved and the size of patient (approximately 5 ml for an injection into the common digital artery or 20 ml for injection into the common carotid).

Diagnostic criteria

Figures 13.1, 13.3(a), page 570 and 13.3(b), page 571 show normal angiograms of the head and distal limb of a horse. A detailed description is

[566]
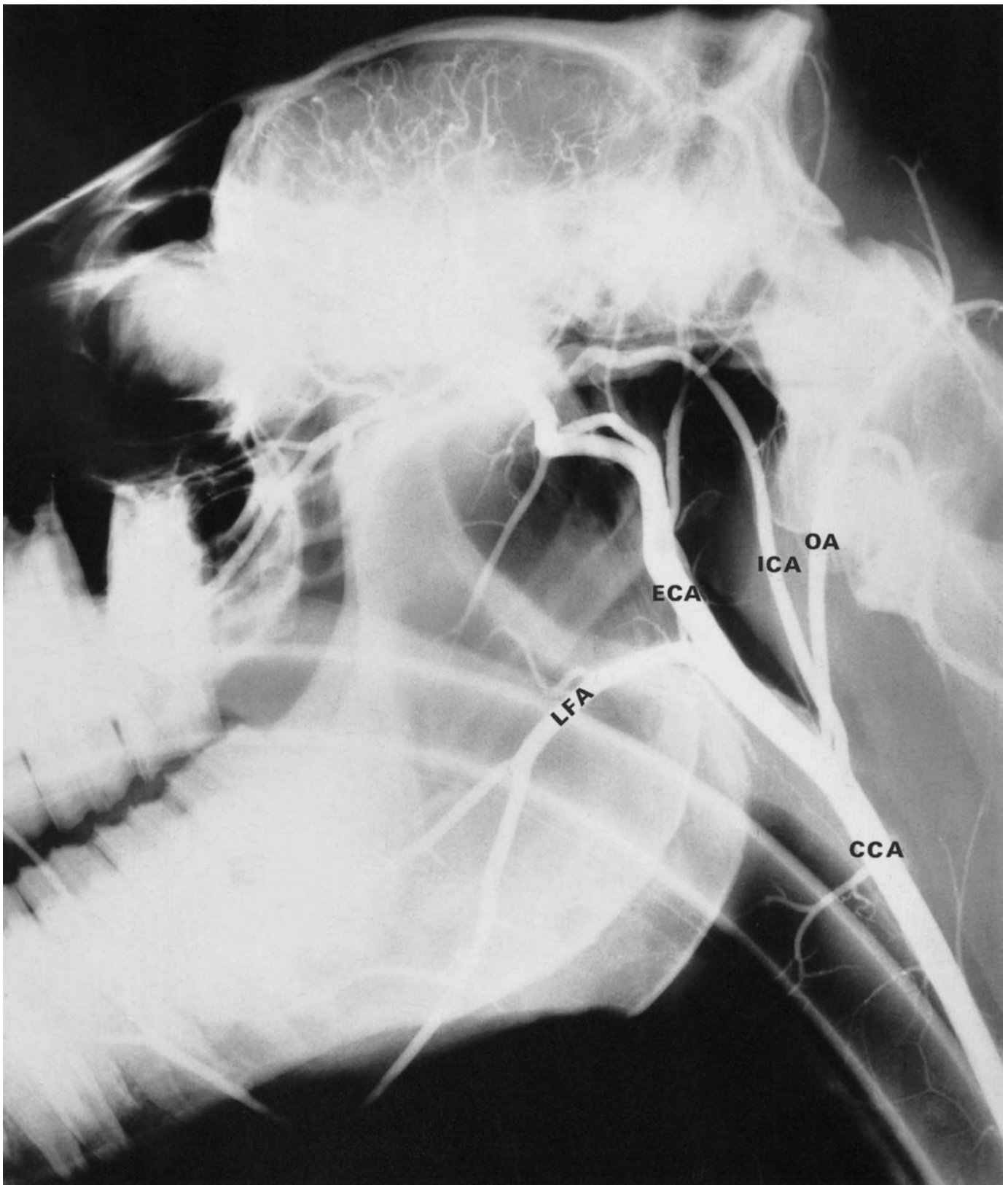
Figure 13.1 Lateral view of the pharyngeal region to show a normal angiogram of the head. The radiograph was obtained with the horse under general anaesthesia. Note the endotracheal tube, common carotid artery (CCA), occipital artery (OA), internal carotid artery (ICA), external carotid artery (ECA) and linguofacial artery (LFA).

not given, since reference to the figures will give adequate information on the normal. More detailed information on the techniques and results can be obtained from the 'Further reading' list given at the end of the chapter. The information that follows gives a general outline of the changes that can be anticipated to be found on angiograms of any area.

Clinically significant lesions found will vary with the site radiographed, but may include those given below.

Irregular arterial wall

1 There may be an irregular 'roughened' appearance to the arterial wall. There may be little overall change in diameter of the arterial lumen, or there may be obvious narrowing of a section or all of the artery. This may indicate arterial disease, e.g. thrombosis. This is seen in the internal carotid in some cases of auditory tube diverticulum mycosis, where it may indicate the initial stages of the artery thrombosing. It also occurs in the digital arteries of many horses, both 'normal' and with conditions such as navicular disease.

2 A condition known as 'beading' may occur, when the arterial wall goes into spasm. This gives regular narrowed bands along the length of the vessel, although the wall appears to have a generally smooth internal surface. This can occur in normal vessels, and is probably triggered by the pressure of the injection. It is most common in vessels that are already sensitive, either from rough handling when being catheterized or if suffering from arterial disease.

Distension of a vessel

1 A vessel may become enlarged because of an increased peripheral resistance or increased flow to an inflamed area, and does not necessarily indicate arterial disease.

2 Outpouchings of a vessel are abnormal. The most common cause is an aneurysm (Figure 13.2). This results from a weakness of the arterial wall, which allows the arterial lining to be forced through a defect in the wall. They are seen on angiograms as an outpouching, with a slight narrowing on the cardiac side of the defect. They may be congenital or acquired. Frequently they will give rise to spontaneous haemorrhage.

Narrowing of a vessel and failure to fill

Narrowing of a vessel and failure to fill have many common causes, which must be determined in the light of the available clinical information:

1 Arterial spasm may prevent a vessel filling or may cause partial filling or beading (see above). If serial radiographs are obtained using a rapid automatic serial plate changer, the vessel may be visible for part of the time, being occluded usually at the start of the injection. Repeat injections may be needed, but may result in repeat occlusion or narrowing of the vessel.

2 Another common cause of failure of an artery to fill is external pressure on the vessel. This may be caused by a haematoma, abscessation, neoplasia, or incorrect positioning of the patient.

[568]

Figure 13.2 Lateral view of the pharyngeal region of a 7-year-old Thoroughbred with a recent history of epistaxis and dysphagia. Endoscopic examination confirmed the presence of auditory tube diverticulum mycosis. This angiogram demonstrates an aneurysm of the internal carotid artery (arrow).

Figure 13.3(a) Lateral view of the foot of a normal pony. This angiogram was obtained 2.5 seconds after injection of the contrast medium into the common digital artery approximately 5 cm distal to the carpus (the pony was under general anaesthesia).

3 Arterial thrombosis may cause partial or complete occlusion of vessels (see also 'Distension of a vessel', above).

4 Inadequate concentration, volume or rate of injection of contrast medium may result in inadequate contrast for visualization of a vessel, or in vessels showing poor contrast.

MYELOGRAPHY

Myelography is the technique of introducing contrast agent into the spinal canal for radiography. It is usually performed to define the site or sites of cervical spinal cord compression in an ataxic horse, when a detailed clinical examination has suggested a lesion involving the cervical spinal cord. It is essential if surgical treatment is being considered. Survey radiographs

[570]
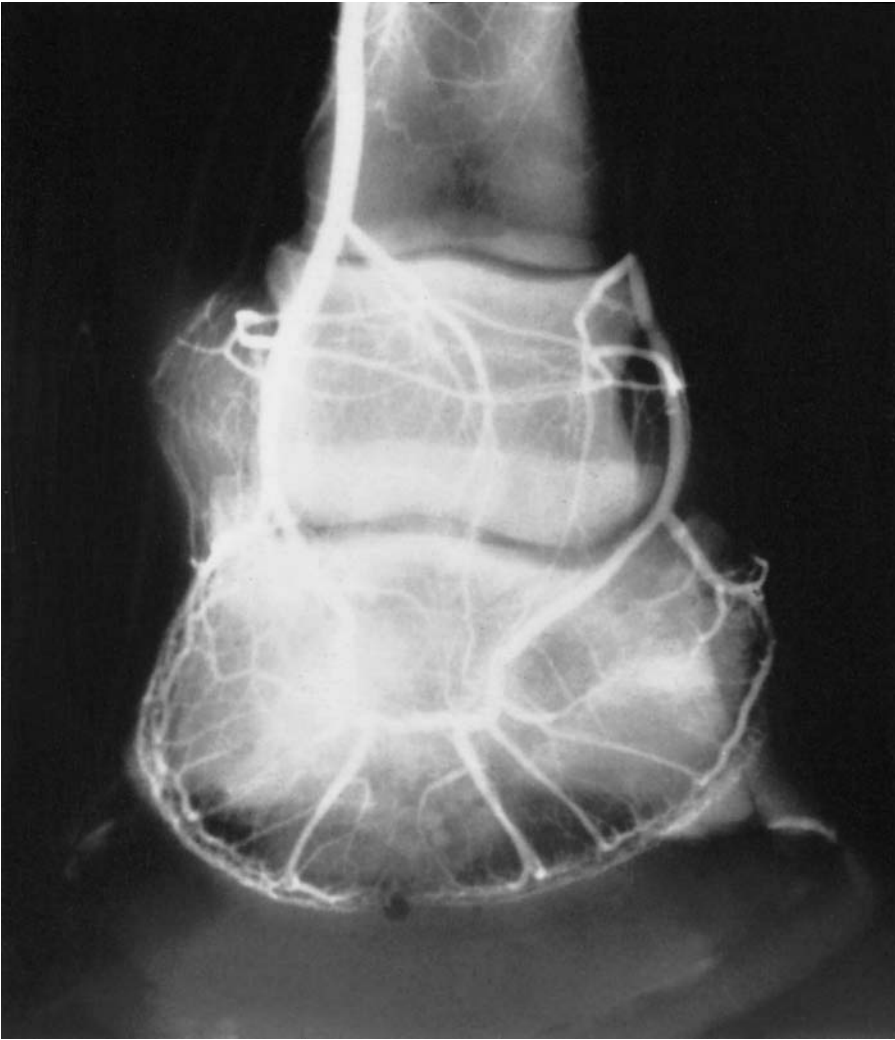
Figure 13.3(b) Dorsoproximal-palmarodistal oblique view of the foot of a normal pony. The angiogram was obtained 2.5 seconds after injection of the contrast medium into the common digital artery approximately 5 cm distal to the carpus (the pony was under general anaesthesia).

should be obtained prior to myelography, and are often suggestive of the site of a lesion.

Technique

Myelography is best performed under general anaesthesia, since it results in fewer untoward side-effects, and the neck can be examined radiographically in the normal, flexed and extended positions. This is essential for identification of dynamic compressive lesions. Ventrodorsal views can also be obtained (see Chapter 9, page 404 for details of the radiographic technique). Myelography has been performed in the standing horse, but is not recommended.

At present, the following anaesthetic regimen is recommended for myelography, since it has been associated with minimal side-effects:

premedication with acepromazine, detomidine or xylazine, followed by induction of anaesthesia using guianfenesin and thiopentone or ketamine, and maintenance using halothane in oxygen. Pretreatment with phenylbutazone is recommended.

The horse is positioned in lateral recumbency and plain lateral survey radiographs are obtained. It is important to support the neck with radiolucent cushions in order to obtain true lateral projections, which are essential for correct interpretation.

The skin over the poll is clipped and prepared as for surgery. The head is elevated approximately 30° and positioned so that the long axis of the head is perpendicular to the long axis of the neck. This prevents cranial passage of contrast material. An 18-gauge 86mm spinal needle is inserted at the intersection of a line joining the cranial borders of the wings of the atlas and the dorsal midline. It is directed perpendicularly to the skin, aiming for the lower incisor teeth. A change of resistance can usually be appreciated as the needle penetrates the dorsal atlanto-occipital membrane and the cervical dura mater. The needle's stilette is withdrawn, and cerebrospinal fluid (CSF) will appear at the hub if the needle is correctly positioned. It is important not to insert the needle too deeply, since spinal cord puncture may result, with severe adverse consequences.

Approximately 40ml of CSF is slowly withdrawn before injecting a similar volume of contrast agent over 3–5 minutes. Once injection is complete the needle is removed.

A superior technique involves the insertion of needles at both the cisterna magna and the lumbosacral subarachnoid cistern. A spinal needle is inserted on the dorsal midline approximately level with the cranial edge of the tubera sacrale and the caudal border of each tuber coxae, between the caudal edge of the dorsal spinous process of the sixth lumbar vertebra and the cranial edge of the second sacral dorsal spinous process. The latter landmarks can be difficult to palpate in a well muscled horse. Care should be taken to advance the needle in the sagittal plane. The needle is advanced into the ventral subarachnoid space, through the interacuate ligament, dorsal dura mater and arachnoid and the conus medullaris. Forty to sixty millilitres of contrast is injected slowly via the cisterna magna, and CSF is allowed to flow from the lumbosacral site. The stilette should be replaced in the needle at the lumbosacral site while images are obtained. This method, although technically more difficult, encourages contrast agent to flow in a caudal direction.

Metrizamide has been successfully used in the horse, although there have been a number of side-effects, including delayed recovery from anaesthesia, muscle fasciculations, depression, pyrexia, and deterioration of ataxia (it is not clear whether this last is due to the contrast agent or the affects of manipulating the neck during myelography and recovery from anaesthesia). Other, less irritant, non-ionic, water-soluble contrast agents have recently been introduced, and the use of either iopamidol (370mg I/ml) or iohexol (350mg I/ml) is strongly recommended. An iodine concentration of 300mg/ml will give an adequate density in a small horse, but contrast may be poor in larger horses.

Approximately 5 minutes after completion of the injection (or 1–2 minutes if the double needle technique is used), the horse's head may be repositioned level with the rest of the body, and radiography can be repeated. Cranial, mid-neck and caudal neck views should be obtained routinely, with the neck in the neutral position. With the neck in flexion, at least cranial and mid-neck views should be repeated, and with the neck in extension, at least a caudal neck view should be repeated. Flexion and extension of the neck should be performed carefully to obtain radiographs in these 'stressed' positions, which will help to define any dynamic component to compression. If necessary, the horse may then be positioned in dorsal recumbency in order to obtain ventrodorsal radiographic views and identify sites of lateral compression. These views are difficult to obtain and are limited to the cranial two-thirds of the neck. The myelographic study should be performed quickly, since radiographic contrast may be reduced with time by dilution and resorption of the contrast agent.

Interpretation of the myelogram

The myelogram should be evaluated with the neck in normal, flexed and extended positions in order to identify both static and dynamic lesions. Using 40 ml of contrast agent there should be complete filling of the subarachnoid space to the cervicothoracic junction. With the neck in the neutral position, the dorsal column of contrast agent is usually of more uniform width, and is wider than the ventral column (Figures 13.4a, page 574 and 13.5, page 576). There is slight widening of the dorsal contrast column at the caudal aspect of each vertebral foramen, and slight narrowing at the cranial aspect of each vertebral foramen. The ventral contrast column usually narrows slightly and is slightly elevated at the intervertebral spaces.

If the neck is flexed, the width of the dorsal contrast column remains uniform (Figure 13.4b, page 575), whereas the ventral column becomes narrower at the intervertebral spaces. This is most marked at the articulations between the third and fourth, and fourth and fifth cervical vertebrae. Extension of the neck results in slight widening of the ventral column in the fifth, sixth and seventh cervical vertebrae, with no change in the dorsal column.

Diagnostic criteria

Focal narrowing of the dorsal contrast column when the neck is extended or flexed (Figures 13.6a, page 578; 13.6b, page 579 and 13.7, page 580), together with narrowing of the ventral contrast column at similar sites, or occlusion of the passage of contrast agent, are indicative of a site of spinal cord compression. Narrowing of the dorsal column by more than 50% is generally considered to be significant. Focal narrowing of the ventral contrast column alone, when the neck is in the normal position or flexed, or of the dorsal column alone when the neck is extended, must be interpreted with extreme care, since these may be normal findings. Overflexion can result in obliteration of both contrast columns in the mid-neck region, especially in small horses, and may potentially accentuate spinal cord damage.

Figure 13.4(a) Lateral view of the second to fifth cervical vertebrae to show a normal myelogram of a mature Thoroughbred. Note that the dorsal dye column is much wider than the ventral column. The ventral column narrows slightly at the intervertebral articulations, but the dorsal column remains of uniform width.

Figure 13.4(b) Flexed lateral view of the third to sixth cervical vertebrae to show a normal myelogram (the same horse as in Figures 13.4a). Narrowing of the ventral dye column is accentuated at the intervertebral articulations, but the dorsal column remains a uniform width.

Figure 13.5 Lateral view of the fourth to seventh cervical vertebrae to show a normal myelogram (same horse as in Figures 13.4a and 13.4b).

The myelogram should be carefully inspected for evidence of more than one site of potential narrowing of the vertebral canal, since this will influence surgical treatment and prognosis. In some instances, interpretation of the myelogram by subjective evaluation of the width of the contrast columns is equivocal. In these cases, measurements of the minimum dural sagittal diameter may be useful, provided that a standardized radiographic technique is employed to allow for magnification, and comparison is made with horses of similar size.

Separation of the dorsal or ventral contrast column from the wall of the vertebral foramen is suggestive of an epidural or extradural space-occupying lesion, e.g. epidural haemorrhage or a prolapsed intervertebral disc. Occasionally false positive results are obtained from myelography. False negative results may occur due to failure to identify a laterally compressive lesion.

PNEUMOCYSTOGRAPHY

Chapter 12, page 556, describes the use of positive contrast cystography. Pneumocystography involves the introduction of air into the bladder, prior to radiographs being obtained. This provides negative (radiolucent) contrast within the bladder, allowing radiographic visualization of the internal surface of the bladder wall. While this can be carried out with the horse standing, the bladder can only be visualized on lateral radiographs of small horses. It is therefore normally necessary to carry out the technique under general anaesthesia, so that the bladder can be radiographed using the standard ventrodorsal views used for the pelvis (see Chapter 10, page 458).

Technique

This technique can be used in conscious foals or, if necessary, under mild sedation. The horse is positioned in dorsal recumbency as for pelvic radiography (see Chapter 10, page 458). A urinary catheter is then introduced into the bladder (a standard equine urinary catheter of approximately 7 mm diameter is adequate for this purpose in either sex). Any urine present should be withdrawn, and air is then introduced into the bladder and a radiograph obtained. The urethra in mares and geldings is sufficiently narrow for little air to escape around the catheter, but some device must be used to prevent egress of air through the catheter during the exposure. In adult Thoroughbreds, up to 5 litres of air may be used.

Diagnostic criteria

In the normal horse, the bladder is seen as a roughly pear-shaped lucent shadow lying in the abdomen and pelvic canal, the broader part being within the abdomen. It is important to realize that the outline of the cranial portion of the bladder may be modified by pressure on the bladder from the intestines. In some horses, there is a tendency for a mineralized 'sandy' deposit to collect in the bladder. Normally this is voided in part or in total with the urine, but if a portion is left in the bladder, it will be evident on

Figure 13.6(a) Lateral view of the second to fifth cervical vertebrae of a yearling Thoroughbred colt with mild hindlimb ataxia. Note the slight dorsal deviation of the fourth cervical vertebra, the suggestion of slight stenosis at its cranial orifice and the prominent caudal epiphysis of the third cervical vertebra. The myelogram was obtained with the neck in a normal (neutral) position. There is subtle narrowing of the dorsal dye column at the articulation between the third and fourth cervical vertebrae. The ventral dye column is narrower at each of the intervertebral articulations – a normal feature.

Figure 13.6(b) Flexed lateral view of the second to fifth cervical vertebrae (the same colt as in Figure 13.6a). Dorsal displacement of the head of the fourth cervical vertebra is accentuated and there is more obvious narrowing of the dorsal dye column at this level, confirming a site of spinal cord compression. This was verified at post-mortem examination.

[579]

Figure 13.7 Lateral view of the fifth to seventh cervical vertebrae of a 3-year-old Thoroughbred filly with severe hindlimb and forelimb ataxia. There is tremendous enlargement of the articular facets of the synovial articulations between the fifth and sixth and seventh cervical vertebrae, with marked irregularity of the joint spaces. These changes are compatible with severe degenerative joint disease. There is marked narrowing of the dorsal and ventral dye columns at the articulations between the fifth and sixth cervical vertebrae and to a lesser extent between the sixth and seventh. This is indicative of two sites of spinal cord compression. The filly was treated by fusion of the fifth, sixth and seventh cervical vertebrae and showed marked clinical improvement associated with some remodelling of the synovial articulation.

radiographs as a rather amorphous radiopacity lying in the dependent part of the bladder.

This technique is particularly useful in foals with suspected rupture of the bladder, where it can be carried out in the standing foal. It is important to look for air escaping from the bladder into the abdominal cavity, and not just to assess the outline of the bladder.

Positive (opaque) and double contrast studies can also be made, either introducing opaque contrast medium into the bladder via a catheter as above, or as a result of intravenous pyelography (see below). Interpretation is similar to that outlined above, but is generally more difficult than with pneumocystography.

INTRAVENOUS PYELOGRAPHY

This technique is of limited value, but can be used to assess the outline of the kidneys, ureters and bladder. It is normally performed under general anaesthesia with the horse in dorsal recumbency. Ventrodorsal views of the pelvic and abdominal areas are required (see Chapters 10 and 12), but lateral views of the abdominal region may also be helpful in thinner horses.

Technique

There is little information available on the use of this technique in the horse, but it can be successfully performed as follows:

The horse is placed in dorsal recumbency, and the bladder catheterized. Any urine present is withdrawn. The jugular vein is catheterized, and 100 ml of Urografin (Schering Chemicals) is injected over 30 seconds. Radiographs are taken at five 5-minute intervals, centring over the kidneys. Good visualization of the kidneys and ureters can be obtained using ventrodorsal views. The exact entrance of the ureters to the bladder is difficult to see on ventrodorsal or lateral views, as it tends to be superimposed upon the pelvis or abdominal viscera. This makes this technique of limited value in cases of suspected ectopic ureter. Within 15–20 minutes, the contrast medium collects in the bladder, and good positive contrast films of the bladder can be obtained.

OTHER TECHNIQUES

Contrast agents can be used to outline sinus tracts (so-called *fistulography*). They may also outline foreign bodies lying within sinuses. The technique varies, depending on the position and size of the sinus. If possible, a Foley catheter should be used, to limit leakage and allow injection under pressure if necessary. In smaller tracts, it may be sufficient to introduce the contrast agent through a flexible catheter of 2–3 mm external diameter, introduced no more than 1 cm into the sinus. In other situations, contrast agent may be introduced by passing a flexible catheter as far into the sinus as possible. Sedation of the patient may be necessary, and the infusion of local

[581]

anaesthetic into the sinus may also be beneficial. Diagnostic ultrasonography may also be useful.

Water-soluble, positive intravenous agents may be used, although contrast agents are manufactured specifically for fistulography. Contrast medium is likely to 'leak' from the sinus during injection, and should be cleaned from the skin surface prior to radiography. As always, more than one view of the area should be obtained. Interpretation of the results should be guarded. Sinuses frequently do not fill fully, and artefactual filling defects are quite common.

The nasolacrimal duct can also be visualized using intravenous contrast agents (*dacryocystorhinography*). The contrast medium is introduced through a flexible catheter most easily via the puncta lacrimalia, but can be retrograde through the nasal ostium. If the duct is blocked, it is important to take care that it is not ruptured, as contrast media may cause a marked soft-tissue reaction.

The duct commences as two separate branches about 1 cm from the medial canthus of the eye. They join at the medial canthus, the duct then passing forward over the outer wall of the frontal sinus to open at the lower commissure of the nostril. The duct generally has a consistent diameter throughout its length, and runs a relatively straight course. There may be several openings into the nostril.

POLAROID RADIOGRAPHS

The polaroid system of producing radiographs has a number of advantages and disadvantages when compared with conventional x-ray film. At the time of going to print only one type of transillumination film is available, which limits the flexibility of the system, and it is unlikely that this will change in the foreseeable future. The film is relatively fast, making it practical for use with portable x-ray machines.

The system has the advantage that it allows instant automatic processing without darkroom facilities, and the processing speed is rapid (usually 1 minute).

The film gives a positive image, i.e. dark structures on a clear background. This takes time to learn to read, but with practice can be read as easily as conventional film. It is particularly good for visualizing relatively lucent structures, such as the hoof wall and small osteophytic lesions.

The film is not as good as conventional film when looking for lucent changes in bone.

The film requires coating before it can be stored, in order that the image does not fade. Prior to coating, the emulsion is more easily scratched than that of conventional film.

FURTHER READING

Arthrography

Arnbjerg, J. (1969) Contrast studies of joints and tendon sheaths in the horse. *Nord. Vet. Med.*, **21**, 318

[582]

Dik, K.J. (1984) Equine arthrography. *Vet. Radiol.*, **25**, 93–96

Meredith, W.J. and Massey, J.B. (1971) *Fundamental Physics of Radiology*, 2nd edn, Wright and Sons, Bristol

Nichols, F. and Sande, R. (1989) Radiographic and arthroscopic findings in the equine stifle. *J. Am. Vet. Med. Ass.*, **181**, 918–924

Nixon, A. and Spencer, C. (1990) Arthrography of the equine shoulder. *Equine Vet. J.*, **22**, 107–113

Stashak, T.S. (1987) *Adams' Lameness in Horses*, 4th edn, Lea and Febiger, Philadelphia, pp. 171–172

Swanstorm, O. and Lewis, R. (1969) Arthrography of the equine fetlock. *Proc. Am. Ass. Equine Pract.*, **15**, 221–225

Tendonography

Hago, B.E.D. and Vaughan, L.C. (1986) Radiographic anatomy of tendon sheaths and bursae in the horse. *Equine Vet. J.*, **18**, 102–106

Stashak, T.S. (1987) *Adams' Lameness in Horses*, 4th edn, Lea and Febiger, Philadelphia, pp. 172–174

Verschooten, F. and De Moor, A. (1978) Tendinitis in the horse: radiographic diagnosis with air tendograms. *J. Am. Vet. Radiol. Soc.*, **19**, 23–30

Angiography

Colles, C.M. and Cook, W.R. (1983) Carotid and cerebral angiography in the horse. *Vet. Rec.*, **113**, 483–489

Colles, C.M., Garner, H.E. and Coffman, J.R. (1979) The blood supply of the horse's foot. *Proc. 25th Am. Ass. Equine Pract.*, pp. 385–398

Herbert, W.W. (1964) Angiographic artefacts which simulate or mask abnormality. *Am. J. Roentgenol.*, **92**, 907–917

Hertsh, B-W. (1983) *Arteriographische Untersuchungen an den Extremitäten beim Pferd*, Habilitationsschrift, Hanover

Lindbom, A. (1957) Arterial spasm caused by puncture and catheterisation. *Acta Radiol.*, **47**, 449–459

Seldinger, S.I. (1953) Catheter replacement of the needle in percutaneous arteriography. *Acta Radiol.*, **39**, 368

Wickbom, I. and Bartley, O. (1957) Arterial spasm in peripheral arteriography. *Acta Radiol.*, **47**, 433–448

Myelography

Beech, J. (1979) Metrizamide myelography in the horse. *J. Am. Vet. Radiol. Soc.*, **20**, 22–31

Burbidge, H., Kannegieter, N., Dickson, L. and Goulden, B. (1988) Iohexol myelography in the horse. *Equine Vet. J.*, **21**, 347–350

Conrad, R. (1984) Metrizamide myelography of the equine cervical spine: 14 case histories. *J. Am. Vet. Radiol. Soc.*, **25**, 73–77

Foley, J., Gatlin, S. and Selcer, B. (1986) Standing myelography in 6 adult horses. *J. Am. Vet. Radiol. Soc.*, **27**, 54–57

Hubbell, J., Reed, S., Myer, C. and Muir, W. (1988) Sequelae of myelography in the horse. *Equine Vet. J.*, **20**, 438–440

May, S., Wyn-Jones, G., Church, S., Brouwer, G. and Jones, R. (1986) Iopamidol myelography in the horse. *Equine Vet. J.*, **18**, 199–202

Nyland, T., Blythe, L., Pool, R., Helphrey, M. and O'Brien, T. (1980) Metrizamide myelography in the horse: clinical, radiographic and pathological changes. *Am. J. Vet. Res.*, **41**, 204–211

Papageorges, M., Gavin, P., Sande, R., Barbee, D. and Grant, B. (1987) Radiographic and myelographic examination of the cervical vertebral column in 306 ataxic horses. *Vet. Radiol.*, **28**, 53–59

Rantanen, N., Gavin, P., Barbee, D. and Sande, R. (1981) Ataxia and paresis in horses,

part ii: radiographic and myelographic examination of the cervical vertebral column. *Comp. Cont. Educ.*, **4**, 161–171

Widmer, W., Blevins, W., Jakovljevic, S. *et al*. (1998) A prospective clinical trial comparing metrizamide and iohexol for equine myelography. *Vet. Radiol. Ultrasound.*, **39**, 106–109

Other techniques

Crispin, S. (1988) Nasolacrimal duct cannulation in the horse. *In Practice*, **10**, 154–156

Lundin, C., Clem, M., DeBowes, R. and Bertone, A. (1988) Diagnostic fistulography in horses. *Comp. Cont. Educ.*, **10**, 639–645

Appendix A
Fusion Times of Physes and Suture Lines

HEAD AND VERTEBRAL COLUMN

Area	Centres	Notes	Closure	
HEAD				
Occipital	Squamous Lateral Basilar		Lateral-basilar Squamous to lateral- basilar Parieto-occipital Spheno-occipital Occipitomastoid	By 4 months 12–24 months 5 years* 5 years* Aged*
Sphenoid	Pre-sphenoid Post-sphenoid		 Spheno-occipital	Uncertain, but in first year 5 years*
Ethmoid	Perpendicular Cribriform			Uncertain, but soon after birth
Parietal	One centre		Parietal suture Parieto-occipital	4 years* 5 years*
Premaxilla	One centre		Left and right	During 4th year*
Nasal	One centre		Left and right Naso-frontal	Do not fuse 1 year*
Mandible	Two halves		Left and right	3 months*
CERVICAL SPINE				

Atlas	Two halves	Faint longitudinal line
		  evident in ventrodorsal
		  view in neonate		

Axis	Dens, head, body, caudal epiphysis		Dens to head Caudal epiphysis	About 7 months Complete 4–5 years

C3–C7	Cranial vertebral
	  physis
	Caudal vertebral
	  physis
				Complete by 2 years
				
				Complete by 4–5 years

THORACOLUMBAR SPINE				

T1–L6	Cranial vertebral
	  physis
	Caudal vertebral
	  physis
				6–12 months
				
				2–4 years

T2–T8	Separate centres of
	  ossification in
	  cartilaginous
	  summits
		Develop at about 12 months
		Gradual ossification
				Remain separate
				  throughout life

*Obliteration of suture; all others are fusion of suture.

[585]

Area	Centres	Notes	Closure	
SCAPULA	Scapular cartilage Body of scapula Cranial glenoid cavity of scapula	Cranial glenoid cavity of scapula and supraglenoid tubercle incompletely ossified at birth	Cranial glenoid cavity with body	About 5 months
	Supraglenoid tubercle		Supraglenoid tubercle	By 12–24 months
HUMERUS Proximal	Diaphysis Humeral head Greater tubercle	Lesser tubercle develops from same ossification centre as humeral head – incompletely ossified at birth	Centres of proximal epiphysis	Merge about 3–4 months
			Proximal physis	24–36 months
Distal	Diaphysis Distal epiphysis Epiphysis of medial epicondyle			11–24 months
RADIUS Proximal	Single epiphysis			11-24 months
Distal	Diaphysis Epiphysis Lateral styloid process		Lateral styloid process with epiphysis	Within 1 year
			Physis	20–24 months
ULNA	Single proximal epiphysis	Incompletely ossified at birth Occasionally a separate centre for anconeal process	Physis	24–36 months
METACARPUS Third metacarpus	Proximal physis Distal physis		Physis Physis	Fused at birth About 6 months
Second and fourth		Distal epiphysis cartilaginous at birth, gradually ossifies	Fuses with shaft	1–9 months
PROXIMAL PHALANX	Proximal epiphysis Diaphysis Distal epiphysis		Proximal physis Distal physis	About 1 year Fused at birth
MIDDLE PHALANX	Proximal epiphysis Diaphysis Distal epiphysis		Proximal physis Distal physis	8–12 months Fused at birth
DISTAL PHALANX	Single centre	Models until about 18 months Palmar processes model over 12 months		–
NAVICULAR BONE	Single centre	Models until about 18 months		–
PROXIMAL	Single centre	Outline complete about 3–4 months		–
SESAMOID BONES		Enlarge until 18 months		
CARPAL BONES	Single centre each	Fully developed about 18 months		–

Area	Centres	Notes	Closure	
PELVIS	Ilium – iliac crest and tuber coxae		Iliac crest and tuber coxae	About 10 months
	Pubis	Symphyseal branches of pubis and ischium fused at birth	Pubic symphysis	Remains open
	Ischium		Caudal portion of bone and tuber ischii	About 10–12 months
			Articular portions of pubis, ilium and ischium to form acetabulum	About 1 year
FEMUR Proximal	Femoral head Trochanter major Trochanter minor		Femoral head Trochanter major to femoral shaft Trochanter minor	24–36 months 18–30 months About 2 years
Distal	Epiphysis Diaphysis	Trochlear ridges develop over about 5 months Medial trochlear ridge becomes more prominent at about 2 months	Physis	24–30 months
TIBIA Proximal	Epiphysis Metaphysis Tibial tuberosity (apophysis)		Apophysis-epiphysis Epiphysis-metaphysis Apophysis-metaphysis	9–12 months 24–30 months 30–36 months
Distal	Lateral malleolus Epiphysis	(distal epiphysis of fibula)	Fuses to epiphysis Epiphysis-metaphysis	By 3 months 17–24 months
TUBER CALCANEI		May be absent at birth, gradually ossified	Fuses to calcaneus	By 16–24 months
FIRST AND SECOND TARSAL BONES				Usually fused at birth
PATELLA	Single centre	Incompletely ossified at birth Fully modelled about 4 months		
FIBULA		Little ossification until 2 months		

DISTAL TO TARSUS: Same as thoracic limb

Appendix B
Exposure Guide and Image Quality

Area/view	RS	FFD (cm)	AWF	Grid	kV	mAs
Head						
Cranium, lateral	600	150	–	CH	65	40
Cranium (under GA)	600	150	–	CH	75/80	64
Sinus, lateral	600	150	–	–	55	12
Pharynx	600	150	–	CH	65	35
Rostral, lateral	600	150	–	CH	60	18
Cervical spine						
Upper	600	150	–	CH	68	45
Mid	600	150	–	CH	70	50
Lower	600	150	–	CH	75	64
Lower/T1	600	150	–	CH	90	90
Thoracolumbar spine						
Withers (DSP)	600	150	yes	CH	65	50
Mid thoracic (DSP)	600	150	yes	CH	65	50
Caudal thoracic (DSP)	600	150	yes	CH	75	64
Cranial lumbar (DSP)	600	150	yes	CH	85	80
Mid thoracic artic./vertebrae	600	150	–	CH	100	160/180
Sacrum (cranial)	600	150	yes	CH	110	80
Sacrum (caudal)	600	150	yes	CH	70	63
Cranial coccygeal	600	150	–	CH	70	40/50
Scapulohumeral joint						
ML, standing	600	150	yes	CH	100/105	100/130
CrM-CdLO, standing	600	120	yes	–	80	25
ML, under GA (cassette tunnel)	600	130	yes	CH	100/105	130/160
Elbow						
ML, standing	600	150	yes	CH	70	20
CrCd, standing	600	120	–	–	66	13
Carpus						
LM and obliques	150	100	–	–	63	10
DPa	150	100	–	–	65	12
DPr-DDiO	150	100	–	–	65	10
Metacarpus/tarsus						
LM and obliques	150	100	–	–	62	9
DPa	150	100	–	–	66	12
RC/T II/IV	150	100	–	–	57	10
Metacarpo/tarsophalangeal joint						
LM and obliques	150	100	–	–	62	9
DPa/DPl	150	100	–	–	65	12
L45°Pr-MDiO	150	105	–	–	60	10
Pastern						
Flexed oblique	150	100	–	–	62	10

Area/view	RS	FFD (cm)	AWF	Grid	kV	mAs
Feet						
Lateral	150	100	–	8:1	70	22
Lateral	150	100	–	–	62	16
DPr-PaDiO, distal phalanx	150	100	yes	8:1	60	9
DPr-PaDiO, navicular	150	100	–	8:1	73	25
PaPr-PaDiO, navicular	150	100	–	–	66	14
DPa, weight-bearing	150	100	–	8:1	70	22
Pelvis						
Ischium	600	130	–	2	120	160
Pelvic canal	600	130	–	2	130	250
Coxofemoral joint	600	130	–	2	135	220
Sacroiliac joint	600	130	–	2	135/140	320
Ilial wing	600	130	–	2	135	220
Stifle						
Cd60°L-CrMO, standing	600	120	yes	–	57	13
CdCr, standing	600	120	yes	–	75	20
LM, under GA	600	120	yes	CH	65	40
CdCr, under GA	600	120	yes	CH	80	64
Patella, CrPr-CrDiO	600	120	yes	–	65	13
Tarsus						
LM	150	100	–	–	60	13
Obliques	150	100	–	–	63	13
DPl	150	100	–	–	70	13
DPl, flexed	150	100	–	–	70	15
Thorax						
Caudodorsal (diaphragm)	600	150	–	CH	80	36
Craniodorsal (aortic arch)	600	150	–	CH	90	36
Caudoventral (caudal heart)	600	150	–	CH	90	36
Cranioventral (cranial heart)	600	150	–	CH	110	40
Sternum, lateral	600	150	yes	CH	85	100
Abdomen						
Lateral, standing (7 day foal)	600	150	–	CH	70	63

Notes:
RS: Relative speed rating of screens.
FFD: Focus/film distance.
AWF: Aluminium wedge filter.
Grids:
   CH – Cross-hatch parallel 12:1 ratio grid.
   2 – Two crossed 12:1 ratio focused grids.
   8:1 – 8:1 ratio focused grid, 47 lines/cm.

ALTERING THE TABLE FACTORS

The exposures above are based on a 500 kg horse of Thoroughbred type. As an approximate guide the kV should be increased by 5% for limb radiography of heavier horses, and reduced for neonatal foals both by 5 kV and halving the mAs. Relative speed rating of screens and distance factors must both be considered when converting the above exposure guide.

[590]

Relative speed (RS)

Speed classification of film/screen combinations in terms of relative speed enables comparison of systems between manufacturers. Although the exposures required will be the same to produce images of similar opacity, the detail and resolution may vary. Some manufacturers use 100, 200, etc., some may use 2, 4, 8, etc., but the interrelationship is the same. Speed 8 requires half the exposure (mA s) needed for speed 4; speed 200 requires double the exposure (mA s) of speed 400 screens, etc. Generally speaking, if using only one screen from a pair (i.e. when used with single emulsion film) the speed of the system will halve, e.g. one screen from a pair rated 400 will give a speed of 200.

Distance

The distance between the source (focus) and the cassette (film) affects the radiopacity of the image produced. When the focal–film distance (FFD) is altered, the total amount of x-rays (mA s) must be increased or decreased to make a comparable exposure. The equation to calculate the exposure for a change in distance is:

$$\text{Old mA s} \times \frac{(\text{new FFD})^2}{(\text{old FFD})^2} = \text{New mA s}$$

i.e. The mA s decreases as the square of the distance.

FACTORS AFFECTING IMAGE QUALITY

There are many factors which have an effect on contrast, sharpness, resolution and opacity of the radiographic image. Choice of screen, film and grid is a major factor and needs to be carefully considered, each having an effect on the sharpness and definition of the final image. Faster screens mean shorter exposure times can be used, reducing the risk of movement blur, but these provide less resolution than slower screens. Individual films have inherent contrast and latitude values. When x-raying structures greater than 10 cm in depth the use of a grid should be considered to reduce scattered radiation. The final choice of factors will be a compromise for any given area radiographed.

Rare earth vs. calcium tungstate screens

Rare earth screens are more efficient and require less exposure than calcium tungstate, the light conversion of rare earth phosphors being approximately four times greater. As a general rule rare earth screens produce better detail radiographs than calcium tungstate screens.

Spectral sensitivity of screens and films

Screens emit light in a specific part of the spectrum. It is therefore important to match the spectral output of the screen to the spectral sensitivity of

[591]

the film. Failure to do so, in general, will result in loss of system speed and loss of information transfer. Calcium tungstate phosphors are blue emitting, rare earth phosphors may be blue, green or ultraviolet. Ensure the darkroom light filtration is correct for the type of film in use.

Single vs. double emulsion film

Single emulsion films, so-called mammography films, offer greater detail than conventional double emulsion films, and are used with a single screen. They do not suffer from parallax unsharpness evident with double emulsion films. They are, however, much slower and are not practical when using low-output portable machines as exposure times are too long, increasing the risk of movement. They can be used in conjunction with medium speed screens, as opposed to specific mammography screens, to increase the speed of the system to a certain degree.

Grids

Scattered radiation has a significant effect on image contrast. This can be improved by good collimation of the primary beam. Grids can also be used to control scattered radiation to improve contrast. However, they require more exposure, resulting in longer exposure times, and increasing the risk of movement blur. Focused grids need careful positioning to avoid grid cut-off and should be used at the correct distance for optimum results. Parallel grids have slightly more latitude when using FFDs greater than 120 cm. The higher the grid ratio and lines per centimetre the more effective the grid in reducing scatter, but the higher the grid factor. The grid factor denotes how much an exposure would need to be increased from non-grid values for comparable opacity, e.g. grid factor 2 – double the mAs. If a grid is unavailable, an air gap between the object and the cassette helps to attenuate scattered radiation.

Exposure factors

Exposure factors affect the opacity and contrast of the radiographic image. The quantity of x-rays reaching the film is a result of mAs (mA × time) and the FFD; these affect opacity, not contrast. The kilovoltage governs the quality of the x-rays and their intensity, and affects both opacity and contrast. A low kilovoltage gives high contrast with low latitude, whereas a high kilovoltage results in low contrast, but has a wide latitude. To obtain a radiograph with the same opacity as an original but decreased contrast, halve the mAs and increase the kilovoltage by 15% (approximately 10 kV). Conversely, to increase contrast levels, double the mAs and reduce the kilovoltage by 15% to achieve the same opacity. For good bone detail ideally the kilovoltage should be less than 70 kV. Attenuation of the x-ray beam is heavily dependent on the atomic number of the tissues, and it is desirable that photoelectric absorption predominates. Increasing the kV also results in more forward scatter.

Unsharpness

Movement is an obvious cause of unsharpness of the radiographic image. This can be reduced by the use of short exposure times and shorter focal–film distances. Unfortunately the use of a shorter FFD increases geometric unsharpness (penumbra). Poor screen/film contact is another cause of image blur. It can be tested for by placing a wire mesh on top of the cassette and making an exposure using a large FFD. Any areas of poor contact will result in unsharpness of the image.

Focal spot size

With high output stationary x-ray machines there is usually a facility to select different size focal spots. A smaller focal spot (e.g. 0.6 mm) usually results in better resolution, but an increased exposure time is required to achieve the same mA s output. Therefore when movement is likely to be a problem, e.g. in most proximal limb examinations, a larger focal spot (e.g. 1.5–2.0 mm) should be used to reduce exposure times to a minimum.

PROCESSING

Processing technique

Processing plays a major part in the quality of the final radiograph. Standard darkroom procedures will give more consistent and higher quality results.
- Change and replenish processing chemicals at regular intervals. Developer will deteriorate when not in use.
- Cover developer to reduce oxidation. Keep at a constant temperature. Do not overheat.
- Develop for the recommended time.
- Prepare the chemicals to the correct dilution.
- Wash thoroughly.
- Separate wet and dry areas to avoid chemical and water splashes. Keep clean to avoid dust and dirt on the screens.

Automatic processors provide a more consistent level of processing. They should be cleaned and serviced regularly.

Identifying processing problems

Overdevelopment: results in overall darkness of the radiograph
– development time too long or developer temperature too high
Underdevelopment: results in pale, washed out image, including background opacity
– development time too short, the developer is too diluted, too cold or exhausted
Uneven development: results in patchy opacities, including the background (manual processing)

[593]

– adjacent films touching in the developer, or uneven temperature in the developer tank caused by insufficient stirring

Yellow stain

– exhausted or old developer, poor fixation or insufficient washing

Milky image: image has not cleared completely

– insufficient fixing: fixer exhausted or overdiluted

Chemical smell (automatic processing)

– insufficient washing: wash tank empty or poor water flow; or chemical contamination

Stored films stained and silver sheen

– insufficient washing: wash tank empty or poor water flow

White marks

– dust, dirt or hair inside the cassette, or fixer splashed on the film before processing.

DEFINITIONS

resolution objective measurement of how much detail can be provided by a film/screen combination, measured in line pairs per millimetre. Indicates size of the smallest object that the system will record, i.e. the smallest distance that must exist between two objects before they can be seen as two separate entities.

definition subjective impression of the amount of detail that is seen in a radiograph. This is difficult to quantify.

Appendix C
Glossary

This glossary is not meant to be comprehensive, but provides brief definitions of some colloquial terms which may differ in usage in different countries, some anatomical terms which have recently been changed or adopted, a few radiological or radiographic terms, and other words not easily found in a dictionary or standard radiology text. Explanations of many technical terms may be found in the text by reference to the Index. Some radiological terms are discussed in greater detail in Chapter 1. Some words have different meanings when used in different circumstances, but only the definition relevant to the context of this book is included.

air gap space (occupied by air) between the object being radiographed and the cassette; the air gap will attenuate scattered radiation, thus a grid is not required.

antebrachiocarpal joint formerly called the radiocarpal joint.

apophysis bony outgrowth with a separate centre of ossification such as a tuberosity or process, under tensile forces.

arthropathy colloquial non-specific term to describe pathological changes within a joint (e.g. steroid arthropathy).

back-scatter deflection or production of radiation back towards the source; it is of most practical importance when high exposures are used; its effect on the film can be minimized by placing a sheet of lead behind the cassette.

Birkeland fracture articular fracture of the proximal palmar or, more commonly, plantar aspect of the proximal phalanx; the term has been used to encompass fragments from a number of different locations; some of these fragments may be developmental in origin.

bucked shins colloquial term used to describe periosteal and endosteal modelling on the dorsal aspect of the third metacarpal (metatarsal) bone resulting in an acquired convex contour to the bone; it is usually preceded by obvious 'shin soreness'.

callus, external new bone formation in response to a fracture on the external side of the bone (periosteal new bone).

callus, internal new bone formation in response to a fracture on the internal side of the cortex (endosteal new bone).

carpitis colloquial term used to describe inflammation of the antebrachiocarpal and/or middle carpal joints. Synovitis may or may not be accompanied by detectable radiographic abnormalities.

centrodistal joint formerly called the distal intertarsal joint (of the tarsus or hock).

chondroid inspissated pus (found in a paranasal sinus or guttural pouch) appearing radiographically as a radiopaque mass.

chondroma tumour composed of cells closely resembling those of normal cartilage, usually appearing radiographically as a space-occupying mass with some mineralization.

Codman's triangle triangular area of new bone adjacent to the cortex which develops as a result of elevation of the periosteum associated with neoplasia, inflammation, infection or trauma.

collimator device for restricting the field covered by the primary x-ray beam.

cone method of collimating the x-ray beam.

contrast degree of definition on an x-ray between adjacent structures of differing radiopacities.

[595]

contrast medium substance used to delineate a structure or structures; a positive contrast medium (agent) is radiopaque; a negative contrast medium is radiolucent.

cross-hatch grid grid composed of two sets of parallel lead lines perpendicular to each other.

definition clarity or distinctness with which radiographic image detail is seen.

delayed union failure of a fractured bone to unite within the expected period; if the cause is corrected healing should occur eventually.

density degree to which a tissue absorbs incident x-rays.

density, tissue weight per unit volume.

dental sac developing tooth.

dentigerous cyst cyst containing all or part of a tooth (or teeth); also called a temporal teratoma. All dentigerous cysts are temporal teratomas although not all temporal teratomas contain dentigerous material.

detail degree of sharpness with which individual shadows appear on the radiograph.

diaphysis shaft of a long bone.

distal interphalangeal joint formerly called the coffin, pedal or coronopedal joint.

distal intertarsal joint now called the centrodistal joint.

dorsal conchus formerly called the dorsal turbinate.

double contrast use of both positive and negative contrast media (agents), e.g. barium and air.

dystrophic mineralization mineralization in soft tissues (due to abnormal nutrition of the tissue). Occurs in areas of cell necrosis.

edge effect or edge enhancement term synonymous with a Mach line or band; a radiolucent line which may be created by one bone edge superimposed on another.

entheseophyte new bone formation at the site of insertion of a tendon, ligament or joint capsule.

epiphysis separate centre of ossification at each end of a long bone.

epiphysitis colloquial term used incorrectly to describe inflammation in the region of a physis or growth plate, most commonly the distal radial physis.

exposure latitude degree of overexposure or underexposure that can be tolerated in a correctly developed film and still produce an image of acceptable radiographic quality.

fatigue fracture synonymous with a stress fracture: an incomplete fracture, the result of repetitive overload and microfractures.

flatness lack of contrast on a radiograph.

fluoroscopy production of a visual image on a fluorescent screen for diagnosis.

fluid line horizontal interface separating a radiopaque area (fluid) distally from a more lucent area (often air) proximally.

focal distance perpendicular distance from a focused grid to the place in space where the planes that pass through the grid would converge.

focal–film distance distance between the x-ray tube focal spot and the plane of the radiographic film.

focused grid grid with lead strips slightly angled so that if they continued they would meet at some line in space, the focal point.

graininess lack of homogeneity in a radiographic image due to a clumping together of silver particles.

grid thin plate consisting of alternating strips of radiolucent and radiopaque (lead) materials which attenuate scattered radiation.

grid cut-off absorption of excessive amounts of primary radiation by the grid (and thus underexposure of part of the film) due to an incorrect angle between the primary x-ray beam and the grid; when a focused grid is used, the x-ray beam must be perpendicular to the grid and centred on the centre of the grid and with the focal spot of the x-ray tube at the proper focus distance to avoid grid cut-off.

grid ratio ratio between the height of the lead strips and the distance between them in a grid.

hairline fracture incomplete non-displaced fracture, sometimes used incorrectly as synonymous with a fatigue or stress fracture.

intercarpal joint now called the middle carpal joint.

involucrum sclerotic bone surrounding a sequestrum.

joint mouse small bony or mineralized fragment within a joint, usually mobile.

kV kilovoltage.

kVp kilovoltage peak (generally synonymous with kV).

kyphosis abnormal flexion of the thoracolumbar spine in the sagittal plane so that the dorsum appears abnormally convex; may be congenital or acquired.

light beam diaphragm method of collimating the x-ray beam by use of adjustable lead sheets incorporating a light beam to indicate the surface area to be exposed.

linear grid grid in which the lead strips are parallel to each other.

lordosis abnormal extension of the thoracolumbar spine in the sagittal plane so that the dorsum appears abnormally concave; may be congenital or acquired.

luxation complete dislocation or displacement of a joint.

Mach line or band synonymous with edge enhancement; a radiolucent line which may be created by one bone edge superimposed on another.

mA milliamperage – number of x-rays produced during an exposure.

margination definition of a bone contour, i.e. well or poorly marginated.

mAs milliamperage-seconds – exposure magnitude expressed as the product of milliamperage and time in seconds.

metaphysis wider part at the end of the diaphysis (shaft) of a long bone, adjacent to the physis.

middle carpal joint formerly called the intercarpal joint.

modelling there is confusion between the histological and radiographic use of the terms 'modelling' and 'remodelling'. Histologically, modelling refers to resorption and formation of bone which is not coupled and occurs at anatomically different sites (bone drift). It is a continuous process which regulates the macroscopic structure according to Wolff's law. Radiographically, modelling has been used to describe the formation of bone relevant to the cartilage model which is being replaced, i.e. the normal formation of bone. Thus the two definitions do not agree, so to avoid confusion, strictly speaking the term 'modelling' should be used to describe the change in shape of a bone as it adapts to the stresses applied to it (see also 'remodelling').

non-focused grid grid in which the lead strips are parallel, perpendicular to the surface of the grid.

non-screen film high-definition x-ray film designed for exposure without intensifying screens; higher exposure factors are required than if screens are used.

non-union cessation of fracture healing without bony union; may be classified radiographically as an atrophic non-union or a hypertrophic non-union.

odontoma tumour arising in tissues which normally produce teeth, usually solid and radiopaque.

opacity degree of whiteness of the object being radiographed.

osselet colloquial term used to describe enlargement on the dorsal aspect of a metacarpophalangeal joint which may be associated with thickening of the joint capsule and/or synovial proliferation, degenerative joint disease or an articular chip fracture. There may be mineralized tissue within the abnormal synovial tissue.

osseous metaplasia formation of bone in a non-bony structure.

osteitis inflammation of bone.

osteoarthritis synonymous with degenerative joint disease.

osteochondroma (a) benign tumour of projecting adult bone capped by cartilage undergoing endochondral ossification; (b) radiopaque body of mineralized cartilage which may be free floating or attached to synovial tissue (synovial osteochondroma).

osteolysis bone destruction and resorption seen more easily in cortical bone than cancellous bone because of greater contrast. There is a delay of at least 10 days between histologic and radiographic evidence of lysis.

osteoma solid, radiopaque tumour of bone, usually well marginated.

osteomalacia decreased bone mass due to insufficient or abnormal mineralization of osteoid.

osteomyelitis infection of a bone which has a medullary cavity.

osteopenia decrease in the radiopacity of bone due to osteoporosis or to osteomalacia.

osteophyte spur of new bone.

osteophyte, marginal or articular spur of new bone at an articular margin at the chondrosynovial junction.

osteoporosis loss of bone mass due to imbalance between bone resorption and formation.

pastern joint correctly called the proximal interphalangeal joint.

periosteal new bone new bone production, the result of elevation of the periosteum

[597]

from the cortex; there is usually a lag of at least 14 days between the initial stimulus and the radiographic detection of new bone.

physeal dysplasia abnormality of development of the physis; in some cases this may be a more appropriate term than physitis for a physeal abnormality.

physis growth plate of a long bone.

physitis inflammation of the physis often incorrectly called 'epiphysitis', characterized radiographically by irregular width of the physis with or without modelling of the adjacent metaphysis. Remnant cartilage cones may be seen as triangular radiolucent areas in the metaphysis.

primary cut-off absorption by a grid of the primary beam (grid cut-off).

podotrochleitis inflammation of the navicular bone (and/or navicular bursa).

primary radiation, primary beam radiation from the x-ray tube which is incident on the subject matter or which continues unaltered in photon energy after passing through it.

proximal interphalangeal joint formerly the pastern joint.

proximal intertarsal joint now called the talocalcaneal-centroquatral joint.

radiocarpal joint now called the antebrachiocarpal joint.

radiography practice of obtaining radiographs.

radiology study of radiographs; the science and application of ionizing radiation.

radiolucency degree of blackness of the object being radiographed.

radiopacity degree of whiteness of the object being radiographed.

rare earth screens intensifying screens that use rare earth phosphors; reduced exposure factors can be used in comparison to calcium tungstate screens.

remodelling there is confusion between the histological and radiographic usage of the terms 'remodelling' and 'modelling'. Histologically, remodelling refers to resorption and formation of bone which is coupled and occurs in basic multicellular units. This regulates the microstructure of bone without altering its shape and is a continuous process, replacing damaged bone with new bone. Thus it cannot be appreciated radiographically. The term has been used radiographically to describe the reshaping of bone to match form and function (e.g. after fracture repair), but strictly speaking the term 'modelling' should be used (see also 'modelling').

resolution objective measurement of how much detail that can be provided by a film/screen combination, measured in line pairs per millimetre. Indicates the size of the smallest object that the system will record, i.e. the smallest distance that must exist between two objects before they can be seen as two separate entities.

ringbone colloquial term used to describe new bone formation in the pastern region, which may encircle the parent bone. It is a non-specific term and its use is discouraged because of confusion caused by the prefixes high and low, true and false, articular and non-articular.

scatter radiation multidirectional radiation resulting from the interaction of the primary x-ray beam and an object; it causes loss of contrast between images on the radiograph.

scintigraphy production of two-dimensional images of the distribution of radioactivity in tissues after systemic administration of a radiopharmaceutical imaging agent.

sclerosis increased opacity of bone.

scoliosis curvature of the thoracolumbar spine from side to side; usually congenital.

secondary radiation particles (such as electrons) or photons (such as x-rays) produced by the interaction of the primary x-ray beam with matter.

seedy toe term with different usage in the USA and the UK. In the USA it describes separation at the white line seen secondary to chronic laminitis and rotation of the distal phalanx. In the UK it describes separation at the white line of unknown aetiology filled with crumbly dry material. It is not generally associated with rotation of the distal phalanx. Unless white line separation is extensive there is usually no associated lameness.

sequestrum necrotic fragment of bone; a sequestrum usually is a sharply demarcated sclerotic fragment separated from the parent bone by a zone of radiolucency and an outer rim of sclerotic bone (the involucrum).

silhouette sign effect produced when two fluid opacities are contiguous and the clear outline of one is lost; the two fluid opacities thus merge into one; often used in thoracic radiology.

soft x-ray beam low-energy, low-penetrating x-ray beam made at low kVp settings.

sore shins see 'bucked shins'.

splint colloquial term used to describe (a) active or inactive periosteal new bone on a second or fourth metacarpal (metatarsal) bone; (b) inflammation of the interosseous ligament.

splint bones second and fourth metacarpal (metatarsal) bones.

standing lateral positioning technique for a lateral projection using a horizontal x-ray beam, vertically positioned cassette and standing patient.

stress fracture synonymous with a fatigue fracture.

stressed radiographs radiographs of a joint obtained with the joint passively manipulated to assess joint integrity and to detect subluxation or luxation.

subluxation partial dislocation (displacement) of a joint.

summation radiopacity created by superimposition of more than one structure.

survey radiograph (a) radiographic study of a large area; (b) plain radiograph obtained prior to performing a contrast study.

talocalcaneal-centroquatral joint formerly called proximal intertarsal joint.

tarsocrural joint formerly called the tibiotarsal joint.

temporal teratoma neoplasm in the temple region comprising of a number of different types of tissue, none of which is native to the area in which it occurs.

tibiotarsal joint correctly called tarsocrural joint.

turbinate bone now called conchus.

ultrasonography imaging of soft tissues using the principle of echography: the variable transmission or reflection of ultrasound waves by tissues of differing densities.

valgus bent outwards: a deformity in which the angulation of the part is away from the midline of the body. Usage is confusing when terms such as carpal valgus are employed since, although the limb distal to the carpus is angled outwards, the carpus often appears 'knock-kneed', i.e. deviates inwards.

varus bent inwards: a deformity in which the angulation of the part is toward the midline of the body. Usage is confusing when terms such as fetlock varus is used: the distal limb is angled inward, but the fetlock appears to deviate outward.

Wolff's law modelling of bone according to the stresses placed on it, to be functionally competent while using the minimum amount of bone tissue.

weight-bearing radiograph radiograph of part of a limb obtained with the horse bearing some weight on the limb, ideally with the foot flat.

xeroradiography dry radiographic process in which the sensitive material consists of a plate carrying an electrical charge on the surface; when radiation interacts with the surface the charge is released; the plate is dusted with a special powder and an image is formed by the powder being attracted and retained in the charged area. Definition is high.

Index